Advanced Structured Materials

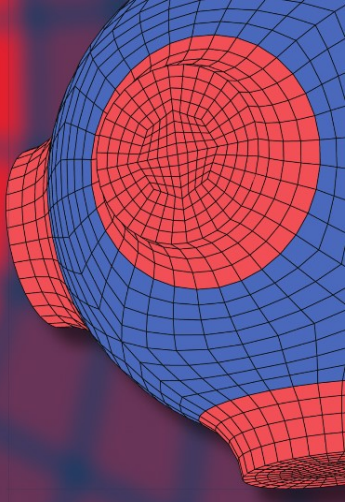

Sabu Thomas
P. M. Visakh
Aji. P. Mathew *Editors*

Advances in Natural Polymers

Composites and Nanocomposites

Springer

Advanced Structured Materials

Volume 18

Series Editors

Andreas Öchsner
Lucas F. M. da Silva
Holm Altenbach

For further volumes:
http://www.springer.com/series/8611

Sabu Thomas · P. M. Visakh
Aji. P. Mathew
Editors

Advances in Natural Polymers

Composites and Nanocomposites

Springer

Editors
Sabu Thomas
Centre for Nanoscience
and Nanotechnology
Mahatma Gandhi University
Kottayam, Kerala
India

Aji. P. Mathew
Department of Applied Physics
and Mechanical Engineering
Lulea University of Technology
Lulea
Sweden

P. M. Visakh
Centre for Nanoscience
and Nanotechnology
Mahatma Gandhi University
Kottayam, Kerala
India

ISSN 1869-8433 ISSN 1869-8441 (electronic)
ISBN 978-3-642-20939-0 ISBN 978-3-642-20940-6 (eBook)
DOI 10.1007/978-3-642-20940-6
Springer Heidelberg New York Dordrecht London

Library of Congress Control Number: 2012952035

Printed on acid-free paper

Springer is part of Springer Science+Business Media (www.springer.com)

Preface

The book on "*Advances in Natural Polymers*: *Their Blends*, *Composites and Nanocomposite*s", summarizes many of the recent technical research accomplishments in the area of natural polymers, such as cellulose, hemicellulose, lignin, chitin, starch, etc. As the title indicates, the book emphasizes on the various aspects of preparation, structure, processing, morphology, properties, and applications of natural polymers. It is written in a systematic and comprehensive manner. Recent advances in the development and characterization of multicomponent polymer blends and composites (macro, micro, and nano) based on natural polymers are discussed here in detail. It is very important to mention that till date, there are not many books published on the recent advances on the synthesis, morphology, structure, properties and applications of natural polymers, their blends, composites, and nanocomposites. In this sense, the content of the present book is unique. It covers an up-to-date record on the major findings and observations in the field of natural polymers. This book is intended to serve as a "one stop" reference resource for important research accomplishments in this area. The various chapters in the book are contributed by prominent researchers from industry, academia, and government/private research laboratories across the globe. This book will be a very valuable reference source for university and college faculties, professionals, post-doctoral research fellows, senior graduate students, polymer technologists, and researchers from R&D laboratories working in the area of natural polymers.

The first chapter on natural polymers: their blends, composites, and nanocomposites, give an over-view of the various natural polymers such as cellulose, hemicellulose, lignin, chitin, starch, etc. This chapter is very essential for the beginners in these fields since it provides a basic thorough understanding of the biopolymer field. The following chapter on cellulose-based blends, composites, and nanocomposites provides an overview of the main characteristics and properties of cellulose, as well as its most promising potential applications emphasizing the use of composites reinforced with lignocellulosic fibers, nanocomposites reinforced with cellulose whiskers, and bacterial cellulose nanocomposites. The first part of this chapter reviews the structure and properties of cellulose at the molecular, supramolecular, and morphological level. The authors also focus on the

cellulose whiskers, their main preparation and processing techniques, as well as the influence of the processing conditions on the characteristics of whiskers. Later in this chapter, the manufacture of cellulose-based blends, composites, and nanocomposites are also discussed. Finally, the authors present several applications for cellulose-based composites and nanocomposites including the biomedical, optoelectronic, and electrical applications along with the use of cellulose in the preparation of high strength "nanopapers" and packaging materials.

A survey on chitin and chitosan-based blends and composites is done in the third chapter. The authors concentrate on the utility of chitin and chitosan as potential materials for various implant applications and also address some of the challenges while dealing with its biocompatibility. The biomedical applications of chitin and chitosan-based blends and nanocomposites, such as tissue engineering scaffolds, wound dressings, separation membranes, antibacterial coatings, stent coatings, and biosensors are addressed. This chapter also brings out new innovative methods for extracting chitin and chitosan nanofibers for such novel applications. The study discloses the recent progress of chitin and chitosan-based fibrous materials, hydrogels, membranes, scaffolds, and sponges in wound dressing applications where the use of chitin, chitosan, and its derivative is immense.

The fourth chapter on starch-based blends and composite systems comprises of different sub-topics. The first section contains the basic introduction, structure, and properties and the second section deals with the preparation of starch-based materials using, casting film, extrusion sheet/film, injection moulding, compression moulding, and reactive extrusion. The possibility and development of blending starch with polyolefins, biodegradable polymers, etc. are explored along with the starch-based composites and nanocomposites. The coming chapter on soy protein provides basic understanding of its structure, mechanical properties, their amino acids composition, and thermal behavior. Moreover the fabrication of soy protein biodegradable films, coatings, and their functional applications in the area of nanocomposites are also dealt with.

Nano- and micro-carriers originating from milk proteins is yet another area in biopolymers. The chemistry of milk proteins, caseins and whey proteins, their structure, self-assembling behavior along with the films, and composites based on such proteins are discussed by giving special consideration to models. This chapter finds the extensive possibility of carriers, films, and coatings based on milk proteins, and the applications of such products in technology and industry. Another chapter based on recent studies on alginates-based blends, composites, and nanocomposites deals with the structure of alginates and their chemical modification such as introduction of hydroxyl and carboxyl groups. These materials have excellent properties such as physicochemical thermal properties, gel formation, rheological properties, and immunogenic properties. A thorough investigation on the preparation of micro-nano-particles and their films, fibers, different application, biomedical and pharmaceutical applications, and environmental applications is also included in this book.

The chapter on effective utilization of lignin in new advanced materials deals with the structure of lignin and its role and occurrence in plants. The lignification

process, lignin composition, and the structural information are observed by giving special attention to the effect of lignin properties such as amorphous structure, solubility, molecular weight, and molecular conformation on its compounds. The other properties of lignin such as antibacterial and antioxidant properties are also discussed. The great possibility of lignin nanoparticles, their properties, and nanolignin applications in composite systems are another important aspect of the study. There is a separate chapter on recent studies on hemicellulose as well as xylans and mannan-based blends, composites, and nanocomposites. Bacterial nanocellulose has a major role in medical implants and the fundamental idea behind its purification and morphological analysis is quite necessary. A distinct chapter on microbial cellulose, their modifications to increase the compatibility between cellulosic surfaces and a variety of plastic materials provides basic and deep knowledge in this area. Furthermore, fascinating current and future applications of bacterial cellulose and their nanocomposites especially in the medical field, such as biomimicking nature were described. Polylactic acid (PLA) has attained wide attention nowaday because of its biodegradability and crystallinity. The chapter on blends, composites, and nanocomposites of PLA offers an introduction to polylactic acid and their plasticized biodegradable and non-biodegradable blends, and also their composites with natural fillers. The nanocomposites of PLA with MMT cause its significant toughening. In addition to this, the notable applications of PLA/CNT and PLA/CNW nanocomposites are also explained. Special care has been taken toward the future aspects of PLA-based blends, composites, and nanocomposites. The last chapter covers the detailed significance and applications of polyhydroxyalkanoates (PHAs). These are another class of biodegradable natural polymers produced from bacterial fermentation. Apart from the introduction, properties, biosynthesis, production, composites, and blends of PHAs, the chapter gives more emphasis to its use in biomedical applications such as cardiovascular, wound treatment, nerve tissue engineering, drug-delivery systems, and dental materials.

Finally, the editors would like to express their sincere gratitude to all the contributors of this book, who made excellent support to the successful completion of this venture. We are grateful to them for the commitment and the sincerity they have shown toward their contribution in the book. Without their enthusiasm and support, the compilation of a book series could have not been possible. We would like to thank all the reviewers who have taken their valuable time to make critical comments on each chapter. We also thank the publisher Springer for recognizing the demand for such a book, and for realizing the increasing importance of the area of ***Natural Polymers*** and for starting such a new project, in which not many other publishers put their hands on.

Sabu Thomas
P. M. Visakh
Aji. P. Mathew
Deepa Lekshmi

Contents

Chapter 1
Natural Polymers: Their Blends, Composites and Nanocomposites: State of Art, New Challenges and Opportunities

P. M. Visakh, Aji P. Mathew and Sabu Thomas

Abstract The present chapter deals with a brief account on various types of natural polymers such as cellulose, chitin, starch, soy protein, casein, hemicelluloses, alginates, polylactic acid and polyhydroxyalkanoates etc. Blends, composites and nanocomposites based on these polymers have been very briefly discussed. Finally the applications, new challenges and opportunities of these biomaterials are also discussed.

1.1 Introduction

A large number of natural polymers could be easily prepared from animals and plants. These include cellulose, chitin, starch, soy protein, casein, hemicelluloses alginates, polylactic acid, polyhydroxyalkanoates etc. They have many attractive

P. M. Visakh · S. Thomas (✉)
Centre for Nanoscience and Nanotechnology, Mahatma Gandhi University,
Kottayam, Kerala 686 560, India
e-mail: sabuchathukulam@yahoo.co.uk

P. M. Visakh
School of Chemical Sciences, Mahatma Gandhi University, Kottayam,
Kerala 686 560, India

P. M. Visakh · A. P. Mathew
Division of Materials Science, Luleå University of Technology, 97187 Luleå, Sweden

S. Thomas
Universiti Teknologi MARA, Faculty of Applied Sciences,
40450 Shah Alam Selongor, Malaysia

S. Thomas
Center of Excellence for Polymer Materials and Technologies, Tehnoloski park 24 1000
Ljubljana, Slovenia

S. Thomas et al. (eds.), *Advances in Natural Polymers*,
Advanced Structured Materials 18, DOI: 10.1007/978-3-642-20940-6_1,

features. They are abundant, natural, renewable and biodegradable. During the past decade, many studies have been devoted to the manufacturing of advanced polymeric materials (blends, composites and nanocomposites) by mixing natural polymers with other polymers (natural and synthetic) and fillers (natural and synthetic).

1.1.1 Cellulose Polymers

Cellulose is the most common organic compound on earth having the chemical formula $(C_6H_{10}O_5)_n$. It is a polysaccharide consisting of a linear chain of several hundred to over 10,000 $\beta(1 \rightarrow 4)$ linked D-glucose units [1, 2]. Cellulose was discovered in 1838 by the French Chemist Anselme Payen. It was used to produce the first successful thermoplastic polymer, celluloid, by Hyatt Manufacturing Company in 1870. Professor Hermann Staudinger who determined the structure of cellulose in 1920. The compound was first chemically synthesized in 1992, by Kobayashi and Shoda [3].

Cellulose is the structural component of the primary cell wall of green plants, and many forms of algaeoomycetes. Some species of bacteria secrete it to form biofilms. About 33 % of all plant matter is cellulose (the cellulose content of cotton is 90 % and that of wood is 40–50 %). Cellulose has no taste, is odorless, is hydrophilic with the contact angle of 20–30° [4], it is insoluble in water and most organic solvents, is chiral and is biodegradable. It can be broken down chemically into its glucose units by treating it with concentrated acids at high temperature. Cellulose is soluble in cupriethylenediamine (CED), cadmiumethylenediamine (Cadoxen), N-methylmorpholine N-oxide and lithium chloride/dimethylformamide [5]. Cellulose is used in the production of regenerated celluloses (as viscose and cellophane) from dissolving pulp. Cellulose is a straight chain polymer unlike starch, no coiling or branching occurs, and the molecule adopts an extended and rather stiff rod-like conformation, aided by the equatorial conformation of the glucose residues. The multiple hydroxyl groups on the glucose from one chain form hydrogen bonds with oxygen atoms on the same or on a neighbor chain, holding the chains firmly together side-by-side and forming microfibrils with high tensile strength. Compared to starch, cellulose is much more crystalline, whereas starch undergoes a crystalline to amorphous transition when heated beyond 60–70 °C in water (as in cooking). Cellulose requires a temperature of 320 °C and pressure of 25 MPa to become amorphous in water [6].

Cellulose is one of the most attractive bio-resources for energy and chemicals [6–9]. Most cellulose is utilized as raw material in the paper industry for the production of paper and cardboard products. Cellulose based nanocomposites have emerged as a new type of advanced materials, attracting great interest in their research and development. Cellulosic nanocomposites are formed by adding cellulose nanoscale fillers in various polymer matrices resulting in mechanical reinforcement and alteration of other properties.

The cellulose found in woody plants (soft and hard woods, wheat, straw, bamboo, etc.) is present together with lignin, hemicelluloses and small amount of extractives [10]. In this case neat cellulose can be obtained by delignification with different processes (sulfite, sulfate or organocell method) in the form of pulp. The content of cellulose strongly depends on its source and the isolation procedure. Cellulose can be synthesized by other living organisms as well. For example, the tunicate is a marine animal that secretes tough cellulose called tunicin [11]. Other cellulose producing organisms are different types of bacteria, algae and some types of fungi [12]. Under the right conditions, some bacteria can synthesize a type of cellulose which is known as bacterial cellulose (BC). Traditionally BC is used as raw material for a Phillipinian dessert called "nata de coco" [13] and it is also present in the mat used for the preparation of a beverage known as "kombucha tea" [8]. BC can be produced by bacteria of different genera, including Gluconacetobacter, Rhizobium, Agrobacterium and Sarcina. BC is different from the cellulose produced in plants. BC is pure cellulose that has no lignin, hemicelluloses or other extractives that are normally found with plant cellulose. Also, BC is produced in the form of nanofibers of around 100 nm in diameter [14, 15]. These fibers form a coherent structured network that exhibits remarkable mechanical properties. BC has been utilized for a wide range of applications such as paper, textile and food industry and as a biomaterial in cosmetic and medicine [16, 17]. Cellulose based composites, blends and nanocomposites are being used for many applications. These include composites materials [18, 19], tissue engineered cartilage scaffolds [20, 21], wound dressings [22–26], artificial skin [23], dental implant, vascular grafos, catheter covering dressing [26], dialysis membrane [27], coatings for cardiovascular stents, cranial stents [26], membranes for tissue-guided regeneration [26], controlled-drug release carriers [26], vascular prosthetic devices [28] and artificial blood vessels [29–31], optoelectronic materials [32–34], Optical coating [35, 36], packaging materials [37] and electrical materials for electrical applications [38, 39].

1.1.2 Chitin and Chitosan Polymers

Chitin is a naturally occurring polysaccharide and is characterized by 2-acetamido-2-deoxy-D-glucose via a β [1–4] linkage. As the second most abundant biopolymer after cellulose, chitin occurs in enormous number of living organisms such as shrimps, crabs, tortoise, and insects, [40] and can also be synthesized by a non-biosynthetic pathway through chitinase-catalyzed polymerization of a chitobiose oxazoline derivative [41–43]. Chitosan, the most important derivative of chitin, can be prepared by its chemical modification. Chitin and chitosan have many excellent properties including biocompatibility, biodegradability, non-toxicity, absorption properties, etc., and thus they can be widely used in variety of areas such as biomedical applications, agriculture, water treatment and cosmetics.

During the last few years, some interesting papers have appeared in the literature about the preparation of composites made of chitin whiskers dispersed in natural and artificial polymers. It is believed that this subject represents at this time an opportunity for a better exploitation of chitin, as well as a challenge in view of solving certain technical difficulties. Paillet and Dufresne [44] was the first to report on the use of chitin whiskers as reinforcing agents for thermoplastics. In 2001 the matrix polymer for the nanocomposites preparation was poly(S-co-BuA). Thereafter, chitin whiskers have been increasingly used in many other polymer matrixes. Paillet and Dufresne [44] have discussed on the use of different types of preparation techniques for the manufacture of nanocomposites with chitin and chitosan. These include casting and evaporating technique, freeze-drying and hot-pressing technique, polymer grafting, non-aqueous solvent dispersion technique, extrusion and impregnation and electrospinning.

Both chitin and chitosan are as potential materials for various implant applications. The eventual realizations of real implants await the take-up of these materials on a more commercial basis that would see the introduction of chitin-based implantable devices. They are very much useful for nanocomposites materials [45] biomedical applications such as tissue engineering scaffolds, wound dressings, separation membranes, antibacterial coatings, stent coatings and sensors. Nano fibrous scaffolds based on chitin or chitosan have potential applications in tissue engineering. Electrospun chitin and chitosan nano fibrous scaffolds could be used to produce tissue engineering scaffolds with improved cytocompatibility, which could mimic the native extracellular matrix (ECM). Additional studies are necessary before clinical applications and for commercialization of the chitin and chitosan based nanofibers. Chitin and chitosan seem to be excellent dressing materials for the wound healing. The recent progress of chitin and chitosan-based fibrous materials, hydrogels, membranes, scaffolds and sponges in wound dressing have been reviewed by many researchers [46–55]. In the area of wound management, the use of chitin, chitosan and its derivative is immense.

As a renewable and biodegradable nanoparticle, chitin whiskers are attracting great attention from both academic and industrial fields. Similar to cellulose whiskers, with so many advantages over conventional inorganic nanoparticles such as low density, non-toxicity, biodegradability, biocompatibility and easy surface modification and functionalization, chitin whiskers with or without modification, are supposed to find extensive application in many areas such as reinforcing agents for polymers, cosmetic, food industry, drug delivery, tissue engineering. In summary there are abundant of opportunities combined with challenges in chitin whisker related scientific and industrial fields.

1.1.3 Starch Polymers

Starch is a polymeric carbohydrate consisting of anhydroglucose units linked together primarily through α-D-(1 → 4) glucosidic bonds. Starch is a heterogeneous material containing two microstructures, the linear (amylose) and the

branched (amylopectin). Amylose is essentially a linear structure of alpha-1,4 linked glucose units and amylopectin is a highly branched structure of short alpha-1,4 chains linked by alpha-1,6 bonds. The linear structure of amylose makes its behavior more closely resemble that of conventional synthetic polymers. Amylopectin, on the other hand, is a branched polymer and its molecular weight is much greater than amylase. Light scattering measurements indicate its molecular weights in the order of millions. The high molecular weight and branched structure of amylopectin reduce the mobility of the polymer chains, and interfere with any tendency for them to become oriented closely enough to permit significant level of hydrogen bounding. Most native starches are semi-crystalline, having a crystallinity of about 20 $\sim$ 45 % [56]. Amylose and the branching points of amylopectin form amorphous regions. The short branching chains in the amylopectin are the main crystalline component in granular starch.

Various conventional processing technologies, such as casting, extrusion, injection and compression moulding, have been adapted for the processing starch-based materials, as well as some new techniques, such as orientation and reactive extrusion. Liao et al. [57] reported biodegradable nanocomposites prepared from poly(lactic acid) (PLA) or acrylic acid grafted poly(lactic acid) (PLA-*g*-AA), titanium tetraisopropylate, and starch. Arroyo et al. [58] reported that thermoplastic starch (TPS) and polylactic acid (PLA) were compounded with natural montmorillonite (MMT). The TPS can intercalate the clay structure and the clay was preferentially located in the TPS phase or at the blend interface. This led to an improvement in tensile modulus and strength, but a reduction in fracture toughness. Multilayer co-extrusion is another technique used in the preparation of starch/biodegradable synthetic polymer sheets or films [59–62]. Thermoplastic starch has been laminated with appropriate biodegradable polymers to improve the mechanical, water-resistance and gas-barrier properties of final products. These products have shown potential for applications such as food packaging and disposable product manufacture. Biodegradable polyesters such as PCL [63], PLA [64] poly(hydroxybutyrate-co-valerate) [63] are often used for the outer layers. These new blends and composites are extending the utilization of starch-based materials into new value-added products [65].

1.1.4 Soy Protein Based Polymers

The soybean (U.S.) or soya bean (UK) (Glycine max) [66] is a species of legume native to East Asia, widely grown for its edible bean which has numerous uses. Due to the high protein amount, soy has a high demand for nitrogen. Similar to other plants, soy protein has the primary function of providing amino acids for germination and protein synthesis. The plant is classed as an oilseed rather than a pulse by the Food and Agricultural Organization (FAO). Fat-free (defatted) soybean meal is a primary, low-cost source of protein for animal feeds and most prepackaged meals. Soy vegetable oil is another product of processing the soybean

crop. For example, soybean products such as textured vegetable protein (TVP) are ingredients in many meat and dairy analogues [67]. Soybeans produce significantly more quantities protein per acre than most other. Traditional nonfermented food uses of soybeans include soy milk, and from the latter tofu and tofu skin. Fermented foods include soy sauce, fermented bean paste, natto, and tempeh, among others. The oil is used in many industrial applications. The main producers of soy are the United States (35 %), Brazil (27 %), Argentina (19 %), China (6 %) and India (4 %). The beans contain significant amounts of phytic acid, alpha-linolenic acid, and the isoflavones genistein and daidzein. Liu et al. [68] prepared soy proteins/calcium carbonate nanocomposites, they reported that adhesive greatly improving the water-resistance and bonding strength of soy protein adhesives. Kumar et al. [69] prepared films based on soy protein isolate (SPI) and montmorillonite (MMT) were prepared using melt extrusion. Morphology, tensile testing, thermal behavior and water vapor barrier measurement were analyzed. The arrangement of MMT in the soy protein matrix ranged from exfoliated at lower MMT content (5 %) to intercalate at higher MMT content (15 %). There was a significant improvement in mechanical, thermal stability, and water vapor permeability of the films with the addition of MMT [69]. Jong et al. [70] prepared soy protein based styrene–butadiene (SB) latex nanocomposites using evaporation method. They have reported, good mechanical properties when they add small amount of soy protein to styrene–butadiene (SB) latex. From the literature they have more work have been reported in the preparation and characterization study of soy based blends, composites and nanocomposites [71–76].

1.1.5 Milk Protein Based Polymers (Casein Polymers)

Caseins are similar in structure and found in milk as nanoparticles called micelle. Casein micelles are composed of several thousand molecules, bonded via calcium phosphate nanoclusters. All other proteins present in milk are grouped together and termed whey proteins. The primary whey protein in cow milk is β-lactoglobulin. A very interesting feature of milk proteins is their potential as nanovehicles for bioactive compounds. The potential of delivering high nutritional value components by milk proteins has opened new opportunities in food and non-food industrial sectors. Fortunately, the huge volume of milk production enables the manufacture of non-expensive purified proteins possible [77].

Milk protein films are widely used in food and non-food sectors such as textile, paper, leather etc. These films and composites are used in different scopes of food science such as coating of meat and fresh-cut fruits, bread wrapping and preparation of antimicrobial packaging. Cow's milk proteins are divided into 2 parts: caseins and whey proteins. The major fraction of milk proteins (approximately 80 %) belongs to casein group which consists of α_{s1}-, α_{s2}-, β-, and κ-casein and their portions are nearly 38, 10, 36 and 12, respectively with the corresponding molecular masses of 23,164, 25,388, 23,983 and 19,038 Da [78].

Proteose peptones and γ-casein are obtained through splitting β-casein by plasmin, a proteolytic enzyme naturally present in milk. Caseins can be distinguished from other milk components by precipitating near their isoelectric pH ($\sim$4.6 at 20 °C). Caseins are amphiphilic molecules with hydrophilic and hydrophobic segments and are widely used as emulsifier in the food industry due to their amphiphilic character [79, 80]. The highest amount of caseins in milk belongs to α_{s1}-casein. Unlike other caseins, in α_{s1}-casein both N- and C-terminal segments of molecules are hydrophobic which leads to the formation of either intra- or inter-molecular interactions [81]. Amino acid sequence in α_{s1}-casein differs from that in α_{s2}-caseins and hence it is normal to possess different physical and chemical properties. Although both α_{s1}- and α_{s2}-caseins are calcium-sensitive, the same as β-casein, α_{s2}-caseinis much more sensitive to Ca^{2+} [82, 83]. Indeed, 2 mM Ca^{2+} at pH 7 is sufficient for precipitation of α_{s2}-casien, while a concentration of 6 mM is needed to precipitate α_{s1}-casien. However, α_{s1}-casien is more sensitive to Ca^{2+} in comparison with β-casein. Several nice research papers have published on mil protein films, composites and blends based on milk proteins and applications of milk proteins-based films and composites [84]. Pojanavaraphan et al. [85] prepared nanocomposites film with casein and sodium montmorillonite clay by freeze-drying process.

1.1.6 Alginate Based Polymers

Alginic acids were first isolated from brown algae by Stanford more than 100 years ago [86–89]. Later, these polysaccharides were detected in all brown algal species without exception as cell wall and intercellular matrix components. Their content in the biomass may amount to 40 % of the dry weight; this strongly depends on the species, growth and stationary conditions [90]. Commercial alginates are currently obtained by extraction from brown seaweeds such as *Laminaria digitata*, *Laminaria hyperborea*, and *Macrocystis pyrifera*. Several bacteria such as the nitrogen-fixing aerobe *Azotobacter vinelandii* and the opportunistic pathogen *Pseudomonas aeruginosa* also produce alginates. However, only alginates synthesized by *A. vinelandii* have a block copolymer structure similar to the one extracted from seaweed species while alginate produced by *Pseudomonas* sp. does not have a G block. In addition, bacterial alginic acids present some of their hydroxyl groups acetylated. Acetyl groups occupy positions 2 or 3 (sometimes, both simultaneously) in D-mannuronic acid residues. The price of algal alginates is generally low but their production is subjected to environmental hazards, natural (i.e. climatic conditions) or not (e.g. pollution). Therefore, alginates from *A. vinelandii* may become major commercial products [91]. In brown seaweed, alginate is present mainly as the calcium salt of alginic acid, although magnesium, potassium, and sodium salts may also be present. These biopolymers are structural polysaccharides of the algae and their biological function is to prevent desiccation, sustain the cell integrity and give the stability to the plant in the water. The

properties of alginates, preparation of micro- and nano-particles, preparation of blends, composites, nanocomposites, films, scaffolds and fibers for biomedical and pharmaceutical and environmental applications have already been reported [92–97].

1.1.7 Lignin Polymers

After cellulose and hemicellulose, lignin represents the next main component of vegetal biomass. Lignin or lignen is a complex chemical compound most commonly derived from wood, and an integral part of the secondary cell walls of plants [98] and some algae [99]. The term was introduced in 1819 by de Candolle and is derived from the Latin word lignum [100], meaning wood. Lignin is employing 30 % of non-fossil organic carbon [101] and constituting from a quarter to a third of the dry mass of wood. As a biopolymer, lignin is unusual because of its heterogeneity and lack of a defined primary structure. Its most commonly noted function is the support through strengthening of wood (xylem cells) in trees.

The estimation of lignin produced annually through biosynthesis indicates a quantity of 2×10^{10} tons. The continuing decline of available oil reserves during the early 21st century will make lignin one of most important source of chemicals for our future society. There are two special reasons to approach researches in the field of lignin: (1) the large accessibility of this compound in the world and it is an inevitable by-product resulted from pulp manufacturing, and (2) it has a huge potential as phenolic raw material. Most part of lignin (about 95 %) is used to produce energy and to recover inorganic chemicals used in wood pulping process, and only 5 % are commercially used; lignosulfonates ($\sim$1,500,000 t/year) as dispersants, binding material and kraft lignins($\sim$60,000 t/year) are processed to obtain high quality surfactants. Lignin is one of the main constituents of the higher plants with vascular structure providing mechanical support to stand upright, having some vital functions which confer resistance to the physical–chemical stress and facilitate water and nutrient transport.

The characteristic features of lignin particles with dimensions below 100 nm are an interesting and important field of studies in wide domains, such as: (a) in medicine to provide drugs; (b) new smart nano-sized coatings beginning to be used on an industrial scale, and also information technology (IT); (c) cars, cosmetics, chemicals and packaging industries and (d) additives for plastic material industry. Excellent reports are available on the use lignin in preparing high performance polymer blends, composites and nanocomposites [102–105].

1.1.8 Hemicellulose-Based Polymers

Hemicelluloses are the most abundant plant polysaccharides other than cellulose. They are biosynthesized in large quantities in the majority of trees and terrestrial plants. In spite of their abundance, the industrial utilization of hemicelluloses is

minor in comparison with the use of starch and cellulose. In many lignocellulosic refining processes, hemicelluloses are partly degraded; they are removed and burnt, or further used as feed raw material. However, methods for separation and isolation of high molar mass hemicelluloses have been developed. Hemicelluloses can be extracted from plant material with alkali; parts of them are extracted also with water. The amount of potential raw material from forestry and agricultural side streams is significant and researchers are currently aiming at finding potential uses for it. Unlike starch, hemicelluloses are not digested by humans but function as a dietary fiber. Therefore they are an interesting raw material e.g. for the food industry. Potential applications include paper making, biodegradable packaging materials, coatings, hydrogels, absorbents, and emulsifyers. Hemicelluloses are a structurally versatile group of polysaccharides. By cross-linking cellulose and lignin they contribute to the cell wall flexibility. Hemicelluloses form the hydrophilic component of the cell wall. Hemicelluloses are classified to different groups according to their structure: xylans, mannans, galactans, arabinans, and β-glucans. Two most common hemicelluloses, namely xylans and mannans are being used as components of polymer blends, composites, and nanocomposites. Plant gum mannans were also included due to their chemical similarity to hemicelluloses. Xylans were blended with other natural polymers, while mannan-based blends were prepared with polysaccharides, proteins, and synthetic polymers. Nanocomposites were made by mixing xylans and mannans with nanosized cellulose or inorganic nanoparticles. In some cases, blending with other polymers was necessary to obtain cohesive self-standing films from hemicelluloses. Often, the hydrophilic character of xylans and mannans enabled the formation of homogeneous blends and strong hydrogen bonding between the blended polymers or with the nanoparticles. The polymers usually had an optimal blend ratio at which the mechanical properties of the films reached a maximum. The effect of hemicellulose content on the water vapour barrier properties of films depended on the film composition. Oxygen permeability was studied on spruce galactoglucomannan—based films and they were generally considered as good oxygen barriers. Blending xylans and mannans with other polymers or making nanocomposites enlarges the number of potential applications of these polysaccharides [106–113].

1.1.9 Bacterial Cellulose

Nanocellulose, such as that produced by the bacteria Gluconacetobacter xylinus (bacterial cellulose, BC), is an emerging biomaterial with great potential in several applications. The performance of bacterial cellulose stems from its high purity, ultra-fine network structure and high mechanical properties in the dry state [114]. These features allow its applications in scaffold for tissue regeneration, medical applications and nanocomposites. A few researchers have used bacterial cellulose mats to reinforce polymeric matrices and scaffolds with wound healing properties [115–121]. BC is pure cellulose made by bacterial fabrication via biochemical

steps and self-assembling of the secreted cellulose fibrils in the medium. Shaping of BC materials in the culture medium can be controlled by the type of cultivation and kind of bioreactor. They may be obtained as BC hydrogel or BC in dry state by methods like freeze-drying. Although chemically identical to plant cellulose, the cellulose synthesized by bacteria has a fibrillar nanostructure which determines it's physical and mechanical properties, which are necessary for modern medicine, biomedical research [122, 123] and develop LED display [124].

The use of bacterial nanocellulose for medical implants, the structural features of microbial cellulose and its properties have been reported in relation to the current and future applications in medicine [125–129]. Bacterial cellulose has proven to be a remarkably versatile biomaterial that can be used in a wide variety of biomedical devices. The extraordinary supramolecular nanofiber network structure and the resulting valuable properties have led to a real challenge and extensive global activity. The ultrafine 3-D BC network structure with its native unique properties is exploited for the synthesis of materials analogous to human and animal soft and hard tissues. From the scientific and economic perspective, these innovative polymers, which are exciting examples of the large and significant biopolymer family of cellulosics, are on the threshold of a breakthrough.

1.1.10 Polylactic Acid

Poly(lactic acid) or polylactide (PLA) is a thermoplastic aliphatic polyester derived from renewable resources, such as corn starch (in the United States), tapioca products (roots, chips or starch mostly in Asia) or sugarcanes (in the rest of world). It can biodegrade under certain conditions, such as the presence of oxygen, and is difficult to recycle. Due to the chiral nature of lactic acid, several distinct forms of polylactide exist: poly-L-lactide (PLLA) is the product resulting from polymerization of L,L-lactide (also known as L-lactide). PLLA has a crystallinity of around 37 %, a glass transition temperature between 60 and 65 °C, a melting temperature between 173 and178 °C and a tensile modulus between 2.7 and 16 GPa [130, 131]. Heat resistant PLA can withstand temperatures of 110 °C (230 F). PLA has similar mechanical properties to PETE polymer, but has a significantly lower maximum continuous use temperature. PLA is currently used in a number of biomedical applications, such as sutures, stents, dialysis media and drug delivery devices. The total degradation time of PLA is a few years [132]. It is also being evaluated as a material for tissue engineering.

Because it is biodegradable, it can also be employed in the preparation of bioplastic, useful for producing loose-fill packaging, compost bags, food packaging, and disposable table wares. In the form of fibers and non-woven textiles, PLA also has many potential uses, for example as upholstery, disposable garments, awnings, feminine hygiene products, and diapers. PLA has been used as the hydrophobic block of amphiphilic synthetic block copolymers used to form the vesicle membrane of polymersomes. PLA is a sustainable alternative to

petrochemical-derived products, since the lactides from which it is ultimately produced can be derived from the fermentation of agricultural by-products such as corn starch [133] or other carbohydrate-rich substances like maize, sugar or wheat. PLA can be an alternative to high-impact polystyrene by using as much as 1 wt % non-PLA due to creating co-polymers which can strengthen PLA plastics.

PLA is more expensive than many petroleum-derived commodity plastics, but its price has been falling as production increases. The demand for corn is growing, both due to the use of corn for bioethanol and for corn-dependent commodities, including PLA. Polylactic acid (PLA) has caught the attention of polymer scientists and proving to be a viable alternative biopolymer to petrochemical based plastics for many applications. PLA is produced from lactic acid, that is derived itself from the fermentation of corn or sugar beet and due to its biodegradation ability, PLA presents the major advantage to enter in the natural cycle implying its return to the biomass. PLA nanocomposites hold the future in biopolymer nanocomposites as there is an urge for the development of 'green' technology from sustainable and renewable resources. Nano-sized filler-based technology has enabled the application of both organic/inorganic fillers with at least one of its dimension in the scale of nanometer, into PLA leading to the formation of PLA nanocomposites. Various types of nanofillers are incorporated into PLA by researchers to explore the suitable nanofiller which contribute to the desired properties of the engineering PLA nanocomposites. In the past decades, layered clay such as montmorillonite (MMT) is commonly used as reinforcement materials due to its nanoscale size and intercalation/exfoliation properties. In its pristine form, they are hydrophilic in nature, and this property makes them very difficult to be well dispersed in PLA. The most common strategy to overcome this difficulty is to replace the interlayer MMT cations with quarternized ammonium cations, preferably with long alkyl chains. The presence of hydrophobic chain within the interlayer of MMT enables PLA chains to diffuse in resulting in separation of the layers.

Despite the current efforts by researchers and polymer engineers in realizing the commercial potential of PLA to create a sustainable environment, there are a number of challenges to be overcome. Challenges from economic aspects and technicality have to be faced to enable PLA to compete with petroleum based plastics in the near future. The high price of PLA at the current market is attributed to the tedious process of obtaining lactic acid and the polymerization process to produce PLA. Whereas from technical point of view, the limited toughness (i.e: impact strength) has urged researchers to develop a biodegradable impact modifier in the recent decade. Another challenge is to be able to identify and utilize process additives (i.e: compatibilizers, plasticizers) including PLA blends, that are derived from renewable resources to be consistent with the concept of sustainable materials. The introduction of natural fibers in PLA however, will have to meet several performance requirements such as expected degradability (biodegradability when required and not before). Resistance to moisture absorption, flameretardancy and embrittlement are also the major setbacks to be tackled. The development of PLA nanocomposites is ought to hold the future in the effort to develop the future

material. Nevertheless, due to low number of effective applications, the acceptance of PLA nanocomposites has been relatively slow. Despite the setback, the properties of these nanocomposites up to now confirm that the promise of a dream material for the 21st century can be fulfilled [134]. Further research is therefore necessary to develop a proper understanding of the formulation/structure/property relationship/toughening mechanisms and interactions involved in PLA nanocomposites system.

1.1.11 Polyhydroxyalkanoates

In 1920 s, a French scientist called Maurice Lemoigne isolated a polymer of 3-hydroxybutyric acid (3HB) from the Gram-positive bacterium *Bacillus megaterium* [135, 136]. But it took nearly 30 years to commercialize the polymer. Later a PHA with 3HB and 3-hydroxyvalerate (3HV) was discovered from activated sludge. Further, mcl-PHAs were discovered in 1983, more than 100 different monomers units have been incorporated into mcl-PHAs in order to produce PHAs with different physical as well as mechanical properties, to be utilized in various applications. PHAs are naturally occurring biodegradable and biocompatible polymers commonly found as storage compounds of carbon and energy in various microorganisms. These are produced in the presence of excess carbon and other nutrient limiting conditions for e.g. nitrogen, phosphorus, sulphur, magnesium or oxygen [137, 138]. There are more than 100 different known types of PHA monomers and more than 300 different PHA producing microorganisms known. The known producers of PHA include *Ralstonia eutropha* reclassified from *Alcaligenes eutrophus*, *Alcaligenes latus*, *Azotobacter vinelandii*, *Azotobacter chroococcum*, Methylotrophs, Pseudomonads, *Rhodobacter sphaeroides* and recombinant *Escherichia coli* [139]. The main properties of PHAs are biodegradability, insolubility in water, nontoxic, biocompatibility, piezoelectric, thermoplastic and/or elastomeric nature, which makes them favorable to be used in the packaging industry, medicine, pharmacy, agriculture, food industry and the paint industry [140].

PHAs have rapidly gained interest both in research and industry due to their structural versatility and characteristics such as biodegradability, insolubility in water, nontoxicity, biocompatibility, piezoelectric property, thermo plasticity and or elastomeric properties, which make them favorable to be used in the packaging industry, medicine, pharmacy, agriculture, food industry and in the paint industry. The chemical and physical properties of the polymer are dependent on the monomeric composition which is determined by the producing microorganism and their nutrition. So far scl-PHAs are being studied extensively due to their easier handling and higher crystallization rates. However, the degradation rate of scl-PHAs in vitro and in vivo has been found to be very slow probably due to the high crystallinity. Therefore, the less crystalline mcl-PHA has become the better prospective material for medical applications with required rate-controlled

degradation. Hence, one major step forward for PHAs is the production of composites and blends to overcome or minimise drawbacks in properties that limit their application. In order to tailor the property of the polymer according to the application, blends and composites of PHAs have been studied which has helped in the progress of tissue engineering, sustained and controlled drug delivery and in other areas of medical/biomedical applications such as the development of devices, artificial organs, therapeutic uses and blends & nanocomposites [141, 142].

However, the high production cost of the PHAs has triggered interest in using cheap raw materials including a variety of waste and byproducts as carbon sources for PHA production. Several strategies have been tried to improve conditions for economical PHA production including different bacterial species for different types of PHA production and recombinant strains, transgenic plants harbouring the microbial PHA biosynthesis genes, inexpensive carbon sources with high growth rate and with high polymer synthesis rate, media ingredients, fermentation conditions, modes of fermentation (batch, fed-batch, continuous) and recovery. And so far, despite all of the hindrances in the production cost of the PHAs, relatively high productivity at large scale has been achieved for P(3HB), P(3HB-co-3HV) and P(3HHx-co- 3HO).

1.2 Summary

In cellulose based chapter, the authors were started with the structure and properties of cellulose at the molecular, supramolecular and morphological level. Then they continue describing the manufacture of cellulose based blends, composites and nanocomposites. Finally, they present several applications for cellulose based composites and nanocomposites and their applications. In the chapter of chitin, the authors were demonstrated the utility of chitin and chitosan as potential materials for various implant applications and some of the challenges in demonstrating biocompatibility. The preparation and tissue engineering applications of chitin and chitosan based nanofibers, and their blends, composites and nanocomposites have also been summarized. Authors described the for tissue engineering applications with chitin and chitosan in the future. From the chapter on starch, we can see that the structure and properties (thermal and rheological) of starch and different preparation method of starch based materials, such as blends, composites and nanocomposites, finally the authors were described the application of starch blends, composites and nanocomposites, for soy protein chapter were discussed about the structure, and mechanical properties, their amino acids composition, structures and thermal behavior of soy proteins, and their biodegradable films, coatings and their functional uses then authors were analyzed about the nanocomposites with soy protein and their applications. The chapter based caseins and whey proteins were discussed about the chemistry of caseins and whey proteins, structure of casein molecules, assembly of caseins and casein micelle models and structure and assembly of whey proteins. Finally in the chapter they were added

the allocation of caseins and whey proteins. In alginates based chapter author discussed about the structure of alginates and chemical modification such as hydroxyl groups, carboxyl groups Then they were discussed about the properties of alginates such as physicochemical thermal properties, gel formation, rheological properties and immunogenic properties. Then they are focused on the preparation of micro-nano-particles and their films and fibers. Finally they analyzed about their different application, biomedical and pharmaceutical applications and environmental applications. In other chapters such as lignin polymers, hemicellulose-based polymers, bacterial cellulose polymers, polylactic acid (PLA) and polyhydroxyalkanoates authors were discussed about the general introduction and their preparation of composites, blends and nanocomposites, and finally discussed about their all kind of applications.

References

1. Crawford, R.L.: Lignin Biodegradation and Transformation. Wiley, New York (1981). ISBN 0-471-05743-6
2. Updegraff, D.M.: Semimicro determination of cellulose in biological materials. Anal. Biochem. **32**(3), 420–424. doi:10.1016/S0003-2697(69)80009-6. PMID 5361396 (1969)
3. Klemm, D., Heublein B., Fink, H-P., Bohn A.: Cellulose, fascinating biopolymer and sustainable raw material. Chem. Inform. **36**(36). doi:10.1002/chin.200536238 (2005)
4. Charles, A. B, (ed.).: Vacuum Deposition onto Webs, Films, and Foils, 0(8155), p. 165. ISBN 0815515359 (2007)
5. Stenius, P.: 1. Forest Products Chemistry. Papermaking Science and Technology. Fapet OY, Finland. p. 35. ISBN 952-5216-03-9
6. Imai, M., Ikari, K., Suzuki, I.: High-performance hydrolysis of cellulose using mixed cellulose species and ultrasonication pretreatment. Biochem. Eng. J. **17**, 19–23 (2003)
7. Jarvis, M.: Cellulose stacks up. Nature **426**, 611–612 (2003)
8. Holtzapple, M.T.: Cellulose. In: Macrae, R., Robinson, R.K., Saddler, M.J. (eds.) Encyclopedia of Food Science Food Technology and Nutrition. London Academic Press, UK (1993)
9. Klemm, D., Philipp, B., Heinze, T., Heinze, U., Wagenknecht, W.: Comprehensive Cellulose Chemistry Fundamentals and Analytical Methods, vol. 1. Wiley-VCH, Germany (1998)
10. Krässig, H.: Cellulose: Structure, Accessibility, and Reactivity Gordon and Breach Sci. Publishers, Switzerland (1993)
11. Matthysse, A.G., Deschet, K., Williams, M., Marry, M., White, A.R., Smith, W.C.: A functional cellulose synthase from ascidian epidermis. Proc. Natl. Acad. Sci. **101**, 986–991 (2004)
12. Jonas, R., Farah, L.F.: Production and application of microbial cellulose. Polym. Degrad. Stab. **59**, 101–106 (1998)
13. Iguchi, M., Yamanaka, S., Budhiono, A.: Review bacterial cellulose—a masterpiece of nature's arts. J. Mater. Sci. **35**, 261–270 (2000)
14. Sreeramulu, G., Zhu, Y., Knol, W.: Kombucha fermentation and its antimicrobial activity. J. Agric. Food Chem **48**, 2589–2594 (2000)
15. Torres, F.G., Troncoso, O.P., Lopez, D., Grande, C., Gomez, C.M.: Reversible stress softening and stress recovery of cellulose networks. Soft Matter **5**, 4185–4190 (2009)

16. Torres, F.G., Grande, C.J., Troncoso, O.P., Gomez, C.M., Lopez, D.: Bacterial cellulose nanocomposites for biomedical applications; In: Kumar, S.A., Thiagarajan, S., Wang, F. (eds.) Biocompatible Nanomaterials: Synthesis, Characterization and Application in Analytical Chemistry. Nova Science Publishers, USA (2010)
17. Ring, D.F., Nashed, W., Dow, T.: Liquid loaded pad for medical applications; US patent 4 588 400 (1986)
18. Dong, H., Strawhecker, K.E., Snyder, J.F., Orlicki, J.A., Reiner, R.S., Rudie, A.W.: Cellulose nanocrystals as a reinforcing material for electrospun poly(methyl methacrylate) fibers: formation, properties and nanomechanical characterization. Carbohydr. Polym. **87**, 2488–2495 (2012)
19. Cristiane, S., Rodrigues F.H.A., Neto,A.G.V.C., Pereira A.G.B., Fajardo, A.R., Radovanovic, E., Rubira, A.F., Muniz, E.C.: Nanocomposites based on poly(acrylamide-co-acrylate) and cellulose nanowhiskers. Eur. Polym. J. Macromol. Nanotechnol. **48**, 454–463 (2012)
20. Svensson, A., Nicklasson, E., Harrah, T., Panilaitis, B., Kaplan, D.L., Brittberg, M., Gatenholm, P.: Bacterial cellulose as a potential scaffold for tissue engineering of cartilage. Biomaterials **26**, 419–431 (2005)
21. Andersson, J., Stenhamre, H., Bäckdahl, H., Gatenholm, P.: Behavior of human chondrocytes in engineered porous bacterial cellulose scaffolds. J. Biomed. Mater. Res., Part A **94**, 1124–1132 (2010)
22. Czaja, W., Krystynowicza, A., Bielecki, S., Malcolm Brown Jr, R.: Microbial cellulose—the natural power to heal wounds. Biomaterials **27**, 145–151 (2006)
23. Czaja, W.K., Young, D.J., Kawecki, M., Brown Jr, R.M.: The future prospects of microbial cellulose in biomedical applications. Biomacromolecules **8**, 1–12 (2007)
24. Cienchanska, D.: Multifunctional bacterial cellulose/chitosan composite materials for medical applications. Fibres Text. East. Eur. **12**, 69–72 (2004)
25. Legeza, V.I., Galenko-Yaroshevskii, V.P., Zinovev, E.V., Paramonov, B.A., Kreichman, G.S., Turkovskii, I.I., Gumenyuk, E.S., Karnovich, A.G., Khripunov, A.K.: Effects of new wound dressings on healing of thermal burns of the skin in acute radiation disease. Bull. Exp. Biol. Med. **138**, 311–315 (2004)
26. Wan, W.K., Millon, L.E.: Poly(vinyl alcohol)-bacterial cellulose nanocomposite; U.S. Patent Appl., Publ. US 2005037082 A1, 16 (2005)
27. Sokolnicki, A.M., Fisher, R.J., Harrah, T.P., Kaplan, D.L.: Permeability of bacterial cellulose membranes. J. Membr. Sci. **272**, 15–27 (2006)
28. Charpentier, P.A., Maguire, A., Wan, W.: Surface modification of polyester to produce a bacterial cellulose-based vascular prosthetic device. Appl. Surf. Sci. **252**, 6360–6367 (2006)
29. Klemm, D., Schumann, D., Udhardt, U., Marsch, S.: Bacterial synthesized cellulose—artificial blood vessels for microsurgery. Prog. Polym. Sci. **26**, 1561–1603 (2001)
30. Backdahl, H., Helenius, G., Bodin, A., Nannmark, U., Johansson, B.R., Risberg, B., Gatenholm, P.: Mechanical properties of bacterial cellulose and interactions with smooth muscle cells. Biomaterials **27**, 2141–2149 (2006)
31. Wan, W.K., Hutter, J.L., Millon, L., Guhados, G.: Bacterial cellulose and its nanocomposites for biomedical applications. ACS Symp. Ser. **938**, 221–241 (2006)
32. Iwamoto, S., Nakagaito, A.N., Yano, H., Nogi, M.: Optically transparent composites reinforced with plant fiber-based nanofibers. Appl. Phys. A Mater. Sci. Process. **81**, 1109–1112 (2005)
33. Ifuku, S., Nogi, M., Abe, K., Handa, K., Nakatsubo, F., Yano, H.: Surface modification of bacterial cellulose nanofibers for property enhancement of optically transparent composites: dependence on acetyl-group DS. Biomacromolecules **8**, 1973–1978 (2007)
34. Yano, H., Sugiyama, J., Nakagaito, A.N., Nogi, M., Matsuura, T., Hikita, M., Handa, K.: Optically transparent composites reinforced with networks of bacterial nanofibers. Adv. Mater. **17**, 153–155 (2005)

35. Podsiadlo, P., Sui, L., Elkasabi, Y., Burgardt, P., Lee, J., Miryala, A., Kusumaatmaja, W., Carman, M., Shtein, M., Kieffer, J., Lahann, J., Kotov, N.: Layer-by-layer assembled films of cellulose nanowires with antireflective properties. Langmuir **23**, 7901–7906 (2007)
36. Legnani, C., Vilani, C., Calil, V.L., Barud, H.S., Quirino, W.G., Achete, C.A., Ribeiro, S.J.L., Cremona, M.: Bacterial cellulose membrane as flexible substrate for organic light emitting devices. Thin Solid Films **517**, 1016–1020 (2008)
37. Svagan, A.J., Samir, M.A.S.A., Berglund, L.A.: Biomimetic foams of high mechanical performance based on nanostructured cell walls reinforced by native cellulose nanofibrils. Adv. Mater. **20**, 1263–1269 (2008)
38. van den Berg, O., Schroeter, M., Capadona, J.R., Weder, C.: Nanocomposites based on cellulose whiskers and (semi)conducting conjugated polymers. Material Chememistry **17**, 2746–2753 (2007)
39. Agarwal, M., Lvov, Y., Varahramyan, K.: Conductive wood microfibres for smart paper through layer-by-layer nanocoating. Nanotechnology **17**, 5319–5325 (2006)
40. Kumar, M.N.V.R.: A review of chitin and chitosan applications. React. Funct. Polym. **46**, 1–27 (2000)
41. Kobayashi, S., Kiyosada, T., Shoda, S.-I.: Synthesis of artificial chitin: irreversible catalytic behavior of a glycosyl hydrolase through a transition state analogue substrate. J. Am. Chem. Soc. **118**, 13113–13114 (1996)
42. Sakamoto, J., Sugiyama, J., Kimura, S., Imai, T., Itoh, T., Watanabe, T., Kobayashi, S. Macromolecules, **33**, 4155-4160 (2000)
43. Kadokawa, J.-I.: Precision polysaccharide synthesis catalyzed by enzymes. Chem. Rev. **111**, 4308–4345 (2011)
44. Paillet, M., Dufresne, A.: Macromolecules, **34**, 6527–6530 (2001)
45. Ahmed Jalal, U., Masahiro, F., Shinichiro, S., Yasuo, G.: Outstanding reinforcing effect of highly oriented chitin whiskers in PVA nanocomposites. Carbohydr. Polym. **87**, 799–805 (2012)
46. Phongying, S., Aiba, S., Chirachanchai, S.: Polymer, **48**, 393–400 (2007)
47. Noh, H.K., Lee, S.W., Kim, J.M., Oh, J.E., Kim, K.H., Chung, C.P., Choi, S.C., Park, W.H., Min, B.M.: Electrospinning of chitin nanofibers: degradation behavior and cellular response to normal human keratinocytes and fibroblasts. Biomaterials. Biomaterials **27**, 3934–3944 (2006)
48. Park, K.E., Jung, S.Y., Lee, S.J., Min, B.M., Park, W.H.: Biomimetic nanofibrous scaffolds: preparation and characterization of chitin/silk fibroin blend nanofibers. Int. J. Biol. Macromol **38**, 165–173 (2006)
49. Park, K.E., Kang, H.K., Lee, S.J., Min, B.M., Park, W.H.: Biomimetic nanofibrous scaffolds: preparation and characterization of PGA/chitin blend nanofibers. Biomacromolecules **7**, 635–643 (2006)
50. Shalumon, K.T., Binulal, N.S., Selvamurugan, N., Nair, S.V., Menon, D., Furuike, T., Tamura, H., Jayakumar, R.: Carbohydr. Polym. **77**, 863–869 (2009)
51. Bhattarai, N., Edmondson, D., Veiseh, O., Matsen, F.A., Zhang, M.: Electrospun chitosan-based nanofibers and their cellular compatibility. Biomaterials **26**, 6176–6184 (2005)
52. Subramaniyan, A., Vu, D., Larsen, G.F., Lin, H.Y. J. Biomater. Sci. Poly. Ed. 7, 861–873 (2005)
53. Mo, X., Chen, Z., Weber, H.J.: Front. Mater. Sci. 1, 20–23 (2007)
54. Zhang, Y.Z., Venugopal, J.R., El-Turki, A., Ramakrishna, S., Su, B., Lim, C.T.: Electrospun biomimetic nanocomposite nanofibers of hydroxyapatite/chitosan for bone tissue engineering. Biomaterials **29**, 4314–4322 (2008)
55. Yang, D., Jin, Y., Zhou, Y., Ma, G., Chen, X., Lu, F.Nie.: In situ mineralization of hydroxyapatite on electrospun chitosan-based nanofibrous scaffolds. Macromolcule. Biosci. **8**, 239–246 (2008)
56. Whistler, R.L., BeMiller, J.N., Paschall, B.F.: Starch: chemistry and technology. Academic Press, New York (1984)

57. Liao, H., Wu, C.: New biodegradable blends prepared from polylactide, titanium tetraisopropylate, and starch. J Appl. Poly. Sci. **108**, 2280–2289 (2008)
58. Carr. L., Parra, D., Ponce, P., Lugão, A., Buchler, P.: Influence of fibers on the mechanical properties of cassava starch foams. J. Polym. Environ. **14**, 179–183 (2006)
59. Gattin, R., Copinet, A., Bertrand, C., Couturier, Y.: Biodegradation study of a starch and poly(lactic acid) co-extruded material in liquid, composting and inert mineral media. Int. Biodeterior. Biodegradation **50**, 25–31 (2002)
60. Wang. L.; Shogren, R. L.; Carriere, C.: Poly. Eng. Sci. **40**, 499–506 (2000)
61. Averous, L.: Biodegradable multiphase systems based on plasticized starch. J. Macromol. Sci.-Poly. Rev. **C44**, 231-274 (2004)
62. Vidal, R., Martinez, P., Mulet, E.: Environmental assessment of biodegradable multilayer film derived from carbohydrate polymers. J. Polym. Environ. **15**, 159–168 (2007)
63. Martin. O.; Schwach. E.; Avérous. L.; Couturier. Y.: properties of biodegradable multilayer films based on plasticized wheat starch. Starch–Stärke **53**, 372–380 (2001)
64. Gattin, R., Copinet, A., Bertrand, C., Couturier, Y.: Int. Biodeterior. Biodegradation **50**, 25–31 (2002)
65. Famá, Lucía., Gañan Rojo, Piedad., Bernal, Celina., Goyanes, Silvia.: Biodegradable starch based nanocomposites with low water vapor permeability and high storage modulus. Carbohydr. Polym. **87**(3), 1989–1993 (2012)
66. Glycine max. Multilingual Multiscript Plant Name Database
67. Riaz, Mian.N.: Soy Applications in Food. CRC Press, Boca Raton (2006). ISBN 0-8493-2981-7
68. Liu, D., Chen, H., Chang, P.R., Qinglin, W., Li, K., Guan, L.: Biomimetic soy protein nanocomposites with calcium carbonate crystalline arrays for use as wood adhesive. Bioresour. Technol. **101**(15), 6235–6241 (2010)
69. Kumar, P., Sandeep, K.P., Alavi, S., Truong, V.D., Gorga, R.E.: Preparation and characterization of bio-nanocomposite films based on soy protein isolate and montmorillonite using melt extrusion. Food Eng. **100**(3), 480–489 (2010)
70. Jong, L., Peterson, S.C.: Effects of soy protein nanoparticle aggregate size on the viscoelastic properties of styrene–butadiene composites. Compos. A Appl. Sci. Manuf. **39**(11), 1768–1777 (2008)
71. Su, J.-F., Yuan, X.Y., Huang, Z., Xia, W.L.: Properties stability and biodegradation behaviors of soy protein isolate/poly (vinyl alcohol) blend films. Polym. Degrad. Stab. **95**(7), 1226–1237 (2010)
72. Kumar, R., Zhang, L.: Aligned ramie fiber reinforced arylated soy protein composites with improved properties. Compos. Sci. Technol. **69**(5), 555–560 (2009)
73. Mariani, P.D.S.C., Allganer, K., Oliveira, F.B., Cardoso, E.J.B.N., Innocentini-Mei, L.H.: Effect of soy protein isolate on the thermal, mechanical and morphological properties of poly (ε-caprolactone) and corn starch blends. Polym. Testing **28**(8), 824–829 (2009)
74. Vega-Lugo, A.-C., Lim, L.T.: Controlled release of allyl isothiocyanate using soy protein and poly(lactic acid) electrospun fibers. Food Res. Int. **42**(8), 933–940 (2009)
75. Wang,W., Wang, A.: Preparation, characterization and properties of superabsorbent nanocomposites based on natural guar gum and modified rectorite. Carbohydr. Polym. **77**, 4, 19, 891–897 (2009)
76. Peles, Z., Zilberman, M.: Novel soyprotein wound dressings with controlled antibiotic release: Mechanical and physical properties. Acta Biomater. **8**(1), 209–217 (2012)
77. Frinault, A., Gallant, D.J., Bouchet, B., Dumont, J.P.: Preparation of casein films by a modified wet spinning process. J. Food Sci. **62**(4), 744–747 (1997)
78. Fox, P.F., Kelly, A.L.: The caseins. In: Yada R.Y (ed.) Proteins In Food Processing. Woodhead Publishing Ltd and CRC Press LLC, Cambridge, UK (2004)
79. Walstra, P., Wouters, J., Geurts, T.: Dairy Science and Technology, 2nd edn. CRC Press LLC, New York, USA (2006)
80. Dickinson, E.: Casein in emulsions: interfacial properties and interactions. Int. Dairy J. **9**, 305–312(1999)

81. Horn, D.S.: Casein interactions: casting light on the black boxes, the structure in dairy products. Int. Dairy J. **8**, 171–177 (1998)
82. Farrell, H.M., Malin, E.L., Brown, E.M., Mora-Gutierrezt. A.: Review of the chemistry of α_{s2}-casein and the generation of the homologous molecular model to explain its properties. J. Dairy Sci. **92**, 1338–1353 (2009)
83. Ginger, M.R., Grignor, M.R.: Comparative aspects of milk caseins. Comp. Biochem. Physiol B Biochem. Mol. Biol. **124**(2), 133–145 (1999)
84. Chen, H.: Functional properties and applications of edible films made of milk proteins. Dairy Sci. **78**, 2563–2583 (1995)
85. Pojanavaraphan, T., Magaraphan, R., Chiou, B.S., Schiraldi, D.A.: Development of biodegradable foamlike materials based on casein and sodium montmorillonite clay. Biomacromolecules **11**, 2640–2646 (2010)
86. Usov, A.I.: Alginic acids and alginates: analytical methods used for their estimation and characterization of composition and primary structure. Russ. Chem. Rev. **68**, 957–966 (1999)
87. Chèze-Lange, H., Beunard, D., Dhulster, P., Guillochon, D., Cazé, A.M., Morcellet, M., Saude, N., Junter, G.A.: Production of microbial alginate in a membrane bioreactor. Enzyme Microb. Technol. **30**, 656–661 (2002)
88. Hernández-Carmona, G., McHuge, D.J., Arvizu-Higuera, D.L., Rodríguez-Montesinos, Y.E.: Pilot plant scale extraction of alginate from *Macrocystis pyrifera.* 1. Effect of pre-extraction treatments on yield and quality of alginate. J. Appl. Phycol. **10**, 507–513 (1999)
89. Gómez, C.G., Pérez Lambrecht, M.V., Lozano, J.E., Rinaudo, M., Villar, M.A.: Influence of extraction-purification conditions on final properties of alginates obtained from brown algae (*Macrocystis pyrifera*). Int. J. Biol. Macromol. **44**, 365–371 (2009)
90. Usov, A.I.: Alginic acids and alginates: analytical methods used for their estimation and characterization of composition and primary structure. Russ. Chem. Rev. **68**, 957–966 (1999)
91. Chèze-Lange, H., Beunard, D., Dhulster, P., Guillochon, D., Cazé, A.M., Morcellet, M., Saude, N., Junter, G.A.: Production of microbial alginate in a membrane bioreactor. Enzyme Microb. Technol. **30**, 656–661 (2002)
92. Draget, K.I., Taylor, C.: Chemical, physical and biological properties of alginates and their biomedical implications. Food Hydrocolloids **25**, 251–256 (2011)
93. Gong, J.P., Katsuyama, Y., Kurokawa, T., Osada, Y.: Double network hydrogels with extremely high mechanical strength. Adv. Mater. **15**, 1155–1158 (2003)
94. Hampson, F.C., Farndale, A., Strugala, V., Sykes, J., Jolliffe, I.G., Dettmar, P.W.: Alginate rafts and their characterisation. Int. J. Pharm. **294**, 137–147 (2005)
95. Becker, T.A., Preul, M.C., Bichard, W.D., Kipke, D.R., McDougall, C.G.: Calcium alginate gel as a biocompatible material for endovascular arteriovenous malformation embolization: six-month results in an animal model. Neurosurgery **56**, 793–803 (2005)
96. Thomas, A., Harding, K.G., Moore, K.: Alginates from wound dressings activate human macrophages to secret tumour necrosis factor-∝. Biomaterials **21**, 1797–1802 (2000)
97. Paul, W., Sharma, C.P.: Chitosan and alginate wound dressings: a short review. Trends Biomater. Artif. Organs **18**, 18–23 (2004)
98. Lebo, S.E. Jr., Gargulak, J.D., McNally, T.J.: Lignin.: Kirk-Othmer Encyclopedia of Chemical Technology. Wiley. doi: 10.1002/0471238961.12090714120914.a01.pub2 (2001)
99. Martone, P.T., Estevez, J.M., Lu, F., Ruel, K., Denny, M.W, Somerville, C., Ralph, J.: Discovery of lignin in seaweed reveals convergent evolution of cell-wall architecture. Curr. Biol. **CB19** (2), 169–75. doi:10.1016/j.cub.2008.12.031. ISSN0960-9822. PMID19167225 (2009)
100. Sjöström, E.: Wood Chemistry: Fundamentals and Applications. Academic Press, ISBN (1993). 012647480X
101. Boerjan, W., Ralph, J., Baucher, M.: Lignin bios. Ann. Rev. Plant Biol, 54(1), 519–549. doi:10.1146/annurev.arplant.54.031902.134938. PMID 14503002 (2003)

102. Darie, R.N., Cazacu, G., Vasile, C.: Melt processing and physico-chemical characterisation of some synthetic polymer (PVA)/natural polymer (lignin) systems, Iasi Academic Days, Progress in Organic and Polymer Chemistry,22nd (edn.), Iasi, Oct 8–10 (2009)
103. Ciolacu, D., Darie, R.N., Cazacu, G.: Polymeric systems based on lignin—poly(vinyl alcohol), in Binders, composites and other applications based on Lignins. In: Totolin, M., Cazacu, G (eds.), pp. 170–194. PIM Publising, Iasi, ISBN 606-520-740-3 (2010)
104. Baumberger, S., Lapierre, C., Monties, B., Della Valle, G.: Use of kraft lignin as filler for starch films. Polym. Degrad. Stab. **59**, 273–277 (1998)
105. Stevens, E.S., Willett, J.L., Shogren, R.L.: Thermoplastic starch—kraft lignin—glycerol blends. J. Biobased Mat. Bioen. **1**(3), 351–359 (2007)
106. Tian, D., Hu, W., Zheng, Z., Liu, H., Xie, H.-Q.: Study on in situ synthesis of konjac glucomannan/silver nanocomposites via photochemical reduction. Appl. Polym. Sci. **100**, 1323–1327 (2006)
107. Ye, X., Kennedy, J.F., Li, B., Xie, B.J.: Condensed state structure and biocompatibility of the konjac glucomannan/chitosan blend films. Carbohydr. Polym. **64**, 532–538 (2006)
108. Wang, B., Jia, D.-Y., Ruan, S.-Q., Qin, S.: Structure and properties of collagen-konjac glucomannan-sodium alginate blend films. Appl. Polym. Sci. **106**, 327–332 (2007)
109. Yu, Z., Jiang, Y., Zou, W., Duan, J., Xiong, X.: Preparation and characterization of cellulose and konjac glucomannan blend film from ionic liquid. Polym. Sci, Part B: Polym. Phys **47**, 1686–1694 (2009)
110. Cheng, L.H., Karim, A.A., Seow, C.C.: Characterisation of composite films made of konjac glucomannan (KGM), carboxymethyl cellulose (CMC) and lipid. Food Chem. **107**, 411–418 (2008)
111. Xiao, C., Liu, H., Gao, S., Zhang, L.: Characterization of poly(vinyl alcohol) –konjac glucomannan blend films. Macromol. Sci. Pure Appl. Chem. **37**(9), 1009–1021 (2000)
112. Mikkonen, K.S., Heikkilä, M.I., Helén, H., Hyvönen, L., Tenkanen, M.: Spruce galactoglucomannan films show promising barrier properties. Carbohydr. Polym. **79**(4), 1107–1112 (2010)
113. Hosseinaei, Omid., Wang, Siqun., Taylor, Adam.M.: Jae-Woo Kim Effect of hemicellulose extraction on water absorption and mold susceptibility of wood–plastic composites. Int. Biodeterior. Biodegradation **71**, 29–35 (2012)
114. Gatenholm, P., Klemm, D.: Bacterial nanocellulose as a renewable material for biomedical applications. MRS Bull. **35**(3), 208–213 (2010)
115. Zugenmaier, P.: Conformation and packing of various crystalline cellulose fibers. Prog. Polym. Sci. **26**, 1341–1417 (2001)
116. Keshk, S.M.A.S., Sameshima, K.: Evaluation of different carbon sources for bacterial cellulose production. Afr. J. Biotechnol. **4**, 478–482 (2005)
117. Jung, J.Y., Park, J.K., Chang, H.N.: Bacterial cellulose production by *Gluconoacetobacter hansenii* in an agitated culture without living non-cellulose producing cells. Enzyme Microb. Technol. **37**, 347–354 (2005)
118. Bodin, A., Concaro, S., Brittberg, M., Gatenholm, P.: Bacterial cellulose as a potential meniscus implant. Tissue Eng. Regen. Med. **1**, 406–408 (2007)
119. Barbara, J.A.: Does A New Cellulose Dressing Have Potential In Chronic Wounds? 2004. http://www.podiatrytoday.com/article/2311, visited 7 Feb 2011
120. Aslan, M., Simsek, G., Dayl, E.: Guided bone regeneration (GBR) on healing bone defects: a histological study in rabbits. J. Contemp. Dent. Pract. **2**(5), 114–123 (2004)
121. Carvalho, R.S., Nelson, D., Keldernian, H., et al.: Guided bone regeneration to repair an osseous defect. Am. J. Orthod. Dentofacial Orthop. **123**, 455–467 (2003)
122. Czaja, W.K., Young, D.J., Kawecki, M.: The future prospects of microbial cellulose in biomedical applications. Biomacromolecules **8**, 1 (2007)
123. Shoda, M., Sugano, Y.: Recent advances in bacterial cellulose production. Biotechnol. Bioprocess Eng. **10**, 1–8 (2005)

124. Ummartyotin, S., Juntaro, J., Sain, M., Manuspiya, H.: Development of transparent bacterial cellulose nanocomposite film as substrate for flexible organic light emitting diode (OLED) display. Ind. Crops Prod. **35**(1), 92–97 (2012)
125. Iamaguti, L.S., Brandão, C.V.S., Pellizzon, C.H., Ranzani, J.J.T., Minto, B.W.: Análise histológica e morfométrica do uso de membrana biossintética de celulose em trocleoplastia experimental de cães. Pesq. Vet. Bras. **28**(4), 195–200 (2008)
126. Helenius, G., Bäckdahl, H., Bodin, A., Nannmark, U., Gatenholm, P., Risberg, B.: In vivo biocompatibility of bacterial cellulose. Biomed. Mater. Res. Part A **76**, 431–438 (2006)
127. Salata, L.A., Hatton, P.V., Devlin, A.J.: In vitro and in vivo evaluation of e-PTFE and alkali-cellulose membranes for guided bone regeneration. Clin. Oral Implants Res. **12**(1), 62–68 (2001)
128. Cockbill, S.M.E.: Evaluation in vivo and in vitro of the performance of interactive dressings in the management of animal soft tissue injuries. In: Veterinary Dermatology, 9(2), 87–98. ISSN 0959-4493 (1998)
129. Macedo, N.L., Matuda, F.S., Macedo, L.G.S., Monteiro, A.S.F., Valera, M.C., Carvalho, Y.R.: Evaluation of two membranes in guided bone tissue regeneration: histological study in rabbits. Braz. J. Oral Sci. **3**, 395 (2004)
130. Södergård, A., Mikael, S.: Properties of lactic acid based polymers and their correlation with composition. Prog. Polym. Sci. **27**(6), 1123–1163 (2002)
131. Middelton, J.C., Tipton, A.J.: Synthetic biodegradable polymers as orthopedic devices. Biomaterial **21**(23), 2335–2346 (2000)
132. Niţă, T.: Concepts in biological analysis of resorbable materials in oro-maxillofacial surgery. Revista de Chirurgie Oro-Maxilo-Facială şi Implantologie, **2**(1), 33–38 (2011)
133. Royte, E.: Corn Plastic to the Rescue. Smithsonian Magazine. (2006)
134. Najafi, N., Heuzey, M.C., Carreau, P.J.: Polylactide (PLA)-clay nanocomposites prepared by melt compounding in the presence of a chain extender. Compos. Sci. Technol **72**(5), 608–615 (2012)
135. Keshavarz, T., Roy, I.: Polyhydroxyalkanoates: bioplastics with a green agenda. Curr. Opin. Microbiol. **13**, 321–326 (2010)
136. Philip, S., Keshavarz, T., Roy, I.: Polyhydroxyalkanoates: biodegradable polymers with a range of applications. J. Chem. Technol. Biotechnol. **82**, 233–247 (2007)
137. Du, G., Si, Y., Yu, J.: Inhibitory effects of medium-chain-length fatty acid on synthesis of Polyhydroxyalkanoates from volatile fatty acid by Ralstonia eutrophus. Biotechnol. Lett. **23**, 1617–1623 (2001)
138. Salehizadeh, H., Van Loosdrecht, M.: Production of polyhydroxyalkanoates by mixed culture: recent trends and biotechnological importance. Biotechnol. Adv. **22**, 261–279 (2004)
139. Stock, U., Sakamoto, T., Hastuoka, S., Martin, D., Nagashima, M., Moran, A., Moses, M., Khalil, P., Schoen, F., Vacanti, J., Mayer, J.: Patch augmentation of the pulmonary artery with bioabsorbable polymers and autologous cell seeding. J. Thorac. Cardiovasc. Surg. **120**, 1158–1168 (2000)
140. Valappil, S., Misra, S., Boccaccini, A., Roy, I.: Biomedical applications of polyhydroxyalkanoates, an overview of animal testing and in vivo responses. Expert Rev. Med. Devices **3**(6), 853–868 (2006)
141. Thibaut, G., Tatiana, B.: Morphology and molten-state rheology of polylactide and polyhydroxyalkanoate blends. Eur. Polym. J. **48**(6), 1110–1117 (2012)
142. Bing, M., Jingjing, D., Qing, L., Zhihua, W., Wei, Y.: Transparent and ductile poly(lactic acid)/poly(butyl acrylate) (PBA) blends: structure and properties. Eur. Polym. J. **48**(1), 127–135 (2012)

Chapter 2
Cellulose Based Blends, Composites and Nanocomposites

F. G. Torres, O. P. Troncoso, C. Torres and C. J. Grande

Abstract Cellulose is the most abundant natural polymer on earth. It is the major constituent of cotton and wood, which together are the basic resources for all cellulose based products such as paper, textiles, construction materials, etc. Cellulose is also used as raw material for the production of blends, composites and nanocomposites which have a variety of different applications. In this chapter we review the main characteristics and properties of cellulose as well as its most promising potential applications emphasizing the use of composites reinforced with lignocellulosic fibers, nanocomposites reinforced with cellulose whiskers and bacterial cellulose nanocomposites. First, we start describing the structure and properties of cellulose at the molecular, supramolecular and morphological level. We present a review of cellulose whiskers, including the main processing techniques used for their preparation, as well as the influence of the processing conditions on the characteristics of such whiskers. We continue describing the manufacture of cellulose based blends, composites and nanocomposites. Composites reinforced with lignocellulosic macro-fibers as well as nanocomposites reinforced with cellulose whiskers and bacterial cellulose nanofibers are reviewed in this section. Finally, we present several applications for cellulose based composites and nanocomposites. This last section includes biomedical, optoelectronic and electrical applications as well as the use of cellulose for the preparation of high strength "nanopapers" and materials for packaging applications.

F. G. Torres (✉) · O. P. Troncoso · C. Torres · C. J. Grande
Department of Mechanical Engineering, Catholic University of Peru.
Av. Universitaria, Lima 32, Lima 1801, Peru
e-mail: fgtorres@pucp.edu.pe

S. Thomas et al. (eds.), *Advances in Natural Polymers*,
Advanced Structured Materials 18, DOI: 10.1007/978-3-642-20940-6_2,

2.1 Introduction

Cellulose is the most abundant natural polymer on earth. It is the primary product of photosynthesis in terrestrial environment and has the potential to be a renewable bioresource for energy and chemicals [1–3]. The amount of cellulose synthesized annually by plants is close to 10 tons [4]. Most cellulose is utilized as raw material in the paper industry for the production of paper and cardboard products. This equates to 10 tons of pulp produced annually. In addition, 4 million tons are used for further chemical processing and only around 4 tons are used for the production of cellulose based advanced materials. Cellulose based nanocomposites have emerged as a new type of advanced materials, attracting great interest in their research and development. They represent an alternative to conventional composites because less of 5 % wt of reinforcement is needed to produce advanced materials with improved properties [5]. Cellulosic nanocomposites are formed by adding cellulose nanoscale fillers in various polymer matrices resulting in mechanical reinforcement and alteration of other properties. Within the nanocellulose family, we can quote cellulose nanowhiskers or nanocrystals, nanofibrillated cellulose, electrospun nanofibers and bacterial cellulose nanofibers. In this chapter, we review the properties and applications of cellulose based blends, composites and nanocomposites. First, we give the main characteristics of native cellulose structures, including their morphology, as well as their fibrillar hierarchy. Then, we discuss the properties of cellulose whiskers and show the influence of preparation conditions on their properties. Different manufacturing techniques used for the production of cellulose based blends, composites and nanocomposites are presented in Sect. 2.5. Finally, we give several examples of cellulose based composites and nanocomposites for different applications including biomedical, optical, optoelectronic and packaging applications.

2.2 Structure and Properties of Cellulose

2.2.1 Sources

Cellulose occurs naturally in a rather pure form in the fibers of textile plants like cotton, ramie, and jute [6] or in flax. The cellulose found in woody plants (soft and hard woods, wheat, straw, bamboo, etc.) is present together with lignin, hemicelluloses and small amount of extractives [7]. In this case cellulose can be obtained by delignification with different processes (sulfite, sulfate or organocell method) in the form of pulp. The content of cellulose strongly depends on its source and the isolation procedure. Cellulose can be synthesized by other living organisms as well. For example, the tunicate is a marine animal that secretes a tough cellulose sac called tunicin [8]. Other cellulose producing organisms are different types of bacteria, algae and some types of fungi [9]. Under the right conditions, some bacteria can synthesize a type of cellulose which is known as Bacterial Cellulose (BC). Traditionally BC is

used as raw material for a Phillipinian dessert called "nata de coco" [10] and it is also present in the mat used for the preparation of a beverage known as "kombucha tea" [11]. BC can be produced by bacteria of different genera, including *Gluconacetobacter*, *Rhizobium*, *Agrobacterium and Sarcina* [9]. BC is different from the cellulose produced in plants. BC is pure cellulose that has no lignin, hemicelluloses or other extractives that are normally found with plant cellulose. Also, BC is produced in form of nanofibers of around 100 nm in diameter [12, 13]. These fibers form a coherent structured network that exhibits remarkable mechanical properties. BC has been utilized in a wide range of applications such as paper, textile and food industry and as a biomaterial in cosmetic and medicine [14, 15].

2.2.2 Structural Levels of Cellulose

Native cellulose is a linear condensation homopolymer with a complex structure. Three structural levels can be considered [4, 7]:

Molecular level (A). The cellulose is treated as a single macromolecule. Its chemical constitution, molecular mass distribution, presence of reactive sites and intramolecular interactions are discussed.

Supramolecular level (nm). The aggregation of the cellulose macromolecules into elementary fibrils, microfibrils and macrofibrils are described in this level. Its intermolecular interactions and crystal lattice are also discussed.

Morphological level (nm to υm). This level describes the organization of the microfibrils and macrofibrils into layers and walls the existence of distinct cell wall layers in native cellulose fibers or in skin core structures in man-made cellulosic fibers are discussed.

2.2.3 Molecular Level

The chemical formula of cellulose is $C_6H_{10}O_5$. Pure cellulose consists of D-glucopyranose units (so called anhydroglucose units) linked together by β-(1, 4)-glycosidic bonds formed between C-1 and C-4 of adjacent glucose units [4, 16–18]. In the solid state, anhydroglucose units are rotated by 180° with respect to each other due to the constraints of β-linkage.

Each anhydroglucose unit (AGU) possesses three reactive hydroxyl groups at C-2, C-3 and C-6 positions, showing the typical behavior of primary and secondary alcohols. The C-1 and C-4 positions possesses reducing end and non-reducing end groups respectively. AGU in cellulose chain generally adopt the thermodynamically more stable $^4C_1$ chair conformation [7]. In this equatorial conformation, the free hydroxyls groups are positioned in the plane of the pyranose ring (consisting of five carbons and one oxygen) with the hydrogen atoms in a vertical position (axial). This result is derived from infrared spectroscopy (IR),

nuclear magnetic resonance NMR and X ray diffraction studies. The degree of polymerization (DP) of cellulose depends on the cellulose source, isolation method and the technique used for measurement [19]. For instance, cotton has a degree of polymerization (DP) higher than 10,000, wood pulp has values of DP between 300 and 1,700, bacterial cellulose and plant fibers have a DP ranging from 800 to 10,000 and the cellulose produced by algae *Valonia ventricosa* has a DP of 25,000. By contrast, the DP of regenerated cellulose fibers is between 250 and 500 [20] and microcrystalline cellulose prepared by acid hydrolysis has a DP between 100 and 200 [4]. The strength of these H-bonds is around 25 kJ/mol [7]. According to X-ray diffraction, infrared spectroscopy and nuclear magnetic resonance (NMR) measurements, two intramolecular H-bonds are formed in native cellulose (C3-OH group) with endocyclic oxygen (C5′-OH group) [21]. Blackwell et al. [22] assumed the existence of a second intramolecular H-Bond (C2′-OH and C6-OH groups). One intermolecular H-Bonds is present (C3′′-OH and C6-OH groups).

Cellulose is considered a semi-flexible polymer. Intramolecular bonds are responsible for the stiffness of cellulose molecules. The chair conformation of the pyranose ring and the beta glucosidic linkage also favor the linear nature, stiffness and stability of cellulose chain [7]. These properties are reflected in its high viscosity in solution, a high tendency to crystallize and its ability to form fibrillar strands. Cellulose is insoluble in common organic solvents and in water. This is due to the fact that the hydroxyl groups are responsible for the extensive hydrogen bonding network. In order to dissolve cellulose the prevailing hydrogen bonding network must be broken.

2.2.4 Supramolecular Level

The first-X ray diffraction pattern of native cellulose was taken by Nishikawa and Ono in 1913 [23]. This finding determined that individual cellulose molecules tend to arrange themselves in a highly organized manner leading to a ‘paracrystalline’ state. Cellulose chains have a strong tendency to align and aggregate forming structural entities such as elementary fibrils, microfibrils and macrofibrils. These molecular alignments are favored by the regular build-up of the cellulose molecule, the stiffness of the molecular chains and the high hydrogen bonding capacity. The fibrillar structure of cellulose can be understood considering the cellulose biosynthesis in higher plants. Cellulose is synthesized in the plasma membrane by a ring of six complexes of six hexagonally arranged cellulose synthase enzymes (CESAs). The CESA proteins produce β-(1, 4)-glucan chains (the glucan chain consist of AGUs) by using uridine diphosphate glucose (UDP-glucose) as a substrate.

Six adjacent β-(1, 4)-glucan chains produced by each of the six CESAs complexes are extruded and probably start associating by Van der Walls forces and hydrogen bonds [24, 25]. The glucan chains coalesce producing the first fibrillar unit called “elementary fibril”. Five or more elementary fibrils aggregate in microfibrils having typical cross sections of 3, 5–10 nm and consisting of

36–90 glucan chains in land plants and some green algae. The amount of glucan chains within the microfibrils can vary depending on the source. Microfibrils can contain up to 1,400 glucan chains in certain green algae as *Valonia macrophysa*.

The aggregation of elementary fibrils in microfibrils forms crystalline units called "elementary crystallites". The size of these crystals is typically 5–6 nm in diameter for bacterial cellulose and 4–5 nm for cotton cellulose [26]. Their length is 10–20 nm for regenerated cellulose fibers and longer for cotton and other natural cellulosic fibers [7]. Finally, the microfibrils aggregate into macrofibrils in order to form the cell wall. Some authors consider that microfibrils are the smallest morphological unit [27] instead of the elementary fibril which is an aggregate of six glucan chains. But, considering the fact that microfibrils undergo large dimension variations due to the varied existing structure of the CSC, we will consider the elementary fibril as the smallest structural unit of cellulose. Larger entities as micro and macrofibrils are thus only aggregates of this elementary entity. Considering the internal build-up of the fibrillar structure, WAXS and ^{13}C CP-MAS NMR results show that the local order of the macromolecules in cellulose is not uniform throughout the whole structure [4]. The supramolecular structure consists of regions of low order (amorphous regions) and region of very high order (crystalline regions) arranged in a fibrillar fashion. This structure can be described by a two-phase model called fringed fibril model. In this model, there are latticeworks of highly ordered (crystalline) regions together with low ordered (amorphous) regions. Elementary fibrils aggregate in elementary crystallites in order to form microfibrils and macrofibrils. Several imperfections occur in this structure such as the less ordered regions in microfibrils, the interstice between microfibrils and the larger voids between microfibrils and macrofibrils [7]. The cohesion of these different entities is ensured by a hydrogen bond network.

Polymorphism of the crystalline regions in cellulose

Cellulose is a polymorphic material that can adopt four different crystal modifications. These crystal modifications are cellulose I, II, III, IV [26]. Cellulose I is the found in nature and it is known as native cellulose. Cellulose I represents a mixture of two sub allomorphs (Iα and Iβ) [28]. Depending on the source, both sub allomorphs coexist in different proportions. Cellulose produced by primitive organisms (bacteria, algae etc.) is believed to be dominated by the Iα phase whereas the cellulose of higher plants (wood, cotton, ramie etc.) consists mainly of the Iβ phase [29]. Cellulose II, which is the most important crystalline form of cellulose from a technical and commercial point of view, is thermodynamically the most stable crystalline form. Cellulose II has been reported to be produced by the bacterium *Gluconacetobacter xylinum* at low temperatures [27] and by the alga Halicystis [30]. It may also be obtained from cellulose I by either regeneration or a mercerization process. The regeneration process is performed by solubilizating cellulose I in an appropriate solvent and then precipitating it in water to give cellulose II. Mercerization is the process of swelling native fibers in concentrated sodium hydroxide, followed by recrystallization of cellulose II upon washing.

The crystalline structures of cellulose I and II differ in the unit cell dimension and the polarity of the chains. Cellulose III1 and III11 [31, 32] are formed by treating cellulose I and II with liquid ammonia or ethylene diamine [33–35]. Polymorphs IV1 and IV11 [36, 37] may be prepared by processing cellulose III1 and III11 respectively. These processes consist in heating celluloses in a suitable liquid such as glycerol at high temperatures and under tension.

2.2.5 The Morphological Level

The morphological structure of cellulose comprises a well organized architecture of fibrillar elements. An elementary fibril, which is the smallest morphological unit, aggregates into fibrillar entities such as microfibrils and macrofibrils. The length, diameter and properties of elementary fibrils depend on the origin of cellulose [38]. In native cellulose, the fibrillar entities are organized in layers with differing fibrillar textures. These layers have different thickness and microfibrils orientations. By contrast, the arrangement into distinct layers does not exist in regenerated cellulose fibers. These man-made fibers consist of elementary fibrils, which are positioned quite randomly in the structure. A skin-core structure is typical morphology for these regenerated cellulose products. The practical consequence of the fibrillar structure of cellulose is the presence of a network structure. The morphology of such a network presents capillarities, cavities, voids and interstices [4]. The total pore volume and pore size distribution are very sensitive to pre-treatments. Mercerization leads to a decrease in pore diameter and an enhancement of micropore surface while enzyme treatments enlarge the existing pores [39]. Acid hydrolysis enhances the pore system by removing amorphous cellulose from the surface and revealing the macrofibrillar structure of cellulose fibers. The network structure and inner surface area of cellulose fibers is considered as a key parameter in the accessibility and reactivity of cellulose in dissolution and derivatization processes [4]. The properties related with the pore system such as size, volume, shape of the pores can be obtained from sorption data, from small-angle X-ray scattering (SAXS) or mercury porosimetry measurements [4]. Figure 2.1 shows a micrograph of a pure bacterial cellulose network produced by *Gluconacetobacter xylinum*. The assembled nanofibers form a highly ordered and coherent 3-D structure. This network has been used as a model microorganism for investigation of the biosynthesis of cellulose because it produces cellulose as an extracellular product [40]. Bacterial cellulose (BC) networks have also been used as a model of the wall of plants to study the wall relaxation process that occurs during the expansive growth of plants cells. Torres et al. [13] have used small oscillatory rheology to measure the storage modulus (G') and loss modulus (G''). They found that the storage and loss modulus decrease after a certain level of stress is reached. This process, called stress softening, is consistent with the overall mechanical behavior of plant cell walls during cell growth.

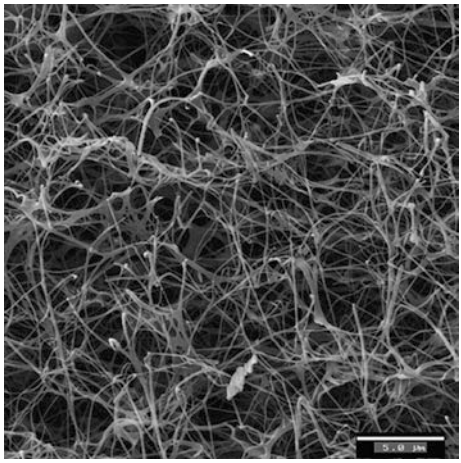

Fig. 2.1 SEM micrograph of a freeze dried bacterial cellulose showing the coherent nanofiber network synthesized by the *Gluconacetobacter* bacteria [13]

2.3 Preparation and Characterization of Cellulose Whiskers

As it has been discussed in Sect. 2.2, the elementary fibrils are composed of consecutive elementary crystallites. These elementary crystallites are often referred to as cellulose nanowhiskers, whiskers, nanocrystals, nanofibers, nanoparticles, microcrystallites, or microcrystals. Hereafter, they will be called "whiskers". Currently, whiskers (diameter 20–40 nm) are being extensively investigated in both research and industry, because of the abundance and renewable nature of cellulose, and the outstanding mechanical properties of cellulose nanocrystals. Due to its high elastic modulus (134 GPa), cellulose nanocrystals are suitable as reinforcement in nanocomposites [41]. Whiskers constitute a generic class of materials having mechanical strengths equivalent to the binding forces of adjacent atoms. The resultant highly ordered structure produces not only unusually high strengths but also significant changes in electrical, optical, magnetic, ferromagnetic, dielectric, conductive, and even superconductive properties. Native cellulose is a typical example of a material that can be described as whisker-like. Microcrystalline cellulose (MCC) is formed by stiff rod-like particles. MCC is prepared by removing the amorphous regions of cellulose by either degradation or dissolution.

Battista [42] synthesized microcrystalline cellulose (MCC). The development of the hydrochloric acid- assisted degradation of cellulose fibers derived from high quality wood pulps, followed by sonification treatment, lead to the commercialization [42, 43]. This MCC has been extensively used for multiple applications. In the pharmaceutical industry, MCC has been used as an excipient for the formulation of solid dosage forms, especially for tableting due to outstanding dry binding properties. In the food industry, MCC has been used as a texturing agent and fat replacer. MCC has also been used as an additive in the paper industry and as reinforcement for the production of composites. Cellulose whiskers are obtained

from natural fibers such as wood [44, 45], sisal [46], ramie [47], cotton stalks [48], wheat straw [49], bacterial cellulose [50, 51], sugar beet [52], chitin [53], potato pulp [54, 55] as well as sea animals called tunicin [56, 57].

2.3.1 Preparation of Cellulose Whiskers

The main process for the isolation of whiskers from cellulose microfibrils is based on acid hydrolysis. Under controlled conditions, this process consists in the disruption of amorphous regions surrounding and embedded within cellulose microfibrils while leaving the microcrystalline regions intact. The amorphous regions are preferentially hydrolyzed whereas crystalline regions remain intact under an acid attack because they have a higher resistance to acid attack than amorphous regions [58, 59]. The differences in the kinetic of hydrolysis between amorphous and crystalline regions produce the acid cleavage event. The hydrolysis carried out over the amorphous regions, produces rod-like crystals called "whiskers". Acid hydrolysis of native cellulose induces a rapid decrease in its degree of polymerization (DP). The DP subsequently decreases much more slowly, even during prolonged hydrolysis times [43, 60–62]. These whiskers are homogeneous crystallites. This is confirmed by X-ray crystal diffraction [63], electron microscopy with iodine-staining [63], small-angle X-ray diffraction [61] and neutron diffraction analyses [64]. Typical procedures currently employed for the production of cellulose whiskers consist of subjecting pure cellulosic material to strong acid hydrolysis under strictly controlled conditions of temperature, agitation, and time. The nature of the acid and the acid-to-cellulosic fibers ratio are also important parameters that affect the preparation of cellulose whiskers. The resulting suspension is subsequently diluted with water and washed with successive centrifugations. Dialysis against distilled water is then performed to remove any free acid molecules from the dispersion. Additional steps such as filtration [65], differential centrifugation [66], or ultracentrifugation (using a saccharose gradient) have been also reported [67].

2.3.2 Influence of Preparation Conditions

2.3.2.1 Dissolution of Cellulose Whiskers

Cellulose is insoluble in water and common organic solvents. This leads to the formation of colloidal suspension when cellulose whiskers are suspended in water. The stability of these suspensions depends on the dimensions of the dispersed particles, their size polydispersity and surface charge. Different acids have been used as solvents for dissolution of cellulose. Sulfuric and hydrochloric acids have been extensively used for whisker preparation, but phosphoric [68] and hydrobromic acids [69] have also been reported for such purposes. When whiskers are

prepared by hydrolysis in hydrochloric acid, the ability to disperse is limited and their aqueous suspensions tend to flocculate [45]. When whiskers are prepared by hydrolysis in sulfuric acid, they tend to remain dispersed in water due to the fact that sulfuric acid reacts with the surface hydroxyl groups of cellulose to yield charged surface sulfate esters that promote their dispersion [44].

2.3.2.2 Effect of Ultrasonic Treatment

Ultrasonic treatments [70] have the potential to change the morphology of the formed whiskers. When hydrolysis is carried out under ultrasonic treatment, a combination of both sulfuric and hydrochloric acids during the hydrolysis appears to generate spherical cellulose nanocrystals instead of rod like nanocrystal which are the typical morphology of whiskers. These spherical cellulose nanocrystals show better thermal stability mainly because they possess fewer sulfate groups on their surfaces [71].

2.3.2.3 Effects of the Temperature and Hydrolysis Time on Microcrystalline Cellulose

The concentration of sulfuric acid in hydrolysis reactions to obtain whiskers has a typical value of 65 % (wt). However, the temperature can range from room temperature up to 70 °C and the corresponding hydrolysis time can be varied from 30 min to overnight depending on the temperature. Dong et al. [72] have investigated the influence of the hydrolysis time on the length of cellulose whiskers and their surface charge. They reported a decrease in the whiskers length and an increase in their surface charge with prolonged hydrolysis time [72]. Beck-Candanedo et al. [73] have investigated the reaction time and acid to pulp ratio on whiskers obtained by sulfuric acid hydrolysis of bleached softwood sulfite pulp. The results determined that shorter nanocrystals with narrow size polydispersity were produce at longer hydrolysis time.

Elazzouzi et al. [65] have studied the size distribution of whiskers resulting from sulfuric acid hydrolysis of cotton treated with 65 % sulfuric acid over 30 min at different temperatures, ranging from 45 to 72 °C. The results showed that shorter crystals were obtained when increasing the temperature. However, no clear influence on the width of the crystal was revealed. Bondenson et al. [50, 74] have tried to optimize the hydrolysis conditions by an experimental factorial design matrix (response surface methodology). The factors that were varied during the process were the concentrations sulfuric acid, the hydrolysis time, temperature and the ultrasonic treatment time. The responses that were measured were the median size of the cellulose particles and the yield of the reaction. The results demonstrated that with a sulfuric acid concentration of 63.5 % (w/w) over a time of approximately 2 h, it was possible to obtain CNs having a length between 200 and 400 nm and a width less than 10 nm with a yield of 30 % (based on initial weight).

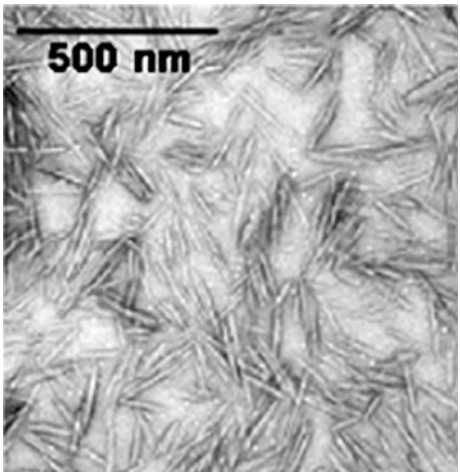

Fig. 2.2 Transmission electron micrograph of cotton whiskers [75]

2.3.3 Characterization of Cellulose Whiskers

Figure 2.2 shows a TEM micrograph of cellulose whiskers prepared from cotton. Geometrical characteristics of cellulose whiskers depend on the origin of cellulose microfibrils and on the conditions of the acid hydrolysis process such as time, temperature, and purity of materials. Samir et al. [75] have reported the dimensions of cotton and tunicin whiskers. The length (L) and lateral dimension (D) of cotton whiskers were around 200 and 5 nm, respectively (ratio L/D = 40). The length and lateral dimension of tunicin whiskers were reported to be around 1,000 and 15 nm, respectively (ratio L/D = 67). De Souza [76] studied cotton and tunicate whiskers in aqueous suspensions as well. The average size whisker dimensions reported were L = 255 nm and D = 15 nm for cotton whiskers (ratio L/D = 17) while the values were L = 1,160 nm and D = 6 nm (ratio L/D = 72.5) for tunicate whiskers.

2.3.3.1 Morphological Characterization

The morphological characteristics of cellulose whiskers are usually studied by microscopy (TEM, AFM, E-SEM, etc.) or light scattering techniques, including small angle neutron scattering (SANS) [77], and polarized and depolarized dynamic light scattering (DLS, DDLS) [76]. Table 2.1 list the geometrical properties of several cellulose whiskers as well as the technique used for their study. AFM has been widely used to provide nanometer scale information about the surface topography of cellulose whiskers under ambient conditions [78–80]. However, AFM topography may show rounded cross sectional profiles in cases where other shapes are expected. For instance, Valonia whiskers shown in AFM images shapes different than the square shape cross section observed under TEM

Table 2.1 Geometrical characteristics, length and width, of cellulose nanocrystals (adapted from ref [38])

Source	Length (nm)	Width (nm)	Technique	References
Bacteria	100–1,000	5–50 × 30–50	TEM	[172, 173]
Cotton	70–300	5–15	TEM, DDLS[a], AFM	[56, 76, 80, 174, 175]
Cotton linter	25–500	6–70	FEG-SEM[b], TEM, AFM	[65, 114, 116]
Ramie	50–250	5–10	TEM	[112, 176]
Sisal	100–500	3–6.5	TEM	[119, 177]
Tunicate	100–1,160	8.8–28	SANS[c], DDLS, TEM	[56, 65, 76, 77, 138]
Valonia	>1,000	10–20	TEM	[178]
Soft wood	100–200	3–5	TEM, AFM	[73, 179]
Hard wood	140–150	4–5	AFM	[73]
MCC	35–270	3–48	TEM	[65, 180]

[a] DDLS: depolarized dynamic light scattering
[b] FEG-SEM: field emission gun scanning electron microscopy
[c] SANS: small angle neutron scattering

images [38] this issue is probably because AFM overestimated the width of the whiskers due to the tip-broadening effect [38, 81]. Besides surface topography, AFM was reported to measure mechanical properties and interactions of the cellulose nanocrystals, such as stiffness and adhesion or pull-off forces [82].

2.3.3.2 Spectroscopic Techniques

Small-angle (Neutron and X-ray) scattering techniques are used to determine the precise shape of whiskers. For instance, the crosses sectional shape of rigid tunicin whiskers is rectangular with a calculated value close to 88 × 182°A [77]. Terech et al. [77] reported the use of Small-angle (Neutron and X-ray) scattering techniques to determine the precise shape of tunicin whiskers. They demonstrated that the cross sectional shape of these rigid whiskers was rectangular with a calculated value close to 88 × 182°A. In addition, cellulose samples can be characterized by its degree of crystallinity. The crystalline regions of cellulose are characterized by an orderly arrangement of molecule chains and are assessed from wide-angle X-ray scattering (WAXS) patterns or from the evaluation of a 13C CP-MAS NMR spectrum. Tashiro and Kobayashi [83] calculated the three dimensional elastic constants for native and regenerated cellulose perfect crystal. The theoretical values of Young's modulus along the chain axis were 167.5 and 162.1 GPa, respectively. Sturcova et al. [84] reported measurements of the elastic modulus of tunicin whiskers using a Raman spectroscopy technique. This technique consists of deforming a dispersed sample of the material using a four-point bending test. As a consequence, the deformation produces a shift in a characteristic Raman band. This shift is used as an indication of the stress in the material. The results showed that the elastic modulus of tunicin whiskers were very high, at about 143 GPa. Rusli et al. [85] reported that the elastic modulus of cotton whiskers by Raman Spectroscopy produced a value about 105 GPa.

2.4 Manufacture of Cellulose Blends, Composites and Nanocomposites

2.4.1 Cellulose Based Blends and Composites

Natural cellulose fibers such as cotton, ramie, etc. have been used in the garment industry as blends. These blends have their own distinctive properties that are affected by the fiber sources, the proportion of fibers blended and the processing techniques. Mayer et al. [86] prepared blends of cellulose acetate (2.5 degree of substitution) and starch using a melt processing technique. The results showed that cellulose acetate/starch blends have acceptable properties for injection-molded applications and that they are biodegradable and nontoxic. Silk fibroin (Bombyx mori)/cellulose blend films have been also studied. The mechanical properties showed that both strength and elongation at break of silk fibroin films were improved by blending with cellulose [87]. Industrial thermoplastics manufacturing techniques have been explored to prepare natural fiber reinforced composites. Torres et al. [88] adapted conventional thermoplastic processing techniques such as extrusion, compression and rotational molding in order to manufacture natural fiber reinforced polymers. They used natural lignocellulosic fibers such as sisal, jute and cabuya to reinforce polyethylene and starch matrices [88–93]. The main processing problems encountered to develop this work were the hydrophilicity of natural fibers, as well as their degradation at low temperatures and the formation of clumps. Grande and Torres [93] have prepared lignocellulosic fiber reinforced composites using a single screw extruder. The polymer matrix employed was polyethylene. Jute and sisal were used as reinforcement with initial lengths varying from 5 to 10 mm. The results showed that at higher processing temperatures, the fibers were more aligned in the flow direction. In the extrusion process, one disadvantage is the presence of bubbles which affect the quality of the extruded rods. A way of controlling the formation of bubbles is by pretreating the fibers. Torres and Aragon [91] have developed the process of rotational molding of natural fiber reinforced polymers. Rotomolded cylinders were made of HDPE powder. Cabuya and sisal with an average length of about 5 mm were added as reinforcement at concentrations varying from 0 to 7.5 % by weight. The results showed that cabuya reinforced composites showed higher impact strengths than the sisal reinforced ones. Impact strength decreased with increasing fiber content. Kuruvilla et al. [94] have also used sisal fibers as reinforcement in low density polyethylene (LDPE) composites. They found that tensile properties of LDPE-sisal composites increase with the increase in fiber content as well as with fiber length. Herrera-Franco et al. [95] introduced henequen cellulosic fibers into a LDPE matrix. The concentration of randomly oriented fibers in the composite ranged between 0 and 30 % by volume. The results showed that the addition of henequen cellulosic fibers in a low-density polyethylene (LDPE) matrix increased the tensile strength by 50 % (from 9.2 to 14 MPa) at a fiber loading of 30 % by volume. The modulus increased from 275 MPa for pure HDPE to 860 MPa for 30 % fiber loading though the strain at failure decreased from 42 to 5 %.

The advantages of using lignocellulosic reinforcements in the production of composites are their low density, low cost, high specific properties, biodegradability and renewability. Also, the organic nature of lignocellulosic reinforcements allows incineration or compostation methods for degradation. The main disadvantages are their hydrophilic nature of cellulose, high moisture absorption and limited thermal stability. The hydrophilic nature of lignocellulosic fibers leads to poor interfacial adhesion and dispersion in olefinic thermoplastic matrix materials [96]. The high moisture absorption promotes dimensional instability of composites [97]. Water, in the liquid or vapor state, can diffuse into composites. As a consequence, their properties are hampered. In order to avoid this issue, modification of cellulose fibers by esterification has been used [98]. Torres et al. [99] have assessed the interfacial properties of lignocellulosic reinforced composites prepared with untreated fibers and with fibers treated with stearic acid. Interfacial shear strength was measured by a single fiber fragmentation test. Figures 2.3 and 2.4 show typical fracture surfaces of sisal reinforced polyethylene composites. Figure 2.3 corresponds to an untreated polyethylene-sisal specimen, while Fig. 2.4 was taken from a treated specimen. A relatively ductile failure can be observed in the matrix region adjacent to the fibers. A relatively large fiber pull-out can be observed in the untreated composite (Fig. 2.3). By contrast, virtually no pull-out can be observed when the composite is prepared with treated fibers (Fig. 2.4). This indicates higher interfacial shear strength for the treated specimens. Also, the results showed that pre-treated fibers with stearic acid increased the interfacial shear strength by 23 % with respect to untreated fibers. It was observed that during dry mixing, the best dispersion was attained when stearic acid was used, compared to a poor dispersion with no fiber treatment.

The limited thermal stability determines low permissible temperatures of processing. The processing temperature for cellulose based reinforced composites is limited to around 200 °C, though higher temperature can be used for short periods of time [100]. Other properties such as thermal conductivity and water absorption have been studied in fiber reinforced composites. Torres et al. [89] have prepared sisal fiber reinforced composites. They determined that their thermal conductivity coefficient, k, are affected mainly by void fraction and moisture content. Water absorption tests indicated that higher natural fiber reinforcement level corresponds to higher masses of water being absorbed over a given period of time because of hydrophilicity of natural fibers. Linear burn rate experiments showed that sisal reinforced polymers burn twice as fast as unreinforced HDPE specimens. However, the reinforced specimens showed better structural integrity during burning than the unreinforced specimens. Biocomposites have also been studied to develop friendly environmental materials. Torres et al. [92] prepared biocomposites of starch and natural fibers. Starch extracted from potato, sweet potato, and corn starch, were used as matrices and lignocellulosic fibers from jute, sisal and cabuya were used as discrete reinforcement. Due to the biodegradable compostable nature of natural fiber-starch composites, Gomez et al. [101] have investigated the effect of plasticizer and different natural fibers on their mechanical, degradation and thermal properties.

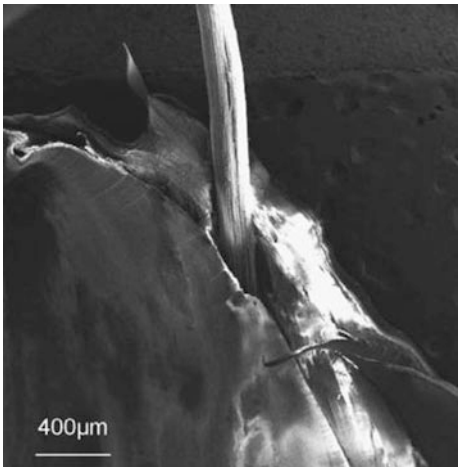

Fig. 2.3 Fracture surface of a polyethylene-sisal composite showing a pulled out fiber [99]

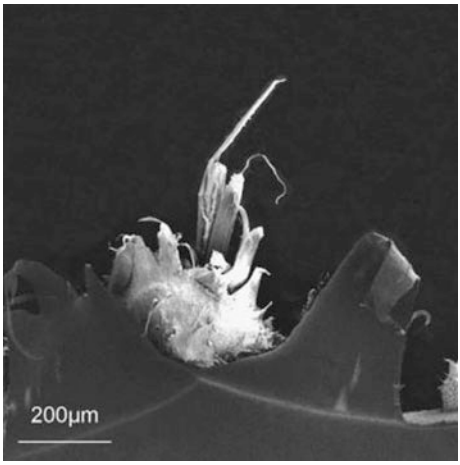

Fig. 2.4 Typical fracture surface of polyethylene-sisal composite for a treated fiber [99]

2.4.2 Cellulose Based Nanocomposites

The cellulose based materials that are used as nano-reinforcements are cellulose nanocrystals (i.e. whiskers and nanospheres), nanofibrillated cellulose, regenerated cellulose nanoparticles and electrospun nanofibers. A wide range of polymer matrices have been used to form cellulose nanocomposites. Synthetic polymers such as polypropylene, poly(vinyl chloride) (PVC) [102], waterborne epoxy [103], waterborne polyurethane [104], polyurethane [105], poly-(styrene-co-butyl acrylate) [106], poly(oxyethylene) [107], polysiloxanes [108], polysulfonates [109], cellulose acetate butyrate [110, 111], poly(caprolactone) [112], poly(vinyl alcohol) [113] and poly(vinyl acetate) [114]. Different biopolymers such as starch-based

polymers [58], soy protein [115], chitosan [116], regenerated cellulose [117], silk fibroin [118], poly (-hydroxyoctanoate) (PHO) [119], poly (lactic acid) and cellulose acetate butyrate (CAB) have also been used as matrices.

Siqueira et al. [120] prepared cellulose nanocomposites to reinforce polycaprolactone (PLC) matrix. As reinforcement, they used two kinds of nanoscale fillers, nanowhiskers and microfibrillated cellulose, both extracted from sisal. They found significant differences according to the nature of the nanoparticle and amount of nanofillers used as reinforcement. Wang et al. [115] produced reinforced soy protein isolate (SPI) plastics using cellulose whiskers extracted from cotton inner pulp. The cellulose whiskers had an average length of 1.2 υm and diameter of 90 nm. The incorporation of cellulose whiskers into the SPI matrix led to an improvement in the water resistance of SPI composites. The addition of cellulose whiskers promoted strong interactions between whiskers and the SPI matrix. The tensile strength and Young's modulus of the SPI/cellulose whisker composites increased from 5.8 to 8.1 MPa and from 44.7 to 133.2 MPa, respectively. The effect of whiskers on the mechanical properties exceeded conventional predictions from traditional classical models applied to filler-reinforced nanocomposites such as the Halpin-Kardos model. Favier et al. [57] explained that this effect is due to the formation of a rigid percolating filler network that is joined together by hydrogen bonds. The existence of such a network was confirmed by electrical measurements [121]. Flandin et al. [121] prepared nanocomposites containing cellulose whiskers that were coated with a conductive polypyrrole. They measured their electrical properties and founded strong interactions between fillers. Factors such as the nature of polymer matrix and the surface energy of the whiskers showed an influence on the formation of this network [38].

Gea et al. [122] prepared biocomposites based on bacterial cellulose (BC) and apple and radish pulp. The bacterial cellulose films formed by a network of cellulose nanofibers were disintegrated to be used as reinforcement in order to produce biocomposites sheets with apple and radish pulp. This nanosize disintegrated BC fibers were blended with apple and radish pulp in the wet state and then hot pressed to produce paper–like sheets. The results showed that the organic matrices such as apple and radish pulp are heavily reinforced with BC. For pure apple and radish pulp, the Young's modulus was around 4.5 GPa while BC reinforced sheets reached values as high as 6.5 GPa. Nishino et al. [123] prepared "all-cellulose" composites, in which both the fibers and the matrix were cellulose. This composite was manufactured using a wet process by controlling the solubility of cellulose through pretreatment conditions. The cellulose self-reinforced composite showed excellent mechanical and thermal properties such that this composite can be used as an alternative of glass-fiber-reinforced composites. Fiber pretreatment enhances the molecular diffusion across the fiber-matrix interface, obtaining improved transverse mechanical properties of the composite.

Gindl and keckes [124] prepared cellulose based nanocomposite films with different ratio of cellulose I and II, The process consist of a partial dissolution of microcrystalline cellulose powder in lithium chloride/N,N-dimethylacetamide and subsequent film casting. The results showed that, by varying the cellulose I and II

ratio, the mechanical performance of the nanocomposites can be tuned. This nanocomposite films were transparent to visible light and of high strength and stiffness with regard to comparable cellulosic materials and they are easily recyclable and biodegradable as well.

2.4.3 Cellulose Based Nanocomposite Manufacturing Techniques

2.4.3.1 Casting-Evaporation Processing

Casting evaporation techniques have been extensively used to transfer cellulose whiskers from an aqueous dispersion into an organic polymer matrix. Nanocomposites films are formed via solution casting, allowing the solvent to evaporate [38]. Two steps are used to prepare nanocomposites films. The first step consists of mixing an aqueous suspension of cellulose nanostructures and the dispersed or solubilized polymer matrix. Homogeneous suspensions are obtained by magnetic stirring at room temperature or by using an autoclave reactor for mixing at high temperatures. The suspensions are generally degassed under vacuum to remove air. Then, the mixture is cast on the Petri dish (e.g. Teflon or propylene dishes) and put in a drying oven under vacuum. An increase of temperature allows the solvent evaporation and the film formation.

2.4.3.2 Sol: Gel Processing

This processing is based on the formation of a three dimensional template of well individualized cellulose whiskers which is filled with a polymer [125, 126]. The first step in this process is the formation of a cellulose nanostructure template through a sol/gel process. This involves the formation of an aqueous cellulose nanostructures dispersion which is converted into a gel through solvent exchange with a water miscible solvent (e.g. acetone). In the second step, the cellulose nanostructures template is then filled with a matrix polymer by immersing the gel into a polymer solution. This polymer solvent must be miscible with the gel solvent and does not disperse the cellulose nanostructures.

2.4.3.3 Melt Compounding Processing

A twin extruder is used to compound a thermoplastic polymer with a whisker suspension. Such suspension is added in an extruder zone where the PLA is melted by means of a peristaltic pump. The extruder has a venting system that is used to remove the liquid phase of the whisker suspension. Kamel [81] has compounded PLA-malic anhydride and poly (ethylene glycol) with cellulose whiskers

suspended in LiCl/dimethyl acetamide. Orts et al. [127] extruded starch plastics reinforced with cotton whiskers that produced and increase of Young's modulus 5 times relative to a control sample with no cellulose reinforcement.

2.4.3.4 Electrostatic Fiber Spinning (Electrospinning)

This is method allows to prepare fibers with diameters ranging from several micrometers down to 100 nm through the action of electrostatic forces. It uses a high electrostatic potential applied to a spinning liquid across a charged nozzle and a grounded screen collector. At the right conditions, a charged stream of the spinning liquid is ejected and ultimately a mat of non-woven fibers is collected on the collector.

Electrospinning processes are used to prepare nanocomposite fiber mats. In order to prepare nanocomposite fiber mats, mixtures containing the polymer solution and cellulose whiskers solution are placed in the appropriated electrospinning setup. Peresin et al. [128] have produced nanocomposite mats of poly (vinyl alcohol) (PVA) reinforced with cellulose nanocrystals using this electrospinning technique. Smooth nonwoven mats with homogeneous nanofibers were obtained. Park et al. [129] have also incorporated cellulose whiskers into nanofibers of polyethylene oxide (PEO) by the electrospinning process.

2.4.3.5 Layer-by-Layer (LBL) Electrostatic Assembly

Layer-by-layer assembly (LBL) is able to produce nanometer-scale multi-layered materials in order to improve highly desirable properties including chemical, mechanical, electrical, magnetic, thermal and optical. In this method, a charged solid substrate is exposed to a solution of oppositely highly charged polyelectrolytes for a short time. These highly charged polyelectrolytes can produce charge reversal upon adsorption on the oppositely-charged substrate. In consequence, when the substrate is exposed to a second solution containing polyelectrolytes of opposite charges, an additional layer is adsorbed on the first layer, thereby forming a second layer. These steps can be repeated cyclically to form multilayer structures on a given substrate. The use of the LBL technique is expected to maximize the interaction between cellulose whiskers and a polar polymeric matrix. It also allows the incorporation of cellulose whiskers with a dense and homogeneous distribution in each layer. De Mesquita et al. [130] obtained a biodegradable cellulose nanocomposite from Layer-by-layer (LBL) technique. This nanocomposite was composed of highly deacetylated chitosan and eucalyptus wood cellulose nanowhiskers. They claimed that the driving forces for the growth of the multilayered films were the hydrogen bonds and electrostatic interactions between the negatively charged sulfate groups on the whisker surface and the ammonium groups of chitosan. Their results showed that cellulose nanowhiskers adsorbed on each chitosan layer presented high density and homogeneous distribution and the

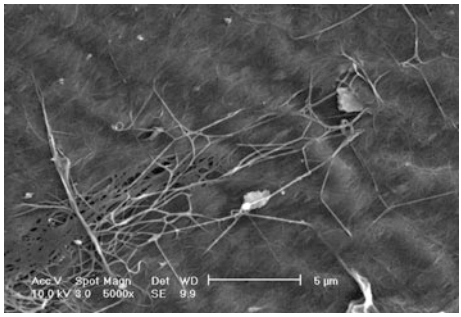

Fig. 2.5 ESEM micrograph of a bacterial cellulose-corn starch composite. Arrows show bacterial cellulose nanofibers [12]

average thickness of a single bilayer was found to be 7 nm. Podsiadlo et al. [131] reported the preparation of cellulose whiskers multilayer composites with a polycation, poly-(dimethyldiallylammonium chloride) (PDDA) using the LBL technique. The average thickness of a single bilayer was found to be 11 nm and the authors concluded that the multilayer films revealed uniform coverage and densely packed cellulose crystal surface. Cranston et al. [132] reported the orientation of the cellulose nanocrystals layer adsorbed onto poly(allyl)amine hydrochloride (PAH) coated silicon surface after long exposure to a strong magnetic field.

2.4.3.6 Bottom-up Manufacture of Bacterial Cellulose Nanocomposites

Grande et al. [133] developed a technique for the production of self assembled bacterial cellulose nanocomposites. This technique is based on the natural bottom-up process found in the synthesis of bacterial cellulose (BC). For instance, BC-Starch nanocomposites were prepared by this technique (Fig. 2.5). Figure 2.6 shows a scheme of the bottom-up manufacturing process. The process is based on the addition of intact starch granules to the culture medium before bacteria are inoculated. After being added to the culture medium, the starch-medium suspension is autoclaved at 121 °C. During this process the starch phase, undergoes a "first gelatinization". Then, bacteria are inoculated and the nanofibers network is formed in the presence of a partially gelatinized starch. The gelatinization of starch allow to partially controlling the diffusion of polymeric chains into an existing fiber network of BC. This controlled diffusion process allows cellulose nanofibrils to grow in the presence of a starch phase. Starch was gelatinized in different stages and formed a layer that covers cellulose nanofibrils. The BC-starch gel formed was hot pressed into sheets. As a consequence, starch was forced to further penetrate the BC network. Nanocomposites produced by this technique showed a high volume fraction (around 90 %) of a strong phase of BC nanofibers covered by a starch phase. This technique has the advantage to be extended for the addition of other materials into the BC network e.g. BC-hydroxyapatite nanocomposites [12]. Nanocomposites produced with this technique could have a variety of potential biomedical applications.

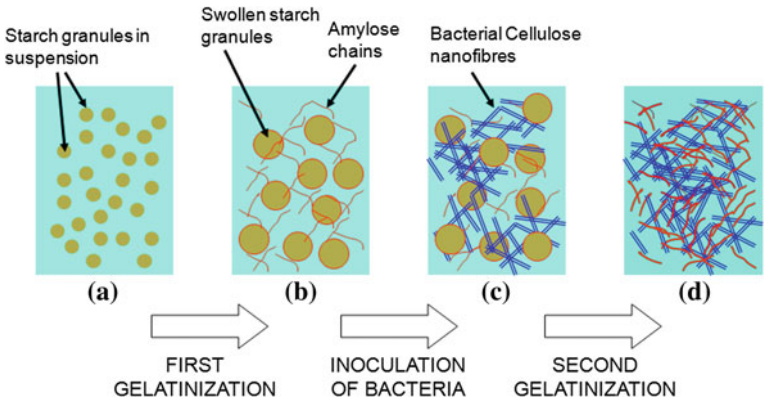

Fig. 2.6 Scheme of the BC-starch bottom-up process. **a** starch granules are in suspension in the culture medium. **b** After autoclaving, starch is partially gelatinized, amylose leaches and granules swell. **c** BC nanofibrils grow in presence of the partially gelatinized starch. **d** After hot pressing, the nanocomposite shows interpenetrating networks of amylose and cellulose [133]

2.5 Characterization of Cellulose Nanocomposites and Blends

2.5.1 Morphological Characterization

Scanning electron microscopy (SEM) as well as atomic force microscopy (AFM) can be used for structure and morphologies determination of cellulose nanocomposites. SEM allows the analysis of the homogeneity of nanocomposite, presence of voids, and dispersion level of the cellulose nanocrystals within the continuous matrix, presence of aggregates and sedimentation possible orientation of cellulose nanocrystals. Figure 2.7 shows an AFM micrograph of a bacterial cellulose network accompanied by the section analysis of the segment indicated in the micrograph. The AFM analysis shows that the diameter of the nanofibres was in the range 100–200 nm.

2.5.2 Spectroscopic Techniques

The structural properties of the nanocomposites such as the size of the cellulose crystallites and the crystallinity index can be characterized using X-ray diffraction. X-ray diffraction is used to elucidate the eventual modifications in the crystalline structure of the matrix after the addition of the whiskers.

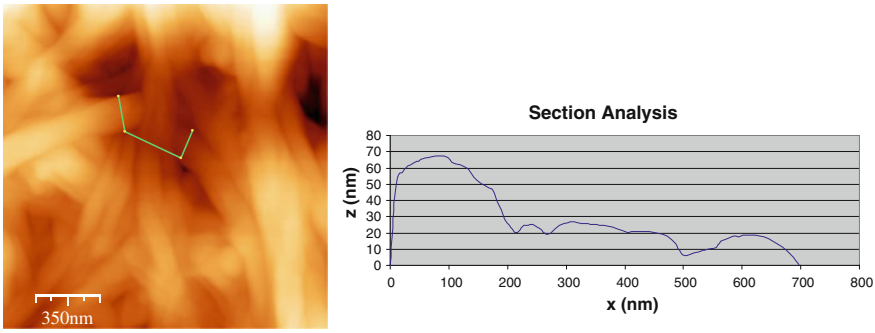

Fig. 2.7 AFM micrograph and section analysis of a bacterial cellulose sheet [12]

2.5.3 Mechanical Properties

Mechanical properties of nanomaterials have been characterized using both tensile test and nanoindentation techniques. Nanoindentation experiments describe the deformation of the volume of material beneath the indenter (interaction volume). The nanoindentation of cellulose composites can be performed by using an AFM.

Zimmermann et al. [134] have used cellulose fibrils obtained from sulphite wood pulp to reinforce water soluble polymers such as polyvinyl alcohol (PVA) and hydroxypropyl cellulose (HPC). The mechanical properties of these nanocomposites were measured by tensile tests showing that the addition of fibrils increase the modulus of elasticity (E) up to three times and the tensile strength up to five times compared to the raw polymer. Zimmermann et al. [135] have determined the 'E' values and the hardness of cellulose/HPC nanocomposites using nanoindentation technique. The results showed that the E values measured by nanoindentation were from two to three times higher than the E values measured by means of tensile tests. Stauss et al. [136] have explained that differences between tensile test and indentation results are due to the fact that they do not test the same material volumes and regions. The large volume used in tensile test includes defects such as pores, cracks and impurities.

2.5.4 Thermal Characterization

The glass transition temperature (Tg) of cellulose reinforced composites is an important parameter which influences different properties of the resulting composite such as mechanical behavior, matrix chains dynamics and swelling behavior. Differential scanning calorimetry (DSC) and dynamic mechanical analysis (DMA) are used to evaluate the Tg value of cellulose nanocomposites. In some cases, the addition of cellulose nanocrystals into polymer matrices does not seem to affect the

glass transition temperature regardless of the nature of the polymeric matrix, the origin of the cellulose nanocrystals, or the processing conditions. For tunicin whisker filled composites, no modification of Tg values was reported when increasing whisker content [50, 137, 138]. Similar results were reported for bacterial cellulose and wheat straw cellulose whisker based nanocomposites. [49]. Hajji et al. [139] showed that the Tg of poly (S-co-BuA) composites is independent of both the whisker content and the processing conditions. Angles and Dufresne [138] have evaluated the effect of whiskers content and water content on the Tg values of cellulose nanocomposites obtained using glycerol plasticized starch as matrix and tunicin whiskers as reinforcing phase. They reported that for lower whiskers content (3.2 % wt) a classical plasticization effect of water was observed and for higher whiskers content (6.2 % wt) an antiplasticization effect was observed. Mathew and Dufresne [140] have reported that the Tg of tunicin whisker-starch nanocomposites depends on the whisker content. A significant increase in crystallinity was observed in the nanocomposites prepared by increasing either moisture content or whiskers content. Roohani et al. [114] have proposed that the modification of Tg values in moisture conditions is due to the plasticization effect of water linked to the strong interaction between cellulose nanocrystals and the matrix.

2.6 Applications of Cellulose Based Blends, Composites and Nanocomposites

Natural cellulose fibers such as cotton, ramie, etc. have been used as blends for textile applications. High modulus regenerated cellulose fibers are produced on a commercial scale. For instance, Lyocell®, a high performance cellulosic fiber, has been used in many nonwoven applications because of its high strength, durability, absorbency, purity and biodegradability.

Lyocell® fibers have been explored in blends. Chang et al. [141] prepared Lyocell® based blends. Poly(vinyl alcohol) (PVA), poly(vinyl alcohol-co-ethylene) (EVOH), and poly(acrylic acid-co-maleic acid) (PAM) were used as fillers in blends with lyocell produced through solution blending. The results showed that blends with PVA exhibit the best tensile properties. Thus, Lyocell® fibers have recently been used as reinforcement for thermoplastic fiber composites.

2.6.1 Biomedical Applications

Bacterial cellulose has a wide range of potential biomedical applications such as tissue engineered cartilage scaffolds [142, 143] wound dressing [144–148]

artificial skin [9, 145], dental implant, vascular grafos, catheter covering dressing [148], dialysis membrane [148, 149], coatings for cardiovascular stents, cranial stents [148], membranes for tissue-guided regeneration [145, 148], controlled-drug release carriers [148], vascular prosthetic devices [150] and artificial blood vessels [151–153]. Bacterial cellulose has been used for the production of scaffolds for tissue engineering [142]. Andersson et al. [143] prepared engineered porous BC scaffolds by fermentation of *Acetobacter xylinum* in the presence of slightly fused wax particles with a diameter of 130–300 υm, which were then removed by extrusion. In this research, human chondrocytes were seeded onto the porous BC scaffolds and the results showed that cells entered the pores of the scaffolds and that they increasingly filled out the pores overtime. The proliferation of human chondrocytes within the porous BC was observed as well.

Hydroxyapatite (Hap) has been used in bone regeneration due to the fact that it is biocompatible, bioactive, non-inflammatory, non-toxic and non-immunogenic. It is believed that BC-Hap nanocomposites are promising in applications of bone tissue engineering. Grande et al. [154] have fabricated BC-Hap nanocomposites by the formation of cellulose nanofibers in the presence of a Hap phase in static culture (Fig. 2.8). The biocompatibility and cell viability of the nanocomposites were confirmed by HEK cell seeding (Fig. 2.9). The results confirmed that these novel nanocomposites are suitable for biomedical applications. It has been reported that bacterial cellulose shows a vast potential as a novel wound healing system. Cellulose nanofibril networks show the ability to absorb and hold large contents of water. Another advantage is that external bacteria cannot penetrate through the hydrated BC network. These features make gel-like BC nanofibril networks suitable as wound dressing [144, 145].

2.6.2 Cellulose Based Materials for Batteries

Azizi Samir et al. [155] have studied the possibility to reinforce thin films of polymer electrolytes for lithium battery applications. They reinforced polyoxyethylene with tunicate whiskers. The results showed that the storage modulus and temperature stability was greatly improved, and the ionic conductivity was maintained.

Nystrom et al. [156] have produced a nanostructured high surface area electrode material for energy storage applications. It was obtained from cellulose fibers of algal origin individually coated with a thin layer of polyrrole. The high surface area and good electronic conductivity of this composites made it suitable for use in electrochemically controlled ion-exchange [157–159] and ultrafast all polymer-based batteries [156]. These investigations open up new possibilities for the production of environmentally friendly, cost efficient, up-scalable and lightweight energy storage systems.

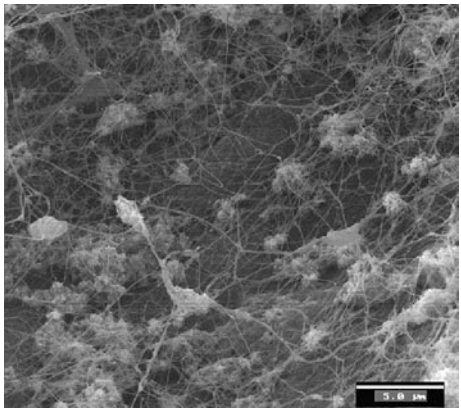

Fig. 2.8 SEM micrographs of a hap-bacterial cellulose composite showing the hap particles inside the cellulose network [154]

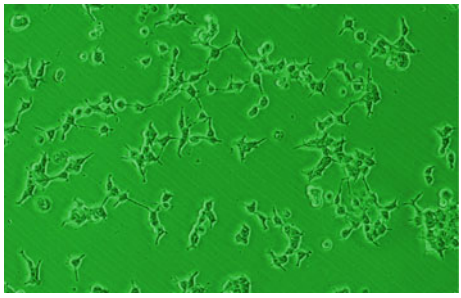

Fig. 2.9 Optical micrographs of HEK cells for one day of culture in a hap-bacterial cellulose nanocomposite [154]

2.6.3 Optoelectronic Applications

Cellulose nanofibers from different sources have showed remarkable characteristics as reinforcement material for optically transparent composites [160, 161]. Iwamoto et al. [160] prepared optically transparent composites of transparent acrylic resin reinforced with cellulose nanofibers extracted from wood pulp fibers by fibrillation process. They showed that cellulose nanofiber-reinforced composites are able to retain the transparency of the matrix resin even at high fiber content (up to70 % wt). The aggregation of cellulose nanofibers also contributes to a significant improvement in the thermal expansion properties of plastics.

Yano et al. [162] obtained polymer resins reinforced with bacterial cellulose nanofibers. This flexible plastic composite maintains the transparency of the original resin even at high fiber contents (70 % wt). This composite has interesting technical properties such as low thermal expansion coefficients (6×10^{-6} °C^{-1}), mechanical strength 5 times higher than the one of engineered plastics (Young's modulus of 20 GPa and tensile strengths reaching 325 MPa) and high transparency.

2.6.4 Optical Coating

Podsiadlo et al. [163] have prepared layer-by-layer assembled films of cellulose nanowires extracted from tunicate. These films showed strong antireflection properties due to porous architecture created by randomly-oriented overlapping nanowires. In addition to their antireflection properties, the remarkable mechanical properties of tunicate nanowires make films suitable for optical coatings. Bacterial cellulose (BC) membranes have been used as flexible substrates for the fabrication of Organic Light Emitting Diodes (OLED). Indium tin oxides were deposited onto the membrane using sputtering technique to improve conductive properties [164].

2.6.5 Packaging Applications

There is a strong interest to replace the use of petroleum based polymers with biodegradable polymers in the packaging industry. Single-use foam packaging is used by manufacturers to protect and preserve a wide array of food and industrial products. Starch has shown a potential use for foaming. The use of fillers as reinforcement has been explored to improve starch based foams. Due to the thin cell walls in the foams, microscale fillers cannot be used efficiently. Nanoscale fibrils have been explored as reinforcements in starch based foams. Svagan et al. [165] successfully reinforced the cell walls in starch based foams with microfibrillated cellulose (MFC). The MFC addition improved the mechanical properties such as Young's modulus, yield strength and work to fracture. At the same time the moisture stability was increased.

2.6.6 Electrical Applications

Van den Ber et al. [166] has prepared nanocomposites of semi conducting polymers reinforced with tunicate cellulose whiskers with a typical diameter or around 20 nm. The results showed that the nanocomposites synergistically combine the electronic characteristic of the conjugated polymers with the improved mechanical properties of the cellulose scaffold. Other studies suggest that cellulose whisker can be used for electrical applications such as the creation of circuitry in a special kind of smart paper [167].

2.6.7 Cellulose Nanopapers

Cellulose nanofibrils are also used to prepare cellulose nanopaper structures of remarkable properties such as high toughness [168]. Large, flat, smooth and optically transparent cellulose nanopaper structures have been developed using several techniques. Sehaqui et al. [169] prepared cellulose nanopaper sheets with diameter of 200 nm and with optical transparency and high tensile strength, indicating well dispersed nanofibrils. In addition, the application of the nanopaper-making strategy to cellulose/inorganic hybrids demonstrated the potential for "green" processing of new types of nanostructured functional materials.

2.6.8 Ceramics with Uniform Nanopores

Cellulose nanocrystals have been used in the elaboration of ceramics [170, 171]. Shin and Exarhos [170] have prepared porous Titania by using a template process with cellulose nanocrystals. A colloid suspension of cellulose nanocrystals was added into titanium (IV) bis(ammonium lactate)dihydroxide (Tyzor-LA) to form a Tyzor-LA-cellulose nanocrystals composite. After calcination at 500 °C in air, a porous structure was obtained.

2.7 Conclusions

In this chapter we have reviewed some of the most important characteristics of cellulose and cellulose based blends, composites and nanocomposites. The intrinsic properties of cellulose such as its remarkable mechanical properties have promoted its use as a reinforcement material for different composites. It has been showed that cellulose is a material with a defined hierarchy that tends to form fibrillar elements such as elementary fibrils, micro fibrils, and macro fibers. Physical and chemical processes allow us to obtain different scale cellulose reinforcements. Macro fibers, such as lignocellulosic fibers of sisal, jute, cabuya, etc. are used for the production of composites, whereas nano-sized fibers, such as whiskers or bacterial cellulose fibers are used to produce nanocomposites. Given that cellulose can be used to obtain macro- and nano-reinforcements, it can be used as raw material for the production of several composites and nanocomposites with many different applications. The understanding of the characteristics and properties of cellulose is important for the development of novel composites and nanocomposites with new applications.

References

1. Imai, M., Ikari, K., Suzuki, I.: High-performance hydrolysis of cellulose using mixed cellulose species and ultrasonication pretreatment. Biochem. Eng. J. **17**, 19–23 (2003)
2. Jarvis, M.: Cellulose stacks up. Nature **426**, 611–612 (2003)
3. Holtzapple, M.T.: Cellulose. In: Macrae, R., Robinson, R.K., Saddler, M.J. (eds.) Encyclopedia of food science food technology and nutrition. London Academic Press, UK (1993)
4. Klemm, D., Philipp, B., Heinze, T., Heinze, U., Wagenknecht, W.: Comprehensive Cellulose Chemistry, Fundamentals and Analytical Methods, vol. 1. Wiley-VCH, Germany (1998)
5. Dufresne, A.: Polysaccharide nanocrystals reinforced nanocomposites. Can. J. Chem. **86**, 484–494 (2008)
6. Wang, W., Cai, Z., Yu, J.: Study on the chemical modification process of jute fiber. J. Eng. Fibers Fabr. **3**, 1–11 (2008)
7. Krässig, H.A.: Cellulose: Structure, Accessibility, and Reactivity. Gordon and Breach Science Publishers, Switzerland (1993)
8. Matthysse, A.G., Deschet, K., Williams, M., Marry, M., White, A.R., Smith, W.C.: A functional cellulose synthase from ascidian epidermis. Proc. Natl. Acad. Sci. **101**, 986–991 (2004)
9. Jonas, R., Farah, L.F.: Production and application of microbial cellulose. Polym. Degrad. Stab. **59**, 101–106 (1998)
10. Iguchi, M., Yamanaka, S., Budhiono, A.: Review bacterial cellulose: a masterpiece of nature's arts. J. Mater. Sci. **35**, 261–270 (2000)
11. Sreeramulu, G., Zhu, Y., Knol, W.: Kombucha fermentation and its antimicrobial activity. J. Agric. Food Chem. **48**, 2589–2594 (2000)
12. Grande, C.J., Torres, F.G., Gomez, C.M., Troncoso, O.P., Canet-Ferrer, J., Martínez-Pastor, J.: Morphological characterisation of bacterial cellulose-starch nanocomposites. Polym. Polym. Compos. **16**, 181–185 (2008)
13. Torres, F.G., Troncoso, O.P., Lopez, D., Grande, C., Gomez, C.M.: Reversible stress softening and stress recovery of cellulose networks. Soft Matter **5**, 4185–4190 (2009)
14. Torres, F.G., Grande, C.J., Troncoso, O.P., Gomez, C.M., Lopez, D.: Bacterial cellulose nanocomposites for biomedical applications. In: Kumar, S.A., Thiagarajan, S., Wang, F. (eds.) Biocompatible Nanomaterials: Synthesis Characterization and Application in Analytical Chemistry. Nova Science Publishers, USA (2010)
15. Ring, D.F., Nashed, W., Dow, T.: Liquid loaded pad for medical applications. US patent **4**(588), 400 (1986)
16. Purves, C.B.: Chemical nature of cellulose and its derivatives. In: Ott, E., Spurlin, H.M. (eds.) Cellulose and Cellulose Derivatives: Part 1. Wiley-Interscience, USA (1954)
17. Marchessault, R.H., Sundararajan, P.R.: Cellulose. In: Aspinall, G. (ed.) The Polysaccharides. Academic Press, USA (1983)
18. Kontturi, E.J.: Surface Chemistry of Cellulose: From Natural Fibres to Model Surfaces. Technische Universiteit Eindhoven, Germany (2005)
19. Krässig, H.: Cellulose, Polymer Monographs Volume 11. Gordon and Breach Science Publishers, Amsterdam (1996)
20. Klemm, D., Heublein, B., Fink, H.-P., Bohn, A.: Cellulose: fascinating biopolymer and sustainable raw material. Angew. Chem. Int. **44**, 3358–3393 (2005)
21. Liang, C.Y., Marchessault, R.H.: Infrared spectra of crystalline polyssacharides II. Native celluloses in the region from 640 to 1700 cm-1. J. Polym. Sci. **39**, 269–278 (1959)
22. Blackwell, J., Kolpak, F.J., Gardner, K.H.: Structures of native and regenerated celluloses. ACS Symp. Ser. **48**, 42–55 (1977)
23. Nishikawa, S., Ono, S.: Transmission of X-rays through fibrous, lamellar and granular substances. Proc. Tokyo Math. Phys. Soc. **7**, 131–138 (1913)

24. Cousins, S.K., Brown Jr, R.M.: Cellulose I microfibril assembly: computational molecular mechanics energy analysis favours bonding by Van de Waals forces as the initial step in crystallization. Polymer **36**, 3885–3888 (1995)
25. Cousins, S.K., Brown Jr, R.M.: X-ray diffraction and ultrastructural analyses of dye-altered celluloses support van der Waals forces as the initial step in cellulose crystallization. Polymer **38**, 897–902 (1997)
26. O'Sullivan, A.C.: Cellulose: the structure slowly unravels. Cellulose **4**, 173–207 (1997)
27. Klemm, D., Schumann, D., Kramer, F., Hebler, N., Hornung, M., Schumauder, H.P., Marsch, S.: Nanocelluloses as innovative polymers in research application. In: Klemm, D. (ed.) Polysaccharides II. Wiley-VCH, Weinheim (2002)
28. Sugiyama, J., Persson, J., Chanzy, H.: Combined IR and electron diffraction study of the polymorphism of native cellulose. Macromolecules **24**, 2461–2466 (1991)
29. Gardner, K.H., Blackwell, J.: The structure of native cellulose. Biopolymers **13**, 1975–2001 (1974)
30. Roberts, E., Saxena, I.M., Brown, Jr.R.M. Does cellulose II occur in nature?. In: Bailey, G.W. (ed.) Proceedings of the 47th Annual Meeting of the Electron Microscopy, Society of America (1989b)
31. Marrinan, H.J., Mann, J.: Infrared spectra of the crystalline modifications of cellulose. J. Polym. Sci. **21**, 301–311 (1956)
32. Hayashi, J., Sufoka, A., Ohkita, J., Watanabe, S.: The conformation of existence of cellulose IIII, IIIII, IVI and IVII by X-ray method. J. Polym. Sci. Polym. Lett. **13**, 23–27 (1975)
33. Davis, W.E., Barry, A.J., Peterson, F.C., King, A.J.: X-ray studies of reactions of cellulose in non-aqueous systems. II. Interaction of cellulose and primary amines. J. Am. Chem. Soc. **65**, 1294–1300 (1943)
34. Sarko, A., Southwick, J., Hayashi, J.: Packing analysis of carbohydrates and polysaccharides 7. Crystal structure of cellulose IIII and its relationship to other cellulose polymorphs. Macromolecules **9**, 857–863 (1976)
35. Sarko, A.: Cellulose: how much do we know about its structure. In: Kennedy, J.F. (ed.) Wood and Cellulosics: Industrial Utilization, Biotechnology, Structure and Properties. Ellis Horwood, UK (1987)
36. Hess, K., Kissig, H.: Zur Kenntnis der Hochtemperatur-Modifikation der Cellulose (Cellulose IV). Z. Phys. Chem. B **49**, 235–239 (1941)
37. Gardiner, E.S., Sarko, A.: Packing analysis of carbohydrates and polysaccharides. 16. The crystal structures of celluloses IVI and IVII. Can. J. Chem. **63**, 173–180 (1985)
38. Habibi, Y., Lucia, L.A., Rojas, O.J.: Cellulose nanocrystals: chemistry, self-assembly, and applications. Chem. Rev. **110**, 3479–3500 (2010)
39. Fink, H.-P., Philipp, B., Zschunke, C., Hayn, M.: Structural changes of LOPD cellulose in the original and mercerized state during enzymatic hydrolysis. Acta Polym. **43**, 270–274 (1992)
40. Cannon, R.E., Anderson, S.M.: Biogenesis of bacterial cellulose. Crit. Rev. Microbiol. **17**, 435–447 (1991)
41. Sakurada, I., Nukushina, Y., Ito, T.: Experimental determination of elastic modulus of crystalline regions in oriented polymers. J. Polym. Sci. **57**, 651–660 (1962)
42. Battista, O.A.: Hydrolysis and crystallization of cellulose. Ind. Eng. Chem. **42**, 502–507 (1950)
43. Battista, O.A., Coppick, S., Howsmon, J.A., Morehead, F.F., Sisson, W.A.: Level-off degree of polymerization. Ind. Eng. Chem. **48**, 333–335 (1956)
44. Revol, J.F., Bradford, H., Giasson, J., Marchessault, R.H., Gray, D.G.: Helicoidal self-ordering of cellulose microfibrils in aqueous solution. Int. J. Biol. Macromol. **14**, 170–172 (1992)
45. Araki, J., Wada, M., Kuga, S., Okano, T.: Flow properties of microcrystalline cellulose suspension prepared by acid treatment of native cellulose. Colloids Surf. **142**, 75–82 (1998)
46. de Rodriguez, N.L.G., Thielemans, W., Dufresne, A.: Sisal cellulose whiskers reinforced polyvinyl acetate nanocomposites. Cellulose **13**, 261–270 (2006)

47. Whistler, R.L., BeMiller, J.M.: Carbohydrate chemistry for food scientists. American Association of Cereal Chemists, St Paul (1997)
48. El-Sakhawy, M., Hassan, M.: Physical and mechanical properties of microcrystalline cellulose prepared from local agricultural residues. Carbohydr. Polym. **67**, 1–10 (2007)
49. Helbert, W., Cavaillé, J.-Y., Dufresne, A.: Thermoplastic nanocomposites filled with wheat straw cellulose whiskers. Part I: Processing and mechanical behavior. Polym. Compos. **17**, 604–611 (1996)
50. Bondeson, D., Mathew, A., Oksman, K.: Optimization of the isolation of nanocrystals from microcrystalline cellulose by acid hydrolysis. Cellulose **13**, 171–180 (2006)
51. Stromme, M., Mihranyan, A., Ek, R.: What to do with all these algae? Mater. Lett. **57**, 569–572 (2002)
52. Dufresne, A., Cavaillé, J.-Y., Vignon, M.R.: Mechanical behavior of sheet prepared from sugar beet cellulose microfibrils. J. Appl. Polym. Sci. **64**, 1185–1894 (1997)
53. Gopalan, N.K., Dufresne, A., Gandini, A., Belgacem, M.N.: Crab shell chitin whisker reinforced natural rubber nanocomposites. 3. Effect of chemical modification of chitin whiskers. Biomacromolecules **4**, 1835–1842 (2003)
54. Dufresne, A., Vignon, M.R.: Improvement of starch film performances using cellulose microfibrils. Macromolecules **31**, 2693–2696 (1998)
55. Dufresne, A., Dupeyre, D., Vignon, M.R.: Cellulose microfibrils from potato tuber cells: processing and characterization of starch-cellulose microfibril composites. J. Appl. Polym. Sci. **76**, 2080–2092 (2000)
56. Heux, L., Chauve, G., Bonini, C.: Nonocculating and chiral-nematic self-ordering of cellulose microcrystals suspensions in nonpolar solvents. Langmuir **16**, 8210–8212 (2000)
57. Favier, V., Dendievel, R., Canova, G., Cavaille, J.-Y., Gilormini, P.: Simulation and modeling of threedimensional percolating structures: case of a latex matrix reinforced by a network of cellulose fibers. Acta Mater. **45**, 1557–1565 (1997)
58. Anglès, M.N., Dufresne, A.: Plasticized starch/tunicin whiskers nanocomposites : 2. mechanical behavior. Macromolecules **34**, 2921–2931 (2001)
59. Ruiz, M.M., Cavaille, J.Y., Dufresne, A., Gerard, J.F., Graillat, C.: Processing and characterization of new thermoset nanocomposites based on cellulose whiskers. Compos. Interfaces **7**, 117–131 (2000)
60. Sharples, A.: The hydrolysis of cellulose and its relation to structure, part 2. Trans. Faraday Soc. **54**, 913–917 (1958)
61. Yachi, T., Hayashi, J., Takai, M., Shimizu, Y.J.: Supermolecular structure of cellulose: stepwise decrease in LODP and particle size of cellulose hydrolyzed after chemical treatment. Appl. Polym. Sci.: Appl. Polym. Symp. **37**, 325–343 (1983)
62. Hakansson, H., Ahlgren, P.: Acid hydrolysis of some industrial pulps, effect of hydrolysis conditions and raw material. Cellulose **12**, 177–183 (2005)
63. Schurz, J., John, K.: Long periods in native and regenerated celluloses. Cellul. Chem. Technol. **9**, 493–501 (1975)
64. Nishiyama, Y., Kim, U.J., Kim, D.Y., Katsumata, K.S., May, R.P., Langan, P.: Periodic disorder along ramie cellulose microfibrils. Biomacromolecules **4**, 1013–1017 (2003)
65. Elazzouzi-Hafraoui, S., Nishiyama, Y., Putaux, J.L., Heux, L., Dubreuil, F., Rochas, C.: The shape and size distribution of crystalline nanoparticles prepared by acid hydrolysis of native cellulose. Biomacromolecules **9**, 57–65 (2008)
66. Bai, W., Holbery, J., Li, K.: A technique for production of nanocrystalline cellulose with a narrow size distribution. Cellulose **16**, 455–465 (2009)
67. de Souza Lima, M.M., Borsali, R.: Static and dynamic light scattering from polyelectrolyte microcrystal cellulose. Langmuir **18**, 992–996 (2002)
68. Okano, T., Kuga, S., Wada, M., Araki, J., Ikuina, J.: Nisshin Oil Mills Ltd., Japan. JP Patent 98/151052 (1999)
69. Filpponen, I. Ph.D. Thesis, North Carolina State University; Raleigh, NC (2009)
70. Wang, N., Ding, E., Cheng, R.: Preparation and liquid crystalline properties of spherical cellulose nanocrystals. Langmuir **24**, 5 (2008)

71. Wang, N., Ding, E., Cheng, R.: Thermal degradation behaviors of spherical cellulose nanocrystals with sulfate groups. Polymer **48**, 3486–3493 (2007)
72. Dong, X.M., Revol, J.F., Gray, D.G.: Effect of microcrystallite preparation conditions on the formation of colloid crystals of cellulose. Cellulose **5**, 19–32 (1998)
73. Beck-Candanedo, S., Roman, M., Gray, D.G.: Effect of reaction conditions on the properties and behavior of wood cellulose nanocrystal suspensions. Biomacromolecules **6**, 1048–1054 (2005)
74. Bondeson, D., Kvien, I., Oksman, K.: Strategies for preparation of cellulose whiskers from microcrystalline cellulose as reinforcement in nanocomposites. In: Oksman, K., Sain, M. (eds.) Cellulose Nanocomposites: Processing, Characterization, and Properties; ACS Symposium Series 938. American Chemical Society, Washington (2006)
75. Samir, M.A.S., Alloin, F., Dufresne, A.: Review of recent research into cellulosic whiskers, their properties and their application in nanocomposite field. Biomacromolecules **6**, 612–626 (2005)
76. de Souza Lima, M.M., Wong, J.T., Paillet, M., Borsali, R., Pecora, R.: Translational and rotational dynamics of rodlike cellulose whiskers. Langmuir **19**, 24–29 (2003)
77. Terech, P., Chazeau, L., Cavaille, J.-Y.: A small-angle scattering study of cellulose whiskers in aqueous suspensions. Macromolecules **32**, 1872–1875 (1999)
78. Kvien, I., Tanem, B.S., Oksman, K.: Characterization of cellulose whiskers and its nanocomposites by atomic force and electron microscopy. Biomacromolecules **6**, 3160–3165 (2005)
79. Hanley, S.J., Giasson, J., Revol, J.F., Gray, D.G.: Atomic force microscopy of cellulose microfibrils: comparison with transmission electron microscopy. Polymer **33**, 4639–4642 (1992)
80. Miller, A.F., Donald, A.M.: Imaging of anisotropic cellulose suspensions using environmental scanning electron microscopy. Biomacromolecules **4**, 510–517 (2003)
81. Kamel, S.: Nanotechnology and its applications in lignocellulosic composites, a mini review; eXPRESS. Polym. Lett. **1**, 546–575 (2007)
82. Lahiji, R.R., Reifenberger, R., Raman, A., Rudie, A., Moon, R.J. Characterization of cellulose nanocrystal surfaces by SPM; Technical Proceedings of the 2008 NSTI Nanotechnology Conference and Trade Show; Boston, Massachusetts (2008)
83. Tashiro, K., Kobayashi, M.: Theoretical evaluation of three dimensional elastic constants of native and regenerated celluloses: role of hydrogen bonds. Polymer **32**, 1516–1526 (1991)
84. Sturcova, A., Davies, G.R., Eichhorn, S.J.: Elastic modulus and stress-transfer properties of tunicate cellulose whiskers. Biomacromolecules **6**, 1055 (2005)
85. Rusli, R., Eichhorn, S.J.: Determination of the stiffness of cellulose nanowhiskers and the fibre-matrix interface in a nanocomposite using Raman spectroscopy. Appl. Phys. Lett. **93**, 033111 (2008)
86. Mayer, J.M., Elion, G.R., Buchanan, C.M., Sullivan, B.K., Pratt, S.D., Kaplan, D.L.: Biodegradable blends of cellulose acetate and starch: production and properties. J. Macromol. Sci. Part A **32**, 775–785 (1995)
87. Freddi, G., Romano, M., Masafra, M.R., Tsukada, M.: Silk fibroin/cellulose blend films: preparation, structure, and physical properties. J. Appl. Polym. Sci. **56**, 1537–1545 (1995)
88. Torres, F.G., Diaz, R.M.: Morphological characterisation of natural fibre reinforced thermoplastics (NFRTP) processed by extrusion, compression and rotational moulding. Polym. Polym. Compos. **12**, 705–719 (2004)
89. Torres, F.G., Flores, R., Dienstmaier, J.F., Quintana, O.A.: Transport and flame properties of natural fibre reinforced polymers. Polym. Polym. Compos. **13**, 753–764 (2005)
90. Torres, F.G., Arroyo, O.H., Gomez, C.: Processing and mechanical properties of natural fiber reinforced thermoplastic starch biocomposites. J. thermoplast. compos. mater. **20**, 207–223 (2007)
91. Torres, F.G., Aragon, C.L.: Final product testing of rotational moulded natural fibre-reinforced polyethylene. Polym. Testing **25**, 568–577 (2006)

92. Torres, F.G., Arroyo, O.H., Grande, C., Esparza, E.: Bio- and photo-degradation of natural fibre reinforced starch: based biocomposite. Int. J. Polym. Mater. **55**, 1115–1132 (2006)
93. Grande, C., Torres, F.G.: Investigation of fiber organization and damage during single screw extrusion of natural fiber reinforced thermoplastics. Adv. Polym. Technol. **24**, 145–156 (2005)
94. Kuruvilla, J., Sabu, T.I., Pavithran, C.: Dynamic mechanical properties of short sisal fiber reinforced low density polyethylene composites. J. Reinf. Plàst. Compos. **12**, 139–154 (1993)
95. Herrera-Franco, P.J., Aguilar-Vega, M.J.: Effect of fiber treatment on mechanical properties of LDPE-henequen cellulosic fiber composites. J. Appl. Polym. Sci. **65**, 197–207 (1997)
96. Youngquist, J.A.: Unlikely partners ? the marriage of wood and nonwood materials. For. Prod. J. **45**, 25–30 (1995)
97. Sanadi, A.R., Caulfield, D.F., Rowell, R.M.: Reinforcing polypropylene with natural fibers. Plast. Eng. **4**, 27–30 (1994)
98. Rowell, R.M.: Recent Advances in Lignocellulosic-Derived Composites. In: Chun, H.L (ed.) Polymers from Biobased Materials; Noyes Data Corp., New Jersey (1991)
99. Torres, F.G., Cubillas, M.L.: Study of the interfacial properties of natural fibre reinforced polyethylene. Polym. Testing **24**, 694–698 (2005)
100. Sanadi, A.R., Caulfield, D.F., Jacobson, R.E., Rowell, R.M.: Renewable agricultural fibers as reinforcing fillers in plastics: mechanical properties of Kenaf fiber: polypropylene composites. Ind. Eng. Chem. Res. **34**, 1889–1896 (1995)
101. Gómez, C., Torres, F.G., Nakamatsu, J., Arroyo, O.H.: Thermal and structural analysis of natural fibre reinforced starch based biocomposites. Int. J. Polym. Mater. **55**, 893–907 (2006)
102. Chazeau, L., Cavaille, J.Y., Canova, G., Dendievel, R., Boutherin, B.: Viscoelastic properties of plasticized PVC reinforced with cellulose whiskers. J. Appl. Polym. Sci. **71**, 1797–1808 (1999)
103. Matos-Ruiz, M., Cavaille′, J.-Y., Dufresne, A., Graillat, C., Gerard, J.-F.: New waterborne epoxy coatings based on cellulose nanofillers. Macromol. Symp. **169**, 211–222 (2001)
104. Cao, X., Habibi, Y., Lucia, L.A.J.: One-pot polymerization, surface grafting, and processing of waterborne polyurethane-cellulose nanocrystal nanocomposites. J. Mater. Chem. **19**, 7137–7145 (2009)
105. Marcovich, N.E., Auad, M.L., Bellesi, N.E., Nutt, S.R., Aranguren, M.I.: Cellulose micro/nanocrystals reinforced polyurethanes. J. Mater. Res. **21**, 870–881 (2006)
106. Favier, F., Chanzy, H., Cavaille, J.-Y.: Polymer nanocomposites reinforced by cellulose whiskers. Macromolecules **28**, 6365–6367 (1995)
107. Cavaille, J.-Y., Dufresne, A., Paillet, M., Azizi Samir, M.A.S., Alloin, F., Sanchez, J.Y.: French Patent FR2841255, (1999)
108. Grunnert, M., Winter, W.T.: Progress in the development of cellulose reinforced nanocomposites. Polym. Mater. Sci. Eng. **82**, 232–233 (2000)
109. Noorani, S., Simonsen, J., Atre, S.: Polysulfone-Cellulose Nanocomposites. In: Oksman, K., Sain, M. (eds.) Cellulose Nanocomposites, Processing, Characterization and Properties, ACS Symposium Series 938, American Chemical Society, Washington (2006)
110. Grunert, M., Winter, W.T.: Nanocomposites of cellulose acetate butyrate reinforced with cellulose nanocrystals. J. Polym. Env. **10**, 27–30 (2002)
111. Petersson, L., Mathew, A.P., Oksman, K.J.: Dispersion and properties of cellulose nanowhiskers and layered silicates in cellulose acetate butyrate nanocomposites. Appl. Polym. Sci. **112**, 2001–2009 (2009)
112. Habibi, Y., Goffin, A.-L., Schiltz, N., Duquesne, E., Dubois, P., Dufresne, : Bionanocomposites based on poly(e-caprolactone)-grafted cellulose nanocrystals by ring-opening polymerizationA. J. Mater. Chem. **18**, 5002–5010 (2008)
113. Paralikar, S.A., Simonsen, J., Lombardi, J.: Poly(vinyl alcohol)/cellulose nanocrystals barrier membranas. J. Membr. Sci. **320**, 248–258 (2008)
114. Roohani, M., Habibi, Y., Belgacem, N.M., Ebrahim, G., Karimi, A.N., Dufresne, A.: Cellulose whiskers reinforced polyvinyl alcohol copolymers nanocomposites. Eur. Polym. J. **44**, 2489–2498 (2008)

115. Wang, Y., Cao, X., Zhang, L.: Effects of cellulose whiskers on properties of soy protein thermoplastics. Macromol. Biosci. **6**, 524–531 (2006)
116. Li, Q., Zhou, J., Zhang, L.: Structure and properties of the nanocomposite films of chitosan reinforced with cellulose whiskers. J. Polym. Sci., Part B: Polym. Phys. **47**, 1069–1077 (2009)
117. Qi, H., Cai, J., Zhang, L., Kuga, S.: Properties of films composed of cellulose nanowhiskers and a cellulose matrix regenerated from alkali/urea solution. Biomacromolecules **10**, 1597–1602 (2009)
118. Noshiki, Y., Nishiyama, Y., Wada, M., Kuga, S., Magoshi, J.: Mechanical properties of silk fibroin-microcrystalline cellulose composite films. J. Appl. Polym. Sci. **86**, 3425–3429 (2002)
119. Dufresne, A.: Dynamic mechanical analysis of the interphase in bacterial polyester/cellulose whiskers natural composites. Compos. Interfaces **7**, 53–67 (2000)
120. Siqueira, G., Bras, J., Dufresne, A.: Cellulose whiskers versus microfibrils: influence of the nature of the nanoparticle and its surface functionalization on the thermal and mechanical properties of nanocomposites. Biomacromolecules **10**, 425–432 (2009)
121. Flandin, L., Bidan, G., Brechet, Y., Cavaille, J.Y.: New nanocomposite materials made of an insulating matrix and conducting fillers: processing and properties. Polym. Compos. **21**, 165–174 (2000)
122. Gea, S., Torres, F.G., Troncoso, O.P., Reynolds, C.T., Vilasecca, F., Iguchi, M., Peijs, T.: Biocomposites based on bacterial cellulose and apple and radish pulp. Int. Polym. Proc. **5**, 497–501 (2007)
123. Nishino, T., Matsuda, I., Hirao, K.: All-cellulose composite. Macromolecules **37**, 7683–7687 (2004)
124. Gindl, W., Keckes, J.: All-cellulose nanocomposites. Polymer **46**, 10221–10225 (2005)
125. Capadona, J.R., van den Berg, O., Capadona, L.A., Schroeter, M., Rowan, S.J., Tyler, D.J., Weder, C.: A versatile approach for the processing of polymer nanocomposites with self-assembled nanofibre templates. Nat. Nanotechnol. **2**, 765–769 (2007)
126. Capadona, J.R., Shanmuganathan, K., Tyler, D.J., Rowan, S.J., Weder, C.: Stimuli-responsive polymer nanocomposites inspired by the sea cucumber dermis. Science **319**, 1370–1374 (2008)
127. Orts, W.J., Shey, J., Imam, S.H., Glenn, G.M., Guttman, M.E., Revol, J.F.: Application of cellulose microfibrils in polymer nanocomposites. J. Polym. Env. **13**, 301–306 (2005)
128. Peresin, M.S., Habibi, Y., Zoppe, J.O., Pawlak, J.J., Rojas, O.J.: Nanofiber composites of polyvinyl alcohol and cellulose nanocrystals: manufacture and characterization. Biomacromolecules **11**, 674–681 (2010)
129. Park, W., Kang, M., Kim, H.-S., Jin, H.-J.: Electrospinning of poly(ethylene oxide) with bacterial cellulose whiskers. Macromol. Symp. **240**(250), 289–294 (2007)
130. de Mesquita, J.P., Donnici, C.L., Pereira, F.V.: Biobased nanocomposites from layer-by-layer assembly of cellulose nanowhiskers with chitosan. Biomacromolecules **11**, 473–480 (2010)
131. Podsiadlo, P., Choi, S.Y., Shim, B., Lee, J., Cuddihy, M., Kotov, N.A.: Molecularly engineered nanocomposites: layer-by-layer assembly of cellulose nanocrystals. Biomacromolecules **6**, 2914–2918 (2005)
132. Cranston, E.D., Gray, D.G.: Formation of cellulose-based electrostatic layer-by-layer films in a magnetic field. Sci. Technol. Adv. Mater. **7**, 319–321 (2006)
133. Grande, C.J., Torres, F.G., Gomez, C.M., Troncoso, O.P., Canet-Ferrer, J., Martínez-Pastor, J.: Development of self-asembled Bacterial cellulose-starch nanocomposites. Mater. Sci. Eng. C **29**, 1098–1104 (2009)
134. Zimmermann, T., Pöhler, E., Geiger, T.: Cellulose fibrils for polymer reinforcement. Adv. Eng. Mater. **6**, 754–761 (2004)
135. Zimmermann, T., Pöhler, E., Schwaller, P.: Mechanical and morphological properties of cellulose fibril reinforced nanocomposites. Adv. Eng. Mater. **7**, 1156–1161 (2005)
136. Stauss, S., Schwaller, P., Bucaille, J.-L., Blank, E., Michler, J.: Determining the stress-strain behaviour of small devices by nanoindentation in combination with inverse methods. Microelectron. Eng. **67**, 818–825 (2003)

137. Favier, V., Canova, G.R., Cavaille, J.-Y., Chanzy, H., Dufresne, A., Gauthier, C.: Nanocomposites materials from latex and cellulose whiskers. Polym. Adv. Technol. **6**, 351–355 (1995)
138. Anglès, M.N., Dufresne, A.: Plasticized starch/tunicin whiskers nanocomposites: 1. Struct. anal. Macromol. **33**, 8344–8353 (2000)
139. Hajji, P., Cavaille, J.Y., Favier, V., Gauthier, C., Vigier, G.: Tensile behavior of nanocomposites from latex and cellulose whiskers. Polym. Compos. **17**, 612–619 (1996)
140. Mathew, A.P., Dufresne, A.: Morphological investigation of nanocomposites from sorbitol plasticized starch and tunicin whiskers. Biomacromolecules **3**, 609–617 (2002)
141. Chang, J.-H., Nam, S.W., Jang, S.-W.: Mechanical and morphological properties of lyocell blends: comparison with lyocell nanocomposites (I). J. Appl. Polym. Sci. **106**, 2970–2977 (2007)
142. Svensson, A., Nicklasson, E., Harrah, T., Panilaitis, B., Kaplan, D.L., Brittberg, M., Gatenholm, P.: Bacterial cellulose as a potential scaffold for tissue engineering of cartilage. Biomaterials **26**, 419–431 (2005)
143. Andersson, J., Stenhamre, H., Bäckdahl, H., Gatenholm, P.: Behavior of human chondrocytes in engineered porous bacterial cellulose scaffolds. J. Biomed. Mater. Res., Part A **94**, 1124–1132 (2010)
144. Czaja, W., Krystynowicza, A., Bielecki, S., Malcolm Brown Jr, R.: Microbial cellulose: the natural power to heal wounds. Biomaterials **27**, 145–151 (2006)
145. Czaja, W.K., Young, D.J., Kawecki, M., Brown Jr, R.M.: The future prospects of microbial cellulose in biomedical applications. Biomacromolecules **8**, 1–12 (2007)
146. Cienchanska, D.: Multifunctional bacterial cellulose/chitosan composite materials for medical applications. Fibres Text. Eastern Eur. **12**, 69–72 (2004)
147. Legeza, V.I., Galenko-Yaroshevskii, V.P., Zinovev, E.V., Paramonov, B.A., Kreichman, G.S., Turkovskii, I.I., Gumenyuk, E.S., Karnovich, A.G., Khripunov, A.K.: Effects of new wound dressings on healing of thermal burns of the skin in acute radiation disease. Bull. Exp. Biol. Med. **138**, 311–315 (2004)
148. Wan, W.K., Millon, L.E.: Poly(vinyl alcohol)-bacterial cellulose nanocomposite. U.S. Pat. Appl. Publ. US 2005037082 A1, 16 (2005)
149. Sokolnicki, A.M., Fisher, R.J., Harrah, T.P., Kaplan, D.L.: Permeability of bacterial cellulose membranes. J. Membr. Sci. **272**, 15–27 (2006)
150. Charpentier, P.A., Maguire, A., Wan, W.: Surface modification of polyester to produce a bacterial cellulose-based vascular prosthetic device. Appl. Surf. Sci. **252**, 6360–6367 (2006)
151. Klemm, D., Schumann, D., Udhardt, U., Marsch, S.: Bacterial synthesized cellulose: artificial blood vessels for microsurgery. Prog. Polym. Sci. **26**, 1561–1603 (2001)
152. Backdahl, H., Helenius, G., Bodin, A., Nannmark, U., Johansson, B.R., Risberg, B., Gatenholm, P.: Mechanical properties of bacterial cellulose and interactions with smooth muscle cells. Biomaterials **27**, 2141–2149 (2006)
153. Wan, W.K., Hutter, J.L., Millon, L., Guhados, G.: Bacterial cellulose and its nanocomposites for biomedical applications. ACS Symp. Ser. **938**, 221–241 (2006)
154. Grande, C.J., Torres, F.G., Gomez, C.M., Bañó, C.: Nanocomposites of bacterial cellulose/hydroxyapatite for biomedical applications. Acta Biomater. **5**, 1605–1615 (2009)
155. Samir, M.A.S., Alloin, F., Sanchez, J.-Y., Dufresne, A.: Cross-linked nanocomposite polymer electrolytes reinforced with cellulose whiskers. Macromolecules **37**, 4839–4844 (2004)
156. Nystrom, G., Razaq, A., Stromme, M., Nyholm, L., Mihranyan, A.: Ultrafast all-polymer paper-based batteries. Nano Lett. **9**, 3635–3639 (2009)
157. Razaq, A., Mihranyan, A., Welch, K., Nyholm, L., Strømme, M.: Influence of the type of oxidant on anion exchange properties of fibrous *Cladophora* cellulose/polypyrrole composites. J. Phys. Chem. B **113**, 426–433 (2009)
158. Gelin, K., Mihranyan, A., Razaq, A., Nyholm, L., Strømme, M.: Potential controlled anion absorption in a novel high surface area composite of *Cladophora* cellulose and polypyrrole. Electrochim. Acta **54**, 3394–3401 (2009)

159. Stromme, M., Frenning, G., Razaq, A., Gelin, K., Nyholm, L., Mihranyan, A.: Ionic motion in polypyrrole—cellulose composites: trap release mechanism during potentiostatic reduction. J. Phys. Chem. B **113**, 4582–4589 (2009)
160. Iwamoto, S., Nakagaito, A.N., Yano, H., Nogi, M.: Optically transparent composites reinforced with plant fiber-based nanofibers. Appl. Phys. A Mater. Sci. Process. **81**, 1109–1112 (2005)
161. Ifuku, S., Nogi, M., Abe, K., Handa, K., Nakatsubo, F., Yano, H.: Surface modification of bacterial cellulose nanofibers for property enhancement of optically transparent composites: dependence on acetyl-group DS. Biomacromolecules **8**, 1973–1978 (2007)
162. Yano, H., Sugiyama, J., Nakagaito, A.N., Nogi, M., Matsuura, T., Hikita, M., Handa, K.: Optically transparent composites reinforced with networks of bacterial nanofibers. Adv. Mater. **17**, 153–155 (2005)
163. Podsiadlo, P., Sui, L., Elkasabi, Y., Burgardt, P., Lee, J., Miryala, A., Kusumaatmaja, W., Carman, M., Shtein, M., Kieffer, J., Lahann, J., Kotov, N.: Layer-by-layer assembled films of cellulose nanowires with antireflective properties. Langmuir **23**, 7901–7906 (2007)
164. Legnani, C., Vilani, C., Calil, V.L., Barud, H.S., Quirino, W.G., Achete, C.A., Ribeiro, S.J.L., Cremona, M.: Bacterial cellulose membrane as flexible substrate for organic light emitting devices. Thin Solid Films **517**, 1016–1020 (2008)
165. Svagan, A.J., Samir, M.A.S.A., Berglund, L.A.: Biomimetic foams of high mechanical performance based on nanostructured cell walls reinforced by native cellulose nanofibrils. Adv. Mater. **20**, 1263–1269 (2008)
166. van den Berg, O., Schroeter, M., Capadona, J.R., Weder, C.: Nanocomposites based on cellulose whiskers and (semi)conducting conjugated polymers. J. Mater. Chem. **17**, 2746–2753 (2007)
167. Agarwal, M., Lvov, Y., Varahramyan, K.: Conductive wood microfibres for smart paper through layer-by-layer nanocoating. Nanotechnology **17**, 5319–5325 (2006)
168. Henriksson, M., Berglund, L.A., Isaksson, P., Lindstrom, T., Nishino, T.: Cellulose nanopaper structures of high toughness. Biomacromolecules **9**, 1579–1585 (2008)
169. Sehaqui, H., Liu, H., Zhou, Q., Berglund, L.A.: Fast preparation procedure for large, flat cellulose and cellulose/inorganic nanopaper structures. Biomacromolecules **11**, 2195–2198 (2010)
170. Shin, Y., Exarhos, G.J.: Template synthesis of porous Titania using cellulose nanocrystals. Mater. Lett. **61**, 2594–2597 (2007)
171. Dujardin, E., Blaseby, M., Mann, S.: Synthesis of *Mesoporous silica* by sol–gel mineralisation of cellulose nanorod nematic suspensions. J. Mater. Chem. **13**, 696–699 (2003)
172. Araki, J., Kuga, S.: Effect of trace electrolyte on liquid crystal type of cellulose microcrystals. Langmuir **17**, 4493–4496 (2001)
173. Roman, M., Winter, W.T.: Effect of sulfate groups from sulfuric acid hydrolysis on the thermal degradation behavior of bacterial cellulose. Biomacromolecules **5**, 1671–1677 (2004)
174. Araki, J., Wada, M., Kuga, S.: Steric stabilization of a cellulose microcrystal suspension by poly(ethylene glycol) grafting. Langmuir **17**, 21–27 (2001)
175. Dong, X.M., Kimura, T., Revol, J.-F., Gray, D.G.: Effects of ionic strength on the isotropic—chiral nematic phase transition of suspensions of cellulose crystallites. Langmuir **12**, 2076–2082 (1996)
176. de Menezes, A.J., Siqueira, G., Curvelo, A., Dufresne, A.: Extrusion and characterization of functionalized cellulose whiskers reinforced polyethylene nanocomposites. Polymer **50**, 4552–4563 (2009)
177. Garcia de Rodriguez, N.L., Thielemans, W., Dufresne, A.: Sisal cellulose whiskers reinforced polyvinyl acetate nanocomposites. Cellulose **13**, 261–270 (2006)
178. Revol, J.F.: On the cross-sectional shape of cellulose crystallites in *Valonia ventricosa*. Carbohydr. Polym. **2**, 123–134 (1982)

179. Araki, J., Wada, M., Kuga, S., Okano, T.: Influence of surface charge on viscosity behavior of cellulose microcrystal suspension. J. Wood Sci. **45**, 258–261 (1999)
180. Capadona, J.R., Shanmuganathan, K., Trittschuh, S., Seidel, S., Rowan, S.J., Weder, C.: Polymer nanocomposites with nanowhiskers isolated from microcrystalline cellulose. Biomacromolecules **10**, 712–716 (2009)

Chapter 3
Chitin and Chitosan Based Blends, Composites and Nanocomposites

Mohammad Zuber, Khalid Mahmood Zia and Mehdi Barikani

Abstract Nature is gifted with several nanomaterials which could be obtained from different animal and plant sources. Cellulose, chitin and starch are abundant, natural, renewable and biodegradable polymers. By intelligent processing techniques they could be used as classical nano reinforcing fillers in polymers i.e., composites. They are often called whiskers.

3.1 Introduction

Nature is gifted with several nanomaterials which could be obtained from different animal and plant sources. Cellulose, chitin and starch are abundant, natural, renewable and biodegradable polymers. By intelligent processing techniques they could be used as classical nano reinforcing fillers in polymers i.e., composites. They are often called whiskers. These whiskers are almost defect free and as a result, their properties are comparable to perfect crystals. The excellent reinforcing properties of these natural whiskers stem from their chemical nature and hierarchical structure. During the past decade, many studies have been devoted to mimic biocomposites by blending natural whiskers from waste and biomass sources with various polymer matrices. The presence of crystalline fibrils in the chitinous integuments has been elucidated several decades ago [1–3]. This chapter intends to

M. Zuber (✉) · K. M. Zia
Department of Applied Chemistry, Government College University, Faisalabad 38000, Pakistan
e-mail: mohammadzuber@gmail.com

M. Barikani
Department of Polyurethane, Iran Polymer and Petrochemical Institute, Tehran, Iran

S. Thomas et al. (eds.), *Advances in Natural Polymers*,
Advanced Structured Materials 18, DOI: 10.1007/978-3-642-20940-6_3,

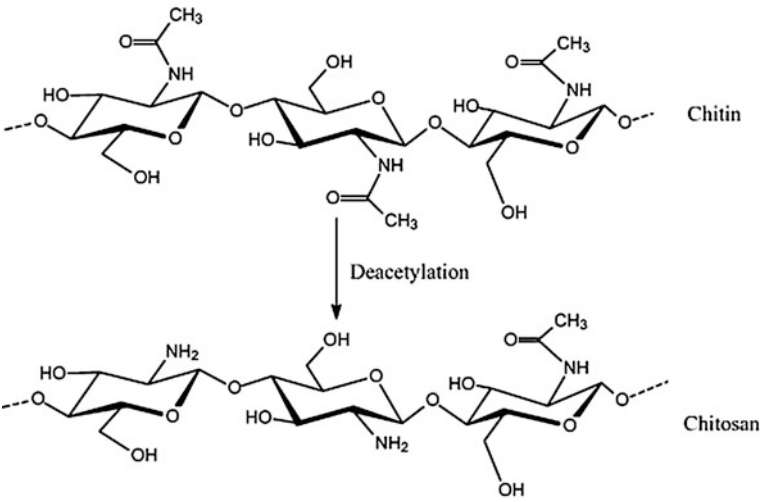

Fig. 3.1 Chemical structure of chitin and deacetylated chitin (chitosan)

focus on the chitin and chitosan based blends, composites and nanocomposites. During the last few years, however, some indications appeared in the literature about the preparation of composites made of chitin whiskers dispersed into natural and artificial polymers. It is believed that this subject represents at this time an opportunity for a better exploitation of chitin, as well as a challenge in view of certain technical difficulties.

Chitin is a naturally occurring polysaccharide and is recognized by consisting of 2-acetamido-2-deoxy- D-glucose via a β (1–4) linkage (Fig. 3.1). As the second most abundant biopolymer after cellulose, chitin occurs in enormous number of living organisms such as shrimps, crabs, tortoise, and insects, [4] and can also be synthesized by a nonbiosynthetic pathway through chitinase-catalyzed polymerization of a chitobiose oxazoline derivative [5–7]. Chitosan, as the most important derivative of chitin, can be prepared by its chemical modification. Chitin and chitosan have many excellent properties including biocompatibility, biodegradability, non-toxicity, absorption properties, etc., and thus they can be widely used in variety of areas such as biomedical applications, agriculture, water treatment and cosmetics. In addition, there is a reactive amino group on the structured units of chitosan (Fig. 3.1). The amino group makes chitosan much easier to be modified by chemical reactions than cellulose. A lot of derivatives of chitosan with different functional properties have been synthesized by chemical modifications. There are many reviews focusing on the properties, modifications and applications of chitin and chitosan [8–10]. This chapter focuses on the other aspects of chitin: chitin nanoparticles and their applications especially in reinforcing polymer nanocomposites. Polymer nanocomposites refer to multiphase materials consisting of a polymer matrix and nanofillers. They show distinctive properties even at minimum loading of nanofillers, due to the nanometric size effect, in comparison

with virgin polymer and conventional polymer composites [11]. Following the successful development of nylon-clay nanocomposites in 1985 [12], the polymer nanocomposites have attracted a great deal of interest from both academic and commercial point of view due to their appealing unique properties [13, 14]. Conventionally used nanofillers are inorganic compounds especially layered nanoclays, such as montmorillonite (MMT) and layered double hydroxides (LDH), with homogeneous dispersion in polymer matrix [15]. Renewable semi-crystalline polysaccharides like cellulose, chitin and starch consisting of crystalline domains and amorphous domains are possible candidates for organic nanofillers, since the amorphous domains can be removed under certain conditions such as acidolysis and the crystalline domains with high modulus can be isolated in nano-scale. Then the nano-sized crystalline particles, usually known as polysaccharide nanocrystals, can be used as reinforcing nanofillers in polymer nanocomposites. Since Favier et al. [16] reported the use of cellulose nanocrystals as reinforcing nanofillers in poly(styrene-co-butyl acrylate) (poly(S-co-BuA))-based nanocomposites in 1995, the polysaccharide nanocrystals have drawn a large interest in polymer nanocomposites due to their excellent intrinsic properties such as nano-sized dimensions, high surface area, biodegradability, non-toxicity, renewability, low density and easy modification conferred by the large amount of surface hydroxyl groups [17–20]. Some recent reviews have been reported on preparation, properties, modifications and applications of cellulose, starch and chitin nanocrystals [15, 17, 21–25].

3.2 Structure of Chitin

The structure of chitin is very analogous to cellulose (Fig. 3.2). They both are supporting materials for living bodies i.e., for both plants and animals, with sizes increasing from simple molecules and highly crystalline fibrils at the nanometer level to composites at the micron level upward [26]. Thus, they intrinsically have

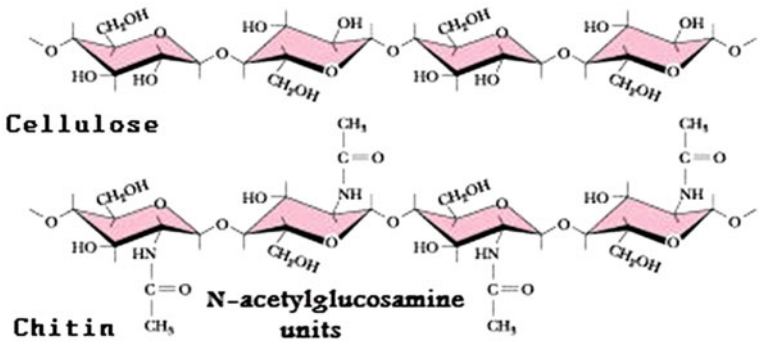

Fig. 3.2 Chemical structure of cellulose and chitin

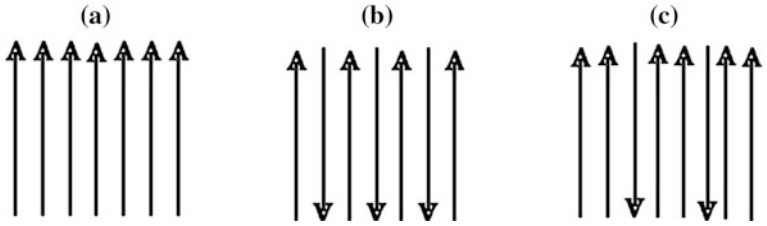

Fig. 3.3 Three polymorphic configuration of chitin **a** α–Chitin, **b** β–Chitin, **c** γ-Chitin

the potential to be converted to crystalline nanoparticles and nanofibers and to find applications in nanocomposite fields. Chitin whisker can be prepared from chitin isolated from chitin containing living organisms by the similar method towards preparation of cellulose whiskers through hydrolysis in aqueous solution of strong acids.

Marchessault et al. [27] for the first time reported a route for preparing suspension of chitin crystallite particles in 1959. In this method, purified chitin was first treated with 2.5 N hydrochloric acid solution under reflux for 1 h, the excess acid was decanted and then distilled water was added to obtain the suspension. They found that acid-hydrolyzed chitin spontaneously dispersed into rodlike particles that could be concentrated to a liquid crystalline phase and self-assemble to a cholesteric liquid crystalline phase above a certain concentration [28, 29]. The chitins are polysaccharides and are present within numerous taxonomic groups. However, on commercial scales chitins are usually isolated from marine crustaceans, mainly because a large amount of waste is available as a by-product of food processing. In this case, α-chitin is produced while squid pens are used to produce β-chitin. The structure of α-chitin has been investigated more extensively than that of either the β- or γ- form, because it is the most common polymorphic form. Very few studies have been carried out on γ- chitin. It has been suggested that γ- chitin may be a distorted version of either α- or β-chitin rather than a true third polymorphic form [30]. In α–chitin, the chains are arranged in sheets or stacks, the chains attaining the same direction or 'sense'. In α- chitin, adjacent sheets along the *c* axis have the same direction; the sheets are parallel, while in β-chitin adjacent sheets along the *c* axis have the opposite direction, as antiparallel arrangement. In γ- chitin, every third sheet has the opposite direction to the two preceding sheets [30]. A schematic representation of the three structures is shown in Fig. 3.3.

The underlying chitin matrix in the crab shell and its microfibrillar structure is shown in Fig. 3.4. This chitin is termed as α-chitin because of its crystal structure. Treatment of this chitin with 20 % NaOH for 1–3 h at 120 °C gives a 70 % deacetylated chitin (chitosan), which is soluble in many dilute acids. The detailed method is given in Sect. 3.4. The repetition of this step can give deacetylation

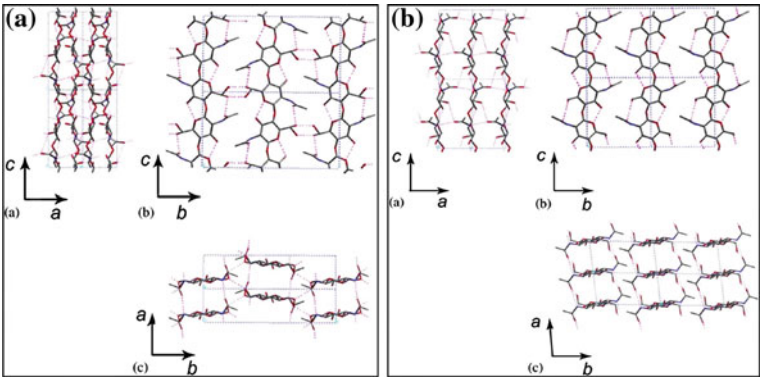

Fig. 3.4 Structures of α-chitin (**a**) and β-chitin (**b**) [215]

values up to 98 %. A more reactive form of chitin is obtained from squid pens [28, 29]. This β-chitin is easily isolated and has a looser chain packing in the crystal, accounting for its higher reactivity and solubility in formic acid. The isolation of β-chitin is accomplished by first washing the squid pens in 1 M HCl for 12 h, followed by a 12 h treatment with 2 *M* NaOH. The final step is to heat the pens at 100 °C for 4 h in fresh 2 *M* NaOH. This procedure yields 35 % chitin from the mass of the pens. The degree of acetylation may be up to 92 %.

It is worth mentioning that crustaceans protect themselves from predators and pathogens by secreting an acellular exoskeleton including calcite crystals within the fibrillar organic network. The organic matrix is made of four superimposed layers (Fig. 3.5a). The epicuticle (ep) and pigmented (pi) layers are deposited before moult; the principal (pr) and membranous (mb) layers are deposited after moult. The matrix, composed of chitin associated with proteins, is produced by an underlying monolayer of epidermal cells (Fig. 3.5b). In a lower ratio, the cells also secrete lipids mostly in the epicuticle and pigments in the pigmented layer. The enzymes, for example alkaline phosphatase and carbonic anhydrase, are also synthesized in relation with the control of calcification, which occurs in the two middle layers (pi and pr) [31]. Carbonic anhydrase producing carbonate ions shows maximum activity during the first stages of calcification just after the moult. The enzyme enhances the precipitation of calcium carbonate; it was shown that diamox, its inhibitor, depresses the growth rate of calcite crystals in the cuticle. In domains where the section plane is transverse to the fibril axis, a honeycomb pattern reveals the elementary chitin protein units (high resolution TEM). Ultrathin section of the principal layer of the chitin-protein fibrils are seen in longitudinal, oblique or transverse view forming well defined strands (Fig. 3.5c). The clear central rods, a few nanometres in diameter, correspond to chitin crystallites; the dark sheath corresponds to the binding proteins (Fig. 3.5d).

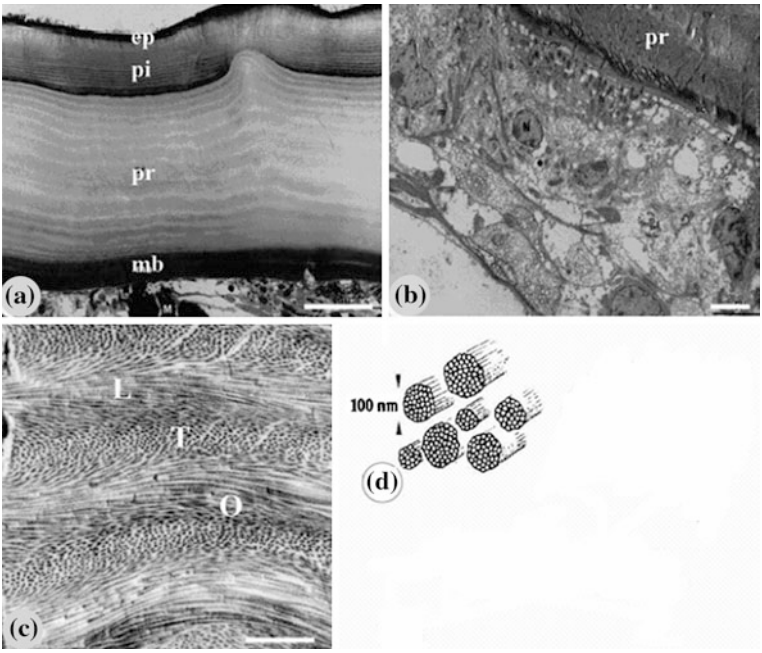

Fig. 3.5 The chitin-protein matrix of the crab cuticle. **a** Semi-thin section normal to the carapace, from top to bottom: epicuticle (*ep*), pigmented layer (*pi*), principal layer (*pr*), membranous layer (*mb*). Optical microscopy, bar = 50 μm. **b** Ultrathin section of the principal layer of the cuticle and the underlying epidermal cells. TEM, bar = 5 μm. **c** Ultrathin section of the principal layer, the chitin-protein fibrils are seen in longitudinal, oblique or transverse view forming well defined strands. TEM, bar = 1 μm. **d** Aspect of the chitin protein fibrils observed at high magnification in TEM; the central electron light chitin crystals are surrounded by a sheath of contrasted proteins [31]

3.3 Properties of Chitin Whiskers

Similar with preparation of cellulose nanocrystals, the main process for isolation of chitin nanocrystals is also based on acid hydrolysis [32]. Disordered and low lateral ordered regions of chitin are preferentially hydrolyzed and dissolved in the acid solution, whereas water-insoluble, highly crystalline residues that have a higher resistance to acid attack remain intact. Thus, following an acid hydrolysis that removes disordered and low lateral ordered crystalline defects, chitin rodlike whiskers are produced [16, 17]. Unlike tunicin whiskers which can only be prepared by hydrolysis in strong sulfuric acid (H_2SO_4) solutions [16, 33], chitin whiskers (CWs) can be prepared by hydrolysis in hydrochloric acid (HCl) solutions. Revol et al. [34] and Li et al. [35] reported an approach towards preparation of suspension of chitin crystallites through acid hydrolysis in detail. In this approach, the purified chitin was hydrolyzed by boiling solution of 3 N HCl for

Table 3.1 Sizes of chitin whiskers prepared from different origins

Chitin origin	Hydrolytic time (hr)	Chitin whisker size		References
		Length	Width (nm)	
Squid pen	1.5	150	10	[36]
Riftia tube	1.5	2200	18	[37]
	1.5	240	15	[39]
	1.5	500	50	[38]
	6	255	31	[53]
Shrimp shell	1.5	417	33	[41, 42]
	1.5	200–500	10–15	[43]
	3	200–560	18–40	[55]
	6	427	43	[202]
	6	549	31	[217]
	6	343	46	[44]

90 min; after acid hydrolysis, the suspensions were diluted with deionized water followed by centrifugation and Decantation of the supernatant; this process was repeated several times until the suspension spontaneously transformed into a colloidal state. The obtained crystallites were rodlike particles with average size of 200 ± 20 nm in length and 8 ± 1 nm in thickness. Because of the nanoscale size, the acicular crystal shaped can be called as nanocrystals or whiskers. Based on these procedures, whiskers have recently been prepared from many chitins of different origins such as squid pen chitin, [36] riftia tubes [37], crab shells [38–40], and shrimp shells [41–44]. The detailed information for CWs prepared from different origins of chitins is summarized in Table 3.1. The obtained rodlike whiskers showed similar size in width and were all in range of 10–50 nm irrespective of their origins and hydrolytic time. However, the lengths of the whiskers vary a lot in the range of 150–2200 nm for different origins of chitin, which may be ascribed to the different original sizes of the chitin particles and the diffusion controlled nature of the acid hydrolysis. The typical morphologies and sizes (average length and width) of dilute CW suspension observed by TEM and AFM are given in Figs. 3.6a and 3.6b [38, 39]. The suspension contains chitin fragments consisting of both individual microcrystals and associated or collapsed microcrystals. The length and width of the rodlike CW can be measured from the micrographs (Table 3.1) depending on the chitin origins. The principle towards preparation of polysaccharide nanocrystals is on the basis of the different hydrolytic kinetics between amorphous and crystalline domains [17]. That is to say, both the amorphous and the crystalline phases of polysaccharides can be hydrolyzed during treatment with aqueous solutions of strong acid. The swelling and hydrolysis of amorphous phases occur much faster than those of crystalline phases due to the regular tight arrangement of molecular chains in the crystalline domains. It is well established, documented and known that the boiling hydrochloric acid can easily dissolve the amorphous domains of chitin [45]; however, it can also break the ether and amide linkages of chitin [46]. So after removal of the amorphous domains,

the surface of crystallites will be attacked by the excess acid thus undergo further hydrolysis. Then controlling hydrolytic extent of chitin is very important for the preparation of CW with desired size and good yield. Except for the original sizes of chitin, concentrations of HCl and hydrolysis time are the two important factors for controlling the particle sizes and yield of chitin nanocrystals. The optimal concentration is 2.5–3 N which was widely used in preparation of CWs from chitin of different origins [32–34, 36–44]. The crystals of chitin are destroyed significantly with increase of HCl concentration, and they are completely dissolved in 8.5 N or higher HCl solutions [32, 46]. When 3 N HCl was applied, the hydrolytic time does not significantly affect the size especially cross-sectional width of the nanocrystals, since the whiskers showed similar lateral diameters in range of 10–50 nm within different hydrolysis times between 1.5 and 6 h, regardless of the original chitin sources. Recently, TEMPO-mediated oxidation (2,2,6,6-tetramethylpiperidine-1-oxyl radical mediated oxidation) method, which succeeded in preparing cellulose nanocrystals [47] and nanofibers [48–50], has also been successfully applied in the preparation of chitin nanocrystals [51] and nanofibers [52]. Almost individualized chitin nanocrystals with width less than 10 nm can be prepared from both α-chitin and β-chitin with this method based on two steps, i.e., oxidation followed by ultrasonic treatment.

TEMPO-mediated oxidation of chitin occurred in water at pH 10 in the presence of NaBr and NaClO. During oxidation, chitin was converted into water-soluble polyuronic acid and water-insoluble particles, and the ratio of contents of both parts can be controlled by the amount of NaClO in the system. The water-soluble polyuronic acid products should be produced by oxidation of disordered domains or outer space of ordered domains of chitin, and the water-insoluble particles were the crystallites of chitin. Some hydroxyl groups of water-insoluble particle surfaces were converted to carboxyl or carboxylated groups during oxidation. When the carboxylated group containing crystallites were subjected to ultrasonic treatment, mostly individualized chitin nanocrystals were obtained, and the aggregation was hampered by existence of carboxylate groups on surface of the nanocrystals. In comparison with the conventional method, TEMPO-mediated oxidation method has many advantages: TEMPO-mediated oxidation is more controllable by the amount of NaClO and the yield of water-insoluble particles can reach 90 %; individualized nanocrystals with narrow width (less than 10 nm) can be obtained; besides, no N-deacetylation of chitin occurs during TEMPO-mediated oxidation. Figure 3.6c shows the TEM image and sizes of the obtained whiskers. In comparison with Fig. 3.6a (conventional CW), much more individual whiskers are formed by TEMPO method although some associated crystals could also be observed.

More recently, individual chitin nano-whiskers have been prepared from partially deacetylated α-chitin by fibril surface cationization. When CWs with degrees of N-acetylation (DNAc) 0.74–0.70 were mechanically disintegrated in water at pH 3–4, individualized nano-whiskers with average width and length of 6.2 ± 1.1 and 250 ± 140 nm respectively, were successfully prepared, as reported by Fan et al. [52] the driving force for individualization of CWs is the same as that in

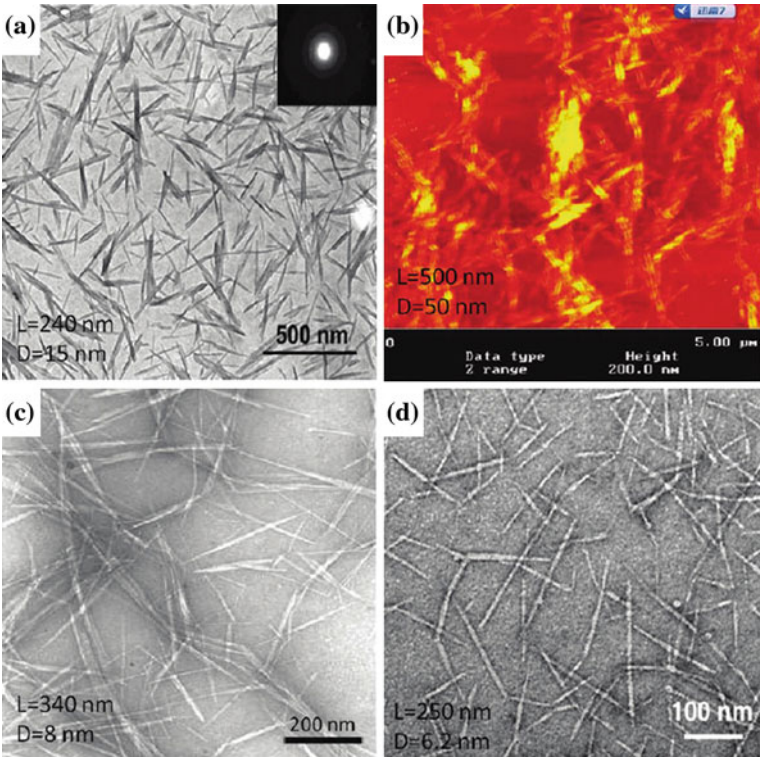

Fig. 3.6 TEM (**a**) [39] and AFM (**b**) [38] images of a dilute suspension of chitin whiskers and TEM images of individual chitin whiskers obtained by TEMPO method (**c**) [51] and surface cationization (**d**) [53]

TEMPO-mediated oxidation method, i.e., surface charge induced electrical repulsion. The difference in the two methods are that TEMPO mediated oxidation endows CW surfaces with anionic charges while cationic charges for the latter. The TEM photograph and size of the individual CW are shown in Fig. 3.6d, some long individual fibrils, with widths similar to those of the whiskers but lengths of more than 500 nm were observed, which have not been reported in previous CWs prepared by the conventional method. The properties of nano-dispersions and casting films of α-chitin nanowhiskers/nanofibers obtained by TEMPO-mediated oxidation method, surface cationization of partially deacetylated chitin and conventional acid hydrolysis were studied and compared with those of squid-pen β-chitin nanofibers, as reported by Fan et al. [53].

The results suggested that squid-pen β-chitin nanofiber dispersion showed the highest shear stress and viscosity due to its highest aspect ratio, that the film of partially deacetylated α-chitin nanowhisker/nanofiber mixture showed the highest tensile strength and elongation at break owning to its relatively higher degree of

crystallinity combined with higher aspect ratio, and that all the samples showed similar thermal stabilities and oxygen permeabilities.

3.4 Preparation of Nano Chitin Whisker

Before the preparation of nano chitin whisker (NCW), chitin has to be isolated from the chitin producing parts of living animals, in which chitin does not occur alone, whereas, chitin always coexists with some other compounds. At present, the major sources of chitin in industry are the shell wastes of crabs and shrimps. The shell wastes are mainly made up of chitin (20–30 %), proteins (30–40 %), calcium carbonate (30–50 %), lipids and astaxanthin (less than 1 %) [54]. Preparation of nano chitin whiskers involves various steps e.g., preparation of raw chitin including isolation, demineralization, deproteinization and finally the extraction of nano chitin whiskers. The raw chitin is obtained from crustacean shells and mycelium of fungi following the detailed procedure given under the following headings:

3.4.1 Isolation of Chitin

Chitin and chitosan do not occur in a pure or in an isolated form. A substantial effort has been made to develop chemical, mechanical, and enzymatic methods to obtain purified materials [54]. The usual method of obtaining chitin involves the chemical treatment of shellfish wastes from the crab and shrimp industries. The first step is to demineralize the shell with dilute hydrochloric acid at room temperature. This is followed by a deproteinization step with warm dilute caustic. This yields a partially deacetylated chitin, which may then be further deacetylated to chitosan. In actual practice the isolation of chitin from shellfish involves the step-by-step removal of the two major constituents of the shell, the intimately associated proteins by deproteinization and inorganic calcium carbonate by demineralization, together with small amounts of pigments, lipids and trace-metals leaving chitin as the final residue [55]. Many methods have been proposed and used over the years. The isolation of chitin begins with the selection of shells. Ideally, shells of the same size and species are chosen. For shrimp shells, the comparatively thin walls make recovery of chitin easier. The cleaning and drying of the shells followed by thorough crushing is the next step in the process. The small shell pieces are treated with dilute hydrochloric acid to remove calcium carbonate. Proteins as well as other organic impurities are removed by an alkali treatment (20 % sodium hydroxide). The pigments, primarily carotenoids are removed by extraction with ethanol or acetone after the demineralization process. A typical procedure of getting the raw chitin is outlined in Fig. 3.7.

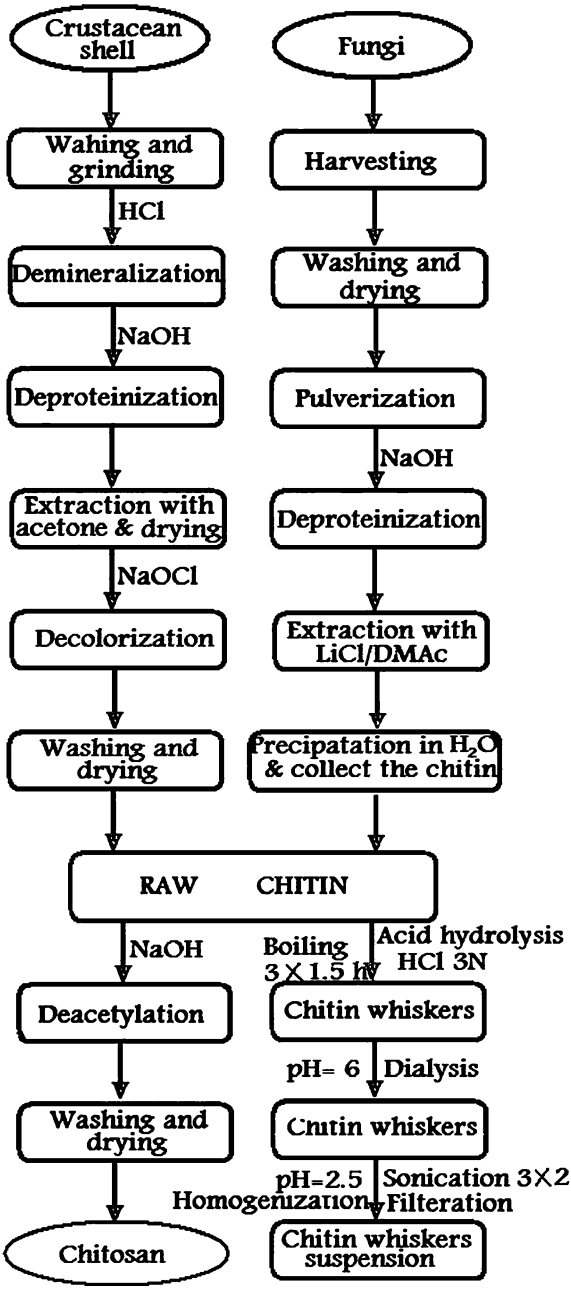

Fig. 3.7 Schematic representations for the preparation of raw chitin and chitosan and chitin whiskers

3.4.2 Demineralization

Demineralization as the term suggests is the removal of minerals, primarily calcium carbonate. A mineral free chitin i.e. very low ash content chitin would be required for applications that have very low impurity tolerance. Demineralization is readily achieved because it involves the decomposition of calcium carbonate into the water-soluble calcium salts with the release of carbon dioxide. The extensively used reagent for this purpose is dilute hydrochloric acid (HCl) that produces water-soluble calcium chloride ($CaCI_2$). Some of the shortcomings of using HCl are that the large volumes of $CaCI_2$ solution must be disposed off and being a strong acid, can cause some hydrolysis of the chitin chains thereby reducing the molecular weight of the biopolymer. Performing demineralization at room temperature or lower can minimize this depolymerization of chitin chains.

3.4.3 Deproteinization

In deproteinization, covalent bonds between the chitin-protein complexes have to be destroyed. This is achieved with some difficulty especially if performed heterogeneously utilizing chemicals that will also depolymerize the biopolymer. The complete removal of protein, possible from shellfish sources, is especially important for biomedical applications. Chemical methods were the first approach used in deproteinization. A wide range of chemicals have been tried as deproteinization reagents including NaOH, Na_2CO_3, $NaHCO_3$, KOH, K_2CO_3, $Ca(OH)_2$, Na_2SO_3, $NaHSO_3$, $Ca(HSO_3)_2$, Na_3PO_4 and Na_2S. NaOH is the preferred reagent on the basis of its performance and typically a 1 M NaOH solution is used with variations in the temperature and duration of treatment parameters. The use of NaOH invariably results in partial deacetylation of chitin and hydrolysis of the biopolymer that lowers the molecular weight of chitin [50, 51]. Normally the protein content in the raw chitin produced from traditional commercial sources is around 1 %. In seeking to raise the deproteinization efficiency and an alternative to the harsh chemical treatment other methods have emerged and are being investigated. The use of proteolytic enzymes such as pepsin, papain or trypsin has been shown to minimize deacetylation and depolymerization in the chitin isolation. Other proteolytic enzymes such as tuna trypsin, Rhozyme-62, cod trypsin and bacterial proteinase have also been demonstrated the removal of proteins from crustacean shells. Bustos and Healy [56] have found that chitin obtained by deproteinization of shrimp shell waste using proteolytic microorganisms such as *Pseudomonas maltophilia, Bacillus subtilis, Streptococcus faecium, Pediococcus pentosaseus* and *Aspergillus oryzae,* had a higher molecular weight compared to chemically prepared chitin. A schematic representation for the preparation of raw chitin and chitosan from crustacean shells and fungi is outlined in Fig. 3.7.

3.4.4 Extraction of Nano Chitin Whiskers

There are various studies in the literature which discuss the extraction of nano chitin whiskers (NCWs) from raw sources [37–40]. Based on the procedure reported [37], the commercial raw chitin was dispersed into a 5 wt% KOH aqueous solution, and then boiled for 6 h with mechanical stirring to remove most of the proteins. The resultant suspension was conditioned at ambient temperature overnight under mechanical stirring followed by filtering and washing with distilled water for several times. Subsequently, the crude product was bleached with 17 g of $NaClO_2$ in 1 L of water containing 0.3 M sodium acetate buffer for 6 h at 80 °C, and then fully rinsed with distilled water. The crude product was finally dispersed into a 5 wt % KOH aqueous solution for 48 h to remove residual proteins followed by centrifugation to produce protein-free chitin. The resulting suspension was centrifuged at 3000 rpm for 20 min. Chitin whisker suspensions were prepared by hydrolyzing the purified chitin sample with boiling solution of 3 N HCl for 1.5 h under stirring. The ratio of 3 N HCl to chitin was 30 mL/g. After acid hydrolysis, the suspensions were diluted with distilled water followed by centrifugation (10,000 trs/min for 5 min). This process was repeated three times. Next, the suspensions were transferred to a dialysis bag and dialyzed for 24 h against distilled water until a pH 6 was reached. The pH was subsequently adjusted to 3.5 by adding HCl. The dispersion of whiskers was completed by a further 2.5 min ultrasonic treatment (B12 Branson sonifier) for every 40 mL aliquot. Morin and Dufresne [37] also prepared the nano chitin whiskers from Riftia. The diameter of these whiskers was 18 nm and length around 120 nm. In another study Gopalan and Dufresne [38] extracted nanochitin whiskers from crab shell. They successfully extracted 100–600 nm length and 4–40 nm width nanocrystal aggregate in the form of 500–1000 μm chitin microcrystal. Rujiravanit and coworkers [39] have reported preparation of chitin whiskers by acid hydrolysis of shrimp shells. The nanochitin whiskers consisted of slender rods with sharp points that had broad distribution in size. The length of the chitin fragments ranged from 150 to 800 nm, the width ranged from 5 to 70 nm. More than 75 % of the whiskers however, had a length below 420 nm. From the group of Zhang and coworkers [40] nanochitin whiskers were prepared from crab shell. It was spindle shaped with broad distribution in length (L) ranging from 100 to 650 nm and diameter (D) ranging from 10 to 80 nm.

3.4.5 Deacetylation of Chitin into Chitosan

Chitosan is prepared by hydrolysis of acetamide groups of chitin. This is normally conducted by severe repetitions of alkaline hydrolysis due to treatment due to the resistance of such groups imposed by the *trans* arrangement of the C2-C3 substituents in the sugar ring [57]. Thermal treatments of chitin under strong aqueous

alkali are usually needed to give partially deacetylated chitin (DA lower than 30 %), regarded as chitosan. The deacetylation of chitin into chitosan is usually achieved by treating chitin with 50 % NaOH at 95 °C for 3 h, cooling down, decanting off the NaOH and washing with water until neutral pH. This procedure is normally repeated twice. Finally the chitosan is extracted with 2 % acetic acid solution, filtered and precipitated in distilled water to give purified chitosan that is dried and stored. In general, two different methods for preparing chitosan from chitin with varying degree of acetylation are known. These are the heterogeneous deacetylation of solid chitin and the homogeneous deacetylation of pre-swollen chitin under vacuum in an aqueous medium. In both, heterogeneous and homogeneous conditions, the deacetylation reaction involves the use of concentrated alkali solutions and long processing times which may vary depending on the heterogeneous or homogeneous conditions from 1 to nearly 80 h. In practice, the maximal degree of deacetylation that can be achieved in a single alkaline treatment is about 75–85 % [58]. For better yield, during deacetylation, the conditions must be properlycontrolled in a reasonable time so that the chitin may be deacetylated tochitosan resulting in better yield.

Several alternative processing methods have also been developed to reduce the long processing times and large amounts of alkali typically needed to deacetylate chitin to an acid-soluble derivative. Examples of these include the use of successive alkali treatments using thiophenol in DMSO [59]; thermo-mechanical processes using a cascade reactor operated under low alkali concentration [60]; flash treatment under saturated steam [61]; use of microwave dielectric heating [62]; and intermittent water washing [63]. There is evidence that in certain bacteria and fungi, enzymatic deacetylation can take place [64]. Deacetylases have been isolated from various types of fungi, namely *Mucorrouxii*, *Aspergillus nidulans* and *Colletotrichum lindemuthianium.* However, the activity of these deacetylases is severely limited by the insolubility of the chitin substrate.

Recently a microwave technique for efficient deacetylation of chitin nanowhiskers to a chitosan nanoscaffold has also been reported [65]. A chitosan nanoscaffold in the form of a colloidal solution was obtained from the deacetylation of chitin whiskers under alkaline conditions by using a microwave technique in only 1/7 of the treatment time of the conventional method (Fig. 3.8). Fourier-

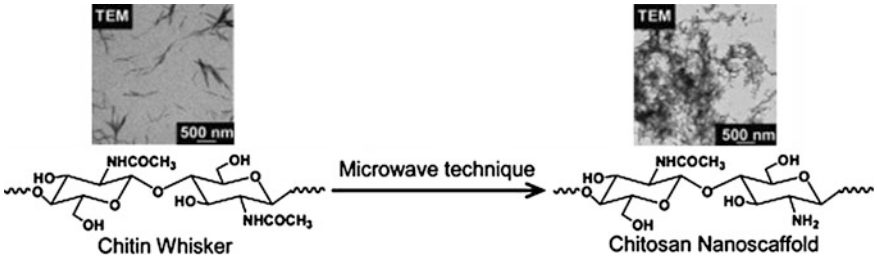

Fig. 3.8 Efficient deacetylation of chitin nanowhiskers to a chitosan nanoscaffold using microwave technique [65]

transform infrared spectroscopy (FTIR) and nuclear magnetic resonance (^{1}H NMR) techniques confirm the degree of deacetylation to be above 90 % within 3 h. The wide-angle X-ray diffraction (WAXD) pattern clearly shows that the highly crystalline chitin whiskers are changed to amorphous chitosan. SEM micrographs show the aggregation of branched nanofibers, whereas the TEM micrographs reveal the scaffold morphology.

3.4.6 Chitosan Nanoparticles Preparation

For the purpose of chitosan nanoparticles preparation, 20 mg chitosan is dissolved in 40 ml of 2.0 % (v/v) acetic acid and 20 ml of 0.75 mg/ml tripolyphosphate TPP is dropped into a beaker at room temperature. After that chitosan solution was sonicated for 5 min and centrifuged for 15 min at 6000 rpm in order to obtain chitosan nanoparticles. These chitosan nanoparticles could be stored in distilled water; however, sonication for 10 s should be applied before a further immobilization step. The morphological characterization of the chitin whisker and chitosan nanoparticles can be evaluated by a Transmission Electron Microscopy (TEM) and Nanosizer.

3.4.7 Depolymerization of Chitosan

The main limitations in the use of chitosan in several applications are its high viscosity and low solubility at neutral pH. Low molecular weight (Mw) chitosans and its oligomers can be prepared by hydrolysis of the polymer chains. For some specific applications, these smaller molecules have been found to be much more useful. Chitosan depolymerization can be carried out chemically, enzymatically or physically. Chemical depolymerization (Fig. 3.9) is mainly carried out by acid

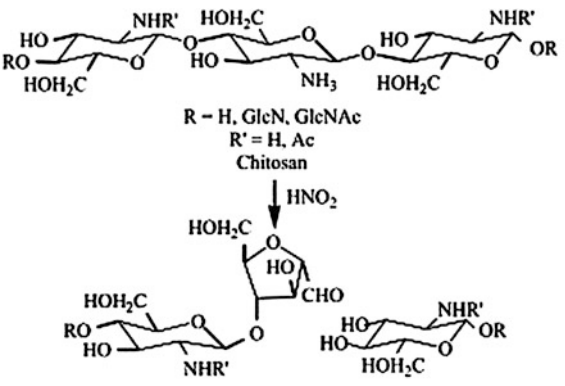

Fig. 3.9 Chemical depolymerization of chitosan with HNO_2 [68]

hydrolysis using HCl or by oxidative reaction using HNO_2 and H_2O_2 [66]. It has been found to be specific in the sense that HNO_2 attacks the amino group of D-units, with subsequent cleavage of the adjacent glycosidic linkage. In case of enzymatic depolymerization, the low molecular weight chitosan with high water solubility can be produced by several enzymes such as chitinase, chitosanase, gluconase and some proteases. Non-specific enzymes including lysozyme, cellulase, lipase, amylase and pectinase that are capable of depolymerization of chitosan are known [67]. In this way, regioselective depolymerization under mild conditions is allowed. Physical depolymerization yielding dimers, trimers and tetramers has been carried out by radiation (Co-60 gamma rays) but low yields have been achieved [68].

3.5 Characterization of Nano Chitin Whiskers

For the determination of physicochemical characteristics of chitin and chitosan, various methods are available in the literature for the purpose. The detailed informations have been presented in the Table 3.2.

The chitin has been characterized by FTIR spectroscopy. The FTIR spectra of original chitin have also been discussed elsewhere [96]. However, FT-IR spectra of original chitin (Fig. 3.10) shows the broad OH stretching vibration band appeared at 3,443 cm^{-1}. The N–H symmetric and asymmetrical stretching vibration bands appeared at 3,289 and 3,105 cm^{-1}, respectively. The C–H symmetric and asymmetric stretching vibrations of CH_2 groups were observed at 2,931 and 2,889 cm^{-1}, respectively. The spectral region of 686–1,661 cm^{-1} is the information-rich region. The faint absorptions at 1,661, 1,626 are due to C=O bond

Table 3.2 Physicochemical characteristics of chitin and chitosan and the determination methods

Sr. no.	Physical characteristics	Determination methods
1	Degree of deacetylation	Infrared spectroscopy [87, 218, 219]
		First derivative UV-spectrophotometry [220, 221]
		Nuclear magnetic resonance spectroscopy (^{1}HNMR) and (^{13}CNMR) [86, 87, 222, 223]
		Conductometric titration [223]
		Potentiometric titration [224]
		Differential scanning calorimetry [225]
2	Average Mw and/or Mw distribution	Viscosimetry [226]
		Gel Permeation chromatography [227]
		Light scattering [216]
3	Crystallinity	X-ray Diffraction [228, 229]
4	Moisture contents	Gravimetric analysis [230]
5	Ash contents	Gravimetric analysis [230]
6	Protein	Bradford method [231]

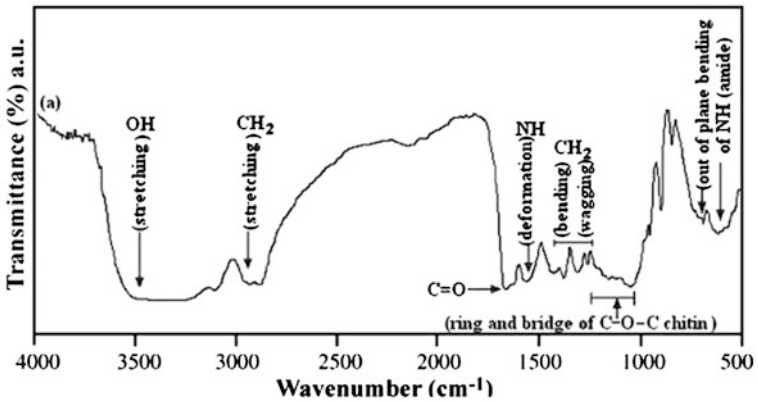

Fig. 3.10 FTIR spectra of chitin [96]

and at 1,563 cm^{-1} is due to NH deformations. The absorption bands at 1,427, 1,377 and 1,307 cm^{-1} were attributed to CH_2 bending vibration, CH bending vibration and CH_2 wagging, respectively. The bands appeared at 1,261 and 1,204 cm^{-1} are due to NH bending vibration and OH in-plane bending. The absorption band appearing at 1,158 cm^{-1} is due to the asymmetric in-plane ring deformation. The absorption bands appearing at 1,046 and 1,026 cm^{-1} are due to C–O and C–C stretching vibration. The two absorption bands at 950 and 896 cm^{-1} are due to C–O ring vibration and ring bending. The broad intense band at 1,000–1,220 cm^{-1} was attributed to the ring and bridge C–O–C vibrations of chitin-ether-type absorption. On the other hand, a weak shoulder at 710 cm^{-1} and well-resolved band at 686 cm^{-1} are assigned to the out-of-plane bending of NH (amide).

Transmission Electron Microscopy (TEM) is very good tool for characterizing the structure of nanosized materials. Nair and Dufresene [70] studied the colloidal suspension of chitin whiskers as the reinforcing phase and latex of both unvulcanized and prevulcanized natural rubber as the matrix. The chitin whiskers, prepared by acid hydrolysis of chitin from crab shell, consisted of slender parallel epiped rods with an aspect ratio close to 16. After the two aqueous suspensions were mixed and stirred, solid composite films were obtained either by freeze-drying and hot pressing or by casting and evaporating the preparations. Figure 3.11 shows TEM image of chitin whiskers obtained from crab shells.

Atomic Force Microscopy (AFM) is also another good tool for detecting the dimension of the nano sized particles. Oksman and coworkers [71] observed that AFM analysis of the chitin and cellulose whiskers is a good alternative to electron microscopy, without any limitations regarding contrast and resolution. The shape of the whiskers appeared, however, different from that observed in TEM. Scanning Electron Microscopy (SEM) is generally employed for the more extensive morphological inspection. It consists of the observation of fractured surface films at liquid nitrogen temperature. This technique allows for conclusions about the

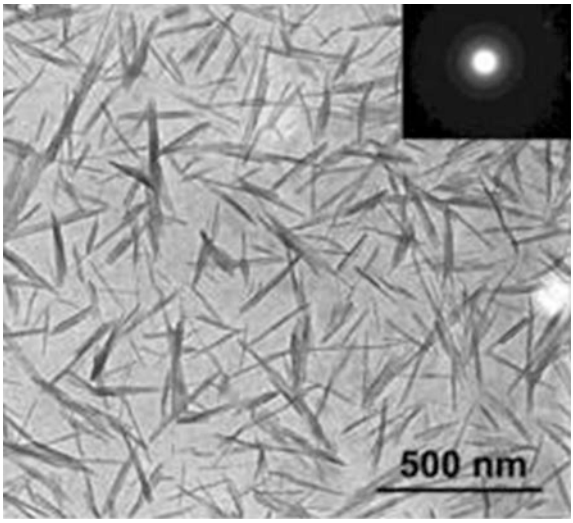

Fig. 3.11 TEM image of chitin whiskers from crab shell [70]

homogeneity of the composite, presence of voids, dispersion level of the whiskers within the continuous matrix, presence of aggregates, sedimentation, and possible orientation of whiskers. Their diameter determined by SEM is much higher than the whiskers diameter. This results from a charge concentration effect due to the emergence of cellulose whiskers from the observed surface. Gopalan et al. [72, 73] have extracted nano chitin whiskers from crab shell. Figure 3.11 shows a transmission electron micrograph of a dilute aqueous suspension of hydrolyzed crab shell chitin. The suspension contains chitin fragments consisting of both individual micro crystals and associated or collapsed micro crystals. These chitin fragments consist of slender rods with sharp ends that have a broad distribution in size. Rujiravanit and coworkers [41] also showed the size of chitin whisker from shrimp shells by using TEM. Michel and Dufresne [74] also showed transmission electron micrographs of nano chitin whiskers from squid pen chitin. AFM analysis of the whiskers was found to be a good alternative to TEM without any limitations regarding contrast and resolution. The shape of the whiskers appeared, however, different than that observed in TEM and FESEM.

X-ray diffraction (XRD) is a versatile, non-destructive technique that reveals detailed information about the chemical composition and crystallographic structure of natural and manufactured materials. Zia et al. [96] reported that the crystalline structure of chitin with dimension $a = 4.85$ Å, $b = 9.26$ Å, $c = 10.38$ Å (fiber axis), and $\gamma = 97.5°$. The unit cell contains two sugar residues related by the two fold screw axis. The structure contains extended polymer chains indicating an anti-parallel arrangement of the chitin chain with strong intermolecular hydrogen bonding [75]. Five crystalline reflections were observed in the 2θ range of 5–30° (Fig. 3.12).

The observed patterns of the crystalline peaks in the 2θ range were indexed as 9.39°, 19.72°, 20.73°, 23.41° and 26.39° for the lower angle for chitin. The outcomes of the results are in accordance with the previous findings [75–77].

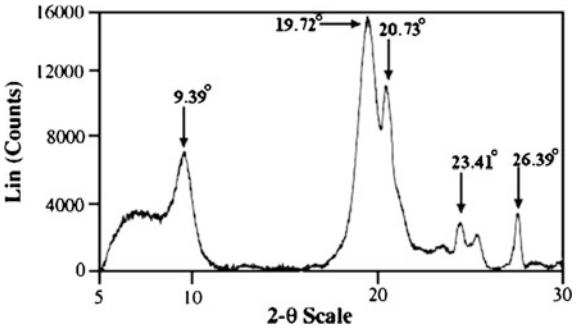

Fig. 3.12 XRD pattern of chitin [96]

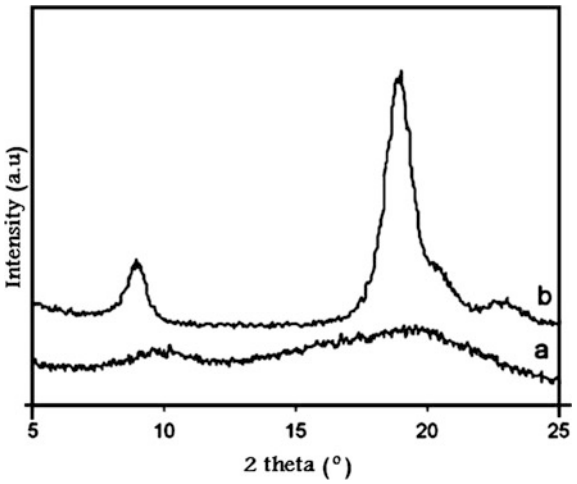

Fig. 3.13 X-ray analysis data of chitosan/chitin crystal nanocomposites

As shown in Fig. 3.12 exhibited a broad signal centered at $2\theta = 19.72°$, which is attributed to the GlcN sequences. Similarly, the intensity of the broad signal centered at $2\theta = 9.39°$ due to GlcNAc sequences [78].

Very recently Mathew et al. [79] reported on the crystal studies of chitosan/chitin crystal nanocomposites. The chitosan (a) exhibits a highly amorphous nature with broad and ill-defined signals at $2\theta = 9–10°$ and 18–20° (Fig. 3.13). The chitin nanocrystals (b) show a strong peak at $2\theta = 8.8$ and 19° and shoulders at $2\theta = 20$ and 22°, confirming its crystalline structure as α-chitin.

3.5.1 Characterization of Chitin and Chitosan for Medicinal Applications (Medical Devices)

It is necessary to prepare several tests, grouped in preliminary, confirmatory and other tests, for characterization of chitin and chitosan used for manufacturing of medical devices [80]. European Pharmacopoeia as well as requirements of ISO

10993-18:2005 [81] and ISO/DIS 10993-1910 [82] Standards for the determination of range of analytical characterization of chitosan must be taken into consideration.

1. *Moisture content and form identification*

Usually moisture contents of chitosan vary from 5.0 to 15.0 % which results changing with humidity and form of chitosan (flakes or powder). The form of the biopolymer is able to give suitable information for quality. The sample of biopolymer should be suspended in water, filtered and dried for detection of water-soluble contaminants.

2. *Ash and protein content in chitosan*

Protein and ash content of chitosan are very important parameters and those should be investigated early in the quality assay protocol. A high quality grade product should have less than 1 % of protein as well as ash content.

3. *Insolubility, turbidity, color and UV absorption of chitosan solution*

For determination of insolubility, turbidity, color and UV absorption of chitosan 1 % (w/v) solution of dried sample ought to be prepared in 1 % acetic acid solution. When the sample is dissolved, the solution is filtered and insolubility of the sample is determined. The insolubility of a good quality chitosan should not exceed 0.1 %. If the appearance of the residues is different from that of chitin and chitosan, one may consider analyzing its nature. The turbidity of 1 % sample solution in 1 % acetic acid should be less than 15 NTU (i.e., nephelometric turbidity units) and should be free from physical contamination by visual examination. The transmittance should be higher than 90 %, both at $\lambda = 400$ nm and $\lambda = 560$ nm. The UV spectrum of chitosan is additionally able to provide the other chromophoric impurities information upon the interference of other chromophores. If during preliminary tests no significant deviation has been found, then further investigations should be conducted for the confirmatory test.

4. *Confirmatory test: Chromatographic and spectroscopic examinations*

Acid hydrolysis of chitosan followed by the HPLC detection of the amount of acetic acid liberated is able to give acetyl content of chitin/chitosan. Due to the high sensitivity, availability, easiness of method and effectiveness in detection of functional groups IR spectroscopy can give useful information about the acetyl content of chitin/chitosan as well as possible cross-contaminations. The results of Differential Thermogravimetric Analysis (DTA) show increased thermostability compared to GlcNAc. Discussed biopolymer shows its main thermal process from 275 to 280 °C respectively.

5. *Further confirmation tests*

In general, one can assure the confirmatory test for chitosan after colorimetric analysis since above-mentioned series of physical and chemical analysis can clearly investigate the identity of sample. But in certain cases, one might encounter

to check the purity of chitosan for very sensitive applications that demand very high purity. Then, NMR spectroscopy will come into consideration as described in ISO 10993-18:20059 and ISO/DIS 10993-1910 Standards [82].

6. *Other characteristics of chitosan*

The remaining parameters of chitosan should be taken into the consideration. Molecular weight of chitosan is one of the important properties affecting chitosan quality and reproductively of results in several medicinal applications requires different range of molecular weights or strictly narrow range of molecular weight. X-ray diffraction is a perfect analytical method to define the crystallinity but IR and NMR spectra are able to provide additional data for intrepretation and understanding sample morphology. Not only heavy metals but nitrogen, chloride, ammonia contents in chitosan are also very important in medical applications. Additionally, extractable residues in non-polar and polar solvents are helpful in identifying the characteristic of investigated samples. Source for manufacture of medical devices should be apyrogenic as well as it should not contain pathogenic contamination. Therefore, it is useful to determine biological contamination defined as viable aerobic microorganisms, fungi, mould and yeast content. The bioburden level should be measured before introduction of new portion of source for production to avoid accidental cross-contamination.

3.6 Manufacture of Chitin Nanocomposites and Blends

Morin and Dufresne [37] prepared nanocomposites from a colloidal suspension of high aspect ratio chitin whiskers as the reinforcing phase and poly (ε-caprolactone) as the matrix. The chitin whiskers, prepared by acid hydrolysis of Riftia tubes, consisted of slender parallel-tubed rods with an aspect ratio close to 120. Films were obtained by both freeze-drying and hot-pressing or casting and evaporating the preparations. Amorphous poly (styrene-co-butyl acrylate) latex was also used as a model matrix. In another work [72] nanocomposite materials were obtained from a colloidal suspension of chitin whiskers as the reinforcing phase and latex of both unvulcanized and prevulcanized natural rubber as the matrix. The solid composite films were obtained either by freeze-drying and hot-pressing or by casting and evaporating the preparations. In another study, Lu et al. [38] prepared environment friendly thermoplastic nanocomposites using a colloidal suspension of chitin whiskers as a filler to reinforce soy protein isolate (SPI) plastics. SPI of desired weight and various contents of chitin were mixed and stirred to obtain a homogeneous dispersion. The dispersion was freeze-dried, and 30 % glycerol was added. The resulting mixture was hot-pressed at 20 MPa at 140 °C for 10 min and then slowly cooled to room temperature. Rujiravanit and coworkers [83] prepared α-chitin whisker-reinforced poly (vinyl alcohol) (PVA) nanocomposite films by solution-casting technique. Casting technique leading to the formation of films was used for the preparation of latex based starch nanocomposites [84]. In another

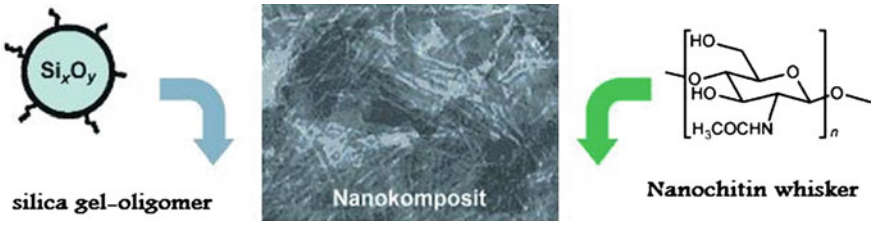

Fig. 3.14 Self-organization and sol–gel chemistry of colloids for the formation of chitin-silica nanocomposites [85]

study Alonso, et al. [85] prepared chitin-silica nanocomposites by self-organization. Self-organization processes of chemical building blocks are the basis for many biological processes (Fig. 3.14).

The synthesis was carried out by sol–gel process techniques. The sol into a desired shape can be "cast" and dried. So a nanocomposite formed from silicon dioxide into a fully-integrated matrix of chitin rods. The mechanism is based on a self-organized storage of chitin and weak forces of attraction between chitin and siloxane oligomers. Different textures and morphologies are accessible by adjusting the evaporation process or by applying external fields.

In another study Feng et al. [86] presented the structure and properties of new thermoforming bionanocomposites based on chitin whiskers-graft-polycaprolactone. The synthesized material was characterized by FTIR, SEM, TEM and XRD. The surface and mechanical properties were also determined and discussed. Hariraksapitak et al. [87] prepared a neat hyaluronan–gelatin scaffolds and chitin-whisker-reinforced hyaluronan–gelatin scaffolds. The obtained cylindrical scaffolds obtained were about 10 mm in diameter and 2 mm in height, whereas the disc-shaped scaffolds were about 1 mm in thickness; these were later cut into a desired shape and size for the mechanical property assessment.

Eectron beam is usually used on the polymeric material to induce effects such as chain scission (which makes the polymer chain shorter) and cross linking. The result is a change in the properties of the polymer which is intended to extend the range of applications for the material. The effects of irradiation may also include changes in crystallinity as well as microstructure. Usually, the irradiation process degrades the polymer. The irradiated polymers may sometimes be characterized using DSC, XRD, FTIR, or SEM. In poly(vinylidene fluoride-trifluoroethylene) copolymers, high-energy electron irradiation lowers the energy barrier for the ferroelectric-paraelectric phase transition and reduces polarization hysteresis losses in the material [88].

Electron beam irradiation is an alternate method to prepare poly(aniline) (PANI) nanocomposite stable at ambient conditions. Ramaprasad et al. [89] synthesized the chitin-polyaniline nanocomposite by electron beam irradiation method (Fig. 3.15). The blends of chitin and PANI with PANI 30, 50, and 70 % (30P, 50P, and 70P) were prepared by mixing 0.5 % (wt%) chitin solution and 0.5 % (wt%) EB solution in DMA with 5 % LiCl in required proportions and irradiated with

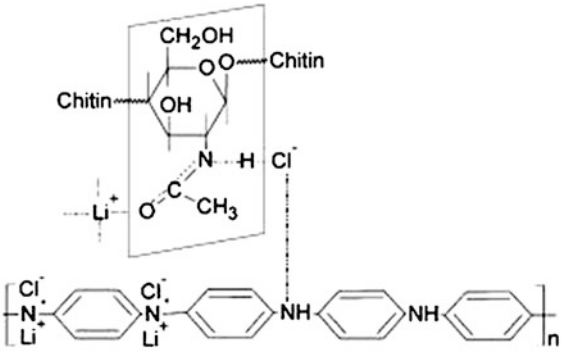

Fig. 3.15 Interaction between chitin and polyaniline [89]

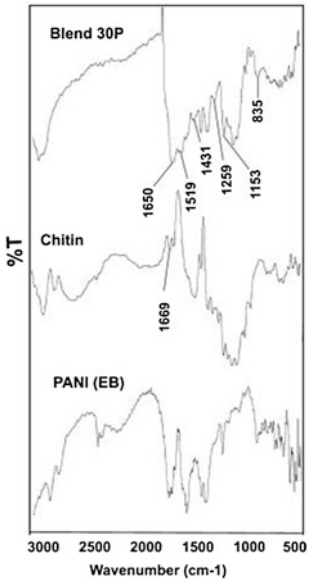

Fig. 3.16 FTIR spectra of PANI (*EB*), chitin and 30P blend [89]

electron beam. During irradiation, the color of the solution turned blue to brown and above 4 kGy, immediately after the irradiation of blend solution, brown particles were obtained at the top of the solution, and after 20–30 min these particles were uniformly distributed in solution. The FTIR spectra of PANI, chitin, and 30P blend is presented in Fig. 3.16.

Preparations of SiO_2-chitin/carbon nanotubes (CNTs) bionanocomposites have also been reported by many researchers [90]. The use of nanomaterials such as CNTs to fabricate matrices for biosensors is one of the most exciting approaches because nanomaterials have a unique structure and high surface to volume ratio [90]. The surfaces of nanomaterials can also be tailored in the molecular scale in order to achieve various desirable properties [91]. The diverse properties of nanocomposite materials such as unique structure and good chemical stability enable them to provide a wide range of applications in sensor technology [92].

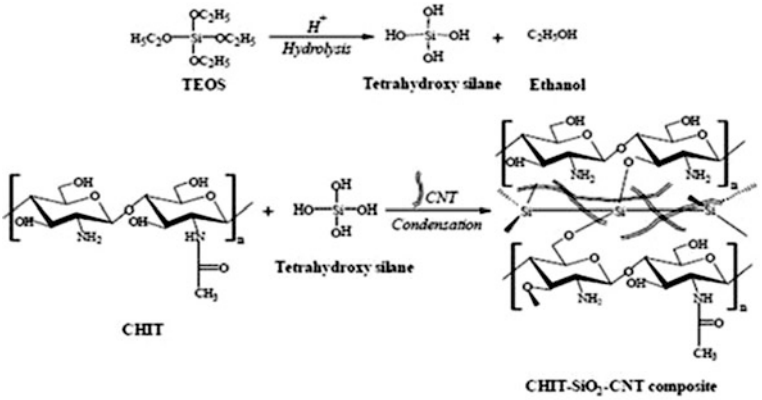

Fig. 3.17 Reaction scheme for the preparation of SiO_2-chitin/CNTs bionanocomposites [90]

Moreover, the nanocomposites do not suffer from the drawback of sensing complications, synthesis complexities; have a long shelf life, and excellent performance. In to this addition, the fundamental electronic characteristics of CNTs could also be used to facilitate the uniform distribution within the nanocomposite biosensing electrodes. There are many reports on integration of CNTs with sol–gel derived SiO_2-chitin to fabricate biosensors to gain synergistic action using organic–inorganic bionanocomposites. The sol–gel SiO_2-chitin is prepared by mixing of alcoholic silica precursor such as tetraethyl orthosilicate (TEOS) and chitin solution under magnetic stirring at room temperature. To this mixture, homogeneously dispersed CNTs in ethanol are added. The mixture initially comprising of two phases is made uniform by stirring vigorously until -SiO_2 is distributed evenly in the aqueous solution while the hydrolysis reaction occurs. After certain time period, the opaque and black sol is formed (Fig. 3.17). In a controlled process, tetraethoxysilane undergone hydrolysis and formed tetrahydroxy silane (silanol) at acidic pH [93]. The resulted silanol then reacted with chitin via a condensation reaction between the -OH groups and led to the formation of a chitin-SiO_2 composite network, in which CNTs are homogeneously dispersed. Both CNTs and SiO_2 improve the mechanical properties of the chitin-SiO_2-CNTs bio- nanocomposite, primarily CNTs enhance the electrical conductivity of the bio- composite.

The fabrication of enzyme-SiO_2-Chitin-CNT bioelectrodes have also been reported [94]. The SiO_2-chitin/CNTs sol thin film is fabricated by spreading it uniformly onto a substrate such as ITO glass plate (i.e., indium tin oxide coatings on *glass* slides) using spin coating technique and subsequently dried at room temperature. SiO_2-chitin/CNTs/substrate electrode is washed with deionized water followed by phosphate buffer saline of pH 7.0 in order to maintain pH over the electrode surface. SiO_2-chitin/CNTs electrode is treated with aqueous glutaraldehyde as a cross-linker. The freshly prepared enzyme solution is uniformly spread onto glutaraldehyde treated SiO_2-chitin/CNTs electrode and is kept in a humid

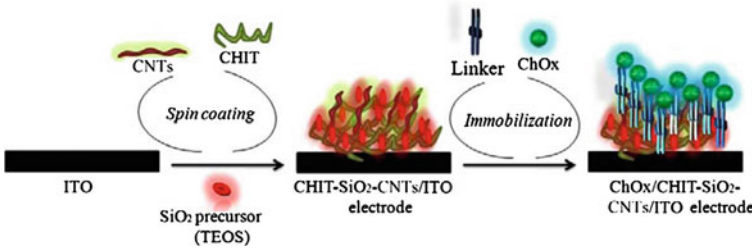

Fig. 3.18 Schematic diagram of the fabrication of CHIT-SiO_2-CNTs/ITO and ChOx/CHIT-SiO_2-MWNT/ITO electrodes

chamber at 4 °C for 12 h, Fig. 3.18. The enzyme-SiO_2-chitin/CNTs bioelectrode is immersed in phosphate buffer solution of pH 7.0 in order to wash out unbound enzyme from the electrode surface.

Extensive work on detailed molecular characterization [95], XRD studies [96], and thermal properties [96] of chitin-based polyurethane elastomers (PUEs) have also been extensively studied and reported in the literature. In vitro biocompatibility and non-toxicity of chitin/1,4-butanediol blends based polyurethane elastomers has also been reported elsewhere [97, 98]. Some reports are also available on molecular characterization and shape memory properties of chitin-based shape memory polyurethane elastomers [99, 100]. For the application of PU, their stability against terrestrial weathering is important. One of the greatest factors in the terrestrial weathering of PUEs is ultraviolet (UV) radiation in the wave-length range 330–410 nm. Attempts have also been made to study the effect of UV-irradiation on surface properties of some common polymers [101–103]. Photo-oxidative behavior and effect of chain extender length in polyurethane on photo-oxidative stability have also been reported [104]. Surface morphology of starch [105], cellulose [106], and chitin–humic acid [107] have also been investigated and well documented. XRD studies and surface characteristics of UV-irradiated and non-irradiated chitin-based polyurethane elastomers have also been presented in different research articles [108–110]. The synthesis and characterization of chitin based polyurethane samples have been reported using chitin as chain extender/crosslinker [116. 132]. The synthetic scheme for the synthesis of chitin based polyurethane is presented in Fig. 3.19.

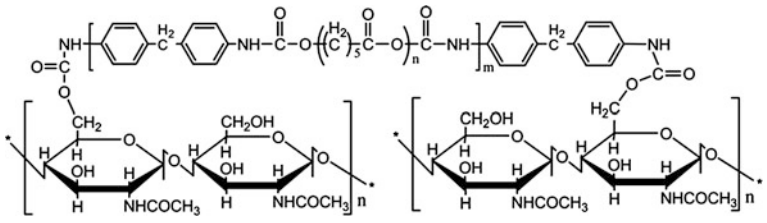

Fig. 3.19 Synthesis of chitin based polyurethane [100]

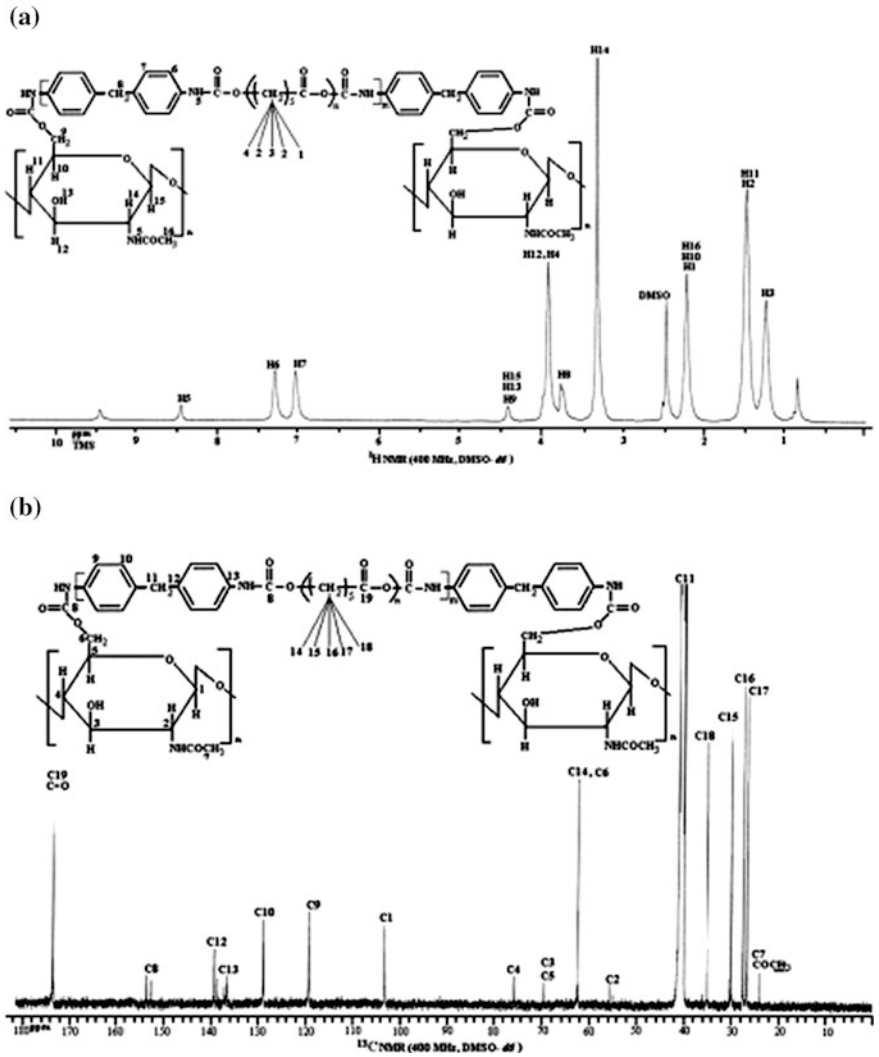

Fig. 3.20 **a** ^{1}H NMR. **b** ^{13}C NMR spectra of chitin based polyurethane [95]

The ^{1}H NMR and ^{13}C NMR spectra of final synthesized chitin based polyurethane (PU) samples were in accordance with proposed structures (Fig. 3.20). ^{1}H NMR spectra obtained for chitin based PU exhibited new peaks at 4.48 ppm which was assigned to the proton of C1, C3 and C6 position of chitin. ^{13}C NMR spectra obtained for the chitin-based PU samples, exhibited peaks at 23.0 and 174 ppm, which were attributed, respectively to the CH_3 (methyl) and C=O (carbonyl) group of chitin [111]. Moreover, the peaks located at about 56.2, 63.3, 69.6, 68.8, 77.5 and 104 ppm were attributed to C2, C6, C3, C5, C4 and C1 positions of chitin,

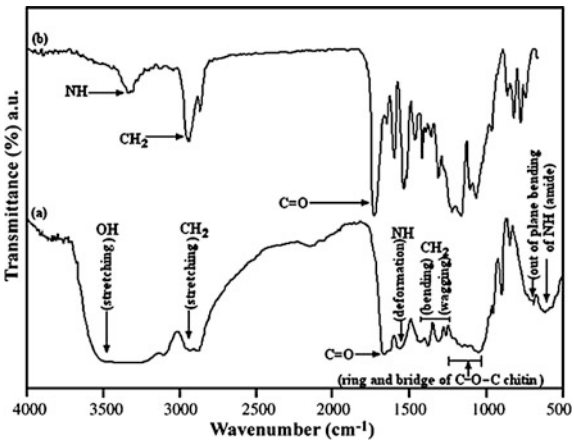

Fig. 3.21 FTIR spectra of **a** original chitin, **b** NCO-terminated pre-polymer extended with chitin [114]

respectively [112, 113], which provides evidence of involvement of chitin in final polyurethane structure. The FTIR spectra confirm the synthesis of chitin based polyurethane. The FTIR spectra of original chitin and polyurethane extended with chitin are shown in Fig. 3.21a and b.

The role chitin as a material of highly ordered crystalline structure has been reported in the study [96]. X-ray diffraction analysis was carried out in order to find the changes of the crystalline structure upon the substitution reaction with NCO terminated prepolymer. The X-ray diffraction studies showed that crystallinity mainly depends on the concentration of chitin in the polyurethane backbone, crystallinity increased as the concentration of chitin into the final PU increased (Fig. 3.22). The crystallinity of some polymers was clearly observed by optical microscopic studies [114]. The results of X-ray diffraction experiments correlate with optical microscopy findings. A crystalline polymer is distinguished from an amorphous polymer by the presence of sharp X-ray lines superimposed on an amorphous halo. Under an optical microscope, the presence of polycrystalline aggregates appear as spherulites [114]. The spherulites are made of small crystallites and grow from a nucleus at their centre. They consist of narrow chain folded lamellae growing radially. Since the fibrous crystals are radial, the chains folded with the lamellae are circumferentially oriented. From the evaluation of the X-ray and optical microscopic studies, it has been observed that the involvement of chitin in the PU formulation and have improved crystallinity of the final polyurethane.

The cell culture tests were used to evaluate both cytotoxicity and cytocompatibility of the specimens. In the cell culture method, the performance of a cell is investigated by comparing it with a negative control. A control is a sample thoroughly compatible with cells and is cultured with the main samples. A material is considered to be biocompatible, if it supports cell attachment and growth.

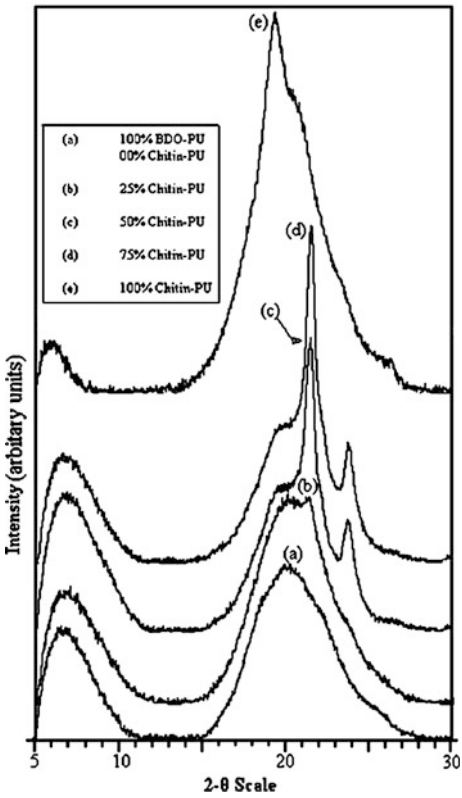

Fig. 3.22 X-ray diffractograms of **a** CPU1–0 % chitin–PU, **b** CPU2–25 % chitin–PU **c** CPU3–50 % chitin–PU **d** CPU4–75 % chitin–PU **e** CPU5–100 % chitin–PU [96]

Zuber, et al. [115] prepared chitin based polyurethane bionanocomposites (PUBNC) by solution polymerization. The formation of well dispersed ordered intercalated assembled layers of bentonite in PU matrix was observed. The results revealed that pure silicate disappears in PU/bentonite nanoclay hybrid and a set of new peaks appear corresponding to the basal spacing of PU/bentonite clay bionanocomposites. Wang et al. [116] reported the synthesis of chitosan-based nanocomposites with montmorillonite. The nanocomposites were prepared by the solution intercalation method in which the chitosan solution was added to the clay dispersion followed by film casting. Morphology and properties of the composites generated with and without acetic acid residue were also compared with the pure polymer. Figure 3.23 shows the TEM micrographs of the composites with varying extents of montmorillonite. It was observed that the dispersion of filler was uniform. At low filler amounts, the morphology was of intercalated-exfoliated type. On the other hand, increasing the filler content led to the shift of morphology to mostly intercalate with occasional flocculation. The thermal performance of the nanocomposites was observed to be better than that of pure polymer. Higher

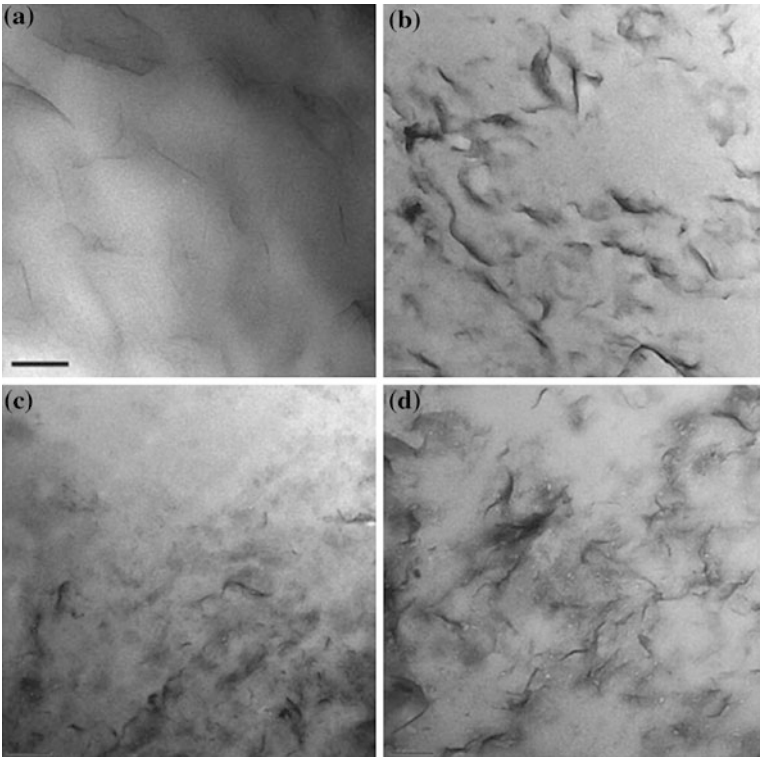

Fig. 3.23 TEM micrographs of chitosan nanocomposites with **a** 2.5 wt % filler, **b** 5 wt % filler, **c** 5 wt % filler as well as acetic acid residue, and **d** 10 wt % filler [116]

hardness and superior mechanical properties were also observed in the composites as compared to pure polymer.

Darder et al. [117] also reported chitosan intercalated montmorillonite nanocomposites. Darder et al. [118] further reported on the reinforcement of chitosan with sepiolite, which is a natural magnesium silicate with micro fibrous texture. The study suggested a considerable interaction between hydroxyl groups belonging to the biopolymer structure of the chitosan polymer and the silanol groups present on the external surface of sepiolite as shown in Fig. 3.24. The crystalline structure of sepiolite was observed to be preserved during the nanocomposite synthesis. Strong interaction between the organic and inorganic components of the system was also confirmed with different characterization methods. The resulting composites were thermally more stable than the pure polymer. As a result of the strong interaction, the mechanical properties of the composites were also superior to those of the pure polymer. Similarly, other fillers like double layer hydroxides have also been incorporated in the polymer matrices [119].

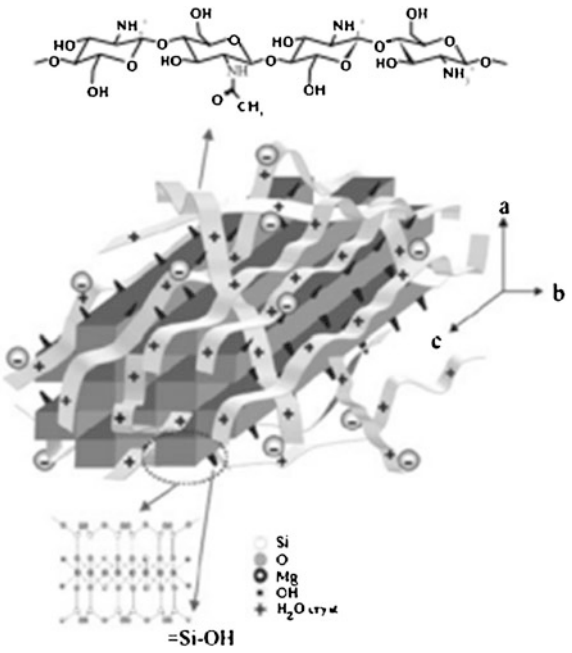

Fig. 3.24 Representation of the chitosan adsorption on sepiolite surface [118]

3.6.1 Chitosan Based Nanocomposites

Recently, much attention has been paid to chitosan as a potential polysaccharide resource due to its excellent properties [120–124]. The polymorphism of chitosan has also been studied, extensively and different conclusions have been drawnunder different study conditions. Nanocomposites based on the intercalation of chitosan in Na^+ montmorillonite are known to be robust and stable three-dimensional materials, since the interaction of the biopolymer with the clay substrate strongly reduces its film-forming tendency. When the chitosan amount exceeds the cationic exchange capacity (CEC) of the clay, the biopolymer is intercalated as a bilayer in the clay interlayer space by means of cationic exchange and hydrogen bonding processes. It was assumed that the excess of $–NH_3^+$ groups, which do not interact electrostatically with the negatively charged sites of the clay, is balanced with the acetate ions from the initial chitosan solution, providing the bidimensional nanostructured material with anionic exchange sites ($–NH_3^+X$). Since chitosan–montmorillonite nanocomposites exhibited good functional and mechanical properties, they were employed in the construction of bulk-modified sensors for the detection of anions [125]. In another study, ionotropic crosslinking methodology was used to synthesize chitosan-tripolyphosphate chelating resin beads to fabricate zero-valent copper-chitosan nanocomposites. The copper nanoparticles were dispersed on chitosan-tripolyphosphate beads, and were thus able to maintain appropriate dispersion and stability, which greatly improved their applicability. The fabrication process contains two steps: using chitosan-tripolyphosphate beads

to adsorb Cu(II) ions, followed by chemical reduction to reduce Cu(II) ions to zero-valent copper [126]. Huang et al. [127] synthesized various metal–chitosan nanocomposites including silver (Ag), gold (Au), platinum (Pt), and palladium (Pd) in aqueous solutions. Metal nanoparticles were formed by reduction of corresponding metal salts with $NaBH_4$ in the presence of chitosan. Cu_2O/CS nanocomposites are prepared by electrochemical deposition. By the joint analysis of photocatalytic performance of Cu_2O/CS nanocomposites with variant mass ratios of Cu_2O in the decoloration of reactive brilliant red X-3B, and the chelation capability of CS and found that when the mass ratio of Cu_2O in the Cu_2O/CS nanocomposites is 50 %, the composites provide with a new feasibility to eliminate the pollutants by visible light irradiation in the advanced treatment of drinking water [128]. The growth of hydroxyapatite (HA) on gelatin–chitosan composite capped gold nanoparticles was done for the first time by employing wet precipitation methods and obtained good yields of HA. High Resolution Transmission Electron Microscope images (HRTEM) of GC–Au–HA nanocomposites showed the size of nanocomposite about 50 nm [129]. Chitosan and chemically modified chitosan (CMC) were chosen matrices for synthesizing and stabilizing the gold, silver and platinum nanoparticles [130]. It was observed that CMC was poor choice as the nanoparticle aggregation and also lack of free amines limited the extent of polymer crosslinking. Lui and Huang in their work on nanocomposites of genipin (excellent natural cross-linker for proteins, collagen, gelatin,and chitosan) crosslinked chitosan silver nanoparticles concluded that silver nanoparticles affect the material characteristics, biological activity and antimicrobial activity. Enhanced micro-structural property of the nanocomposites reduced the biodegradation rate under enzymatic digestion [130].

Molecularly imprinted polymer (MIP) represents a new class of materials that have artificially created receptor structures. This potential technology is a method for making selective binding sites in synthetic polymers by using a molecular template. MIPs have steric and chemical memory toward the template and hence could be used to rebind it (Fig. 3.25).

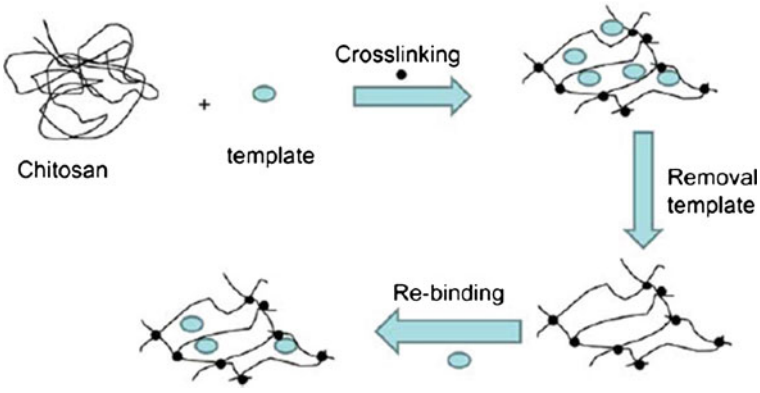

Fig. 3.25 Schematic representation of imprinted chitosan-based matrix preparation [130]

3.6.2 Bionanocomposites: From New Sources to New Processes

In recent years a number of research studies on the synthesis of clay-based nanocomposites have been reported [112]. Nanocomposites, by virtue of the interactions between the organic and inorganic components, can have different morphologies [131]. In the intercalated morphology, the clay layers are still ordered. However, the exfoliated or delaminated morphology provides maximum benefit as the filler is completely delaminated and the platelet ordering is lost. This morphology has maximum interfacial contact with the polymer; thus, polymer properties like mechanical performance, barrier properties and biodegradability are significantly affected. Nanocomposites have also been prepared by different synthetic routes [132, 133]. In situ polymerization for preparation of nanocomposites, as described in the earlier section, is based on the swelling of the clay in the monomer followed by polymerizing the monomer in the presence of clay, thus trapping the delaminated clay in the polymer structure. Melt intercalations, also described earlier, is the method where the preformed high molecular weight polymer can be directly used for the synthesis of the polymer nanocomposite. In this case, the polymer is melted at high temperature, and the filler is slowly added to this melt under shearing in the compounder. The filler platelets are sheared during compounding and kneading in the compounder and thus are well mixed with the polymer phase. Another method for synthesizing polymer nanocomposites is solvent intercalation. In this case, the polymer is dissolved in the same solvent in which the clay is dispersed. Evaporation of the solvent leads to entrapment of the polymer chains in between the filler platelets. One can also synthesize thermoset polymer nanocomposites by this route. The prepolymer is dissolved in the solvent in which the filler is dispersed. The crosslinking is then initiated by the addition of the crosslinker. The simultaneous evaporation of solvent and crosslinking of the polymer matrix leads to delaminated filler in the polymer matrix. A more comprehensive review has been reported by Bordes et al. [134].

3.6.3 Polymer/Chitin Whisker Bionanocomposites Processing

Similar to cellulose nanocrystals, chitin whiskers also showed high values of different modulii. The longitudinal modulus and transverse modulus of the CW are 150 and 15 GPa, respectively. Thus, CWs can be used as potential nanofillers in reinforcing polymer nanocomposites. Following the use of cellulose nanocrystals in reinforcing poly(styrene-co-butyl acrylate) (poly(S-co-BuA))-based nanocomposites in 1995, the application of polysaccharide nanocrystals in reinforcing polymer nanocomposites have attracted a great deal of interests due to their appealing intrinsic properties [135–139]. Paillet et al. [36] first time reported the use of CWs in reinforcing thermoplastic nanocomposites in 2001, the same polymer, poly(S-co-BuA), was used as the matrix for the nanocomposites.

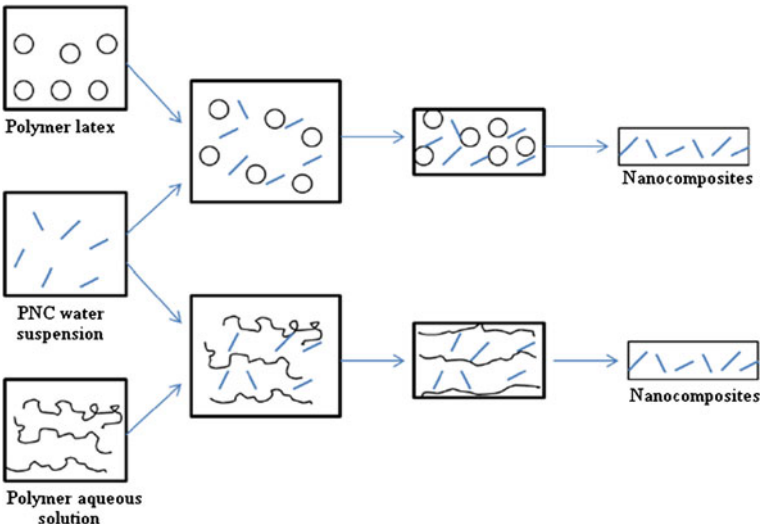

Fig. 3.26 Casting-evaporating procedures for preparation of polymer/CW nanocomposites

Thereafter, CWs have been increasingly used in many other polymer matrices. Following processing steps are involved in the manufacturing of polymer/chitin whisker bio nanocomposites.

1. *Casting and evaporating technique*

The processing techniques have an important influence on the final properties of nanocomposites. The techniques that are employed should take into account the intrinsic properties of CWs, the nature of polymer matrix, and the desired final properties of the composites. Good dispersibility of CWs in polymer matrix is the prerequisite to prepare high performance polymer/CW nanocomposites. So for uniform composition CWs are homogenously dispersed in water and are usually obtained as aqueous suspensions. Thus, water is the best medium for preparation of CWs reinforced nanocomposites, and most investigations preferred to use water-soluble, water-dispersible and latex-form polymers as the polymer matrixes to make nanocomposites. In the process, as shown in Fig. 3.26, the polymer aqueous solution or dispersion was first mixed with CW aqueous suspension to obtain homogenous dispersion which was then casted onto a container; afterwards, the nanocomposites with CWs incorporated into polymer matrix were obtained by evaporation of water, this method is so-called casting and evaporating technique.

Most of the recent reported polymer/CW nanocomposites were prepared by this method. The reported polymer matrixes contain poly(styrene-co-butyl acrylate) [36], poly(caprolactone) [37], natural rubber [39, 140, 141], soy protein isolate [38], poly(vinyl alcohol) [42, 44], chitosan [41, 141], silk fibroin, [142], alginate [44], starch [143], hyaluronan–gelatin [55], and waterborne polyurethane [144, 145].

2. *Freeze-drying and hot-pressing technique*

Another method called freeze-drying and hot-pressing has also been used to prepare polymer/CW nanocomposites [37, 39, 40]. In this method, the blends of polymer and CW were also prepared in water medium to get well-dispersed aqueous mixtures, which were then freeze-dried to give nanocomposite powders, and the powders were consequently processed into specimen by hot-pressing. This method can be used only when a thermoplastic polymer is used as the matrix. If those polymers which would undergo crosslinking or have lower decomposition temperature than their melting temperature were used as the matrix polymers, their CW based nanocomposites cannot be prepared by this method since they are unable to be hot-pressed. Such polymers include waterborne polyurethane [144], vulcanized rubber [39, 141], chitosan [41, 141], and poly(vinyl alcohol) [42]. Their CW filled nanocomposites were predominantly prepared by casting and evaporating method. Polymer/CW nanocomposites produced by the two techniques usually showed different physical properties due to the different morphology of the composite and the fact that different interactions between whiskers can establish [37, 39, 141]. The distribution morphologies of CW in polymer matrix may be different for the composites obtained by casting and evaporating and freeze-drying and hot-pressing methods although aqueous mediums were used for the two techniques. The cryo-fractured surfaces for unvulcanized natural rubber/CW nanocomposties prepared by the two methods were comparatively observed by SEM as reported by Nair et al. [39] The SEM micrographs are shown in Fig. 3.27. In Fig. 3.27a, the CWs appear as white dots, which are distributed evenly throughout the evaporated unvulcanized natural rubber matrix.

It seems there is no significant difference between Figs. 3.27a (casted and evaporated film) and 3.27b (freeze-dried and hot-pressed film), however, there are broader smooth unfilled regions in Fig. 3.27b, which is an indication of poorer whisker distribution in freeze-dried and hot-pressed composites. The reason for the relatively poorer distribution might be ascribed to the self aggregation of CW during hot-pressing. So, casting-evaporating technique is a more effective way to prepare well-dispersed CW nanocomposites.

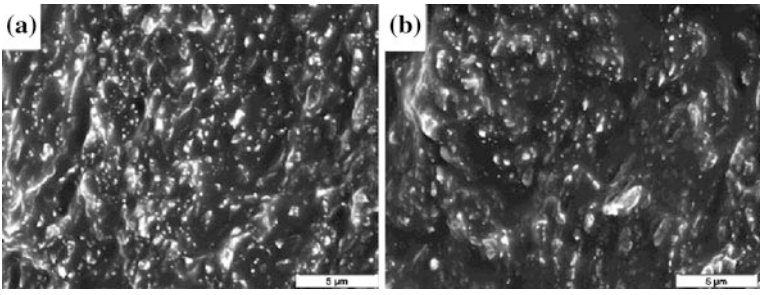

Fig. 3.27 Scanning electron micrographs of the cryo-fractured surfaces of unvulcanized natural rubber/CW obtained by casting and evaporating (**a**) and freeze-drying and hot-pressing (**b**) [39]

3. *Polymer grafting*

A solvent free technique, "graft from" strategy, was reported to prepare chitin whisker-graft polycaprolactone (CW-g-PCL) nanocomposites [146] CW powders were first obtained by lyophilization of CWs suspension. The CW-g-PCL nanocomposites were prepared by bulk ring-opening polymerization of caprolactone in the presence of CWs of which the surface hydroxyl groups work as initiation sites. The resulting products can be shaped by thermoforming. The shortcoming of this technique is that the amount of CWs is limited (less than 2 wt%) since high-molecular-weight PCL is unobtainable when the content of CWs is too high. Thus, strong reinforcement may not be anticipated with such small content of CWs.

4. *Non-aqueous solvent dispersion technique*

Same as other traditional nanoparticles, polysaccharide nanocrystals are also easy to self-aggregate and even form the agglomerates in micrometer scale. The self-aggregation reduces positive function of nanocrystals in nanocomposites [146]. There are a large number of hydroxyl groups on the surface of the polysaccharide nanocrystals, which make them hydrophilic. These hydroxyl groups endow two characteristics with polysaccharide nanocrystals. On one hand, they make polysaccharide nanocrystals thermodynamically immiscible with most of hydrophobic polymers; thus, it is difficult to achieve well dispersed nanocomposites through simple melt compounding of hydrophobic polymers with polysaccharide nanocrystals. PCL/CW nanocomposites were reported to be processed by melt compounding of poly(caprolactone) and freeze-dried CW, however, the morphology of the nanocomposite has not been shown thus the dispersion of whiskers in the polymer matrix cannot be evaluated [4]. On the other hand, these hydroxyl groups are very reactive thus make their modification very easy by various surface chemical reactions which are able to improve the hydrophobicity of polysaccharide nanocrystals [147, 148]. With improved hydrophobicity, these nanocrystals can disperse in non-aqueous solvents and be more compatible with hydrophobic polymers [149]. Therefore, melt compounding and non-aqueous solution mixing techniques are possible for preparing well dispersed polymer/polysaccharide nanocrystals reinforced nanocomposites. After surface hydrophobic modification, CWs can form a good dispersion in non-aqueous solvent, then, nanocomposites can be prepared in non-aqueous medium. The surface of crab shell CWs were chemically modified using different reactive compounds such as alkenyl succinic anhydride (ASA), phyenyl isocyanate (PI), and isopropenyl-α, α'-dimethylbenzyl (TMI). Figure 3.28 shows TEM images of CWs before and after modification. After surface chemical modification with ASA and PI, the appearance of the chitin fragments changed to be entangled, and individual whiskers were difficult to observe. The surface modified CWs can disperse in toluene and form stable dispersion, whereas, unmodified CWs cannot disperse in toluene. The natural rubber/CWs nanocomposites were prepared using toluene as a medium. The removal of toluene resulted in nanocomposites films in which CWs and natural rubber matrix showed improved adhesion [141].

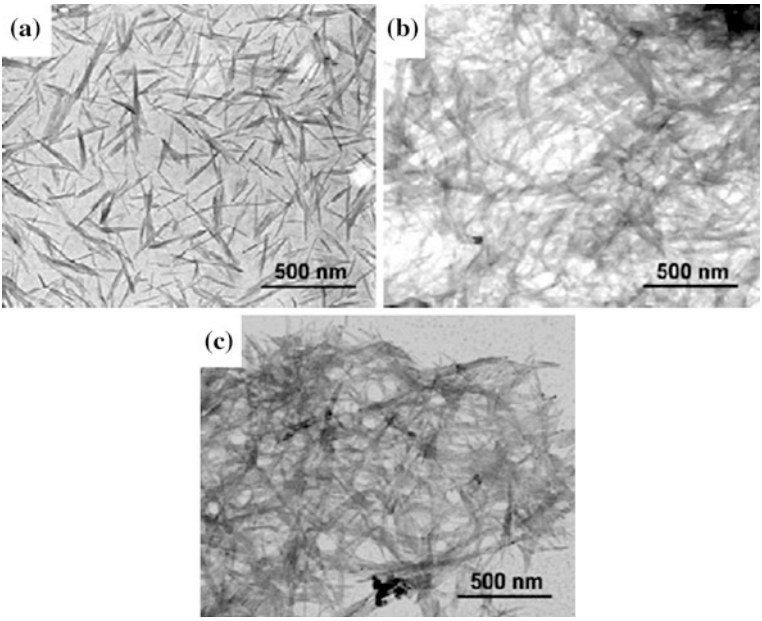

Fig. 3.28 Transmission electron micrographs of a dilute suspension of **a** unmodified, **b** ASA modified, and **c** PI-modified chitin whiskers [141]

5. *Extrusion and impregnation*

Very few studies have been reported concerning the processing of polysaccharide nanocrystal-reinforced nanocomposites by extrusion methods. The hydrophilic nature of polysaccharides causes irreversible agglomeration during drying and aggregation in non-polar matrices because of the formation of additional hydrogen bonds between amorphous parts of the nanoparticles. Therefore, the preparation of cellulose whiskers reinforced poly lactic acid (PLA) nanocomposites by melt extrusion was carried out by pumping the suspension of nanocrystals into the polymer melt during the extrusion process [150]. An attempt to use PVA as a compatibilizer for promoting the dispersion of cellulose whiskers within the PLA matrix was reported [151]. Organic acid chlorides-grafted cellulose whiskers were extruded with LDPE [152]. The homogeneity of the ensuing nanocomposite was found to increase with the length of the grafted chains.

An attempt to use a recently patented concept (Dispersed Nano-Objects Protective Encapsulation—DOPE process) intended to disperse carbon nanotubes in polymeric matrices was reported. Physically cross-linked alginate capsules were successfully formed in the presence of either cellulose whiskers or microfibrillated cellulose [153]. The resulting capsules were extruded with a thermoplastic material. Another possible processing technique of nanocomposites using cellulosic nanoparticles in the dry state present in the filtration of the aqueous suspension to obtain a film or dried mat of particles followed by immersion in a

polymer solution. The impregnation of the dried mat was performed under vacuum. Composites were processed by filling the cavities with transparent thermosetting resins such as phenol formaldehyde [154, 155], epoxy 178], acrylic [155–158] and melamine formaldehyde [159].

Nonwoven mats of cellulose microfibrils were also used to prepare polyurethane composite materials via film stacking method [160]. Water-redispersible nanofibrillated cellulose in powder form was recently prepared from refined bleached beech pulp by carboxymethylation and mechanical disintegration [161]. However, the carboxymethylated sample displayed a loss of crystallinity and strong decrease in thermal stability limiting its use for nanocomposite processing.

6. *Electrospinning*

Electrostatic fiber spinning or "electrospinning" is a versatile method to prepare fibers with diameters ranging from several microns down to below 100 nm through the action of electrostatic forces. It uses an electrical charge to draw a positively charged polymer solution from an orifice to a collector. Electrospinning shares characteristics of both electrospraying and conventional solution dry spinning of fibers. The process is non-invasive and does not require the use of coagulation chemistry or high temperatures to produce solid threads from solution. This makes the process particularly suited for the production of fibres using large and complex molecules. Bacterial cellulose whiskers were incorporated into POE nanofibers with a diameter of less than 1 μm by the electrospining process to enhance the mechanical properties of the electrospun fibers [162]. The whiskers were found to be globally well embedded and aligned inside the fibers, even though they were partially aggregated. Electrospun polystyrene (PS) [163], PCL [164] and PVA [165] microfibers reinforced with cellulose nanocrystals were obtained by electrospinning. Nonionic surfactant sorbitan monostearate was used to improve the dispersion of the particles in the hydrophobic PS matrix.

7. *Multilayer films*

The layer-by-layer assembly (LBL) is a method by which thin films particularly of oppositely charged layers are deposited. Thin film LBL assembly technique can also be utilized for nanoparticles. In general the LBL assembly is described as sequential adsorption of positive or negative charged species by alternatively dipping into the solutions. The excess or remaining solution after each adsorption step is rinsed with solvent and thus a thin layer of charged species on the surface ready for next adsorption step is obtained. There are many advantages of the LBL assembly technique and these include simplicity, universality and thickness control in nanoscale. Further the LBL assembly process does not require highly pure components and sophisticated hardware. For almost all-aqueous dispersion of even high molecular weight species, it is easy to find an LBL pair that can be useful for building thin layer. In each adsorption step, either a monolayer or a sub monolayer of the species is obtained and, therefore the number of adsorption steps needed for a particular nanoscale layer can be determined. The use of the LBL technique is expected to maximize the interaction between cellulose whiskers and a polar

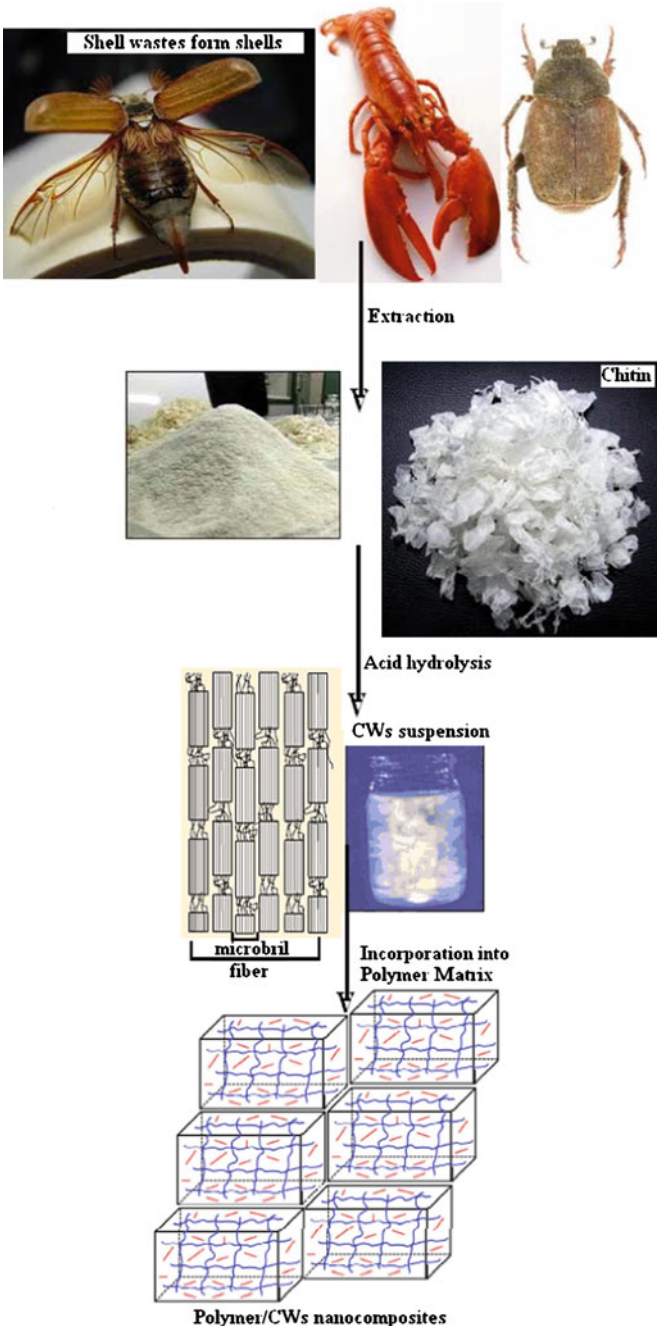

Fig. 3.29 Synthetic routes for the synthesis of polymer/chitin nanocomposites

polymeric matrix, such as chitosan [166]. It also allows the incorporation of high amounts of cellulose whiskers, presenting a dense and homogeneous distribution in each layer. Podsiadlo et al. [167] reported the preparation of cellulose whiskers multilayer composites with a polycation, poly-(dimethyldiallylammonium chloride) (PDDA), using the LBL technique. The authors concluded that the multilayer films presented high uniformity and dense packing of nanocrystals.

Orientated self-assembled films were also prepared using a strong magnetic film [168] or spin coating technique [169]. The preparation of thin films composed of alternating layers of orientated rigid cellulose whiskers and flexible polycation chains was reported [170]. Alignment of the rod-like nanocrystals was achieved using anisotropic suspensions of cellulose whiskers. Green composites based on cellulose nanocrystals/xyloglucan multilayers have been prepared using the non-electrostatic cellulose-hemicellulose interaction [171]. The thin films were characterized using neutron reflectivity experiments and AFM observations. More recently, biodegradable nanocomposites were obtained from LBL technique using highly deacetylated chitosan and cellulose whiskers [166]. Hydrogen bonds and electrostatic interactions between the negatively charged sulfate groups on the surface of nanoparticles and the ammonium groups of chitosan were the driving forces for the growth of the multilayered films. A high density and homogeneous distribution of cellulose nanocrystals adsorbed on each chitosan layer, each bilayer being around 7 nm thick, were reported. Self-organized films were also obtained using only charge-stabilized dispersions of celluloses nanoparticles with opposite charges [172] from the LBL technique.

The overall processing for the polymer chitin whiskers nanocomposites is outlined in Fig. 3.29.

3.7 Characterization of Chitin Nanocomposites and Blends

The properties of high performance chitin filled natural rubber (NR) nanocomposites were carefully analyzed by Gopalan et al. [72]. It was concluded that the whiskers form a rigid network in the NR matrix which is assumed to be governed by a percolation mechanism. A percolated filler–filler net work is formed by hydrogen bonding interaction between chitin particles above the percolation threshold. The values of diffusion coefficient, bound rubber content, and relative weight loss also supported the presence of a three-dimensional chitin network within the NR matrix. The mechanical behavior of the composites gives additional insight and evidence for this fact. Rujiravanit and coworkers [42] studied thermal stability of the chitin nanocomposites by TGA. The presence of the whiskers did not affect much the thermal stability and the apparent degree of crystallinity of the chitosan matrix. The tensile strength of α-chitin whisker-reinforced chitosan films increased from that of the pure chitosan film with initial increase in the whisker content to reach a maximum at the whisker content of 2.96 wt% and decreased gradually with further increase in the whisker content, while the percentage of

elongation at break decreased from that of the pure chitosan with initial increase in the whisker content and leveled off when the whisker content was greater than or equal to 2.96 wt %. The crystallinity of the PVA/chitin nanocomposites; the presence of the whiskers did not have any effect on the crystallinity of the PVA matrix [42]. They suggested that the cast PVA film was essentially amorphous for the α-chitin whiskers, their WAXD pattern exhibits two major scattering peaks at 2θ angles of about 9 and 19°, respectively, for the resulting α-chitin whisker reinforced PVA films. The WAXD patterns were intermediate to those of the pure components with the strong scattering peaks of α-chitin whiskers (i.e. at about 9 and 19°) being more pronounced with increasing whisker content. To verify whether or not incorporation of α-chitin whiskers into PVA resulted in an increase in the crystallinity of the PVA matrix, FT-IR spectra were considered. The peak at 1144 cm^{-1} (C–O of doubly H-bonded OH in crystalline regions) was useful for indication of the crystallinity of PVA. Apparently, the relative intensity of this peak was not found to increase with increasing whisker content, indicating that incorporation of α-chitin whiskers did not have an effect on the crystallinity of the PVA matrix. Lu et al. [38] described that the chitin filled SPI composites showed an increase in Young's modulus and tensile strength from 26 to 158 MPa and 3.3 to 8.4 MPa with increasing chitin contents from 0 to 20 wt%. As the chitin whiskers increase in the SPI matrix, the composites showed greater water-resistance. The improvement in all of the properties of these novel SPI/chitin whisker nanocomposites may be ascribed to three-dimensional networks of intermolecular hydrogen bonding interactions between filler and filler and between filler and SPI matrix. Spriupayo and co-workers [42] have determined the TGA thermograms of pure PVA, α-chitin whiskers, and α-chitin whisker-reinforced PVA nanocomposites films having whisker content of 14.8 and 29.6 wt %, respectively. All of the samples showed initial weight loss at about 60–80 °C, due to the loss of moisture upon heating. The moisture content in these samples was almost similar (i.e. about 8 %). According to the derivative TGA curves, pure PVA film exhibited a major degradation peak at 274 °C while as prepared α-chitin whiskers showed a major degradation peak at 347 °C curve (d)). The major degradation peaks for PVA films reinforced with 14.8 and 29.6 wt% α-chitin whiskers were intermediate to those of the pure components, with the thermal stability of the nanocomposite films increased with increasing α-chitin whisker content.

In another study, the bare and enzyme immobilized SiO_2-chitin/CNTs bio-nanocomposite was characterized with Fourier transform infrared spectroscopy (FTIR), scanning electron microscopy (SEM) and cyclic voltammetry (CV). In the FTIR spectra, the infrared peaks of chitin in SiO_2-chitin become wider and sharper due to overlap of functional groups of chitin and SiO_2, i.e., stretching vibration bands of Si–O–Si, Si–O–C and C–O bond. In addition, two new peaks appear at 1,300 and 785 cm^{-1} pertaining to stretching vibration of C–Si and bending vibration of C–H corresponding to CH_3-Si group [173]. On incorporation of CNTs in CH-SiO_2 hybrid, the infrared band corresponding to SiO_2 becomes broader and a new infrared band appears at 890 cm^{-1} revealing presence of CNTs that affects vibration mode of chitin and SiO_2 resulting in the formation of SiO_2-chitin/CNTs

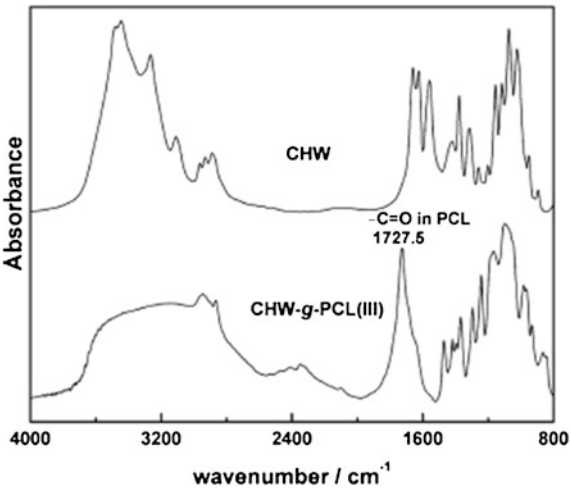

Fig. 3.30 FTIR spectra of the CW and CW-g-PCL(III) powders, where the CW-g-PCL(III) is used as the representative of grafted CW [174]

bio- nanocomposite. After immobilization of enzyme, FTIR bands corresponding to -NH/-OH group in nanobiocomposite become broader suggesting interaction between amino and hydroxyl group of chitin. However, presence of peaks at 1,672 and 1,442 cm^{-1} (corresponding to amide bands) indicates immobilization of enzymes. The surface morphology of SiO_2-chitin/CNTs reveals the monodispersed rope like structure of CNTs surrounded with globular appearance of SiO_2 particles into chitin matrix indicating that CNTs and SiO_2 are uniformly dispersed into the backbone of chitin. So it can be speculated that CNTs are rapped with chitin and SiO_2 via electrostatic interactions. The surface morphology of SiO_2-chitin/CNTs nanobiocomposite further changes after the immobilization of enzyme revealing attachment of enzymes over the electrode surface. Feng et al. [174] reported the structure and properties of new thermoforming bionanocomposites based on chitin whisker-graft-polycaprolactone (chitin-g-PCL).

FTIR spectra of the chitin-g-PCL(III) and chitin powders are depicted in Fig. 3.30. The spectrum of pure chitin was compared with that of spectrum of-chitin-g-PCL, the prominent change observed after grafting process was the appearance of one distinct peak located at 1727.5 cm^{-1} assigned to ester-carbonyl group of grafted PCL chains. It indicated that the PCL and chitin were successfully linked together. The SEM and TEM images of CW and CW-g-PCL(III) nano-particles are presented in Figs. 3.31 and 3.32 respectively.

Ramaprasad et al. [89] synthesized the chitin-polyaniline nanocomposite by electron beam irradiation method. UV–Vis spectra showed the decrease in the intensity of peak at 630 nm due to formation of low-energy electron beam *(*LEB*)* during irradiation. IR analysis showed the interaction between chitin and PANI. SEM micrograph showed the formation of chitin-PANI nanocomposite. XRD analysis confirmed the formation PANI particles in the blend solution.

Electrical study showed the increase in the conductivity due to irradiation up to certain level and then conductivity decreases. TGA analysis showed that blends

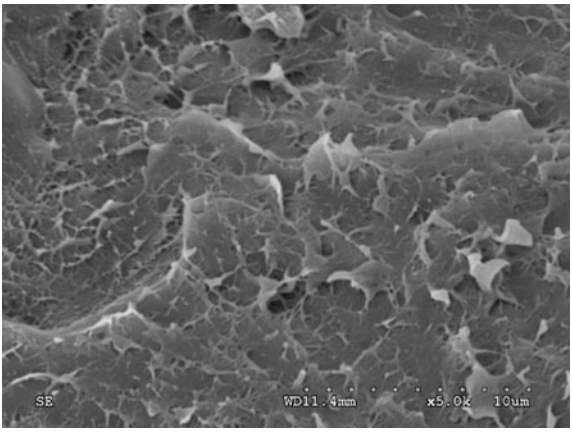

Fig. 3.31 SEM image of fractured surface for the thermoforming CW-g-PCL(III) sheet as the representative of all the sheets [174]

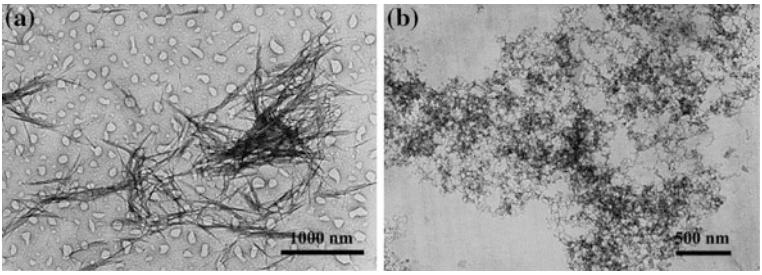

Fig. 3.32 TEM images of the CW and CW-g-PCL(III) nanoparticles, where the CW-g-PCL(III) is used as the representative of grafted CW [174]

are more stable after irradiation. Finally, the formation of PANI particle during irradiation in the blend solution is due to the presence of chitin, where as no particle formation is observed in pure PANI solution irradiated with electron beam. The detailed presentation of effect of radiation on chitin and PANI is presented in Fig. 3.33.

Zia et al. [115] presented that nanostructure and morphological pattern of chitin/bentonite clay based polyurethane bionanocomposites. The clay dispersion within chitin was characterized by both XRD and optical microscopy (OM), which is the most frequently, used and approachable methods to study the structure of nanocomposites. There are one acetamide ($-NHCOCH_3$) group at C-2 position and two (two hydroxy (–OH)) groups at C-3 (C3–OH) and C-6 (C6–OH) positions on chitin chains which can serve as the coordination and reaction sites [95]. The crystalline structure of chitin has been reported by many researchers [96].

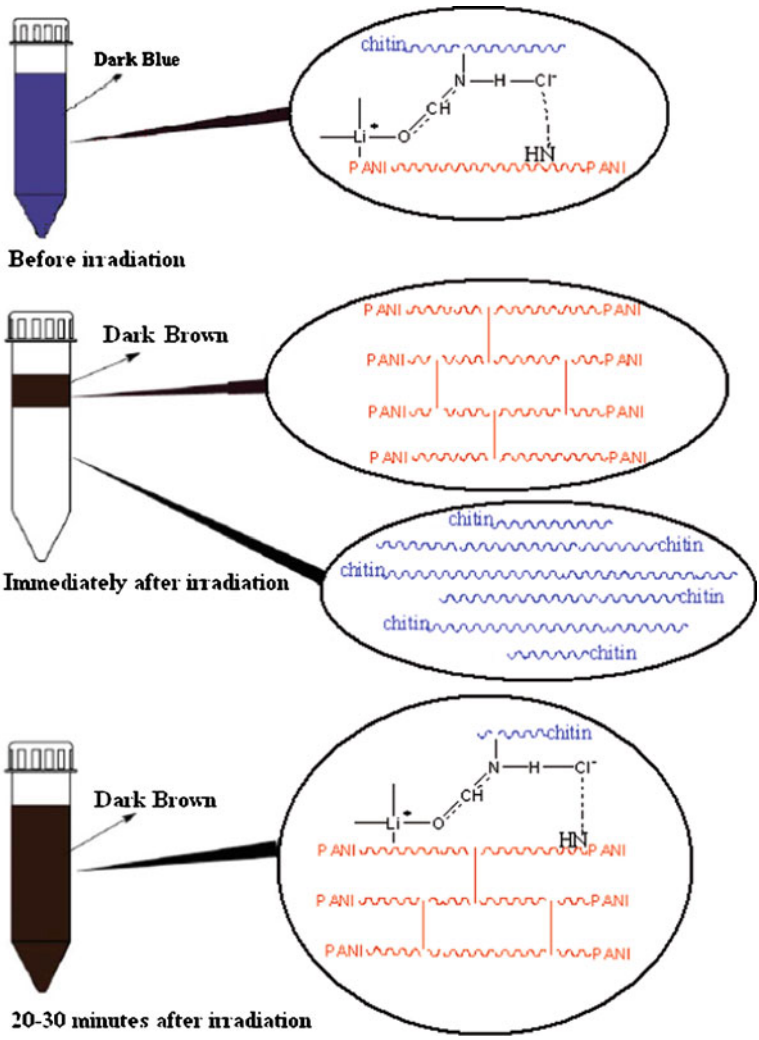

Fig. 3.33 Effect of radiation onto chitin and polyaniline [89]

3.7.1 Properties of Polymer/CW Nanocomposites

1. *Mechanical properties*

Tensile testing of single crystalline metallic microwhiskers can also be studied following the experimental tensile testing constructed by Brenner and (b) results of whisker fracture strength as a function of whisker size, showed the clear size dependence (Fig. 3.34). The chitin whiskers are usually incorporated into polymer matrix to prepare CWs reinforced polymer nanocomposite. Thus, the mechanical

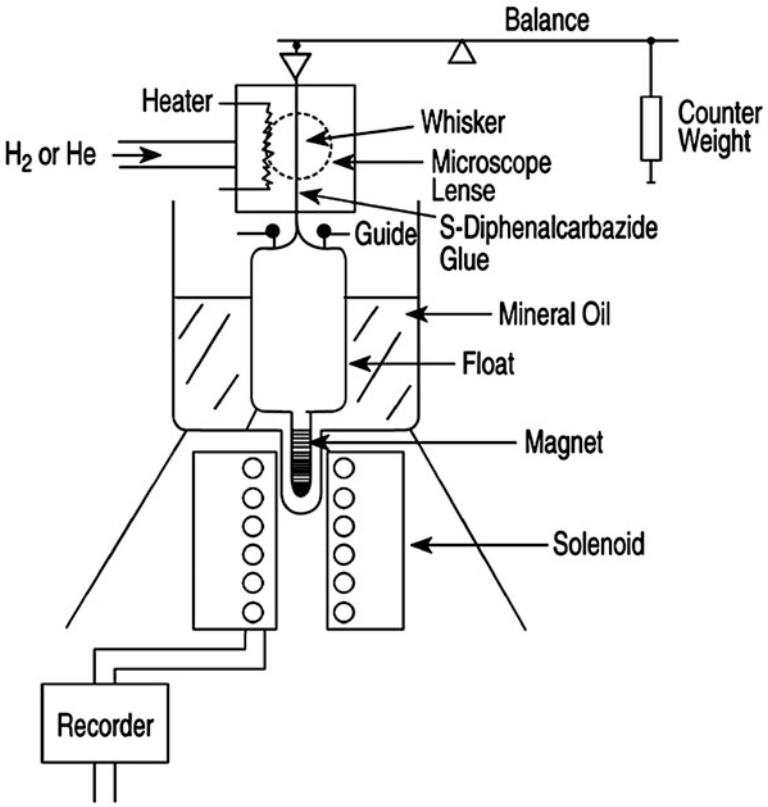

Fig. 3.34 Tensile testing of single crystalline metallic microwhiskers [175]

properties are of the first importance for CW reinforced nanocomposites. The improvement in mechanical properties especially modulus has been achieved in many polymer/CW systems. There are several factors which affect the reinforcing effect of polymer/CW nanocomposites, including the glass transition temperature of polymer matrix, the aspect ratio (L/D ratio) of CWs, the loading of CW, and nanocomposite processing techniques. Taking poly(S-*co*-BuA)/CW system for an example [175], at temperature range lower than *T*g of poly(S-*co*-BuA), the increase in storage shear modulus was very limited with CW obtained from squid pen chitin introduced or increased; however, when the temperature increased to higher than *T*g of poly(S-*co*-BuA), the relaxed modulus of the nanocomposites increased significantly when the loading of CW was more than 10 wt%, and more than 25 and 160 times improvement in modulus were achieved when CW loadings were 10 and 20 wt% at $\sim$300 K (*T*g + 25 °C), respectively. It was found that when CW loading was less than 5 wt%, almost no reinforcement occurred for poly(S-*co*-BuA)/CW nanocomposite. The reinforcing effect of the CW is much less pronounced than the one observed for tunicin whisker filled composites.

The differences in reinforcing effect of the two kinds of whiskers are ascribed to their different aspect ratios.

The reinforcing effect strongly depends on the aspect ratio of nanocrystals, and higher aspect ratio usually brings about greater reinforcement as been proved in comparative study of starch and cellulose nanocrystals [176]. The aspect ratio for tunicin whisker is around 50–200 [19], but that of squid pen chitin whisker is only about 15. When riftia tubes CWs with aspect ratio of 120 was used as nanofillers for poly(S-*co*-BuA), a significant modulus increase was observed even with only 1 wt% whisker loading [37]. The effects of processing methods on the mechanical properties of natural rubber/crab shell CW nanocomposites were investigated in detail by Nair et al. [39, 140]. The nanocomposites with unvulcanized natural rubber as the polymer matrix were prepared by two techniques, freeze-drying and hot-pressing method and casting and evaporating method. The samples prepared by casting and evaporating method showed higher reinforcing efficiency than those prepared by freeze-drying and hot-pressing method. It is believed that a three-dimensional CWs network was formed driving by the strong hydrogen bonding during evaporation method, as been proved by swelling behavior of composite films. The three dimensional network of cellulose whiskers was also reported to be formed during preparation of poly(S*co*-BuA)/CW and Mcl-PHA/CW nanocomposites by evaporation methods [17, 33]. The tensile properties of polymer matrix could be changed greatly by incorporation of CWs. Generally speaking, the tensile strength and Young's modulus could be improved at the cost of ductility. The CW loading plays an important role in the improvement of tensile properties of the nanocomposites. The optimum loadings are various for different polymer matrices and CW origins and usually less than 5 wt% since CW tends to aggregate with higher CW content, which will lead to negative effects on the mechanical properties. For poly (vinyl alcohol)/CW and chitosan/CW nanocomposites, the highest tensile strength was obtained with CW loading at 2.96 wt% [41, 42]. The maximum tensile strength for glycerol plasticized-potato starch (GPS)/CW [143] waterborne polyurethane/CW [145] and hyaluronan–gelatin/CW [55] nanocomposites happened at the CW loading of 5, 3, and 2 wt%, respectively. The elongation at break of all the related nanocomposites gradually decreased with increase of CW loading. CWs were also reported to reinforce polymer nanocomposites/nanofibers. The polymer/CW nanocomposites nanofibers are prepared by electrospinning or wet spinning of mixture of water soluble polymer aqueous solution and CW suspension. PVA/CW nanocomposite fiber mats with different amounts of CW were prepared by electronspinning, and the Young's modulus of the nanocomposite fiber mat was 4–8 times higher than that of neat PVA fiber mat. The storage modulus of PVA nanofiber mat increased with CW loading in the considered range. Alginate/CW nanocomposite fibers with 0.5–2.0 wt% CW were prepared by wet spinning. The incorporation of such low amount of CW in the nanocomposite fibers improved the mechanical properties significantly due to possible specific interactions, i.e., hydrogen bonding and electrostatic interactions, between the alginate molecules and the homogeneously dispersed CWs [44]. The surface modification of CW could also affect the mechanical properties of

polymer/CW nanocomposites. The crab shell CW was reported to be treated with PI, ASA and TMI separately and then incorporated into natural rubber matrix. The interactions between natural rubber matrix and CW increased by the surface treatment of CW, however, rubber/modified CW showed poorer mechanical properties compared to rubber/unmodified CW composites. The poorer reinforcing effect may be ascribed to lack of formation of whisker network after surface modification which would reduce the driving force of network formation and hydrogen bonding [141].

On the basis of the influence factors of reinforcing efficiency when using CW as reinforcing filler, we can conclude that high reinforcing effects are easier to be obtained when low *T*g polymers such as natural rubber and polycaprolactone were used as matrixes and that the reinforcing efficiency increased with aspect ratio of CW, which were similar to other nanocomposites consisting of polymer and inorganic nanofillers [177]. Although surface hydrophobic modification of CW could improve compatibility with polymers, the reinforcing effect could not be simultaneously improved since whisker network is difficult to be formed after surface modification.

2. *Swelling behavior*

The interaction of polymeric materials with solvents is a problem from technological points of view, since the dimensions and physical properties of materials may be changed due to the penetration of solvents into specimens. A rigid cellulose network can be formed within polymer matrix by three-dimensional hydrogen bonding between cellulose whiskers during the films formation, which is very helpful for hindering diffusion of solvent in the polymer matrix, thus improve solvent resistance of polymer/CW nanocomposites. Although the hydrogen bonding of chitin is somewhat weaker than cellulose, a similar rigid network can also be formed during the preparation of polymer/CW nanocomposites by casting-evaporation method. The swelling of vulcanized natural rubber/chitin whisker (PCH) nanocomposites, prepared by casting-evaporation, in toluene were investigated by Dufresne et al [39]. The toluene uptake of the PCH nanocomposites is rapid in the initial zone ($t < 5$ h), afterwards, the sorption rate decreases leading to a plateau, corresponding to equilibrium absorption. The equilibrium toluene uptake value of neat vulcanized natural rubber was 488 %, which gradually decreases to 413, 331, 282, and 239 % for the PCH nanocomposites with CW loading of 5, 10, 15 and 20 % respectively. The diffusion coefficient of toluene gradually decreases with increasing the loading of CW, down to 4.4×10^{-8} cm^2 s^{-1} for 20 % loading. The results were ascribed to the increased stiffness of chitin network and interactions between VNR and CW with increase of CW loading. Water resistance of hydrophilic polymers can also be improved by incorporation of CW to form nanocomposites. The water swelling of glycerol plasticized soy protein isolate/chitin whiskers (SPI/CW) nanocomposites was investigated by Lu et al. [38]. The water uptake SPI sheet was about 40 %, whereas that of the SPI/chitin nanocomposites decreases with increasing CW content, e.g., only about 23 % for SPI-30 composite, suggesting an improvement of water resistance. The

diffusion coefficient of water in SPI/CW nanocomposites was much lower than in SPI sheet. The results were also attributed to the formation of stronger chitin network with increase of CW content. The water absorption of other CW filled nanocomposites such as PVA/CW [42] and CS/CW [41] was also studied and similar results were obtained with incorporation and increasing loading of CW.

3. *Barrier properties*

Barrier properties increase shelf life period by protecting the inside product from deteriorations through oxidation, humidity or bacteria [16]. Polymer nanocomposites with well-dispersed nano-clay showed improved barrier properties compared with the neat polymer matrix. Starch nanocrystal showing platelet morphology similar to clay nanosheet can improve barrier properties of polymer matrix by forming nanocomposites [16, 178, 179]. Although cellulose whisker shows rodlike morphology, the improvement in barrier properties was also observed for polymer/CW nanocomposite [49, 180]. CW possesses similar morphology to cellulose whisker. The barrier properties of polymer/CW nanocomposites have not been investigated widely. Only Chang et al. [143] investigated the water vapor permeability (WVP) of glycerol plasticized starch/chitin nanoparticle (GPS/CNP) composites. WVP of GPS reached a peak value when the CNP content increased from 1 to 3 w %. The improvement in water vapor barrier by incorporation CNP was ascribed to the tortuous path for water molecules to pass through the composites [181].

4. *Thermal properties*

It has been reported that the glass transition temperature (Tg) of host polymers seems independent of CW concentration [37]; however, the Tg value of the host polymer was usually lower than those of their CW nanocomposites prepared by casting-evaporation technique [37, 145]. The increased Tg was ascribed to the fact that the existence of high specific area of CW in the composites would restrict the molecular mobility of polymer chains. For CW-g-PCL copolymer nanocomposites, the α-relaxation temperature determined by DMA gradually increased with increase of CW concentration, indicating that the segment mobility of PCL gradually decreased with CW concentration [146]. The melting point temperature (Tm) was also reported to be independent of the CW concentration for PCL/CW nanocomposites; however, the enthalpic changes at melting transition (ΔHm) and the deduced degree of crystallinity (xc) of PCL in nanocomposites were systemically lower than those of neat PCL, which might be due to the fact that CWs might slow down the crystallization kinetics of PCL [37, 40]. Nevertheless, the Tm and ΔHm of CW-g-PCL copolymer nanocomposites almost keep unchanged with CW concentration in the range of 1 ∼1.42 wt% has been reported by Feng [146]. The thermal stability of polymer/CW nanocomposites has been investigated occasionally. Most studies suggested that incorporation of CWs into polymer matrix improves thermal stability of the matrix very slightly especially when the content of CW was less than 10 % [41, 42, 55]. Some published references indicated that the onset decomposition temperature gradually increased with CW

content [40]. Limited researches demonstrated that the quite visible distinct increase in thermal stability could be achieved when the content of CW was high enough, for example 30 wt%, the improvement in thermal stability was ascribed to the increased matrix-CW interaction and the formed CW network with increase of CW content [144].

5. *Other properties*

Because of the reinforcing effect, CWs were incorporated into some potential biomedical materials, such as hydrogels and scaffolds, in which the materials have to possess non-cytotoxicity. When CW was incorporated into silk fibroin to form reinforced nanocomposite sponges, it not only improved the dimensional stability but also promote the cell spreading on the nanocomposite materials [142]. Zhang et al. [182] introduced three different polysaccharide nanocrystals into cyclodextrin/polymer inclusion supramolecular hydrogels to enhance mechanical strength and regulate drug release behavior of the hydrogels, and the in vitro cell viability of the extracted leached media from the nanocomposite and native hydrogels was evaluated by the MTT Cell *Proliferation* Assay using the L929 cell line. The results showed that incorporation of chitin whisker as well as cellulose and starch nanocrystals did not increase the cytotoxicity of the nanocomposite materials since they showed similar cell viability with native hydrogel. Hariraksapitak et al. [55] incorporated CW into hyaluronan–gelatin to manufacture reinforced nanocomposite scaffolds and investigated their cytotoxicity. The results suggested that with 10 wt% CW incorporated in the nanocomposite scaffold showed the greatest cell viability even higher than native scaffold. All the results suggested that CW is non-toxic and can be used in biomedical materials. One of the advantages of polysaccharide nanocrystals over inorganic nanofiller in reinforcing polymer nanocomposites is their biodegradability, which makes them very competitive particularly in reinforcing biodegradable thermoplastics since fully biodegradable nanocomposites can be produced. Watthanaphanit et al. [44] incorporated CW into alginate to produce reinforced nanocomposite fibers by wet spinning process. The biodegradation of the nanocomposite fibers was investigated in Tris–HCl buffer solution containing lysozyme and the results suggested that the addition of the CWs in the nanocomposite fibers could accelerate the biodegradation process.

3.8 Applications of Chitin and Their Nanocomposites and Blendes

3.8.1 Applications of Chitin Whicker and Chitosan Nano-Fibers

The blood compatibility of chitin and chitosan remains a prime aspect almost 20 years after Hirano reported his studies on chitosan and its acyl derivatives in 1985 [183]. A resurgence of these initial studies was reported by Lee et al. [184]

who confirmed the blood compatibility properties of N-acylchitosans. An N-acylation of 20–50 % was achieved and their susceptibility to lysozyme degradation was found to be comparable to acetyl-chitosan. Recent reports by Hirano et al. [185] concentrate on the production of chitosan collagen fibers that again were chemically modified and evaluated for their blood compatibility. The chitosan fiber was improved when collagen was added to chitosan as well as when the resultant chitosan-collagen fibers were N-derivatized. Anti-thrombogenic activity was obtained for collagen coated on N-acyl derivatized fibers similar to the results obtained in 1985. The chitosan fibers offer the potential of being fabricated into blood vessels and their blood compatibility results demonstrated in the recent work predicts well for applications where hemocompatibility is sought. Another noteworthy variation is the preparation of chitosan material that is subsequently chemically modified with an azide functionality to impart UV activation. Ishihara et al. [186] prepared a UV sensitive chitosan material that was crosslinked with lactose moieties to improve water solubility. The material, intended as a bioadhesive, was found to be non-cytotoxic and shown to have adhesive strength comparable to fibrin glue [187].

In order for chitin and chitosan to take their place as approved biomedical materials, two principal issues, biocompatibility and sterility, must be resolved [188]. These matters should be briefly discussed to reinforce their significance. Ikada and Tomihita [189] studied the degradation of chitin and chitosan films by lysozyme action and subcutaneous implant in a rat model. The rate of in vivo degradation was high for chitin reduction as the degree of deacetylation increased. Interestingly, the authors noted mild tissue reaction to chitosan. Similarly, Onishi and Machida [190] investigated the in vivo biodegradation of water-soluble chitosan using a mouse model. The approximately 50 % deacetylated material was found to be readily degraded and cleared by the animal suggesting no concerns in bioaccumulation. Other workers have looked at the effect of chitin and chitosan on biological systems. Tanaka et al. [191] found that when chitin and chitosan were administered orally or injected intra-peritoneally into a mice model, chitosan invoked a bigger reaction compared to chitin. Mori et al. [192] using cell culture assay, reported that chitin did not produce an acceleratory effect on L929 mouse fibroblasts proliferation. It was noted, however, that chitosan appeared to exhibit an inhibitory effect, attributing to the interaction of chitosan with growth factors thereby immobilizing the growth factors. This is in contrast to the report by Prasitsilp et al. [193] who found that a high degree of deacetylation in chitosan was more favorable for supporting cell growth, proliferation and attachment. This behavior was attributed to the electropositive nature of the amino group permitting interactions between chitosan and cells. It is clear that chitosan's effect on cell proliferation requires further study. Taking a different viewpoint, Fujinaga et al. [194] have chosen to study the effect of chitosan on wound healings. They found that chitosan accelerated the infiltration of polymorphonuclear (PMN) cells at the wound site. PMN also stimulated the production of osteopontin that promotes cell attachment, essential in tissue reorganization at the wound site. Okamoto et al. [195] found that chitin; neither chitosan nor glucosamine (chitosan monomer)

affected the proliferation of mouse 3T6 fetal fibroblasts or HUVEC (human umbilical vascular endothelial cells). However, the migration of cells, important during tissue reorganization, was affected by chitosan and glucosamine, warranting further study as to the effects of these biopolymers for wound healing applications. The authors suggest that further work should be performed to elucidate the mechanisms that chitin and chitosan invoke during wound healing [196]. Chitosan products intended for parenteral administration and those in contact with wounds will have to be sterilized before use. Common methods for the sterilization of pharmaceutical and medical products include exposure to dry heat, saturated steam, and ethylene oxide or γ radiation. Before any of these methods are endorsed for the sterilization of chitosan products, their effects on the properties and end performance of the polymer will have to be documented.

Lim et al. [197] have been active in evaluating the effects of dry heat, saturated steam and γ-irradiation on chitosan based membranes. Ethylene oxide was not evaluated as it involves a chemical reactant that may be more reactive with chitosan to generate by-products and warranted a separate and specifically designed study. Exposure to dry heat resulted in lower aqueous solubility for chitosan and in extreme cases, insolubility in acidic aqueous media. This was found to be related to interchain crosslink formation involving the NH_2 groups in chitosan. A reduction of 60 % in tensile strength and 53 % reduction in the strain at break point were also experienced [198]. Saturated steam was also found to significantly accelerate the rate and extent of thermal events in chitosan. Chitosan became water insoluble and lost 80 % of its original tensile strength retaining only 28 % of the original strain at break point. The γ- irradiation caused main chain scission events in chitosan [199]. Chitosan membranes irradiated with 2.5 M-rad in air experienced a 58 % increase in tensile strength and a 22–33 % decrease in the swelling index of the membrane. Applying anoxic conditions during irradiation significantly reduced the changes to membrane properties. On the basis of these findings, it may be concluded that γ-irradiation at 2.5 M-rad under anoxic conditions provides the best means of sterilization for chitosan products. This study is in contrast to the findings by Rao and Sharma, [200] who recommended steam autoclaving although irradiation was not included in their study. The long-term storage effects have also to be thoroughly investigated as it will have implications on the integrity of chitin and chitosan materials [201]. Therefore, there remains a lot of scope to explore in the area of sterilization and storage before the method of sterilization and storage conditions can be optimized.

3.8.2 Applications of Chitin Nanocomposites and Blends

New products are anticipated to be produced and the related physical properties for diverse applications need to be further investigated to take full advantage of the inexpensive and abundant annually occurring natural product, which coincides with sustainable development of human society. Recently, nano fibrous scaffolds

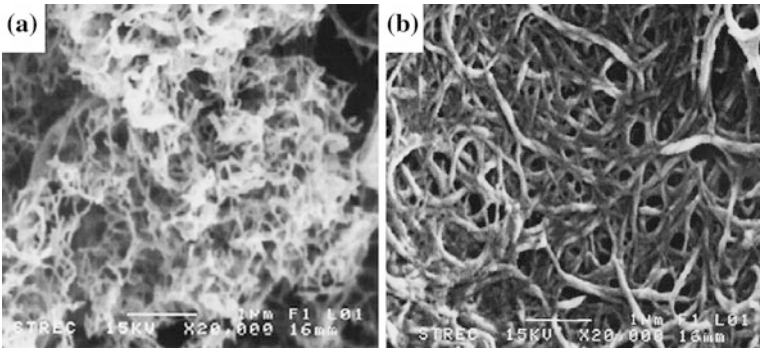

Fig. 3.35 SEM micrographs of **a** chitin flakes (×20,000), **b** chitosan flakes (×20,000) [216]

based on chitin or chitosan have potential applications in tissue engineering. Tissue engineering is one of the most exciting interdisciplinary and multidisciplinary research areas today, and there has been exponential growth in the number of research publications in this area in recent years. It involves the use of living cells, manipulated through their extracellular environment or combined process to develop biological substitutes for implantation into the body and/or to foster remodeling of tissues in some active manners. It was reported that CWs can be used as raw materials to produce chitosan nanoscaffolds [202–204]. Phongying et al. [202] found that three times treatment of CWs by 40 % w/v NaOH aqueous solution at 150 °C for 7 h for each time would generate chitosan with degree of deacetylation of as high as 98 %. The micrographs from scanning electron microscope (SEM) and transmission electron microscope (TEM) confirm that the short fiber of CWs develop itself to be a network in nano-scale of chitosan or chitosan nanoscaffold by the alkali treatment. The aggregation and packing morphology of CW and morphology of chitosan nanoscaffolds are shown in Fig. 3.35. The chitosan nanoscaffolds showed porous structure with the pore diameter of ~200 nm. The produced nanoscaffolds are assumed to be nontoxic since the treatments were carried out in aqueous solution and the polymer matrix was natural polysaccharide, thus, are able to be used as tissue engineering materials. Because of non-toxicity, biocompatibility and biodegradability, CWs themselves or modified products have the potential to be used in many food and biomedical related areas.

Chitin nanofibers were found to promote cell attachment and spreading of normal human keratinocytes and fibroblasts compared to chitin microfibers [205]. This may be a consequence of the high surface area available for cell attachment due to their three-dimensional features and high surface area to volume ratios, which are favorable parameters for cell attachment, growth, and proliferation. The cell studies conducted on chitin/poly(glycolic acid) (chitin/PGA) [206] and chitin/silk fibroin (SF) [207] fibrous mats proved that a matrix consisting of 25 % PGA or SF and 75 % chitin had the best results. The chitin/PGA fibers had a bovine serum albumin coating and are considered as a good candidate for use in tissue-

engineering scaffold because normal human epidermal fibroblasts (NHEF) attached and spread. The chitin/SF fibrous mats had the highest spreading of NHEF and normal human epidermal keratinocytes (NHEK). Therefore, this scaffold is suggested for wound tissue engineering applications. Shalumon et al. [208] developed carboxymethyl cellulose/polyvinyl alcohol (CMC/PVA) blend nanofibrous scaffold for tissue engineering applications. The prepared nanofibers were bioactive and biocompatible. Cytotoxicity and cell attachment studies of the nanofibrous scaffold indicate that the nanofibrous CMC/PVA scaffolds can be safely used for tissue engineering applications. Bhattarai et al. [209] reported that the chitosan/polyethylene oxide (PEO) nanofibrous scaffolds promoted the attachment of human osteoblasts and chondrocytes and maintained characteristic cell morphology and viability throughout the period of study. This nanofibrous matrix is of particular interest in tissue engineering for controlled drug release and tissue remodeling. Similarly, Subramaniyan et al. [210] prepared chitosan/PEO nanofibers for cartilage tissue engineering. Cells were attached to the chitosan/PEO nanofiber mats slowly in the fist week. After 10 days, the more cells were attached on the surface of the nanofibers. These results indicated that the electrospun chitosan/PEO mats have been used for cartilage tissue repair. Mo et al. [211] also reported the smooth muscle cells attachment to the electrospun chitosan/collagen nanofibers after 30 days of culture.

The biological evaluations of chitosan/hydroxyapatite (HAp) nanfibrous composite scaffolds have been reported [212]. The chitosan/HAp nanofibrous scaffolds have significantly stimulated the bone forming ability as shown by the cell proliferation, mineral deposition, and morphology observation, due to the excellent osteoconductivity of HAp compared to the controlled chitosan. The results obtained from this study highlight the great potential of using the chitosan/HAp nanocomposite nanofibers for bone tissue engineering applications. A biocomposite of HAp with electrospun nanofibrous scaffolds was prepared by using chitosan/PVA and *N*-CECS/PVA for tissue engineering applications [213]. The cell studies showed that the L929 cell culture revealed the attachment and growth of mouse fibroblast on the surface of biocomposite scaffolds. Similarly, the potential use of the *N*-CECS/PVA electrospun fiber mats as scaffolding materials for skin regeneration was evaluated in vitro using L929 [214]. Indirect cytotoxicity assessment of the fiber mats indicated that the *N*-CECS/PVA electrospun mat was nontoxic to the L929 cell. Cell culture results showed that fibrous mats were good in promoting the cell attachment and proliferation. This novel electrospun matrix would be used as potential wound dressing for skin regeneration.

Liver tissue engineering requires a perfect extracellular matrix (ECM) for primary hepatocytes culture to maintain high level of liver-specific functions and desirable mechanical stability. Feng et al. [214] developed novel galactose/chitin (GC) nanofibers with surface galactose ligands to enhance the bioactivity and mechanical stability of primary hepatocytes in culture. The GC nanofibrous scaffolds displayed slow degradation and suitable mechanical properties as an ECM for hepatocytes according to the evaluation of disintegration and Young's modulus testing. The hepatocytes cultured on GC nanofibrous scaffold formed

stably immobilized 3D flat aggregates and exhibited superior cell bioactivity with higher levels of liver-specific function maintenance in terms of albumin secretion, urea synthesis and cytochrome P-450 enzyme than 3D spheroid aggregates formed on GC films. These results suggested that the GC-based nanofibrous scaffolds could be useful for various applications such as bioartificial liver-assist devices and tissue engineering for liver regeneration as primary hepatocytes culture substrates.

The plant and animal nanofibers (derived from waste and biomass) are uniformly mixed with resins and other polymers like plastics and rubbers to create natural based composite materials. A variety of plant fibers with high tensile strength can be used including kenaf, industrial hemp, flax, jute, sisal, coir etc. Fibers can be combined with traditional resins or newer plant based resins. The resulting component is a plant based alternative for many traditional steel and fiberglass applications. Advantages of bionanocomposites over traditional composites are reduced weight, increased flexibility, greater moldability, reduced cost, sound insulation and renewable nature. For environmental awareness and the international demand for green technology, nanobiocomposites have the potential to replace present petrochemical-based materials. They represent an important element of future waste disposal strategies. In true bionanocomposites, both the reinforcing material such as a natural fiber and the matrix are biodegradable. Cellulose, chitin and starch are the most abundant organic compounds in nature; they are also inexpensive, biodegradable, and renewable. They obviously receive a great attention for non-food applications. The use of natural fibers instead of traditional reinforcement materials, such as glass fibers, carbon, and talc, provides several advantages including low density, low cost, good specific mechanical properties, reduced tool wear, and biodegradability. These important applications include packaging, environment-friendly biodegradable composites, biomedical composites for drug/gene delivery, tissue engineering applications and cosmetic orthodontics. They often mimic the structures of the living materials involved in the process in addition to the strengthening properties of the matrix that was used but still providing biocompatibility, e.g. in creating scaffolds in bone tissue engineering.

3.9 Conclusion and Future Prospective

This chapter has demonstrated the utility of chitin and chitosan as potential materials for various implant applications and some of the challenges in demonstrating biocompatibility as well as sterility that must be addressed. The eventual realizations of real implants await the take-up of these materials on a more commercial basis that would see the introduction of chitin-based implantable devices. Chitin and its deacetylated derivative, chitosan, are non-toxic, biodegradable biopolymers currently being developed for use in biomedical applications such as tissue engineering scaffolds, wound dressings, separation membranes, antibacterial coatings, stent coatings, and sensors. Nano fibrous scaffolds based on chitin or chitosan have potential applications in tissue engineering. Electrospun

chitin and chitosan nano fibrous scaffolds would be used to produce tissue engineering scaffolds with improved cytocompatibility, which could mimic the native extracellular matrix (ECM). The preparation and tissue engineering applications of chitin and chitosan based nanofibers has also been summarized. Additional studies are necessary before clinical applications and for commercialization of the chitin and chitosan based nanofibers. This chapter will help to bring about newer innovative ideas for chitin andchitosan nanofibers for tissue engineering and other biomedical applications inthe future. Chitin and chitosan seem to be excellent dressing materials for the wound healing. The recent progress of chitin and chitosan-based fibrous materials, hydrogels, membranes, scaffolds and sponges in wound dressing has been overviewed. In the area of wound management, the use of chitin, chitosan and its derivative is immense.

As renewable and biodegradable nanoparticles, chitin whiskers are attracting and will continuously draw attention from both academic and industrial fields. Similar to cellulose whisker, with so many advantages over conventional inorganic nanoparticles such as low density, non-toxicity, biodegradability, biocompatibility and easy surface modification and functionalization, chitin whiskers, within or without modification, are supposed to find extensive application in many areas such as reinforcing nanocomposites, cosmetic, food industry, drug delivery, tissue engineering. However, recent studies have mainly focused on the preparation and applications of nanocomposite based on chitin whiskers; less attention has been paid on other application areas. For the future studies, more attention should be focused on developing novel applications of chitin whiskers. Even for the chitin reinforced nanocomposites, there will still be a lot of valuable works to be done for future research, for example, developing new simple and effective processing methods so as to commercialize high performance polymer/chitin whisker composites, producing polymer nanocomposites filled with individual chitin whiskers which would create much more reinforcing efficiency than the conventional chitin whisker due to the high aspect ratio of individual chitin whisker. Then, great endeavors are necessary to make this area more prosperous and fruitful. In a word, there are abundant of opportunities combined with challenges in chitin whisker related scientific and industrial fields.

References

1. Richard, A.G.: The Integument of Arthropods. University of Minnesota Press, Minneapolis (1951)
2. Rudall, K.M.: Conformation of chitin-protein complexes. In: Ramachandran, G.N. (ed.) Conformation of Biopolymers. Academic, London (1967)
3. Weis-Fogh, T.: Structure and formation of insect cuticle. Symposia R. Entomolo. Soc. **5**, 165–183 (1970)
4. Kumar, M.N.V.R.: A review of chitin and chitosan application. React. Funct. Polym. **46**, 1–27 (2000)
5. Kobayashi, S., Kiyosada, T.: Shoda, S.-i.: Synthesis of artificial chitin: irreversible catalytic behavior of glycosyl hydrolase through a transition state analogue substrate. J. Am. Chem. Soc. **118**, 13113–13114 (1996)

6. Sakamoto, J., Sugiyama, J., Kimura, S., Imai, T., Itoh, T., Watanabe, T., Kobayashi, S.: Artificial Chitin Spherulites Composed of Single Crystalline Ribbons of alpha-Chitin via Enzymatic Polymerization. Macromolecules. **33**, 4155–4160 (2000)
7. Kadokawa J.-i.: Precision polysaccharide synthesis catalyzed by enzymes. Chem. Rev. 111, 4308–4345 (2011)
8. Ravikumar, M.N.V.B.: Chitin and chitosan fibres: a review. Mater. Sci.C. 22, 905–915 (1999)
9. Rinaudo, M.: Chitin and chitosan: Properties and applications. Prog. Polym. Sci. **31**, 603–632 (2006a)
10. Pillai, C.K.S., Paul, W., Sharma, C.P.: Chitin and chitosan polymers: Chemistry, solubility and fiber formation. Prog. Polym. Sci. **34**, 641–678 (2009)
11. Bordes, P., Pollet, E., Averous, L.: Nano-biocomposites: Biodegradable polyester/nanoclay systems. Prog. Polym. Sci. **34**, 125–155 (2009a)
12. Okada, A., Usuki, A.: Macromolecular Materials and Engineering Twenty Years of Polymer-Clay Nanocomposites. Macromol. Mater. Eng. **291**, 1449–1476 (2006)
13. Usuki, A., Hasegawa, N., Kato, M.: Polymer-clay nanocomposites. Adv. Polym. Sci. **179**, 135–195 (2005)
14. Chen, B.Q., Evans, J.R.G.: Impact strength of polymer-clay nanocomposites. Soft Matter. **5**, 3572–3584 (2009)
15. Le Corre, D., Bras, J., Dufresne, A.: Starch Nanoparticles: A Review. Biomacromolecules. **11**, 1139–1153 (2010)
16. Favier, V., Chanzy, H., Cavaille, J.Y.: Polymer nanocomposites reinforced by cellulose whiskers. Macromolecules. **28**, 6365–6367 (1995)
17. Habibi, Y., Lucia, L.A., Rojas, O.: Cellulose nanocrystals: chemistry, self-assembly, and applications. Chem Review. J. Chem. Rev. **110**, 3479–3500 (2010)
18. Chen, L., Zhu, M.F., Song, L.Y., Yu, H., Zhang, Y., Chen, Y.M., Adler, H.: Crystallization behavior and thermal properties of blends of poly(3-hydroxybutyrateco-3-valerate) and poly(1,2-propandiolcarbonate). J. Macromol. Symp. **210**, 241–250 (2004)
19. Angles, M.N., Dufresne, A.: Plasticized starch/tunicin whiskers nanocomposites. 1. Structural analysis. Macromolecules. **33**, 8344–8353 (2000)
20. Angles, M.N., Dufresne, A.: A. Plasticized starch/tunicin whiskers nanocomposite materials. 2. Mechanical behavior. Macromolecules. **34**, 2921–2931 (2001)
21. Samir, M.A.S.A., Alloin, F., Dufresne, A.: Review of recent research into cellulosic whiskers, their properties and their applications in nanocomposite field. Biomacromolecules. **6**, 612–626 (2005)
22. Siqueira, G., Bras, J., Dufresne, A.: Cellulosic BioNCs: A review of preparation. Properties and applications. Polymers. **2**, 728–765 (2010a)
23. Klemm, D., Kramer, F., Moritz, S., Lindstrom, T., Ankerfors, M., Gray, D., Dorris, A.: "Nanocelluloses: A new family of nature-based materials. Angew. Chem. Int. Ed. **50**, 5438–5466 (2011)
24. Siqueira, G., Bras, J., Dufresne, A.: Cellulose Whiskers versus Microfibrils: Influence of the Nature of the Nanoparticle and its Surface Functionalization on the Thermal and Mechanical Properties of Nanocomposites. Biomacromolecules. **10**, 425–432 (2009)
25. Dufresne, A.: Cellulose Whiskers versus Microfibrils: Influence of the Nature of the Nanoparticle and its Surface Functionalization on the Thermal and Mechanical Properties of Nanocomposites. Can. J. Chem. **86**, 484–494 (2008)
26. Fan, Y., Saito, T., Isogai, A.: Preparation of chitin nanofibers from squid pen beta-chitin by simple mechanical treatment under acid conditions. Biomacromolecules. **9**, 1919–1923 (2008a)
27. Revol, J.-F., Marchessault, R.H.: In vitro nematic ordering of chitin crystallites. Int. J. Biol. Macromol. **15**, 329–335 (1993a)
28. Marchessault, R.H., Morehead, F.F., Walter, N.M.: Liquid crystal systems from fibrillar polysaccharides. Nature. **184**, 632–633 (1959a)

29. Li, J., Revol, J.F., Naranjo, E., Marchessault, R.H.: Effect of electrostatic interaction on phase separation behaviour of chitin crystallite suspensions. Int. J. Biol. Macromol. **18**, 177–187 (1996a)
30. Roberts, G.: Chitin Chemistry. Macmillan, London (1998a)
31. Giraud-Guille, M.M., Belamie, E., Mosser, G.: Organic and mineral network in carapaces, bones and biomimetic materials. Comptes Rendus Palevol. **3**, 503–513 (2004)
32. Marchessault, R.H., Morehead, F.F., Walter, N.M.: Liquid crystal systems from fibrillar polysaccharides. Nature. **184**, 632–633 (1959b)
33. Dufresne, A., Kellerhals, M.B., Witholt, B.: Transcrystallization in mcl-PHAs/ cellulose whiskers composites. Macromolecules. **32**, 7396–7401 (1999)
34. Revol, J.-F., Marchessault, R.H.: In vitro chiral nematic ordering of chitin crystallites. Int. J. Biol. Macromol. **15**, 329–335 (1993b)
35. Li, J., Revol, J.F., Marchessault, R.H.: Rheological properties of aqueous suspensions of chitin crystallites. J. Colloid Interface Sci. **183**, 365–373 (1996b)
36. Paillet, M., Dufresne, A.: Chitin whiskers reinforced thermoplastic nanocomposites. Macromolecules. **34**, 6527–6530 (2001)
37. Morin, A., Dufresne, A.: Nanocomposites of chitin whiskers from Riftia tubes and poly(caprolactone). Macromolecules. **35**, 2190–2199 (2002)
38. Lu, Y.S., Weng, L.H., Zhang, L.N.: Morphology and properties of soy protein isolate thermoplastics reinforced with chitin whiskers. Biomacromolecules. **5**, 1046–1051 (2004)
39. Nair, K.G., Dufresne, A.: "Crab shell chitin whisker reinforced natural rubber nanocomposites. 1. Biomacromolecules. **4**, 657–665 (2003a)
40. Wu, X., Torres, F.G., Vilaseca, F., Peijs, T.: Influence of the processing conditions on the mechanical properties of chitin whisker reinforced poly(caprolactone) nanocomposites. J. Biobased Mater. Bio. **1**, 341–350 (2007)
41. Sriupayo, J., Supaphol, P., Blackwell, J., Rujiravanit, R.: Preparation and characterization of @a-chitin whisker-reinforced chitosan nanocomposite films with or without heat treatment. Carbohydr. Polym. **62**, 130–136 (2005a)
42. Sriupayo, J., Supaphol, P., Blackwell, J., Rujiravanit, R.: Preparation and characterization of α-chitin whisker-reinforced poly(vinyl alcohol) nanocomposite films with or without heat treatment. Polymer. **46**, 5637–5644 (2005b)
43. Goodrich, J.D., Winter, W.T.: α-Chitin Nanocrystals Prepared from shrimp shells and their specific surface area measurement. Biomacromolecules. **8**, 252–257 (2007)
44. Watthanaphanit, A., Supaphol, P., Tamura, H., Tokura, S., Rujiravanit, R.: Fabrication, structure and properties of chitin whisker-reinforced alginate nanocomposite fibers. J. Appl. Polym. Sci. **110**, 890–899 (2008)
45. Clark, G.L., Smith, A.F.: X-ray diffraction studies of chitin, chitosan and derivatives. J. Phys. Chem. **40**, 863–879 (1936a)
46. Montanari, S., Rountani, M., Heux, L., Vignon, M.R.: Topochemistry of carboxylated cellulose nanocrystals resulting from TEMPO-mediated oxidation. Macromolecules. **38**, 1665–1671 (2005)
47. Saito, T., Nishiyama, Y., Putaux, J.L., Vignon, M., Isogai, A.: Natural Polymers: Volume 2: Nanocomposites. Biomacromolecules. **7**, 1687–1691 (2006)
48. Fukuzumi, H., Saito, T., Wata, T., Kumamoto, Y., Isogai, A.: Transparent and high gas barrier films of cellulose nanofibers prepared by TEMPO-mediated oxidation. Biomacromolecules. **10**, 162–165 (2009)
49. Ishii, D., Saito, T., Isogai, A.: Viscoelastic Evaluation of Average Length of Cellulose Nanofibers Prepared by TEMPO-Mediated Oxidation. Biomacromolecules. **12**, 548–550 (2011)
50. Saito, Y., Putaux, J.-L., Okano, T., Gaill, F., Chanzy, H.: Structural aspects of the swelling of chitin in HCl and its conversion into α-chitin. Macromolecules. **30**, 3867–3873 (1997)
51. Fan, Y., Saito, T., Isogai, A.: Chitin nanocrystals prepared by TEMPO-mediated oxidation of alpha-chitin. Biomacromolecules. **9**, 192–198 (2008b)

52. Fan, Y.M., Saito, T., Isogai, A.: Individual chitin nano-whiskers prepared from partially deacetylated α-chitin by fibril surface cationization. Carbohydr. Polym. **79**, 1046–1051 (2010)
53. Hariraksapitak, P., Supaphol, P.: Preparation and properties of a-chitin-whisker-reinforced hyaluronangelatin nanocomposite scaffolds. J. Appl. Polym. Sci. **117**, 3406–3418 (2010)
54. Bustos, R.O., Healy, M.G.: Proceedings Icheme Research Event. London **4–6**, 126–128 (1994)
55. Phongying, S., Aiba, S., Chirachanchai, S.: Direct chitosan nanoscaffold formation via chitin whiskers. Polymer. **48**, 393–400 (2007)
56. Horton, D., Lineback, D.R.: N-deacetylation, chitodan from chitin. In: Whistler, R.L., Wolfson, M.L. (eds.) Methods in Carbohydrate Chemistry, p. 403. Academic, New York (1965)
57. Park, S.-I., Zhao, Y.: Incorporation of a high concentration of mineral or vitamin into chitosan-based films. J. Agric. Food Chem. **52**, 1933–1939 (2004)
58. Domard, A., Rinadudo, M.I.: Preparation and characterization of fully deacetylated chitosan. J. Biol. Macromol. **5**, 49–52 (1983)
59. Pelletier, A., Lemire, I., Sygusch, J., Chornet, E., Overend, R.P.: Chitin/chitosan transformation by thermo-mechano-chemical treatment including characterization by enzymatic depolymerization. Biotechnol. Bioeng. **36**, 310–315 (1990)
60. Focher, B., Beltrane, P.L., Naggi, A., Torri, G.: Alkaline N-deacetylation of chitin enhanced by flash treatments: Reaction kinetics and structure modifications. Carbohydr. Polym. **12**, 405–418 (1990)
61. Goycoolea, F.M., Higuera, C.I., Hernandez, J.L.J., García, K.D.: Advances in Chitin Science. Lyon: Jacques André, pp. 78–83 (1998)
62. Mima, S., Miya, M., Iwamoto, R., Yoshikawa, S.: Microwave technique for efficient deacetylation of chitin nanowhiskers to a chitosan nanoscaffold. J Appl. Polym. Sci. **28**, 1909–1917 (1983)
63. Gooday, G.W., Prosser, J.I., Hillman, K., Cross, M.G.: Functional characterization of chitin and chitosan. Biochem. Syst. Ecol. **19**(5), 395–400 (1991)
64. Lertwattanaseri, T., Ichikawa, N., Mizoguchi, T., Tanaka, Y., Chirachanchai, S.: Natural Chelating Polymers. Carbohydr. Res. **344**, 331–335 (2009a)
65. Aranaz, I., Mengíbar, M., Harris, R., Paños, I., Miralles, B., Acosta, N., Galed, G., Heras, A.: Functional characterization of chitin and chitosan. Curr. Chem. Biol. **3**, 203–230 (2009a)
66. Muzzarelli, R.A.A.: In: Muzzarelli, R.A.A. (ed.) Chitin Handbook, pp. 153–65. Grottamore, European Chitin Society (1977)
67. Choi, W., Ahn, K., Lee, D., Byun, M., Park, H.: Preparation of chitosan oligomers by irradiation. Polym. Degrad. Stabil. **78**, 533–538 (2002)
68. Kassai, M.: A review of several reported procedures to determine the degree of N-acetylation for chitin and chitosan using infrared spectroscopy. Carbohydr. Polym. **71**, 497–508 (2008)
69. Nair, K.G., Dufresne, A.: Crab shell chitin whisker reinforced natural rubber nanocomposites. Biomacromolecules. **4**, 657–665 (2003b)
70. Kvien, I., Bjørn, S.T., Oksman, K.J.: Characterization of cellulose whiskers and their nanocomposites by atomic force and electron microscopy. Biomacromolecules. **6**, 3160–3165 (2005)
71. Gopalan, K.N., Dufresne, A.: Effect of chemical modification of chitin whiskers. J. Biomacromolecules. **4**, 1835–1842 (2003a)
72. Gopalan, N.K., Dufresne, A.: Crab shell chitin whisker reinforced natural rubber nanocomposites. 1. Processing and swelling behavior. J. Biomacromolecules. **4**, 657–665 (2003b)
73. Michel, P., Dufresne, A.: Chitin Whisker Reinforced Thermoplastic Nanocomposites. J. Macromolecules. **34**, 19 (2001)
74. M. Wada., Y. Saito.: J. Polym. Sci. B: Lateral thermal expansion of chitin crystals. Polym. Phys. 39, 168–174 (2001)

75. Feng, F., Liu, Y., Hu, K.: Influence of alkali-freezing treatment on the solid state structure of chitin. Carbohydr. Res. **339**, 2321–2324 (2004)
76. Li, J., Revol, J.F., Marchessault, R.H.: Effect of degree of deacetylation of chitin on the properties of chitin crystallites. J. Appl. Polym. Sci. **65**, 373–380 (1997)
77. Jayakumar, R., Tamura, T.: Synthesis, characterization and thermal properties of chitin-&-poly(€-caprolactone) copolymers by using chitin gel. Int. J. Biol. Macromol. **43**, 32–36 (2008)
78. Mathew, A.P., Laborie, M.P.G., Oksman, K.: Cross-linked chitosan α-chitin whiskers nanocomposites with improved permeation selectivity and pH stability. J. Biomacromolecules. **10**, 1627–1632 (2009)
79. Hein, S., Ng, C. H., Chandrkrachang, S., Stevens, W.F.: A systematic approach to quality assessmentsystem of chitosan. Chitin and Chitosan: Chitin and Chitosan in Life Science. Yamaguchi. 327–335 (2001)
80. ISO 10993-18:200s5 Biological evaluation of medical devices, Part 18: Chemical characterizations of material
81. ISO/DIS 10993-19 Biological evaluation of medical devices, Part 19: Physico-chemical, mechanical and morphological characterization
82. Sriupayo, J., Supaphol, P., Blackwell, J., Rujiravanit, R.J.: Preparation and characterization of α-chitin whisker-reinforced poly(vinyl alcohol) nanocomposite films with or without heat treatment. Polymer. **46**, 5637–5644 (2005c)
83. Angellier, H., Boisseau, S.M., Lebrun, L., Dufresne, A.: Processing and structural properties of waxy maize starch nanocrystals reinforced natural rubber. J. Macromolecules. **38**, 3783–3792 (2005a)
84. Alonso, B., Belamie, E.: Chitin–Silica Nanocomposites by Self-Assembly. Angewandte. Chemie. **122**(44), 8377–8380 (2010)
85. Feng, L., Zhou, Z., Dufresne, L., Huang, J., Wei, M., An, L.J.: Structure and Properties of New Thermoforming Bionanocomposites Based on Chitin Whisker-Graft-Polycaprolactone. Appl. Polym. Sci. **112**, 2830–2837 (2009a)
86. Van de Velde, K., Kiekens, P.: Structure analysis and degree of substitution of chitin, chitosan and dibutyrylchitin by FT-IR spectroscopy and solid state ^{13}C NMR. Carbohydr. Polym. **58**, 409–416 (2004)
87. Varum, K.M., Antohonsen, M.W., Grasdalen, H., Smidsrod, O.: Determination Of The Degree Of N-Acetylation And The Distributionof N-Acetyl Groups In Partially N-Deacetylated Chitins (Chitosans)By High-Field NMR-Spectroscopy. Carbohyd. Res. **211**, 17–23 (1991)
88. Ramaprasad, T., Rao, V., Sanjeev, G.: Synthesis of chitin-polyaniline nanocomposite by electron beam irradiation. J. Appl. Polym. Sci. **121**, 623–633 (2011)
89. Ruiz-Hitzky, E., Darder, M.: Special Issue on trends in Biohybrid Nanostructured Materials. Curr. Nanosci. **2**, 153–294 (2006)
90. Pandey, J.K., Kumar, A.P., Misra, M., Mohanty, A.K., Drzal, L.T., Singh, R.P.: Recent advances in biodegradable nanocomposites. J. Nanosci. Nanotech. **5**, 497–526 (2005)
91. Ikoma, T., Muneta, T., Tanaka, J.: Key Engineering Materials. Key Eng. Mater. **192–1**, 487–490 (2000)
92. Kikuchi, M., Itoh, S., Ichinose, S., Shinomiya, K., Tanaka, J.: Self-Organization Mechanism in a Bone-like Hydroxyapatite/Collagen Nanocomposite Synthesized in vitro and Its Biological Reaction in vivo. Biomaterials. **22**, 1705–1711 (2001)
93. Wang, K.: In: Yin Y CRC Press, pp. 339–406, ISBN: 978-1-4398-2114-5
94. Zia, K.M., Barikani, M., Zuber, M., Bhatti, I.A., Sheikh, M.A.: Molecular engineering of chitin based polyurethane elastomers. Carbohydr. Polym. **74**, 149–158 (2008a)
95. Zia, K.M., Barikani, M., Bhatti, I.A., Zuber, M., Bhatti, H.N.: Synthesis and characterization of novel biodegradable thermally stable chitin based polyurethane elastomers. J. App. Polym. Sci. **110**, 769–776 (2008b)

96. Zia, K.M., Zuber, M., Bhatti, I.A., Barikani, M., Sheikh, M.A.: Evaluation of biocompatibility and mechanical behavior of polyurethane elastomers based on chitin/1,4-butane diol blends. Int. J. Biolog. Macromol. **44**, 18–22 (2009a)
97. Zia, K.M., Zuber, M., Bhatti, I.A., Barikani, M., Sheikh, M.A.: Evaluation of biocompatibility and mechanical behavior of chitin polyurethane elastomers, Part-II: Effect of diisocyanate structure. Int. J. Biol. Macromol. **44**, 23–28 (2009b)
98. Barikani, M., Zia, K.M., Bhatti, I.A., Zuber, M., Bhatti, H.N.: Molecular engineering and properties of chitin based shape memory polyurethane elastomers. Carbohydr. Polym. **74**(3), 621–626 (2008)
99. Zia, K.M., Zuber, M., Barikani, M., Bhatti, I.A., Khan, M.B.: Surface characteristics of chitin based shape memory polyurethane elastomers. Colloids Surf. B. **72**, 248–252 (2009c)
100. Kaczmarek, H., Chaberska, H.: The influence of UV-irradiation and support type on surface properties of poly(methyl methacrylate) thin films, Journal of Photochemistry and Photobiology. App. Surf. Sci. **252**, 8185–8192 (2006)
101. Kaczmarek, H., Podgorski, A.: J. Photochem. Photobiol. A: The effect of UV-irradiation on poly(vinyl alcohol) composites with montmorillonite. Journal of Photochemistry and Photobiology. Journal of Photochemistry and Photobiology. Chemi. **191**, 209–215 (2007)
102. Zia, K.M., Bhatti, H.N., Bhatti, I.A.: Methods for polyurethane and polyurethane composites, recycling and recovery. Funct. Polym. 67, 675–692
103. Zia, K.M., Barikani, M., Zuber, M., Bhatti, I.A.: Surface Characteristics of UV-irradiated Polyurethane Elastomers extended with alkane Diols Islam-ud-Din. App. Surf. Sci. **254**, 6754–6761 (2008c)
104. Matsushita, Y., Suzuki, A., Sekiguchi, T., Saito, K., Imai, T., Fukushima, K.: Mapping of the cationic Starch adsorbed on pulp fibers by tof-SIMS App. Surf. Sci. **255**, 1022–1024 (2008)
105. Yokota, S., Kitaoka, T., Wariishi, H.: Surface morphology of cellulose films prepared by spin coating on silicon oxide substrates pretreated with cationic polyelectrolyte. App. Surf. Sci. **253**, 4208–4214 (2008)
106. Santosa, S.J., Siswanta, D., Sudiono, S., Utarianingrum, R.: Chitin–humic acid hybrid as adsorbent for Cr(III) in effluent of tannery wastewater treatment. Journal of Photochemistry and Photobiology. App. Surf. Sci. **254**, 7846–7850 (2008)
107. Zia, K.M., Barikani, M., Khalid, A.M., Honarkar, H.: Surface characteristics of polyurethane elastomers based on chitin/1,4-butanediol blends. Ehsan-ulHaq. Carbohydr. Polym. **77**, 621–627 (2009d)
108. Zia, K.M., Barikani, M., Zuber, M., Bhatti, I.A., Barmar, M.: Surface characteristics of polyurethane elastomers based on chitin/1,4-butanediol blends. Int. J. Biol. Macromol. **44**, 182–185 (2009e)
109. Zia, K.M., Barikani, M., Zuber, M., Bhatti, I.A., Barmar, M.: "XRD studies of UV irradiated chitin-based polyurethane elastomers. Carbohydr. Polym. **77**, 54–58 (2009f)
110. Zia, K.M., Bhatti, I.A., Barikani, M., Zuber, M., Bhatti, H.N.: XRD studies of polyurethane elastomers based on chitin/1,4-butane diol blends. Carbohydr. Polym. **76**, 183–187 (2009g)
111. Nishio, Y., Koide, T., Miyashita, Y., Kimura, N., Suzuki, H.J.: Water-Soluble Polymer Blends with Partially Deacetylated Chitin: A Miscibility Characterization. Appl. Polym. Sci. **37**, 1533–1538 (1999)
112. Kim, J.Y., Ha, C.S., Jo, N.J.: Synthesis and properties of biodegradable chitin-*graft*-poly(L-lactide) copolymers Polym. Int. **51**, 1123–1128 (2002)
113. Zuber, M., Zia, K.M., Mahboob, S., Hassan, M., Bhatti, I.A.: Synthesis of chitin-bentonite clay based polyurethane bio-nanocomposites Int. J. Biol. Macromol. **47**, 196–200 (2010)
114. Cardenas, G., Cabrera, G., Taboada, E., Miranda, S.P.: Chitin characterization by SEM, FTIR, XRD, and 13C cross polarization/mass angle spinning NMR. J. Appl. Polym. Sci. **93**, 1876–1885 (2004)
115. Wang, S.F., Shen, L., Tong, Y.J., Chen, L., Phang, I.Y., Lim, P.Q., Liu, T.X.: Biopolymer Chitosan/Montmorillonite Nanocomposites: Preparation and Characterization. Polym. Degrad. Stab. **90**, 123 (2005)

116. Darder, M., Colilla, M., Ruiz-Hitzky, E.: Biopolymer-clay Nanocomposites based on chitosan intercalated in montmorillonite. NMR. Chem. Mater. **15**, 3774–3780 (2003a)
117. Darder, M., Lopez-Blanco, M., Aranda, P., Leroux, F., Ruiz-Hitzky, E.: Bionanocomposites Based on layered double hydroxides. Chem. Mater. **17**, 1969–1977 (2005)
118. Darder, M., Lopez-Blanco, M., Aranda, P., Aznar, A.J., Bravo, J., Ruiz-Hitzky, E.: Microfi brous chitosan-sepiolite nanocomposites. Chem. Mater. **18**, 1602–1610 (2006)
119. Darder, M., Colilla, M., Ruiz-Hitzky, E.: Biopolymer-clay nanocomposites based on Chitosan intercalated in montmorillonite. Chem. Mater. **15**(20), 3774–3780 (2003b)
120. Xin, Y., Guanghan, L., Xiaogang, W., Tong, Z.: Studies on Electrochemical Behavior of Bromideat a Chitosan-Modified Glassy Carbon Electrode. Electroanalysis. **13**, 923–926 (2001)
121. Lu, G., Yao, X., Wu, X., Zhan, T.: Determination of the total iron by chitosan-modified Glassy carbon electrode. Microchem. J. **69**, 81–87 (2001)
122. Zhao, C.-Z., Egashira, N., Kurauchi, Y., Ohga, K.: Electrochemiluminescence sensor having a pt electrode coated with a ru(bpy)(3)(2-modified chitosan silica-gel membrane. Anal. Sci. **14**, 439–441 (1998)
123. Khan, T.A., Peh, K.K.: Ch'ng, H.S.: Reporting degree of deacetyla-tion values of chitosan: The influence analytical methods. J. Pharm. Pharm. Sci. **5**, 205–212 (2002)
124. Giles, C.H., MacEwan, T.H., Nakhwa, S.N., Smith, D.J.: A system of classification of solution adsorption isotherms and its use in diagnosis of adsorption mechanisms and in measurements of specific Areas of soils. Chem. Soc. 3973–3993 (1960)
125. Miller, R., Fainerman, V.B.: Möhwald, H.: Adsorption behaviour of oxyethylated surfactants at the air/water interface. J. Colloid Interface Sci. **247**, 193–199 (2002)
126. Huang, H., Yuan, Q., Yang, X.: Preparation and characterization of metal-chitosan nanocomposites. Colloid Surf.B. 39(1–2):31–37
127. Clark, G.L., Smith, A.F.: X Ray diffraction studies of Chitin. Chitosan and Derivatives. J. Phys. Chem. **40**, 863–879 (1936b)
128. Van Olphen, H.: Preparation and characterization of metal-chitosan nanocomposites. An introduction to clay colloid chemistry, 2nd edn. Wiley-Interscience, New York (1977)
129. Aranaz, I., Mengíbar, M., Harris, R., Paños, I., Miralles, B., Acosta, N., Galed, G., Heras, A.: Functional characterization of chitin and chitosan. Curr. Chem. Biol. **3**, 203–230 (2009b)
130. Ray, S.S., Yamada, K., Okamoto, M., Ueda, K.: New polylactide-layered silicate nanocomposites. 2. Concurrent Improvements of material properties, biodegradability and melt rheology. Polymer. **44**, 857–866 (2003)
131. Alexandre, M., Dubois, P. Mater. Polymer-layered silicate nanocomposites: Preparation, properties and uses of a new class of materials. Sci. Eng. R: Rep. 28, 1–63 (2000)
132. Pavlidoua, S., Papaspyrides, C.D.: A review on polymer–layered silicate nanocomposites. Prog. Polym. Sci. **33**, 1119–1198 (2008)
133. Bordes, P., Pollet, E., Averous, L.: Nano-biocomposites: Biodegradable polyester/nanoclay systems. Prog. Polym. Sci. **34**, 125–155 (2009b)
134. Dufresne, A., Cavaille, J.Y., Helbert, W.: New nanocomposite materials: microcrystalline starch reinforced thermoplastic. Macromolecules. **29**, 7624–7626 (1996)
135. Dubief, D., Samain, E., Dufresne, A.: Polysaccharide microcrystals reinforced amorphous poly(β-hydroxyoctanoate) nanocomposite materials. Macromolecules. **32**, 5765–5771 (1999a)
136. Grunert, M., Winter, W.T.: Nanocomposites of cellulose acetate butyrate reinforced with cellulose nanocrystals. J. Polym. Environ. **10**, 27–30 (2002)
137. Samir, M.A.S.A., Alloin, F., Paillet, M., Dufresne, A.: Tangling effect in fibrillated cellulose reinforced nanocomposite. Macromolecules. **37**, 4313–4316 (2004a)
138. Samir, M.A.S.A., Alloin, F., Sanchez, J.Y., El Kissi, N., Dufresne, A.: Preparation of cellulose whiskers reinforced nanocomposites from an organic medium suspension. Macromolecules. **37**, 1386–1393 (2004b)

139. Nair, K.G., Dufresne, A.: Crab Shell Chitin Whisker Reinforced Natural Rubber Nanocomposites. 2. Mechanical Behavior. Biomacromolecules. **4**, 666–674 (2003c)
140. Nair, K.G., Dufresne, A., Gandini, A., Belgacem, M.N.: Crab shell chitin whiskers reinforced natural rubber nanocomposites. 3. Effect of chemical modification of chitin whiskers. Biomacromolecules. **4**, 1835–1842 (2003)
141. Li, Q., Zhou, J.P., Zhang, L.N.: J. Polym. Sci.Part B: Starch-based composites reinforced with novel chitin nanoparticles. Polym. Phys. 47, 1069–1077 (2009)
142. Chang, P.R., Jian, R.J., Yu, J.G., Ma, X.F.: Chitin whiskers: an overview. Carbohydr. Polym. 80, 420–425, (4123–4135) (2010)
143. Zeng, J-B., He, Y-S., Li, S-L., Wang, Y-Z.: Biomacromolecules. dx.doi.org/10.1021/bm201564a (2012)
144. Huang, J., Zou, J.W., Chang, P.R., Yu, J.H., Dufresne, A.: New waterborne polyurethane-based nanocomposites reinforced with low loading levels of chitin whisker. Express Polym. Lett. **5**, 362–373 (2011)
145. Feng, L.D., Zhou, Z.Y., Dufresne, A., Huang, J., Wei, M., An, L.J.: Structure and properties of new thermoforming bionanocomposites based on chitin whisker-graft-polycaprolactone. J. Appl. Polym. Sci. **112**, 2830–2837 (2009b)
146. Yuan, H.H., Nishiyama, Y., Wada, M., Kuga, S.: Surface acylation of whiskers by drying aqueous emulsion. Biomacromolecules. **7**, 696–700 (2006)
147. Siqueira, G., Bras, J., Dufresne, A.: New process of chemical grafting of cellulose nanoparticles with a long chain isocyanate. Langmuir. **26**, 402–411 (2010b)
148. Gousse, C., Chanzy, H., Excoffier, G., Soubeyrand, L., Fleury, E.: Stable suspensions of partially silylated cellulose whiskers dispersed in organic solvents. Polymer. **43**, 2645–2651 (2002)
149. Oksman, K., Mathew, A.P., Bondeson, D., Kvien, I.: Manufacturing process of cellulose whiskers/polylactic acid nanocomposites. Compos. Sci. Technol. **66**, 2776–2784 (2006)
150. Bondenson, D., Oksman, K.: Polylactic acid/cellulose whisker nanocomposites modified by polyvinyl alcohol. Compos. Part A. **38**, 2486–2492 (2007)
151. de Menezes, A.J., Siqueira, G., Curvelo, A.A.S.: Extrusion and characterization of functionalized cellulose whisker reinforced polyethylene Nanocomposites. Polymer. **50**, 4552–4563 (2009)
152. Pan, J.R., Huang, C., Chen, S., Chung, Y.-C.: Evaluation of a modified chitosan biopolymer for coagulation of colloidal particles. Colloids Surf. A. **147**, 359–364 (1999)
153. Nakagaito, A.N., Yano, H.: The effect of morphological changes from pulp fiber towards nano-scale fibrillated cellulose on the mechanical properties of high-strength plant fiber based composites. Appl. Phys. A. **78**, 547–552 (2004)
154. Nakagaito, A.N., Iwamoto, S., Yano, H.: Bacterial cellulose: the ultimate nano-scalar cellulose morphology for the production of high-strength composites. Appl. Phys. A. **80**, 93–97 (2005)
155. Shimazaki, Y., Miyazaki, Y., Takezawa, Y., Nogi, M., Abe, K., Ifuku, S., Yano, H.: Excellent thermal conductivity of transparent cellulose nanofiber/epoxy resin nanocomposites. Biomacromolecules. **8**, 2976–2978 (2007)
156. Nogi, M., Handa, K., Nakagaito, A.N., Yano, H.: Optically transparent bionanofiber composites with low sensitivity to refractive index of the polymer matrix. Appl. Phys. Lett. **87**, 243110–243112 (2005)
157. Iwamoto, S., Abe, K., Yano, H.: The effect of hemicelluloses on wood pulp nanofibrillation and nanofiber network characteristics. Biomacromolecules. **9**, 1022–1026 (2008)
158. Henriksson, M., Berglund, L.A.: Structure and properties of cellulose nanocomposite films containing melamine formaldehyde. J. Appl. Polym. Sci. **106**, 2817–2824 (2007)
159. Seydibeyoğlu, M.Ö., Oksman, K.: Novel nanocomposites based on polyurethane and micro fibrillated cellulose. Compos. Sci. Technol. **68**, 908–914 (2008)
160. Eyholzer, Ch., Bordeanu, N., Lopez-Suevos, F., Rentsch, D., Zimmermann, T., Oksman, K.: Preparation and characterization of water-redispersible nanofibrillated cellulose in powder form. Cellulose. **17**, 19–30 (2010)

161. Park, I., Kang, M., Kim, H.S., Jin, H.J.: Electrospinning of poly(ethylene oxide) with bacterial cellulose whiskers. Macromol. Symp. **249–250**, 289–294 (2007)
162. Rojas, O.J., Montero, G.A., Habibi, Y.: Electrospun nanocomposites from polystyrene loaded with cellulose nanowhiskers. J. Appl. Polym. Sci. **113**, 927–935 (2009)
163. Zoppe, J.O., Peresin, M.S., Habibi, Y., Venditti, R.A., Rojas, O.J.: Reinforcing poly(-caprolactone) nanofibers with cellulose nanocrystals. ACS Appl. Mater. Interfaces. **1**, 1996–2004 (2009)
164. Peresin, M.S.: Habibi, Y, Zoppe, J.O., Pawlak, J.J., Rojas, O.J.: Nanofiber composites of polyvinyl alcohol and cellulose nanocrystals: manufacture and characterization. Biomacromolecules. **11**, 674–681 (2010)
165. de Mesquita, J.P., Donnici, C.L., Pereira, F.V.: Biobased nanocomposites from layer-by-layer assembly of cellulose nanowhiskers with chitosan. Biomacromolecules. **11**, 473–480 (2010)
166. Podsiadlo, P., Choi, S.Y., Shim, B., Lee, J., Cuddihy, M., Kotov, N.A.: Molecularly engineered nanocomposites: layer-by-layer assembly of cellulose nanocrystals. Biomacromolecules. **6**, 2914–2918 (2005)
167. Cranston, E.D., Gray, D.G.: Formation of cellulose-based electrostatic layer-by-layer films in a magnetic field. Sci. Technol. Adv. Mater. **7**, 319–321 (2006a)
168. Cranston, E.D., Gray, D.G.: Morphological and optical characterization of polyelectrolyte multilayers incorporating nanocrystalline cellulose. Biomacromolecules. **7**, 2522–2530 (2006b)
169. Jean, B., Dubreuil, F., Heux, L., Cousin, F.: Structural details of cellulose nanocrystals/polyelectrolytes multilayers probed by neutron reflectivity and AFM. Langmuir. **24**, 3452–3458 (2008)
170. Jean, B., Heux, L., Dubreuil, F., Chambat, G., Cousin, F.: Non-electrostatic building of biomimetic cellulose-xyloglucan multilayers. Langmuir. **25**, 3920–3923 (2009)
171. Aulin, C., Johansson, E., Wågberg, L., Lindström, T.: Self-organized films from cellulose I nanofibrils using the layer-by-layer technique. Biomacromolecules. **11**, 872–882 (2010)
172. Qiu, J.-D., Xie, H.-Y., Liang, R.-P.: Preparation of porous chitosan/carbon modified electrode for biosensor application. Microchim. Acta. **162**, 57–64 (2008)
173. Feng, L., Zhou, Z., Dufresne, A., Huang, J., Wei, M., An, L.: Structure and properties of new thermoforming bionanocomposites based on chitin whisker-graft-polycaprolactone. J. Appl. Polym. Sci. **112**, 2830–2837 (2009c)
174. Brenner, S.S.: Tensile strength of whiskers. J. App. Phys. **27**, 1484 (1956)
175. Dubief, D., Samain, E., Dufresne, A.: Polysaccharide microcrystals reinforced amorphous poly(β-hydroxyoctanoate) nanocomposite materials. Macromolecules. **32**, 5765–5771 (1999b)
176. Paul, D.R., Robeson, L.M.: Polymer nanotechnology: nanocomposites. Polymer. **49**, 3187–3204 (2008)
177. Kristo, E., Biliaderis, C.G.: Physical properties of starch nanocrystal-reinforced pullulan films. Carbohydr. Polym. **68**, 146–158 (2007)
178. Angellier, H., Molina-Boisseau, S., Lebrun, L., Dufresne, A.: Processing and structural properties of waxy maize starch nanocrystals reinforced natural rubber. Macromolecules. **38**, 3783–3792 (2005b)
179. Paralikara, S.A., Simonsen, J., Lombardi, J.: Physical properties of starch nanocrystal-reinforced pullulan films. J. Membr. Sci. **320**, 248–258 (2008)
180. Yu, J., Yang, J., Liu, B., Ma, X.: Preparation and characterization of glycerol plasticized-pea starch/ZnO-carboxymethylcellulose sodium nanocomposites. Bioresour. Technol. **100**, 2832–2841 (2009)
181. Zhang, X.L., Huang, J., Chang, P.R., Li, J.L., Chen, Y.M., Wang, D.X., Yu, J.H., Chen, J.H.: Structure and properties of polysaccharide nanocrystal-doped supramolecular hydrogels based on Cyclodextrin inclusion. Polymer. **51**, 4398–4407 (2010)

182. Wang, X., Ma, J., Wang, Y., He, B.: Structural characterization of phosphorylated chitosan and their applications as effective additives of calcium phosphate cements. Biomaterials. **22**, 2247–2255 (2001)
183. Hirano, S., Noishiki, Y.: The blood compatibility of chitosan and N-acylchitosans. J. Biomed. Mater. Res. **19**, 413–417 (1985)
184. Kuen, Y.L., Wan, S.H.: Won, H.P.:Blood compatibility and biodegradability of partially N-acylated chitosan derivatives. Biomaterials. **16**, 1211–1216 (1995)
185. Hirano, S., Midorikawa, T.: Novel method for the preparation of N-acylchitosan fiber and N-acylchitosancellulose fiber. Biomaterials. **19**, 293–297 (1998)
186. Ono, K., Saito, Y., Yura, H., Ishikawa, K., Kurita, A., Akaike, T., Ishihara, M.: Photocrosslinkable chitosan as a biological adhesive. J. Biomed. Mater. Res. **49**, 289–295 (2000)
187. Khor, E.: Chitin: a biomaterial in waiting. Mater. Sci. **6**, 313–317 (2002)
188. Tomihata, K., Ikada, Y.: In vitro and in vivo degradation of films of chitin and its deacetylated derivatives. Biomaterials. **18**, 567–575 (1997)
189. Onishi, H., Machida, Y.: Biodegradation and Distribution of Water-soluble Chitosan in Mice. Biomaterials. **20**, 175–182 (1999)
190. Tanaka, Y., Tanioka, S.-I., Tanaka, M., Tanigawa, T., Kitamura, Y., Minami, S., Okamoto, Y., Miyashita, M., Nanno, M.: Effects of chitin and chitosan particles on BALB/c mice by oral and parenteral administration. Biomaterials. **18**, 591–595 (1997)
191. Mori, T., Okumura, M., Matsuura, M., Ueno, K., Tokura, S., Okamoto, Y., Minami, S., Fujinaga, T.: Effects of chitin and its derivatives on proliferation and cytokine production of fibroblasts in vitro. Biomaterials. **18**, 947–951 (1997)
192. Prasitsilp, M., Jenwithisuk, R., Kongsuwan, K., Damrongchai, N., Watts, P.: Cellular responses to chitosan in vitro: The importance of deacetylation. J. Mater. Sci. Mater. Med. **11**, 773–778 (2000)
193. Ueno, H., Murakami, M., Okumura, M., Kadosawa, T., Uede, T., Fujinaga, T.: Chitosan accelerates the production of osteopontin from polymorphonuclear leukocytes. Biomaterials. **22**, 1667–1673 (2001)
194. Okamoto, Y., Watanabe, M., Miyatake, K., Morimoto, M., Shigemasa, Y., Minami, S.: Effects of chitin/chitosan and their oligomers/monomers on migration of fibroblasts and vascular endothelium. Biomaterials. **23**, 1975–1979 (2002)
195. Usami, Y., Okamoto, Y., Takayama, T., Shigemasa, Y., Minami, S.: Chitin and chitosan stimulate caine polymorphonclear cells to release leukotrien B4 and prostaglandin E2. J. Biomed. Mater. Res. **42**, 517–522 (1998)
196. Lim, L.Y., Khor, E., Ling, C.E.: Effects of dry heat and saturated steam on the physical properties of chitosan. J. Biomed. Mater. Res. **48**, 111–116 (1999)
197. Lim, L.Y., Khor, E.: Permeability and tensile strength of heated chitosan films. Proceedings of Conference on Challenges for Drug Delivery and Pharmaceutical Technology. p. 196, June 9–11, Tokyo, Japan (1998)
198. Lim, L.Y., Khor, E., Koo, O.: Effects of dry heat and saturated steam on the physical properties of chitosan. J. Biomed. Mater. Res. **43**, 282–290 (1998)
199. Rao, S.B., Sharma, C.P.: Use of chitosan as a biomaterial: studies on its safety and hemostatic potential. J. Biomed. Mater. Res. **34**, 21–28 (1997)
200. Kam, H.M., Khor, E., Lim, L.Y.: Storage of partially deacetylated chitosan films. J. Biomed. Mater. Res. B: Appl. Biomater. **48**, 881–888 (1999)
201. Phongying, S., Aiba, S.I., Chirachanchai, S.: A novel soft and cotton-like chitosan-sugar nanoscaffold. Biopolymers. **83**, 280–288 (2006)
202. Wongpanit, P., Sanchavanakit, N., Pavasant, P., Bunaprasert, T., Tabata, Y., Rujiravanit, R.: Characterization of Chitin Whisker-Reinforced Silk Fibroin Nanocomposite Sponges Eur. Polym. J. **43**, 4123–4135 (2007)
203. Lertwattanaseri, T., Ichikawa, N., Mizoguchi, T., Tanaka, Y., Chirachanchai, S.: Microwave technique for efficient deacetylation of chitin nanowhisker to a chitosan nanoscaffold. Carbohydr. Res. **344**, 331–335 (2009b)

204. Noh, H.K., Lee, S.W., Kim, J.M., Oh, J.E., Kim, K.H., Chung, C.P., Choi, S.C., Park, W.H., Min, B.M.: Electrospinning of chitin nanofibers: degradation behavior and cellular response to normal human keratinocytes and fibroblasts. Biomaterials. **27**, 3934–3944 (2006)
205. Park, K.E., Jung, S.Y., Lee, S.J., Min, B.M., Park, W.H.: Biomimetic nanofibrous scaffolds: preparation and characterization of chitin/silk fibroin blend nanofibers. Int. J. Biolog. Macromol. **38**, 165–173 (2006a)
206. Park, K.E., Kang, H.K., Lee, S.J., Min, B.M., Park, W.H.: Biomimetic nanofibrous scaffolds: Preparation and characterization of PGA/chitin blend nanofibers. Biomacromolecules. **7**, 635–643 (2006b)
207. Shalumon, K.T., Binulal, N.S., Selvamurugan, N., Nair, S.V., Menon, D., Furuike, T., Tamura, H., Jayakumar, R.: Electrospinning of carboxymethyl chitin/poly(vinyl alcohol) nanofibrous scaffolds for tissue engineering applications. Carbohydr. Polym. **77**, 863–869 (2009)
208. Bhattarai, N., Edmondson, D., Veiseh, O., Matsen, F.A., Zhang, M.: Electrospun chitosan-based nanofibers *and* their cellular compatibility. Biomaterials. **26**, 6176–6184 (2005)
209. Subramaniyan, A., Vu, D., Larsen, G.F., Lin, H.Y.: Preparation and evaluation of the electrospun chitosan/PEO fibers for potential applications in cartilage tissue engineering. J. Biomat. Sci.: Polymer Edition. 7, 861–873 (2005)
210. Mo, X., Chen, Z., Weber, H.: Electrospun nanofibers of collagen-chitosan and P(LLA-CL) for tissue engineering. J. Frontier in Material Science. **1**, 20–23 (2007)
211. Zhang, Y.Z., Venugopal, J.R., El-Turki, A., Ramakrishna, S., Su, B., Lim, C.T.: Electrospun biomimetic nanocomposite nanofibers of hydroxyapatite/chitosan for bone tissue engineering. Biomaterials. **29**, 4314–4322 (2008)
212. Yang, D., Jin, Y., Zhou, Y., Ma, G., Chen, X., Lu, F., Nie, J.: In situ mineralization of hydroxyapatite on electrospun chitosan-based nanofibrous scaffolds. Macromol. Biosci. **8**, 239–246 (2008)
213. Zhou, Y.S., Yang, D., Chen, X., Xu, Q., Lu, F., Nie, J.: Electrospun water-soluble carboxyethylchitosan/poly(vinyl alcohol) nano-fibrous membrane as potential wound dressing for skin regeneration. Biomacromolecules. **9**, 349–354 (2008)
214. Feng, Zhang-Qi, Chu, Xuehui, Huang, Ning-Ping, Wang, Tao, Wang, Yichun, Shi, Xiaolei, Ding, Yitao: Zhong-Ze Gu.: The effect of nanofibrous galactosylated chitosan scaffolds on the formation of rat primary hepatocyte aggregates and the maintenance of liver function. Biomaterials. **30**, 2753–2763 (2009d)
215. Rinaudo, M.: Chitin and chitosan: Properties and applications Prog. Polym. Sci. **31**, 603–632 (2006b)
216. Yen, M., Yang, J., Mau, J.: Physicochemical characterization of chitin and chitosan from crab shells Carbohydr. Polym. **75**, 15–21 (2009)
217. Junkasem, J., Rujiravanit, R., Supaphol, P.: Fabrication of a-chitin whisker-reinforced poly(vinyl alcohol) nanocomposite nanofibres by electrospinning. Nanotechnology. **17**, 4519–4528 (2006)
218. Brugnerotto, J., Lizardi, J., Goycoolea, F.M., Arguelles-Monal, W., Desbrieres, J., Rinaudo, M.: An infrared investigation in relation *with* chitin and chitosan characterization. Polymer. **42**(8), 3569–3580 (2001a)
219. Muzzarelli, R.A.A., Rocchetti, R.: Determination of the degree of acetylation of chitosans by first derivative ultraviolet spectrophotometry. Carbohydr. Polym. **6**, 61–72 (1985)
220. Wu, T., Zivanovic, S.: Determination of the degree of acetylation (DA) of chitin and chitosan by an improved first derivative UV method. Carbohyd. Polym. **73**, 248–253 (2008)
221. Duarte, M.L., Ferreira, M.C., Marvao, M.R.: Determination of the degree of acetylation of chitin materials by 13C CP/MAS NMR spectroscopy. I J Biol. Macromol. **28**(5), 359–363 (2001)
222. Raymond, L.: Morin. F.G., Marchessault, R.H.: Degree of deacetylation of chitosan using conductometric titration and solid-state NMR. Carbohydr. Res. **246**(1), 331–336 (1993)
223. Jiang, X., Chen, L., Zhong, W.: A new linear potentiometric titration method for the determination of deacetylation degree of chitosan. Carbohydr. Polym. **54**, 457–463 (2003)

224. Guinesi, L., Cavalheiro, E.: The use of DSC curves to determine the acetylation degree of chitin/chitosan samples. Termochim. Acta. **444**, 128–133 (2006)
225. Rinaudo, M., Milas, M., Le Dung, P.: Characterization of chitosan. Influence of ionic stregth and degree of acetylation on chain expansion. I. J. Biol.Macromol. 15, 281–285 (1993)
226. Brugnerotto, J., Desbrieres, J., Roberts, G., Rinaudo, M.: Characterization of chitosan by steric exclusion chromatography. Polymer. **42**(25), 9921–9927 (2001b)
227. Terbojevich, M.: Cosani, A. In: Muzzarelli, R.A.A., Peter, M.G. (eds.) Chitin Handbook, pp. 87–101. European Chitin Society, Grotammare (1997)
228. ASTM. F2103-01 Standard guide for characterization and testing of chitosan salts as starting materials intended for use in biomedical and tissue-engineered medical product applications (2001)
229. Zia, K.M., Bhatti, I.A., Barikani, M., Zuber, M., Sheikh, M.A. Int. XRD studies of chitin-based polyurethane elastomers. J. Biol. Macromol. 43, 136–141 (2008)
230. Bradford, M.: A rapid and sensitive method for the quantitation of microgram quantities of protein utilizing the principle of protein dye binding. Anal. Biochem. **72**, 248–254 (1976)
231. Roberts, G.: Chitin Chemistry. Macmillan, London (1998b)

Chapter 4
Starch Based Blends, Composites and Nanocomposites

Long Yu, Xingxun Liu, Eustathios Petinakis, Katherine Dean and Stuart Bateman

Abstract The development and production of biodegradable starch-based materials has attracted more and more attention in recent years due to the depletion in the world's oil resources and the growing interest in easing the environmental burden from petrochemically derived polymers. Furthermore, the unique microstructures of different starches can be used as an outstanding model system to illustrate the conceptual approach to understanding the relationship between the structures and properties in polymers.

Abbreviations

BC	Bacterial cellulose
MC	Moisture content
MDI	Methylenediphenyl diisocyanate
MMT	Montmorillonite
PBSA	Poly(butylene succinate adipate)
PCL	Poly(caprolactone
PFRR	Polymer from renewable recourse
PHB	Poly(3-hydroxybutyrate)
PHBV	Polyhydroxybutyrate-valerate
PLA	Poly(lactic acid)
REX	Reactive extrusion
SA	Starch acetate
TPS	Thermoplastic starch

L. Yu (✉) · X. Liu · E. Petinakis · K. Dean · S. Bateman
Materials Science and Engineering, CSIRO, Melbourne, VIC 3168, Australia
e-mail: long.yu@csiro.au

X. Liu
Centre for Polymer from Renewable Resources, South China University of Technology, 510640 Guangzhou, China

S. Thomas et al. (eds.), *Advances in Natural Polymers*,
Advanced Structured Materials 18, DOI: 10.1007/978-3-642-20940-6_4,

4.1 Introduction

The development and production of biodegradable starch-based materials has attracted more and more attention in recent years due to the depletion in the world's oil resources and the growing interest in easing the environmental burden from petrochemically derived polymers. Furthermore, the unique microstructures of different starches can be used as an outstanding model system to illustrate the conceptual approach to understanding the relationship between the structures and properties in polymers.

Like most polymers from petroleum, starch-based materials are rarely used by themselves. Starch was initially used as filler blended with various polymers, especially with polyolefins. Recently, blending starch with biodegradable polymers has attracted great interest. Starch-based materials are hydrophilic and are water-soluble. Water solubility raises degradability and increases the speed of degradation; however, this moisture sensitivity limits their application. Blending and compositing of starch with other kinds of polymers can be used to improve their properties. Blends can also aid in the development of new low-cost products with better performance. However, hydrophobic synthetic polymers and hydrophilic starch are thermodynamically immiscible, leading to poor adhesion between the two components, and hence poor and irreproducible performance. Various compatibilizers and additives have been investigated and have been found to improve the interfacial interactions of these blends.

Fibers have been widely used in polymeric composites to improve mechanical properties. Cellulose is the major substance obtained from vegetable fibers, and applications for cellulose fiber-reinforced polymers have again come to the forefront with the focus on renewable raw materials. Hydrophilic cellulose fibers are very compatible with most natural polymers. The reinforcement of starch with cellulose fibers is a perfect example of a polymer from renewable recourses (PFRR). The reinforcement of polymers using rigid fillers is another common method in the production and processing of polymeric composites. The interest in new nanoscale fillers has rapidly grown in the last two decades, since it was discovered that a nanostructure could be built from a polymer and layered nanoclay. This new nanocomposite showed dramatic improvement in mechanical properties with low filler content. Various starch-based nano-composites have been developed.

This chapter discusses the development of starch based blends, composites and nanocomposites from a fundamental viewpoint, such as designing principle and mechanism, as well as processing techniques and application areas. The knowledge of unique microstructure of starch and its multiphase transitions during thermal processing provides scientific and technological guides to improve the performance of starch based materials through blending and compositing. Various conventional processing techniques such as extrusion, injection and compression moulding, and casting, as well as some new techniques such as reactive extrusion, have been adapted for processing starch-based blends and composites.

4.2 Structure of Starch

Starch is a polymeric carbohydrate consisting of anhydroglucose units linked together primarily through α-D-(1 → 4) glucosidic bonds. Figure 4.1 shows the chemical structure and a schematic representation of amylose and amylopectin starches. Although the detailed microstructures of starch are still being elucidated, it has generally been established that starch is a heterogeneous material containing two microstructures—the linear (amylose) and the branched (amylopectin). Amylose is essentially a linear structure of alpha-1,4 linked glucose units, and amylopectin is a highly branched structure of short alpha-1,4 chains linked by alpha-1,6 bonds. The linear structure of amylose makes its behavior more closely resemble that of conventional synthetic polymers. The molecular weight of amylose is about $\times 10^6$, depending on its source and the processing conditions employed during its extraction, which is 10 times higher than conventional synthetic polymers. Amylopectin, on the other hand, is a branched polymer and its molecular weight is much greater than amylose, with light scattering measurements indicating molecular weights in millions. The high molecular weight and branched structure of amylopectin reduce the mobility of the polymer chains, and interfere with any tendency for them to become oriented closely enough to permit significant level of hydrogen bounding. Most native starches are semi-crystalline, having a crystallinity of about 20 $\sim$ 45 % [1]. Amylose and the branching points of amylopectin form amorphous regions. The short branching chains in the amylopectin are the main crystalline component in granular starch.

Starch granules contain both crystalline and amorphous regions, and are thus semi-crystalline, which in native starch granules manifests itself in a hierarchical structural periodicity which originates from the hilum [2, 3]. The granules are organised into concentric rings radiating out from the central hilum to the surface of the granule. The number and size of the rings depends on the botanical origin of the starch, and it is generally believed to consist of alternating 120–400 nm thick amorphous and semi-crystalline growth rings [4]. The amorphous growth rings contain both amylopectin and amylose macromolecules in relatively disordered conformations, whereas the semicrystalline growth rings consist of amylopectin clusters that contain alternating crystalline and amorphous regions of approximately 9–11 nm thickness, organised in a lamellar arrangement [5–7].

4.3 Properties of Starch

4.3.1 Thermal Properties

Thermal processing of starch-based polymers involves multiple chemical and physical reactions, e.g. water diffusion, granule expansion, gelatinization, decomposition, melting and crystallization [8]. Among the various phase

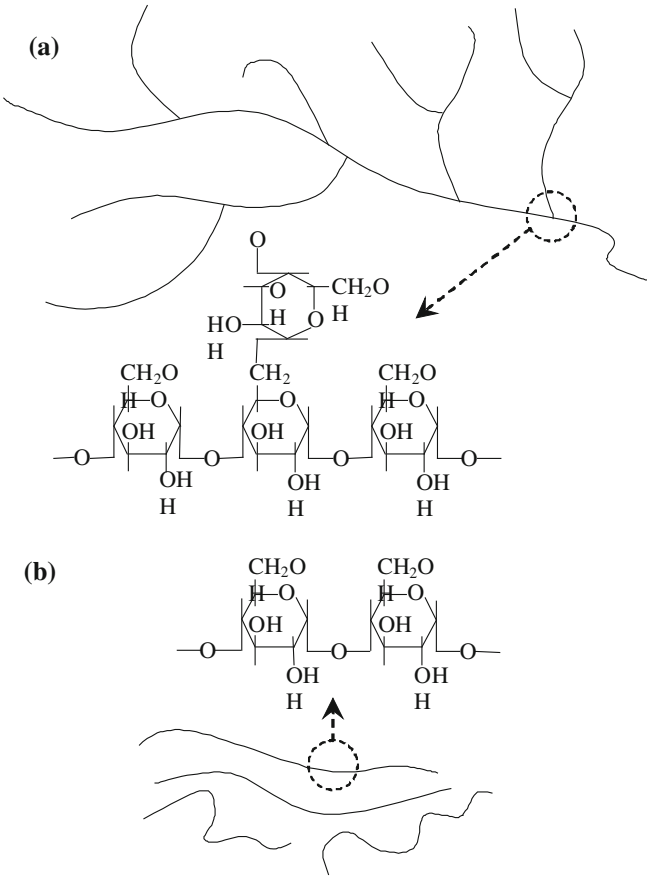

Fig. 4.1 Chemical structures and physical schematic representation of **a** amylopectin starch, and **b** amylose starch

transitions, gelatinization is particularly important because it is closely related to the others, and it is the basis of the conversion of starch to a thermoplastic. Furthermore, the decomposition temperature of starch is higher than its melting temperature before gelatinization. The well-accepted concept of "gelatinization" refers to the destruction of the crystalline structure in starch granules [9, 10], which is an irreversible process that includes, in a broad sense and in time sequence, granular swelling, native crystalline melting (loss of birefringence) and molecular solubilization [11, 12].

Unlike most conventional polymers, starch granules undergo unique and complicated phase changes during thermal processing (normally an aqueous environment), including starch swelling, loss of birefringence, melting and solubilization [10, 13–16]. Without physical force (shear stress), the process of gelatinization depends mainly on water content and temperature conditions. During the

initial stage of thermal processing as the temperature is increased from 20 to 60 °C, water is thought to be reversibly complexed with starch molecules, thus decreasing its mobility [17]. Full gelatinization of starch under shearless conditions requires excess water, which Wang et al. [18] have defined as >63 %. However, if the water concentration is too high, the crystallites in starch might be pulled apart by swelling, leaving none to be melted at higher temperatures [19], and if the water concentration is limited, the swelling forces will be much less significant, and complete gelatinization will not occur in the usual temperature range [19]. However, as the temperature increases, starch granules will become progressively more mobile and eventually the crystalline regions will melt [20], and the starch would then be expected to show the usual viscoelastic behavior exhibited by thermoplastic melts [21] The process of gelatinization in a low moisture content environment could more accurately be defined as the "melting" of starch.

In addition to the effects of water content, pressure can also influence the gelatinization/melting behavior of starch. For example, Kokini et al. [22] found that for amioca at both 20 and 30 % moisture content (MC), increasing the pressure from 15 to 200 psi induced a 57 °C increase in gelatinization temperature, and that at 150 and 200 psi, two thermally induced transitions were observed, in contrast to the monophasic melting at 15 psi. Pressure is also significant in terms of its effect on the extent of conversion, as measured by rheological techniques. Herh and Kokini [23] studied the effect of pressure on starch conversion at both high and low moisture content using a pressure rheometer. The change observed in amioca cornstarch in the presence of water was of the order of 1 K/bar, compared to the change in melting temperature with pressure of polyethylene (a typical polymer), which is of the order of 0.04 K/bar [24]. This indicates that starch is much more sensitive to changes in pressure than traditional petroleum-based polymers.

Because extrusion processing involves high-shear and high-pressure conditions, gelatinization is typically achieved at low MC, since the shear forces physically tear apart the starch granules, allowing faster transfer of water into the interior molecules [25]. Therefore during extrusion, loss of crystallinity is not caused by water penetration, but by the mechanical disruption of molecular bonds due to the intense shear fields within the extruder [26]. In fact, during extrusion at low MC, small amounts of gelatinized and melted starch, as well as starch fragmentation (also degradation or decomposition), exist simultaneously [19].

A study [26] has shown that shear stress can result in fragmentation of starch granules during extrusion. Indeed, both the mechanical and thermal energy transferred to starch dough during extrusion will affect the breakdown of the main and secondary valence bonds, and the hydrogen bonds between neighbouring starch polymers in a starch structure [27]. These structural changes increase the susceptibility of starch to enzyme action, reduce the hydrogen bonds and increase the free hydroxyl groups. Extrusion can also affect amylopectin much more than amylose [19]. Colonna et al. [28], for example, found that the average molecular weight of amylose and amylopectin decreased by factors of 1.5 and 15, respectively, during extrusion.

Another important thermal property of starch-based materials is their glass transition temperature (T_g). The glass transition temperature (T_g) of starch is one of the critical thermal properties for starch-based products. However, measurement of T_g by DSC is difficult since the change of heat capacity or the signal on heat flow is usually weaker than that of conventional polymers. Liu et al. [29] has studied the T_g of cornstarch using a Hyper-DSC with heating rate up to 250 °C/min. The high heating rate increases the temperature of the thermal event, which allows the weak T_g of starch to be visible. The results showed that the extrapolated T_g of cornstarch film with 13.3, 11.6 and 8.7 % moisture content is 59.2, 61.4, and 67.3 °C, respectively. Xie et al. [30] confirmed this technique through comparing the results from DSC and MDSC. Liu et al. [31] also studied the glass transition temperatures (T_g) of starch with different amylose/amylopectin ratios, which were systematically studied by a high-speed DSC. It was found that T_g was increased with increasing amylose content. The microstructure and phase transition were used to explain this phenomenon, in particular the multiphase transitions that occur in high-amylose starches at higher temperatures, and gel-ball structure of gelatinized amylopectin.

4.3.2 Rheological Properties

One of the unique characteristics of starch-based polymers is their rheological properties, which are much more complex than conventional polymers, due to the multiple chemical and physical reactions that may occur during processing. Native starches are non-plastic due to the intra- and intermolecular hydrogen bonds between the hydroxyl groups in starch molecules, which represent their crystallinity. Thermal processing is used to disrupt and transform the semi-crystalline structure of starch granules to form a homogeneous and amorphous material. This transformation is usually accomplished using small amounts of molecular substances commonly known as gelatinization agents or plasticizers [32–35]. The transformed materials is normally called thermoplastic starch (TPS), and the techniques used to produce TPS products include extrusion [32–46], injection/compression molding [47–51], intensive mixing [52–55] and hot pressing [56].

The most commonly used technique for studying the rheological properties of TPS is capillary rheometry. For most TPS, the dependence of apparent viscosity on shear rate is linear on double-logarithmic plots, indicating that the power-law model could describe the rheological behavior of TPS [37, 39, 41, 43, 49, 51, 57–69] as:

$$\eta = \mathrm{K}\dot{\gamma}^{\mathrm{n}-1}$$

where η is the molten viscosity, K is the consistency, $\dot{\gamma}$ is the shear rate, and n is the power-law (pseudo-plasticity) index. The power-law behavior of TPS is mainly ascribed to the gradual reduction of starch intermolecular bonds [43]. The apparent viscosity η of TPS normally decreases with an increase in plasticizer (and/or water) content at constant temperature [37, 39, 41, 43, 49, 58, 60]; it also decreases

with increasing temperature at the same plasticizer weight content [39, 43, 51]. Moreover, starches with higher amylose contents have higher melt viscosities [37, 70].

K decreases with increasing plasticizer weight content [61–63, 66–68], because plasticizers can form strong bonding interactions with starch and weaken the interaction of starch molecules, facilitating movement among starch molecules. Some researchers have proposed other explanations for decreasing K values for TPS using specific plasticizers. For example, Yu et al. [43] found that in the presence of citric acid, the acidolysis of starch resulted in decreasing K with increasing temperature, which is similar to conventional polymers.

On the other hand, the effect of plasticizer on n has been widely reported. Yu et al. [43] found that n decreased with increasing citric acid weight content, and a similar pattern has also been observed using glycerol as a plasticizer [41, 67]. However, in a study of the shear viscosity of cornstarch, Willett et al. [71] found that n varied only slightly at different water contents, but it decreased significantly when the content of certain co-plasticizers was increased. In further work, Willett and co-workers [61] reported that n increased as the water content of waxy maize was increased; however others [65, 67, 69] have reported the reverse pattern. In fact, the relationship between n and plasticizer content is quite complicated and depends on a number of parameters, such as processing history, plasticizer type and the presence of other additives.

It has been commonly considered that a higher temperature will increase n and thus make a starch melt less pseudoplastic and more Newtonian [64, 67, 71]. In addition, the effect of amylose content on n has attracted much attention, with some reports [64, 67] showing that n decreased as amylose content increased, indicating that a lower amylose starch will exhibit greater Newtonian behavior in the melt state. Decreasing n with increasing amylose content is generally attributed to an increase in entanglements within the amylose content, with the highly branched amylopectin not expected to form entanglements well [71]. However, González et al. [60] discovered that the opposite applied in the results of their study. Recently, Xie et al. [72] have systematically studied the rheological properties of cornstarch with different amylose/amylopectin contents. It can be seen that the higher the amylose content, the higher the apparent viscosity under the same shear rate range. These rheological behaviors are attributed to the higher gelatinization temperature of amylose-rich starches, in particular the multiphase transitions that occur in these starches at higher temperatures, and the gel-ball structure of gelatinized amylopectin (see Fig. 4.2).

4.4 Preparation of Starch-Based Materials

Various conventional processing technologies, such as casting, extrusion, injection and compression moulding, have been adapted for processing starch-based materials, as well as some new techniques, such as orientation and reactive extrusion.

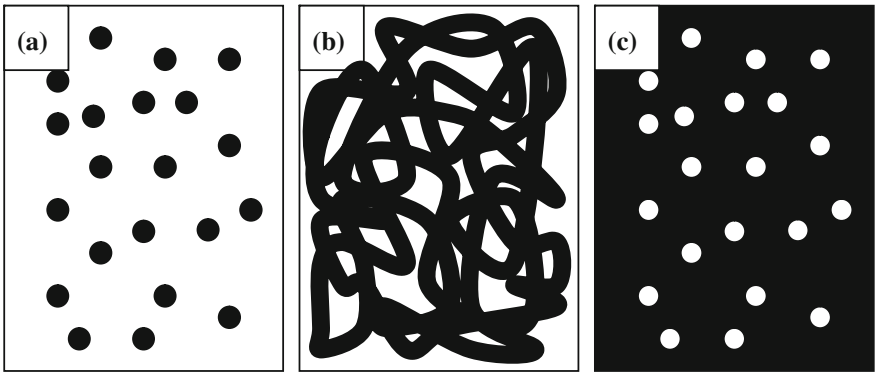

Fig. 4.2 Schematic representation of possible morphologies of polyolefin/starch blends (*black* part represents polyolefin phase; and *white* part represents starch phase)

4.4.1 Casting Film

The technique of casting starch-based films has been widely reported [73–98], and typically includes solution preparation, gelatinization, casting and drying. Starch and plasticizers are directly mixed to about 3–10 % solid concentration in water, and this film-forming solution is then transferred quantitatively to, for example, a Brabender viscograph cup, in which the solution is heated from room temperature to 95 °C, where it is maintained for 10 min while being constantly shaken or blended. A higher temperature is used when another plasticizer like glycerol is added to the formulation. The gelatinized suspensions are then immediately poured onto a flat Teflon or acrylic plate, and left to dry for ~24 h in an oven at about 40–75 °C to constant weight. The final thickness of cast films is normally 0.02–0.10 mm, which is controlled by calculating the quantity of starch suspension poured onto the plate.

Plasticizers not only play an important role in processing, but also in improving the mechanical properties of starch-based films. For example, plasticizers can increase film flexibility by reducing the internal hydrogen bonding between polymer chains by increasing intermolecular space. Although water is an excellent plasticizer for starch, it has the disadvantage that its content varies with humidity—at low humidity there are problems with brittleness, and at high humidity there are problems with softness. Glycerol and sorbitol are widely used as plasticizers to make brittle films more flexible. Other chemicals such as sugars, sucrose, glucose, xylose, fructose, urea and various glycols have also been evaluated [98–100]. Different plasticizers have regularly been used in combination with water in order to approach the conditions suitable for gelatinization.

However, plasticizers can make brittle films less strong and, as a result, blending [101] or laminating [102] with other materials has been used to overcome this disadvantage. Aqueous blends of soluble starch and cellulose acetate have been studied intensively [103–107] as they have properties that make them suitable

for a wide range of biomedical applications, from bone replacement to engineering of tissue scaffolds, to drug-delivery systems. For example, antibacterial starch/chitosan blended films formed under the action of irradiation have been reported by Zhai et al. [107].

An unique method of preparing starch films by electrospraying was reported by Pareta and Edirisinghe [77]. Firstly, 5 % starch in deionized water was gelatinized at 120 °C for 30 min, and then small quantities of dispersant and ethanol were added and ultrasonic disruption was employed to make a stable modified starch solution. Subsequently, the solution was electrosprayed in cone-jet mode and films were collected on a rotating plate. In this method, the solvent evaporated very quickly due to the large surface area of the droplets generated, which resulted in instantaneous films. Films of different thicknesses were obtained by varying the electrospraying time.

Previous studies have shown that films cast from high-amylose starch have better film-forming and mechanical properties [80, 108, 109]. Furthermore, both amylose and amylopectin have shown excellent oxygen-barrier characteristics, which is one of the advantages of using edible hydrophilic starch-based films for food protection [110].

4.4.2 Extrusion Sheet/Film Extrusion

A simple and well-established technique for producing sheets or films by extrusion is the use of a twin-screw extruder with a slit or flat film die, followed by a take-off device for orientation and collection [111–115]. During extrusion, viscoelastic starch-based material are forced through a die to form sheet or film products [116]. A two-stage sheet/film extrusion processing technique has also been practiced by some researchers [117–120], in which starch blends are first extruded in a twin-screw extruder to form ribbons that are subsequently dried and ground into a powder, and then flat sheets or films are extruded using a single-screw extruder with a slit die. Although this two-stage extrusion technique may be more time-consuming, it offers easier and more stable extrusion of starch sheets or films because the high pressure capacity of the single-screw extruder overcomes the high viscosity and poor processibility of starch-based materials. The thickness of the extruded material can be controlled by adjusting the outlet of the slit die, thus determining whether the end product is a sheet or film. In addition, with the appropriate die as a substitute for the slit/flat film die, the two-stage technique can also be used to produce the much thinner blown films [117, 119–125].

Sheets and films based on high-amylose starch (especially high-amylose cornstarch [66, 126]) normally exhibit greater mechanical performance [50] than those based on other starches. The extrusion of high-amylose starch, however, is more difficult than normal TPS because a higher die pressure is required due to the higher melt viscosity [127, 128], and unstable flow [37]. However, by increasing MC, the barrel and die temperature, the compression ratio of the screw and the screw rotation speed [37], these problems can be reduced or eliminated.

To successfully produce sheets or films by extrusion, native starches are normally blended with other additives and plasticizers to enhance their processibility and to improve the properties of the final products. The most commonly used plasticizers are water and/or glycerol [37, 111–115, 117, 118, 129, 130], however various others have been evaluated for a wide range of purposes. Urea has been reported to improve the gelatinization of starch at low water levels, thus allowing direct extrusion of a uniform film from a semi-dry blend (~16 % MC) [112, 113, 122–124]. Thuwall et al. [37] used a fluoroelastomer lubricant to reduce the tendency of a material to stick to the die and clog it, and they used dextrin to lower the viscosity by virtue of its low molecular mass. Stearic acid and poly(ethylene glycol) have been used to improve the rheological behavior of starch blends [112, 113], and blending poly(vinyl alcohol) (PVOH) with starch can produce excellent mechanical properties in final products [117].

In blown film processing, starch-based materials are required to have sufficiently high melt strength and extensibility to form a good bubble. As a result, starch is blended with high contents of other low-viscosity polymers, such as poly(ethylene-co-vinyl alcohol) [125], PBSA [121] and PVOH [117], to overcome the naturally poor processibility of native starch, and a high glycerol content (30 %) is used to improve extensibility during the blowing process [117].

The orientation of polymer materials plays an important role in determining the performance of films or sheets. Products with "designed-in" orientation are increasingly important in the polymer industry, and include filaments with uniaxial orientation, and films and bottles with biaxial orientation. Yu and Christie [131] investigated the effect of orientation in starch-based sheets, and found that it increased both modulus and yield stress, but decreased elongation. In particular, elongation in the cross-extrusion direction decreased significantly in amylopectin-rich materials. Fishman et al. [117] studied pectin/starch/PVOH/glycerol blends, and found that tensile strength and initial modulus of extruded sheets were slightly higher in the machine direction than in the cross direction, while the reverse was true for elongation to break. For blown films, tensile strength tended to be higher in the cross direction than in the machine direction, while the reverse was seen for initial modulus.

4.4.3 Injection Moulding

The high viscosity and poor flow properties of starch-based materials present difficulties during injection moulding, and furthermore the lack of reliable parameters makes it difficult to design the optimum processing conditions. For example, since almost all formulations of starch-based materials comprise of water, which tends to evaporate during heating, it is impossible to measure the melt flow index using a conventional facility. However, efforts have been made to gain a better understanding of the injection moulding behavior of starch-based materials. Stepto [48, 49] used a given mould (shot) volume, screw speed and

temperature profile, then measured the variation of refill times for materials to feed in front of a screw at different screw-rotation speeds and under different applied back pressure. By using this technique, the shear rate of the screw was determined by its rotational speed, and the back pressure defined the reverse pressure drop along the metering zone of the screw [20, 132]. Abbes et al. [133] used numerical simulation of a TPS injection molding process to determine the optimal moulding parameters. The moulding of a standardized sample for tensile testing was considered, and it was shown that the conventional continuum mechanics equations can be used for modelling the injection moulding of TPS.

Due to the poor mechanical properties and instability of native starches, it is frequently reinforced with fibers [134–136] or blended with synthetic polymers [137–140]. Recently, much emphasis has been put on blending starch with biodegradable polyesters like PLA [141, 142], PCL [120, 143–145] and PBS [143, 144]. The injection conditions depend on the polyesters incorporated; generally, blending with these synthetic polymers decrease the overall viscosity of starch.

4.4.4 Compression Moulding

Compression moulding has been intensively investigated for processing starch-based plastics, particularly for producing foamed containers, and generally involves starch gelatinization, expanding and drying. Apart from gelatinization agents, mould-release agents such as magnesium stearate and steric acid are often used in formulations to prevent the starch sticking to the mold.

Explosion puffing is the oldest technique used to create starch-based foams from starch feedstock with low moisture content. A typical example of this is making popcorn: a kernel explosion puffs naturally at about 177 °C and requires only 10–15 % moisture to achieve maximum volume [146]. Explosion puffing can produce low-density starch-based foams within several seconds, however the performance of the foamed products is poor.

Another simple method [147, 148] of producing moulded starch-based foam containers is a baking technique that is similar to that used for making wafer cookies, whereby a measured amount of dough-like material containing 70–80 % moisture is placed in a heated mold, and the steam generated by the moisture acts as a blowing agent to create foam. The high moisture content of the dough results in a longer processing time (1–2 min) compared with that needed for making conventional polymer containers, but the excess steam generated in the sample forges channels throughout the matrix of the foam, which can contribute to the strength of the finished product. The properties of baked starch foam products will vary with moisture content, starch type and additives, used in the dough formulations [50, 149–152].

Glenn and Orts [153] describe another technique for making starch-based foams using a compression–explosion process. Starch feedstock is compressed in a heated mould at 230 °C under a 3.5 MPa clamping force for 10 s, which is then

instantaneously released, allowing the feedstock to expand into a foam that partially fills, completely fills or overfills the mold cavity, depending on the moisture content of the feedstock. The advantage of this method is that it produces moulded starch-based foams with physical and mechanical properties similar to traditional commercial food packaging products. Zhou et al. [154] reported on a foaming technique in which starch-based materials are initially formed into pellets by extrusion, and then the pellets are foamed by microwave heating. Lightweight end-products such as containers, end caps, edges or corner cushions for protective packaging, can be produced if the pellets are placed in appropriate moulds prior to heating using a microwave.

Various fillers such as $CaCO_3$ [155], natural rubber latex [155, 156] and various fibers [157–162] have been used to improve the mechanical properties of foamed products. Baked starch-based foam properties can be further improved by chemical modification. For example, moisture resistance can be improved by including additives in the dough formulation, e.g. monostearyl citrate [159] or a moisture-resistant polymer such as PVOH [151, 159]. Moisture resistance can also be achieved by applying a protective coating to foamed products following the baking process. The efficiency and cost effectiveness of coatings can be enhanced by baking and coating starch-based containers in a single step. Glenn et al. [163] developed a method of forming baked starch foam with paper coated with PVA or PVC; Martin et al. [164] reported on multilayer films based on plasticized wheat starch and various biodegradable aliphatic polyesters, produced by flat film co-extrusion and compression moulding.

4.4.5 Reactive Extrusion

Unlike the techniques mentioned above, and as the name suggests, reactive extrusion (REX) involves concurrent reaction and extrusion. The technology was originally developed in the 1980s primarily for the modification of synthetic polymers [165], but has evolved quickly and is now applied in various areas such as polymerization, grafting and crosslinking. Although the use of REX in starch modification is a relatively new area, it continues to receive wide focus due to a number of reasons, e.g.: the many advantages of extrusion itself, as already discussed. Chemically modified starches with improved properties for non-food applications have gained increasing importance in industry, mainly due to the biodegradable polysaccharide component of products and the pursuit of high-efficiency and low-cost product manufacture. Various starch-based products have been prepared using REX, including starch-grafted-copolymers [166, 167], cationic starch [168–170], oxidized starch [171], esterified starch [172] and glycosides [173–175]. REX has also been employed to produce controlled-release starch-encapsulated pesticides [176–182].

The process of reactive extrusion has advantages since it is a solvent-less process that allows the combination of several chemical manipulations in a

continuous fashion. Jun [183] reported reactive blends of starch/PLA with a reactive agent during the extrusion process. The affects of the reactive blending were investigated and significant improvements were confirmed by measuring the tensile strength and elongation at break, IR spectra and DSC. Interfacial compatibilization can be achieved via two different strategies depending on the nature of the polyester chains [184]. In the case of starch/PLA compositions, PLA chains were grafted with maleic anhydride through a free radical reaction conducted by reactive extrusion. The maleic anhydride-grafted PLA chains (MAG-PLA) enhanced the interfacial adhesion with granular starch. As far as starch/PLA blends were concerned, the compatibilization was achieved via the interfacial localization of amphiphilic graft copolymers formed by the grafting of PCL chains onto a polysaccharide backbone such as dextran. The PCL-grafted polysaccharide copolymers were synthesized by controlled ring-opening polymerization of ε-caprolactone, which proceeded via a coordination-insertion mechanism. These compatibilized starch/PLA compositions displayed improved mechanical properties as determined by tensile testing, and more rapid biodegradation as measured by composting testing.

Bossard et al. [185] studied linear viscoelastic, steady shear behaviors, and morphologies of starch formate/poly(caprolactone) (PCL) blends, compatibilized by oligomers and obtained by reactive extrusion. In presence of formic acid, starch is destructured to starch formate and oligomers are used as plasticizers. The linear viscoelastic response of blends is quite similar to that of nanocomposite materials; the low frequency behavior is attributed to a percolated network of destructured starch particles, and the high frequency behavior is that of the polymer matrix. The viscosity curves present a profile characterized by two plateau regions, at low and high shear rates. The plateau region at low shear rates correspond to the viscous response of the blend while the region observed at high shear rates can be attributed to the PCL matrix. The compatibilization is enhanced in the presence of starch formate and increases with increasing the oligomer molecular weight. The use of PCL oligomer was shown to improve this compatibilization effect.

4.5 Development of Starch-Based Blends

4.5.1 Blending with Polyolefin

In order to obtain a cost-effective biodegradable plastic, the blends of polyolefin with starch are still one of the best alternatives due to their low price, better properties, broad suppliers, and mature processing facilities and techniques etc. However, starch and polyolefin blends are incompatible at the molecular level, which often leads to poor performance. In order to overcome this drawback, either polyolefins or starch can be modified by introducing a compatibilising agent into the blend.

The properties of polyolefin/starch blends depend on starch content, degree of dispersion in the polymer matrix, on sample morphology, interactions between components, degree of crystallinity, presence of structural defects as well as preparation or processing conditions. Starch was initially added into polymers as a filler to decrease the price of products. Typical examples are blends of starch with PE, PVC and rubber. Since the 1990s, starch has been blended with conventional polymers to facilitate biodegradation of polymers, in particular polyolefins.

Like many other binary systems, there are three possible morphologies of polyolefin/starch blends. Figure 4.2a represents the morphology that starch is a continuous phase while polyolefins appear as particles distributed in starch. Wool [186] reported the biodegradation kinetics and mechanisms of starch-based polyethylene blends with volume fractions of PE ranging from 0 to 20 %. Since the rigidity of polyolefin particles are not very high there is no clear commercial benefit for this kind of blend except for developing understanding of fundamental science issues.

Figure 4.2b represents a co-continuous or possible interpenetrating network (IPN) structure. However, due to differences in viscosities of both polyolefins and starch, it is not easy to produce this kind of co-continuous or IPN microstructure. Bajpai and Saxena [187] have tried to synthesise a semi-IPN material by aqueous polymerization of methacrylamide in the presence of polyethylene glycol (PEG) and natural polysaccharides. Rodriguez-Gonzalez et al. [188] reported co-continuous blends prepared through gelatinized starch with glycerol. A one-step combined twin -screw/single screw extrusion setup is used to carry out the melt–melt mixing of the components. Glycerol was used as the starch plasticiser and its content in the TPS (thermoplastic starch) was varied from 29 to 40 %. Under the particular one-step processing conditions used it was possible to develop continuous TPS (highly interconnected) and co-continuous polymer/TPS blend extruded ribbon which possessed a high elongation at break, modulus and strength in the machine direction. The PE/TPS (55:45) blend prepared with TPS containing 36 % glycerol maintains 94 % of the elongation at break and 76 % of the modulus of polyethylene. At a composition level of 71:29 PE/TPS for the same glycerol content, the blend retains 96 % of the elongation at break and 100 % of the modulus of polyethylene.

In most polyolefin/starch blends, the polyolefin is a continuous phase while starch appears as particles distributed in the polyolefin phase (see Fig. 4.2c). Starch can be added into polyolefins as granular particles or gelatinised starch (thermoplastic starch, TPS or TS). St-Pierre et al. [189] has studied the morphologies and performance of gelatinised starch and granular starch in PE. The behaviours of gelatinised starch plasticised with glycerol were studied as the dispersed component in a polyethylene (LDPE or LLDPE) matrix. A processing technique was developed to compound the blends in one continuous process in a co-rotating twin-screw extruder fed by a single-screw extruder. The use of the single-screw as a side feeder allowed for gelatinisation of the starch before feeding it into the twin-screw at controlled temperature and pressure. The screw configuration of the twin-screw extruder maintained high pressure (>0.9 MPa) during blending to prevent

early evaporation of water. These materials displayed morphological characteristics typical of immiscible polymer–polymer blends. The number-average diameter of the dispersed phase increased from 4 μm with 8 wt % TPS to 18 μm with 36 wt % TPS in LDPE blends. It ranged from 3 to 8 μm in LLDPE blends containing 7–39 wt % TS. These results therefore indicate the possibility of achieving a level of morphological control with respect to the size and shape of the dispersed phase in these systems. Dry granular starch, on the other hand, typically is dispersed as a spherical like particle with a fixed morphology of approximately 10 μm.

Increased elastic modulus and ultimate stress of low density polyethylene has been achieved by incorporating coco-yam, water-yam and guinea-corn starches into low density polyethylene using a standard hot-melt compounding technique [190]. Some mechanical properties of compression moulded dumbbell shaped films of low density polyethylene containing up to a maximum of 20 wt % of each starch was reported. The effect of starch content and granular size of starch on the mechanical properties of PE film was reported [191]. It was found that as starch content increased, tensile strength, % elongation and light transmittance decreased and film thickness increased. Small-particle corn starch (2 μm average diameter) film had the highest elongation rate and tensile and yield strength. Similar work has also been reported by Wu et al. [192]. It was found that along with the reduction in starch granularity, the MFI of the blend melt decreases, but there was no significant change in viscosity. The decrease in starch granularity improves the processing and mechanical properties of the blend. Blending polyolefins with TPS showed similar results. Smaller particle size of TPS phase in the polyolefin phase showed improvements in the mechanical performance. For example, the number-average diameter of the dispersed phase increased from 4 μm with 8 wt % TPS to 18 μm with 36 wt % TPS in LDPE blends. It ranged from 3 to 8 μm in LLDPE blends containing 7–39 wt % TPS [189]. The LDPE blend containing 22 % TPS had 240 % elongation at break and its modulus was 109 MPa. The LLDPE blend containing 39 % TS had more than 540 % elongation at break, while the modulus was 136 MPa.

4.5.2 Blending with Biodegradable Polymers

Blending with biodegradable aliphatic polyesters has been found to be an effective method to improve the performance of starch-based materials [121, 184]. Aliphatic polyesters are usually biodegradable thermoplastic polymers with good processability, thermal stability, excellent mechanical properties, good water resistance, and dimensional stability [193]. In addition, some aliphatic polyesters such as poly(lactic acid) (PLA) [193, 194], poly(butylene succinate) (PBS) [195, 196] and poly(3-hydroxyalkanoates) (PHA) [197] can also be derived from renewable resources. So blending with these bio-derived aliphatic polyesters can improve performance without negatively influencing the biodegradability and reduce our dependence on fossil fuels for production of these materials. While natural

polymers are usually hydrophilic, aliphatic polyesters are hydrophobic polymers, so these two polymers are usually thermodynamically immiscible, which would result in poor adhesion between the two components and hence poor performance [198]. To achieve improved properties of blends, the compatibility between natural polymers and aliphatic polyesters has to be enhanced, and considerable progress has been made in this regard [199–202].

Blending starch with PLA is one of the most promising efforts, because starch is an abundant and cheap biopolymer and PLA is biodegradable with good mechanical properties. The effect of starch moisture content is an important issue and has been investigated [203]. Starch moisture (10–20 %) had a negative effect on the interfacial bonding between starch and PLA [203]. The tensile strength and elongation of the blend both decreased as starch moisture content increased. At 20 % moisture level, starch granules embedded in the PLA matrix were observed to be swollen, resulting in poor strength properties and high water absorption in the blend. Ke and Sun [141] characterized blends of starch and PLA in the presence of various water contents. It was found that the initial moisture content of the starch had no significant effect on its mechanical properties, but had a significant effect on the water absorption of the blends. The thermal and crystallization properties of PLA in the blend were not affected by moisture content. The blends prepared by compression moulding had higher crystallinities than those prepared by injection moulding. However, the blends prepared by injection moulding had higher tensile strengths and elongations and lower water absorption values than those made by compression moulding. The crystallinities of the blends increased greatly with annealing treatment at the PLA second crystallization temperature. The decomposition of PLA indicated that PLA degraded slightly in the presence of water under the processing temperatures used.

The detailed thermal behaviours of the starch/PLA blends have been studied by DSC [204]. The experimental data was evaluated using the well-known Avrami kinetic model. Starch effectively increased the crystallization rate of PLA, even at a 1 % content, but the effect was less than that of talc. The crystallization rate of PLA increased slightly as the starch content in the blend was increased from 1 to 40 %. An additional crystallization of PLA was observed, and it affected the melting point and degree of crystallinity of PLA.

The effect of amylose content in starches on the mechanical properties of the PLA/starch blends has been studied [142]. Four dry cornstarches with different amylose content were blended at 185 °C with PLA at various starch/PLA ratios. Starch with 30 % moisture content was also blended with PLA at a 1:1 ratio. Starch was used as a filler in the PLA continuous matrix phase, but the PLA phase became discontinuous as the starch content increased beyond 60 %. Blends made with high-amylose starches had lower water absorption than the blends with normal and waxy corn-starches. On the other hand, Park and Im [205] studied blends of PLA with gelatinized starch. Starch was firstly gelatinized with various ratios of water/glycerol using a twin-screw mixer. Gelatinization of starch was found to lead to the destruction or diminution of hydrogen bonding in granules and a decrease in crystallinity of starch. DSC data showed that starch acted as a

nucleating agent and glycerol as a plasticizer, contributing to an improvement in the crystallinity of the PLA blends. When the content of starch increased, the size of the spherulites in PLA blends were smaller and less regular. In the case of PLA/pure starch blends, voids appeared that were formed by the separation of starch particles from the matrix. These voids were not observed in the PLA/gelatinized starch. Similar blends were also reported by Martin and Averous [206]. The mechanical properties gave a strong indication that a low level of compatibility existed in these blends. The blends showed two distinct T_g values. However, the T_g due to the PLA phase shifted toward the T_g of TPS with the blend composition, indicating some degree of interaction. Microscopic observations revealed non-uniformly dispersed PLA inclusions in the TPS matrix, confirming that phase separation had occurred.

Blending starch with various thermoplastic resins to produce foams using a twin-screw extruder has been reported [207]. Foams of corn-starch with PLA, poly(hydroxyester ether) (PHEE) or PHBV had significantly lower densities and greater radial expansion ratios than the control starch. Blends with other polyesters and cellulose acetate had densities and expansion ratios between those of the control starch and the other polyesters. Most of the polymer occupied spherical to elongated domains 1–10 μm long, although PLA domains were much smaller. Surface polymer concentrations were larger than the bulk, and correlated with foam expansion and resistance to fragmentation.

Various compatibilizers and additives have been investigated to improve the interfacial interactions of these blends. Wang et al. [208] used methylenediphenyl diisocyanate (MDI) to improve the interface and studied a blend of 55/45 (%w/w) mixture of PLA and dried wheat starch in an intensive mixer with or without a low level of MDI. Blends with MDI had enhanced mechanical properties that could be explained by the in situ formation of a block copolymer acting as a compatibilizer. SEMs showed reduced interfacial tension between the two phases. The presence of MDI also enhanced the mechanical properties of the blend at temperatures above T_g. Water uptake by the PLA/starch blends with and without MDI did not differ.

The blends of PLA with various levels of wheat starch and MDI that were hot mixed at 180 °C then hot-pressure moulded at 175 °C [209]. The blend with 45 % wheat starch and 0.5 wt % MDI gave the highest tensile strength. Dynamic mechanical analysis showed that storage modulus increased and tanδ decreased as starch level increased, but almost leveled off when the starch level reached 45 % or higher. Water absorption of the blends increased significantly with starch content. Yet the blend, if waterproofed on its surface, has potential for short-term disposable applications. The effect of physical aging on the properties of the blends with or without MDI was also studied [210]. In this study, blends of PLA (1/1, %w/w) and starch with or without MDI were evaluated for thermal and mechanical properties, as well as morphology, during the course of physical aging when stored for up to 12 months at 25 °C and 50 % relative humidity. The blends were prepared by thermally blending PLA with wheat starch, corn-starch and/or high amylose corn-starch, with or without MDI. All samples exhibited the phenomena of physical aging. The samples with MDI aged more slowly, showing a

slower reduction rate of excess enthalpy relaxation, than those without MDI. The mechanical properties decreased slowly as aging proceeded. The microstructure of these blends showed a reduced interaction between starch and PLA around the interface with aging.

Zhang and Sun [211] used dioctyl maleate (DOM) as a compatibilizer in blends of PLA/starch. Using DOM as a compatibilizer markedly improved the tensile strength of the blend, even at low concentrations (below 5 %). When DOM functioned as a plasticizer at concentrations over 5 %, significant enhancement in elongation was observed. Compatibilization and plasticization took place simultaneously, which was indicated by the mechanical properties and thermal behaviour of the blends. With DOM as a polymeric plasticizer, thermal loss in the blends was not significant. Water absorption of PLA/starch blends increased with DOM concentration, whereas DOM leaching in an aqueous environment was inhibited.

Other compatibilizers were also studied for the starch/PLA blends, such as poly(vinyl alcohol) (PVOH) [212] and PHEE (Poly(hydroxyester ether) [213]. PVOH containing unhydrolytic residual groups of poly(vinyl acetate) was shown to have a good compatibility with starch. It was added to a starch and PLA blend (50/50, w/w) to enhance compatibility and improve mechanical properties. The increasing molecular weight of PVOH was also shown to affect water absorption. The blend containing gelatinized starch had higher tensile strength. However, gelatinized starch also resulted in increased water absorption. A study of injection moulded tensile bars composed of native corn-starch, PLA and PHEE showed that the rates of weight loss increased in the order; pure PLA ($\sim$0 %/year) $<$ starch/PLA (0–15 %/year) $<$ starch/PHEE/PLA (4–50 %/year), and increased with increasing starch and PHEE contents.

In addition to PLA, other polyesters have also been blended with starch. Zhang et al. [214] studied blends of poly(3-hydroxybutyrate) (PHB) and starch acetate (SA), and found that the PHB/SA blends were immiscible. Melting temperatures of PHB in the blends showed some shift with an increase of SA content. Melting enthalpy of the PHB phase in the blend was close to the value for pure PHB. The glass transition temperatures of PHB in the blends remained constant at 9 °C. FTIR absorptions of hydroxyl groups of SA and carbonyl groups of PHB in the blends were found to be independent of the second component at 3,470 and 1,724 cm^{-1}, respectively. Crystallization of PHB was affected by the addition of the SA component, both from the melt on cooling and from the glassy state on heating. Temperature and enthalpy of non-isothermal crystallization of PHB in the blends were much lower than those of pure PHB. Crystalline morphology of PHB crystallized from the melt under isothermal conditions varied with SA content. The cold crystallization peaks of PHB in the blends shifted to higher temperatures compared with that of pure PHB. Willett et al. [215]. utilized grafted copolymers of starch and glycidyl methacrylate (starch-*g*-PGMA) to improve the mechanical properties of composites with PHBV. In general, the tensile and flexural strengths of the composites were greater with starch-*g*-PGMA compared to untreated starch, and increased with increasing graft content. Grafting did not significantly change

the modulus and elongation of these blends. All samples gained weight after immersion in water for 28 days. Tensile strength and modulus decreased with water sorption, while the fracture toughness significantly increased with grafted starch. SEMs of cryogenic fracture surfaces showed improved adhesion between the starch-*g*-PGMA and the PHBV matrix.

Maliger et al. [216] have reported on a compatible blend of starch and polyester through reactive extrusion using maleic anhydride (MA) and dicumyl peroxide (DCP) as compatilizer and initiator, respectively. It was found that distributing di-isocyanate in the polyester phase prior to blending resulted in better mechanical properties than distribution in starch phase [194, 196].

4.6 Development of Starch-Based Composites

4.6.1 Starch/Mineral Filler Composites

The introduction of inorganic fillers to the matrix of starch-based materials can increase its strength and stiffness and sometimes creates special properties, originating from the synergetic effect between the component materials. Among inorganic compounds, special attention has been paid to clay because of their small particle size and intercalation properties. An increase of 50 % in the modulus for starch/calcined kaolin composite containing kaolin when compared with a sample prepared without calcined kaolin, was observed [217]. Dynamic mechanical analyses showed that the composite films gave rise to three relaxation processes, attributable to a transition of the glassy state of the glycerol-rich phase, to water loss including the interlayer water from the clay structure, and to the starch-rich phase.

Plasticized starch/clay composite films can be prepared by casting aqueous solutions containing oxidized corn-starch [218]. Different concentrations of glycerol as a plasticizer and 5 % clay on the basis of dry starch were investigated. Both montmorillonite (MMT) and organically modified montmorillonite (OMMT) were utilized to reinforce the thermoplastic acetylated starch (TPAS) composite [219]. After the addition of layered silicates, the restriction of the motion of the intercalated acetylated starch molecular chains by the clay layer sheets led to an increase in melt viscosity and equilibrium torque. As expected, the tensile strength and storage modulus of the TPAS composite were remarkably enhanced due to the interaction of layered silicates with the TPAS matrix, but the thermal stability of the TPAS composite was not obviously improved. The greater reinforcing effect of OMMT than that of MMT could be attributed to the better dispersion of OMMT in the TPAS matrix, resulting from the larger distance between OMMT layers after the modification by organic ammonium cations with long alkyl chains. Clay has also been widely used in starch-based compression moulded products (see Sect. 4.4.4).

4.6.2 Starch/Cellulose Fibre Composites

Cellulose has been widely used in polymeric composites to improve mechanical properties. Hydrophilic cellulose fibers are very compatible with starch-based materials. An almost linear relationship between fiber content and the tensile properties was found [220]. The unidirectional and crossed-ply arrangements act important role during processing [221]. During loading the acoustic emission (AE) was recorded. Burst type AE signal characteristics (amplitude, width) were traced to the failure mechanisms and supported by fractographic inspection. The mechanical response and failure mode of the composites strongly depended on the flax content and the flax fiber lay-up. The flax fiber reinforcement increased the tensile modulus of the pure starch by several orders of amplitude.

Unripe coconut fibers were used as fillers in a biodegradable polymer matrix of starch/ethylene vinyl alcohol (EVOH)/glycerol [222]. At low fiber content, blends were more flexible, with higher tensile strength oberved than at higher fiber levels. The temperature at the maximum degradation rate slightly shifted to lower values as fiber content increased. Comparing blends with and without fibers, there was no drastic change in melt temperature of the matrix with increase of fiber content, indicating that fibers did not lead to significant changes in crystalline structure. The micrographs of the tensile fractured specimens showed a large number of holes resulting from fiber pull-out from the matrix, which is indicative of poor adhesion between fiber and matrix. Rosa et al. [223] studied the coir fibers treated by three ways, namely washing with water, alkali treatment (mercerization) and bleaching, incorporated in starch/ethylene vinyl alcohol copolymers (EVOH) blends. All treatments produced surface modifications and improved the thermal stability of the fibers and consequently of the composites. The mercerization improved fiber–matrix adhesion, allowing an efficient stress transfer from the matrix to the fibers. The increased adhesion between fiber and matrix was also observed by SEM. Treatment with water also improved values of Young's modulus which were increased by about 75 % as compared to the blends without the fibers. Lee et al. [224] prepared biodegradable composites of cellulose diacetate and starch. Epoxidized soybean oil, as a lubricant, and triacetine, as a plasticizer, were added to the composites.

Colloidal suspension of cottonseed linter cellulose crystallite was used as a filler to reinforce glycerol plasticized starch [225]. The cellulose crystallites, having lengths of 350 ± 70 nm and diameters of 40 ± 8 nm on average, were prepared from cottonseed linters by acid hydrolysis. It was found that the strong interactions between fillers and between the filler and starch matrix play a key role in reinforcing the resulting composites. Incorporating cottonseed linter cellulose crystallites into starch matrix leads to an improvement in water resistance for the resulting bio-composites.

Comparing with glycerol-plasticized thermoplastic pea starch (TPS)/carboxymethyl cellulose (CMC) and TPS/microcrystalline cellulose (MC) composites [226], scanning electron microscope (SEM) showed that there was good adhesion

between starch and CMC or MC, but these superfluous cellulose derivatives resulted in the conglomeration in TPS matrix. MC increased the thermal stability, while CMC impaired it. DMTA revealed that the addition of CMC or MC enhanced the storage modulus and the glass transition temperature of the composites. At the low contents of cellulose derivatives (<9 wt %), the greater the content of CMC or MC, the greater the tensile strength of the composite. The values of WVP decreased with the increasing of cellulose derivatives. TPS/MC composites exhibited improved water vapor barrier properties than TPS/CMC composites. Coconut, sisal and jute fibers were added as reinforcement materials in a biodegradable polymer matrix comprised of starch/gluten/glycerol [227]. Addition of lignocellulosic fibers in the matrix decreased the water absorption at equilibrium.

Alvarez et al. [228] developed biodegradable composites based on cellulose derivatives/starch blends reinforced with sisal short fibers, by injection molding. The addition of sisal fibers to the polymeric matrix promotes a significant improvement in creep resistance of the composite. The composites with different fiber content, ranging from 5 to 20 wt %, showed a significant increase in the crack initiation resistance under quasistatic loading [229]. This was caused by the incorporation of sisal fibers to the matrix and the development of failure mechanisms induced by the presence of the fibers. On the other hand, a modest increase in resistance to crack initiation with fiber loading was detected. An improved fracture behaviour was also observed when the impact loading was parallel to the thickness direction. The composites exhibited higher values of ductility index, energy at initiation and total fracture energy than the plain matrix.

Recently, bacterial cellulose, produced by Acetobacter Xylinum, was used as reinforcement in composite materials with a starch thermoplastic matrix [230]. The composites prepared with bacterial cellulose displayed better mechanical properties than those with vegetable cellulose fibers.

4.7 Development of Starch-Based Nano-Composites

The interest in new nanoscale fillers has rapidly grown in the last two decades, since it was discovered that a nanostructure could be built from a polymer and layered nano-filler, such as nanoclay. This new technique has been widely used in starch-based materials.

4.7.1 Reinforcement by Nano-Fillers

Montrorillonite (MMT) is the most popular filler used for developing thermoplastic starch (TPS)/clay nanocomposites. Nanocomposites showed a significant improvement in tensile properties compared to the pure matrix [231].

Natural montrorillonite and organically modified MMT with methyl tallow bis-2-hydroxyethyl ammonium cations located in the silicate gallery (Cloisite 30B) were evaluted in starch-based nanocomposite [232]. It was observed that the TPS/Cloisite Na+ nanocomposites showed higher tensile strength and thermal stability, better barrier properties to water vapor than the TPS/Cloisite 30B nanocomposites, as well as the pristine TPS, due to the formation of the intercalated nanostructure. Pérez et al. [233] compared three different clays (Cloisite Na+, Cloisite 30B and Cloisite 10A) and found the best properties were achieved with Cloisite 10A due to their greatest compatibility with the matrix.

Modified kaolinite/carboxymethyl starch (CMS) nanocomposite was synthesized with a displacement method with dimethyl sulfoxide modified kaolinite as an intermediate [234]. The analyses showed that kaolinite was dispersed as nanometer-scale segments, in the CMS matrix. Several starch/poly(vinylalcohol)/montmorillonite nanocomposites have been subjected to surface modification by physical treatments such as dielectric barrier discharge (DBD) exposure and coating with proteins (albumin) or polysaccharides (chitosan), for improving their biocompatibility [235]. It has been established that enhancement of the surface characteristics depends on the type and number of incorporated nanoparticles as well as on the treatment applied. Coupling of DBD exposure and coating techniques appears to be highly efficient. Zhang et al. [236] found that the increase in *d*-spacing of organically modified clay was due to starch molecular intercalation while the increase in *d*-spacing of pristine clay was mostly caused by glycerol intercalation because of the narrow valid *d*-spacing of pristine clay and special ring-like monomer of starch.

Various techniques have been developed to modify MMT, in particular to exfoliate clay. Liao et al. [237] produced nanocomposites from metallocene polyethylene-octene elastomer (POE), montmorillonite and starch. It was found that organophillic clay could be well dispersed into acrylic acid grafted polyethylene-octene elastomer (POE-g-AA) in nanoscale sizes since cetyl pyridium chloride was partially compatible with POE-g-AA and allows POE-g-AA chains to intercalate into clay layers. The new partly biodegradable POE-g-AA/clay/starch hybrid could obviously improve the elongation and the tensile strength at break of the POE-g-AA/starch hybrid since the former can give the smaller starch phase size and nanoscale dispersion of silicate layers in the polymer matrix. Mathew et al. [238] reported nanocomposite materials using sorbitol plasticized waxy maize starch as matrix and tunicin whiskers as the reinforcement. The nanocomposites exhibit good mechanical strength due to the strong interaction between tunicin whiskers, matrix, plasticizer (sorbitol), and water, and due to the ability of the cellulose filler to form a rigid three-dimensional network. A decrease in crystallinity of the amylopectin phase is observed at high filler loads, due to the resistance to chain rearrangement imposed by the whiskers. The mechanical strength increased proportionally with filler loads, showing an effective stress transfer from the matrix to the whiskers.

Plasticizers used for TPS can also exfoliate clay during processing. Maksimov et al. [239] investigated an unmodified-montmorillonite (MMT)-filled

nanocomposite based on plasticized starch. It is found that the resistance to water permeation of plasticized starch can be improved considerably by introducing a rather small amount of the filler into it. Ma et al. [240] prepared thermoplastic starch/montmorillonite nanocomposites plasticized by sorbitol. Dai et al. [241] reported that N-(2-Hydroxyethyl) formamide (HF) was synthesized efficiently and used as a new additive to prepare TPS/MMT. HF acted as both plasticizer for TPS and swelling agent for MMT. Two steps extrusion processing was developed to prepare TPS/glycerol modified-montmorillonite (GMMT) nanocomposites [242]. Glycerol can enlarge the d-spacing and destruct the multilayer structure of MMT) effectively using high speed emulsifying machine in the first modification step. So the enlarged d-spacing and destructed platelets of MMT are favorable to form intercalated or exfoliated TPS/GMMT nanocomposites in the second melt extrusion processing. In addition, citric acid (CA) can increase the plasticization of TPS and dispersion of MMT in nanocomposites effectively. Majdzadeh-Ardakani et al. [243] studied the starch/clay nanocomposites prepared via solution casting method and the effects of starch source, clay cation, glycerol content, and mixing mode on clay intercalation and Young's modulus of nanocomposites. Nanocomposites prepared with MMT modified with citric acid demonstrated the highest Young's modulus compared to pristine MMT and organoclay. A combined mechanical and ultrasonic mixing mode led to an extensive dispersion of silicate layers and thus the highest Young modulus in nanocomposites. Schlemmer et al. [244] reported starch and clay nanocomposite plasticized by pequi (Caryocar brasiliense) oil. Exfoliation is the predominant mechanism of clay dispersion for low filler loading. X-ray diffraction and transmission electron microscopy demonstrated that plasticizer could enlarge the d-spacing and destruct the layered structure of MMT effectively during the pre-processing of MMT [245]. The enlarged d-spacing and fragmentized platelets of glycerol activated-MMT were a precondition to form intercalated or exfoliated TPS-based nanocomposites during the melt extrusion processing. These highly dispersive and compatible TPS/activated-MMT nanocomposites had increased thermal stability and tensile properties as compared with non-activated composites.

Ren et al. [246] developed TPS and nanocomposite (TPS/OMMT) with 15 % carbamide, 15 % ethanolamine and different contents of organic activated montmorillonite (OMMT) by twin-screw extruder. Scanning electron microscope revealed that the lower contents of OMMT could disperse well in the matrixes of TPS. The carbamide, ethanolamine and the OMMT could destroy the crystallization behavior of starch, but only the OMMT restrained this behavior for long-term storing. Tensile strength and modulus of TPS/OMMT nanocomposites were better than those of TPS, while the elongation at break was descended with the increasing of OMMT contents. Zeppa et al. [247] investigated nanocomposites based on starch, glycerol and a urea/ethanolamine mixture. The significant reduction of oxygen permeability obtained with natural montmorillonite was related to the high dispersion state of this clay. For urea–ethanolamine composites, specific compatibilizer/clay interactions led to an improvement again in the barrier properties. Similarly Cyras et al. [248] reported glycerol-plasticized starch/clay

nanocomposites films from potato starch and three different loadings of montmorillonite aqueous suspensions.

Dean et al. [111] studied a series of gelatinized starch–clay nanocomposites which exhibit intercalated and exfoliated structures. Various nanoclay dispersions were prepared (either by standard mixing or through the use of ultrasonics) prior to their combination with a high amylose content starch, using high-speed mixing and extrusion technology. A range of plasticiser levels were evaluated in conjunction with different unmodified nanoclays (sodium montmorillonite (Na-MMT) and fluorohectorite (Na-FHT)) having different cationic exchange capacities. It was shown that an optimum level of both plasticiser and nanoclay existed to produce a gelatinized starch film with the highest levels of exfoliation, resulting in superior properties. The use of ultrasonics was only advantageous in terms of clay dispersions at medium clay concentrations in the Na-MMT nanocomposites and higher clay concentrations in the Na-FHT, most probably due to the difference in cationic exchange capacity; however when the level of clay, water and starch was optimised an exfoliated structure was produced via standard mixing which exhibited comparable improvements in mechanical properties to ultrasonically treated samples. Dean et al. [249] also reported a series of thermoplastic starch/PVOH/montmorillonite micro- and nanocomposites. Fourier transform infrared spectra of the thermoplastic starch and starch nanocomposites showed a number or variants in H-bonding between starch chains, PVOH and Na-MMT during extrusion processing. The addition of small amounts of PVOH to the starch nanocomposite produced a very ordered intercalated structure. The relative concentrations of PVOH and Na-MMT could be directly correlated to changes in intergallery spacings. Although good dispersion of clay platelets was important in improving mechanical properties in these nanocomposites, the interfacial interactions of filler and matrix played just as important a role (the more agglomerated composites) containing both Na-MMT and PVOH, which showed significant increases in tensile strength and tensile modulus as compared to the more well dispersed composites without PVOH. The improvements in properties were attributed to both interfacial interactions.

Mondragón et al. [250] used unmodified and modified natural rubber latex (uNRL and mNRL) to prepare thermoplastic starch/natural rubber/montmorillonite type clay (TPS/NR/Na+-MMT) nanocomposites by twin-screw extrusion. Transmission electron microscopy showed that clay nanoparticles were preferentially intercalated into the rubber phase. Elastic modulus and tensile strength of TPS/NR blends were dramatically improved as a result of rubber modification. Properties of blends were almost unaffected by the dispersion of the clay except for the TPS/mNR blend loading 2 % MMT. This was attributed to the exfoliation of the MMT.

The performance of the TPS/MMT nanocomposities using different kinds of starch have been studied. Nejad et al. [251] developed nanocomposites through the melt intercalation of nanoclays and starch esters from high amylose starch. Starch acetates (SAs) and starch propionates (SPs) were tested in combination with glycerol triacetate (triacetin) as a plasticizer for concentrations up to 30 and 20 wt %, respectively, with different types of organomodified and unmodified

montmorillonites (MMTs). Mondragon et al. [252] used three types of maize starch with different amounts of amylose and amylopectin to prepare plasticized starch/clay nanocomposite films by casting. The plasticized waxy starch molecules were the easiest of them all to be intercalated/exfoliated, which was reflected in the highest increment of the stress at peak of these nanocomposites. Moreover, the lowest water uptake was showed by the plasticized high-amylose starch/clay nanocomposites. It was concluded that varying contents of amylose and amylopectin influenced the formation of intercalated/exfoliated clay structures and also affected the interactions of clay with water. Zeppa et al. [247] investigated nanocomposites based on potato starch, glycerol and a urea/ethanolamine mixture. The significant reduction of oxygen permeability obtained with natural montmorillonite was related to the high dispersion state of this clay. For urea–ethanolamine composites, specific compatibilizer/clay interactions led to an improvement again in the barrier properties. Similarly Cyras et al. [248] developed glycerol-plasticized starch/clay nanocomposites films from potato starch and three different loadings of montmorillonite aqueous suspensions.

Other nano-fillers have also investigated. Cao et al. [253] reported the utilization of multiwalled carbon nanotubes (MWCNTs) as filler-reinforcement to improve the performance of plasticized starch (PS). The PS/MWCNTs nanocomposites were prepared by a simple method of solution casting and evaporation. The results indicated that the MWCNTs dispersed homogeneously in the PS matrix and formed strong hydrogen bonding with PS molecules. Besides the improvement of mechanical properties, the incorporation of MWCNTs into the PS matrix also led to a decrease in the water sensitivity of the PS-based materials.

4.7.2 Reinforcement by Nano-Fibres

More recently, various nano-fibre reinforced nanocomposites have been developed. Viguié et al. [254] developed nanocomposite films processed from a filler and a matrix having the same nature: waxy maize starch. The filler consists of nanoplatelet-like starch particles obtained as an aqueous suspension by acid hydrolysis of starch granules and the matrix was prepared by plasticization and disruption of starch granules with water and sorbitol. Nanocomposite films were obtained by casting and evaporating the mixture of the aqueous suspension of starch nanocrystals with the gelatinized starch. The resulting films were conditioned before testing and the effect of accelerated ageing in a moist atmosphere was investigated. Similarly, García et al. [255] reported nanocomposites of cassava starch reinforced with waxy starch nanocrystals. The materials showed a 380 % increase of the rubbery storage modulus and a 40 % decrease in the water vapor permeability. X-ray spectra show that the composite was more amorphous than the neat matrix, which was attributed to higher equilibrium water content in the composites. TGA confirmed this result and its thermal derivative suggested the formation of hydrogen bonding between glycerol and the nanocrystals.

The reinforcing effect of starch nanocrystals was attributed to strong filler/matrix interactions due to the hydrogen bonding. The decrease of the permeability suggests that the nanocrystals were well dispersed, with few filler/filler interactions.

Cao et al. [256] developed nanocomposite films from a mixed suspension of hemp cellulose nanocrystals (HCNs) and thermoplastic starch by the casting. The cellulose nanocrystals dispersed in the TPS matrix homogeneously and resulted in an increase in the glass-transition temperature, which was ascribed to the fact that the flexibility of the starch molecular chains in the starch-rich phase was reduced because of the strong intermolecular interactions between the starch and stiff HCNs. The films exhibited significant increases in the tensile strength and Young's modulus with increasing HCN content. In addition to the improvement in mechanical properties, the incorporation of HCNs into the PS matrix also led to a decrease in the water sensitivity of the final composite materials. Therefore, the HCNs played an important role in improving the mechanical properties and water resistance of the starch-based materials. Kaushik et al. [257] characterized the properties of cellulose nanofibril/TPS based nanocomposites. The cellulose nanofibrils were extracted from wheat straw using steam explosion, acidic treatment and high shear mechanical treatment. These nanofibrils were dispersed in thermoplastic starch using a Fluko high shear mixer in varying proportions and films were casted out of these nanocomposites. The fiber diameter was in the range from 30 to 70 nm. TGA depicted an increasing in residue left with increase in cellulose nanofibrils content. Mechanical properties increased with nanofiber concentration. Barrier properties also improved with addition of nanofillers up to 10 % but further addition deteriorated properties due to possible fiber agglomeration.

Grande et al. [258] reported a bioinspired bottom-up process to produce self-assembled nanocomposites of cellulose synthesized by Acetobacter bacteria and native starch. This process takes advantage of the way some bacteria extrude cellulose nanofibres and of the transport process that occurs during the gelatinization of starch. Potato and corn starch were added into the culture medium and partially gelatinized in order to allow the cellulose nanofibrils to grow in the presence of a starch phase. The bacterial cellulose (BC)–starch gels were hot pressed into sheets that had a BC volume fraction higher than 90 %. During this step starch was forced to further penetrate the BC network.

Teixeira et al. [259] reported that cellulose cassava bagasse nanofibrils (CBN) were used as reinforcing nanoparticles in a thermoplastic cassava starch matrix plasticized using either glycerol or a mixture of glycerol/sorbitol (1:1) as plasticizer through a melting process. The tensile tests depend on the nature of the plasticizer employed. For the glycerol-plasticized matrix-based composites, it was limited especially due to additional plasticization by sugars originating from starch hydrolysis during the acid extraction. This effect was evidenced by the reduction of glass vitreous temperature of starch after the incorporation of nanofibrils in TPSG and by the increase of elongation at break in tensile test. On the other hand, for glycerol/sorbitol plasticized nanocomposites the transcrystallization of amylopectin in nanofibrils surface hindered good performances of CBN as reinforcing

agent for thermoplastic cassava starch. The incorporation of cassava bagasse cellulose nanofibrils in the thermoplastic starch matrices has resulted in a decrease of its hydrophilic character especially for glycerol plasticized sample.

4.8 Summary

Blending and compositing have been successfully used in starch-based materials. Starch was initially used a fillers blended with various polymers, especially with polyolefin. Blending starch with biodegradable polymers has attracted more and more attention. The interest in new nanoscale fillers has rapidly grown since it was discovered that a nanostructure could be built from a polymer and a layered nanoclay. These new nanocomposites show dramatic improvement in mechanical properties with low filler content. Cellulose is the major substance obtained from vegetable fibers, and applications for cellulose fiber-reinforced polymers have again come to the forefront with the focus on renewable feedstocks. Hydrophilic cellulose fibers are very compatible with most natural polymers.

In practice, the techniques of blending, compositing and nano-reinforcement are often used together. Thermoplastic starch/poly(vinyl alcohol) (PVOH)/clay nanocomposites exhibited the intercalated and exfoliated structures [260]. Montmorillonite (MMT) with three types of cation or modifier (Na^+, alkyl ammonium ion, and citric acid) was examined. The prepared nanocomposites with modified montmorillonite indicated a mechanical improvement in the properties, in comparison with pristine MMT.

Liao et al. [261] reported biodegradable nanocomposites prepared from poly(lactic acid) (PLA) or acrylic acid grafted poly(lactic acid) (PLA-*g*-AA), titanium tetraisopropylate, and starch. Arroyo et al. [262] reported that thermoplastic starch (TPS) and polylactic acid (PLA) were compounded with natural montmorillonite (MMT). The TPS can intercalate the clay structure and that the clay was preferentially located in the TPS phase or at the blend interface. This led to an improvement in tensile modulus and strength, but a reduction in fracture toughness.

Multilayer co-extrusion is another technique used in the preparation of starch/synthetic sheets or films [164, 263–266], in which TPS is laminated with appropriate biodegradable polymers to improve the mechanical, water-resistance and gas-barrier properties of final products. These products have shown potential for applications such as food packaging and disposable product manufacture. Three-layer co-extrusion is most often practiced, in which a co-extrusion line consists of two single-screw extruders (one for the inner starch layer and the other for the outer polymer layers); a feedblock; a coat-hanger-type sheet die; and a three-roll calendering system [164]. Biodegradable polyesters such as PCL [164, 264], PLA [164, 263], and polyesteramide, PBSA and poly(hydroxybutyrate-co-valerate) [164] are often used for the outer layers. These new blends and composites are extending the utilization of starch-based materials into new value-added products.

References

1. Whistler, R.L., BeMiller, J.N., Paschall, B.F.: Starch: Chemistry and Technology. Academic Press, New York (1984)
2. Chen, P., Yu, L., Simon, G., Petinakis, E., Dean, K., Chen, L.: J. Cereal Sci. **50**, 241–247 (2009)
3. Blazek, J., Salman, H., Rubio, A.L., Gilbert, E., Hanley, T., Copeland, L.: Carbohydr. Polym. **75**, 705–711 (2009)
4. French, D.: Organization of starch granules. In: Whistler, R.L., Bemiller, J.N., Parschall, E.F. (eds.) Starch, Chemistry and Technology, pp. 183–247. Academic Press, New York (1984)
5. Qi, X., Tester, R.F., Snape, C.E., Yuryev, V., Wasserman, L.A., Ansell, R.: J. Cereal Sci. **39**, 57–66 (2004)
6. Cameron, R.E., Donald, A.M.: Polymer **33**, 2628–2635 (1992)
7. Kozlov, S., Noda, T., Bertoft, E., Yuryev, V.: J. Therm. Anal. Calorim. **86**, 291–301 (2006)
8. Liu, H., Xie, F., Yu, L., Chen, L., Li, L.: Prog. Polym. Sci. **34**, 1348–1368 (2009)
9. Atwell, W.A., Hood, L.F., Lineback, D.R., Varrianomarston, E., Zobel, H.F.: Cereal Foods World **33**, 306–311 (1988)
10. Lelievre, J.: J. Appl. Polym. Sci. **18**, 293–296 (1974)
11. Sullivan, J.W., Johnson, J.A.: Cereal Chem. 41, 73–77 (1964)
12. Yu, L., Christie, G.: Carbohydr. Polym. **46**, 179–184 (2001)
13. Biliaderis, C.G., Page, C.M., Slade, L., Sirett, R.R.: Carbohydr. Polym. **5**, 367–389 (1985)
14. Svensson, E., Eliasson, A.-C.: Carbohydr. Polym. **26**, 171–176 (1995)
15. Lelievre, J.: Polymer **17**, 854–858 (1976)
16. Russell, P.L.: J. Cereal Sci. **6**, 133–145 (1987)
17. Olkku, J., Rha, C.: Food Chem. **3**, 293–317 (1978)
18. Wang, S.S., Chiang, W.C., Zhao, B., Zheng, X.G., Kim, I.H.: J. Food Sci. **56**, 121–124 (1991)
19. Lai, L.S., Kokini, J.L.: Biotechnol. Prog. **7**, 251–266 (1991)
20. Donovan, J.W.: Biopolymers **18**, 263–275 (1979)
21. Levine, H., Slade, L.: Influences of the glassy and rubbery states on the thermal, mechanical and structural properties of doughs and baked products. In: Faridi, H., Faubion, J.M. (eds.) Dough Rheology and Baked Product Texture, pp. 157–330. Van Nostrand Reinhold, New York (1990)
22. Kokini, J.L., Baumann, G.C., Bresslauer, K., Chedid, L.L., Herh, P., Lai, L.S.: A kinetic model for starch gelatinization and effect of starch/protein interactions on rheological properties of 98 % amylopectin and amylose rich starches. In: Spiess, W.E.L., Schubert, H. (eds.) Engineering and Foods, Advanced Process, pp. 109–121. Elsevier/Applied Science Publishers, New York (1990)
23. Herh, P.K., J.L. Kokini: The effect of pressure on gelatinization of starch using small amplitude oscillatory measurements under pressure. Paper presented at the proceedings of the institute of food technologists 51st annual meeting Anaheim, CA
24. Wunderlich, B.: The basis of thermal analysis. In: Turi, E.A. (ed.) Thermal Characterization of Polymeric Materials, pp. 92–234. Academic Press, New York (1981)
25. Burros, B.C., Young, L.A., Carroad, P.A.: J. Food Sci. 52, 1372–1376 (1987)
26. Wen, L.F., Rodis, P., Wasserman, B.P.: Cereal Chem. **67**, 268–275 (1990)
27. Klingler, R.W., Meuser, F., Niediek, E.A.: Starch–Stärke **38**, 40–44 (1986)
28. Colonna, P., Doublier, J.L., Melcion, J.P., Demonredon, F., Mercier, C.: Cereal Chem. **61**, 538–543 (1984)
29. Liu, P., Yu, L., Liu, H., Chen, L., Li, L.: Carbohydr. Polym. **77**, 250–253 (2009)
30. Xie, F., Liu, W.-C., Liu, P., Wang, J., Halley, P.J., Yu, L.: Starch–Stärke **62**, 350–357 (2010)
31. Liu, P., Yu, L., Wang, X., Li, D., Chen, L., Li, X.: J. Cereal Sci. **51**, 388–391 (2010)

32. Ma, X.F., Yu, J.G., Wan, J.J.: Carbohydr. Polym. **64**, 267–273 (2006)
33. Yang, J.-h., Yu, J.-g., Ma, X.-f.: Starch—Stärke **58**, 330–337 (2006)
34. Yang, J.-h., Yu, J.-g., Ma, X.-f.: Carbohydr. Polym. **66**, 110–116 (2006)
35. Yang, J.-H., Yu, J.-G., Ma, X.-F.: Carbohydr. Polym. **63**, 218–223 (2006)
36. Follain, N., Joly, C., Dole, P., Roge, B., Mathlouthi, M.: Carbohydr. Polym. **63**, 400–407 (2006)
37. Thuwall, M., Boldizar, A., Rigdahl, M.: Carbohydr. Polym. **65**, 441–446 (2006)
38. Keszei, S., Szabó, A., Marosi, G., Anna, P., Nagy, S.: Macromolecular Symposia **239**, 101–104 (2006)
39. Ma, X.F., Yu, J.G., Ma, Y.B.: Carbohydr. Polym. **60**, 111–116 (2005)
40. Ma, X., Yu, J.: J. Appl. Polym. Sci. **93**, 1769–1773 (2004)
41. Rodriguez-Gonzalez, F.J., Ramsay, B.A., Favis, B.D.: Carbohydr. Polym. **58**, 139–147 (2004)
42. Ma, X., Yu, J.: Carbohydr. Polym. **57**, 197–203 (2004)
43. Yu, J.G., Wang, N., Ma, X.F.: Starch-Starke **57**, 494–504 (2005)
44. Teixeira, E.D., Da Roz, A.L., de Carvalho, A.J.F., Curvelo, A.A.D.: Macromolecular Symposia **229**, 266–275 (2005)
45. Ma, X.F., Yu, J.G., Jin, F.: Polym. Int. **53**, 1780–1785 (2004)
46. Ma, X.F., Yu, J.G.: Acta Polymerica Sinica, 240–245 (2004)
47. Stepto, R.F.T.: Macromolecular Symposia 245–246, 571–577 (2006)
48. Stepto, R.F.T.: Macromolecular Symposia **201**, 203–212 (2003)
49. Onteniente, J.-P., Abbès, B., Safa, L.H.: Starch–Stärke **52**, 112–117 (2000)
50. Soest, J.J.G.V., Borger, D.B.: J. Appl. Polym. Sci. **64**, 631–644 (1997)
51. Stepto, R.F.T.: Polym. Int. **43**, 155–158 (1997)
52. Teixeira, E.M., Da Róz, A.L., Carvalho, A.J.F., Curvelo, A.A.S.: Carbohydr. Polym. **69**, 619–624 (2007)
53. Da Roz, A.L., Carvalho, A.J.F., Gandini, A., Curvelo, A.A.S.: Carbohydr. Polym. **63**, 417–424 (2006)
54. Forssell, P.M., Mikkilä, J.M., Moates, G.K., Parker, R.: Carbohydr. Polym. **34**, 275–282 (1997)
55. Shi, R., Zhang, Z., Liu, Q., et al.: Carbohydr. Polym. **69**, 748–755 (2007)
56. Zhang, S.-D., Zhang, Y.-R., Zhu, J., Wang, X.-L., Yang, K.-K., Wang, Y.-Z.: Starch–Stärke **59**, 258–268 (2007)
57. Carvalho, A.J.F., Zambon, M.D., Curvelo, A.A.S., Gandini, A.: Polym. Degrad. Stab. **79**, 133–138 (2003)
58. Altskär, A., Andersson, R., Boldizar, A., et al.: Carbohydr. Polym. **71**, 591–597 (2008)
59. Wiedmann, W., Strobel, E.: Starch-Stärke **43**, 138–145 (1991)
60. González, R.J., Torres, R.L., De Greef, D.M., Guadalupe, B.A.: J. Food Eng. **74**, 96–107 (2006)
61. Walia, P.S., Lawton, J.W., Shogren, R.L., Felker, F.C.: Polymer **41**, 8083–8093 (2000)
62. Della Valle, G., Buleon, A., Carreau, P.J., Lavoie, P.A., Vergnes, B.: J. Rheol. **42**, 507–525 (1998)
63. Aichholzer, W., Fritz, H.-G.: Starch-Stärke **50**, 77–83 (1998)
64. Della Valle, G., Colonna, P., Patria, A., Vergnes, B.: J. Rheol. **40**, 347–362 (1996)
65. Valle, G.D., Boché, Y., Colonna, P., Vergnes, B.: Carbohydr. Polym. **28**, 255–264 (1995)
66. Willett, J.L., Jasberg, B.K., Swanson, C.L.: Polym. Eng. Sci. **35**, 202–210 (1995)
67. Lai, L.S., Kokini, J.L.: J. Rheol. **8**, 1245–1266 (1990)
68. Valle, G.D., Vergnes, B., Tayeb, J.: Entropie **169**, 59–63 (1992)
69. Kokini, J.L., Chang, C.N., Lai, L.S.: The role of rheological properties on extrudate expansion. In: Kokini, J.L., Ho, C.T., Karwe, M.V. (eds.) Food Extrusion Science and Technology, pp. 631-652. Marcel Dekker, New York (1992)
70. Tester, R.F., Morrison, W.R.: Cereal Chem. **69**, 258–262 (1992)
71. Willett, J.L., Millard, M.M., Jasberg, B.K.: Polymer **38**, 5983–5989 (1997)
72. Xie, F., Yu, L., Su, B.et al.: J. Cereal Sci. **49**, 371–377 (2009)

73. Zamudio-Flores, P.B., Vargas-Torres, A., Pérez-González, J., Bosquez-Molina, E., Bello-Pérez, L.A.: Starch-Stärke **58**, 274–282 (2006)
74. Parandoosh, S., Hudson, S.M.: J. Appl. Polymer Sci. **48**, 787–791 (1993)
75. Otey, F.H., Westhoff, R.P., Russell, C.R.: Product R&D **16**, 305–308 (1977)
76. Cinelli, P., Chiellini, E., Gordon, S.H., Imam, S.H.: Macromolecular Symposia **197**, 143–155 (2003)
77. Pareta, R., Edirisinghe, M.J.: Carbohydr. Polym. **63**, 425–431 (2006)
78. Yavuz, H., Babaç, C.: J. Polym. Environ. **11**, 107–113 (2003)
79. Mali, S., Sakanaka, L.S., Yamashita, F., Grossmann, M.V.E.: Carbohydr. Polym. **60**, 283–289 (2005)
80. Lawton, J.W.: Carbohydr. Polym. **29**, 203–208 (1996)
81. Bengtsson, M., Koch, K., Gatenholm, P.: Carbohydr. Polym. **54**, 1–11 (2003)
82. Chen, L., Imam, S.H., Gordon, S.H., Greene, R.V.: J. Environ. Polym. Degrad. **5**, 111–117 (1997)
83. Chen, L., Imam, S.H., Stein, T.M., Gordon, S.H., Hou, C.T., Greene, R.V.: Am. Chem. Soc., Polym. Prepr., Div. Polym. Chem. **37**, 461–462 (1996)
84. Cyras, V.P., Zenklusen, M.C.T., Vazquez, A.: J. Appl. Polym. Sci. **101**, 4313–4319 (2006)
85. Jayasekara, R., Harding, I., Bowater, I., Christie, G.B.Y., Lonergan, G.T.: J. Polym. Environ. **11**, 49–56 (2003)
86. Jayasekara, R., Harding, I., Bowater, I., Christie, G.B.Y., Lonergan, G.T.: Polym. Test. **23**, 17–27 (2004)
87. Kampeerapappun, P., Aht-ong, D., Pentrakoon, D., Srikulkit, K.: Carbohydr. Polym. **67**, 155–163 (2007)
88. Khan, M.A., Bhattacharia, S.K., Kader, M.A., Bahari, K.: Carbohydr. Polym. **63**, 500–506 (2006)
89. Lawton, J.W., Fanta, G.F.: Carbohydr. Polym. **23**, 275–280 (1994)
90. Lee, W.-J., Youn, Y.-N., Yun, Y.-H., Yoon, S.-D.: J. Polym. Environ. **15**, 35–42 (2007)
91. Mali, S., Grossmann, M.V.E., García, M.A., Martino, M.N., Zaritzky, N.E.: Carbohydr. Polym. **56**, 129–135 (2004)
92. Ramaraj, B.: J. Appl. Polym. Sci. **103**, 1127–1132 (2007)
93. Ramaraj, B.: J. Appl. Polym. Sci. **103**, 909–916 (2007)
94. Rioux, B., Ispas-Szabo, P., Ait-Kadi, A., Mateescu, M.-A., Juhász, J.: Carbohydr. Polym. **50**, 371–378 (2002)
95. Thiré, R.M.S.M., Simão, R.A., Andrade, C.T.: Carbohydr. Polym. **54**, 149–158 (2003)
96. Vorwerg, W., Dijksterhuis, J., Borghuis, J., Radosta, S., Kröger, A.: Starch-Stärke **56**, 297–306 (2004)
97. Wu, Q., Zhang, L.: J. Appl. Polym. Sci. **79**, 2006–2013 (2001)
98. Kalichevsky, M.T., Jaroszkiewicz, E.M., Blanshard, J.M.V.: Polymer **34**, 346–358 (1993)
99. Poutanen, K., Forssell, P.: Trends Polym. Sci. **4**, 128–132 (1996)
100. Shogren, R.L., Swanson, C.L., Thompson, A.R.: Starch-Stärke **44**, 335–338 (1992)
101. Chandra, R., Rustgi, R.: Prog. Polym. Sci. **23**, 1273–1335 (1998)
102. Coffin, D.R., Fishman, M.L.: J. Agric. Food Chem. **41**, 1192–1197 (1993)
103. Pereira, C.S., Cunha, A.M., Reis, R.L., VÁzquez, B., San RomÁn, J.: J. Mater. Sci.: Mater. Med. **9**, 825–833 (1998)
104. Espigares, I., Elvira, C., Mano, J.F., Vázquez, B., San Román, J., Reis, R.L.: Biomaterials **23**, 1883–1895 (2002)
105. Arvanitoyannis, I., Biliaderis, C.G.: Carbohydr. Polym. **38**, 47–58 (1999)
106. Lepeniotis, S., Feuer, B.I., Bronk, J.M.: Chemometr. Intell. Lab. Syst. **44**, 293–306 (1998)
107. Zhai, M., Zhao, L., Yoshii, F., Kume, T.: Carbohydr. Polym. **57**, 83–88 (2004)
108. Tharanathan, R.N.: Trends Food Sci. Technol. **14**, 71–78 (2003)
109. Rindlav-Westling, A., Stading, M., Hermansson, A.-M., Gatenholm, P.: Carbohydr. Polym. **36**, 217–224 (1998)
110. Forssell, P., Lahtinen, R., Lahelin, M., Myllärinen, P.: Carbohydr. Polym. **47**, 125–129 (2002)

111. Dean, K., Yu, L., Wu, D.Y.: Compos. Sci. Technol. **67**, 413–421 (2007)
112. Walenta, E., Fink, H.-P., Weigel, P., Ganster, J., Schaaf, E.: Macromol. Mater. Eng. **286**, 462–471 (2001)
113. Walenta, E., Fink, H.-P., Weigel, P., Ganster, J.: Macromol. Mater. Eng. **286**, 456–461 (2001)
114. Soest, J.J.G.V., Knooren, N.: J. Appl. Polym. Sci. **64**, 1411–1422 (1997)
115. Fishman, M.L., Coffin, D.R., Onwulata, C.I., Konstance, R.P.: Carbohydr. Polym. **57**, 401–413 (2004)
116. Chiang, B.Y., Johnson, J.A.: Cereal Chem. **54**, 436–443 (1977)
117. Fishman, M.L., Coffin, D.R., Onwulata, C.I., Willett, J.L.: Carbohydr. Polym. **65**, 421–429 (2006)
118. Myllymäki, O., Myllärinen, P., Forssell, P., et al.: Packag. Technol. Sci. **11**, 265–274 (1998)
119. Matzinos, P., Tserki, V., Gianikouris, C., Pavlidou, E., Panayiotou, C.: Eur. Polym. J. **38**, 1713–1720 (2002)
120. Matzinos, P., Tserki, V., Kontoyiannis, A., Panayiotou, C.: Polym. Degrad. Stab. **77**, 17–24 (2002)
121. Ratto, J.A., Stenhouse, P.J., Auerbach, M., Mitchell, J., Farrell, R.: Polymer **40**, 6777–6788 (1999)
122. Arévalo-Niño, K., Sandoval, C.F., Galan, L.J., Imam, S.H., Gordon, S.H., Greene, R.V.: Biodegradation **7**, 231–237 (1989)
123. Fanta, G.F., Swanson, C.L., Shogren, R.L.: J. Appl. Polym. Sci. **44**, 2037–2042 (1992)
124. Otey, F.H., Westhoff, R.P., Doane, W.M.: Ind. Eng. Chem. Res. **26**, 1659–1663 (1987)
125. Stenhouse, P.J., Ratto, J.A., Schneider, N.S.: J. Appl. Polym. Sci. **64**, 2613–2622 (1997)
126. van Soest, J.J.G., Essers, P.: J. Macromol. Sci., Part A: Pure Appl. Chem. **34**, 1665–1689 (1997)
127. Shogren, R.L.: Carbohydr. Polym. **19**, 83–90 (1992)
128. Shogren, R.L., Jasberg, B.K.: J. Polym. Environ. **2**, 99–109 (1994)
129. Delville, J., Joly, C., Dole, P., Bliard, C.: Carbohydr. Polym. **49**, 71–81 (2002)
130. Fishman, M.L., Coffin, D.R., Konstance, R.P., Onwulata, C.I.: Carbohydr. Polym. **41**, 317–325 (2000)
131. Yu, L., Christie, G.: J. Mater. Sci. **40**, 111–116 (2005)
132. Sachetto, J.-P., Stepto, R., Zeller, H.: Destructurized starch essentially containing no bridged phosphate groups and process for making same. UK Patent
133. Abbégs, B., Ayad, R., Prudhomme, J.-C., Onteniente, J.-P.: Polym. Eng. Sci. **38**, 2029–2038 (1998)
134. Funke, U., Bergthaller, W., Lindhauer, M.G.: Polym. Degrad. Stab. **59**, 293–296 (1998)
135. Avérous, L., Fringant, C., Moro, L.: Polymer **42**, 6565–6572 (2001)
136. Averous, L., Boquillon, N.: Carbohydr. Polym. **56**, 111–122 (2004)
137. Ramkumar, D., Vaidya, U.R., Bhattacharya, M., Hakkarainen, M., Albertsson, A.C., Karlsson, S.: Eur. Polymer J. **32**, 999–1010 (1996)
138. Ramkumar, D.H.S., Bhattacharya, M., Vaidya, U.R.: Eur. Polymer J. **33**, 729–742 (1997)
139. Mani, R., Bhattacharya, M.: Eur. Polymer J. **34**, 1467–1475 (1998)
140. Mani, R., Bhattacharya, M.: Eur. Polymer J. **34**, 1477–1487 (1998)
141. Ke, T., Sun, X. J.: Appl. Polym. Sci. **81**, 3069–3082 (2001)
142. Ke, T., Sun, S.X., Seib, P.: J. Appl. Polym. Sci. **89**, 3639–3646 (2003)
143. Sen, A., Bhattacharya, M.: Polymer **41**, 9177–9190 (2000)
144. Sen, A., Bhattacharya, M., Stelson, K.A., Voller, V.R.: Mater. Sci. Eng., A **338**, 60–69 (2002)
145. Mani, R., Bhattacharya, M.: Eur. Polymer J. **37**, 515–526 (2001)
146. Hoseney, R.C., Zeleznak, K., Abdelrahman, A.: J. Cereal Sci. **1**, 43–52 (1983)
147. Tiefenbacher, K.F.: J. Macromol. Sci., Part A: Pure Appl. Chem. **30**, 727–731 (1993)
148. Haas, F., (Vienna, AT), Haas, J., (Klosterneuburg, AT), Tiefenbacher, K., (Vienna, AT).: Process of manufacturing rottable thin-walled starch-based shaped elements. US Patent

149. Andersen, P.J., (Santa Barbara, CA), Hodson, S.K., (Santa Barbara, CA).: Molded articles having an inorganically filled organic polymer matrix. US Patent
150. Shogren, R.L., Lawton, J.W., Doane, W.M., Tiefenbacher, K.F.: Polymer **39**, 6649–6655 (1998)
151. Shogren, R.L., Lawton, J.W., Tiefenbacher, K.F., Chen, L.: J. Appl. Polym. Sci. **68**, 2129–2140 (1998)
152. Lawton, J.W., Shogren, R.L., Tiefenbacher, K.F.: Cereal Chem. **76**, 682–687 (1999)
153. Glenn, G.M., Orts, W.J.: Ind. Crops Prod. **13**, 135–143 (2001)
154. Zhou, J., Song, J., Parker, R.: Carbohydr. Polym. **63**, 466–475 (2006)
155. Kiatkamjornwong, S., Surunchanajirasakul, P., Tasakorn, P.: Plast. Rubber Compos. **30**, 318–327 (2001)
156. Shey, J., Imam, S.H., Glenn, G.M., Orts, W.J.: Ind. Crops Prod. **24**, 34–40 (2006)
157. Glenn, G.M., Orts, W.J., Nobes, G.A.R.: Ind. Crops Prod. **14**, 201–212 (2001)
158. Lawton, J.W., Shogren, R.L., Tiefenbacher, K.F.: Ind. Crops Prod. **19**, 41–48 (2004)
159. Shogren, R.L., Lawton, J.W., Tiefenbacher, K.F.: Ind. Crops Prod. **16**, 69–79 (2002)
160. Cinelli, P., Chiellini, E., Lawton, J.W., Imam, S.H.: Polym. Degrad. Stab. **91**, 1147–1155 (2006)
161. Shibata, S., Cao, Y., Fukumoto, I.: Polym. Testing **24**, 1005–1011 (2005)
162. Carr, L., Parra, D., Ponce, P., Lugão, A., Buchler, P.: J. Polym. Environ. **14**, 179–183 (2006)
163. Glenn, G.M., Orts, W.J., Nobes, G.A.R., Gray, G.M.: Ind. Crops Prod. **14**, 125–134 (2001)
164. Martin, O., Schwach, E., Avérous, L., Couturier, Y.: Starch-Stärke **53**, 372–380 (2001)
165. Brown, S.B., Orlando, C.M.: Reactive extrusion. In: Mark, H.F., Bikales, N.M., Overberger, C.G., Menges, G., Kroschwitz, J.I. (eds.) Encyclopedia of Polymer Science and Engineering, pp. 169–189. Wiley, New York (1988)
166. Carr, M.E., Kim, S., Yoon, K.J., Stanley, K.D.: Cereal Chem. **69**, 70–75 (1992)
167. Yoon, K.J., Carr, M.E., Bagley, E.B.: J. Appl. Polym. Sci. **45**, 1093–1100 (1992)
168. Dellavalle, G., Colonna, P., Tayeb, J.: Starch-Starke **43**, 300–307 (1991)
169. Carr, M.E.: J. Appl. Polym. Sci. **54**, 1855–1861 (1994)
170. Gimmler, N., Lawn, F., Meuser, F.: Starch-Stärke **47**, 268–276 (1995)
171. Wing, R.E., Willett, J.L.: Ind. Crops Prod. **7**, 45–52 (1997)
172. Miladinov, V.D., Hanna, M.A.: Ind. Crops Prod. **11**, 51–57 (2000)
173. Carr, M.E., Cunningham, R.L.: Cereal Chem. **66**, 238–243 (1989)
174. Carr, M.E., Cunningham, R.L.: Abstracts of papers of the American chemical society **203**, 562-POLY (1992)
175. Roth, D.: Continuous process for preparing polyol glycosides. US Patent
176. Carr, M.E., Wing, R.E., Doane, W.M.: Cereal Chem. **68**, 262–266 (1991)
177. Trimnell, D., Wing, R.E., Carr, M.E., Doane, W.M.: Starch-Starke **43**, 146–151 (1991)
178. Wing, R.E., Carr, M.E., Trimnell, D., Doane, W.M.: J. Control. Release **16**, 267–278 (1991)
179. Trimnell, D., Carr, M.E., Doane, W.M.: Starch-Stärke **43**, 146–151 (1991)
180. Carr, M.E., Wing, R.E., Doane, W.M.: Starch-Stärke **46**, 9–13 (1994)
181. Powers, J., (W.B., MO), Choate, D.G., (Everton, MO), Mcmasters, K.T., (Springfield, MO).: Method of and apparatus for automatically inspecting an exposed and bent lithographic plate. US Patent
182. Doane, W.M.: Ind. Crops Prod. **1**, 83–87 (1992)
183. Jun, C.L.: J. Polym. Environ. **8**, 33–37 (2000)
184. Dubois, P., Narayan, R.: Macromolecular Symposia **198**, 233–244 (2003)
185. Bossard, F., Pillin, I., Aubry, T., Grohens, Y.: Polym. Eng. Sci. **48**, 1862–1870 (2008)
186. Wool, R.P., Cole, M.A., Peanasky, J.S., Willett, J.L.: Abstracts of papers of the American chemical society **195**, 39-MACR (1988)
187. Bajpai, S.K., Saxena, S.: J. Appl. Polym. Sci. **100**, 2975–2984 (2006)
188. Rodriguez-Gonzalez, F.J., Ramsay, B.A., Favis, B.D.: Polymer **44**, 1517–1526 (2003)
189. StPierre, N., Favis, B.D., Ramsay, B.A., Ramsay, J.A., Verhoogt, H.: Polymer **38**, 647–655 (1997)
190. Oogbobe, Okeke, C.N., Otashu, M.: Indian J. Eng. Mater. Sci. **4**, 134–138 (1997)

191. Lim, S.T., Jane, J.L., Rajagopalan, S., Seib, P.A.: Biotechnol. Prog. **8**, 51–57 (1992)
192. Wu, J., Wen, Q.-Z., Xie, S.-H., Xie, B.-J.: Gaofenzi Cailiao Kexue Yu Gongcheng/ Polymeric Materials Science and Engineering **21**, 141–144 (2005)
193. Gupta, B., Revagade, N., Hilborn, J.: Prog. Polym. Sci. **32**, 455–482 (2007)
194. Yu, L., Petinakis, E., Dean, K., Liu, H., Yuan, Q.: J. Appl. Polym. Sci. (2010)
195. Song, H., Lee, S.Y.: Enzyme Microb. Technol. **39**, 352–361 (2006)
196. Yu, L., Dean, K., Yuan, Q., Chen, L., Zhang, X.M.: J. Appl. Polym. Sci. **103**, 812–818 (2007)
197. Sudesh, K., Abe, H., Doi, Y.: Prog. Polym. Sci. **25**, 1503–1555 (2000)
198. Yu, L., Dean, K., Li, L.: Prog. Polym. Sci. **31**, 576–602 (2006)
199. Ohkita, T., Lee, S.H.: J. Adhes. Sci. Technol. **18**, 905–924 (2004)
200. Nabar, Y., Raquez, J.M., Dubois, P., Narayan, R.: Biomacromolecules **6**, 807–817 (2005)
201. Li, Y.-D., Zeng, J.-B., Wang, X.-L., Yang, K.-K., Wang, Y.-Z.: Biomacromolecules **9**, 3157–3164 (2008)
202. Raquez, J.-M., Nabar, Y., Narayan, R., Dubois, P.: Polym. Eng. Sci. **48**, 1747–1754 (2008)
203. Wang, H., Sun, X.Z., Seib, P.: J. Polym. Environ. **10**, 133–138 (2002)
204. Ke, T.Y., Sun, X.Z.: J. Appl. Polym. Sci. **89**, 1203–1210 (2003)
205. Park, J.W., Im, S.S., Kim, S.H., Kim, Y.H.: Polym. Eng. Sci. **40**, 2539–2550 (2000)
206. Martin, O., Averous, L.: Polymer **42**, 6209–6219 (2001)
207. Willett, J.L., Shogren, R.L.: Polymer **43**, 5935–5947 (2002)
208. Wang, H., Sun, X.Z., Seib, P.: J. Appl. Polym. Sci. **82**, 1761–1767 (2001)
209. Wang, H., Sun, X.Z., Seib, P.: J. Appl. Polym. Sci. **84**, 1257–1262 (2002)
210. Wang, H., Sun, X.Z., Seib, P.: J. Appl. Polym. Sci. **90**, 3683–3689 (2003)
211. Zhang, J.F., Sun, X.Z.: J. Appl. Polym. Sci. **94**, 1697–1704 (2004)
212. Ke, T.Y., Sun, X.Z.S.: J. Polym. Environ. **11**, 7–14 (2003)
213. Shogren, R.L., Doane, W.M., Garlotta, D., Lawton, J.W., Willett, J.L.: Polym. Degrad. Stab. **79**, 405–411 (2003)
214. Zhang, L.L., Deng, X.M., Zhao, S.J., Huang, Z.T.: Polym. Int. **44**, 104–110 (1997)
215. Willett, J.L., Kotnis, M.A., O'Brien, G.S., Fanta, G.F., Gordon, S.H.: J. Appl. Polym. Sci. **70**, 1121–1127 (1998)
216. Maliger, R.B., McGlashan, S.A., Halley, P.J., Matthew, L.G.: Polym. Eng. Sci. **46**, 248–263 (2006)
217. de Carvalho, A.J.F., Curvelo, A.A.S., Agnelli, J.A.M.: Carbohydr. Polym. **45**, 189–194 (2001)
218. Yu, J., Wang, J., Wu, X., Zhu, P.: Starch-Stärke **60**, 257–262 (2008)
219. Qiao, X., Jiang, W., Sun, K.: Starch-Stärke **57**, 581–586 (2005)
220. Nättinen, K., Hyvärinen, S., Joffe, R., Wallström, L., Madsen, B.: Polym. Compos. **31**, 524–535 (2010)
221. Romhány, G., Karger-Kocsis, J., Czigány, T.: Macromol. Mater. Eng. **288**, 699–707 (2003)
222. Rosa, M.F., Chiou, B., Medeiros, E.S., et al.: J. Appl. Polym. Sci. **111**, 612–618 (2009)
223. Rosa, M.F., Chiou, B.-S., Medeiros, E.S., et al.: Bioresour. Technol. **100**, 5196–5202 (2009)
224. Lee, S.Y., Cho, M.S., Nam, J.D., Lee, Y.: Macromolecular Symposia **242**, 126–130 (2006)
225. Lu, Y., Weng, L., Cao, X.: Macromol. Biosci. **5**, 1101–1107 (2005)
226. Ma, X., Chang, P.R., Yu, J.: Carbohydr. Polym. **72**, 369–375 (2008)
227. Corradini, E., Imam, S.H., Agnelli, J.A.M., Mattoso, L.H.C.: J. Polym. Environ. **17**, 1–9 (2009)
228. Alvarez, V.A., Kenny, J.M., Vázquez, A.: Polym. Compos. **25**, 280–288 (2004)
229. Alvarez, V., Vázquez, A., Bernal, C.: Polym. Compos. **26**, 316–323 (2005)
230. Martins, I.M.G., Magina, S.P., Oliveira, L., et al.: Compos. Sci. Technol. **69**, 2163–2168 (2009)
231. Kvien, I., Sugiyama, J., Votrubec, M., Oksman, K.: J. Mater. Sci. **42**, 8163–8171 (2007)
232. Park, H.M., Lee, W.K., Park, C.Y., Cho, W.J., Ha, C.S.: J. Mater. Sci. **38**, 909–915 (2003)
233. Pérez, C.J., Alvarez, V.A., Mondragón, I., Vázquez, A.: Polym. Int. **56**, 686–693 (2007)
234. Zhao, X., Wang, B., Li, J.: J. Appl. Polym. Sci. **108**, 2833–2839 (2008)

235. Pascu, M.C., Popescu, M.C., Vasile, C.: J. Phys. D Appl. Phys. **41**, 175407–175407 (2008)
236. Zhang, Q.X., Yu, Z.Z., Xie, X.L., Naito, K., Kagawa, Y.: Polymer **48**, 7193–7200 (2007)
237. Liao, H., Wu, C.: J. Appl. Polym. Sci. **97**, 397–404 (2005)
238. Mathew, A.P., Thielemans, W., Dufresne, A.: J. Appl. Polym. Sci. **109**, 4065–4074 (2008)
239. Maksimov, R.D., Lagzdins, A., Lilichenko, N., Plume, E.: Polym. Eng. Sci. **49**, 2421–2429 (2009)
240. Ma, X., Yu, J., Wang, N.: Macromol. Mater. Eng. **292**, 723–728 (2007)
241. Dai, H., Chang, P.R., Geng, F., Yu, J., Ma, X.: J. Polym. Environ. **17**, 225–232 (2009)
242. Wang, N., Zhang, X., Han, N., Bai, S.: Carbohydr. Polym. **76**, 68–73 (2009)
243. Majdzadeh-Ardakani, K., Navarchian, A.H., Sadeghi, F.: Carbohydr. Polym. **79**, 547–554 (2010)
244. Schlemmer, D., Angélica, R.S., Sales, M.J.A.: Compos. Struct. **92**, 2066–2070 (2010)
245. Wang, X., Zhang, X., Liu, H., Wang, N.: Starch-Stärke **61**, 489–494 (2009)
246. Ren, P., Shen, T., Wang, F., Wang, X., Zhang, Z.: J. Polym. Environ. **17**, 203–207 (2009)
247. Zeppa, C., Gouanv, F., Espuche, E.: J. Appl. Polym. Sci. **112**, 2044–2056 (2009)
248. Cyras, V.P., Manfredi, L.B., Ton-That, M.-T., Vázquez, A.: Carbohydr. Polym. **73**, 55–63 (2008)
249. Dean, K., My Do, Petinakis, S., Yu, L.: Compos. Sci. Technol. **68**, 1453–1462
250. Mondragón, M., Hernández, E.M., Rivera-Armenta, J.L., Rodríguez-González, F.J.: Carbohydr. Polym. **77**, 80–86 (2009)
251. Nejad, M.H., Ganster, J., Volkert, B.: J. Appl. Polym. Sci. **118**, 503-510 (2010)
252. Mondragon, M., Mancilla, J.E., Rodriguez-Gonzalez, F.J.: Polym. Eng. Sci. **48**, 1261–1267 (2008)
253. Cao, X., Chen, Y., Chang, P.R., Huneault, M.A.: J. Appl. Polym. Sci. **106**, 1431–1437 (2007)
254. Viguié, J., Molina-Boisseau, S., Dufresne, A.: Macromol. Biosci. **7**, 1206–1216 (2007)
255. García, N.L., Ribba, L., Dufresne, A., Aranguren, M.I., Goyanes, S.: Macromol. Mater. Eng. **294**, 169–177 (2009)
256. Cao, X., Chen, Y., Chang, P.R., Stumborg, M., Huneault, M.A.: J. Appl. Polym. Sci. **109**, 3804–3810 (2008)
257. Kaushik, A., Singh, M., Verma, G.: Carbohydr. Polym. **82**, 337–345 (2010)
258. Grande, C.J., Torres, F.G., Gomez, C.M., Troncoso, O.P., Canet-Ferrer, J., Martínez-Pastor, J.: Mater. Sci. Eng., C **29**, 1098–1104 (2009)
259. Teixeira, E., Pasquini, D., Curvelo, A.A.S., Corradini, E., Belgacem, M.N., Dufresne, A.: Carbohydr. Polym. **78**, 422–431 (2009)
260. Majdzadeh-Ardakani, K., Nazari, B.: Compos. Sci. Technol. **70**, 1557–1563 (2010)
261. Liao, H., Wu, C.: J. Appl. Polym. Sci. **108**, 2280–2289 (2008)
262. Arroyo, O.H., Huneault, M.A., Favis, B.D., Bureau, M.N.: Polym. Compos. **31**, 114–127 (2010)
263. Gattin, R., Copinet, A., Bertrand, C., Couturier, Y.: Int. Biodeterior. Biodegradation **50**, 25–31 (2002)
264. Wang, L., Shogren, R.L., Carriere, C.: Polym. Eng. Sci. **40**, 499–506 (2000)
265. Averous, L.: J. Macromol. Sci.-Polym. Rev. **C44**, 231–274 (2004)
266. Vidal, R., Martinez, P., Mulet, E., et al.: J. Polym. Environ. **15**, 159–168 (2007)

Chapter 5
Recent Studies on Soy Protein Based Blends, Composites and Nanocomposites

Lucia H. Innocentini-Mei and Farayde Matta Fakhouri

5.1 Introduction

With the environmental appeal around the planet for a sustainable development, there is the need to develop new materials from renewable resources, which can be degraded in a short time in the environment, thereby maintaining the proper balance of the carbon cycle. The utilization of hydrocolloids, such as soy protein, to prepare biodegradable materials with suitable properties, has been a great challenge for the scientific community, since these materials do not possess all the desirable characteristics of the synthetic polymers, being mostly often, highly hydrophilic and also presenting poor mechanical properties to be used as engineering's materials. In this context, the studies with application of nanotechnology to biodegradable polymers can open new possibilities to improve not only the properties of these materials, but also its efficiency.

Although the oil is important as energy source, its main utilization is directed toward the industrial production of raw material for packaging. For those industries that manufacture plastics packaging's, there is an enormous challenge to ensure the sustainability of the raw material since the conventional plastics, when discarded, will take decades or centuries to degrade. Among the most used plastic, in food packaging industries, are: (1) low density polyethylene (LDPE), which has low cost and is used in general to pack dehydrated products, pasteurized milk and in the manufacture of laminated packing; (2) high density polyethylene (HDPE), which is mainly used to produce plastic bags for supermarkets, (3) polystyrene (PS), used in the preparation of expanded trays (Styrofoam) for various food

L. H. Innocentini-Mei (✉) · F. M. Fakhouri
School of Chemical Engineering, State University of Campinas—UNICAMP, Av. Albert Einstein 500, CP 6066 13083-970 Campinas, São Paulo, Brazil
e-mail: lumei@feq.unicamp.br

S. Thomas et al. (eds.), *Advances in Natural Polymers*,
Advanced Structured Materials 18, DOI: 10.1007/978-3-642-20940-6_5,

products; (4) poly vinyl chloride (PVC), widely used for packaging of vinegar, mineral water, edible oils, sauces and food wraps, among others; (5) oriented and bi–oriented polypropylene (PP), used for foods containing high fat content, possess excellent gloss and transparency; (6) poly ethylene terephthalate (PET), used mainly in carbonated beverages and (7) poly ethylene naphthalate (PEN), which has more specific applications than PET, such as fruit juices and preserves beer, wine and returnable packaging, due to its high price [1]. The four alternatives to treat plastic waste are incineration, recycling, landfills and biodegradation. The incineration of plastic waste will always produce a large amount of carbon dioxide causing global warming and sometimes producing toxic gases that contribute to environmental pollution [2]. Furthermore, recycling is a great option in this context, but requires education on the proper disposal of garbage and a subsequent processing to obtain the recycled plastic, which leads to higher cost packaging with inferior quality compared to those plastics produced with virgin resin. To attend the growing appeal for environmentally friendly materials to replace some traditional plastics packages, that take decades or centuries to decompose in landfills and dumps, many scientists around the world have dedicated themselves to transform the raw material from renewable sources in packages which have good properties and which have a very short life after its discharge [2].

The properties required for plastic packaging mainly depend on the alterations presented by the product being protected and the conditions where it is stored. When a flexible packaging is required for food packing, the bioplastic must: (1) present good sensory properties of gas barrier and mechanical properties, (2) sufficient biochemical, physical–chemical and microbiological stability, (3) be free of toxic and be safe for consumption, (4) has a simple manufacturing technology, (5) should not be polluting and, finally, (6) have good availability and low cost, both with respect to raw material and with the process of obtaining [3]. Among the main natural materials for the production of bioplastics are proteins, such as gelatin and soy protein, cellulose derivatives, alginate, pectin, starch and other polysaccharides. The water solubility of films based on polysaccharides is advantageous in situations where the film is consumed with the product, resulting in minor changes in the sensory properties of food [4]. Edible films based on proteins, polysaccharides or lipids, in addition to increasing food quality, minimize special care with the final package [5].

Bioplastics can be simple (made with a simple macromolecule), compounds (two or more macromolecules), and be compounded with two or more layers. The compounds have the advantage of bringing together the strengths of each component, since hydrophobic films have good barrier to water vapor and hydrophilic films have good barrier to gases, in addition to providing effective mechanical properties [6]. As commented by Sorrentino et al., the application of nanotechnology to biodegradable polymers can open new possibilities to improve not only the properties of these materials, but at the same time improve the cost and the efficiency [7]. The cultivation of raw materials and the industrial production of nanocomposites based on natural polymers may contribute for employment

generation, thereby promoting social inclusion, especially considering the vast potential of productive family farms.

5.2 Biodegradable Films and Coatings

As defined by the term "biodegradable material" [8] is used to describe those materials that can be degraded by the enzymatic action of living organisms such as bacteria, yeasts and fungi, presenting as end products of the degradation process: CO_2, H_2O and biomass under aerobic conditions, and hydrocarbons, methane and biomass under anaerobic conditions. Biopolymers have been proposed to formulate edible films. Polysaccharides, proteins and lipids has been used in several ways: simple or composite materials or films or multiple layers [9]. Bioplastics, or organic plastics, are derived from renewable biomass sources, such as vegetable oil, corn starch, pea starch, or microbiota, rather than fossil-fuel plastics which are derived from petroleum. Some, but not all, bioplastics are designed to be biodegradable. They can be molded by the action of heat and pressure, like the conventional plastics, and are potential alternatives to conventional thermoplastic of petrochemical origin, such as polyolefins and polyesters [10], in strategic applications such as packaging area that generates much waste. Industries that produce bioplastics generally use microbes, or their enzymes, to convert biomass to feedstocks, building blocks for biodegradable plastics. The water solubility of films from polysaccharides is advantageous in situations where the film is consumed with the product, resulting in minor changes in the sensory properties of food [4]. Edible films based on proteins, polysaccharides or lipids, in addition to increasing food quality, minimize special care with the final package [11].

Edible films differ from edible coatings since they are formed before their application to the product, while the cover is formed during the application on it. Edible coatings can be defined as a layer of edible material formed around the food or placed between the components thereof [12].

For the development of edible and biodegradable bioplastics, it is required solvents and a pH regulating agent, when necessary, in addition to the plasticizer and polymer. The pH adjustment in the case of proteins is necessary to control the solubility of the polymer. Some regulators of pH found in the literature [13]: acetic acid and sodium hydroxide. The solvents commonly used to prepare these bioplastics are: water, ethanol or a combination of both [14]. A crucial aspect in the preparation of films is the solubility of proteins and the ability to interact with the same solvent used, since the total solubility of the protein is required for films' formation [15]. The dispersion of the protein molecule in water is possible due to the large number of amino acid residues that interact with the polar solvents. These interactions can be improved depending on the dielectric constant of the solvent, since this constant is inversely proportional to the strength of intermolecular attraction. Films can be simple, made with one type of macromolecule or composed by two or more types of macromolecules, and can be formed with two or

more layers. The composed films have the advantage of bringing together the strengths of each component, as in the case of hydrophobic films that have good water vapor barrier, and hydrophilic films which have good barrier to gases, propitiating effective mechanical properties [6].

5.3 Soy Protein Isolate

5.3.1 Structure of Soy Protein

The soybean (U.S.) or soya bean (UK) (*Glycine max*) is a species of legume native of East Asia [16]. Soybean consists of 36–42 % protein and is also rich in oil (18–22 %). Due to the high protein amount, soy has a high demand for nitrogen. It is an annual plant that has been used in China for 5,000 years to primarily add nitrogen into the soil as part of crop rotation. Similar to other plants, soy protein has the primary function of providing amino acids for germination and protein synthesis. It is estimated that the polypeptide chain of soybean has a molecular weight between 300–600 $\times$ 10^3 Da and a complex structure with bonds of type SS and hydrogen [17].

Soybean production in the United States, Argentina and Brazil accounted for 82 % of world production. According to the report of February 2009 the Department of Agriculture (USDA) soybean production worldwide was 224.15 million tons, while in Brazil it was around 57 and in Argentine 43,8 [18]. For the 2010/2011 harvest, second the United States Department of Agriculture, the world production of soybeans was 2,637 million tons.

5.3.2 Amino Acids Composition, Structures and Thermal Behaviour of Soy Proteins

The largest portion of the soy proteins is present as globulins and its incorporation in amino acids can be seen in Table 5.1.

The soy protein isolate (SPI) comprises a set of macromolecules with different structures, formed by 18 different amino acids and with a molecular weight that may reach 600.000 gmol. When a solution containing SPI is subjected to ultra-filtration, it generally reveals about fifteen distinct fractions and four dominant fractions identified as 2S (20–22 %) 7S (37 %), 11S (31–40 %) and 15S (10–11 %), according to Schmidt et al. [19, 20]. To these four dominant fractions are attributed the characteristics of SPI. Like other proteins, can be organized into four different types of structures, i.e., the primary structure, secondary, tertiary and quaternary what will depend on their amino acids sequence.

The primary structure of proteins consists of a sequence of amino acids, linked together by peptide bonds (Fig. 5.1a). In the case of soy, the sequence consists of the amino acids of Table 5.1. All the protein structures, like other proteins, are

Table 5.1 Amino acids composition of SPI

Amino acids	Composition (g, 16 g N)
Isoleucine	4,54
Leucine	7,78
Lysine	6,38
Methionine	1,26
Cysteine	1,33
Phenylalanine	4,94
Tyrosine	3,14
Threonine	3,86
Tryptophan	1,28
Valine	4,80
Arginine	7,23
Histidine	2,53
Alanine	4,26
Aspartic acid	11,70
Glutamic acid	18,70
Glycine	4,18
Proline	5,49
Serine	5,12

Source [19]

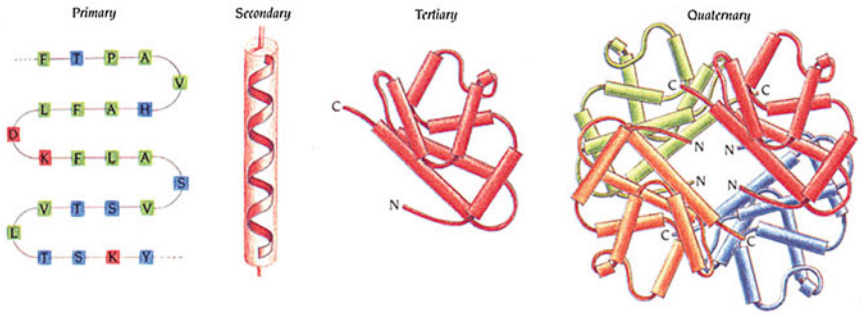

Fig. 5.1 Amino acids forming peptide bonds (**a**) and protein (**b, c, d**) structures [22]

illustrated in Fig. 5.1b. The peptide bond is formed between the carbon atom (C) of the carboxylic group and nitrogen atom (N) of the amino group with elimination of water. The two ends of the chain thus formed are termed "amino terminal" and terminal carboxylic acid or N-terminus and C-terminus [21].

The secondary structure includes the spatial arrangement of peptides' segments, stabilized by H bonding between carboxyl and amine groups of atoms. There are two types of arrangement, i.e., α helix (occurs between groups of the same chain segments, parallel to the chain) or β sheet (occurs between groups of different inter-chain segments, perpendicular to the chain). The tertiary structure describes the folding of the tertiary structural elements, including the lateral chains. The

quaternary structure appears only in oligomeric proteins, with a spatial distribution comprising more than one polypeptide chain in space, which are the subunits of the molecule mainly linked by covalent forces, like disulfide bonds, and noncovalent linkages, like hydrogen bonding and hydrophobic interactions [4]. The secondary, tertiary and quaternary structures of these macromolecules can be changed by the protein denaturation. Denaturating promotes increased interaction between chains of amino acids without the breaking of peptide bonds, thus improving the quality of films and gels formed.

Protein denaturation can be made through mechanical, physical (heat, radiation, ultra violet, ultrasonic, etc.) or chemical (guanidinium chloride, urea, lithium bromide, organic solvents, detergents, and extremes of pH) agents, affecting mainly the quaternary, tertiary and secondary structures. Some proteins are more stable at cooling temperature while some are more stable at ambient temperature. Usually between 40–50 °C the majority becomes unstable and there is the tendency of a change in the original conformation (denaturation) [23]. Denaturing presents several advantages such as: (1) Improves digestibility/bioavailability, i.e., improves enzymatic hydrolysis; (2) destruction of antinutritional factors; (3) Create desirable functional conditions for processing and (4) destroys toxines. Some of the disadvantages presented are: (a) destruction of amino acids, decreasing nutritional value and (b) complex formation (Maillard reaction) [24]. When the denaturation is done smoothly, it can be reversible. The studies linking soy protein denaturation, according to Kumar et al. [25], show that for this protein, structural modifications have been promoted by the use of bases, enzymes, surface-active agents (sodium dodecyl sulfate and sodium dodecylbenzenesulfonate). Such treatment promotes the exposure of polar functional groups, facilitating possible interactions with other molecules.

5.3.3 Functional Uses of Soy Protein Isolate

Soy protein is used for emulsification and texturizing. Specific applications include adhesives, asphalts, resins, cleaning materials, cosmetics, inks, pleather, paints, paper coatings, pesticides/fungicides, plastics, polyesters, and textile fibres [26]. Foods originating from plants have non-nutrient compounds (phytochemicals) with biological activities said health-promoting activities such as antioxidant, inflammatory and hypocholesterolemic like the soy isoflavones [27]. Soybean and its derivatives provide varying levels of isoflavones (daidzein, genistein and glycitein), bioactive compounds with diverse biological activities apparently associated with their forms [28].

The isoflavones exist in four chemical forms with a total of 12 isomers: the aglycones daidzein, genistein and glycitein; the β-glycosides daidzin, genistin and glycitin, and derivatives 6-O-acetylated such as 6-O-acetyldaidzin, 6-O-acetylgenistin, 6-O-acetylglycitin; and glucosyl-O-malonyl derivatives, as 6-O-malonyldaidzin, 6-O-malonylgenistin and 6-O-malonylglycitin [29]. Soy protein derivatives,

such as flours, isolates, concentrates and textured protein are widely used in food industry due to its functional properties. These products contain appreciable amounts of isoflavones, which during the processing stage of soybeans may be lost or modified. The main isoflavones present in soy non-processed, i.e., malonylgenistin, genistin, daidzein and malonyldaidzin are transformed into other forms during processing, such as acetylglicosides and aglycones [30]. Wang et al. [31] comment that the antioxidant activity of isoflavones has been linked to the number of hydroxyl groups present in their chemical structure. Pratt and Birac [32] reported that defatted flour, concentrate and isolated soy protein showed significant antioxidant activity by the method of co-oxidation of both β-caroteno and linoleic acid.

Besides the soybeans commercialization, the food industries also sell flour, concentrates, and soy isolates, and textured soy, fermented foods like miso, soy sauce and still the extract of soy or soy milk (soymilk) [29]. There are also other possibilities for the use of soy, like the elaboration of bioplastics, which have opened a new range of option for soy products, such as the use of Soy Protein Isolate (SPI) in the production of films and edible coatings. As published [25, 33], the separation of (SPI) from the other components of soybeans goes through a process of purification, based on chemical reactivity and solubility. A process for obtaining the SPI starts after the removal of bark and oil of soya beans, resulting in defatted flour. From this stage, and performed a typical process of aqueous extraction based in dissolution with pH lower than 5 or greater than 6.5, the SPI precipitation occurs. It is possible to study the SPI solubility as a function of the pH used in the protein extraction process [20]. The SPI has always been used as ingredient in food products due to their nutritional properties and physiological function, and have capacity for hydration, solubility, colloidal stability, gelation and also acts as emulsifier (technological functional properties) [34]. The IPS contains at least 90 % protein (N $\times$ 6.25) having as main components, the fractions β-conglycinin and glycinin, being free of fat and carbohydrate [35]. Moreover, lowering cholesterol in humans, due to consumption of soy protein isolates, is related to its isoflavone content [31].

5.3.4 Mechanical Properties

Films based on IPS, according to Gontard [9], the mechanical properties or barrier to water vapor unsatisfactory for practical applications, what became become worse under conditions of high humidity. Several studies have been made to improve the properties of the films based on IPS. It is reported that the addition of cross linking agents the film-forming solutions, or other physical methods, can improve the mechanical properties and/or the water vapor permeation (WVP) of films based on proteins [36]. Ou et al. [37] prepared films with 5.0 g of SPI, 3.0 g glycerol and different amounts (0, 50, 100, 150, 200 mg) of ferulic acid in two pH levels (8.0 and 9.0). At pH 9, the films showed better mechanical properties, as shown in Table 5.2.

Table 5.2 Effect of ferulic acid on tensile strength (TS) and percentage of elongation at break (E) of SPI films plasticized with glycerol

Feluric acid (mg/100 g)	Tensile strength (MPa)		Elongation (%)		Thickness (μm)	
	pH = 8,0	pH = 9,0	pH = 8,0	pH = 9,0	pH = 8,0	pH = 9,0
0	1.472 ± 0.044^{a}	1.598 ± 0.056^{a}	61.7 ± 7.8^{a}	156.3 ± 7.1^{a}	70.3 ± 0.4^{a}	70.8 ± 1.6^{a}
50	1.688 ± 0.139^{b}	2.065 ± 0.138^{b}	94.7 ± 3.9^{a}	167.0 ± 3.5^{b}	72.4 ± 3.2^{a}	72.8 ± 1.5^{b}
100	1.622 ± 0.057^{b}	2.602 ± 0.073^{d}	85.1 ± 10.9^{b}	165.3 ± 7.2^{b}	71.0 ± 1.2^{a}	70.2 ± 1.0^{a}
150	1.638 ± 0.098^{b}	2.438 ± 0.059^{c}	93.0 ± 12.4^{b}	166.5 ± 5.3^{b}	71.4 ± 1.8^{a}	71.8 ± 1.3^{a}
200	1.476 ± 0.062^{a}	2.172 ± 0.175^{b}	86.4 ± 7.6^{b}	155.4 ± 8.5^{a}	71.4 ± 0.7^{a}	$72.2 \pm 1.3^{a.b}$

[a–h] Values (mean ± standard deviation, $n = 5$), with different letters in the same column are significantly different at 5 % level

Source [37]

Physical properties of films consisting of isolated soy protein and gelatin has been studied [38]. Film forming solutions with 10 % protein and 0.1 % glycerol were prepared by mixing different proportions of IPS solutions and gelatin (10:0, 8:2, 6:4, 4:6, 2:8; 0:10). The results showed that the tensile strength of films prepared increased with the content of gelatin. The film made only with IPS was stiffer and less flexible. With the addition of gelatin, the film became more transparent, homogeneous and easier to handle. An important factor to be considered is related to the hydrophilicity/hydrophobicity of films prepared with proteins, what may interfere in the mechanical properties, beyond the barrier property. To control the balance desired on mechanical and barrier properties, one may control the hydrophilicity of the hydrocolloidal films and the formation of composite films, by preparing double-layer films or even a single homogeneous layer, formulated to combine the advantages of a hydrophobic lipid with the protein hydrocolloid, reducing the disadvantages that each one presented separately [39]. There are several publications reporting the development of composite films with the addition of beeswax and/or fatty acids such as palmitic, stearic and lauric acids in hydrocolloids. Rhim et al. [40] observed an increase in water solubility of films based on soy protein isolate, when lauric acid was added.

5.4 Protein Extrusion

It is well established that the extrusion of proteins is a potential for obtaining edible films on a large scale [41]. For these authors, the incorporation of polysaccharides and inclusion of nanoparticles in these films tend to improve their mechanical properties. Park et al. [42] studied bioplastics made from extruded gelatin plasticized with glycerol, sorbitol or a mixture of both. In this study, they discard sorbitol as a plasticizer because of low flow in the extrusion of the material.

Liu et al. [43] studied the incorporation of corn oil and olive oil in biofilms based on gelatin and sodium alginate, prepared by extrusion. The addition of oil caused an increase in the thickness of biofilms, also causing a decrease in tensile strain and an increase in the elongation. Both corn oil as olive oil reduced the water vapor permeability of biofilms, but no significant difference was observed regarding the use of different concentrations of the same. Extruded flexible films produced with thermoplastic potato starch and glycerol, were studied by Thunwall et al. [44]. The authors concluded that with appropriate control of process conditions, the amount of plasticizer and moisture of the mixture, it is possible to obtain extruded films of this material. The authors also reported that the preparation of biofilms from native starch, by this process, was significantly more difficult.

5.5 Nanocomposites

Nanocomposites are finding several applications as new researches prove their efficiency in the areas that they are used, mainly engineer. They are more popular among researchers from academia and industry, due to their excellent properties that are superior compared to the virgin polymers and conventional composites [45]. They can cover a wide area of applications such as automotive, medical, packaging and aerospace among others, since they have better thermal, mechanical and barrier properties that exceed those found in conventional composites [46]. Nanocomposites are a class of hybrid materials consisting of organic and inorganic components, where the inorganic phase in nanometer level is dispersed in a polymeric [47–49]. Montmorillonite (MMT), hectorite and saponite are the most used clays (phyllosilicates 2:1) in the preparation of polymer nanocomposites (PN). Details of the formula and chemical structure of these clays are presented in Table 5.3 and Fig. 5.2 [2].

5.5.1 Structure of Clays and Nanoclays

Clays have a layered structure consisting of 2 types of sheets, the silica tetrahedral and alumina octahedral sheets. The silica tetrahedral sheet consists of SiO4 groups linked together to form a hexagonal network of the repeating units of composition Si4O10. The alumina sheet consists of two planes of close packed oxygens or hydroxyls between which octahedrally coordinated aluminum atoms are imbedded in such a position that they are equidistant from six oxygens or hydroxyls. The two tetrahedral sheets sandwich the octahedral, sharing their apex oxygens with the latter. These 3 sheets form one clay layer. See Fig. 5.2.

If the octahedral positions were occupied by alumina, we would not be looking at clay at all, but the inert mineral *pyrophyllite*. So, extremely important to the structure of clays is the phenomena of *isomorphous substitution*. Replacement of trivalent aluminum by divalent magnesium or iron II results in a negative crystal charge. The excess negative charge is compensated on the clays' surface by cations that are too large to be accommodated in the interior of the crystal. Further, in low pH environments, the edges of the clay crystal are positive, and compensated by anions. The result is a polyionic, supercharged nano-wafer that is unique in the world of minerals.

Table 5.3 Chemical formula and the characteristic parameters of phyllosilicates 2:1

Phyllosilicates 2:1	Chemical formula[a]	CEC (meq/100 g)	Particle size (nm)
Montmorillonite	$Mx(Al_{4-x}Mg_x)Si_8O_{20}(OH)_4$	110	100–150
Hectorite	$Mx(Mg_{6-x}Li_x)Si_8O_{20}(OH)_4$	120	200–300
Saponite	$MxMg_6(Si_{8-x}\ Al_x)\ Si_8O_{20}(OH)_4$	86,6	50–60

[a] M = monovalent cation; x = degree of isomorphous substitution (between 0,5 and 1,3)
CEC = Cation exchange capacity

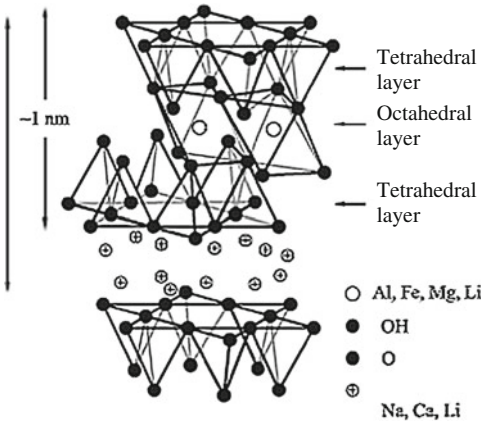

Fig. 5.2 Illustration of clay structure [2, 45]

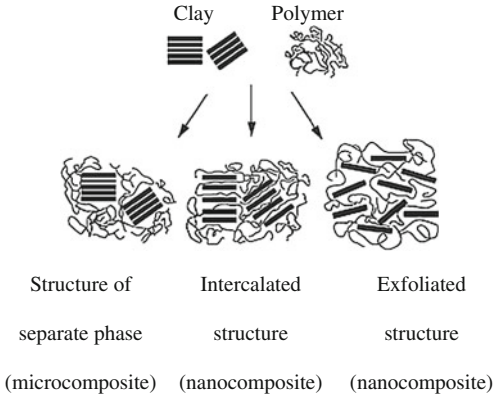

Fig. 5.3 Illustrative structures of micro and nanocompósitos [45]

Three main types of structures, which are shown in Fig. 5.3, can be obtained when a clay is dispersed in a polymer matrix: (1) phase-separated structure, where the polymer chains did not intercalate the clay layers, leading to a structure similar to those of a conventional composite, (2) intercalated structure, where the polymer chains are intercalated between clay layers, forming a well ordered multilayer structure, which has superior properties to those of a conventional composite, and (3) structure exfoliated, where the clay is completely and uniformly dispersed in a polymeric matrix, maximizing the interactions polymer–clay and leading to significant improvements in physical and mechanical properties [2, 50–52]. Production of nanocomposites based on polymer/clay can be done basically in three ways: (a) in situ polymerization, (b) prepared in solution and (c) preparation of the melt or melt blending [53].

The structures of nanocomposites have been characterized mainly by the techniques of X-Ray Diffraction (XRD) and transmission electron microscopy (TEM). The TEM analysis gives qualitative information of the sample as a whole, helping to understand the internal structure, partial distribution of various phases

and a vision of a structural defect by direct visualization, while the peaks in low angle XRD allow qualifying changes in the interlayer [45].

5.6 Conclusions

Based on text above and the references included in it, it is possible to note that there is great interest in other bioplastics based on natural sources of polysaccharides and proteins due to its low cost. However, the use of biofilms for food packaging has been greatly limited due to poor barrier properties and mechanical properties presented by natural polymers. Recent studies are exploring blends composed of soy protein isolate with other hydrocolloids and other biodegradable materials as an alternative to improve the properties of these materials. Compatibilizers have been incorporated into these blends to reach more uniformity in the material and influence directly its characteristics. Another possibility much studied is the preparation of nanocomposites from soy protein isolate. The fillers added to these materials have been clays, in general, which have shown good results. Finally, it is feasible to study biodegradable plastics based on soy protein isolate since it is possible to get this raw material in great amount and in a good price.

References

1. Fakhouri, F.M.: Bioplásticos Flexíveis e Biodegradáveis a Base de Amido e Gelatina. Campinas State University, Campinas (2009)
2. Ray, S.S., Bousmina, M.: Biodegradable polymers and their layered silicate nano composites: In greening the 21st century materials world. Prog. Mater Sci. **50**(8), 962–1079 (2005)
3. Debeaufort, F., Quezada-Gallo, J.A., Voilley, A.: Edible films and coatings: Tomorrow's packagings: A review. Crit. Rev. Food Sci. Nutr. **38**(4), 299–313 (1998)
4. Donhowe, I. G., Fennema, O.: Edible films and coatings: characteristics, formation, definitions and testing methods. In Edible coating and films to improve food quality, (pp. 1–21). Lancaster: Technomic Pub. Co (1994)
5. Chen, P., Zhang, L.: Interaction and properties of highly exfoliated soy protein/montmorillonite nanocomposites. Biomacromolecules **7**(6), 1700–1706 (2006)
6. Amarante, C., Banks, N.H.: Postharvest Physiology and Quality of Coated Fruits and Vegetables. In Horticultural Reviews, (pp. 161–238): John Wiley, Inc (2010)
7. Sorrentino, A., Gorrasi, G., Vittoria, V.: Potential perspectives of bio-nanocomposites for food packaging applications. Trends Food. Sci. Technol. **18**(2), 84–95 (2007)
8. Doi, Y., Fukuda, K.: Biodegradable Plastic and Polymers. Elsevier Science, Amsterdam (1994)
9. Guilbert, S., Guillard, V., Gontard, N.: Mass transport within biodegradable protein based materials: Application to the design of active biopackaging. Abstracts of papers of the American chemical society **229**, U302–U302 (2005)
10. Queiroz, A.U. B., Collares-Queiroz, Z.F.P: Innovation and industrial trends in bioplastics. Polymer Reviews, in press (2009)
11. Chen, H.: Functional properties and applications of edible films made of milk proteins. J. Dairy Sci. **78**(11), 2563–2583 (1995)

12. Krochta, J.M., DeMulderJohnston, C.: Edible and biodegradable polymer films: Challenges and opportunities. Food Technol. **51**(2), 61–74 (1997)
13. Leaver, J., Horne, D.S., Law, A.J.R.: Interactions of proteins and surfactants at oil–water interfaces: influence of a variety of physical parameters on the behaviour of milk proteins. Int. Dairy J. **9**(3–6), 319–322 (1999)
14. Kester, J.J., Fennema, O.R.: Edible films and coatings: A review. Food Technol. **40**, 47–59 (1986)
15. Sgabieri, V.: Proteinas em alimentos protéicos. Editora Varela, São Paulo (1996)
16. Mabberley, D.J.: The Plant-Book: A Portable Dictionary of the Vascular Plants, 2nd edn. Cambridge University Press, Cambridge (1997)
17. Nielsen, N.C.: Structure of Soy Proteins. In: Altschul, A.M. (ed.) New Protein Foods, vol. 5, pp. 27–64. Academic Press, New York (1985)
18. Wool, R. P., Sun, X. S.: Bio-based polymers and composites: Elsevier (2005)
19. Schmidt, V., Giacomelli, C., Soldi, M.S., Soldi, V.: Soy protein isolate based films: Influence of sodium dodecyl sulfate and polycaprolactone-triol on their properties. Macromolecular Symposia **229**, 127–137 (2005)
20. Schmidt, V., Giacomelli, C., Soldi, V.: Thermal stability of films formed by soy protein isolate-sodium dodecyl sulfate. Polym. Degrad. Stab. **87**(1), 25–31 (2005)
21. Lehninger, A.L., Nelson, D.L., Cox, M.M.: Lehninger: Principles of Biochemistry (4th ed.): Sarvier (2007)
22. Dror, O., Benyamini, H., Nussinov, R., Wolfson, H.J.: Multiple structural alignment by secondary structures: Algorithm and applications. Protein Sci. **12**(11), 2492–2507 (2003)
23. Neurath, H., Greenstein, J.P., Putnam, F.W., Erickson, J.A.: The chemistry of protein denaturation. Chem. Rev. **34**(2), 157–265 (1944)
24. Fennema, O.R.: Food Chemistry, 3rd edn. Marcel Dekker Inc, New York (1996)
25. Kumar, R., Choudhary, V., Mishra, S., Varma, I.K., Mattiason, B.: Adhesives and plastics based on soy protein products. Ind. Crops Prod. **16**(3), 155–172 (2002)
26. Riaz, M. N.: Soy applications in food: CRC Press (2006)
27. Harborne, J.B., Willians, C.A.: Advances in flavonoids research since 1992. Phytochemistry **55**, 481–504 (2000)
28. Miniello, V.L., Moro, G.E., Tarantino, M., Natile, M., Granieri, L., Armenio, L.: Soy-based formulas and phyto-oestrogens: A safety profile. Acta Paediatr. **92**, 93–100 (2003)
29. Shigemitsu, K., Yvette, F., Dieter, W., Daniele, M., Teiji, U., Keisuke, K., Kazuyoshi, O.: Malonyl isoflavone glycosides in soybean seeds (Glycine max MERRILL)(food and nutrition). Agric. Biol. Chem. **55**(9), 2227–2233 (1991)
30. Wang, H., Murphy, P.A.: Isoflavone composition of American and Japanese soybeans in Iowa: Effects of variety, crop year, and location. J. Agric. Food. Chem. **42**(8), 1674–1677 (1994)
31. Lopes Barbosa, A.C., Lajolo, F.M., Genovese, M.I.: Influence of temperature, pH and ionic strength on the production of isoflavone-rich soy protein isolates. Food Chem. **98**(4), 757–766 (2006)
32. Pratt, D.E., Birac, P.M.: Source of antioxidant activity of soybeans and soy products. J. Food Sci. **44**(6), 1720–1722 (1979)
33. Lodha, P., Netravali, A.N.: Thermal and mechanical properties of environment-friendly 'green' plastics from stearic acid modified-soy protein isolate. Ind. Crops Prod. **21**(1), 49–64 (2005)
34. Lui, M.C.Y., Aguiar, C.L., Alencar, SMd, Scamparini, A.R.P., Park, Y.K.: Isoflavonas em isolados e concentrados protéicos de soja. Ciência e Tecnologia de Alimentos **23**, 206–212 (2003)
35. Singh, M., Mohamed, A.: Influence of gluten–soy protein blends on the quality of reduced carbohydrates cookies. LWT—Food Sci. Technol. **40**(2), 353–360 (2007)
36. Marquie, C., Aymard, C., Cuq, J.L., Guilbert, S.: Biodegradable packaging made from cottonseed flour: Formation and improvement by chemical treatments with gossypol, formaldehyde, and glutaraldehyde. J. Agric. Food Chem. **43**(10), 2762–2767 (1995)

37. Ou, S., Wang, Y., Tang, S., Huang, C., Jackson, M.G.: Role of ferulic acid in preparing edible films from soy protein isolate. J. Food Eng. **70**(2), 205–210 (2005)
38. Cao, N., Fu, Y., He, J.: Preparation and physical properties of soy protein isolate and gelatin composite films. Food Hydrocolloids **21**(7), 1153–1162 (2007)
39. Greener, I.K., Fennema, O.: Evaluation of edible, bilayer films for use as moisture barriers for food. J. Food Sci. **54**(6), 1400–1406 (1989)
40. Rhim, J.W., Wu, Y., Weller, C.L., Schnepe, M.: Physical characteristics of emulsified soy protein-fatty acid composite filmes. Sciences des Aliments **19**, 57–71 (1999)
41. Hernandez-Izquierdo, V.M., Reid, D.S., McHugh, T.H., De Berrios, J., Krochta, J.M.: Thermal transitions and extrusion of glycerol-plasticized whey protein mixtures. J. Food Sci. **73**(4), E169–E175 (2008)
42. Park, J.W., Scott Whiteside, W., Cho, S.Y.: Mechanical and water vapor barrier properties of extruded and heat-pressed gelatin films. LWT—Food Sci. Technol. **41**(4), 692–700 (2008)
43. Liu, L., Kerry, J.F., Kerry, J.P.: Effect of food ingredients and selected lipids on the physical properties of extruded edible films/casings. Int. J. Food Sci. Technol. **41**(3), 295–302 (2006)
44. Thunwall, M., Kuthanová, V., Boldizar, A., Rigdahl, M.: Film blowing of thermoplastic starch. Carbohydr. Polym. **71**(4), 583–590 (2008)
45. Ray, S.S., Okamoto, M.: Polymer/layered silicate nanocomposites: a review from preparation to processing. Prog. Polym. Sci. **28**(11), 1539–1641 (2003)
46. Mariani, P.D.S.C., Allganer, K., Oliveira, F.B., Cardoso, E.J.B.N., Innocentini-Mei, L.H.: Effect of soy protein isolate on the thermal, mechanical and morphological properties of poly (epsilon-caprolactone) and corn starch blends. Polym. Testing **28**(8), 824–829 (2009)
47. Fornes, T.D., Yoon, P.J., Keskkula, H., Paul, D.R.: Nylon 6 nanocomposites: the effect of matrix molecular weight. Polymer **42**(25), 09929–09940 (2001)
48. Kim, J.-T., Lee, D.-Y., Oh, T.-S., Lee, D.-H.: Characteristics of nitrile–butadiene rubber layered silicate nanocomposites with silane coupling agent. J. Appl. Polym. Sci. **89**(10), 2633–2640 (2003)
49. Yang, F., Ou, Y., Yu, Z.: Polyamide 6/silica nanocomposites prepared by in situ polymerization. J. Appl. Polym. Sci. **69**(2), 355–361 (1998)
50. Krishnamoorti, R., Yurekli, K.: Rheology of polymer layered silicate nanocomposites. Curr. Opin. Colloid Interface Sci. **6**(5–6), 464–470 (2001)
51. LeBaron, P.C., Wang, Z., Pinnavaia, T.J.: Polymer-layered silicate nanocomposites: An overview. Appl. Clay Sci. **15**(1–2), 11–29 (1999)
52. Zhu, L., Wool, R.P.: Nanoclay reinforced bio-based elastomers: Synthesis and characterization. Polymer **47**(24), 8106–8115 (2006)
53. Souza, M.A., Pessan, L.A., Rodolfo Jr, A.: Nanocompósitos de Poli(Cloreto de Vinila) (PVC)/argilas organofílicas. Polímeros **16**, 257–262 (2006)

Chapter 6
Nanocarriers, Films and Composites Based on Milk Proteins

Ashkan Madadlou and Fatemeh Azarikia

6.1 Introduction

The dominant milk proteins, caseins are similar in structure and found in milk as nanoparticles called micelle. Casein micelles (300-600 nm) are composed of several thousand molecules, bonded via calcium phosphate nanoclusters. All other proteins present in milk are grouped together and termed whey proteins. The primary whey protein in cow milk is β-lactoglobulin. Here we firstly review the chemistry of caseins and whey proteins including presented models and theories for the structure of casein micelles. Then, an interesting feature of milk proteins i.e., their potential as nano-vehicles for bioactive compounds is introduced. The potential of delivering high nutritional value components by milk proteins has opened new opportunities in food and non-food industrial sectors. Finally, films and composites based on milk proteins are discussed. Fortunately, the huge volume of milk production enables the manufacture of non-expensive purified proteins possible [1]. Milk protein films are widely used in food and non-food sectors such as textile, paper, leather and etc. These films and composites are used in different scopes of food science such as coating of meat and fresh-cut fruits, bread wrapping and preparation of antimicrobial packaging.

A. Madadlou (✉)
Department of Food Technology, Institute of Chemical Technologies, Iranian Research Organization for Science & Technology (IROST), Tehran, Iran
e-mail: Ashkan.madadlou@gmail.com

F. Azarikia
Department of Food Science & Technology, Faculty of Agriculture, Tarbiat Modarres University, Tehran, Iran

S. Thomas et al. (eds.), *Advances in Natural Polymers*,
Advanced Structured Materials 18, DOI: 10.1007/978-3-642-20940-6_6,

6.2 Chemistry of Caseins and Whey Proteins

6.2.1 Structure of Casein Molecules

Cow's milk proteins are divided into 2 parts: caseins and whey proteins. The major fraction of milk proteins (approximately 80 %) belongs to casein group which consists of α_{s1}-, α_{s2}-, β-, and κ-casein and their portions are nearly 38, 10, 36 and 12, respectively, with respective molecular masses of 23,164, 25,388, 23,983 and 19,038 Da [2]. Proteose peptones and γ-casein are obtained through splitting β-casein by plasmin, a proteolytic enzyme naturally present in milk. Caseins can be distinguished from other milk components by precipitating near their isoelectric pH ($\sim$4.6 at 20 °C). Caseins are amphiphilic molecules with hydrophilic and hydrophobic segments [3] and are widely used as emulsifier in the food industry due to their amphiphilic character [3, 4].

The highest amount of caseins in milk belongs to α_{s1}-casein [2, 3]. Unlike other caseins, in α_{s1}-casein both N- and C-terminal segments of molecules are hydrophobic which leads to the formation of either intra- or inter-molecular interactions [5]. Amino acid sequence in α_{s1}-casein differs from that in α_{s2}-caseins and hence it is normal to possess different physical and chemical properties. Although both α_{s1}- and α_{s2}-caseins are calcium-sensitive, the same as β-casein, α_{s2}-casein is much more sensitive to Ca^{2+} [6, 7]. Indeed, 2 mM Ca^{2+} at pH 7 is sufficient for precipitation of α_{s2}-casien, while a concentration of 6 mM is needed to precipitate α_{s1}-casien [6]. However, α_{s1}-casien is more sensitive to Ca^{2+} in comparison with β-casein [5].

According to a recent reanalyzing of primary structure of α_{s2}-casein sequence, this molecule can be separated to 5 precise sections: 1–41, 42–80, 81–125, 126–170 and 171–207 that are termed a1, a2, b1, a3 and b2, respectively. Characteristic of a1 is being hydrophobic, having negative charge and having 4 phosphorylated serine residues. The a2 area has the highest negative charge and 3 phosphorylated serine residues; while, b1 is positively charged region with hydrophobic character. The a3 region has the lowest negative charge, and also the lowest phosphorylated serine, only 2 residues. The last region, b2, which suggests being surface-accessible is highly positive charged residue and hydrophile. It seems that the latter region has an important role in interaction with negatively charge molecules; hydrocolloids such as κ-carrageenan as well as phosphate [6]. On the other hand, interaction of α_{s2}- casein with cations, like Ca^{2+} is possible via negatively charged N-terminal segment [8]. Notably, among all caseins the most positively charged segment belongs to C-terminal region of α_{s2}-casein [6].

N-terminal portion of β-casein (1–40 residues) exhibits high negative charge; it seems that most of the net charge of molecule concentrates in this region. Furthermore, all 5 phosphorylated serine residues are located in this hydrophilic portion of molecule [9, 10]. On the contrary, amino acids in the C-terminal portion of β-casein are generally apolar and this region is hydrophobic [10]. Self-association of β-casein occurs in aqueous solutions and its reversion is a function of β-casein concentration, temperature, pH as well as ionic strength [9]. It has been observed that

self-association of β-casein is directly related to the C-terminal region of the molecule [10] and increase in the ionic strength of solution results in an increase in degree of polymerization, while increasing the pH diminishes the polymerization [5].

It is believed that high level of proline; comprising 17 of 199 amino acid residues in α_{s1}-casein, 10 of 207 amino acid residues in α_{s2}-casein, 35 of 209 amino acid residues in β-casein and 20 of 169 amino acid residues in κ-casein; prevents from formation of secondary structure in caseins and thus a minute amount of α-helix and β-sheet have been observed in caseins [2]. According to investigations on κ-casein, secondary structure is determined in this protein [11]; in particular, helix structure in macropeptide portion and sheet structure in para-κ-casein portion of the molecule [12]. Recent publications have reported the presence of α-helix and β-sheet structures in α_{s2}-casein molecule [6, 8]. It is predicted that loop structure might be found in α_{s1}-, α_{s2}- and β-caseins [8, 13].

Phosphorylation in which the hydroxyl groups of serine and threonine are esterified to phosphate groups [3] is observed in all caseins. Notably α_{s1}-, α_{s2} and β-casein are extremely phosphorylated peptides in comparison with κ- casein. It is noteworthy that phosphate groups of α_{s1}-, α_{s2} and β-casein have the capacity to bind with cations; for instance Ca^{2+}, leading to their precipitation because of charge neutralization. The presence of κ- casein with a very low number of phosphate groups however, prevents from this precipitation [2]; the mechanism is discussed in Sect. 6.2.2. Lowering the pH and/or action of rennin which splits κ- casein leads to lose this protection character [3]. Splitting of κ-casein by rennin exactly happens at Phe_{105}–Met_{106} linkage in the C-terminal of molecule [2, 11]. As a result, para-κ-casein and macropeptide (caseinomacropeptide or glycomacropeptide) are obtained which are originally the hydrophobic N-terminal peptide and glycosylated C-terminal region in κ-casein molecule, respectively [7, 12]. As the insoluble para-κ-casein is formed, aggregation of casein molecules occurs and this phenomenon leads to the instability of system which is really significant in cheese making process [3]. Unlike phosphorylation, glycosylation is just seen in κ-casein. Hydroxyl groups of threonine in C-terminal portion are linked to saccharide groups; thereupon, galactose, N-acetyl galactosamine and N-acetyl neuraminic (sialic) acid are found in κ-casein molecules [2, 7]. That is the why κ- casein is called a glycoprotein. Fucose and N-acetyl glucosamine are two other carbohydrates that are found in human milk [7].

In contrast with α_{s1}- and β-caseins, the presence of systein residues in α_{s2}- and κ-caseins leads to the formation of disulphide bonds. The number of molecules that bond to each other in κ-casein differs from that in α_{s2}-casein. That is to say that in κ-casein not less than 10 molecules join each other via disulphide linkages, while in most of α_{s2}-caseins only 2 molecules are linked by disulphide bonds and form a dimer. As well, intermolecular disulfide bonds have been reported for α_{s2}- and κ-caseins [6, 11]. The joint of two classes of caseins; for instance α_{s2}-casein–κ-casein, has also been reported [6] due mainly to the different charges of C-terminal regions in these two molecules [8].

6.2.2 Assembly of Caseins and Casein Micelle Models

Casein molecules in milk exist as colloidal nanoparticles with a mean diameter of ~150 nm containing calcium phosphate. These nanoparticles are called casein micelles [14]. Calcium phosphate present in micelles is currently referred as colloidal calcium phosphate (CCP) and has an undeniable significant impact on the formation of micelle as well as their functional properties. Omitting the CCP from casein micelle, for instance with the addition of Ethylenediaminetetraacetic acid (EDTA), acidification and dialysis, can lead to the dissolution of micelle [15–17]. There are some important factors that contribute to the formation of casein micelles namely CCP, hydrogen bonds, hydrophobic interactions [18] and electrostatic interactions [19]. It has been known for over 45 years that individual caseins or a mixture of them can form micelle-like structures in aqueous solutions [19–22] even in the absence of calcium [23]. This is because of self-assembly tendency of casein monomers [24] which is attributed to their amphiphilic nature [20]. The term self-assembled casein nanoparticles is used for associative structures of re-micellised casein in an aqueous solution (Madadlou et al., Self-data"). Mounsey et al. [22] successfully re-assembled casein micelles from insoluble acid casein while retaining good functionality. Vitamin D2 was encapsulated in self-assembled casein micelles prepared from a commercial sodium caseinate powder [21]. Recently, ultrasonic disruption of self-assembled casein nanoparticles was compared at two frequencies of 35 and 130 kHz and it was observed that sonochemical ultrasound (130 kHz) was more effective than power ultrasound (35 kHz) in particle disruption [25]. Then an approach based on dual-frequency sonication of casein solutions by 130 and 24 kHz ultrasounds was elaborated for disrupting the self-assembled casein nanostructures [26]. The self-assembled casein structures whilst not identical are similar to their native counterparts [22, 27] and can be properly used as model biosystems. Euston and Horne [20] found by computer simulation of self-association behavior of four types of casein that the micelles formed by all the simulated casein molecules are stabilized by a layer of hydrophilic segments like the native counterparts. Experts believe that the interaction of positively and negatively charged segments have an important role in self-association of proteins [6]. It has been reported that the appropriate pH ranges for self-assembly of caseins to form micelles are 2.0–3.0 and 5.5–12. At lower pH values micelles have a compact structure, whilst at higher values the structure becomes loose [19, 28]. Despite the huge amount of research carried out in the field, structure of casein micelles is still not clear and various models have been proposed during the past decades.

According to one of the well-known models for the structure of casein micelle which proposed by Morr in 1967, the micelle is composed of submicelles [2]. Submicelles are spherical aggregates of caseins and linked to each other via CCP. In fact, CCP acts as cement to hold submicelles together. In this model each submicelle is comprised of α_{s1}-, α_{s2}- and β-casein in the internal part of it, making hydrophobic core and κ-casein is located on its surface. The important point is that hydrophobic segment of κ-casein molecule is toward to the core, whilst it's

hydrophilic segment protrudes from micelles surface, causing the negative charge of micelles [2, 3, 29]. Kappa-casein does not cover the micelle entirely, but heterogeneously [30]. Therefore, two regions might be found on the surface: highly hydrophilic region and hydrophobic region [2, 3]. Besides, κ-caseins might interact with each other via disulphide bonds [30]. The negatively charged C-terminal segment which protrudes from the surface of the micelle forms hairy layer with thickness of almost 7 nm around the micelle. It is declared that protein chains within the structure of micelle are immobile, except the hairy layer part. This layer causes steric and electrostatic repulsions that result in the stability of micelle [3, 31]. Some conditions such as hydrolysis of κ-casein by rennet, diminishing the pH to 4.6, addition of Ca^{2+} ions or ethanol as well as high pressure treatment collapse the hairy layer of κ-casein [2, 3, 14]. Thus, the steric hindrance is removed and consequently aggregation of micelles would happen. For years, experts tried to find a replacement for κ-casein in order to maintain the stability of acidified milk products. Anionic hydrocolloids are adsorbed on the surface of micelles and prevent from aggregation via steric and electrostatic repulsions or by increasing the viscosity [31–34].

Gel-like structure is another model that states casein molecules are located in micelle in a tangle manner and complicated situation, forming a sphere. In addition, κ-caseins stretch out of the micelle and form a hairy layer. In this model, which was proposed by Holt [35], calcium phosphate nanoclusters act as linkers of thread-like casein monomers by cross-linking [2, 29, 36, 37]. In this model the calcium phosphate nanoclusters are responsible for linking the caseins molecules to each other whereas in previous proposed model nanoclusters are the joiners for submicelles.

Submicelle model was modified by Walstra et al. [38, 39] depicting that CCP nanoclusters are not linker of submicelles but are found within them. They hypothesized that submicelles are linked together via secondary forces [2, 3]. Actually, hydrophobic bonds among protein groups and cross-links among peptide chains are important in holding submicelles together. It is notable that calcium phosphate nanoclusters are not only composed of inorganic phosphate and calcium, but might contain phosphoseryl residues as well as glutaminic acid residues [3]. Nowadays, some researchers cast doubt on the submicellar structure using new analyzing techniques [2, 15, 37, 40].

Founded on the next proposed model which is called dual-binding model, formation of casein micelles depends on hydrophobic segments of casein molecules as well as the presence of CCP that helps to link the caseins molecules. In the structural arrangement of a casein micelle, positively charged calcium phosphate nanoclusters do not just cross link the casein molecules but also bind to negatively charged phosphoserine residues to reduce the repulsive forces among casein molecules leading to domination of attractive interactions between the hydrophobic regions of caseins [5]. α_{s1}-, α_{s2}- and β-casein include 2, 2 and 1 hydrophobic segments, respectively. Their molecules are therefore capable to link with each other and micelle grows in this manner. In addition, formation of CCP-mediated linkages among caseins that contain phosphoseryl residues hands in micelle growth.

However, joining of κ-casein to any of other caseins via its hydrophobic region leads to the termination of micelle growth because κ-casein just owns 1 hydrophobic segment and does not interact with CCP nanoclusters due to the lack of phosphoseryl residues [2, 40]. This model is basically different in comparison with previous models in term of internal structure of micelles; however, the cement role of CCP and location of κ-casein on the surface of micelle are identical.

Based on a new proposed model, each CCP nanocluster is assumed as a core and α_{s1}-, α_{s2}- and β-caseins are linked to this core. Since β-casein just contains 1 hydrophobic site, it links to only 1 CCP nanocluster; in essence, as soon as β-casein links to CCP (core) the growth of micelle in that direction ceases. Contrary, α_{s1}- and α_{s2}-caseins are multi-functional (bi-functional) caseins and own 2 hydrophobic sites. These caseins develop the network via cross-linking since each α_s-casein that is linked to a CCP is able to interact with the next CCP and in this way nanoclusters link to each other. The tendency of Ca-sensitive caseins to interact with CCP is directly related to their phosphoseryl residues. The multi-functional caseins continually link CCP nanoclusters to each other and this process continues till the end nanocluster links to the first one, and a loop is formed. Bacause multi-functional caseins link randomly to each other a variety range of micelle size is obtained. The location of κ-casein and its role in the stability of micelle appear to be unclear in this model [15].

In 2007, a fibril-like structure was proposed for casein micelle. This model might justify why casein undergoes high temperature without denaturation, as fibril proteins resist against heating [37]. Supramolecular structure of casein micelle was proposed as an interlocking lattice model in 2008. Based on this model, nanoclusters are the responsible for holding the casein molecules together and cause the integrity of micelles. In brief, this model states that the phosphoseryl residues of casein molecules are locked by calcium phosphate nanoclusters to form a spherical micelle. Therefore, the unity of casein network is directly related to calcium phosphate nanoclusters In addition, hydrophobic interactions which cause the association of caseins and chain formation, hydrogen bonds and electrostatic interactions are actually effective in micelle's integrity. Since these interactions altogether are responsible for joining the caseins to each other, omitting one of these locking elements does not lead to the complete dissociation of micelle. Like most of the proposed models, κ-casein acts as the terminator of association and locates at the surface of micelle [41]. The latest introduced model is core-shell, in which core part is composed of casein proteins attached to each other and create a network via oval-shaped calcium phosphate nanoparticles. Likewise the previous models, here the term "shell part" is related to κ-casein branches [42].

6.2.3 Structure and Assembly of Whey Proteins

Whey proteins are consisted of β-lactoglobulin, α-lactalbumin, proteose peptone, serum albumin, immunoglobulins and lactoferrin. In contrast with caseins, they are

not heat-resistant and heat treatment causes their denaturation [43] leading to their precipitation onto the casein micelles in milk [3]. However, they are soluble when caseins precipitate at isoelectric pH of milk [43]. Secondary α-helical and β-sheet, and tertiary structures have been observed in whey proteins [44].

The dominant protein in whey is β-lactoglobulin which includes 162 residues with a molecular weight of about 18,300. It comprises 10 % of the total milk protein or about 58 % of the whey proteins. Two disulfide and 1 free sulfhydryl groups are found in this molecule [43, 45]. The sulfhydryl group has a significant role in the interaction of β-lactoglobulin with another β-lactoglobulin molecule, with an α-lactalbumin molecule and in particular with κ-casein during heat treatment [3]. Polymerization of β-lactoglobulin depends on pH; monomers are found at pH values lower than 3.0 and higher than 8.0. At pH 3.1 up to 5.1, 8 β-lactoglobulin molecules are linked to each other forming an octamer. At normal pH of milk β-lactoglobulin is present as dimmers [43] due to hydrophobic linkages. It has the capability to link with apolar molecules such as retinol and some kinds of fatty acids in reason of its extreme hydrophobic character [3]. In addition, its capability to bind with some ligands such as cholesterol and vitamin D_2 has been reported. The ends of β-lactoglobulin molecule are suspected to link with these ligands and the interaction is pH dependent. In cholesterol-β-lactoglobulin complex, the carbonyl of Pro38 residue is found as important factor due to its capability to form a hydrogen bond. In vitamin D_2-β-lactoglobulin complex carbonyl of Lys69 forms the hydrogen bond. The interaction of Pro38 with Lys60 is also significant in the latter complex [45]. Recently, β-lactoglobulin is widely considered as a source for bioactive peptides. The derived peptides from hydrolysis of β-lactoglobulin can act as antihypertensive and antioxidant substances. The other benefits of this protein are the reduction of cholesterol and prevention from cancer by inducing the production of glutathione. In addition, its positive impact on antimicrobial activities has been confirmed. Beta-lactoglobulin is effective on *Esherihia coli*, *Bacillus subtilis* and *Staphylococcus aureus*; whilst, it is not very impressive on γ-negative bacteria [46].

Alpha-lactalbumin is the other significant whey protein that has notable beneficial characteristics such as destroying bacteria, anticancer activity and ability to increase the performance of brain [47]. It is composed of 123 amino acids and 4 disulfide bridges. Low ionic strength induces the association of α-lactalbumin. It is claimed that presence of calcium increases the resistance of α-lactalbumin against heating since intramolecular ionic linkages are formed due to a specific site in α-lactalbumin for linking with calcium ions [3, 43]. Other cations such as Mn^{2+}, Mg^{2+}, K^+ and Na^+ can also link the same site and enhance the resistance against high temperature, except Zn^{2+} which does the opposite [44]. It has been reported that self-assembly of α-lactalbumin, after enzymatic hydrolysis using a serine protease from *Bacillus licheniformis* caused the constitution of nanotubular structures [47]. These structures are discussed in Sect. 6.3. Notably, β-lactoglobulin cannot be used for these purposes because self-assembly of hydrolyzed β-lactoglobulin leads to the formation of aggregates [48]. Although only 60 % of β-lactoglobulin protein contributes in this assembly process, it continues with a linkage rate of one monomer in

each second until a gel phase is obtained [47]. Alpha-lactalbumin might exhibit anticancer activity by binding to cations, for example Zn^{2+} [44].

Contrary to other whey proteins, a Fe^{3+} ion is present in lactoferrin molecule [3]. Similarly to immunoglobulins, it has the antimicrobial character [46]. Whey is appropriate for extraction of lactoferrin and cation-exchange chromatography is proposed for its purification. Heat treatment at pH 4.0 does not denature the protein; therefore, this pH is suitable for its pasteurization. Recently, some beneficial aspects of lactoferrin on human's health have been regarded. Its exceptional properties such as antiinfective, anticancer, antioxidant and antimicrobial activities enhance its utility in pharmaceutical and food industries. Remarkably, lower pH values (2–3) enhance its antibacterial activity. The results of clinical studies about positive effects of lactoferrin on human and animals' health have been published [49].

Proteose peptones is defined as the part of whey proteins that resist against heating and precipitation at pH 4.6; while, 12 % trichloroacetic acid leads to their sedimentation. Being glycoprotein, proteose peptones are known as derivatives of β-casein emerged by plasmin. However, a kind of proteose peptone, termed 8 slow, is not related to proteolytic interaction of casein. Immunoglobulins which are important for their antimicrobial properties are classified to four groups: IgG1, IgG2, IgA and IgM. IgM has an important role in cold agglutination of milk. IgG is composed of 2 light and 2 heavy chains that are joined via disulfide linkages. It is reported that hydrogen bonds, hydrophobic bonds and electrostatic attractions take a part in their polymerization. The last whey protein is serum albumin which contains 17 disulfide bridges and 1 sulfhydryl groups [3, 43].

6.3 Nano and Microcarreirs Based on Milk Proteins

For many years, milk proteins especially caseins, have been used as emulsifying, foaming and gelation agents. However, their structural properties allow their application for delivery of various bioactives. For instance, α_{s1}-, α_{s2}- and β-caseins are inherently carriers of high value nutritional components, in particular calcium and calcium phosphate nanoparticles via their phosphoserine residues [50]. In recent years, milk proteins have extremely been attended for delivery and protection of nutraceuticals such as vitamins, essential oils, probiotics, antioxidants, bioactive peptides and etc. Using milk proteins for encapsulation of nutraceuticals helps the experts of food science to produce functional foods with positive effects on human's health. On the other hand, nutritional benefit of milk proteins should not be neglected. Investigations based on milk proteins as nanocarriers have an undeniable role in nanobiotechnology, in which the particles with the size less than $\sim$1,000 nm are employed. Milk proteins are attended because of their potential to entrap the nutraceuticals and drugs in order to protect and transport them until arriving to target. In fact, the remarkable benefit of encapsulation is delivery of entrapped material to appropriate place without being

harmed. For example, in many cases the core material should be protected from the strong acidic environment of stomach by the wall material in a good encapsulation process [51]. The list of milk proteins that are used for delivery of bioactives in micro and nanoencapsulation processes has been summarized by Livney [21].

The reassembly character of caseins is a positive point which can be really practical for retaining and delivery of nutraceuticals. Self-assembled casein nanoparticles in aqueous solutions have been suggested for nanoencapsulation of hydrophobic nutraceuticals. The reassembling character of casein not only used for entrapping and delivery of vitamin D_2, but also for protecting this vitamin from photochemical degradation. It is supposed that vitamin D_2, is entrapped within the reassembled casein micelle because of adhering to hydrophobic parts of caseins, which tend to locate in the core of particles. It is declared that some amount of vitamin D_2 may link to soluble caseins, which do not incorporate in the reassembly of casein structures. However, the amount of vitamin in reassembled casein micelles is nearly 5.5 times greater than that in the surrounding serum. Moreover, the reassembled casein micelle showed no significant difference in morphology and average size in comparison with their natural counterparts. Consequently, nanoencapsulation in this way can be applicable for enrichment of low fat or free fat dairy products with vitamin D_2, as an oil-soluble vitamin, which has undeniable role in adsorption of Ca^{2+} [21].

In recent years, enzyme transglutaminase has been widely attended because of its capacity to cross-link casein molecules. This ability of transglutaminase was used for cross-linking of casein molecules in casein micelles leading to the formation of nanogel particles. Elimination of CCP from casein nanogel particles does not interrupt their integrity. These particles exhibit no significant difference in terms of size, zeta potential and substructure in comparison with native casein micelles. The nanogel particles are suggested to be used for encapsulation processes in both food and pharmaceutical industries. It is aimed to use casein nanogel particles (after removing the CCP) as a substitute for caseinate in industry. Investigations based on the colloidal stability of cross-linked micelles show that casein nanogel particles are more resistant to heat coagulation than natural casein micelles. This is due to the cross-linking of κ-caseins, which are responsible for stability of micelles by steric repulsion, resulting in lower dissociation of κ-caseins at higher temperatures. However, casein nanogel particles are really susceptive to acid coagulation in comparison with natural casein micelles; in essence, they flocculate at pH $\sim$5.1. Sensitivity of casein nanogel particles to acid-flocculation is again attributed to cross-linking of κ-caseins. The hairy layer losses its capability to move freely due to participation in the cross-linking reactions. As a result, the entropy of conformation diminishes and consequently, the steric repulsion decreases. Completely cross-linked casein micelles are highly stable against ethanol, urea or citrate [52]. Caseinate gel has been utilized for microencapsulation of probiotic cells. The ability of transglutaminase to cross-link the casein molecules was applied to form a gel structure by caseinate. Transglutaminase-induced caseinate gel can protect probiotics against low pH (pH 2.5 and 3.6, at 37 °C for

90 min) which is similar to human's stomach condition. The yield of encapsulation is notably high, especially for *Bifidobacterium lactis Bb*12 that is 90 % [53]. Gelation of casein by enzyme is related to cross-linking of γ-carboxamide group of a glutamyl residue and ε-amino group of a lysine residue leading to the formation of ε-(γ-glutamyl) lysine bond. The potential of casein hydrogel to entrap and release the vitamin B_{12} has also been observed [54].

The same as caseins, whey proteins have a significant role as vehicles for nutraceuticals. Whey proteins can be used in cold-set gelation process as a novel encapsulation technique. The first step is the heat treatment which causes the denaturation of whey proteins and formation of soluble aggregates. After cooling, addition of Ca^{2+} ions at room temperature forms the gel. Cross-linking of carboxyl groups with Ca^{2+} ions has a key role in the formation of network. Cold-gel formation can also be induced by reducing pH to the isoelectric point of proteins. Polypeptide chains of denatured protein and nutraceuticals can interact with each other via hydrogen-bonding, hydrophobic and electrostatic interactions. The method cold-set gelation is highly applicable for entrapping heat-sensitive molecules such as riboflavin, drugs, probiotics and yeasts [50, 51]. Beta-lactoglobulin can be used as a nanocarrier for hydrophobic molecules such as vitamin D, retinol and ω-3 fatty acids [50]. This protein links to hydrophobic molecules through its free thiol group. Based on this fact, a ω-3 fatty acid (DHA) was added to functional beverages via nanoencapsulation with β-lactoglobulin. This procedure prevents from the oxidation of DHA and enhances its solubility. It has also been suggested to use low methoxyl pectin for stabilizating the system at pH 4.5 which is under isoelectric point of β-lactoglobulin. This makes possible to produce dilutable nanoparticle dispersions, which form transparent solutions containing β-lactoglobulin and DHA, with a very good colloidal stability and average particle size of w 100 nm. Low methoxyl pectin causes stability by impeding the precipitation of β-lactoglobulin. As well, pectin protects the complex of protein-DHA against degradation [55]. Biopolymer nanoparticles are formed by heating the mixture of β-lactoglobulin and high or low methoxyl pectin (HMP and LMP, respectively) at temperatures higher than thermal denaturation temperature (80 °C) under pH conditions where the biopolymers form electrostatic complexes (pH 5). These biopolymer nanoparticles are proposed for encapsulation of hydrophobic molecules. Morphological experiments reveal a spherical shape for these biopolymer nanoparticles and thus it is presumed that β-lactoglobulin is surrounded by pectin at low pH values (lower than isoelectric point of protein) via electrostatic attraction. Complexes of HPM-β-lactoglobulin exhibit more stability than those of LMP-β-lactoglobulin at low pH values, indicating that charge of polysaccharide has a notable impact on complex stability [56]. Similarly, HMP has a better effect than LMP in stabilizing the acidified milk drinks [57]. Addition of sodium chloride enhances the resistance of HMP-β-lactoglobulin complexes against low pH, while it has a reverse effect on LMP-β-lactoglobulin complexes [56]. At ambient temperature, addition of sorbitol causes an appreciable decrease in the critical pH where insoluble protein–pectin complexes are formed, whereas addition of glycerol has little impact. They also impact the temperature where biopolymer

aggregation occurs during heating. Both glycerol and sorbitol increase the aggregation temperature, due to their ability to decrease the biopolymer collision rate and increase the thermal denaturation temperature. Hence it is not possible to form pH-stable biopolymer particles by heat treatment when glycerol or sorbitol is present at the temperature (85 °C) that they could be formed in their absence [58].

Serum Albumin, which is found in milk and blood serum, is naturally responsible for delivery of small ligands in blood serum. Therefore, serum albumin as well as lactoferrin has been utilized for delivery of hydrophobic drugs [50, 59]. Alpha-lactalbumin is considered as a novel subject in food science and medicine due to its potential to form hallow nanotubes with a diameter of $\sim$20 nm and length of $\sim$110 nm. The nanotubes are formed trough partial hydrolysis of α-lactalbumin with a serine protease from *B. licheniformis* and α-lactalbumin concentration impacts the structure of assembly. At protein concentrations of 30 g L^{-1} or higher, the tubular assembles are formed whilst, at lower concentrations linear fibrillar aggregates with diameter of almost 5 nm are emerged. Presence of Ca^{2+} ions is necessary to obtain nanotubes because they are responsible for jointing α-lactalbumin dimmers to form tubular structure [48]. Other divalent and trivalent ions such as Mn^{2+}, Zn^{2+}, Cu^{2+} and Al^{3} can also play this serious role. In contrast, Ba^{2+} and Mg^{2+} have a negative effect on tubes formation by directing the self-assembly process toward obtaining fibrillar aggregates. Interestingly, Ca^{2+} may leave its position in α-lactalbumin nanotubes by the addition of EDTA or diluting the solution with a Ca^{2+}-free buffer. This elaboration leads to the disassembly of nanotubes. As well, altering the pH to higher than 9.0 and lower than 3.0 and addition of urea lead to the dissociation of this nanotubes. It has been suggested to cross-link the nanotubes via transglutaminase enzyme to enhance their stability. It is declared that presence of other proteins, for instance β-lactoglobulin, interrupt the self-assembly of α-lactalbumin to form nanotubes due to resulting in accidental aggregation. It is widely feasible to utilize α-lactalbumin nanotubes as viscosifier and gelling agents; notably, they affect even in low concentrations. The remarkable points about the gels which are based on α-lactalbumin nanotubes are their transparency and reversible character. Their firmness is changeable via controlling the disassembly of tubes though omitting Ca^{2+}. Alpha-lactalbumin nanotubes are recently attended in nano-encapsulation process. Some factors including the structure (nanometer-sized cavity and length), controllable disassembly and the ability of being manipulated make α-lactalbumin nanotubes appropriate to be used in nanotechnology. An extremely unique character of α-lactalbumin nanotubes is the possibility to easily make a hole in their wall due to their softer wall in comparison with other nanotubes. Alpha-lactalbumin nanotubes are not affected by some treatments that are necessary for a number of processes in food industry. It is proven that either pasteurization (at 72 °C for 40 s) or freeze-drying has no negative impact on the structure of tubes. It is worthy to note that applications of α-lactalbumin nanotubes are not limited to food science but widely considered in other areas of science, for example in tissue engineering [47].

Recently, whey protein isolate (WPI) was used for coating zinc oxide (ZnO) nanoparticles in ambient temperature and weak basic condition. The average size

of obtained ZnO-WPI nano-composites was approximately 300 nm. It is stated that electrostatic attraction, hydrogen bonding or O–Zn–O bonding are probably responsible for interaction of WPI and ZnO. When pH of solution is basic i.e., 8.0, whey proteins become negatively charged and hence interact with Zn^{2+} electrostatically. Zn^{2+} has a positive impact on human's growth and moral; therefore, consumption of these nano-composites may be suitable for the societies that face with lack of Zn^{2+} [60]. Whey protein concentrate (WPC) has been used as one of the components of wall material in order to reduce the surface tension of emulsion in encapsulation of oils [61, 62]. Whey proteins micro particles can be used for encapsulation of vitamin B_2 [51]. As well, whey proteins and milk fat has been introduced as practical composite for microencapsulation of theophylline, a water-soluble drug. Presence of milk fat, as one of the components of wall material improved protecting the water-soluble core and diminished the core's releasing processes [59].

6.4 Films and Coatings Based on Milk Proteins

6.4.1 Milk Protein Films

Because of environmental pollutions caused by synthetic plastic films, it is requisite to develop edible and biodegradable films for improving waste disposal issues [63]. The easily biodegradable packaging provides a new market for the materials used in the manufacture of environmentally-friendly coatings [64]. These films and coatings carry out an important role in the protection and conservation of foods and are usually used to control moisture transfer, limit gas transport, retard oil and fat migration, prevent solute or flavor absorption and carry additives such as antimicrobial agents and antioxidants [65]. They can extend shelf life of a product by providing a boundary to biological or chemical damage e.g., reduce the exchange of water between the food and the environment, in particular drying of moist foods [66]. Natural polymers such as casein, collagen, zein, wheat gluten, whey proteins, gelatin, and soy protein or their derivatives have been broadly studied due to their special features such as availability, mechanical strength, biodegradability and environmental compatibility [63]. Moreover, films made from proteins can elevate the nutritional value of the food [67]. Milk protein-based films are used in edible packaging as barrier of gases, moisture or oil to protect the foods [68]. They are flavorless and colorless; however, addition of some ingredients to the film formulation can change the taste of films [65]. Oxygen permeability of milk protein-based films is dependent on the amount of protein i.e., higher protein contents leads to better barrier characteristics. On the other hand, protein concentration has an inverse effect on water vapor permeability of films since a more aggregated structure and denser protein matrix is formed in higher protein concentrations leading to larger pores in the matrix [69, 70].

Sodium caseinate is one of the appropriate materials for making edible films. Film forming capability of caseinate and casein is attributed to their random coil nature and ability to form intermolecular hydrogen, electrostatic and hydrophobic bonds [70–73]. Among casein proteins, β- and κ-caseins are more suitable materials for making emulsion films [74]. The most hydrophobic protein of milk, β-casein acts as a potent barrier for water vapor. Interestingly, water vapor permeability of β-casein films is even lower than the lipid-incorporated caseinate films. Moreover, β-casein films have higher tensile strength and elongation than other milk proteins' films. Investigations show that different storage temperatures do not have any significant impact on water vapor permeability, elongation and structure of β-casein films [75]. Calcium caseinate is produced through replacing sodium by calcium in sodium caseinate. Calcium caseinate films are stronger barriers for water vapor in comparison with sodium caseinate films since presence of Ca^{2+} ions increases the cross-linking interactions among protein chains leading to the formation of a tighter structure. The undesired property of these films is their lower transparency than sodium caseinate films. The substitution degree of sodium by calcium is important as a higher substitution degree leads to the more stiffness of film. It is worthy to note that appropriate properties are achieved for films by a combination of calcium and sodium caseinates in the film formulation [73].

Extraction process of casein from milk influences film properties as the films obtained from CO_2-precipitated casein (CO_2CAS) exhibit higher resistance against the humidity of the environment in comparison with calcium or sodium caseinate films. This is due to the lower solubility of CO_2CAS in water [75] and hence its films are extremely hydrophobic. Furthermore, CO_2CAS films are highly suitable as oxygen barriers for foods [76]. Interestingly, protein particle size has a profound impact on characteristics of CO_2CAS films. When protein particle size is diminished to 111 μm, the tensile strength of film is increased and its water vapor permeability is reduced. However, no positive effect is observed in film opacity. It is required to reduce the size of protein particles to less than 86 μm to obtain a transparent film from CO_2CAS. This however, has negative effects on tensile strength and water vapor permeability of films and hence, reduction of protein particle size has a limit [77].

Whey protein-based films are also considered as edible films for food packaging. Intermolecular disulphide, hydrogen and hydrophobic interactions have an important role in the production of whey protein-based films. Heating is essential for the formation of interactive bonds and arrangement of the network [78]. Whey protein films are colorless and odorless, the same as casein-based films, while they are extremely better oxygen barriers in comparison with other biopolymers [79, 80]. In contrast with casein-based films that are water soluble [74] whey protein-based films are partially insoluble because of their intermolecular disulfide bonds [80]. Notably, WPC and WPI films exhibit higher elongation in comparison with caseinate-based films. WPC films are extensively suggested to be used in food packaging since these films present better water vapor permeability and mechanical characteristics than other milk protein-based films [81]. Films based on WPI exhibit better barrier properties at higher pH values due to the enhanced

reactivity of SH groups at alkaline pH, which leads to the formation of intermolecular disulphide bonds during drying [82]. Drying kinetics, which probably affect the structure of films, highly depends on film thickness [69, 78] that is related to film formulation, the used procedure and the area of casting surface [69, 83]. In fact, higher concentration of protein or higher amount of plasticizer leads to a thicker film [69].

A pointed weakness of films based on milk proteins is their brittleness [70, 78] and definitely any created pin, hole or crack on the film during the production or handling processes interrupts the film's role as a good barrier [75]. It is common to use plasticizers, polyol molecules like sugars or even water in the formulation of milk proteins films to improve their mechanical properties and increase flexibility and extensibility [69, 70, 76–78, 84]. Plasticizer is termed to a low volatile organic ingredient that enhances the flexibility and extensibility; as well, reduces the glass transition temperature (T_g) of a polymer [71, 85]. One of the common plasticizers, glycerol is attended due to its high boiling point and polar, water-soluble, non-volatile and protein miscible character [69, 80]. Plasticizers compete with protein chains in forming hydrogen and electrostatic bonds [84] leading to lower intermolecular interactions among protein chains and therefore an increased molecular space for chains in the film matrix [70, 76, 77, 84].

6.4.2 Composites Based on Milk Proteins

Although protein films are excellent oxygen and carbon dioxide barriers, they tend to absorb large quantities of water under elevated relative humidity conditions due to proteins hydrophilicity. As a consequence, their mechanical properties are weakened and their water vapor permeability is increased [86] which is attributed to the plasticizing effect of water on protein films [87]. As well, alteration of the sensory properties of product is not acceptable for consumers e.g., if fresh fruits lose their moisture or dried fruits gain moisture their quality decreases [74]. The drawback is usually palliated through elaboration in the molecular structure of films by using chemical reactions such as cross linking or by physical treatments such as heat, ultrasound or radiation [88]. The formation of cross-linkages in protein-involved composites by the enzyme transglutaminase is an interesting approach. The cross-links form high molecular mass polymers, resulting in changes in the mechanical properties and water vapor permeability of the films [64]. Films based on α_{s1}-casein and cross-linked by transglutaminase are insoluble; whereas, the enzyme treated whey protein-based films show a moderate solubility [83]. Gamma-irradiation affects proteins by causing conformational changes, oxidation of amino acids, formation of protein free radicals, and recombination and polymerization reactions [86]. In caseinate-whey protein films more ordered and more stable structures were adapted because of modifications in conformation of proteins by γ-irradiation [89]. It has been reported that heat pressing of a starch-casein composite film with the help of hot iron box caused a

drastic decrease in water vapor transmission rate. As well, application of heat had a toughening effect on the film and enhanced the thermal stability of film [90]. Addition of hydrophobic materials as lipids, fatty acids and waxes and laminating the hydrophilic film with a hydrophobic layer [87] are other strategies to improve film properties. The blending of varying ratios of biopolymers offers another possibility for manufacturing composite films with improved properties to meet consumer expectations [88, 91]. Gamma-irradiation carried out before or after admixing of composite solutions induces further improvements [92].

It is well known that edible films are improved by combining protein and polysaccharide sources [88]. In general, the incorporation of polysaccharides results in a decrease in tensile strength and elastic modulus and an increase in elongation values. So, the films prepared with polysaccharides are more flexible and more stretchable than the films prepared without them. The presence of polysaccharide in the film matrix causes an increase in the chain mobility that modifies the mechanical response. This leads to a more plasticized structure, especially at low concentrations in the matrix and depending on the protein–polysaccharide interactions; k-carrageenan has a greater depressing effect on tensile properties of sodium caseinate films than alginate [93]. In numerous researches films obtained by combining milk proteins with polysaccharides have been prepared and characterized. Methylcellulose–whey protein composite films have been suggested as appropriate alternatives for moisture-sensitive food products since these composite films posses lower water vapor permeability compared to each biopolymer alone. Also, the addition of pullulan to a whey protein film has shown to decrease water vapor and oxygen permeability, although these barrier properties got worse as the amount of polysaccharide increased [91]. WPI and mesquite gum, a natural exudate from the mesquite tree show high compatibility to make solutions and composite films. Structure of these films is a continuous network of protein aggregates that enlarge in size as the gum content increases. As well, increased gum content in formulation results in films with improved flexibility without increasing plasticizer content and consequently without affecting negatively others characteristics such as water vapor permeability. Researchers have suggested the use of mesquite gum to improve mechanical properties of WPI films as an alternative for larger amounts of low molecular weight plasticizers [94]. Sodium caseinate and pullulan are incompatible when used in the weight ratio 1:1. This is evidenced by similar thermomechanical behavior of pure polymers and composite blends and attributed to substantial different structure of two polymers [95]. Increasing the weight ratio of pullulan to sodium caseinate decreases the Young's modulus, the tensile strength and increases the elongation at break, suggesting that pullulan imparts flexibility and sodium caseinate stiffness to the composite film [96]. The preparation of chitosan–whey protein blend films at higher pH values (5–7) is not successful due to the insolubilization of one of the polymers or the formation of insoluble complexes. However, careful control of pH and polymer concentration enables miscibility and solubility of different biopolymers in the film-forming solutions. These elaborations enabled to produce blend chitosan–whey protein films, at

acidic pH, even though under these conditions a pure whey protein film could not be obtained, since the reactivity of SH groups decreases significantly at low pH values, hindering the formation of intermolecular disulphide bonds necessary to form intact self-supported films, thereby resulting in poor film properties [91].

Composite films that combine hydrocolloids with fatty emulsions or fatty layers could be of particular interest. In these composite films the lipids help to lessen water vapor transmission and the proteins or polysaccharides give the necessary film strength and structural integrity [96] and at the same time keep the low oxygen barrier values. Addition of lipids leads either to the stabilization of film emulsion or laminating the film via forming a new layer, resulting in bilayer films [73]. According to microstructural observations, self association of saturated fatty acid molecules during drying of film results in a bilayer structure [97]. Definitely, the extent of improvement of water vapor permeability depends on the kind and chain length of fatty acids [74]. Presence of saturated fatty acid in the formulation of sodium caseinate-based films has a better effect in terms of reducing the water vapor permeability than oleic acid. Oleic acid in single or combined form with beeswax exhibits a plasticizing effect and has an extremely positive impact on mechanical properties of film. Higher hydrophobic character of waxes makes it possible to use them in lower amount in comparison with lipids [98]. Sohail et al. [63] reported that wax application significantly decreased the tensile strengths and elastic modulus of casein films. Incorporation of low melting point lipids such as soy oil into composite films may provide more organoleptic acceptability than those containing higher melting point lipids [99]. Because protein and lipid base compounds are immiscible, two alternatives are possible: obtain composite films through emulsification of components or obtain multilayer film through their extension in successive layers. In the first case, the development of component interactions, gives rise to the particular functional properties of the film that are unexpected for films formed with the lipid dispersed in a separated phase [73]. Bilayer and multilayer films have been shown to be mechanically weaker than emulsion films [100]. Sodium caseinate-lipid composite films show microstructural discontinuities due to the lack of miscibility of components [97]. When mixtures of two thermodynamically incompatible biopolymers exceed a certain threshold, the mixed biopolymer solution separates into two liquid phases with the different biopolymers concentrated in the separate phases. Thermodynamic incompatibility is viewed at a macromolecular level as immiscibility of two phases [101]. The pure casein films are visually transparent and yellow while, the films with wax applications exhibit hazy/opaque appearance with dark yellow colors [63, 100]. This can be attributed to the formation of lipid aggregates in both the internal and surface parts of the film [98], the level of which increases with the increasing proportion of lipid in the film forming formulation [99]. In sodium caseinate based composites, at the presence of lipids (oleic acid and beeswax) κ-carrageenan modifies lightly the film properties, but the addition of alginate produces less flexible, less stretchable and more permeable films [93]. At high proportions alginate led to the films with lower tensile strength values for WPI-gelatin-sodium alginate composites. An open structure of continuous alginate

phase with small WPI aggregates dispersed in the alginate matrix, or more typically, in the alginate and gelatin matrix were observed for the films. This microstructural feature arises due to the electrostatically-associated complexes, and additionally, via hydrophobic interactions and the formation of hydrogen bonds [88]. Similarly, addition of potato starch to calcium caseinate or calcium caseinate-WPI blend results in somewhat weaker gels due to the incompatibility of calcium caseinate and starch in the presence of $CaCl_2$. Linear polysaccharides such as alginate are less compatible toward proteins than the branched polysaccharides (starch) and thus form softer gels [92].

The electrochemical synthesis of polysaccharide-protein composites as a facile and reproducible method for continuous preparation of a wide variety of composites [102, 103] has been applied to synthesize a range of polysaccharide complexes with milk proteins. In this method, an electrochemical cell is filed with aqueous solution of polysaccharide and protein at room temperature after which a potential is applied across the cell. The composite is formed either as sediment on the cell bottom or more usually as gel on the anode within minutes. The polarization (passivation) of anode with the in-synthesis composite usually causes a significant reduction in the current intensity as process continues [102, 104, 105]. It is therefore required to mechanically remove the gel from surface of anode in time intervals to recover the current intensity. Air-dried pectin/casein, pectin/WPI and potato starch-WPI composites are insoluble in dimethyl sulfoxide, 7M urea and 2M guanidinium thiocyanate. These solutions are potent solvents for polysaccharides and proteins, suggesting that a strong interaction between pectin and proteins is present in composites. In these composites, NH- and OH-groups of both components are involved in the complexation resulting in intermolecular protein NH–polysaccharide COO^- bond formation [103, 104, 106]. In potato starch-casein composites, the phosphate moieties of amylopectin and hydroxyl groups of amylose and amylopectin, as well, amino and carboxylic groups of casein are likely involved [107]. In contrast to potato starch-casein composites with covalent bonds, in CMC-casein composites, components are interacted solely by electrical charges and van der Waals forces causing their solubility in urea and guanidinium thiocyanate. The conformation and supramolecular structure of CMC is regarded as the responsible for the lack of covalent bonding between CMC and casein [105]. Electrochemical synthesis of biopolymer composites has been neglected by researchers despite the obvious profits as a rapid method to generate composites with various characteristics.

6.4.3 Applications of Milk Proteins-Based Films and Composites

Milk proteins-based films and composites are used in different scopes of food science, some of them explained by Chen [74]. Coating of meat and fish with

caseins results in diminished oil absorption during the frying process [108]. Sodium caseinate-based films plasticized with glycerol can be used for bread wrapping [84] and WPC-olive oil composites are appropriate for packaging dried peanut kernels to protect the quality of product by delaying in oxidative rancidity, retaining sensory properties and reducing moisture and oxygen penetration [68]. Whey protein-based pouches which are sealed by heat are useful for packaging milk powders and dry foods. Heat-sealing of film happens at temperatures near to the beginning of glass transition temperature and thickness of film has a significant role in sealing strength [109]. In pharmaceutical sector, casein films plasticized with oleic acid can be used as tablet coating in reason of their acceptable tensile strength. Drug release properties are important and in most cases the drug should not be released immediately. Therefore, it is recommended to apply post-coating using heat treatment at temperatures higher than 100 °C. This leads to intermolecular cross-linking due to the interaction of carboxylic and amino groups of caseins resulting in controlled drug release. In addition, this thermally induced cross-linking causes an improvement in tensile strength [67].

Edible films and coatings can offer a possibility to extend the shelf life of fresh-cut fruits by providing a semipermeable barrier to gases and water vapor, and therefore, reducing respiration, enzymatic browning, and water loss. The use of WPI-beeswax coating reduced the enzymatic browning of *Golden Delicious* apple slices significantly [110]. Whey protein-based coatings are more effective in reducing enzymatic browning of *Golden Delicious* apple slices than hydroxypropyl methylcellulose-based coatings, probably due to the antioxidant effect of amino acids, such as cysteine and/or the higher oxygen barrier that the protein exerts [111]. Emulsion coatings with 20 % solid content gave a whitish appearance that made the apples unacceptable. The optimum solid content of the emulsion and beeswax content to reduce browning were 16 and 20 %, respectively [110]. Incorporation of ascorbic acid or cysteine to WPC-beeswax coatings reduces the enzymatic browning of apples significantly, compared to the use of antioxidants alone [112]. Heat-denatured WPI-coated low-density polyethylene (LDPE) films have excellent oxygen-barrier properties, much better than uncoated LDPE films, at low to intermediate relative humidity. The coated films also have excellent gloss, as well as low haze and color. Therefore, WPI coatings have great potential for replacing existing synthetic oxygen-barrier coatings on LDPE films [113].

It is worthy to note that nutritional nature of protein-based films impels the scientists to use antimicrobial agents such as potassium sorbet in the formulation of films. The presence of potassium sorbet in antimicrobial films leads however, to an increase in water vapor permeability. This can be hindered by incorporating lipids [65]. Hence, it is possible to produce antimicrobial packaging from milk proteins. Addition of antimicrobial ingredients, sodium lactate or ε-polylysine to whey protein-based films prevents the spoilage of beef and increases its shelf life [82]. Whey protein-based films preserved by potassium sorbet are suggested to be used for packaging the biscuits, cookies, nuts and chocolate and for coating chesses, sausages and salamis [65].

References

1. Frinault, A., Gallant, D.J., Bouchet, B., Dumont, J.P.: Preparation of casein films by a modified wet spinning process. J. Food Sci. **62**(4), 744–747 (1997)
2. Fox, P.F., Kelly, A.L.: The caseins. In: Yada, R.Y. (ed.) Proteins in Food Processing. Woodhead Publishing Ltd and CRC Press LLC, Cambridge (2004)
3. Walstra, P., Wouters, J., Geurts, T.: Dairy Science and Technology, 2nd edn. CRC Press LLC, New York (2006)
4. Dickinson, E.: Casein in emulsions: interfacial properties and interactions. Int. Dairy J. **9**, 305–312 (1999)
5. Horn, D.S.: Casein interactions: casting light on the black boxes, the structure in dairy products. Int. Dairy J. **8**, 171–177 (1998)
6. Farrell, H.M., Malin, E.L., Brown, E.M., Mora-Gutierrezt, A.: Review of the chemistry of α_{s2}-casein and the generation of the homologous molecular model to explain its properties. J. Dairy Sci. **92**, 1338–1353 (2009)
7. Ginger, M.R., Grignor, M.R.: Comparative aspects of milk caseins. Comp. Biochem. Physiol. B: Biochem. Mol. Biol. **124**(2), 133–145 (1999)
8. Hoagland, P.D., Unruh, J.J., Wickham, E.D., Farrell, H.M.: Secondary structure of bovine α_{s2}-casein: theoretical and experimental approaches. J. Dairy Sci. **84**, 1944–1949 (2001)
9. Gaudin, J., Le Parc, A., Castrec, B., Ropers, M., Choiset, Y., Shchutskaya, J., Yousefi, R., Muronetz, V.I., Zuev, Y., Chobert, J.M., Haertlé, T.: Engineering of caseins and modulation of their structures and interactions. Biotechnol. Adv. **27**, 1124–1131 (2009)
10. Farrell, H.M., Wickham, E.D., Unruh, J.J., Qi, P.X., Hoagland, P.D.: Secondary structural studies of bovine caseins: temperature dependence of β-casein structure as analyzed by circular dichroism and FTIR spectroscopy and correlation with micellization. Food Hydrocolloids **15**, 341–354 (2001)
11. Kumosinski, T.F., Brown, E.M., Farrell, H.M.: Three-dimensional molecular modeling of bovine caseins: κ-casein. J. Dairy Sci. **74**, 2879–2887 (1991)
12. Creamer, L.K., Plowman, J.E., Liddell, M.J., Smith, M.H., Hill, J.P.: Micelle stability: κ-casein structure and function. J. Dairy Sci. **81**, 3004–3012 (1998)
13. Swaisgood, H.E.: Symposium: genetic perspectives on milk proteins: comparative studies and nomenclature, review and update of casein chemistry. J. Dairy Sci. **76**, 3054–3061 (1993)
14. Fox, P.F., Brodkorb, A.: The casein micelle: historical aspects, current concepts and significance. Int. Dairy J. **18**, 677–684 (2008)
15. Horne, D.S.: Casein structure, self-assembly and gelation. Curr. Opin. Colloid Interface Sci. **11**, 148–153 (2006)
16. Smyth, E., Clegg, R.A., Holt, C.: A biological perspective on the structure and function of caseins and casein micelles. Int. J. Dairy Technol. **57**, 121–126 (2004)
17. Zhang, Z.P., Fujii, M., Aoli, T.: Behavior of calcium and phosphate in artificial casein micelles. J. Dairy Sci. **79**, 1722–1727 (1996)
18. De Kruif, C.G., Holt, C.: Casein micelle structure, functions and interactions. In: Fox, R.F., McSweeney, P.L.H. (eds.) Advanced Dairy Chemistry. Kluwer Academic Plenum, New York (2003)
19. Liu, Y., Guo, R.: pH-dependent structure and properties of casein micelles. Biophys. Chem. **136**, 67–73 (2008)
20. Euston, S.R., Horne, D.S.: Simulating the self-association of caseins. Food Hydrocolloids **19**, 379–386 (2005)
21. Semo, E., Kesselman, E., Danino, D., Livney, Y.D.: Casein micelle as a natural nano-capsular vehicle for nutraceuticals. Food Hydrocolloids **21**, 936–942 (2007)
22. Mounsey, J.S., O'kennedy, B.T., Kelly, P.M.: Comparison of re-micellised casein prepared from acid casein with micellar casein prepared by membrane filtration. Lait **85**, 419–430 (2005)

23. Payens, T.A.J.: Association of caseins and their possible relation to structure of the casein micelle. J. Dairy Sci. **49**, 1317–1324 (1966)
24. Farrer, D., Lips, A.: On the self-assembly of sodium caseinate. Int. Dairy J. **9**, 281–286 (1999)
25. Madadlou, A., Mousavi, M.E., Emam-Djomeh, Z., Ehsani, M., Sheehan, D.: Comparison of pH-dependent sonodisruption of re-assembled casein micelles by 35 and 130 kHz ultrasounds. J. Food Eng. **95**, 505–509 (2009)
26. Madadlou, A., Mousavi, M.E., Emam-Djomeh, Z., Sheehan, D.: Dual-frequency sonication for disrupting the self assembled casein nanoparticles. Milchwissenschaft. **67**, 78–81 (2012)
27. Madadlou, A., Mousavi, M.E., Emam-Djomeh, Z., Ehsani, M., Sheehan, D.: Sonodisruption of re-assembled casein micelles at different pH values. Ultrason. Sonochem. **16**, 644–648 (2009)
28. Huppertz, T., Vaia, B., Smiddy, M.A.: Reformation of casein particles from alkaline-disrupted casein micelles. J. Dairy Res. **75**, 44–47 (2008)
29. Madadlou, A., Mousavi, M.E., Emam-Djomeh, Z., Sheehan, D., Ehsani, M.: Alkaline pH does not disrupt re-assembled casein micelles. Food Chem. **116**, 929–932 (2009)
30. Farrell, H.M., Malin, E.L., Brown, E.M., Qi, P.X.: Casein micelle structure: what can be learned from milk synthesis and structural biology? Curr. Opin. Colloid Interface Sci. **11**, 135–147 (2006)
31. Dalgleish, D.G., Spagnuolo, P.A., Goff, H.D.: A possible structure of the casein micelle based on high-resolution field-emission scanning electron microscopy. Int. Dairy J. **14**, 1025–1031 (2004)
32. Nilsson, L.-E., Lyckand, S., Tamime, A.Y.: Production of drinking products. In: Tamime, A.Y. (ed.) Fermented Milks. Blackwell Science Ltd, UK (2006)
33. Azarikia, F., Abbasi, S.: On the stabilization of doogh (Iranian yoghurt drink) by Gum Tragacanth. Food Hydrocolloids **24**(4), 358–363 (2010)
34. Azarikia, F., Abbasi, S., Azizi, M.H.: Comparison of the efficiency and mechanisms of some hydrocolloids on preventing the serum separation of Doogh. Iran. J. Nutr. Sci. Food Technol. **4**(1), 11–22 (2009). (in Persian)
35. Tuinier, R., Rolin, C., de Kruif, C.G.: Electrosorption of pectin onto casein micelles. Biomacromolecules **3**, 632–638 (2002)
36. Holt, C.: Structure and stability of the bovine casein micelle. In: Anfinsen, C.B. (ed.) Advances in Protein Chemistry, vol. 43. Academic, San Diego, California, (1992)
37. Phadungath, C.: Casein micelle structure: a concise review. Songklanakarin J. Sci Technol **27**(1), 201–212 (2005)
38. Lencki, R.W.: Evidence for fibril-like structure in bovine casein micelles. J. Dairy Sci. **90**, 75–89 (2007)
39. Walstra, P.: Scientific commons: casein sub-micelles: do they exist?. Archive of Wageningen University and Research center, The Netherlands (1999)
40. Walstra, P.: Xasein sub-micelles: do they exist? Int. Dairy J. **9**, 189–192 (1999)
41. Horne, D.S.: Casein micelle structure: models and muddles. Curr. Opin. Colloid Interface Sci. **7**, 456–461 (2002)
42. McMahon, D.J., Oommen, B.S.: Supramolecular structure of casein micelle. J. Dairy Sci. **91**, 1709–1721 (2008)
43. Shukla, A., Narayanan, T., Zanchi, D.: Structure of casein micelles and their complexation with tannins. Soft Matter **5**, 2884–2888 (2009)
44. Kilara, A.: Whey proteins. In: Yada, R.Y. (ed.) Proteins in Food Processing. Woodhead Publishing Ltd and CRC Press LLC, Cambridge (2004)
45. Permyakov, E.A., Berliner, L.J.: α-Lactalbumin: structure and function. FEBS Lett. **473**, 269–274 (2000)
46. Kontopidis, G., Holt, C., Sawyer, L.: Invited review: β-Lactoglobulin: binding properties, structure, and function. J. Dairy Sci. **87**, 785–796 (2004)
47. Hernandez-ledesma, B., Recio, I., Amigo, L.: β-Lactoglobulin as source of bioactive peptides. Amino Acids **35**, 257–265 (2008)

48. Graveland-Bikker, J.F., de Kruif, C.G.: Unique milk protein based nanotubes: food and nanotechnology meet. Trends Food Sci. Technol. **17**, 196–203 (2006)
49. Ipsen, R., Otte, J.: Self-assembly of partially hydrolysed α-lactalbumin. Biotechnol. Adv. **25**, 602–605 (2007)
50. Wakabayashi, H., Yamauchi, K., Takase, M.: Lactoferrin research, technology and applications. Int. Dairy J. **16**, 1241–1251 (2006)
51. Livney, Y.D.: Milk proteins as vehicles for bioactives. Curr. Opin. Colloid Interface Sci. **15**, 73–83 (2010)
52. Chen, L., Remondetto, G.E., Subirade, M.: Food protein-based materials as nutraceutical delivery systems. Trends Food Sci. Technol. **17**, 272–283 (2006)
53. Huppertz, T., de Kruif, C.G.: Structure and stability of nanogel particles prepared by internal cross-linking of casein micelles. Int. Dairy J. **18**, 556–565 (2008)
54. Heidebach, T., Forst, P., Kulozik, U.: Transglutaminase-induced caseinate gelation for the microencapsulation of probiotic cells. Int. Dairy J. **19**, 77–84 (2009)
55. Song, F., Zhang, L.M., Shi, J.F., Li, N.N.: Novel casein hydrogels: formation, structure and controlled drug release. Colloids Surf. B **79**, 142–148 (2010)
56. Zimet, P., Livney, Y.D.: Beta-lactoglobulin and its nanocomplexes with pectin as vehicles for ω-3 polyunsaturated fatty acids. Food Hydrocolloids **23**, 1120–1126 (2009)
57. Jones, O.G., Lesmes, U., Dubin, P., McClements, D.J.: Effect of polysaccharide charge on formation and properties of biopolymer nanoparticles created by heat treatment of β-lactoglobulin-pectin complexes. Food Hydrocolloids **24**, 374–383 (2010)
58. Koksoy, A., Kilic, M.: Use of hydrocolloids in textural stabilization of a yoghurt drink, Ayran. Food Hydrocolloids **18**, 593–600 (2004)
59. Chanasattru, W., Jones, O.G., Decker, E.A., McClements, D.J.: Impact of cosolvents on formation and properties of biopolymer nanoparticles formed by heat treatment of β-lactoglobulin-pectin complexes. Food Hydrocolloids **23**, 2450–2457 (2009)
60. Lee, S.J., Rosenberg, M.: Microencapsulation of theophylline in composite wall system consisting of whey proteins and lipids. J. Microencapsul. **18**, 309–321 (2001)
61. Shi, L., Zhou, J., Gunasekaran, S.: Low temperature fabrication of ZnO-whey protein isolate nanocomposite. Mater. Lett. **62**, 4383–4385 (2008)
62. Jafari, S.M., Assadpoor, E., Bhandari, B., He, Y.: Nano-particle encapsulation of fish oil by spray drying. Food Res. Int. **41**, 172–183 (2008)
63. Jafari, S.M., He, Y., Bhandari, B.: Role of Powder particle size on the encapsulation efficiency of oils during spray drying. Drying Technol. **25**, 1091–1099 (2007)
64. Sohail, S.S., Wang, B., Biswas, M.A.S., Oh, J.-H.: Physical, morphological, and barrier properties of edible casein films with wax applications. J. Food Sci. **71**(4), 255–259 (2006)
65. Chambi, H., Grosso, C.: Edible films produced with gelatin and casein cross-linked with transglutaminase. Food Res. Int. **39**, 458–466 (2006)
66. Ozdemir, M., Floros, J.D.: Optimization of edible whey protein films containing preservatives for water vapor permeability, water solubility and sensory characteristics. J. Food Eng. **86**, 215–224 (2008)
67. Fabra, M.J., Talens, P., Chiralt, A.: Water sorption isotherms and phase transitions of sodium caseinate–lipid films as affected by lipid interactions. Food Hydrocolloids **24**, 384–391 (2010)
68. Abu, Diak O., Bani-Jaber, A., Amro, B., Jones, D., Andrews, G.P.: The manufacture and characterization of casein films as novel tablet coatings. Food Bioprod. Process. **85**(3), 284–290 (2007)
69. Javanmard, M.: Effect of whey protein edible film packaging on the quality and moisture uptake of dried peanuts. J. Food Process Eng. **31**, 503–516 (2008)
70. Gounga, M.E., Xu, S.Y., Wang, Z.: Whey protein isolate-based edible films as affected by protein concentration, glycerol ratio and pullulan addition in film formation. J. Food Eng. **83**, 521–530 (2007)
71. Audic, J., Chaufer, B., Daufin, G.: Non-food applications of milk components and dairy co-products: a review. Lait **83**, 417–438 (2003)

72. Khwaldia, K., Banon, S., Perez, C., Desobry, S.: Properties of sodium caseinate film-forming dispersions and films. J. Dairy Sci. **87**, 2011–2016 (2004)
73. Siracusa, V., Rocculi, P., Romani, S., Rosa, M.D.: Biodegradable polymers for food packaging: a review. Trends Food Sci. Technol. **19**, 634–643 (2008)
74. Fabra, M.J., Talens, P., Chiralt, A.: Influence of calcium on tensile, optical and water vapour permeability properties of sodium caseinate edible films. J. Food Eng. **96**, 356–364 (2010)
75. Chen, H.: Functional properties and applications of edible films made of milk proteins. J. Dairy Sci. **78**, 2563–2583 (1995)
76. Mauer, L.J., Smith, D.E., Labuza, T.P.: Water vapor permeability, mechanical, and structural properties of edible β-casein films. Int. Dairy J. **10**, 353–358 (2000)
77. Tomasula, P.M., Yee, W.C., Parris, N.: Oxygen permeability of films made from CO_2-precipitated casein and modified casein. J. Agric. Food Chem. **51**, 634–639 (2003)
78. Dangaran, K.L., Cooke, P., Tomasula, P.M.: The effect of protein particle size reduction on the physical properties of CO2-precipitated casein films. J. Food Sci. **71**, 196–201 (2006)
79. Kokoszka, S., Debeaufort, F., Lenart, A., Voilley, A.: Water vapour permeability, thermal and wetting properties of whey protein isolate based edible films. Int. Dairy J. **20**, 53–60 (2010)
80. Hong, S.I., Krochta, J.M.: Oxygen barrier performance of whey-protein-coated plastic films as affected by temperature, relative humidity, base film and protein type. J. Food Eng. **77**, 739–745 (2006)
81. Galietta, G., Gioia, L.D., Guilbert, S., Cuq, B.: Mechanical and thermomechanical properties of films based on whey proteins as affected by plasticizer and crosslinking agents. J. Dairy Sci. **81**, 3123–3130 (1998)
82. Banerjee, R., Chen, H.: Functional properties of edible films using whey protein concentrate. J. Dairy Sci. **78**, 1673–1683 (1995)
83. Zinoviadou, K.G., Koutsoumanis, K.P., Biliaderis, C.G.: Physical and thermo-mechanical properties of whey protein isolate films containing antimicrobials, and their effect against spoilage flora of fresh beef. Food Hydrocolloids **24**, 49–59 (2010)
84. Mahmoud, R., Savello, P.A.: Mechanical properties of and water vapor transferability through whey protein films. J. Dairy Sci. **75**, 942–946 (1992)
85. Schou, M., Longares, A., Montesinos-Herrero, C., Monahan, F.J., O'Riordan, D., O'Sullivan, M.: Properties of edible sodium caseinate films and their application as food wrapping. LWT-Food Sci. Technol. **38**, 605–610 (2005)
86. Audic, J.L., Chaufer, B.: Influence of plasticizers and cross linking on the properties of biodegradable films made from sodium caseinate. Eur. Polymer J. **41**, 1934–1942 (2005)
87. Ouattara, B., Canh, L.T., Vachon, C., Mateescu, M.A., Lacroix, M.: Use of γ-irradiation cross-linking to improve the water vapor permeability and the chemical stability of milk protein films. Radiat. Phys. Chem. **63**, 821–825 (2002)
88. Ghanbarzadeh, B., Oromiehi, A.R.: Biodegradable biocomposite films based on whey protein and zein: barrier, mechanical properties and AFM analysis. Int. J. Biol. Macromol. **43**, 209–215 (2008)
89. Wang, L., Auty, M.A.E., Kerry, J.P.: Physical assessment of composite biodegradable films manufactured using whey protein isolate, gelatin and sodium alginate. J. Food Eng. **96**, 199–207 (2010)
90. Lacroix, M., Le, T.C., Ouattara, B., Yu, H., Letendre, M., Sabato, S.F., Mateescu, M.A., Patterson, G.: Use of γ-irradiation to produce films from whey, casein and soya proteins: structure and functionals characteristics. Radiat. Phys. Chem. **63**, 827–832 (2002)
91. Jagannath, J.H., Radhika, M., Nanjappa, C., Murali, H.S., Bawa, A.S.: Antimicrobial, mechanical, barrier, and thermal properties of starch–casein based, Neem (*Melia azardirachta*) extract containing film. J. Appl. Polym. Sci. **101**, 3948–3954 (2006)
92. Ferreira, C.O., Nunes, C.A., Delgadillo, I., Lopes-da-Silva, J.A.: Characterization of chitosan–whey protein films at acid pH. Food Res. Int. **42**, 807–813 (2009)
93. Ciesla, K., Salmieri, S., Lacroix, M.: γ-Irradiation influence on the structure and properties of calcium caseinate-whey protein isolate based films. Part 2. Influence of polysaccharide

addition and radiation treatment on the structure and functional properties of the films. J. Agric. Food Chem. **54**, 8899–8908 (2006)
94. Fabra, M.J., Talens, P., Chiralt, A.: Effect of alginate and λ-carrageenan on tensile properties and water vapour permeability of sodium caseinate–lipid based films. Carbohydr. Polym. **74**(3), 419–426 (2008)
95. Osés, J., Fabregat-Vázquez, M., Pedroza-Islas, R., Tomás, S.A., Cruz-Orea, A., Maté, J.I.: Development and characterization of composite edible films based on whey protein isolate and mesquite gum. J. Food Eng. **92**, 56–62 (2009)
96. Kristo, E., Biliaderis, C.G.: Water sorption and thermo-mechanical properties of water/sorbitol-plasticized composite biopolymer films: caseinate–pullulan bilayers and blends. Food Hydrocolloids **20**, 1057–1071 (2006)
97. Kristo, E., Biliaderis, C.G., Zampraka, A.: Water vapour barrier and tensile properties of composite caseinate-pullulan films: biopolymer composition effects and impact of beeswax lamination. Food Chem. **101**, 753–764 (2007)
98. Fabra, M.J., Talens, P., Chiralt, A.: Microstructure and optical properties of sodium caseinate films containing oleic acid–beeswax mixtures. Food Hydrocolloids **23**, 676–683 (2009)
99. Fabra, M.J., Jimenez, A., Atares, L., Talens, P., Chiralt, A.: Effect of fatty acids and beeswax addition on properties of sodium caseinate dispersions and films. Biomacromolecules **10**, 1500–1507 (2009)
100. Shaw, N.B., Monahan, F.J., O'Riordan, E.D., O'Sullivan, M.: Effect of soya oil and glycerol on physical properties of composite WPI films. J. Food Eng. **51**, 299–304 (2002)
101. Chick, J., Hernandez, R.J.: Physical, thermal, and barrier characterization of casein-wax-based edible films. J. Food Sci. **67**(3), 1073–1079 (2002)
102. Longares, A., Monahan, F.J., O'Riordan, E.D., O'Sullivan, M.: Physical properties of edible films made from mixtures of sodium caseinate and WPI. Int. Dairy J. **15**, 1255–1260 (2005)
103. Dejewska, A., Mazurkiewicz, P., Tomasik, P., Zaleska, H.: Electrochemical synthesis of polysaccharide-protein complexes. Part 1: preliminary studies on apple pectin-albumin complexes. Starch 47(6), 219–223 (1995)
104. Zaleska, H., Ring, S.G., Tomasik, P.: Apple pectin complexes with whey protein isolate. Food Hydrocolloids **14**, 377–382 (2000)
105. Zaleska, H., Ring, S.G., Tomasik, P.: Electrosynthesis of potato starch-whey protein isolate complexes. Carbohydr. Polym. **45**, 89–94 (2001)
106. Zaleska, H., Tomasik, P., Lii, C.-y: Formation of carboxymethyl cellulose-casein complexes by electrosynthesis. Food Hydrocoloids **16**, 215–224 (2002)
107. Zaleska, H., Mazurkiewicz, J., Tomasik, P., Baczkowicz, M.: Electrochemical synthesis of polysaccharide-protein complexes. Part 2. Apple pectin-casein complexes. Nahrung **43**(4), 278–283 (1999)
108. Zaleska, H., Ring, S., Tomasik, P.: Electrosynthesis of potato starch-casein complexes. Int. J. Food Sci. Technol. **36**, 509–515 (2001)
109. Debeaufort, F., Quezada-Gallo, J.A., Voilley, A.: Edible films and coatings: tomorrow's packagings: a review. Crit. Rev. Food Sci. **38**(4), 299–313 (1998)
110. Hernandez-Izquierdo, V.M., Krochta, J.M.: Thermal transitions and heat-sealing of glycerol-plasticized whey protein films. Packag. Technol. Sci. **22**, 255–260 (2009)
111. Perez-Gago, M.B., Serra, M., Alonso, M., Mateos, M., del RÍo, M.A.: Effect of solid content and lipid content of whey protein isolate-beeswax edible coatings on color change of fresh-cut apples. J. Food Sci. **68**(7), 2186–2191 (2003)
112. Perez-Gago, M.B., Serra, M., Alonso, M., Mateos, M., del RÍo, M.A.: Effect of whey protein- and hydroxypropyl methylcellulose-based edible composite coatings on color change of fresh-cut apples. Postharvest Biol. Technol. **36**, 77–85 (2005)
113. Perez-Gago, M.B., Serra, M., del RÍo, M.A.: Color change of fresh-cut apples coated with whey protein concentrate-based edible coatings. Postharvest Biol. Technol. **39**, 84–92 (2006)
114. Hong, S.-I., Krochta, J.M.: Whey protein isolate coating on LDPE film as a novel oxygen barrier in the composite structure. Packag. Sci. Technol. **17**, 13–21 (2004)

Chapter 7
Recent Studies on Alginates Based Blends, Composites, and Nanocomposites

M. M. Soledad Lencina, Noemí A. Andreucetti, César G. Gómez and Marcelo A. Villar

Abstract Alginate is the generic name given to the salts of alginic acids. Alginic acids are polyuronides, i.e., polysaccharides molecules which are built up of uronic acid residues, molecules with a carboxyl group on the carbon that is not part of the ring, Commercial alginates are currently obtained by extraction from brown seaweeds such as *Laminaria digitata*, *Laminaria hyperborea*, and *Macrocystis pyrifera*. However, several bacteria such as the nitrogen-fixing aerobe *Azotobacter vinelandii* and the opportunistic pathogen *Pseudomonas aeruginosa* also produce alginate. Alginates are unique in terms of their properties such as emulsifiers, thickeners, stabilizers, gelling and film forming, resulting in several applications for the food and pharmaceutical industries. Alginate has been regarded as an excellent polysachaccharide for gel systems because of its unique features such as biocompatibility, biodegradability, immnogenecity, and non-toxicity. In the biomedical area, alginates have been used as devices in several human health applications, such as excipients in drug delivery (DDS), wound dressings, as dental impression materials and in some formulations preventing gastric reflux, among others. Main characteristics and chemical modification, along with some interesting properties and applications are reviewed along this chapter.

M. M. S. Lencina (✉) · M. A. Villar
Planta Piloto de Ingeniería Química (PLAPIQUI), Departamento de Ingeniería Química, Universidad Nacional del Sur (UNS), Consejo Nacional de Investigaciones Científicas y Técnicas (CONICET), Camino "La Carrindanga" Km. 7 8000 Bahía Blanca, Argentina
e-mail: mvillar@plapiqui.edu.ar

N. A. Andreucetti
Departamento de Química, Universidad Nacional del Sur (UNS), Av. Alem 1253 8000 Bahía Blanca, Argentina

C. G. Gómez
Departamento de Química Orgánica, Facultad de Ciencias Química, (IMVIB-CONICET), Universidad Nacional de Córdoba, Haya de la Torre y Medina Allende, Edificio de Ciencias II, Ciudad Universitaria 5000 Córdoba, Argentina

S. Thomas et al. (eds.), *Advances in Natural Polymers*,
Advanced Structured Materials 18, DOI: 10.1007/978-3-642-20940-6_7,

7.1 Sources of Alginates

Alginic acids were first isolated from several brown algae by Stanford more than 100 years ago. Later, these polysaccharides were detected in all brown algal species without exception as cell wall and intercellular matrix components. Their content in the biomass may amount to 40 % of the dry weight; this strongly depends on the species, growth and stationary conditions [1].

Commercial alginates are currently obtained by extraction from brown seaweeds such as *Laminaria digitata*, *Laminaria hyperborea*, and *Macrocystis pyrifera*. Several bacteria such as the nitrogen-fixing aerobe *Azotobacter vinelandii* and the opportunistic pathogen *Pseudomonas aeruginosa* also produce alginate. However, only alginates synthesized by *A. vinelandii* have a block copolymer structure similar to the one extracted from seaweed species while alginate produced by *Pseudomonas* sp. does not have a G block. In addition, bacterial alginic acids present some of their hydroxyl groups acetylated. Acetyl groups occupy positions 2 or 3 (sometimes, both simultaneously) in D-mannuronic acid residues. The price of algal alginates is generally low but their production is subjected to environmental hazards, natural (i.e. climatic conditions) or not (e.g. pollution). Therefore, alginates from *A. vinelandii* may become major commercial products [2].

In brown seaweed alginate is present mainly as the calcium salt of alginic acid, although magnesium, potassium, and sodium salts may also be present. These biopolymers are structural polysaccharides of the algae and their biological function is to prevent desiccation, sustain the cell integrity and give the stability to the plant in the water.

Since only the sodium and potassium salts of alginic acid are soluble in water, the first aim of the extraction process is to convert the insoluble calcium and magnesium salts into sodium alginate. If the seaweed is treated with alkali, then the process necessary for extraction is an ion exchange:

$$\mathrm{Ca\ (Alg)_2 + 2\ Na^+ \rightarrow 2\ NaAlg + Ca^{2+}}$$

However it has been stated by many authors that a more efficient extraction is obtained by first treating the seaweed with dilute mineral acid:

1. Pre-extraction:

$$\mathrm{Ca(Alg)_2 + 2\ H^+ \rightarrow 2\ HAlg\ + Ca^{2+}}$$

2. Extraction:

$$\mathrm{HAlg + Na^+ \rightarrow NaAlg\ + H^+}$$

According to several authors, the calcium alginate is converted to alginic acid and this is more readily extracted with alkali than the original calcium alginate [3]. The industrial process for the extraction of alginates from brown algae, is basically

constituted by the following steps: (1) collected algae are ground and treated with acidulated water in order to extract and remove insoluble material; (2) then, alginate is solubilized by the addition of sodium carbonate (Na_2CO_3) until the pH value arise to approximately 10; (3) the insoluble residues are eliminated by filtration, so that, the solution is clarified. Regarding the purification process, at least three ways are presented in the literature [4]: (4) the alginate is precipitated in a calcium salt form or as alginic acid, through the addition of calcium chloride ($CaCl_2$) or hydrochloric acid (HCl) respectively; (5) the calcium precipitate is washed with HCl, and finally (6) the alginic acid formed is converted in the required salt by mixing it with the corresponding carbonate and at the end it is dried. The third method implies a precipitation of the sodium alginate directly from the solution obtained in (3), by addition of ethanol, until reaching a proportion 1:1 in volume, respectively. This precipitation is follow by an exhaustive washing with ethanol by soxhlet and finally the polymer is dried. Scheme 7.1 shows the extraction and purification routes presented. In order to avoid the degradation of the polymer, it is convenient neither acidify nor alkalize in extreme and it is necessary to eliminate the humidity of the sample as much as possible. Three different routes of extraction-purification of sodium alginate are possible, (1) ethanol route, (2) calcium alginate route and (3) alginic acid route [4]. All the purification processes are based on consecutive steps of solubilization and precipitation to eliminate insoluble impurities and all the multivalent cations, in order to obtain the sodium salt. The advantage of the calcium alginate method is that water can be squeezed out relatively easy, but the disadvantage is that it requires an additional step [5].

The calcium alginate obtained is converted to alginic acid with an acid treatment; however, part of the calcium remains in the fibrous of alginic acids. If a high viscosity product is required, it can be controlled during the conversion step from calcium alginate to alginic acid, leaving a certain amount of calcium without reacting. This can be used only if its application does not imply the use of a calcium sequestering agent [5].

To predict the effect of calcium on the viscosity of the alginate solution, it is necessary to know the M and G blocks composition. Most commercial alginates made with the calcium alginate process contain residual quantities of calcium; for example, the food grade sodium alginate from Kelco contains up to 1.2 % calcium [6].

The production of very high-viscosity alginate is debatable; the desired product is much more prone to breakdown with a decreasing in the properties when stored for 6–12 months than a medium-viscosity alginate. Therefore, some manufacturers produce medium- and low-viscosity alginates and for applications that require very high viscosity, they ensure that the product contains sufficient calcium ions to produce the necessary viscosity [5].

The alginic acidic route does not require calcium chloride; however more quantities of HCl and ethanol are necessaries in comparison with the calcium alginate route, being the last one less expensive (the cost of the reagents can vary according to market fluctuations and influence the final cost of the method applied; for this reason, this observation should be considered as a reference). Another

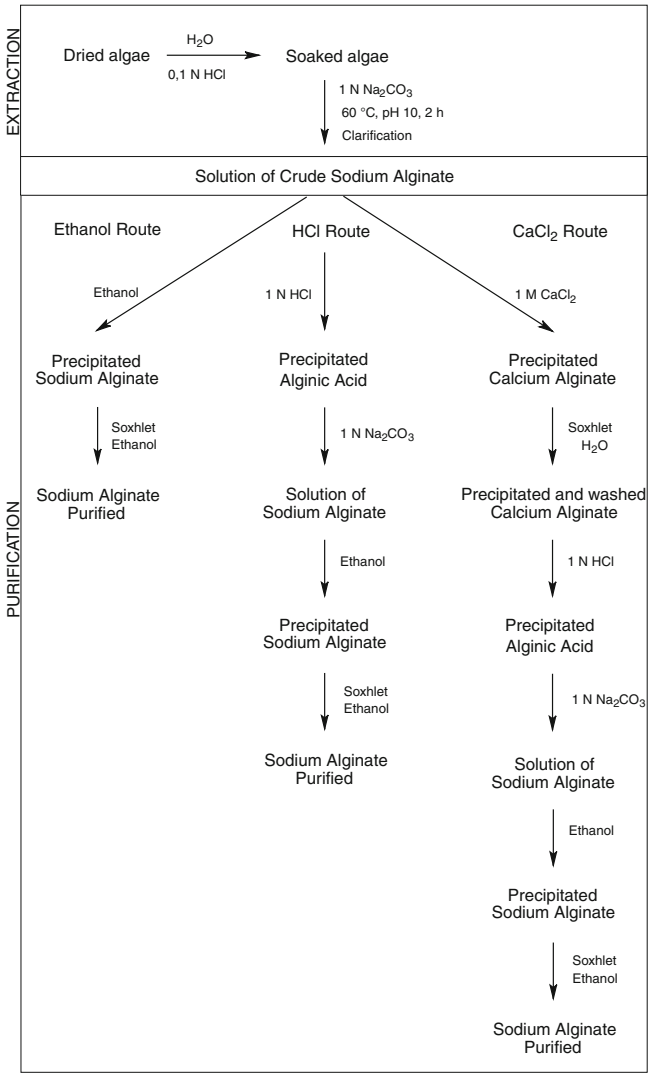

Scheme 7.1 Schematic representation of extraction-purification of sodium alginate from brown algae

disadvantage of direct precipitation with acid is that gelatinous fibers are obtained, which are difficult to handle. On the other hand, alginic acid retains a higher amount of water, even after having been squeezed out, so that more ethanol must be used [6]. Furthermore, with the acid precipitation, the product is exposed a longer time to low pH values, which may degrade the alginic acid and reduce the molar mass and the properties of final product. Alginates obtained by the alginic acid route contain negligible amounts of calcium, so that lower viscosity alginates

are achieved [5]. The alginate yield is not affected by the extraction-purification method used; however, a higher viscosity is observed for the alginates obtained by the calcium alginate route compared to those obtained by the alginic acid route.

A comparative study of the extraction-purification methods concluded that ethanol route results the most successful process, using the lowest number of steps and leading the best yield [4].

As it was mentioned alginates are currently manufactured by harvesting brown algae, but in nature the polymer is also produced by some bacteria belonging to the genera *Azotobacter* and *Pseudomonas*. The biosynthesis of alginate has been mostly studied in *Pseudomonas aeruginosa*, where many of the involved proteins and genes have also been identified. In both algae and bacteria the polymer is first produced as mannuronan, which is then epimerized by the enzyme mannuronan C-5-epimerase [7].

A. vinelandii and *P. aeruginosa* produce alginate as an extracellular polysaccharide in vegetative cells, whereas the alginate production by *A. vinelandii* is involved in a differentiation process called "cyst". This cyst is formed by the intracellular accumulation of poly(hydroxybutyrate) delimited within the cytoplasm by a double wall lipoprotein membrane when the bacterial cell is in an environment with large amounts of carbon source and a limitation in nitrogen, phosphorus, or oxygen source. When there is carbon source exhaustion, these cysts oxidize quickly (through the activation of the PHB depolymerase enzymes) and are used as energy sources.

The extracellular accumulation of alginate acts as a barrier to oxygen diffusion or heavy metals or as protection against other environmental insults [8].

Most studies on microbial exopolysaccharides production have been performed so far using batch fermentation conditions and polymer macromolecules are recovered from fermentation broths by simple chemical and physical techniques, e.g. precipitation and centrifugation. In Scheme 7.2 the route of production of alginate is presented [8]. Some attempts have been made to apply immobilized-cell cultures to the production of alginate and other bacterial polysaccharides. Immobilization techniques are likely to allow the permanent separation of microbial cells from the incubation broth. In the last few years, however, membrane processes have been increasingly used to separate microbial cells from the production medium. A number of studies have therefore focused on the microfiltration of fermentation broths after batch incubation and the mechanisms of membrane fouling by cells, debris, colloidal particles and macromolecules, e.g. for recovery of polysaccharides from fermentation broths [2].

The continuous production of bacterial alginate from *A. vinelandii* coupled to membrane-based extraction appears to be possible but more detailed investigation must still being performed in order to optimize the process. However, it should be remarked the possibility of controlling the structure of resultant alginates obtained by using genetically modified bacteria.

The potential of alginate produced by bacteria as an industrial polymer is still a controversial subject. However, the possibility of using raw materials free of seasonal and geographical variations employing selected strains under carefully

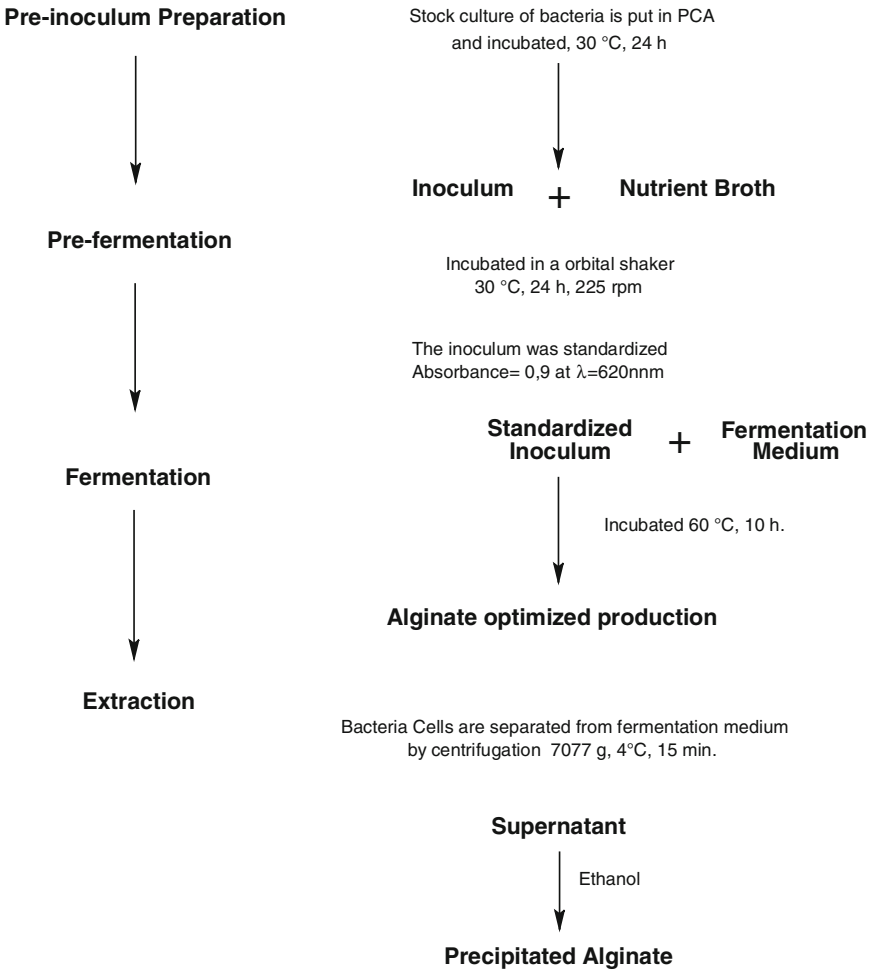

Scheme 7.2 Scheme of bacterial alginate production

controlled operating conditions, so as to meet specific applications in biotechnology and biomedicine may be sufficient to compensate the relatively low production and relatively high degree of acetylation in bacterial alginates [8].

7.2 Structure of Alginates

Alginate is the generic name given to the salts of alginic acids. Alginic acids are polyuronides, i.e., polysaccharide molecules which are built up of uronic acid residues, molecules with a carboxyl group on the carbon that is not part of the ring [9].

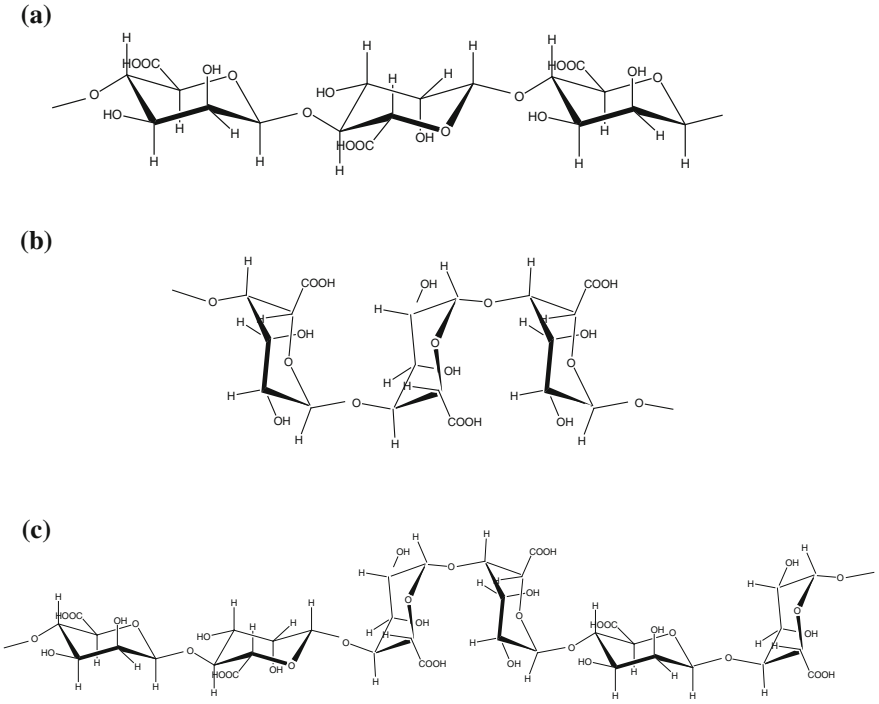

Fig. 7.1 Structure of M-block (**a**), G-block (**b**), and MG-block (**c**)

Alginic acids are a complex mixture of secuences of poly(mannuronic acid) (M-blocks), poly(guluronic acid) (G-blocks) and random MG blocks as it is shown in Fig. 7.1 [10]. The mannuronic acid forms β (1–4) linkages, so that M-block segments show linear and flexible conformation while the guluronic acid, its C5-epimer, gives rise to α (1–4) linkages, introducing in this way a steric hindrance around the carboxyl groups; for this reason G-block segments provides folded and rigid structural conformations, responsible of a pronounced stiffness of the molecular chains [11, 12]. Figure 7.1 shows the basic structures for M-blocks, G-blocks and MG-blocks along with their spacial distribution.

In water solution this particular conformation creates spatial conditions for the tight binding of bivalent metal cations with G-blocks. Moreover, the coordination with such cations favours the cooperative binding of different molecules of the polymer, eventually resulting in the formation of ionotropic gels. Therefore, the total content of α-L-guluronic acid (in a first approximation) or, more precisely, the relative length of G-blocks is an important criteria and the most valuable property of alginates, viz. their ability to form gels. Block structure is also responsible for many other characteristics of alginates including their biological activity [1].

Thus, alginic acids form water-soluble salts with monovalent cations but are precipitated in the presence of polyvalent cations, such as Ca^{2+}, Sr^{2+}, and Ba^{2+}, among others. pH of the medium has also an important role in the solubility of

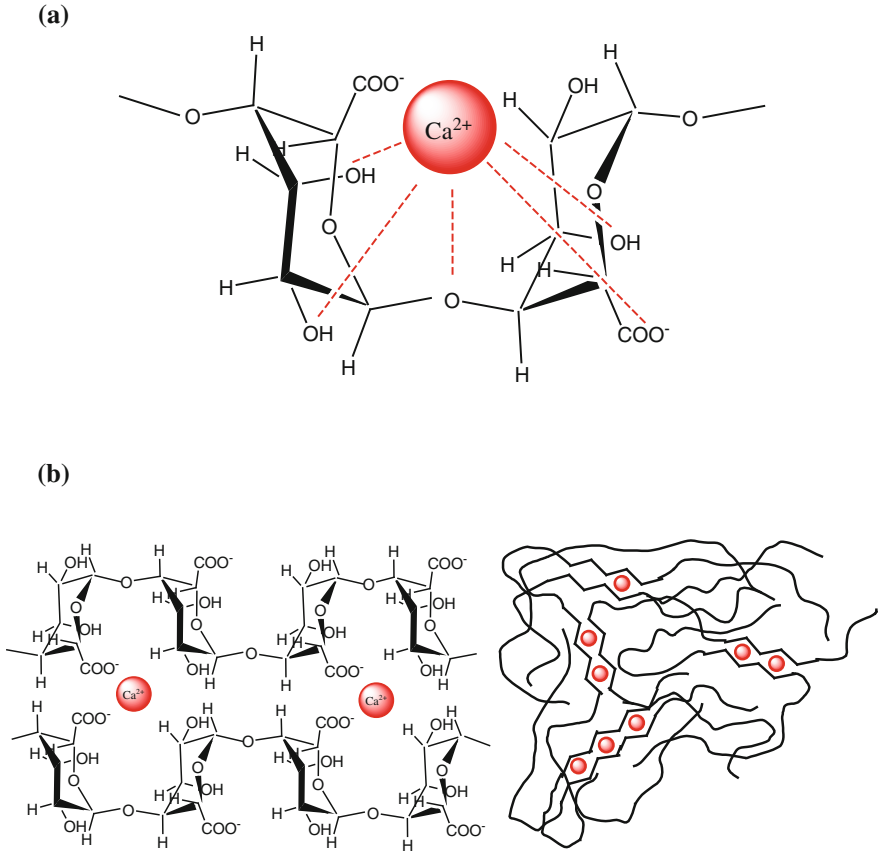

Fig. 7.2 Electrostatic interactions between guluronic (*G*) block and bivalent calcium ions (**a**) and the "egg-box" representation (**b**)

these compounds. Alginates precipitate upon acidification because they are transformed into alginic acids, insoluble in water. Among various cations, Ca^{2+} has received particular attention, since a unique "egg-box structure" is formed in calcium alginate between Ca^{2+} ions and G-blocks as it is shown in Fig. 7.2 [13].

This selective binding of multivalent cations, which is the basis for gel formation is the most important feature of alginate′s physical properties, and the fact that the sol/gel transition of alginates is not particularly influenced by temperature [14].

7.2.1 Chemical Modification

Alginate structure can be used in order to design smart materials for special applications. However, when a modification of the backbone is carried out we always must ask what happens to the stability of the pyranoside ring. Since the acetal

group is a labile bond, alginate chains can be hydrolyzed at a pH less than 4, which together with other variables such as temperature and ionic strength determine the success of the derivative formation [4]. Given that alginate has a number of free hydroxyl and carboxyl groups distributed along the backbone, it is an ideal candidate for chemical functionalization. Therefore, the reactivity of alginate functional groups can be exploited as a potential tool for the modification of interesting properties such as solubility, hydrophobicity, and physicochemical and biological characteristics [12]. The best reaction conditions should be used during chemical modification in order to attain those properties for which the material is generated, while secondary reactions such as backbone hydrolysis should be avoided. Several synthetic methods of alginate derivatives will be summarized, where the most frequently used techniques are oxidation, sulfation, esterification, amidation, and grafting methods, among others. Moreover, the characteristics and applications of some alginate derivatives are also discussed [12].

7.2.1.1 Chemical Modification of Hydroxyl Group

Oxidation Reactions

Modification of carbohydrates by periodate ion oxidation (glycol cleavage) was a classical method used for structure determination of complex carbohydrates [15]. Although this method was abandoned by more sophisticated ones in the last years, periodate reaction has been introduced in order to introduce dialdehydes into polysaccharides or glycoproteins [16]. Nowadays, periodate oxidation is the most frequently used method for modification of alginate. In this reaction, hydroxyl groups on carbons 2 and 3 of the repetitive unit are oxidized by sodium periodate (Scheme 7.3), which leads, by rupture of the carbon–carbon bond, to the formation of two aldehyde groups in each oxidized monomeric unit. Therefore, higher rotational freedom and new reactive groups along the backbone are obtained [17].

However, when applied to polysaccharides, periodate oxidation seems in many cases to be accompanied by depolymerization, such as the case of alginates and chitosans [18, 19]. In turn, the exposed reducing ends consume additional periodate, thereby leading to ‘over oxidation’ [20, 21].

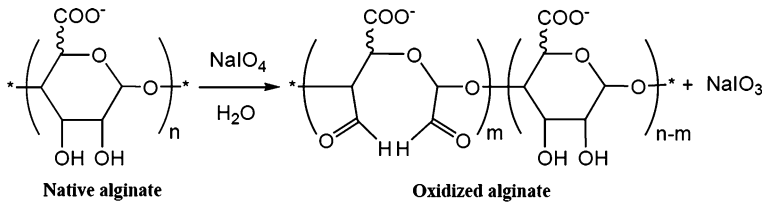

Scheme 7.3 Oxidation reactions with sodium periodate on hydroxyl groups at C-2 and C-3 positions of the uronic units. Formation of aldehyde groups on main backbone of sodium alginate

There are multiple mechanisms of depolymerization, since many of the dialdehyde derivatives are highly susceptible to alkali-catalyzed β-elimination, even at moderate temperatures and pH values. Moreover, the degradation of polysaccharide chains caused by free radicals may occur [22, 23]. Periodate itself is unstable and decomposes over time to form radicals, especially in the presence of light. Oxidations are therefore preferentially carried out in the dark and in the absence of oxygen, using freshly prepared periodate solutions. Also, small amounts of trace metals should be removed as they can also catalyse the formation of free radicals. It has been demonstrated that presence of free radical scavenges such as 1-propanol reduces the extent of depolymerization, and it has therefore been routinely added during oxidation, typically at concentrations around 10 % (v/v) [16].

A general procedure often used for periodate oxidation of alginate is detailed as follows: a 1 wt% sodium alginate aqueous solution is oxidized at room temperature under stirring during 24 h, using sodium periodate in the dark [17]. The mole ratio of sodium periodate to uronic units of alginate used is varied in order to reach different degrees of oxidation. After 24 h, the reaction is quenched by the addition of an excess of ethylene glycol under stirring for 0.5 h. Alginate derivative is purified from reaction mixture by precipitation with an organic solvent such as acetone or ethanol. First, the pH of the reaction mixture is adjusted to 7, and the ionic strength is increased by addition of sodium chloride to reach a 1 M aqueous solution in order to screen the electrostatic interactions between chains and to exchange counter ions other than sodium. Insoluble polymer aggregates are eliminated by filtering the reaction mixture using a filter number 3. Then, a 1.5 volume ratio of organic solvent to aqueous solution is commonly used to precipitate the alginate derivative. This product is washed, under a high stirring, with a mixture of organic solvent–water with a volume ratio higher than 1.5, in order to eliminate the impurities from the system. This washing procedure is used on the derivative in progressive increase of the organic solvent. It is important to highlight that the solid derivative must be dried at room temperature without the use of vacuum to avoid the formation of polymer aggregates.

On the other hand, a limited degree (typically 1–20 %) of periodate oxidation of polysaccharides may give rise to derivatives with improved chemical and physical properties. Notably, the ring opening caused by sodium periodate leads to the formation of highly flexible 'hinges' in otherwise rather semiflexible or rigid structures [16]. Macromolecular properties such as solubility, crystallinity, physical interactions with other biopolymers, and gelling properties can be also included in this discussion. A second aspect of partially oxidized polysaccharides is the chemical properties of the oxidized residues, and in particular the hydrolytic lability, which may provide a basis for biomaterials with increased biodegradability [16]. Gomez et al. found that weight-average molar mass of alginates oxidized with sodium periodate decreases rapidly even for low oxidation values such as 5 mol % [17]. Weight-average molar mass (M_w) decreases with an increase in both concentration of sodium periodate and reaction time. Oxidation of alginate chains produces a decrease in the stiffness of the polymer by breaking C_2-C_3 bond with chain scission as an undesired side reaction. From Size Exclusion Chromatography analysis could be

demonstrated that stiffness of the molecule decreases, in agreement with data calculated from viscosity measurements. The ability for gelation of oxidized alginates was examined and no gels were formed in excess of calcium for alginates with a degree of oxidation higher than 10 mol %. Two effects were proposed for this behaviour: a relatively low molar mass of the modified polymer due to its oxidation and decrease of the stiffness, which reduces the cooperative interaction between carboxylate groups and calcium ions, in particular if guluronic units are first oxidized. By limiting the degree of oxidation to 5 mol %, the ability to form gels with Ca^{2+} ion was retained, whereas the oxidized (dialdehyde) residues provided degradability at physiological conditions [17].

Others authors have studied the use of alginate for biomedical applications due to its biocompatibility and ability to form hydrogels [24]. Oxidized alginates show a slow and uncontrollable degradation under physiological conditions, which represents an undesirable feature, since hydrolytically sensitive sites were introduced in alginate by periodate oxidation. Alginates with different degrees of oxidation were characterized for their degradation behaviour and ability to form gels in the presence of Ca^{2+} ions. The obtained results showed that oxidized alginates exhibited degradation under physiological conditions (pH 7.4 and 37 °C) while their gelling ability was preserved for samples with oxidation degrees up to 5 mol %. In addition, interpenetrated polymer networks (IPNs), based on 1–5 mol % oxidized alginate, and dextran-HEMA were prepared, characterized, and evaluated for protein release. These IPNs showed properties similar to the IPNs networks composed by native alginate, confirming the suitability of IPNs based on dextran-HEMA and oxidized alginate as an in situ forming protein releasing hydrogels [24]. Moreover, Bouhadir et al. [25] recognized that periodate oxidation could be applied to produce biodegradable alginates suitable for tissue engineering.

Another way of alginate oxidation was carried out in aqueous solution using H_2O_2 [26]. In this study, several reactions were performed under different conditions in order to obtain low molar mass alginate with potential application in tissue engineering. The oxidation reaction using H_2O_2 is an effective method for alginate depolymerization whose extent depends on reaction time, temperature, solution pH, and H_2O_2 concentration. The chemical structure was characterized by FTIR, elemental analysis, and ^{13}C-NMR, indicating that rupture of glucoside bonds in alginate chains into low molar mass chains is the basic process during H_2O_2 depolymerization. Oxidation of alginate under weak conditions (H_2O_2 0.6 w/v %, 50 °C, and 1 h) did not significantly affect the formation of ionic junctions with calcium ions. Crosslinked alginate scaffolds prepared with the oxidized alginate showed a faster degradation rate than unmodified alginate. This behaviour was attributed to the low molar mass of oxidized alginate and the susceptibility to hydrolysis of formed aldehyde groups [26].

Reductive Amination of Oxidized Alginate

The reductive amination, widely used in the field of organic chemistry and biochemistry, allows for conversion of carbonyl groups into amines [27].

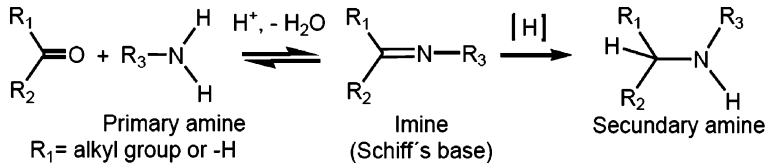

Scheme 7.4 Reductive-amination of aldehydes or ketones

The reaction starts with the coupling of an aldehyde or ketone to a primary amine to give an imine (Schiff's base), which is stable enough for isolation. This pathway is straightforward and proceeds in high yields at a pH near 4.5. Then, the imine is reduced to give a secondary amine (Scheme 7.4). The reduction reaction is usually carried out using sodium borohydride ($NaBH_4$) or sodium cyanoborohydride ($NaCNBH_3$), among others reducing agents.

In the particular case of polysaccharides, this reaction has been used for the modification of several types of biopolymers with different applications [28, 29]. As an example, a monoaldehyde derivative of β-CD (**2**) was prepared from the hydrolysis of product 1 and then grafted, by a reductive amination-type reaction, onto an alginate derivative selectively modified with adipic dihydrazide (alg-ADH) (Scheme 7.5). The new polymeric materials obtained, alg-ADH intermediate and β-CD-grafted alginate were fully characterized in terms of chemical integrity and purity by high-resolution NMR spectroscopy [30].

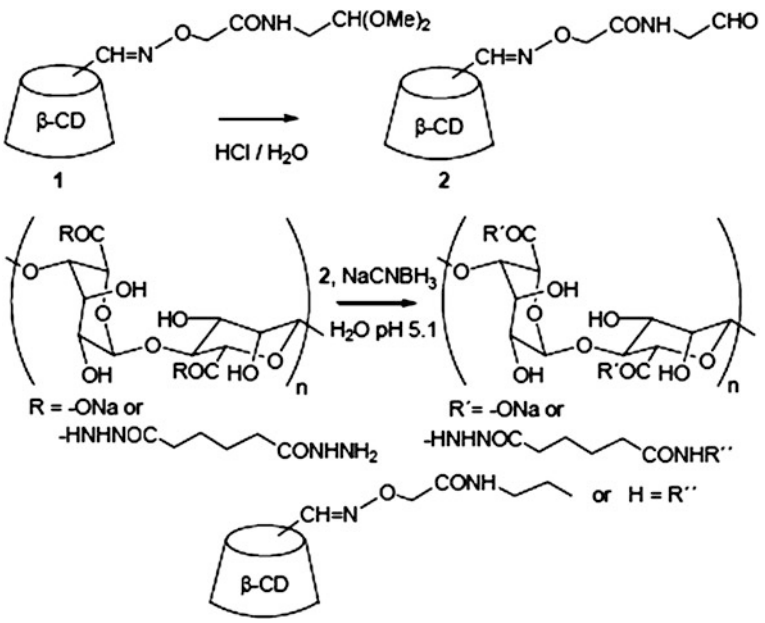

Scheme 7.5 Synthesis of alg-CD employing reductive-amination

Inclusion of sodium adamantane acetate as a model guest, into the grafted β-CD, was investigated by isothermal titration calorimetry. Similar enthalpy values were obtained, suggesting similar mechanisms of binding. However, the association constant for the grafted CD was found to be slightly lower as a result of less favourable entropy due to the fixation onto the polymer. All alginate derivatives were shown to produce hydrogels in the presence of calcium ions. However, rheological measurements performed on the hydrogels demonstrated that backbone chemical modification leads to a lower cooperative ability for calcium interaction as a consequence of a decrease in the content of G-blocks. In addition, the steric effect of the cyclic oligosaccharide (CD) grafted onto alginate plays a negative role on ionic cross-linking. Therefore, G' and G'' values decrease in the following order: alg > alg-ADH > alg-CD, which shows that softer gels are obtained [30].

Another interesting application based on the reaction between aldehyde and amino groups was studied by Boanini et al., where low concentrations of dialdehyde alginate (ADA) were used to crosslink and stabilize gelatin films [31]. However, it should be noted that alginate derivative ADA generated by periodate oxidation was used as a cross-linker agent of gelatine chains through formation of imine groups, where the reduction pathway of this group was not carried out. In this study, films from gelatin solutions at different concentrations (5, 10, and 15 wt%) containing different amounts of oxidized alginate (0, 1, and 3 wt% with respect to the weight of gelatin) were prepared. The extent of crosslinking increases as a function of ADA concentration, up to about 23 %. The product of periodate oxidation—alginate dialdehyde (ADA)—is a better crosslinking agent for gelatin than natural alginate, as verified for composite hydrogels [32]. The crosslinking reaction is due to the reaction of free amino groups of lysine or hydroxylysine amino acid residues of the polypeptide chains with the aldehyde groups of ADA. The presence of oxidized alginate reduces the degree of swelling and gelatin release in phosphate-buffered saline solution, enhancing the effect of gelatin concentration. Furthermore, the values of Young's modulus (E) and stress at break (σ_b), increase with an increase in ADA concentration. On the other hand, an increase in thermal stability was found by differential scanning calorimetry and supported by X-ray diffraction results [31].

Microsphere beads were prepared with alginate-derived polymeric surfactants in aqueous solution of sodium and calcium chloride [33]. Ibuprofen, a hydrophobic drug, was loaded on the modified alginate beads and the in vitro control release was studied. It was found that drug loading level was higher than those obtained for unmodified alginated with a well controlled release rate [33].

Sulfation Reactions

It is known that sulfated polysaccharides, including natural and synthesized ones, had great blood-compatibility or even anticoagulant activity [34]. After sulfation of sodium alginate, its derivative contains both sulfate and carboxyl groups, whose chemical structure is analogous to the natural blood anticoagulant heparin. Fan et al.

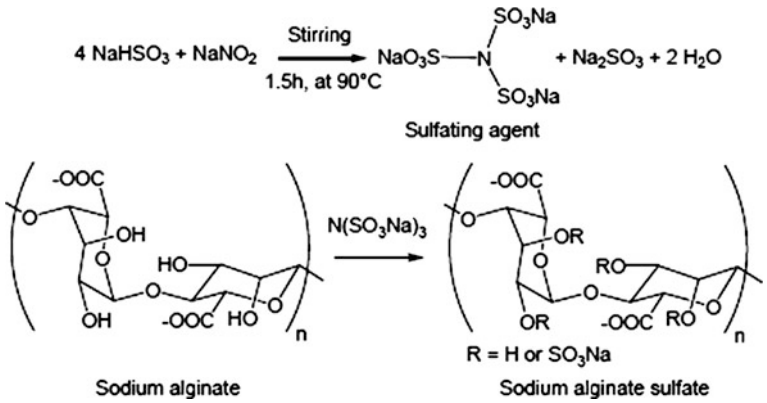

Scheme 7.6 Synthesis of sodium alginate sulphate

prepared an uncommon sulphating agent ($N(SO_3Na)_3$) from sodium bisulfite and sodium nitrite in aqueous solution (Scheme 7.6). This agent was reacted with sodium alginate, and sodium alginate sulfates were obtained [35].

In this work, the reaction conditions that could affect the degree of substitution (DS) of sodium alginate sulphates were investigated. The in vitro coagulation assay of human plasma containing sodium alginate sulfates was determined with respect to activated partial thromboplastin time (APTT), thrombin time (TT) and prothombin time (PT). It was found that the activity strongly depended on the degree of substitution, weight average molar mass (Mw), and concentration of sodium alginate sulfates. The presence of sulfate groups in the polymer backbone greatly increases the APTT and TT. Howevere, either a low sulfur content or a low concentration of sodium alginate sulfates showed little anticoagulant activity. A high value of degree of substitution and a high concentration could inhibit the activity of IIa and Xa to prolong APTT and TT. Moreover, a low molar mass resulted in a higher anti-factor Xa activity to promote anticoagulant activity. On the other hand, sulfate groups could not increase PT, and also they had little effect on coagulation factors in the extrinsic pathway [35].

Grafting Reactions

Considerable interest has been shown on chemical modification of natural polymers by means of graft copolymerization of vinyl monomers onto natural polysaccharides. By the process of grafting, physical and chemical properties of synthetic monomers are superimposed onto the properties of different natural polymers using redox system [36, 37]. In this case, the reaction can take place between two polymers or a polymer and a second monomer and they are based on classical organic chemistry (Scheme 7.7). Kennedy reviewed many of the possibilities of further reactions after polymerization, and distinguished between grafting “onto” and “from” [38].

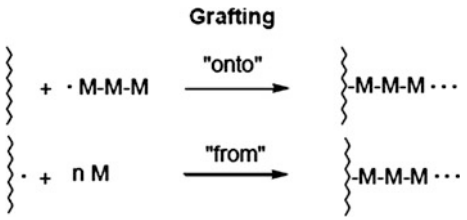

Scheme 7.7 Grafting reactions developed on the polymer backbone, where M represents a monomer or a repetitive unit of another polymer

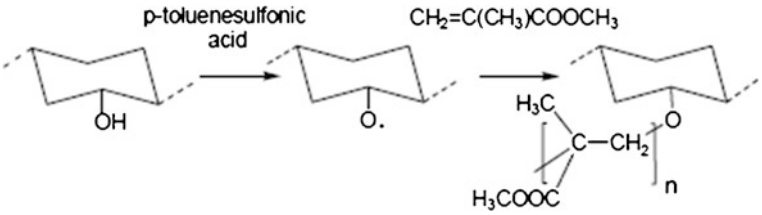

Scheme 7.8 Grafting "from" reaction of MMA onto alginate backbone

Methyl methacrylate (MMA) was rarely used to graft with sodium alginate, although it has good mechanical and biological properties. Yang et al. investigated the grafting reaction of MMA onto sodium alginate in the presence of a radical initiator [39]. Then, hydroxyapatite (HA), with good bioactivity and biocompatibility properties, was introduced into the reaction system to prepare the composite of MMA-NaAlg copolymer and HA (Scheme 7.8).

The grafting reactions of MMA onto alginates lead to partly replace inter or intramolecular hydrogen bonds in sodium alginate. Composites had better water contact angle than sodium alginate, indicating that the strong hydrophilic character of pure sodium alginate was improved. As a consequence, composites should have improved biological properties. Molecular dynamics simulations suggested that when uronic units of alginate are grafted with MMA, the copolymer would have a more stable structure. MMA-NaAlg/HA composites show a relatively lower interface energy, which indicates that copolymers have an stronger linking with HA than either poly(methylmetacrylate) or NaAlg [39].

Another interesting work of grafting reaction was developed by Işiklan et al. where itaconic acid was grafted onto alginate backbone using ceric ammonium nitrate as a radical initiator [40]. A series of alginate-g-poly(itaconic acid) (NaAlg-g-PIA) microspheres, cross-linked by glutaraldehyde (GA), were prepared as drug delivery matrices of nifedipine. The release of nifedipine from grafted microspheres shown to be pH dependent, and it was slower in a pH 1.2 solution than that in a pH 7.4 buffer solution, which can be also attributed to less swelling of NaAlg-*g*-PIA in acid medium. It has been observed that an increase in exposure time, drug amount, glutaraldehyde, and NaAlg-g-PIA concentrations causes a decrease in nifedipine release from the microspheres, whereas an increase in graft yield leads to an increase in the nifedipine release [40].

Poly(*N*,*N*dimethylacrylamide) (PDMAM) is being used in many fields due to its remarkable properties such as water solubility and biocompatibility. Homo- and copolymers of DMAM have been applied in various fields such as oil recovery and slow release of drug. Alginate-*g*-poly(*N*,*N*-dimethylacrylamide) (AG-*g*-PDMAM) was synthesized in order to increase the properties of alginate like swellability, metal ion uptake and flocculation thereby increasing its potential applications [41].

7.2.1.2 Chemical Modification of Carboxyl Group

Esterification Reactions

Native alginate can be modified by direct esterification with several alcohols in the presence of a catalyst, where the alcohol is often present in excess to ensure the product formation [12]. Esterification reaction is often used as a simple method whereby alkyl groups are attached to the backbone of alginate increasing its hydrophobic nature. However, alkyl moieties grafted onto polysaccharides generally lead to intermolecular association in semi-dilute regime, which can be a problem in certain circumstances. As an alternative, Colinet et at. studied the modification of alginate using poly(ε-caprolactone) (PCL), a biodegradable and biocompatible aliphatic polyester [42]. A new route of synthesis was proposed in order to obtain water soluble polysaccharides, based on alginate, grafted with PCL (Alg-*g*-PCL). The coupling reaction between alginate and PCL was carried out by terminal alcohol groups of the commercial PCL (Scheme 7.9) and carboxylic groups of protonated alginate using a carbodiimide activator (EDC) in heterogeneous phase, stabilized by sodium dodecyl sulfate (SDS) as surfactant.

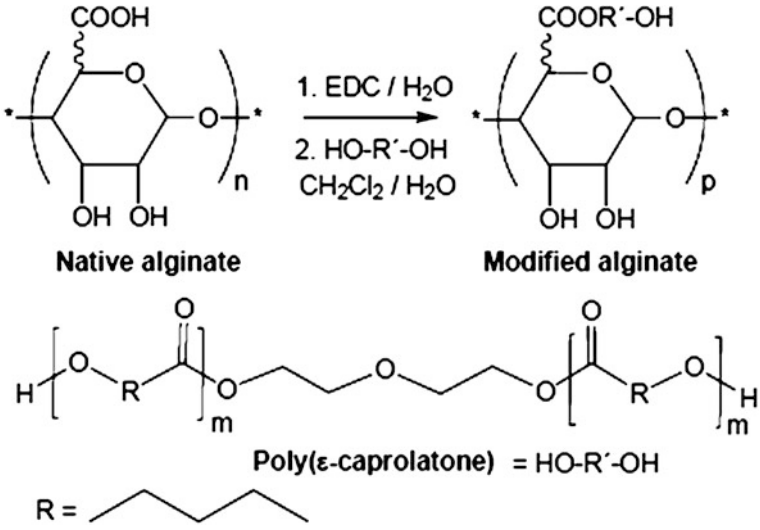

Scheme 7.9 Synthesis of Alg-*g*-PCL through an esterification reaction using a carbodiimide as an activating agent of the carboxyl group

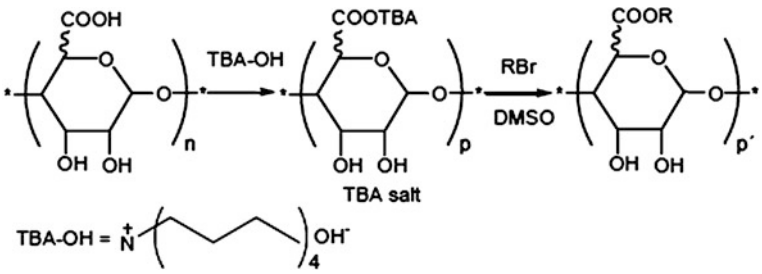

Scheme 7.10 Esterification of alginate with alkyl bromide

Physico-chemical behaviour in aqueous solution was studied by viscosity measurements. Expected associative behaviour has been evidenced in pure water, while in salt media, the associative behaviour strongly depends on PCL chains length. For shorter PCL chains, intramolecular hydrophobic interactions are predominant, even in the semi-dilute regime. This non-classical behaviour for an associative polyelectrolyte opens the way to the conception of amphiphilic matrices with hydrophobic clusters for controlled release applications.

Several authors introduced the idea that the ester of alginate can be prepared by the reaction, in a homogeneous media, between an alkyl halide and the carboxylic groups of alginate, previously transformed into their tetrabutylammonium (TBA) salt (Scheme 7.10) [43]. A simple procedure is summarized as follows: sodium alginate is first transformed into its acidic form, by treatment with ethanolic HCl. After filtration, the resulting acidic polysaccharide is washed with ethanol (70 %) until any trace of chloride ion is removed, and then with acetone. After drying at room temperature and reduced pressure, this compound is dispersed in water and neutralized (pH 7.0) by tetrabutylammonium hydroxide (TBA-OH) under controlled conditions. The TBA salt of alginic acid is dissolved in an organic solvent (DMSO) and the alkyl halide is introduced at an adequate stoichiometry and left to react for 24 h at room temperature under stirring. The reaction mixture is then dialyzed against bidistilled water containing NaN_3 used both as bactericide and to ensure the exchange of TBA^+ by Na^+ ions [44].

In another interesting study where alginate is modified through esterification a hydrophobic alginate derivative of oleyl alginate ester (OAE) was prepared by modification of alginate by hydrochloric acid reaction using oleoyl chloride. This ester was confirmed by FT-IR and ^{1}H-NMR, and its degree of substitution (DS) of OAE was determined by ^{1}H-NMR [45]. Self assembled nanoparticles were formed using OAE at low concentrations in aqueous medium, and nanoparticles retained their structural integrity in simulated gastric fluid (SGF) and simulated intestinal fluid (SIF). The loading and release of nanoparticles based on OAE were investigated using vitamin D_3 as a model nutraceutical. As the concentration of vitamin D_3 increased, the loading capacity (LC) increased, whereas the loading efficiency (LE) decreased. Nanoparticles could release vitamin D_3 at a sustained rate in gastrointestinal fluid. These results revealed the potential of OAE nanoparticles as oral carriers for sustained release of vitamin D_3 [45].

Amidation Reactions

The concept of mucoadhesion was first introduced in the early 1980s as a new approach to improve drug release, targeting and absorption. Mucoadhesion, a key element in the design of mucoadhesive polymer, is defined as the ability to adhere to the mucus gel layer [46]. The most common type of interactions are non-covalent bonds, including hydrogen bonds, van der Waals forces, ionic interactions and/or chain entanglements [47]. It was found that adding linear PEG chains to hydrogel matrices enhanced their adhesion to the mucus due to chain interpenetration at the hydrogel-mucus interface.

A novel approach for the synthesis of the mucoadhesive polymer alginate-poly(ethylenglycolacrylate) (alginate-PEGA) was proposed as a new biomaterial able to promote bioadhesion with mucus-covered surfaces while displaying sustained release ability [48]. The synthesis of Alg-PEGA was designed as a two-step procedure in which the synthesis of an alginate-thiol is performed first, followed by the conjugation of PEGA to the alginate backbone (Scheme 7.11).

Alginate-thiol was obtained when alginate carboxylic groups were activated with the use of a carbodiimide (EDAC) and reacted with the amino group of cystein. The resulting alginate-thiol was disolved in tris (2-carboxyethyl)phosphine hydrochloride solution (TCEP), and a Michael-type addition reaction took place, from a nucleophilic addition of the thiolated alginate to the vinyl group on the acrylate-functionalized PEG. Lack of cytotoxicity, adhesion to mucus surfaces and drug-release ability were demonstrated using in vitro measurements. Apparently, the addition of PEGA to other degradable polymers can open the way for the development of many other biomaterials for a variety of biotechnological and biomedical applications. In the last decade much effort has been invested in developing multifunctional polymer systems that can offer several characteristic properties. One example is biosynthetic tissue engineering scaffolds that combine biological, degradable components that allow and promote cell growth with a

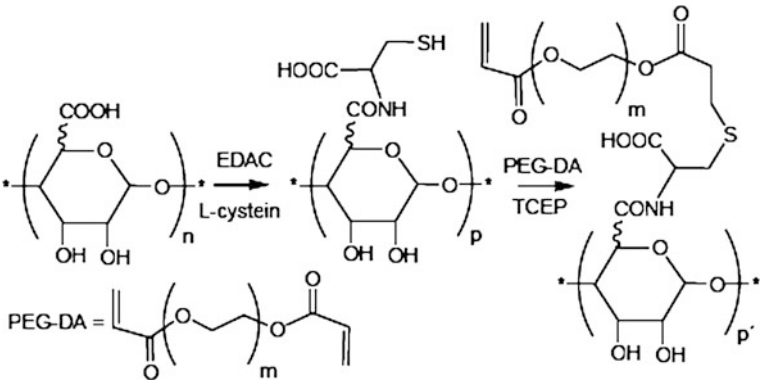

Scheme 7.11 Formation of alginate-PEGA. Amidation reaction of alginate followed by a Michael-type addition

synthetic component that provides mechanical stability and controlled properties [49]. Other examples can be found in the drug-release area where developing a biodegradable polymer system that can offer a controlled release of drugs over time is desirable. These new biomaterials can be also referred to as a ''multi-functional hybrid polymers" due to its characteristics [48]. These functionalities include its ability to enhance bioadhesion with mucus-covered surfaces under physiological conditions, drugs release in a sustained fashion, and control its cross-linking density by two different paths: chemically via acrylate end groups and physically due to the alginate backbone. Moreover, these new biomaterials are expected to be biodegradable due to its polysaccharide backbone, and non-toxic due to its copolymer building blocks which are also non-toxic.

Ugi Reaction

The Ugi reaction is a multi-component organic chemistry reaction (Scheme 7.12), which includes the participation of either a ketone or an aldehyde, an amine, an isocyanide, and a carboxylic acid to form a bis-amide [50]. The particular case shown in Scheme 7.12 corresponds to the study carried out by Bu et al. [51]. First, the imine formation is carried out by the reaction between the aldehyde compounds and the amine. Then, the carbon atom of the synthesized imine is attacked by the nucleophilic carbon atom of the isocianide, which yields an adduct as reaction product. In other pathway, the oxygen atom of a carboxylic acid is added to the previous product, and a new adduct is obtained. After an internal rearrangement of the latter molecular structure, a diamide compound is obtained. It is known that for a successful reaction a pH of 3.6 should be used in the reaction media [52]. This important reaction has been often used to prepare hydrophobically modified alginates [52, 53].

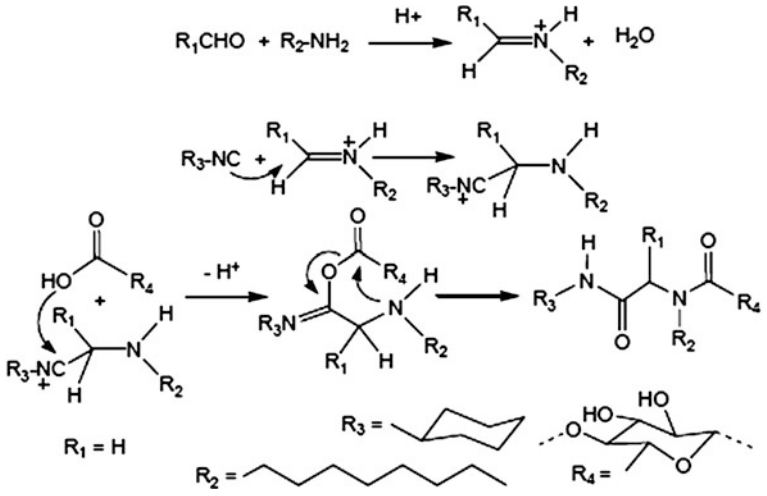

Scheme 7.12 Chemical modification of alginate through Ugi multicomponents reaction

Although alginate hydrogels with versatile properties can be generated through several gel-forming methods, they all involve labor-consuming work in the modification of alginate or the synthesis of an specific cross-linker [54, 55]. A more simple and direct procedure for the synthesis of chemical hydrogels is the Ugi multicomponent condensation reaction on carboxylated polysaccharides [52].

7.3 Properties of Alginates

Alginic acids isolated from different sources can differ in the ratio of mannuronic and guluronic acids (M/G) and in the distribution of the monomers along the polymeric chain. The size and distribution of individual blocks strongly affect the properties of alginic acids and alginates [1].

Its importance manly lies in its hydrocolloid property, e.g., the ability to hydrate in hot or cold water to form viscous solutions, dispersions, or gels. Alginate has been regarded as an excellent polysachaccharide for gel systems because of its unique features such as biocompatibility, biodegradability, immunogenecity, and non-toxicity [56]. Alginates are, in this way, unique in terms of their properties such as emulsifiers, thickeners, stabilizers, gelling and film forming, resulting in several applications for the food and pharmaceutical industries [57].

7.3.1 Physicochemical Properties

Chemical composition and sequence may vary widely between algae species and even between different parts of the algae and the time of the year when it is harvested. Alginate with a very high content of guluronic acid, which is of importance for the mechanical properties of the alginate gel, can be prepared from special algal tissues such as the outer cortex of old stipes of *Laminari*a *hyperborea*. On the other hand, alginates with more extreme compositions containing up to 100 % mannuronate can be isolated from bacteria. Alginates may also be sequentially modified by post-polymerisation enzymatic modification applying mannuronan C-5 epimerases from *Azotobacter vinelandii*, which convert M–G within the polymer chain. Alginates with tailored physical and chemical properties can thus be made. Alginate monomer composition and sequence have a profound effect on the final properties of calcium alginate gels since selective binding of ions is a pre-requisite for gel formation [14].

7.3.2 Thermal Properties

Differential scanning calorimetry (DSC) and thermogravimetric analysis (TGA) have been used to characterize the thermal behavior of native and chemically modified alginates.

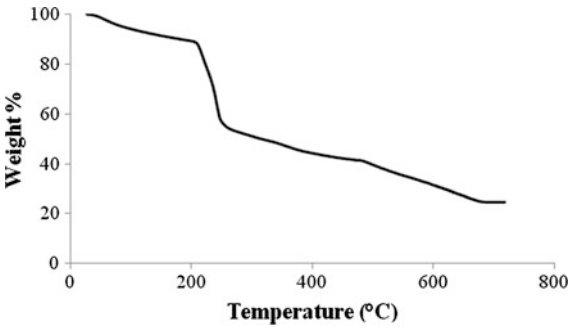

Fig. 7.3 TGA thermogram of a commercial sodium alginate in N_2 atmosphere at 10 °C/min

In a typical DSC characterization, sodium alginate dried powder is heated, in a standard aluminum pan, from 20 to 350 °C at a heating rate of 10 °C/min using nitrogen as purgue gas [58]. The thermogram obtained for alginate showed an initial endothermic peak at 78.9 °C and exothermic peaks at 224.3, 247.1, and 260.7 °C. Endothermic peak is correlated with loss of water associated to hydrophilic groups of alginate while exothermic peaks result from alginate degradation due to dehydration and depolymerization reactions most probably to the partial decarboxylation of the protonated carboxylic groups and oxidation reactions [59].

A TGA thermogram of a commercial sodium alginate is shown in Fig. 3. TGA curve presents an initial weight loss due to dehydration of the sample and a second weight loss attributed to carbon decompositions, reported as a degradation in two steps in previous works [60]. An analysis of the TGA curve reveals dehydration with ∼20 % weight loss, a first decomposition step with an additional ∼30 % weight loss and a second decomposition step with a additional ∼30 % weight loss and a total remaining ash of ∼20 % of the initial weight. In some previous works three different regimes of alginate dehydration, depending on the type and strength of interaction with water molecules, were found: release of free water at 40–60 °C, breakage of hydrogen bonds at 80–120 °C and loss of polar interactions with carboxylic groups at temperatures up to 160 °C. These regions could not be detected separately in the thermogram shown in Fig. 7.3; however, we obtain a mass loss of approximately 20 % at temperatures of up to 200 °C, which is similar to the value reported by Soares et al. [59].

7.3.3 Gel Formation

Alginates can form stable hydrogels by interaction with polyvalent cations, such as Ca^{2+}. The conditions of the media can also induce a gelation even in the ausence of cations which is known as acidic gelation. Alginate's gel strength is a function of the average length of G-blocks larger than one unit ($N_G > 1$). Marked effects on gel strength are observed when N_G changes from 5 to 15, which coincides with typical G-block lengths found in commercially available alginates [14].

Diffusion properties of alginate hydrogels are determined by the pore size and the pore size distribution. It has been reported that calcium alginate forms networks characterized by a pore size between 5 and 150 nm [61].

7.3.3.1 Internal Gelation

Gels obtained by this method shown relatively high homogeneity. The internal gelation method uses an inactive form of Ca^{2+} as a cross-linker, either in bound form to a chelating agent (Ca-EDTA) or as an insoluble salt ($CaCO_3$ or tricalcium citrate). Solutions of a slowly hydrolyzing lactone, generally glucono-d-lactone (GDL), are then added to the aqueous solution or suspension of alginate and the inactive cross-linker [62].

The GDL hydrolyzes in solution to form gluconic acid, thus lowering the pH of the solution. Since the solubility of calcium salt is pH dependent, Ca^{2+} is liberated, resulting in gelation of the alginate solution. With this method, a uniform distribution of Ca^{2+} in the alginate solution is obtained and gelation occurs simultaneously throughout the solution [63].

When water-insoluble calcium salts are used as cross-linker, particle size is a parameter for gelation since it affects the liberation and sedimentation rates prior to gel setting [64]. The pH of the system also affects the gelation behavior. Thus, the gelation properties of alginate are controlled by selecting source and proportion of calcium salt, acidic material, and chelating agent [63, 64].

To produce alginate pellets or micro-pellets, a partial insoluble calcium salt is added to the alginate solution as mentioned before and the resultant mixture is extruded into oil. Then the solution is acidified to bring about the release of calcium ions from the insoluble salt for alginate cross-linking [65].

7.3.3.2 External Gelation

External gelation or dialysis gelation method implies a rapidly migration of the gelation agents, such as Ca^{2+}. Due to diffusion of cross-linker from the surface, gels obtained are more heterogeneous than those prepared by internal gelation; the concentration of Ca^{2+} ions decreases from the surface up to the center of the gel. These gels could be prepared as beads or pellets, as tubes, using a dialysis membrane, or as films from sodium alginate films.

In the production of micropellets by external gelation, the alginate solution is extruded as droplets into a solution of calcium salt. Beads formed are maintained in the calcium solution for a determinated period of time in order to control the degree of cross-linking.

Using a dialysis membrane, gels are prepared by pouring a sodium alginate solution into dialysis bag. This bag, generally with a cylindrical shape, is later introduced in a recipient containing $CaC1_2$ or $NaCl/CaC1_2$ solution of the appropriate concentration. The system is left a determinated period of time to

allow the calcium to form the gel and the cylindrical gel piece is then removed from the bag. The resulting cylinder has a radial gradient of cross-linking concentration because of the restriction in the diffusion once the gel is formed in the vicinity of the membrane [63, 65].

Other way of obtaining calcium alginate gels, is by introducing sodium alginate films already prepared by casting in a $CaCl_2$ solution of a chosen concentration in order to obtain the degree of cross-linking and the rate of cross-linking desired.

7.3.3.3 Acidic Gelation

In this method, the gelation takes place at pH values below the pKa value of the uronic residues. Alginic acid gels are homogeneouos and have the advantage that involve not only guluronic block but also manuronic block. The obtained gels are due to the hydrogen bonds between carboxylic groups present in the molecular structure.

For the acidic gels, an increase in the fraction of homopolymeric G-block yields higher shear modulus, similar to the influence of this residual sequence on the ionotropic gels. Homopolymeric M-block also forms junctions under acidic conditions; however, their contribution is smaller than those of the G-block. Alternating MG-block, with an approximately degree of polymerization of 15, does not contribute to form junctions and rather perturb gel formation [62].

In all cases the final step is the washing with distilled water in order to eliminate the ions that are not part of the gel formed.

7.3.4 Rheological Properties

Rheology is widely applied for two aspects: to get some insight into the processing behavior of polymer and to have information on the molecular structure of polymers [66].

The rheological behavior of alginates in aqueous dispersions depends both on its molar mass (i.e. the length of the polymer chain) and the proportion and arrangement of the monomeric units. Then for a given industrial application it is necessary to select the most appropriate alginate [67].

The intrinsic viscosity (η) is a characteristic value of a single macromolecule in a given solvent and it is a measure of the hydrodynamic volume occupied by the polymer itself. It depends primarily on the molar mass (M_w), chain rigidity, and solvent quality. For anionic polyelectrolytes the presence of macroions and counterions in aqueous media causes coil expansion by intrachain electrostatic repulsion and extra dissipation of energy, thus explaining why the intrinsic viscosity of a polyelectrolyte can be higher than that of a neutral rodlike macromolecule of equal size. Thus, (η) usually increases with an increase in the charge density of the macroion.

Smidsrϕd (1970) demonstrated that intrinsic viscosity of different alginates at infinite ionic strength was independent of the counterion used and representative of the uncharged alginate molecule, being also identical to that obtained for the alginic acid form in 0,1 M HCl, when the macromolecule do not contain charged groups [68]. In this case, the intrinsic viscosity is correlated to the average molar mass by the well-known Mark-Houwink equation [67].

Aqueous dispersions of alginates obtained from bacteria were found to behave as pseudo-plastic liquids, similarly to those containing algal alginates. It was also observed that at a constant alginate concentration and temperature the thickening properties of several bacterial and algal alginates depend only on the molar mass, regardless of their origin [69]. Formation of alginate gels is quite a complex process, depending on the type of alginate used (i.e. high-guluronic 'G' or high-mannuronic 'M' alginates), degree of conversion into calcium alginate, source of calcium ions (viz. calcium chloride, phosphate, lactate, or acetate) and methods of preparation [70, 71].

Viscoelastic properties of algal alginate gels have been assessed so far using either static or dynamic tests. The results of stress-relaxation exhibited a solid-like behaviour that was described by a mechanical model consisting of two Maxwell elements in parallel with one spring [72]. On the contrary, the results of creep experiments showed a liquid-like viscoelastic behaviour that was described by a mechanical model consisting of one Maxwell element in series with two Kelvin–Voigt elements [73]. In dynamic tests, the mechanical spectra of these gels were found to be characterized by a flat dependency of the shear storage modulus (G') and loss modulus (G'') on frequency (ω) for ω ranging from about 10^{-2}–10^{2} s^{-1}; beeing G' one or two orders of magnitude higher than G'' [74]. The viscoelastic properties of several algal alginates of high-mannuronic (M) and -guluronic (G) types, as determined by small amplitude oscillatory dynamic tests, were discriminated in terms of their different orders of the relaxation function and 'gel stiffness' values. The latter was approximately 4–5 times greater in high-G alginate gels than high-M ones, while the former was practically constant and equal to about 0.08 and 0.057 for high-G or -M alginates, respectively [74].

Several mechanisms, such as shifting of cross-linked alginate chains, development of internal hydrostatic pressures causing water exudation through the network, or junction zones breakdown, have been suggested to explain such discrepant results. However, a series of compression-decompression tests carried out at different crosshead speeds suggested that the rapid build-up of a hydraulic pressure, registered as a normal stress representing the overall resistance of the gel network to liquid sleepage, affects the amount of water exuded and consequently the permanent deformation of the samples. Therefore, no mechanical model, consisting of spring and dashpot elements is, in principle, capable of forecasting the phenomena mentioned above and describing the rheological behaviour of alginate gels [74].

7.3.5 Immunogenic Properties

Alginates with high M content possess antitumor and cytokine production stimulatory activities. In bioassays, induction of tumor necrosis factor (TNF) and interleukin 1 (IL-1) showed that the inducibility depends of both chemical structure (mannuronate content) and molecular size of alginate sample [75]. Immunological response and proinflamatory cytokine induction of alginates with high mannuronate content involves pattern recognition receptors, especially toll-like receptors TLR4 or TLR2 [76]. Even when the exact characteristics of alginate molecules responsible for TLR activation is not well established, it is known that neither pure poly(mannuronate) nor alginates containing G-blocks initiate this activation [14].

Suzuki et al. (2011) studied the effect of mannuronate content and molar mass of alginates on in vitro intestinal immunological activity through Peyer's patch cells of C3H/HeJ mice. Alginates containing a high fraction of mannuronate have the ability of stimulate intestinal immunological activity through Peyer′s patch cells. The cytokines secreted in culture medium by Peyer′s patch cells incubated with alginates could affect the proliferation of bone marrow cells [77].

7.4 Preparation of Micro- and Nano-Particles

It has been proved that nanoparticles made of safe materials, as natural biopolymers, have the potential for overcoming important mucosal barriers, such as the intestinal, nasal and ocular barriers.

Alginates form gels by ionically cross-linking polymer chains with bi-valent cations such as Ca^{+2} or positively charged polymers such as chitosan, among others. The formation of beads or particles from alginate gel can be achieved by the techniques described in Sect. 7.3.3. While techniques suitable for the production of relatively large alginate particles (above than 100 μm) are well established, reproducible formation of uniforme alginate gel particles in the range of 10 μm still remains a challenge [78]. When alginate microparticles are to be used for controlled release or delivery of active substances, close control of the particle size and morphology is necessary. One option could be the use of inkjet technology which is based on emitting liquid droplets from a printhead by the action of suitable impulses that can be thermal, acoustic, or piezoelectric. The typical size of droplets ejected from inkjet devices are in the range of 10 μm. The main advantage of inkjet technology is good uniformity of the droplet size and relatively easy scale-up (by replication) [78].

Ciofani et al. (2008) studied the preparation and properties of a drug delivery system based on calcium alginate microgels. For the experiments were used gels in three different forms (spheres, films, and fibers) obtained from 100 μL of a 1 %w/w sodium alginate solution containing the tested protein. Spheres were prepared by

dropping the aqueous alginate + protein solution into a 30 %w/w $CaCl_2$ solution through a needle (23 G) [79].

Cefadroxil has a biological half-life of 1.2–2 h for a dose containing between 0.5 and 1.5 g of the drug. Its short half-life can be enhanced by using a hydrogel matrix for delivery. A 4 % sodium alginate solution in distilled water or the same solution containing gelatin or egg albumin (5 or 10 %w/w based on sodium alginate dry mass) was prepared. Then a 20 % of cefadroxil was added and homogeneously mixed. The polymer solution containing cefadroxil was then added drop-wise into methanol containing 1 % glutaraldehyde and 1 % of 1 N HCl using a hydpodemic syringe through a needle (21) under constant stirring [80].

The success of cell-encapsulating hydrogels is also determined by their abilities to facilitate the influx and efflux of biological molecules into and from the encapsulated cells. The biological transport through the hydrogels is regulated on the basis of pore size, specifically; the diameter of surface pores for a calcium cross-linked alginate hydrogel commonly varies from 5 to 200 nm. This pore size allows the diffusion of small molecules, like albumin. Then, the pore size is further controlled by forming polyelectrolyte complex layers on the gel surface. Exposing alginate hydrogels to polycations such as poly(L-lysine) (PLL) reduces the diffusivity of small molecules. Also, decreasing the molar mass of poly(L-lysine) and extending exposure time led a significant decrease in the average diameter of pores on the gel surfaces [81].

7.5 Preparation of Films and Fibers

Fibers have been extensively used in wound dressing applications because of their unique/advantageous properties, such as high surface area, softness, absorbency and ease of fabrication into many product forms. On the other hand, gel forming properties of alginate helps in removing the dressing without much trauma reducing the pain experienced by the patient during dressing changes.

Alginate/alginic acid fibers were produced by a conventional wet spinning technique using a multi-functional laboratory extruder. Spinning sodium alginate solution (1–6 %w/v) were extruded under pressure through a spinneret (200 holes, 76 μm diameter) into a coagulation bath containing either hydrochloric acid (0.2 M) and/or calcium chloride (1–3 %w/v) to obtain the corresponding alginic acid and/or calcium alginate fibers. The fibers/filaments were then drawn between a first and second set of rolls and were then passed through a water washing bath. After that, the fibers were squeezed between rollers to remove excess of water and placed in a treatment bath containing unhydrolysed and/or hydrolysed chitosan (0–5 %w/v in AcOH, 1 %v/v) for 10 min, rinsed with deionised water and dried using acetone baths of increasing concentration. Achieved levels of unhydrolysed chitosan incorporation ($\sim$0–6 %w/w) into alginate fibers were significantly higher than previous reported values [82]. Fibers strength did not increase indicating that chitosan was more like a coating and it does not penetrate the alginate fibers.

Fibers of sodium alginate and starch loaded with salicylic acid, as a model drug, were obtained by spinning an aqueous solution through a spinneret into a coagulating bath containing $CaCl_2$ and ethanol [83].

Small calcium alginate films were obtained by pouring an alginate-protein solution in a circular mold and then adding drops of 30 % $CaCl_2$ solution. On the other hand, calcium alginate fibers were prepared by passing the alginate-protein solution through a small diameter tube inserted into the 30 % w/w Ca Cl_2 solution [79].

Oxidized alginate/gelatin hydrogels were prepared by using a double syringe fibrin glue applicator, in which one syringe was filled with the solution of an alginate dialdehyde (ADA) in 0.1 M borax and the other with equal volume of gelatin in water fitted with a 20 G needle. The obtained hydrogels were found to possess many critical elements desirable in a wound dressing such as good water absorptivity, conformability, optimal water vapor transmission rate, mild antiseptic properties, and biodegradability [32].

7.6 Applications

7.6.1 Biomedical and Pharmaceutical Applications

Alginates have been used as devices in several human health applications, such as excipients in drug delivery (DDS), wound dressings, as dental impression materials and in some formulations preventing gastric reflux. Alginates used in oral tablet formulation have the advantage of preserving a solid-like characteristic (gel) also at gastric (acid) conditions due to the formation of an alginic acid gel. This property allows for the protection of delicate compounds against the acid influence of gastric juice, both by preventing convection flow and by acting as a buffering agent in the stomach when tablets are manufactured using Na- or Ca-alginate. Also, non-woven alginate fiber wound dressings have been used in the treatment of epidermal and dermal wounds. It is known that applying Ca-alginate dressings appears to be an appropriate topical treatment of diabetic foot lesions with respect to both healing and tolerance. This effect would be attributed to Ca^{2+} ions, which can play an important role in the normal homeostasis of mammalian skin serving as a modulator in keratinocyte proliferation and differentiation. These ions may be released from Ca-alginate fibers promoting early stage wound healing [14, 84].

Alginate anti-reflux preparations are used for the treatment for gastro-oesophageal reflux disease providing a physical barrier upon contact with the stomach contents in the form of a neutral floating gel or ‘raft’. Commercial products contain a high G sodium alginate, calcium carbonate and sodium (or potassium) bicarbonate which are formulated to undergo ionic gelation in the stomach. Alginate rafts are formed by the action of gastric acid on a soluble sodium alginate to form an insoluble gel of alginic acid. The insoluble calcium carbonate release Ca^{+2} on contact with the acid to improve mechanical strength of alginic acid gel.

Simultaneously, action of gastric acid on bicarbonate source produces CO_2 which became trapped within the alginic gel to provide aeration and buoyancy [85].

Recently, it was reported that magnetic resonance imaging (MRI) allows visualization of labeled cells in vivo in real time, providing new insights into the biodynamics of cell migration. This technique has been used to track the efficacy of stem cell therapy, primarily by using cells labeled with super paramagnetic metal contrast agents. This technique need a versatile micro-scale capsule embedded with nano-sized particles able to enhance real-time visualization with magnetic resonance imaging (MRI) as well as deliver a powerful therapeutic strike to diseases in animal models. Then, magnetic microcapsules made of alginate containing ferric oxide and filled with human insulin islets were tested and they safely produced therapeutic levels of insulin in swine for up to four weeks. The magnetic nanoparticles are inserted in a microcapsule with a diameter of 350 μm and they are concentrated to increase the sensitivity of MRI. In addition, the openings in the capsules are large enough to release their therapeutic load (insulin), although small enough to prevent the contents from coming under attack by the immune response system of the body [86].

However those capsules are not limited to diabetes; they have other applications with hepatocytes and stem cells. Applications of stem cells for therapy of neurological conditions, such as Parkinson's disease, Alzheimer's disease, multiple sclerosis, or stroke, are promissory therapies for the irreversible damage of the central nervous system produced in these cases. In that sense, the transplantation of stem cells into the mouse brain, and MRI of the cells both in vivo and *post-mortem* have been analyzed [87]. Also labeling of stem cells with superparamagnetic iron oxides (SPIOs) have been developed for using MRI to visualize these cells in myocardial infarct [88].

Alginate-poly(L-lysine)-alginate (APA) microcapsules have been explored as vehicles for therapeutic drug and cell delivery using barium sulfate, bismuth or a perflurocarbon emulsion instead of ferric oxide nanoparticles. Using these microcapsules other imaging techniques, such as computerized tomography, X-ray, ultrasound or fluorine imaging can be applied [89].

In other experience, it was proven that transplantation of intrathecal and intravenous administration of autologous mesenchymal stem cells (MSCs) (also called mesenchymal stromal cells) in patients with multiple sclerosis (MS) and amyotrophic lateral sclerosis (ALS) is a clinically feasible and relatively safe procedure and induces immediate immunomodulatory effects [90].

7.6.1.1 Control of Type II Diabetes and Obesity

Alginate is a non-digestible polysaccharide and can be classified as dietary fiber. Dietary alginate can produce an improvement in the gastro-intestinal barrier function and a reduction in the damaging potential of the luminal contents with changes in the colonic microflora. On the other hand, dietary alginate reduces intestinal nutrient absorption and promotes satiety both of which have implications for the control of Type II diabetes and obesity [91].

Alginates have shown to modulate appetite and energy intake in models of acute feeding. In those studies alginate formulations undergo ionic gelation upon reaction with gastric acid to form an alginate gel that can slow gastric emptying, stimulate gastric stretch receptors and reduce intestinal nutrient uptake and influence the glycaemic response. A sodium alginate satiety beverage was designed to undergo enhanced ionic gelation within the stomach but independent of gastric acidity. This ability to gel regardless of endogenous acid secretion and pH was achieved by addition of an acidulant (glucono-δ-lactone, GDL). Desired properties of this satiety beverage are obtained when the right alginate is used, high G content (65–75 %) and high molar mass (150,000–200,000 g/mol). Reconstitution of the dry powder (12.5 g) in water (100 mL) hydrolyses the GDL to glucuronic acid giving a reduction in the pH of the beverage. This change in pH controls the solubilization of calcium carbonate which control the rate of gelling of alginate [92].

Dettmar et al. (2011) evaluated the influence of one-off dose of the sodium alginate satiety beverage (or control) upon test meal consumption and perceptions of fullness and hunger. In clinical cases 1.5 g pre-load alginate in the studied satiety beverage reduced the onset of hanger following a test meal, the desire to eat between meals and blood cholesterol and glucose levels in subjects with Body Mass Index >25 compared to control. The use of alginate to address the features important in the development of overweight and obesity was shown to be clinically effective. However, the choice of alginate and the formulation design are essential factors in functionality to bring about satiety and to have an impact upon the global obesity epidemic [92].

7.6.1.2 Dental Impression

Dental impression materials are used to produce dental molds in order to have the information of patient' oral structure. Alginates are used to produce dental impressions by the reaction between a sparingly soluble calcium salt and a soluble alginate with a resulting irreversible hydrocolloid impression. Viscous and elastic properties of impression materials as the cure are essential for the estimation of clinical characteristics such as working and setting time. Alginate irreversible hydrocolloids usually have a chromogenic system intended to allow the clinician to compensate for slight variations in temperature of mixing and working times [93].

7.6.1.3 Dura Mater Repair

Adhesive material can be used as sealant for minor dural defects while large dural defects require patches. In the case of minor dural defects, sutures or adhesives are used as dural sealants. However, suture alone are quick but do not provide adequate sealing of approximated tissue. The implantation of neural prosthetic devices such as deep brain stimulators and penetrating cortical electrodes for motor and

sensory prostheses have necessitated the creation of large dural defects [94]. Thus, engineering biocompatible materials need to be developed for dural replacement patches, and the feasibility of using hydrogels for both applications (dural sealant and dural replacement patches) has been demonstrated in animal models.

Alginates show promise due to its rapid gel formation, biocompatibility, and mild reaction conditions that allow hydrogel cross-linking while in direct contact with the surrounding meningeal and neural tissue [95]. In the presence of polivalent cations alginate participates in an accelerated cross-linking reaction that allow for quick sealing of any size dural defect with an alginate-based hydrogel which do not induce seizure activity or a significant inflammatory response [95].

The mechanism of gelation may dictate alginate's success as a dural sealant or patch. Two methods of gelation using calcium carbonate to cross-link alginate have been extensively described and used to create alginate hydrogels: diffusion gelling and internal gelling. Calcium chloride ($CaCl_2$) is a commonly used calcium source for cross-linking alginate by diffusion versus calcium carbonate ($CaCO_3$) which is utilized in internal gelling through the release of calcium ions in situ [96].

The rate of gel formation should be sufficient to rapidly close a dural defect (small or large) minimizing cerebrospinal fluid leaking and brain swelling. After application of the dural sealant or dura mater replacement, the gel is subjected to a constant intracranial pressure as well as pulsation of the brain with heart rate and respiratory rate that compresses the gel between the brain and the skull. Although the gelation rate of alginate with $CaCO_3$ is slower than that of $CaCl_2$, the components can be mixed and then applied as a single viscous solution to a large dural defect. Site-specific application can be further improved by waiting for the alginate:$CaCO_3$-reacted mixture to reach a high, but still usable, viscosity before filling the dural defect. $CaCO_3$ results in more homogeneous and uniform gels than $CaCl_2$, and is thereby more appropriate for use as dural patch [97]. The hydrogel must be able to retain its shape and orientation to the tissue while accommodating some motion of the dura. The ideal dural patch would exhibit elastic solid behavior enabling the hydrogel to maintain its original form. Therefore, $CaCO_3$ is potentially more appropriate to use as cross-linking alginate when used as a dural patch because of an increased need for long-term stability [97].

7.6.1.4 Mucoadhesion

Mucoadhesion, defined as the ability to adhere to the mucus gel layer, is a key element in the design of polymer systems for specific applications. Mucus gel is composed of 95 % water and about 5 % mucus glicoproteins, called mucin, plus a number of minor components [47].

The first line of mucoadhesive polymers were based on polymer-mucin interaction through physical and/or chemical non-covalent bonds. However, there have been attempts to improve mucoadhesive properties via covalent bonds such as disulfide links between the polymer and the mucin-type glycoproteins. This approach has lead to the development of thiolated polymers where a small

molecule (ligand) consisting on a thiol functional group is attached to the polymer chain [98]. Mucoadhesive systems based on alginate-thiol molecules were unable to display good adhesive properties in a hydrated environment. The benefit achieved by adding thiol groups was flawed in the hydrated crosslinked form due to the formation of intermolecular disulfide bonds [99].

Alginate is an anionic mucoadhesive polymer which is known for its ability to create hydrogen bonds with mucin-type glycoproteins through carboxyl-hydroxyl interactions. Another polymer recognized for its mucoadhesive ability is poly(ethylenglicol), PEG. A non-toxic, non-immunogenic, non antigenic polymer characterized by a high solubility in water, and a rapid in vivo clearance which depends on its molecular weight. In addition to its pharmacological and biological advantages, PEG shows mucoadhesive properties due to its ability to create hydrogen bonds with sugar residues on glycosylated proteins [100].

It has also been shown that alginate G-blocks are able to transiently modify mucin network structures. Such effects may provide a basis for the treatment of pathological respiratory conditions as well as for a general manipulation of mucosal surfaces for e.g. drug delivery systems. In the case of cystic fibrosis the highly viscous mucus combined with a hyperinflammatory state leads to malfunctioning of the mucociliary clearance. The possibility of applying oligoguluronatos to normalize the rheology of mucus by a shielding off the interaction sites between mucin and other macromolecular components therefore became pertinent. Then these types of interactions could be eliminated through electrostatic competitive inhibition by charged oligomers too small to create intermolecular cross-links. G-blocks, typically degree of polymerization 10–20, were chosen as an appropriate candidate for this purpose as they are known to be non-immunogenic [101].

A novel approach for the synthesis of a mucoadhesive polymer based on alginate-PEGAc was designed as a two-step procedure in which the synthesis of alginate-thiol is performed first, followed by the conjugation of PEG-DA to the alginate backbone [48]. The addition of PEG acrylate to other degradable polymers can be used for the development of other biomaterials for a variety of biotechnological and biomedical applications. Biosynthetic tissue engineering scaffolds that combine biological, degradable components that allow and promote cell growth with a synthetic component that provides mechanical stability and controlled properties is an example.

A frequent problem is encountered with the conventional topical delivery of ophthalmic drugs produced by the rapid pre-corneal loss caused by the tear drainage. The design of a mucoadhesive carrier system with improved drug delivery properties to the ocular surface would be a promising step towards the management of external ocular diseases. Since the cornea and conjunctiva have a negative charge, it was proposed that the use of mucoadhesive polymers, which may interact intimately with these extraocular structures, would increase the concentration and residence time of the associated drug. Among others mucoadhesive polymers, cationic chitosan (CS) and anionic alginate have been chosen because of their biodegradability, and biocompatibility. CS solutions prolong the corneal residence time of antibiotic drugs and it was founded that CS-coated

nanocapsules were more efficient in the intraocular penetration of some specific drugs. Also, alginates are hemocompatible and have not been found to accumulate in any major organs and show evidence of in vivo degradation [102].

It was reported that most of colloidal particles used as drug carriers are rapidly taken up from the blood flow by the mononuclear phagocytes system (MPS), especially by cells in the liver. This phenomenon is the great interest for targeting a drug to organs of MPS. Promising results were recently reported in alginate loaded nanoparticles to treat in vivo liver metastasis in mice. However, the rapid capture by MPS becomes a disadvantage to gain access to other target sites in the body keeping drug carriers in the blood flow for a prolonged time. To avoid the rapid clearance of colloidal particles from the blood flow by MPS, some authors have prepared more hydrophilic nanoparticles. In this sense, they choose colloidal particles made from a hydrophilic polymer as sodium alginate. The preparations were based on the gel properties of alginate and on its ability to form stable polyelectrolyte complexes in the presence of polyamines. A broad-spectrum antibacterial agent used in the treatment of ocular infections, was successfully formulated in the form of chitosane-alginate nanoreservoir system. This new mucoadhesive formulation is a viable alternative to conventional eye drops by virtue of its ability to sustain the drug release with an ease administration and a reduced dosing frequency [103].

7.6.1.5 Wound Dressing

Wound dressings based on alginates are a commonly used product, especially in the case of exudating wounds. Calcium alginate is a natural haemostat; then alginate based dressings are indicated for bleeding wounds. Wound healing is a dynamic process and the performance requirements of a dressing can change as healing progresses. Alginate within the dressing absorbs the exudates resulting in a hydrophilic gel over the wound which provides a good moist environment for healing. A fluid balance in burn injury is very important since heavy loss of water from the body by exudation and evaporation may lead to a fall in body temperature and increase the metabolic rate. Different alginates properties, high G (gel strength) and high M (flexibility) are often exploited for this application. Hydrogels combine the features of moist wound healing with good fluid absorbance and are transparent to allow the monitoring of healing [104].

Some commercial alginate-based dressings include AlgiSite™ (non-woven calcium alginate fibers, Smith & Nephew, Inc.), Algosteril® (calcium alginate, Johnson & Johnson), Kaltocarb® (calcium alginate fibers, ConvaTec), Kaltogel® (calcium/sodium alginate gelling fiber, ConvaTec), Kaltostat® (calcium alginate fibers in non-woven pads, ConvaTec), Melgisorb® (calcium/sodium alginate gelling fibers, Molnlycke), Restore® (calcium alginate and carboxymethylcellulose non-woven pad, Hollister Wound Care LLC), Seasorb™ (calcium/sodium alginate gelling fibers, Coloplast Sween Corp.), Sorbalon® (calcium alginate, Hatrman), Sorbsan® (calcium alginate fibers in non-woven pads, Dow Hickam), and

Tegagen™ HG (calcium alginate fibers in non-woven pads, 3 M Health Care) [81, 105]. Certain alginate dressings, such as Kaltostat® can enhance wound healing by the stimulation of human monocytes to produce elevated levels of tumor necrosis factors such as α-interleukin-6. Production of these cytokines at the wound site gives a pro-inflammatory stimulus advantageous to wound healing. The high level of bioactivity of these dressings was attributed to the presence of endotoxin in the alginates [104].

As an alternative to standard alginate dressing, new alginate dressings with superior properties have also been obtained [32, 82]. Knill et al. (2004) prepared alginate fibers modified by absorption into/coating onto this core fiber unhydrolysed and hydrolysed chitosans. Alginate essentially manages excess liquid/exudates and chitosan provide antibacterial, haemostatic and wound healing properties. On the other hand, significant increases in levels of chitosan incorporation (∼7–25 %w/w) are reported for hydrolysed chitosan/alginate fibers. Lowering the molar mass of the chitosan increase its ability to penetrate the alginate fibers, not only increasing fiber chitosan content, but also reinforcing the fiber structure and thus enhancing the tensile properties (compared with unhydrolysed chitosan/alginate fibers). Antibacterial testing of hydrolysed chitosan/alginate fibers demonstrated their antibacterial effect with initial use, and their ability to provide a slow release/leaching of antibacterially active components [82].

Balakrishnan et al. [32] studied the wound healing efficacy of in situ forming oxidized alginate/gelatin hydrogels. An ideal wound dressing must control the water loss from a wound at an optimal rate. A value of approximately 200 g/m^2/day was reported as the evaporative water loss for normal skin, while water loss of injured skin can range from 280 g/m^2/day for a first degree burn to 5140 g/m^2/day for a granulating wound. The water vapor permeability of a wound dressing should prevent excessive dehydratation as well as build up of exudates [32]. A value of 2,000–2,500 g/m^2/day would provide an adequate level of moisture without risking wound dehydratation [106]. The oxidized alginate/gelatin hydrogels obtained by Balakrishnan et al. (2005) showed values of water vapor permeability of approximately 2,700 g/m^2/day close to the range appropriate to maintain a proper fluid balance on the wound which can facilitate cellular migration and enhance re-epithelialization [32].

Wound healing is a complex process that can be compromised by several factors. The wound healing efficacy of calcium alginate fibers in non-woven pads or ropes as well as in situ formed hydrogels can be further improved by incorporating drugs or growth factors.

7.6.1.6 Metal Loaded Nanoparticles

Silver and Gold Nanoparticles

Gamma radiation offers many advantages for the preparation of metallic nanoparticles in solution. Free electrons produced during water radiolysis are hydrated in solution. Hydrated electrons can reduce metal ions to zero-valence metal

particles, avoiding the use of additional reducing agents. Furthermore, the amount of zero-valence nuclei can be controlled by varying the dose of the irradiation. Homogeneous formation of nuclei is favourable as it results in uniformly dispersed nanoparticles. The growth of silver nanoparticles by reduction of Ag^+ to Ag is stepwise. Silver atoms primarily reduced by hydrated electrons rapidly combined with silver ions to form dimmer clusters. Continued reduction of the Ag^+ solution causes the aggregation of tetramer clusters into nanoparticles. The metallic clusters and the nanoparticles formed via gamma irradiation are then capped with sodium alginate chain [107].

After irradiation of $AgNO_3$ solution, the dispersion became yellow, indicating the formation of highly stable and uniform-sized silver nanoparticles. It was found that Ag-NPs dispersion could be stored for more than 6 months without obvious sedimentation, demonstrating a long-term stability of silver particles. This indicates that sodium alginate is a good stabilizer of silver nanoparticles [107].

The preparation of gold nanoparticles with controllable size is also an attractive field of research. Since these particles can be used in biological application such as DNA sensors, drug delivery, cancer diagnostic and therapy, preparation of biocompatible and non toxic systems containing Au–NPs is very important. Gold nanoparticles (Au–NPs) with different size have specific properties that are suitable for utilizations in biomedicine and cosmetics. However, the methods for the preparation of Au–NPs using chemicals, such as citrate, borohydride, or other organic compounds, as reducing and/or stabilizing agents are being associated with environmental toxicity or biological hazards. Then gamma radiation is an alternative method to obtain Au–NPs, from Au^{3+} solutions containing alginate as a stabilizer, with pre-selected size in the range of 5–40 nm. Larger size (40 nm) and more monodisperse Au–NPs were obtained by enlargement of 20 nm-seed particles at $[Au^{3+}]/[Au^0] = 6$. Alginates stabilized Au–NPs with different sizes from 5 to 40 nm may be useful for biological applications owing to biocompatibility of sodium alginate [108].

Iron Nanoparticles

The synthesis of biocompatible nanostructured magnetic materials has long been of interest in biomedical applications such as magnetic resonance imaging for clinical diagnosis, magnetic drug delivery, hyperthermia anti-cancer strategy, and cell-sorting systems. Magnetic resonance imaging is one of the most useful non-invasive methods in the field of diagnostic imaging, which is characterized by its high resolution of soft-tissues and by its non-exposure to radiation. Compared to gadolinium based contrast agents, superparamagnetic iron oxide nanoparticles can produce enhanced relaxation rates in specific organs at lower dose than paramagnetic ions, because of their larger magnetic moment [109]. Superparamagnetic iron oxide nanoparticles are distributed in reticuloendothelial cells according to phagocytic activity and can produce a strong decrease in magnetic resonance intensity (negative enhancement) in the tissues where they accumulate, such as the liver, spleen, bone marrow, and lymph node [109]. Another promising application

of magnetic nanoparticles is in drug delivery as carriers to specific sites. Magnetic nanoparticles with high saturation magnetization and high susceptibility are appropriate to induce controlled release of drug after magnetic stimuli. Iron oxides such as magnetite (Fe_3O_4) and maghemite (γ-Fe_2O_3) have been suggested for these applications because of their biocompatibility and magnetic properties [110]. Llanes et al. (2000) prepared maghemite nanoparticles using the alginate network as the matrix. An aqueous sodium alginate solution in distilled water was added dropwise to a degassed ferrous chloride tetrahydrated solution to form alginate beads. The ferrous alginate beads were separated by filtration and washed several times with methanol/water 1:1. Ferrous alginate beads were then suspended in methanol/water and an aqueous solution of sodium hydroxide was added. The suspension was then placed in a 65 °C water bath and a solution of hydrogen peroxide was added dropwise and the suspension was stirred at that temperature for 60 min. By a well-controlled oxidative reaction using alkaline hydrogen peroxide the ferrous ions were converted to nanometer maghemite particles [111]. Guluronic-rich alginates (M/G < 1) retain large amounts of iron in the gel and more magnetic oxide is formed and retained inside the matrix compared to other alginates in a single oxidative reaction. However, alginate beads are unstable in alkaline solutions, as used in this study, then a ′hardening′ or dual cross-linking on the beads must be done in order to maintain the integrity [111]. Iron oxide nanoparticles were also prepared from Fe^{3+} and Fe^{2+} solutions in the presence of NH_4OH at 60 °C. Calcium alginate beads were prepared at room temperature by dropping a sodium alginate solution into an aqueous Ca^{2+} solution [112]. Two types of alginate spheres were prepared: with iron oxide nanoparticles grown in preformed calcium alginate beads and by encapsulation of preformed iron oxide nanoparticles in calcium alginate beads. In both cases diameter of alginate spheres was approximately 400 μm. Iron oxide particles produced before alginate gelation were significantly larger than iron oxide produced after alginate cross-linking. Usually iron oxide nanoparticles prepared by coprecipitation of Fe^{3+} and Fe^{2+} salts have diameters or around 10 nm. However, a decrease in particle size of about 50 % was found for in situ prepared particles since calcium alginate limits the size of iron oxide particles [112].

Several superparamagnetic iron oxide preparations have already been approved for clinical use: Ferumoxides, composed of iron particles of about 5 nm covered with a layer of dextran with a hydrodynamic diameter of about 80–150 nm, have been used in liver, spleen, and myocardial perfusion magnetic resonance imaging; Ferumoxtran, composed of iron particles of about 4–6 nm covered with a layer of dextran with a hydrodynamic diameter of 20–40 nm, can be used as blood pool agent during early phase of intravenous administration and in lymph nodes in the late phase; and Ferumoxsil, composed of iron particles of about 10 nm coated with a non-biodegradable and insoluble matrix of siloxane and suspended in viscosity-increasing agents such as starch and cellulose with a hydrodynamic diameter of about 300 nm, used in bowel magnetic resonance imaging [113].

Superparamagnetic iron oxide particles stabilized with alginate have been successfully prepared by Ma et al. (2007). Ferric and ferrous chlorides (molar ratio

2:1.5) were dissolved in distilled water and chemical precipitation was achieved by adding NaOH at 60 °C. Sodium alginate solution was added to the suspension and it was vigorously stirred for 30 min, heated at 80 °C with slow stirring for 1 h and then sonicated for 20 min. The obtained suspension was dialyzed against deionized water for the total elimination of $FeCl_2$ and $FeCl_3$, and then centrifuged at 10,000 rpm for 20 min. to remove the solid material; the black supernatant was used as the superparamagnetic iron oxide stabilized by alginate [114]. The pharmacokinetics and tissue distribution of alginate beads containing iron oxide were also examined. After that, the efficacy for the detection of liver cancers was evaluated in two kinds of tumor models: VX2 liver tumor in rabbit and primary liver cancer in rats [115].

7.6.1.7 Biosensors

The modification of alginate, usually by means of the carboxylic groups on the alginate backbone (Sect. 7.2.1.2), with functional groups capable of forming cross-links increases the stability and reduces the swelling of alginate-based hydrogels. With this objective, the Staudinger covalent ligation has been used as a novel method for the formation of stable alginate-based hydrogels. This method possess numerous biological applications because is cell compatible, efficient, chemo selective and catalyst-free [116]. The reacting groups include an azide and a phosphine moiety with an electrophilic trap. First, an azide-functionalized alginate polymer is pre-mixed with a high molar mass poly(ethylene glycol) (PEG) terminated with 1-methyl-2-diphenylphosphino-terephthalate (MDT), prior to cellular incorporation. Then, the cell-compatible Staudinger ligation scheme is used to cross-link phosphine-terminated PEG chemoselectively to azide-functionalized alginate, resulting in XAlgPEG hydrogels. XAlgPEG microbeads were formed by co-incubation the two polymers, followed by ionic cross-linking of the alginate using barium ions. Therefore, a ‘‘gel and lock” system was created, where ionically cross-linked alginate/PEG hydrogels were ‘‘locked” into place through the additional formation of interlocking covalent linkages. The resulting microbeads exhibit significant enhancement in hydrogel stability compared with standard alginate controls. These cross-linked microbeads retain diffusional and permeability properties similar to standard barium cross-linked alginate and exhibit undetectable cytotoxicity. Also, XAlgPEG microbeads were found to be highly cell compatible with insulinoma cell lines, as well as rat and human pancreatic islets [117].

It has been widely applied an interesting property between biotin, a small organic molecule found in every cell, and the avidin a much larger protein that binds biotin with high affinity, and forming an essentially irreversible union. Because of their high affinity, biotin has been used to tag a molecule of interest and avidin to extract the biotin-tagged protein. For example, it is possible to add biotin to all proteins on the outside of a cell and then use avidin to purify (through affinity chromatography) these proteins away from the rest of the proteome. However,

avidin has some disadvantages when is used in immunocytochemical detection systems but these problems can be overcome with the substitution of streptavidin for avidin. Streptavidin is a protein isolated from *Streptomyces avidinii*, and like avidin, has four high affinity binding sites for biotin. The most sophisticated and sensitive extension of the streptavidin–biotin technique employs pre-formed complexes, usually in antigen–antibody systems. Alginates have been used in the preparation of model cells or tissue-specific drug delivery systems in which lectins were attached by means of an avidin–biotin interaction to the surface of spermine alginate microcapsules. In the first step of the latter two step process, avidin was covalently bound to the capsule surface via carbodiimide chemistry [118]. In a second step, avidin-coated capsules were bound to different biotinylated lectins. Also, a new biotin-alginate conjugate was used for the encapsulation of bioluminescent reporter cells into microspheres. In this case, biotin was linked to the carboxylic residues of alginate to provide the alginate with a new conjugation property. Coupling of biotin to the alginate was achieved by using aqueous-phase carbodiimide activation chemistry, followed by the binding of biotin hydrazide. The use of biotin-alginate allows to entrap reporter cells in a spherical geometry and to couple those microspheres onto the optical transducer surfaces. The microsphere-based method has a variety of advantages, specially the possibility of placing a mixture of microspheres containing different biospecificities onto the same fiber, thus facilitating the creation of nonspecific probes with a triggering system sensitive to a wider range of toxics. The biotinylated alginate microspheres may be coupled to the transducer surface with the aid of the widely used avidin–biotin affinity system. Then, a biosensor was prepared by conjugating these biotinylated alginate microspheres to the surface of a streptavidin-coated optical fiber, and the performance of the biosensor was tested in a particular bioluminescent response of *E. coli* strain DPD1718 entrapped within biotin-alginate microspheres that had been conjugated to the optical fibers and exposed to various concentrations of mitomycin C [118].

In a previous study it was also demonstrated that in both, liquid culture and an adlayer-alginate immobilized form, this strain responds to DNA-damaging agents such as mitomycin C, nalidixic acid, or UV radiation, by a dose-dependent increase in bioluminescence of blue-green radiation at 490 nm [119].

The method of deposition of the biological macromolecules employed in the fabrication of a biosensor is a very important aspect because it should be in large amounts, with the maximal retention of their specific activity. These biomolecules can be deposited and absorbed directly onto the surface, or by means of cross-linking and covalent binding, or entrapment via the gelation mechanism. The last alternative is one of the few methods that allow a stable deposition of bioreceptors into a biocompatible environment. Then, alginate is an interesting option because its biocompatibility and a porous structure which allowed for high diffusion rates. But it is necessary to adjust the porosity since macromolecules such as enzymes will leach out into the surrounding aqueous medium. However, the diminution of the porosity will affect its permeability, by reducing the diffusion of the analyte's ability to reach its corresponding enzyme placed on the transducer electrode. For

hydrogels the speed of response is also limited by its ability to deliver the electrical stimuli efficiently throughout the gel. The synthesis of new conducting polymer–hydrogel hybrid molecule alginate-poly(pyrrole), Alg-Py can overcome these disadvantages. Then a highly sensitive biosensor was designed for glucose using this hybrid molecule. The biosensor was built by covalent attachment of the enzyme glucose oxidase with the Alg-Py matrix, followed by pyrrole polymerization and casting the biocomposite onto the surface of a platinum electrode (Pt). Poly(pyrrole) is a conductive polymer widely used in fuel cells and sensors, which combined with alginate allows to obtain hydrogels with better properties that both homopolymers separately. This type of sensor is based on the biomolecule immobilization on electrode surfaces by entrapment or attachment to an electrochemically polymerized film. By selectivity and sensibility, enzymes are the biomolecules most widely used in molecular recognition to build biosensors [120].

An interesting amperometric biosensor for hydrogen peroxide was fabricated by using sodium alginate and polyvinyl butyral (PVB) as matrices. The horseradish peroxidase (HRP) and sodium alginate were electro-co-deposited onto the surface of a gold electrode, and the HRP-alginate/Au electrode was further coated with PVB. The electrocatalytic reactivity of the enzyme electrode was investigated by cyclic voltammetry. Results indicate that HRP-alginate composite shows good catalytic activity toward hydrogen peroxide. The reaction mechanism of the H_2O_2 biosensor can be summarized as follow: in the presence of H_2O_2, HRP (Fe^{2+}) is efficiently converted to its oxidized form, HRP (Fe^{3+}) and HRP (Fe^{3+}) then reduced at the electrode surface according to direct electron transfer [121].

The activation of the reporter luciferase genes was obtained by means of genetic manipulation techniques modifying different *E. coli* strains into both luminescent and specifically responsive reporters for the determination of air toxicity. The activation will produce a readily detectable light signal as a consequence of bacterial response in real-time. Eltzov et al. [122] used TV1061 (sensitive to cytotoxic damage) and DPD2794 (sensitive to genotoxic damage) immobilized in different matrices, as the reporter bacteria in a fiber optic based biosensor. Bacteria were fixed and exposed to environmental pollutants and a direct correlation between the immobilization method (i.e. porosity of the matrix) and sensitivity with time response of the bioreporter bacteria was found. The TV1061 strain immobilized in alginate showed the best sensitivity to the tested compound. Direct correlation between the volume of the immobilization bed and corresponding bacterial response and viability was found. The main advantage of these biosensors is their ability to measure the biological effects of tested indoor air pollutants for various types of toxicities as cyto/neuro/geno toxicities or endocrine disrupting effects [122].

7.6.1.8 Tissue Engineering

Stimuli-responsive polymers have been attracting a lot of attention and have been applied to a variety of fields. Poly(vinyl methyl ether) (PVME) undergoes a phase transition at around 38 °C, going from a fully hydrated water soluble polymer at

temperatures lower than the transition point to an hydrophobic polymer, releasing water molecules at higher temperatures. It is possible to obtain a porous gel fiber by mixing a PVME solution (50 wt%) and a sodium alginate solution (5 wt%) and extruded through nozzles into a coagulation bath containing calcium chloride (20 wt%) at 40 °C. A fibrous gel is formed as alginate is crosslinked in the coagulation bath by the formation of cross-linking points with calcium ions. Since calcium chloride decreased the lower critical solution temperature of PVME, PVME aggregate and it does not dissolve in the warm bath. Then, fibers consisting of PVME and calcium alginate were irradiated by gamma rays with a dose of 100 kGy. The capacity of radiation to act as an initiator of cross-linking has been used in PVME modification with an added advantage of reducing, at the same time, the microbial load of products. On the other hand, radiation promotes chain scission of alginate and since PVME was covalently crosslinked, calcium alginate was completely degraded remaining only the PVME fiber. After the degraded alginate is washed out, a fibrous hydrogel of PVME with a highly porous structure is obtained. Since PVME gel fibers are thin (400–600 μm in diameter) and very porous, swells and shrinks very fast. Then, several thermo-responsive model devices like as an artificial muscle, an artificial finger and an automatic gel valve were constructed taking advantage of this behaviour [123].

Endothelial cells (EC) have a variety of important roles: create a non thrombogenic surface through the expression of anti-coagulant and fibrinolytic agents; form a selectively permeable barrier for the exchange and active transport of macromolecular substances into the vessel wall; and regulate the overall vessel tone through the release of small molecules that regulate vasodilation and vasoconstriction. ECs maintain the basement collagen membrane and proteoglycans upon which they rest and have the ability to oxidize liproproteins as they are transported into the artery wall. They also provide a non adherent surface for leukocytes and platelets. A variety of materials including extracellular matrix (ECM)-based proteins, surface or bulk modified synthetic polymers and synthetic peptides, are substrates for ECs. In the pre-vascularization approach, scaffolds are seeded with ECs under static or dynamic (e.g. perfusion) conditions to ensure the penetration of ECs deep within the scaffold. The ECs form new blood vessels (vasculogenesis) and grow outwards to anastomose (connecting) with the host's vasculature. Recently, a modified macroporous alginate that incorporated the Arg-Gly-Asp (RGD) cell adhesion sequence was used as an in vivo depot for what was termed endothelial progenitor cells and showed success with respect to angiogenesis and cell engraftment when implanted into ischemic mouse hindlimb musculature. The congestive heart failure (CHF) is a chronic disease with a high mortality rate. Scaffold materials have been predominantly investigated in acute myocardial infarction (MI) studies and have shown promising improvement in left ventricular function. The RGD peptides conjugated to alginate improved human umbilical vein endothelial cell (HUVEC) proliferation and adhesion when compared to a non-modified alginate group. Injection of the alginate hydrogel into the infarct area of rats 5 weeks post-MI demonstrated that both modified and non-modified alginate improve heart function. Both the RGD modified alginate and

non-modified alginate increased the arteriole density compared to control, with the RGD modified alginate having the greatest angiogenic response. These results suggest that in situ use of modified polymers may influence the tissue microenvironment and serve as a potential therapeutic agent for patients with chronic heart failure [124].

Endothelialized biomaterials are essential components for the next generation of medical devices. Such artificial supports have become more complex with technical developments, transforming from simple polymer films to fibrous matrices with decreasing fiber-size scale and increasing porosity, designed to closely resemble the natural extracellular matrix (ECM), which supports tissue growth and repair in vivo.

The ECM is composed of a meshwork of macromolecules that provide biochemical and biophysical cues for cell function. Through different combinations, spatial organizations, and biochemical interactions of these macromolecules, the different tissues of the body are formed. The fibrous structure allows for cell guidance and provides a hydrated porous network that allows for chemical interaction with the surrounding environment. Successful tissue scaffolds, in analogy with the natural mammalian extracellular matrix (ECM), are multi-component, fibrous, and on the nanoscale. In addition, artificial scaffolds must have mechanical, chemical, surface, and electrical properties that match the ECM or basement membrane of the specific tissue desired. In particular, these material properties may vary significantly for the four primary tissues in the body: nerve, muscle, epithelial, and connective. Nervous tissue is mainly comprised of neurons and supporting glial cells, which allow the transfer of chemical and electrical signals to the neurons to mediate a response. Muscle is a tissue specialized for contraction and has three main derivatives: skeletal, cardiac, and smooth. Epithelial tissue is primarily used to form membranes from the inner to outer surfaces of the human body, including the skin (the largest organ of the human body based on surface area and depth) to the lining of the organs of the gastrointestinal tract. Connective tissue provides structural and mechanical support for the body and works in conjunction with muscle tissue for coordinated and reflexive movements by acting as the lever arm. In order to address this complex array of attributes with a polymeric material, a nanocomposite approach, employing a blend of materials, addition of particles to enhance particular properties, or a surface treatment, is likely to be required [125].

Current technologies that allow the fabrication of nanofibrous composite scaffolding are limited to three main processes: phase separation, self-assembly, and electrospinning. Electrospinning is the most common technique because of its relatively low cost, versatility, and overall simplicity. The two main classifications of materials are matrix materials (used to fabricate the fiber structure itself) and the functional material (which can either be a reinforcing particle or a surface coating). The strong focus on bioresorbable scaffolds is because of the short-term nature of the function of the scaffold (which will be replaced by a natural ECM secreted by the cells), and the desire for it to degrade such that no foreign materials remain. Alternatively, a non-bioresorbable scaffold may be of interest if, for instance, the scaffold is filled with a material (such as a nanoparticle) that may

have toxicological concerns. In that case, permanent encapsulation ensures that the functional particle will remain trapped, and therefore 'invisible' to the body. The tissue engineering field has had a strong focus on bone and cartilage tissue, with developing high stiffness scaffolds as a significant priority. The generation of functional cartilage tissues is motivated for the millions of people who suffer from degeneration of articular cartilage due to primary osteoarthritis or trauma. Damaged articular cartilages ordinarily demonstrate a very limited capability for self-healing. Many strategies have focused on the incorporation of rigid particles (such as hydroxyapatite, calcium carbonate, and beta-tricalcium phosphate) into the fibrous matrix to improve strength and stiffness [125].

Neural engineering is an emerging discipline that uses engineering techniques to investigate the function and manipulate the behavior of the central or peripheral nervous systems. Neural engineering is highly interdisciplinary and relies on expertise from computational neuroscience, experimental neuroscience, clinical neurology, electrical engineering and signal processing of living neural tissue, and encompasses elements from robotics, computer engineering, neural tissue engineering, materials science, and nanotechnology. The aim is to learn the fundamental mechanisms and details of cell-to-cell signaling via synaptic transmission, and then develop the technologies to replicate these mechanisms with artificial devices and interface them to the neural system at the cellular level. In this way, are important experiences that shown that carbon nanotubes, like the nervous cells of our brain, are excellent electrical signal conductors and form intimate mechanical contacts with cellular membranes, thereby establishing a functional link to neuronal structures.

Different biomedical devices implanted in the central nervous system, so-called neural interfaces, already have been developed to control motor disorders or to translate willful brain processes into specific actions by the control of external devices. Examples of existing brain implants include brain pacemakers, to ease the symptoms of such diseases as epilepsy, Parkinson's disease, dystonia and recently depression; retinal implants that consist of an array of electrodes implanted on the back of the retina, a digital camera worn on the user's body, and a transmitter/image processor that converts the image to electrical signals sent to the brain. This coating is made of three components that together allow electrodes to interface more smoothly with the brain. The nanobiomaterial consists of a special electrically-conductive nanoscale polymer; a natural gel-like buffer (alginate hydrogel); and biodegradable nanofibers loaded with a controlled-release anti-inflammatory drug. The process includes electrospinning of dexamethasone (DEX)-incorporated biodegradable nanofibers, encapsulation of these nanofibers by an alginate hydrogel layer, and then electrochemical polymerization of the conducting polymer on the electrode site, around the DEX-loaded nanofibers, and within the hydrogel matrix. Then, electrical properties of neural microelectrodes have been significantly improved with these coatings. Especially, it is remarkable that alginate hydrogel coatings could decrease the burst effect of the drug (DEX) release for controlling the long-term release patterns. Also this controlled release should reduce the risk of exposure to high systemic doses of DEX that are associated with serious side effects such as diabetes, hemorrhagic ulcer, skin atrophy, and osteoporosis [126].

The intervertebral disc (IVD) is a fibro-cartilaginous tissue that confers flexibility to the spine by permitting limited bending and twisting movements between vertebral bodies. The disc is a heterogeneous structure divided into three anatomical regions: the outer and inner annulus fibrosus (AF) and the nucleus pulposus (NP). The loss of proteoglycans from the NP that occurs with disc degeneration as a result of age or excessive trauma gives rise to a variety of health problems, ranging from lower back pain to paraplegia. Many naturally derived materials such as alginate hydrogels have been examined for IVD tissue reconstruction. Most studies approximate the NP with a hydrogel-like scaffold that maintains the cells in a chondrocyte-like morphology. Then, the synthesis of in situ photo-crosslinkable polymers may provide an alternative method for producing alginate hydrogels for NP replacement. In this system, polymers are modified with functional groups (i.e. methacrylates) that undergo free radical polymerization in the presence of a photoinitiator and upon exposure to UV light. This polymerization reaction induces a fluid–solid phase transformation under physiologic conditions and is ideal for in situ encapsulation of cells. Chou et al. [127] obtained modified alginate hydrogels ionically and photo cross-linked, and they were cultured in vitro (4 weeks) as well as evaluated in vivo using a murine subcutaneous pouch model (over 8 weeks). These hydrogels were analyzed for gene expression, ECM accumulation and distribution, and mechanical properties [127].

Large bone defects present a difficult challenge to orthopaedic surgeons accentuated by the limited effectiveness of current treatment options. A graft obtained from a donor (allografts) is often used to bridge the defects, but these frequently fail to revascularize and remodel. The delivery of recombinant proteins is a particularly attractive therapeutic strategy to promote endogenous repair mechanisms and tissue regeneration. Recently, bone morphogenetic protein-2 (rhBMP-2) has been used to promote spinal fusion and repair of challenging bone defects. Boerckel et al. [128] found that the effective dose of this protein vary with delivery system, demonstrating the importance of biomaterial carrier properties in the delivery of recombinant proteins. They compared the dose–response relationship for rhBMP-2 delivered to 8-mm rat bone defects in a hybrid nanofiber mesh/alginate delivery system with the current clinically-used carrier absorbable collagen sponge. Compared to collagen sponge delivery at the same dose (1.0 mg), the hybrid system yielded greater connectivity and greater bone volume. These differences may be explained by the significantly greater protein retention in the hybrid system [128].

7.6.1.9 Delivery Systems

Drug Delivery

The use of hydrophilic polymers in the development of controlled release formulations for the delivery of drugs for oral route has proven to be advantageous over conventional drug delivery systems. Polymeric delivery systems have the

potential to maintain therapeutic levels of a drug reducing side effects and facilitating the delivery of drugs in specific sites with short in vivo half-lives.

Diclofenac sodium produces side effects such as ulcer bleeding or perforation of intestinal wall. In view of its short biological half-life and the associated side effects, the controlled release from alginate cross-linked beads was studied by Kulkarni et al. [129]. A 4 % sodium alginate solution in distilled water was prepared and different amounts of diclofenac sodium were added. 5 mL of alginate solution containing diclofenac sodium was added into methanol maintained at either 25 or 40 °C containing 1 % glutaraldehyde and 1 % of 10 N HCl solution using a hypodermic syringe under constant stirring [80]. The beads formed were removed from methanol at a particular time and washed with distilled water. Diclofenac sodium in different amounts was successfully encapsulated in alginate cross-linked by gluraldehyde. The percentage entrapment efficiency was varied with pH, the temperature of methanol solution and the time of exposure to the cross-linking agent. The release of diclofenac sodium from the beads is subjected to physical and chemical variables including those directly related to the release medium (pH), the release conditions (temperature and stirring rate) as well as those resulting from the characteristics of beads. Cross-linking degree of alginate beads is more dependent from time of exposure to the crosslink agent than the effect of temperature of methanol [129].

By the use of interpenetrated polymer networks of alginate with either gelatin or egg albumin was possible to prepare cefadroxil-loaded beads with high encapsulation efficiencies (up to 88 %) and low burst release rates. A remarkable delay in the release of cefadroxil was observed for interpenetrated polymer network beads obtained by co-crosslinking alginate and either egg albumin or gelatin [80].

Heparin is a very important anticoagulant drug and there has been a growing interest in the development of effective administration methods. With this purpose, heparine has been encapsulated into microbeads, with a controlled release under physiological conditions. Alginate-hydroxypropylcellulose systems are very promising in this respect. The fact that hydroxypropylcellulose (HPC) is a thermoresponsive polysaccharide provide an additional way to control the behaviour of these materials. An aqueous solution of sodium alginate (2 %w/v) was mixed with the appropriate amount of hydroxypropylcellulose. After that, heparin was added to this solution and the Alg/HPC/heparin solution was added dropwise to a solution composed by cyclohexane and calcium chloride in the presence of a stabilizing agent, to achieve the physical cross-linking of the heparin loaded microbeads. Spherical hydrogel microparticles of ca. 3 μm in diameter were obtained and no significant aggregation was observed. All Alg/HPC gels were thermosensitive showing the LCST transition in the physiological range of temperatures. The morphology of the wet surface shows the network of pores with sizes estimated to be in the range of 30–60 nm [130].

In a previous article related with the addition of cellulose derivatives to sodium alginate prior to microbead formation, Chan et al. [131] observed that efficiency of encapsulation of a model drug (sulphaguanidine) and its release profiles were strongly dependent on the hydrophilicity of the cellulose derivatives used and the

viscosity of these formulations. Only hydroxypropylcellulose (HPC) added to the alginate formulation retarded the drug release from the microspheres, and this was explained based on the markedly higher viscosity of the alginate-HPC solution compared with those of other derivatives [131].

Drug delivery to the central nervous system (CNS) remains a challenge despite the advances in understanding the mechanisms involved in the development of neurodegenerative disorders and the actions of neuroactive agents. Drug accessibility to the CNS is limited by the blood–brain barriers. On the other hand, the systemic administration of neuroactive biomolecules to support neuronal regeneration has several intrinsic problems, including the toxicity and poor stability associated to many bioactive factors [132].

Ciofani et al. (2008) studied the preparation and properties of a drug delivery system based on calcium alginate microgels. Bovine serum albumin (BSA) was employed as model protein for in vitro experiments, while biotinylated *Wisteria floribunda* agglutinin (bio-WFA) was used as model protein for in vivo tests. Preliminary in vivo assays show that alginate fibers result the best choice for application in the central nervous system in terms of release efficiency, minimal invasion, and a simple surgery procedure. The release kinetics of alginate fibers reveals a two phase behavior, with an initial very fast phase (burst) followed by a slow and time sustained release phase. The presence of labeled cells around alginate hydrogels 24 h after the implantation demonstrated the in vivo release and the preservation of the protein properties employing calcium alginate fibers. This kind of behavior can be useful for those treatments where a strong therapeutic initial dose is required followed by a maintenance therapy with lower doses (such as lupus cerebritis, vasculitis, and multiple sclerosis as well as for experimental treatment of Alzheimer disease) [79].

Dual cross-linked beads based on alginate and chitosan were prepared by Xu et al. (2007). For these dual cross-linked beads a homogeneous solution containing 2 %w/v of sodium alginate and chitosan, and 20 %w/w of bovine serum albumin (BSA), based on alginate+chitosan content, was first dripped in a $CaCl_2$ solution (2 %w/v) and spherical beads were formed under mechanical stirring for 15 min. The Ca^{2+} cross-linked beads were then dipped in a Na_2SO_4 solution (2 %w/v) for 15 min [133].

Release of BSA from single alginate beads as well as dual cross-linked beads were investigated in simulated gastric fluid (SGF), simulated intestinal fluid (SIF) and simulated colonic fluid (SCF). Less than 3 % BSA release was obtained after 4 h in SGF and dual cross-linked beads were stable after 10 days in SGF. BSA release after 4 h in SIF depends on alginate/chitosan content in the beads; however BSA total release after 4 h vary between 20 and 40 % and between 60 and 80 % after 8 h. In SCF the release of BSA increased compared to SIF since calcium cross-linked alginate is less stable at pHs higher than 7. BSA release from dual cross-linked beads was also studied by incubating the beads for 4 h in SGF, then for 3 h in SIF, and finally for 3 h in SCF. BSA release increased with an increase in the content of alginate in the beads. BSA release was less than 3 % after 4 h in SGF, after transferring into the SIF, the BSA release rate after 4 h was higher than

SIF only, and BSA release was accelerated with the increase of alginate in the beads. Once in SCF, the rest of BSA was almost completely released in 3 h [133].

Release of salicylic acid from fibers of sodium alginate and starch was studied in vitro in a phosphate buffer with pH 7.4 and ionic strength of 0.145 M [83]. The release of salicylic acid increased with an increase in the starch content in the fibers, which was attributed to solubilization of starch originating pores that accelerate the release of the drug from the matrix fiber. The effect of solution pH in the range of 1.0–7.4, for a constant ionic strength, was also studied. The highest and lowest release rate was obtained at pH 7.4 and 1.0 respectively. A higher pH increased both the swelling ability of alginate as well as the solubility of salicylic acid increasing the drug release rate [83].

Nanospheres are submicron particles containing entrapped drugs intended for enteral and parenteral administration that may prevent or minimize drug degradation and metabolism as well as cellular efflux. To form stable uniform alginate nanospheres is frequent the addition of poly(L-lysine), PLL, a cationic, natural polymer that envelop the negatively charged calcium alginate complex. But, replacement of PLL it has been investigated because it could be toxic and immunogenic when injected. Then, chitosan was chosen as an alternative cationic polymer for the preparation of nanospheres. In the last case, formation of nanospheres requires a low concentration of calcium chloride to form the negatively charged, calcium alginate pre-gel that is subsequently enveloped by the positively charged chitosan. Also, the relative mass ratios of sodium alginate, calcium chloride, and chitosan are critical to form nanospheres rather than microspheres [134].

Films of alginate and gelatin, cross-linked with Ca^{2+} and containing ciprofloxacin hydrochloride as model drug in different concentrations, were obtained by a casting/solvent evaporation method. The film can lead to a successful application for localized drug delivery in vivo or in vitro environments [135].

Considering some controlling drug delivery/controlled drug release systems containing antibacterial agents, alginate is related with ophthalmic delivery of ciprofloxacin hydrochloride from different polymer formulations used in vitro and in vivo studies with very good results. Reservoir-type ocular inserts were fabricated using sodium alginate containing ciprofloxacin hydrochloride as the core (drug reservoir) that was sandwiched between Eudragit and/or poly(vinylacetate) films. Ocular inserts were packed in aluminum foil and sterilized by γ-radiation and they were evaluated for in vitro and in vivo release rate studies, microbial efficacy against induced bacterial conjunctivitis in rabbit's eyes, concentration in the aqueous humor, and stability [136, 137]. The effects of irradiation on those systems have a dual role: as sterilizing agent of loaded systems and as polymerization initiator and/or cross-linker in polymeric drug carriers before their being loaded with drugs.

Yang et al. [138] produced high-performance nanoparticles for photodynamic detection of colorectal cancer, where alginate is physically complexed with folic acid-modified chitosan to form nanoparticles with improved drug release in the cellular lysosome. They are excellent vectors for colorectal-specific delivery of 5-aminolevulinic acid for fluorescent endoscopic detection [138].

Mladenovska et al. [139] prepared chitosan-calcium alginate microparticles for prolonged and colon-specific delivery of 5-aminosalicylic acid (5-ASA), a common drug used in the treatment of inflammatory bowel diseases (IBD). It was observed a size-dependent particle deposition in the inflamed area of the colon. Also charge interactions were reported, so that negatively charged particles adhered more readily to the inflamed tissue. Then, anionic alginate showed more potent mucoadhesion in comparison with cationic chitosan. A spray-drying technique was applied to 5-ASA/sodium alginate aqueous solution to obtain spherical particles having a mean diameter of less than 10 μm. The microparticles formed were cross-linked and coated into solution of $CaCl_2$ and chitosan to obtain a stable microsystem. By using confocal laser scanning microscopy (CLSM) it was determined that chitosan was dominantly localized in the particle wall, while a homogeneous distribution throughout the particles was observed for alginate, giving the particles negative charge. Also, they were not found covalent interactions between the drug and the polymer. The potential of 5-ASA loaded microparticles for intensive mucoadhesion and controlled colon-specific delivery was confirmed by dissolution and biodistribution studies of ^{131}I-labeled 5-ASA after peroral administration of these microparticles to rats [139, 140].

Alginate is widely used in the food industry as a thickener, emulsifier, and stabilizer. Also it is modified to enhance the stability, viscosity, and peculiar rheological properties, introducing various hydrophobic groups such as n-octylamine groups, alkyl chains (C12 and C18), and cholesteryl to the alginate backbone by different procedures. Microspheres prepared by alkyl chain-grafted sodium alginate show high protein encapsulation yields and controlled release properties. As an example amphiphilic derivatives of alginate bearing poly(ε-caprolactone) (PCL) chains prepared by new aqueous micellar grafting technique, allowed the retention of a model poorly water soluble drug and slowed its release considerably [42].

Also, it has been reported that cholesteryl-grafted sodium alginate was able to self-aggregate as nanoparticles through hydrophobic interactions, which are able to encapsulate pyrene, a hydrophobic compound [37]. But the synthesis was performed using organic solvents that may be harm to the human body or to the environment. To overcome this aspect, hydrophobic alginate derivative was prepared by modification of alginate by hydrochloric acid using oleoyl chloride without organic solvents. The obtained oleoyl alginate ester (OAE) formed self assembled nanoparticles at low concentrations in aqueous medium, and nanoparticles retained their structural integrity both in simulated gastric fluid (SGF) and simulated intestinal fluid (SIF). After that, the loading and release characteristics of nanoparticles based on OAE were investigated using vitamin D3 as a model nutraceutical. Vitamin D is of great importance in health and disease prevention since it takes part in calcium and phosphate metabolism, in the formation of osteoblasts, and fetal development, among others. However, vitamin D insufficiency is a public health problem, since it is a fat-soluble vitamin. The release of vitamin D3 from loaded alginate nanoparticles in gastrointestinal fluid was studied by Li et al. [45].

Mesoporous synthetic clays are obtained when polymer-containing silicate gels are hydrothermally crystallized to form layered magnesium silicate hectorite clays. In this process,1,3-didecyl-2-methylimidazolium chloride (DDMI) has been used as pore directing agent. After that, quinine (QUI), an antimalarial drug was adsorbed onto these mesoporous synthetic hectorites (MSH) forming nanocomposites. These nanocomposites were added to an alginate solution and MSH-QUI/Alginate nanocomposite beads were obtained by dripping the above prepared solution into a calcium chloride solution. The drug release rate in the gastric environments was controlled by alginate coating [141].

Cells and Enzymes Delivery

Recently, cells have been increasingly exploited as alternative drug delivery devices. Cells can act as drug depots enabling the delivery of therapeutic molecules over an extended time period. Cells are capable of delivering drugs in response to an external stimulus, which is highly advantageous to maintain homeostasis for patients suffering from chronic diseases, like diabetes or Parkinson. In addition, cells secrete therapeutic proteins and cytokines that may not be purified or synthesized in a test tube. This provides the potential to treat various diseases that cannot be cured with currently available technologies. A variety of stem cells, progenitor cells, lineage-committed cells, and genetically engineered cells are being tested in preclinical and clinical trials as drug delivery vehicles. Stem and progenitor cells secrete a diverse array of growth factors, including vascular endothelial growth factor (VEGF) and nerve growth factor, which are used to treat ischemia and neuronal damage, respectively. Islet cells, kidney cells, and parathyroid cells are examples of lineage-committed cells, which naturally secrete insulin, erythropoietin, and parathyroid hormone, respectively. These therapeutic proteins are used in the treatment of diabetes, anemia, and hyperthyroidism. Many cells, such as kidney cells, ovary cells, fibroblasts, and myoblasts have been genetically engineered to secrete specific therapeutic proteins. Such proteins include endostatin to suppress cancer metastasis, erythropoietin to treat ischemia, nerve growth factor to treat Alzheimer's disease, and β-endorphin to alleviate pain. Encapsulating cells into biomaterials has shown promising results for reducing the immune response and increasing the efficacy and viability of transplanted cells. Biomaterials are commonly processed into hydrogels acting as permeable membranes to block the access of immune cells to the transplanted ones [142].

The relative mild gelation process of alginate has enabled the incorporation of proteins, cells, and DNA into alginate matrices with retention of full biological activity. Furthermore, pore size, degradation rate, and release kinetics can be controlled by selecting the type of alginate and coating agent. Biocompatibilty of alginate is discussed in the literature: alginate is stable against breakdown by mammalian enzymes but it can be dissolved and eliminated in vivo through the kidneys. Alternatively, partial oxidation of uronic units of sodium alginate can be used to make alginate susceptible to hydrolytic breakdown in vivo [17, 143, 144].

However, there are relatively few works related to in vivo applications, especially in the nervous system.

To achieve non-invasive delivery of alginate gels for biomedical applications, variations on the concept of internal gelation have been employed to create *self-gelling* formulations of alginate that facilitate injection of alginate followed by in situ cross-linking in vivo. Recently, a self-gelling alginate hydrogel formulation based on alginate microspheres as calcium reservoirs mixed with soluble alginate solutions was developed. When calcium-reservoirs microspheres were mixed with a solution of alginate containing cells and injected subcutaneously into mice, the solutions formed stable gels in vivo within approximately one hour [145].

Relatively stable gels were formed for matrices loaded with approximately 6 mM Ca^{2+}, whether provided by microspheres only in vitro or by a combination of ions from the reservoir microspheres and surrounding tissue fluid in vivo. Cellular infiltration of the gels was supported by the macroporous morphology of gels formed in situ following injection. The ability to incorporate soluble immunomodulatory factors like interleukin-2 (IL-2) directly into the matrix and the use of microspheres as modular components for slow release CpG oligonucleotides electrostatic anchored to the surface may provide a potent platform for immunotherapy when combined with delivery of immune cells [146].

When a cell suspension is mixed with a (osmolytically balanced) sodium alginate solution and the mixture dripped into a solution containing Ca^{2+}, the droplets instantaneously form gel-spheres entrapping the cells in a three-dimensional lattice. A most exciting prospect for alginate immobilized cells is their potential use in cell transplantation, where the main purpose of the gel is to act as a barrier between the transplant and the immune system of the host. Cell lines that have been suggested for such transplantation include parathyroid cells for the treatment of hypocalcemia and dopamine producing adrenal chromaffin cells for treatment of Parkinson's disease.

A considerable amount of research has been made on insulin producing cells for the treatment of Type I diabetes. Transplantation of a microcapsule-shaped bioartificial pancreas, which contains enclosed islets in an immunoisolatable membrane, has been suggested as one method of more effectively treating this disease because it requires no immunosuppressive therapy and no regular self-injection of insulin. Transplanted islets can secret insulin into the host because the surrounding semipermeable membrane is impermeable to higher molar mass antibodies, protecting the islets from host immune rejection. Alginate-poly(L-lysine) capsules containing pancreatic Langerhans islets have been shown to reverse diabetes in large animals and have also been clinically tested in humans [147].

Calcium alginate cross-linked hydrogels reinforced by poly(L-lysine) remain intact in vitro longer than simple alginate hydrogels. However, after implantation, their structural stability varies with the site of implantation, either subcutaneous or intraperitoneal, and the host organism, either canine or murine. The long-term mechanical stability of hydrogels may be further enhanced with semi-interpenetrating network gels [81].

The presence of polycations on the surface of hydrogels-encapsulating islet cells induced protein adsorption and subsequently decreased the therapeutic efficacy of the cells. Gradual loss of cell viability due to the immune response was often observed from in vivo experiments. Despite concerns about the immunogenicity, the advantageous roles of polycations encouraged clinical trials for the treatment of diabetes with islet cells. The potential impact of this drug delivery approach is that the serious risks associated with the administration of immune suppressors can be eliminated. Then, the biocompatibility of the microcapsules and their biomaterials components is a critical issue for the long-term efficacy of this technology [148].

Sakai et al. [149] prepared alginate-based microcapsules by adding a porous silicate layer to allow the diffusion of lower molar mass molecules, such as glucose or insulin, but not higher molar mass molecules such as γ-globulin. A sodium alginate solution (1.5 %w/w) was dripped through a 22-gauge needle into a $CaCl_2$ solution under gentle stirring. The resulting beads were rinsed and suspended in distilled water, mixed with n-hexane and kept at 4 °C in an ice-bath. The silicon alkoxide precursors were added to the n-hexane containing the calcium alginate gel beads, and the mixture was stirred for 2 min. After the sol–gel process, the gel beads coated with aminopropyl-silicate were rinsed with distilled water and suspended in sodium alginate solution (0.05 %w/w) for 3 min. Finally alginate/aminopropyl silicate/alginate particles were obtained with the aminopropyl silicate layer sandwiched between the alginate core gel and the outer alginate layer [149]. The utilization of 3-aminopropyltrimethoxysilane as silicon precursor to coat the microcapsule surface with anionic alginate polymer led to the suppression of cell adhesion and overgrowth. Even when the mechanism of cellular adhesion and overgrowth is not yet clear, some authors have reported that cellular overgrowth is the consequence of not only an inadequate membrane matrix biocompatibility but also of antigens leaking from microcapsules containing the islets. An optimal molar ratio of silicon alkoxide precursors was found in order to prepare a membrane impermeable to γ-globulin with good permeability to substances of lower molar mass retaining their viability for insulin secretion. These results indicate that alginate/aminopropyl silicate/alginate microcapsules are a promising development in the attempt to design a microcapsule-shaped bioartificial pancreas [149].

In an exhaustive review, Orive et al. (2002) considered that more detailed and in-depth knowledge will lead to the production of standardized transplantation-grade biomaterials and biocompatible microcapsules. Among other aspects, a fundamental role in the validation of alginate for implantation purposes is an efficient purification process to remove some contaminants as endotoxins, certain proteins, and polyphenols. Also industrial processes used for extracting alginates from seaweed could introduce further contaminants. On the other hand, alginate composition (M/G) has a relevant role in some of the main properties of implantable microcapsules including stability, size, biocompatibility and permeability [150]. Although the presence of contaminants had a higher impact on the immune response than alginate composition, the quantity of contamination appeared to be related to composition; since it was observed that high-M alginates presented a higher content in polyphenol, endotoxins, and proteins.

Since charged PLL is known to be immunogenic, PLL coated alginate beads undergo a final incubation in alginate to form alginate-PLL-alginate (APA) systems. However, some studies suggested that external alginate coating is not effectively masking and/or neutralizing the immunogenic PLL. As a consequence, is necessary to improve the knowledge about the biocompatibility, including surface structure, chemistry, and topography of the capsules. On the other hand, it is relevant the amount of electrostatic interactions between PLL and alginate, which is certainly related to M/G content. This interaction plays a major role in determining the final configuration, and therefore the reactivity of the polycation. Spherical shape and suitable size of the microcapsule are also a major difficulty for optimal immunocompatibility. It was determined that, the bigger the grafted encapsulated tissue volume, the more frequent the incidence of adverse side effects in the recipients [151].

It has been shown that the implantation procedure of the microcapsules itself, has a continuous effect in attracting and activating immune cells. Although this non-specific reaction, as well as the peritoneal inflammatory response to microcapsules, is limited to a period of few weeks. Bunger et al. (2005) have achieved the removal of the tissue response against alginate-PLL capsules by temporary release of co-encapsulated steroids [152].

Another form to improve the clinical results of cell-based drug delivery is taking into account the physiological environments of cell-hydrogel implants. The majority of cell-hydrogel capsules are implanted in the peritoneum cavity, but the under vascularized structure leads to hypoxic conditions, which limits the transport of oxygen, nutrients, and therapeutic molecules. Several tissue-engineering technologies to promote the capillary vascular network formation (e.g., delivery of angiogenic growth factors, transplantation of endothelial progenitor cells) may facilitate the transport of biological molecules from and into the hydrogels.

A new technique for artificial cell microencapsulation using carbon nanotubes (CNT) has shown the potential to carry molecules and enter mammalian and bacterial cells. CNT can be functionalized with a variety of molecules for specific purposes and beneficially used to deliver proteins, genes and nucleic acids, drugs and other therapeutics into cells. It was reported the successful incorporation of CNT in alginate capsules. On the other hand, nanotubes were observed to be better distributed on alginate-PLL capsule surfaces compared to pure alginate capsule surfaces. This finding validates the hypothesis that PLL, on account of its positive charge, could electrostatically interact with and attract negatively charged carboxylated single-walled nanotubes. This study could serve as a first step towards the design of efficient nanotube bearing capsule devices for in vivo targeted delivery of therapeutic-functionalized nanotubes [153]. The biocompatibility of the nanotubes and the encapsulation materials, which has been already established through various studies, makes it possible to use this device for therapeutic purposes. Also it was demonstrated the formation of PLL and alginate layers on alginate cores carrying CNTs. In addition, CNTs functionalized with enzymes, can be used as reusable biocatalytic structures, for both therapeutic and industrial application [154].

Human fetal kidney 293/GFP cells were entrapped in calcium alginate beads using a novel microfluidic device that utilizes a silicon micro-nozzle array enabling to prepare beads of 50–200 μm in diameter [155]. A 1.5 % sodium alginate solution containing $1{\cdot}10^7$ cells/mL was fed into the flow of soybean oil through the silicon micro-nozzle in the upper stream solution of soybean oil flow, while an 0.1 M $CaCl_2$ containing 0.14 M NaCl was fed in the downstream area of the oil flow. The droplets of sodium alginate containing cells collide with $CaCl_2$ droplets and the reaction between the alginate and Ca^{2+} proceeds by coalescence of the droplets. The beads were formed under sterile conditions and without chemically irritant materials such as surfactants, which enabled successful encapsulation of living cells in cross-linked calcium alginate. The beads prepared by this method would be useful as sophisticated biomaterials for use in medical, pharmaceutical, and bioengineering fields [155].

Osseous tumours, trauma and other debilitating diseases can create a need to fill defects. Most bone tissue engineering strategies rely on the use of temporary scaffolds that can be seeded with cells prior to implantation, or designed to induce the formation of bone from the surrounding tissue after implantation. Depending on the specificity of the illness, bioactive agents such as growth factors or other protein drugs can be locally released and potentially accelerate the process of bone regeneration. Ribeiro et al. (2004) prepared microspheres of calcium titanium phosphate-alginate and hydroxiapatite-alginate to be used as enzyme delivery matrices and bone regeneration templates [156].

Enzymes are well-known green catalysts that possess a high degree of specificity. The specificity involves discrimination between substrates, similar parts of molecules (regiospecificity), and optical isomers (stereospecificity). The specificity of enzymes increases their applications in pharmaceutical synthesis, food processing, biosensors fabrication, bioremediation, and protein digestion in proteomic analysis. Enzyme immobilization is a requisite for its stability since the multiple-point attachment to the support can restrict the undesirable conformational change of enzyme proteins in unfriendly environments and enables repeated use. Different functional groups such as amino, hydroxyl, epoxy, carboxyl, and phenolic groups are adequate to covalent enzyme immobilization. Also, a multienzyme system can be obtained by means of polymer modification. Among the methods of polymer modification, graft copolymerization may impart a variety of new functional groups to a polymer. One of them is the photografting, performed by irradiating the polymer in the solvent containing selected monomers. UV radiation has been extensively applied for surface graft polymerization employing a photoinitiator. It has been reported that glycidyl methacrylate (GMA) is an attractive monomer and benzophenone (BP) is an efficient initiator for photochemical grafting. GMA has a reactive epoxide group which can form stable covalent bonds with biomolecules without linkers. Such epoxy-modified polymers are stable and resistant against hydrolysis, and proteins can be covalently coupled by opening the epoxide bridge in alkaline media. Then, it is possible an appropriate enzyme immobilization onto a suitable support material and to develop a model which enables reactions catalyzed with different enzymes. Sodium alginate was used as immobilization material and glycidyl methacrylate was grafted onto

sodium alginate; thus reactive epoxy groups were added to sodium alginate. After that, GMA grafted sodium alginates were used for urease immobilization by mean of carboxyl groups at low pH or by mean of epoxy groups at high pH. By this way, enzyme immobilization could be done according to pH selectivity during immobilization. Urease, a frequent enzyme in biological systems, catalyzes the hydrolysis of urea. Immobilized form of urease has found broad applications, such as blood detoxification in artificial kidneys, removal of urea from beverages in food industry, and reduction of urea content in effluent treatment in agriculture [157].

7.6.2 Environmental Applications

7.6.2.1 Active Packaging

The concept of *active packaging* is related to the mode of interaction between the package, the product, and the environment to extend shelf life or enhance safety or sensory properties, while maintaining the nutritional quality of the product. In the last decades numerous studies concerning to edible or biodegradable films and coatings has been proven with the objective of extending the shelf life of foods and to increase their quality. Alginate, as other biopolymers, act as selective barrier for moisture, gas, and solute migration but also as a food additive carrier. In the last case, antimicrobial effects of alginate-based film containing essential oils for the preservation of whole beef muscle has been reported [158].

It is known that essential oils (EOs) extracted from herbs and their components have many applications in medicine, in fragrance, and also in food flavoring and preservation. Among them, oregano, savory, and cinnamon EO-based films have been reported to prevent lipid oxidation when added in various food systems avoiding oxidative deterioration of foods. Then EO natural antioxidant agents were added to alginate/polycaprolactone-based films. Moreover the films were then treated in 2 or 20 %w/v $CaCl_2$ solutions in order to generate insoluble films. Oregano-based films showed the highest antiradical properties, while cross-linking by $CaCl_2$ (20 %) decreased their solubility, and improved their mechanical properties [159].

Also, the microbial quality decay kinetics during storage of Mozzarella cheese was evaluated. Lemon extract, at three different concentrations, was used as active agent, in combination with brine and with a gel solution made of sodium alginate. Results show an increase in the shelf life of all active packaged Mozzarella cheeses, confirming that investigated substance may exert an inhibitory effect on the microorganisms responsible for spoilage phenomena [160].

7.6.2.2 Biodiesel and Bioethanol Production

Biodiesel is a clean-burning fuel produced from vegetable oils or animal fats. Biodiesel is produced by transesterification of oils with short-chain alcohols or by

the esterification of fatty acids. By transesterification triglycerides are transformed into fatty acid alkyl esters, in the presence of an alcohol, such as methanol or ethanol, and a catalyst, such as an alkali or acid, with glycerol as a byproduct. The transesterification of algae oil into fatty acid methyl ester (biodiesel) is one of the well known routes to obtain biofuel from algae and it has been in practice for many years. While microalgae strains that are rich in oil content can be used for producing biodiesel, other strains of microalgae and macroalgae can also be used as energy feedstock. Fuels such as ethanol, methane, hydrogen and other hydrocarbon fuels can be derived from these, through a variety of processes.

Alginate has a potential as substrate for the production of bioenergy. However, enzymatic saccharification of alginate producing oligoalginates is a prerequisite when alginate is going to be used as the renewable source for biofuel. In biocatalytic processes for the production of value-added bioproducts, re-use of enzymes by immobilization is often the key to enhance the economic feasibility. Recombinant alginate lyase was efficiently immobilized onto two types of magnetic nanoparticles, super paramagnetic iron oxide nanoparticle, and hybrid magnetic silica nanoparticle. An alginate oligosaccharide mixture consisting of dimer and trimer was prepared by the immobilized alginate lyase. The immobilized enzymes were re-used repeatedly more than ten times after magnetic separation [161].

Ethanol technology uses fermentation to convert algae directly from culture to ethanol. From a collection of 10,000 strains of algae and using molecular biology some strains have been enhanced. Some of these new strains have the ability of produce some sugars and produce ethanol enzymaticaly by fermentation. Then, bioethanol production from algae is a promising approach that resolves problems associated with biofuel production from land biomass, such as bioethanol–food conflicts and the indirect land use change. However, there are some technical difficulties because existing ethanologenic microbes can neither degrade alginate, a major component of brown algae, nor assimilate alginate degradation products. Then it was necessary to develop an integrated bacterial system for converting alginate to ethanol using a metabolically modified, alginate-assimilating, pit-forming bacterium, *Sphingomonas* sp. A1 (strain A1) [162].

7.6.2.3 Ultra- and Nano-Filtration

Hybrid (inorganic/organic) tubular ultrafiltration and nanofiltration (UF/NF) ceramic membranes functionalized with alginate, allowed for cadmium ions removal from waste water at low pressure(s) and high throughput rates. The tubes consisted of a macroporous alumina support and the deposition and stabilization of alginates was carried out via physical (filtration/cross-linking) and chemical (grafting) procedures. An advantage of membrane-based sorbents is that functional groups can be attached to the membrane pores as polymeric ligands. The interaction with heavy metal ions is enhanced because functional groups are available along the path where contaminated solutions flow through the porous structure [163].

De Moura et al. (2005) prepared thermo-sensitive porous hydrogels composed of interpenetrated networks (IPN) of alginate-Ca^{2+} and poly(N-isopropilacrilamida) (PNIPAAm). Hydrogels were prepared by cross-linking sodium alginate with Ca^{2+} ions inside PNIPAAm networks. Warming IPN hydrogels induced the collapse of the PNIPAAm chains, becoming hydrophobic with a prevalence of intramolecular interactions. Then, polymer chains may be re-arranged in order to occupy the empty spaces (pores occupied by water), thus decreasing the pore size of the hydrogel. Among other, these thermo-responsible materials could be used as separation membranes [164].

7.7 Concluding Remarks

Alginates have been considered for medical applications such as drug delivery, wound coverage material, and cell encapsulation/transplantation based on its unique properties such as emulsifiers, thickeners, stabilizers, gelling and film forming resulting in several applications.

On the other hand, alginate structure can also be chemically modified in order to design smart materials for special applications. The reactivity of alginate functional groups can be exploited as a potential tool for the modification of interesting properties such as solubility, hydrophobicity, and physicochemical and biological characteristics.

Alginate has been regarded as an excellent polysachaccharide for the food and pharmaceutical industries because of its unique features such as biocompatibility, biodegradability, immnogenecity, and non-toxicity.

Acknowledgments We express our gratitude to the Consejo Nacional de Investigaciones Científicas y Técnicas de la República Argentina (CONICET) and the Universidad Nacional del Sur (UNS, Argentina).

References

1. Usov, A.I.: Alginic acids and alginates: analytical methods used for their estimation and characterization of composition and primary structure. Russ. Chem. Rev. **68**, 957–966 (1999)
2. Chèze-Lange, H., Beunard, D., Dhulster, P., Guillochon, D., Cazé, A.M., Saude, N., Morcellet, M., Junter, G.A.: Production of microbial alginate in a membrane bioreactor. Enzym. Microb. Technol. **30**, 656–661 (2002)
3. Hernández-Carmona, G., McHuge, D.J., Arvizu-Higuera, D.L., Rodríguez-Montesinos, Y.E.: Pilot plant scale extraction of alginate from *Macrocystis pyrifera*. 1. Effect of pre-extraction treatments on yield and quality of alginate. J. Appl. Phycol. **10**, 507–513 (1999)
4. Gómez, C.G., Pérez Lambrecht, M.V., Lozano, J.E., Rinaudo, M., Villar, M.A.: Influence of the extraction-purification conditions on final properties of alginates obtained from brown algae (*Macrocystis pyrifera*). Int. J. Biol. Macromol. **44**, 365–371 (2009)
5. McHugh, D.J.: Production, properties and uses of alginates. In: McHugh, D.J. (ed.) Production and utilization of products from commercial seaweeds. FAO Fish. Aquaculture Tech. Pap. **288**, 58–115 (1987)

6. Arvizu-Higuera, D.L., Hernández-Carmona, G., Rodríguez-Montesinos, Y.E.: Efecto del tipo de precipitación en el procesos de obtención de alginato de sodio: Método de alginato de calcio y método de ácido algínico. Cien. Marinas **23**, 195–207 (1997)
7. Ertesvåg, H., Valla, S.: Biosynthesis and applications of alginates. Polym. Degrad. Stab. **59**, 85–91 (1998)
8. Navarro da Silva, A., García-Cruz, C.H.: Biopolymers by *Azotobacter vinelandii*. In: Elnashar, M. (ed) Biopolymers 2010, InTech—Open Access Publisher, Chapter 21, 413–438 (2010)
9. Klöck, G., Pfefferman, A., Ryser, C., Gröhn, P., Kuttler, B., Hahn, H.J., Zimmermann, U.: biocompatibility of mannuronic acid-rich alginates. Biomaterials **18**, 707–713 (1997)
10. Rowley, J.A., Madlambayan, G., Mooney, D.J.: Alginate hydrogels as synthetic extracellular matrix materials. Biomaterials **20**, 45–53 (1999)
11. Avella, M., Di Pace, E., Immirzi, B., Impallomeni, G., Malinconico, M., Santagata, G.: Addition of glycerol plasticizer to seaweeds derived alginates: Influence of microstructure on chemical-physical properties. Carbohydr. Polym. **69**, 503–511 (2007)
12. Yang, J.S., Xie, Y.J., He, W.: Research progress on chemical modification of alginate: A review. Carbohydr. Polym. **84**, 33–39 (2011)
13. Nakamura, K., Nishimura, Y., Hatakeyama, T., Hatakeyama, H.: Thermal properties of water insoluble alginate films containing di- and trivalent cations. Thermochim. Acta **267**, 343–353 (1995)
14. Draget, K.I., Taylor, C.: Chemical, physical and biological properties of alginates and their biomedical implications. Food Hydrocolloids **25**, 251–256 (2011)
15. Sharon, N.: Complex carbohydrates, their chemistry, biosynthesis, and functions. Addison-Wesley Pub Co Reading, Massachussets (1975)
16. Kristiansen, K.A., Potthast, A., Christensen, B.E.: Periodate oxidation of polysaccharides for modification of chemical and physical properties. Carbohydr. Res. **345**, 1264–1271 (2010)
17. Gómez, C.G., Rinaudo, M., Villar, M.A.: Oxidation of sodium alginate and characterization of the oxidized derivatives. Carbohydr. Polym. **67**, 296–304 (2007)
18. Vold, I.M.N., Christensen, B.E.: Periodate oxidation of chitosans with different chemical compositions. Carbohydr. Res. **340**, 679–684 (2005)
19. Vold, I.M.N., Kristiansen, K.A., Christensen, B.E.: A study of the chain stiffness and extension of alginates, in vitro epimerized alginates, and periodate-oxidized alginates using size exclusion chromatography combined with light scattering and viscosity detectors. Biomacromolecules **7**, 2136–2146 (2006)
20. Larsen, B., Painter, T.J.: The periodate-oxidation limit of alginate. Carbohydr. Res. **10**, 186–187 (1969)
21. Perlin, A.S.: Glycol-cleavage oxidation. Adv. Carbohydr. Chem. Biochem. **60**, 183–250 (2006)
22. Andresen, I.L., Painter, T., Smidsrød, O.: Concerning the effect of periodate oxidation upon the intrinsic viscosity of alginate. Carbohydr. Res. **59**, 563–566 (1977)
23. Painter, T.J.: Control of depolymerisation during the preparation of reduced dialdehyde cellulose. Carbohydr. Res. **179**, 259–268 (1988)
24. Pescosolido, L., Piro, T., Vermonden, T., Coviello, T., Alhaique, F., Hennink, W.E., Matricardi, P.: Biodegradable IPNs based on oxidized alginate and dextran-HEMA for controlled release of proteins. Carbohydr. Polym. **86**, 208–213 (2011)
25. Bouhadir, K.H., Lee, K.Y., Alsberg, E., Damm, K.L., Anderson, K.W., Mooney, D.J.: Degradation of partially oxidized alginate and its potential application for tissue engineering. Biotechnol. Prog. **17**, 945–950 (2001)
26. Li, X., Xu, A., Xie, H., Yu, W., Xie, W., Ma, X.: Preparation of low molecular weight alginate by hydrogen peroxide depolymerization for tissue engineering. Carbohydr. Polym. **79**, 660–664 (2010)
27. Cosenza, V.A., Navarro, D.A., Stortz, Carlos A.: Usage of α-picoline borane for the reductive amination of carbohydrates, ARKIVOC **7**, 182–194 (2011)

28. Rinaudo, M.: New amphiphilic grafted copolymers based on polysaccharides. Carbohydr. Polym. **83**, 1338–1344 (2011)
29. Creuzet, C., Kadi, S., Rinaudo, M., Auzély-Velty, R.: New associative systems based on alkylated hyaluronic acid. Synthesis and aqueous solution properties. Polymer **47**, 2706–2713 (2006)
30. Gómez, C.G., Chambat, G., Heyraud, A., Villar, M.A., Auzély-Velty, R.: Synthesis and characterization of a β-CD-alginate conjugate. Polymer **47**, 8509–8516 (2006)
31. Boanini, E., Rubini, K., Panzavolta, S., Bigi, A.: Chemico-physical characterization of gelatin films modified with oxidized alginate. Acta Biomater. **6**, 383–388 (2010)
32. Balakrishnan, B., Mohanty, M., Umashankar, P.R., Jayakrishnan, A.: Evaluation of an in situ forming hydrogel wound dressing based on oxidized alginate and gelatine. Biomaterials **26**, 6335–6342 (2005)
33. Zhiyong, L., Caihua, N., Cheng, X., Qian, L.: Preparation and drug release of hydrophobically modified alginate. Chemistry **1**, 93–96 (2009)
34. Alban, S., Schauerte, A., Franz, G.: Anticoagulant sulfated polysaccharides: Part I. Synthesis and structure-activity relationships of new pullulan sulphates. Carbohydr. Polym. **47**, 267–276 (2002)
35. Fan, L., Jiang, L., Xu, Y., Zhou, Y., Shen, Y., Xie, W., Long, Z., Zhou, J.: Synthesis and anticoagulant activity of sodium alginate sulphates. Carbohydr. Polym. **83**, 1797–1803 (2011)
36. Laurienzo, P., Malinconico, M., Motta, A., Vicinanza, A.: Synthesis and characterization of a novel alginate-poly(ethylene glycol) graft copolymer. Carbohydr. Polym. **62**, 274–282 (2005)
37. Yang, L., Zhang, B., Wen, L., Liang, Q., Zhang, L.M.: Amphiphilic cholesteryl grafted sodium alginate derivative: Synthesis and self-assembly in aqueous solution. Carbohydr. Polym. **68**, 218–225 (2007)
38. Kennedy, J.P.: Recent advances in polymer blends, grafts, and blocks. In: Sperling, L.H. (ed.) Plenum, New York (1974)
39. Yang, W., Zhang, L., Wu, L., Li, J., Wang, J., Jiang, H., Li, Y.: Synthesis and characterization of MMA-NaAlg/hydroxyapatite composite and the interface analyse with molecular dynamics. Carbohydr. Polym. **77**, 331–337 (2009)
40. Işiklan, N., Inal, M., Kurşun, F., Ercan, G.: pH responsive itaconic acid grafted alginate microspheres for the controlled release of nifedipine. Carbohydr. Polym. **84**, 933–943 (2011)
41. Yadav, M., Sand, A., Behari, K.: Synthesis and characterization of graft copolymer (alginate-g-poly(N, N-dimethylacrylamide). Chin. J. Polym. Sci. **28**, 673–683 (2010)
42. Colinet, I., Dulong, V., Hamaide, T., Le Cerf, D., Picton, L.: New amphiphilic modified polysaccharides with original solution behaviour in salt media. Carbohydr. Polym. **75**, 454–462 (2009)
43. Babak, V.G., Skotnikova, E.A., Lukina, I.G., Pelletier, S., Hubert, P., Dellacherie, E.: Hydrophobically associating alginate derivatives: Surface tension properties of their mixed aqueous solutions with oppositely charged surfactants. J. Colloid Interface Sci. **225**, 505–510 (2000)
44. De Boisseson, M.R., Leonard, M., Hubert, P., Marchal, P., Stequert, A., Castel, C., Favre, E., Dellacherie, E.: Physical alginate hydrogels based on hydrophobic or dual hydrophobic/ionic interactions: Bead formation, structure, and stability. J. Colloid Interface Sci. **273**, 131–139 (2004)
45. Li, Q., Liu, C.G., Huang, Z.H., Xue, F.F.: Preparation and characterization of nanoparticles based on hydrophobic alginate derivative as carriers for sustained release of vitamin D_3. J. Agric. Food Chem. **59**, 1962–1967 (2011)
46. Lee, J.W., Park, J.H., Robinson, J.R.: Bioadhesive-based dosage forms: The next generation. J. Pharm. Sci. **89**, 850–866 (2000)
47. Bernkop-Schnurch, A.: Mucoadhesive polymers. In: Dumitriu, S. (ed.) Polymer Biomaterial, pp. 147–165, Marcel Dekker, New York (2002)

48. Davidovich-Pinhas, M., Bianco-Peled, H.: Alginate-PEGAc. A new mucoadhesive polymer. Acta Biomater. **7**, 625–633 (2011)
49. Almany, L., Seliktar, D.: Biosynthetic hydrogel scaffolds made from fibrinogen and polyethylene glycol for 3D cell cultures. Biomaterials **26**, 2467–2477 (2005)
50. Ugi, I.: The α-addition of immonium ions and anions to isonitriles accompanied by secondary reactions. Angew. Chem. Int. Ed. **1**, 8–21 (1962)
51. Bu, H., Kjøniksen, A.L., Elgsaeter, A., Nyström, B.: Interaction of unmodified and hydrophobically modified alginate with sodium dodecylsulfate in dilute aqueous solution. Calorimetric, rheological, and turbidity studies. Colloids Surf. A Physicochem. Eng. Aspects **278**, 166–174 (2006)
52. Bu, H., Kjøniksen, A.L., Knudsen, K.D., Nyström, B.: Rheological and structural properties of aqueous alginate during gelation via the Ugi multicomponent condensation reaction. Biomacromolecules **5**, 1470–1479 (2004)
53. García, A., Hernández, K., Chico, B., García, D., Villalonga, M.L., Villalonga, R.: Preparation of thermostable trypsin-polysaccharide neoglycoenzymes trough Ugi multicomponent reaction. J. Mol. Catal. B: Enzym. **59**, 126–130 (2009)
54. Eiselt, P., Lee, K.Y., Mooney, D.J.: Rigidity of two-component hydrogels prepared from alginate and poly(ethylene glycol)-diamines. Macromolecules **32**, 5561–5566 (1999)
55. Lee, K.Y., Rowley, J.A., Eiselt, P., Moy, E.M., Bouhadir, K.H., Mooney, D.J.: Controlling mechanical and swelling properties of aginate hydrogels independently by cross-linker type and cross-linking density. Macromolecules **33**, 4291–4294 (2000)
56. Kim, W.T., Chung, H., Shin, I.S., Yam, K.L., Chung, D.: Characterization of calcium alginate and chitosan-treated calcium alginate gel beads entrapping allyl isothiocyanate. Carbohydr. Polym. **71**, 566–573 (2008)
57. Ribeiro, A.C.F., Sobral, A.J.F.N., Simões, S.M.N., Barros, M.C.F., Lobo, V.M.M., Cabral, A.M.T.D.P.V., Veiga, F.J.B., Santos, C.I.A.V., Esteso, M.A.: Transport properties of aqueous solutions of sodium alginate at 298.15 K. Food Chem. **125**, 1213–1218 (2011)
58. Gazori, T., Khoshayand, M.R., Azizi, E., Yazdizade, P., Normani, A., Haririan, I.: Evaluation of alginate/chitosan nanoparticles as antisense delivery vector: Formulation, optimization and in vitro characterization. Carbohydr. Polym. **77**, 599–606 (2009)
59. Soares, J.P., Santos, J.E., Chierice, G.O., Cavalheiro, E.T.G.: Thermal behavior of alginic acid and its sodium salt. Eclética Química **29**, 57–63 (2004)
60. Davidovich-Pinhas, M., Bianco-Peled, H.: Physical and structural characteristics of acrylated poly(ethylene glycol)-alginate conjugates. Acta Biomater. **7**, 2817–2825 (2011)
61. Andresen, I.L., Smidsørod, O.: Temperature dependence of the elastic properties of alginate gels. Carbohydr. Res. **58**, 271–279 (1977)
62. Funami, T., Fang, Y., Noda, S., Ishihara, S., Nakauma, M., Draget, K.I., Nishinari, K., Phillips, G.O.: Rheological properties of sodium alginate in an aqueous system during gelation in relation to supermolecular structures and Ca^{2+} binding. Food Hydrocolloids **23**, 1746–1755 (2009)
63. Walsh, P.K., Isdell, F.V., Noone, S.M., O′Donovan, M.G., Malone, D.M.: Growth patterns of *Saccharomyces cerevisiae* microcolonies in alginate and carrageenan gel particles: Effect of physical and chemical properties of gels. Enzym. Microb. Technol. **18**, 366–372 (1996)
64. Draget, K.I., Østgaard, K., Smidsrød, O.: Homogeneous alginate gels: A technical approach. Carbohydr. Polym. **14**, 159–178 (1990)
65. Chan, L.W., Lee, H.Y., Heng, P.W.S.: Mechanisms of external and internal gelation and their impact on the functions of alginate as a coat and delivery system. Carbohydr. Polym. **63**, 176–187 (2006)
66. Münstedt, H., Auhl, D.: Rheological measuring techniques and their relevance for the molecular characterization of polymers. J. Non-newton. Fluid Mech. **128**, 62–69 (2005)
67. Mancini, M., Moresi, M., Sappino, F.: Rheological behaviour of aqueous dispersions of algal sodium alginates. J. Food Eng. **28**, 283–295 (1996)
68. Smidsrϕd, O.: Solution properties of alginate. Carbohydrate research **13**, 359–372 (1970)

69. Clementi, F., Mancini, M., Moresi, M.: Rheology of alginate from *Azotobacter vinelandii* in aqueous dispersions. J. Food Eng. **36**, 51–62 (1998)
70. Moe, S.T., Draget, K.I., Skjåk-Bræk, G., Smidsrød, O.: Alginate, In: Stephen, A.M. (ed.) Food Polysaccharides and their Applications, pp. 245–286. Marcel Dekker, Inc., New York (1995)
71. Sime, W.J.: Alginates. In: Harris, P. (ed.) Food gels, pp. 53-78. Elsevier Science Pub., London (1990)
72. Mancini, M., Moresi, M., Rancini, R.: Uniaxial compression and stress relaxation tests on alginate gels. J. Texture Stud. **30**, 639–657 (1999)
73. Mitchell, J.R., Blanshard, J.M.V.: Rheological properties of alginate gels. J. Texture Stud. **7**, 219–234 (1976)
74. Moresi, M., Mancini, M., Bruno, M., Rancini, R.: Viscoelastic properties of alginate gels by oscillatory dynamic tests. J. Texture Stud. **32**, 375–396 (2001)
75. Kurachi, M., Nakashima, T., Miyajima, C., Iwamoto, Y., Muramatsu, T., Yamaguchi, K., Oda, T.: Comparison of the activities of various alginates to induce TNF-α secretion in RAW264.7 cells. J. Infect. Chemother. **11**, 199–203 (2005)
76. Espevik, T., Rokstad, A.M., Kulseng, B., Strand, B., Skjåk-Bræk, G.: Mechanisms of the host immune response to alginate microcapsules. In: Hallé, J.P., de Vos, P., Rosenberg, L. (eds.) The bioartificial pancreas and other biohybrid therapies, Transworld Research Network, pp. 279–290 (2009)
77. Suzuki, S., Christensen, B.E., Kitamura, S.: Effect of mannuronate content and molecular weight of alginates on intestinal immunological activity through Peyer′s patch cells of C3H/HeJ mice. Carbohydr. Polym. **83**, 629–634 (2011)
78. Dohnal, J., Štěpánek, F.: Inkjet fabrication and characterization of calcium alginate microcapsules. Powder Technol. **200**, 254–259 (2010)
79. Ciofani, G., Raffa, V., Pizzorusso, T., Menciassi, A., Dario, P.: Characterization of an alginate-based drug delivery system for neurological applications. Med. Eng. Phys. **30**, 848–855 (2008)
80. Kulkarni, A.R., Soppimath, K.S., Aminabhavi, T.M., Rudzinski, W.E.: In vitro release kinetics of cefadroxil-loaded sodium alginate interpenetrating networks beads. Eur. J. Pharm. Biopharm. **51**, 127–133 (2001)
81. Gong, J.P., Katsuyama, Y., Kurokawa, T., Osada, Y.: Double network hydrogels with extremely high mechanical strength. Adv. Mater. **15**, 1155–1158 (2003)
82. Knill, C.J., Kennedy, J.F., Mistry, J., Miraftab, M., Smart, G., Groocock, M.R., Williams, H.J.: Alginate fibres modified with unhydrolysed and hydrolysed chitosans for wound dressing. Carbohydr. Polym. **55**, 65–76 (2004)
83. Wang, Q., Hu, X., Du, Y., Kennedy, J.F.: Alginate/starch blend fibers and their properties for drug controlled release. Carbohydr. Polym. **82**, 842–847 (2010)
84. Lansdown, A.B.G.: Calcium: a potent central regulator in wound healing in the skin. Wound Repair Regeneration **10**, 271–285 (2002)
85. Hampson, F.C., Farndale, A., Strugala, V., Sykes, J., Jolliffe, I.G., Dettmar, P.W.: Alginate rafts and their characterisation. Int. J. Pharm. **294**, 137–147 (2005)
86. Herranz, F., Almarza, E., Rodríguez, I., Salinas, B., Rosell, Y., Desco, M., Bulte, J.W., Ruiz-Cabello, J.: The application of nanoparticles in gene therapy and magnetic resonance imaging. Microsc. Res. Tech. **74**, 577–591 (2011)
87. Berman, S.M., Walczak, P., Bulte, J.W.: MRI of transplanted neural stem cells. Methods Mol. Biol. **711**, 435–449 (2011)
88. Kraitchman, D.L., Kedziorek, D.A., Bulte, J.W.: MR imaging of transplanted stem cells in myocardial infarction. Methods Mol. Biol. Part 2. **680**, 141–152 (2011)
89. Barnett, B.P., Kraitchman, D.L., Lauzon, C., Magee, C.A., Walczak, P., Gilson, W.D., Arepally, A., Bulte, J.W.: Radiopaque alginate microcapsules for X-ray visualization and immunoprotection of cellular therapeutics. Mol. Pharm. **3**, 531–538 (2006)
90. Karussis, D., Karageorgiou, C., Vaknin-Dembinsky, A., Gowda-Kurkalli, B., Gomori, J.M., Kassis, I., Bulte, J.W., Petrou, P., Ben-Hur, T., Abramsky, O., Slavin, S.: Safety and

immunological effects of mesenchymal stem cell transplantation in patients with multiple sclerosis and amyotrophic lateral sclerosis. Arch. Neurol. **67**, 1187–1194 (2010)
91. Brownlee, I.A., Allen, A., Pearson, J.P., Dettmar, P.W., Havler, E., Atherton, M.R., Onsøyen, E.: Alginate as a source of dietary fiber. Crit. Rev. Food Sci. Nutr. **45**, 497–510 (2005)
92. Dettmar, P.W., Strugala, V., Richardson, J.C.: The key role alginates play in health. Food Hydrocolloids **25**, 263–266 (2011)
93. King, S., See, H., Thomas, G., Swain, M.: Determining the complex modulus of alginate irreversible hydrocolloid dental material. Dent. Mater. **24**, 1545–1548 (2008)
94. Maynard, E.M., Fernández, E., Normann, R.A.: A technique to prevent dural adhesions to chronically implanted microelectrode arrays. J. Neurosci. Methods **97**, 93–101 (2000)
95. Becker, T.A., Preul, M.C., Bichard, W.D., Kipke, D.R., McDougall, C.G.: Calcium alginate gel as a biocompatible material for endovascular arteriovenous malformation embolization: six-month results in an animal model. Neurosurgery **56**, 793–803 (2005)
96. Mammarella, E.M., Rubiolo, A.C.: Crosslinking kinetics of cation-hydrocolloid gels. Chem. Eng. J. **94**, 73–77 (2003)
97. Nunamaker, E.A., Otto, K.J., Kipke, D.R.: Investigation of the material properties of alginate for the development of hydrogel repair of dura mater. J. Mech. Behav. Biomed. Mater. **4**, 16–33 (2011)
98. Leitner, V.M., Walker, G.F., Bernkop-Schnurch, A.: Thiolated polymers: Evidence for the formation of disulfide bonds with mucus glycoproteins. Eur. J. Pharm. Biopharm. **56**, 207–214 (2003)
99. Davidovich-Pinhas, M., Harari, O., Bianco-Peled, H.: Evaluating the mucoadhesive properties of drug delivery systems based on hydrated thiolated alginate. J. Controlled Release **136**, 38–44 (2009)
100. Wang, Y.Y., Lai, S.K., Suk, J.S., Race, A., Cone, R., Hanes, J.: Addressing the PEG mucoadhesivity paradox to engineering nanoparticles that "slip" through the human mucus barrier. Angew. Chem. Int. **47**, 9726–9729 (2008)
101. Taylor, C., Pearson, J.P., Draget, K.I., Dettmarc, P.W., Smidsrød, O.: Rheological characterisation of mixed gels of mucin and alginate. Carbohydr. Polym. **59**, 189–195 (2005)
102. Rajaonarivony, M., Vauthier, C., Couarraze, A., Puisieux, F., Couvreur, P.: Development of a new drug carrier made from alginate. J. Pharm. Sci. **2**, 912–917 (1993)
103. Motwani, S.K., Chopra, S., Talegaonkar, S., Kohli, K., Ahmad, F.J., Khar, R.K.: Chitosan-sodium alginate nanoparticles as submicroscopic reservoirs for ocular delivery: Formulation, optimization and in vitro characterization. Eur. J. Pharm. Biopharm. **68**, 513–525 (2008)
104. Thomas, A., Harding, K.G., Moore, K.: Alginates from wound dressings activate human macrophages to secret tumour necrosis factor-α. Biomaterials **21**, 1797–1802 (2000)
105. Paul, W., Sharma, C.P.: Chitosan and alginate wound dressings: A short review. Trends Biomater. Artif. Organs **18**, 18–23 (2004)
106. Queen, D., Gaylor, J.D.S., Evans, J.H., Courtney, J.M., Reid, W.H.: The preclinical evaluation of the water vapour transmission rate through burn wound dressings. Biomaterials **8**, 367–371 (1987)
107. Liu, Y., Chen, S., Zhong, L., Wu, G.Z.: Preparation of high-stable silver nanoparticle dispersion by using sodium alginate as a stabilizer under gamma radiation. Radiat. Phys. Chem. **78**, 251–255 (2009)
108. Anh, N.T., Phu, D.V., Duy, N.N., Du, B.D., Hien, N.Q.: Synthesis of alginate stabilized gold nanoparticles by γ-irradiation with controllable size using different Au^{3+} concentration and seed particles enlargement. Radiat. Phys. Chem. **79**, 405–408 (2010)
109. Corot, C., Robert, P., Idee, J.M., Port, M.: Recent advances in iron oxide nanocrystal technology for medical imaging. Adv. Drug Delivery Rev. **58**, 1471–1504 (2006)
110. Gupta, A.K., Gupta, M.: Synthesis and surface engineering of iron oxide nanoparticles for biomedical applications. Biomaterials **26**, 3995–4021 (2005)

111. Llanes, F., Ryan, D.H., Marchessault, R.H.: Magnetic nanostructured composites using alginates of different M/G ratios as polymeric matrix. Int. J. Biol. Macromol. **27**, 35–40 (2000)
112. Morales, M.A., Finotelli, P.V., Coaquira, J.A.H., Rocha-Leão, M.H.M., Diaz-Aguila, C., Baggio-Saitovitch, E.M., Rossi, A.M.: In situ synthesis and magnetic studies of iron oxide nanoparticles in calcium-alginate matrix for biomedical applications. Mater. Sci. Eng. C **28**, 253–257 (2008)
113. Leung, K.: Molecular imaging and contrast agent database (MICAD), National Institute of Health (2011)
114. Ma, H.L., Xu, Y.F., Qi, X.R., Maitani, Y., Nagai, T.: Preparation and characterization of super paramagnetic iron oxide nanoparticles stabilized by alginate. Int. J. Pharm. **333**, 177–186 (2007)
115. Ma, H.L., Xu, Y.F., Qi, X.R., Maitani, Y., Nagai, T.: Super paramagnetic iron oxide nanoparticles stabilized by alginate: Pharmacokinetics, tissue distribution, and applications in detecting liver cancers. Int. J. Pharm. **354**, 217–226 (2008)
116. Gololobov, Y.G., Zhmurova, I.N., Kasukhin, L.F.: Sixty years of Staudinger reaction. Tetrahedron **198**(37), 437–472
117. Hall, K.K., Gattás-Asfura, K.M., Stabler, C.L.: Microencapsulation of islets within alginate/poly(ethylene glycol) gels cross-linked via Staudinger ligation. Acta Biomater. **7**, 614–624 (2011)
118. Polyak, B., Geresh, S., Marks, R.S.: Synthesis and characterization of a biotin-alginate conjugate and its application in a biosensor construction. Biomacromolecules **5**, 389–396 (2004)
119. Polyak, B., Bassis, E., Novodvorets, A., Belkin, S., Marks, R.S.: Bioluminescent whole cell optical fiber sensor to genotoxicants: System optimization. Sens. Actuators B **74**, 18–26 (2001)
120. Abu-Rabeah, K., Marks, R.S.: Impedance study of the hybrid molecule alginate-pyrrole: Demonstration as host matrix for the construction of a highly sensitive amperometric glucose biosensor. Sens. Actuators B **136**, 516–522 (2009)
121. Liu, C., Guo, X., Cui, H., Yuan, R.: An amperometric biosensor fabricated from electro-co-deposition of sodium alginate and horseradish peroxidase. J. Mol. Catal. B Enzym. **60**, 151–156 (2009)
122. Eltzov, E., Pavluchkov, V., Burstin, M., Marks, R.S.: Creation of a fiber optic based biosensor for air toxicity monitoring. Sens. Actuators B **155**, 859–867 (2011)
123. Ichijo, H., Hirasa, O., Kishi, R., Oowada, M., Sahara, K., Kokufuta, E., Kohno, S.: Thermo-responsive gels. Radiat. Phys. Chem. **46**, 185–190 (1995)
124. Yu, J., Gu, Y., Du, K.T., Mihardja, S., Sievers, R.E., Lee, R.J.: The effect of injected RGD modified alginate on angiogenesis and left ventricular function in a chronic rat infarct model. Biomaterials **30**, 751–756 (2009)
125. Mc Cullen, S.D., Ramaswamy, S., Clarke, L.I., Gorga, R.G.: Nanofibrous composites for tissue engineering applications. Wiley Interdiscip. Rev. Nanomed. Nanobiotechnol. **1**, 369–390 (2009)
126. Abidian, M.R., Martin, D.C.: Multifunctional nanobiomaterials for neural interfaces. Adv. Funct. Mater. **19**, 573–585 (2009)
127. Chou, A.I., Akintoye, S.O., Nicoll, S.B.: Photo-crosslinked alginate hydrogels support enhanced matrix accumulation by nucleus pulpous cells in vivo. Osteoarthritis Cartilage **17**, 1377–1384 (2009)
128. Boerckel, J.D., Kolambkar, Y.M., Dupont, K.M., Uhrig, B.A., Phelps, E.A., Stevens, H.Y., García, A.J., Guldberg, R.E.: Effects of protein dose and delivery system on BMP-mediated bone regeneration. Biomaterials **32**, 5241–5251 (2011)
129. Kulkarni, A.R., Soppimath, K.S., Aminabhavi, T.M., Controlled release of diclofenac sodium from sodium alginate beads crosslinked with glutaraldehyde. Pharm. Acta Helv. **74**, 29–36 (1999)

130. Karewicz, A., Zasada, K., Szczubiałka, K., Zapotoczny, S., Lach, R., Nowakowska, M.: "Smart" alginate-hydroxypropylcellulose microbeads for controlled release of heparin. Int. J. Pharm. **385**, 163–169 (2010)
131. Chan, L.W., Heng, P.W.S., Wan, L.S.C.: Effect of cellulose derivatives on alginate microspheres prepared by emulsification. J. Microencapsul. **14**, 545–555 (1997)
132. Maysinger, D., Morinville, A.: Drug delivery to the nervous system. Trends Biotechnol. **15**, 410–418 (1997)
133. Xu, Y., Zhan, C., Fan, L., Wang, L., Zheng, H.: Preparation of dual croslinked alginate-chitosan blend gel beads and in vitro controlled release in oral site-specific drug delivery systems. J. Pharm. **336**, 329–337 (2007)
134. De, S., Robinson, D.: Polymer relationships during preparation of chitosan-alginate and poly(L-lysine)-alginate nanospheres. J. Controlled Release **89**, 101–112 (2003)
135. Dong, Z., Wang, Q., Du, Y.: Alginate/gelatin blend films and their properties for drug controlled release. J. Membr. Sci. **280**, 37–44 (2006)
136. Razem, D., Katusin-Razem, B.: The effects of irradiation on controlled drug delivery/controlled drug release systems. Radiat. Phys. Chem. **77**, 288–344 (2008)
137. Charoo, N.A., Kohli, K., Ali, A., Anwer, A.: Ophthalmic delivery of ciprofloxacin hydrochloride from different polymer formulations: In vitro and in vivo studies. Drug Dev. Ind. Pharm. **29**, 215–221 (2003)
138. Yang, S.J., Lin, F.H., Tsai, H.M., Lin, C.F., Chin, H.C., Wong, J.M., Shieh, M.J.: Alginate-folic acid-modified chitosan nanoparticles for photodynamic detection of intestinal neoplasms. Biomaterials **32**, 2174–2182 (2011)
139. Mladenovska, K., Cruaud, O., Richomme, P., Belamie, E., Raicki, R.S., Venier-Julienne, M.C., Popovski, E., Benoit, J.P., Goracinova, K.: 5-ASA loaded chitosan-Ca-alginate microparticles: Preparation and physicochemical characterization. Int. J. Pharm. **345**, 59–69 (2007)
140. Mladenovska, K., Raicki, R.S., Janevik, E.I., Ristoski, T., Pavlova, M.J., Kavrakovski, Z., Dodov, M.G., Goracinova, K.: Colon-specific delivery of 5-aminosalicylic acid from chitosan-Ca-alginate microparticles. Int. J. Pharm. **342**, 124–136 (2007)
141. Joshi, G.V., Pawar, R.R., Kevadiya, B.D., Bajaj, H.C.: Mesoporous synthetic hectorites: A versatile layered host with drug delivery application. Microporous Mesoporous Mater. **142**, 542–548 (2011)
142. Schmidt, J.J., Rowley, J., Kong, H.J.: Hydrogels used for cell-based drug delivery. J. Biomed. Mater. Res. Part A **87A**, 1113–1122 (2008)
143. Boontheekul, T., Kong, H.J., Mooney, D.J.: Controlling alginate gel degradation utilizing partial oxidation and bimodal molecular weight distribution. Biomaterials **26**, 2455–2465 (2007)
144. Kong, H.J., Kaigler, D., Kim, K., Mooney, D.J.: Controlling rigidity and degradation of alginate hydrogels via molecular weight distribution. Biomacromolecules **5**, 1720–1727 (2004)
145. Hori, Y., Winans, A.M., Huang, C.C., Horrigan, E.M., Irvine, D.J.: Injectable dendritic cell-carrying alginate gels for immunization and immunotherapy. Biomaterials **29**, 3671–3682 (2008)
146. Hori, Y., Winans, A.M., Irvine, D.J.: Modular injectable matrices based on alginate solution/microsphere mixtures that gel in situ and co-deliver immunomodulatory factors. Acta Biomater. **5**, 969–982 (2009)
147. Soon-Shiong, P., Heintz, R.E., Merideth, N., Yao, Q.X., Yao, Z., Zheng, T.: Insulin independence in a type 1 diabetic patient after encapsulated islet transplantation. Lancet **343**, 950–951 (1994)
148. De Castro, M., Orive, G., Hernandez, R.M., Gascon, A.R., Pedraz, J.L.: Comparative study of microcapsules elaborated with three polycations (PLL, PDL, PLO) for cell immobilization. J. Microencapsul. **22**, 303–315 (2005)
149. Sakai, S., Ono, T., Ijima, H., Kawakami, K.: Synthesis and transport characterization of alginate/aminopropyl-silicate/alginate microcapsule: Application to bioartifificial páncreas. Biomaterials **22**, 2827–2834 (2001)

150. Orive, G., Hernández, R.M., Gascón, A.R., Igartua, M., Pedraz, J.L.: Encapsulated cell technology: From research to market. Trends Biotechnol. **20**, 382–387 (2002)
151. Orive, G., Tam, S.K., Pedraz, J.L., Halle, J.P.: Biocompatibility of alginate-poly(L-lysine) microcapsules for cell therapy. Biomaterials **27**, 3691–3700 (2006)
152. Bunger, C.M., Tiefenbach, B., Jahnke, A., Gerlach, C., Freier, T.H., Schmitz, K.P.: Deletion of the tissue response against alginate-PLL capsules by temporary release of co-encapsulated steroids. Biomaterials **26**, 2353–2360 (2005)
153. Kulamarva, A., Raja, P.M.V., Bhathena, J., Chen, H., Talapatra, S., Ajayan, P.M., Nalamasu, O., Prakash, S.: Microcapsule carbon nanotube devices for therapeutic applications. Nanotechnology **20**, 025612(1–7) (2009)
154. Rege, K., Raravikar, N.R., Kim, D.Y., Schadler, L.S., Ajayan, P.M., Dordick, J.S.: Enzyme-polymer-single walled carbon nanotube composites as biocatalytic films. Nano Lett. **3**, 829–832 (2003)
155. Sugiura, S., Oda, T., Izumida, Y., Aoyagi, Y., Satake, M., Ochiai, A., Ohkohchi, N., Nakajima, M.: Size control of calcium alginate beads containing living cells using micro-nozzle array. Biomaterials **26**, 3327–3331 (2005)
156. Ribeiro, C.C., Barrias, C.C., Barbosa, M.A.: Calcium phosphate-alginate microspheres as enzyme delivery matrices. Biomaterials **25**, 4363–4373 (2004)
157. Akkaya, A., Uslan, A.H.: Sequential immobilization of urease to glycidyl methacrylate grafted sodium alginate. J. Mol. Catal. B Enzym. **67**, 195–201 (2010)
158. Oussalah, M., Caillet, S., Salmieri, S., Saucier, L., Lacroix, M.: Antimicrobial effects of alginate-based film containing essential oils for the preservation of whole beef muscle. J. Food Prot. **69**, 2364–2369 (2006)
159. Salmieri, S., Lacroix, M.: Physicochemical properties of alginate/poly-caprolactone-based films containing essential oils. J. Agric. Food Chem. **54**, 10205–10214 (2006)
160. Conte, A., Scrocco, C., Sinigaglia, M., Del Nobile, M.A.: Innovative active packaging systems to prolong the shelf life of Mozzarella cheese. J. Dairy Sci. **90**, 2126–2131 (2007)
161. Shin, J.W., Choi, S.H., Kim, D.E., Kim, H.S., Lee, J.H., Lee, I.S., Lee, E.Y.: Heterologous expression of an alginate lyase from *Streptomyces* sp. ALG-5 in *Escherichia coli* and its use for preparation of the magnetic nanoparticle-immobilized enzymes. Bioprocess Biosyst. Eng. **34**, 113–119 (2011)
162. Takeda, H., Yoneyama, F., Kawai, S., Hashimoto, W., Murata, K.: Bioethanol production from marine biomass alginate by metabolically engineered bacteria. Energy Environ. Sci. **4**, 2575–2581 (2011)
163. Athanasekou, C.P., Romanos, G.E., Kordatos, K., Kasselouri-Rigopoulou, V., Kakizisa, N.K., Sapalidisa, A.A.: Grafting of alginates on UF/NF ceramic membranes for wastewater treatment. J. Hazard. Mater. **182**, 611–623 (2010)
164. de Moura, M.R., Guilherme, M.R., Campese, G.M., Radovanovic, E., Rubira, A.F., Muniz, E.C.: Porous alginate-Ca^{2+} hydrogels interpenetrated with PNIPAAm networks: Interrelationship between compressive stress and pore morphology. Eur. Polymer J. **41**, 2845–2852 (2005)

Chapter 8
Advances Concerning Lignin Utilization in New Materials

Georgeta Cazacu, Mirela Capraru and Valentin I. Popa

8.1 Introduction

After cellulose, lignin represents the second main component of vegetal biomass. The estimation of lignin produced annually through biosynthesis indicates a quantity of 2×10^{10} tons.

The continuing decline of available oil reserves during the early 21st century will make lignin one of more important source of chemicals for our future society. There are two special reasons to approach researches in the field of lignin: (1) the large accessibility of this compound in the world and it is an inevitable by-product resulted from pulp manufacturing, and (2) it has a huge potential as phenolic raw material.

Significant quantities from this product resulted by chemical processing of the wood and annual plants recommend lignin as an important source of aromatic compounds. Thus, the producing potential of lignin in pulp industry, at the world level, is 3×10^8 t/year and depending on the present technologies of products based on lignin; this quantity could be used more efficiently than fossil raw materials. Obviously, most part of lignin (about 95 %) is used to produce energy and to recover inorganic chemicals used in wood pulping process, and only 5 % are commercially used; lignosulfonates ($\sim$1,500,000 t/year) as dispersants, binding material and kraft lignins ($\sim$60,000 t/year) are processed to obtain high quality surfactants. Having this in mind, the pulp industry has essential conditions to produce lignin on the large scale, representing a chemical platform for "green polymers", chemicals, high quality materials and fuels which can substitute the products based on oil.

G. Cazacu
"Petru Poni" Institute of Macromolecular Chemistry, Iasi, Romania

M. Capraru · V. I. Popa (✉)
"Gheorghe Asachi" Technical University of Iasi, Iasi, Romania
e-mail: vipopa@ch.tuiasi.ro; vipopa15dece@yahoo.com

S. Thomas et al. (eds.), *Advances in Natural Polymers*,
Advanced Structured Materials 18, DOI: 10.1007/978-3-642-20940-6_8,

However, although mechanical and chemical wood processing industries are developed with a great rate, an efficient and complete utilization of biomass remains still an incompletely solved problem, mainly from point of view lignin.

From this reason, at world level a series of organizations and governmental institutions has appeared, which are well organized having as main objective financing fundamental research to find of new solutions regarding the isolation and capitalization of lignin component from vegetable biomass. Among these it could be mentioned: United States Department of Agriculture (USDA) and Forest Products Laboratory (FPL)—USA; Royal Institute of Technology—Sweden; National Institute of Materials and Chemicals Research—Japan; Kyoto University—Japan; University Trois-Rivere—Canada; Centre de Recherche sur les Macromolecule Vegetables (CNRS)—France; International Lignin Institute—Lausanne, Swiss; etc.

In 2000 US Department of Energy (DOC) by the Energy Efficiency and Renewable Energy Office of the US initiated and directly supported the Biomass Program. The main goal of this program was to find a convenient solution to complex processing of lignocellulosic materials—the integrated biorefinery—an overall concept of an integrated and diversified processing plant where biomass feedstock are converted into a wide range of valuable products including fuels and high-value chemicals and other materials, having oil refineries as model.

In Europe, in 2000 years, a first Concerted Action Network—EUROLIGNIN-was created having as main goal to promote the cooperation between industry (lignin production and its using), research institutes and universities to develop fundamental and applied knowledge in the field of lignin.

Researches on the use of lignin are not news, but these have known a setback while the materials produced by chemical synthesis had low costs and environmental restrictions were not implemented as they are in present. As a result, it can affirm that there is stagnation or a slow growth of funds allotted for investigations. In recent years, demand for new cheaper, renewable and biodegradable materials created the premises for intensification of researches at least in some areas with high development potential (plastics, adhesives, additives for building materials, agricultural applications, biological systems).

From ecological point of view, the current researches in the field of lignin chemistry have to pursue the following aspects:

1. The processing of wood and annual plants by non-pollutant processes which could lead to isolation of sulphur-free lignin and with high-purity with the great potential to be used as raw materials for chemical industry;
2. The elucidation of structure and the chemical and/or bio-chemical transformation of lignin in order to be used in specific high-tech and high added value fields;
3. The use partial or integral of isolated lignin in bio- and nano-materials;
4. To stimulate the replacement of more hazardous materials by lignin-derived products: biocides and bio-stabilizers in textiles, cosmetics, animal feed (hygienic prevention in food chain) and health prevention by action of lignin as polyphenolic compound with specific characteristics like anti-microbial, anti-oxidant etc.

The application of biorefining principle will allow obtaining lignin as one of the main product which will be added to that offered by pulp industry creating thus new opportunities to introduce lignin in a lot of materials with new properties and fields of utilization. That is why this chapter is dedicated to the aspects concerning recent directions in the lignin investigation, special stress being laid on blends, composites and nanomaterials.

8.2 Structure of Lignin

8.2.1 Role and Occurrence of Lignin in the Plants

Lignin is one of the main constituents of the higher plants with vascular structure providing mechanical support to stand upright, having some vital functions which confer resistance to the physical–chemical stress and facilitate water and nutrient transport [1].

It is common accepted that the ability to synthesize lignin has been essential in the evolutionary adaptation of plants from an aquatic environment to a terrestrial life. Lignin is crucial for structural integrity of the cell wall and stiffness and strength of the stem [2]. As, lignin is a substance unique of vascular plants which imparts the rigidity to the cell wall, Barghoorn [3] has regarded the development of the capacity of cells to lignify as a property on which forces of natural selection could operate in the process of adaptation of plants to life on land.

Lignin functions as a composite with cellulose fibers providing strength to the higher plants and as a matrix of phenolic and aliphatic substances protecting carbohydrates and other components by prevent penetration of destructive enzymes and microorganisms through the cell wall and insects attack. Lignin participates to processes by which the organisms conserves, recovers and reuses highly significant atoms and small molecules essential for cambial and cytoplasm functioning. Also, lignin acts in the plants as: a permanent binding agent between cells, system to energy storage, antioxidant, stabilizer to UV radiation action, hydrophobic agent.

After the death of the plant, the lignin undergoes degradation in nature by soil microorganisms to produce humic substances contributing to soil properties, [4, 5] and the latter probably some additional decomposition processes to form carbonaceous substances and even coal occurring in the nature [6]. Thus, the formation of lignin has an important role both in the physiology of vascular plants and in the carbon cycle, contributing significantly to the ecological balance of the earth.

Though, many years have believed that lignin is absent in primitive forms as fungi, lichens, alga and mosses, the recent studies have detected that lignin, especially syringyl lignin, is present in the bryophytes *Marchantia polymorpha,* the lycophytes *Selaginella martensii, Isoetes fluitants*, and ferns *Ceratopteris thalicroides, Pteridium aquilinium* [7], and in the marine red alga *Calliathron*

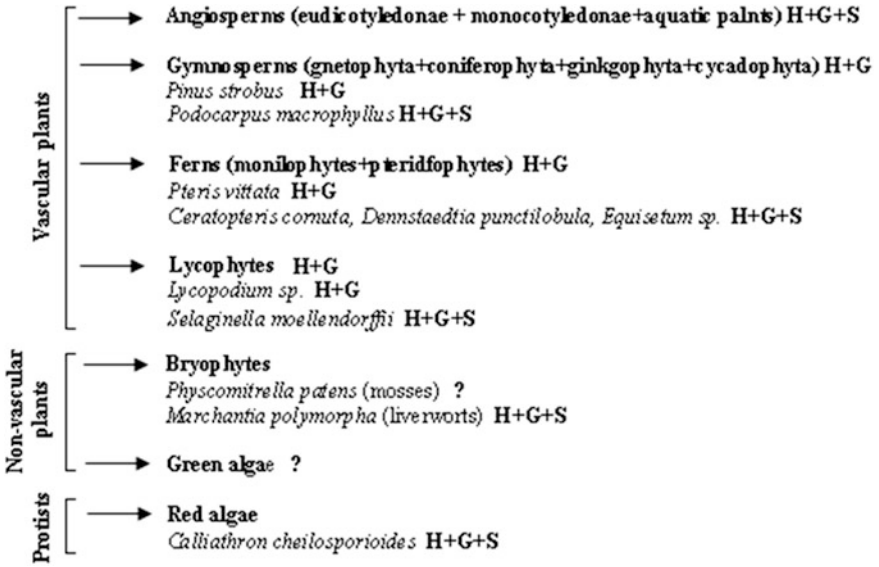

Fig. 8.1 The schematic distribution of the lignin types (guaiacyl, G, syringyl, S, and p-hydroxyphenyl lignin, H) in the major classes' plants [7, 8, 10–12]

cheilosporioides [8], expands the distribution of lignin, to non-vascular plants [9] (Fig. 8.1). These latter findings have opened new questions about the biosynthesis and occurrence of lignin in plants, being necessary the additional research on the genes, enzymes and the pathways of monolignol synthesis.

The lignin content in plants varies in a very large range (Tables 8.1 and 8.2) [13]. Variation in lignin content is caused by species type, growing conditions (temperature, precipitations regime, altitude, soil nature, geographic position, etc.), age, the parts of the plant tested, and numerous other factors [14].

The amount and composition of lignins vary among taxa, cell types, and individual cell wall layers and middle lamella, and are influenced by developmental and environmental conditions [18].

Lignin is not uniformly distributed in the components of the woody tissue, and furthermore, different anatomical regions are lignified at different stages of the life cycle of living cell [6] in different anatomical and morphological regions. Lignin occurs in woody tissues incrusting cellulose fibers in cell walls and filling the space between the cells, i.e. middle lamella acting as an intercellular binder.

It is known that the cell walls consist of various layers: the primary wall (P), the secondary wall which is divided into three sublayers (the outer S1, middle S2, and inner S3), and the midlle lamella (ML). Lignin deposition proceeds in different phases, each preceded by the deposition of carbohydrates, and starts at the cell corners in the region of the middle lamella and the primary wall when S1 formation has initiated. When the formation of the polysaccharide matrix of the S2 layer is completed, lignification proceeds through the secondary wall. The bulk of lignin is

Table 8.1 Limits of chemical composition variations of some plant species from Romania forest land[a] [15]

Species of plant	Cellulose (%)	Lignin (%)	Pentosans (%)	Easy hydrolysable polysaccharides (%)	Hard hydrolysable polysaccharides (%)
Softwood (coniferous wood)					
Fir (*Abies alba* Mill, *Abies balsamea*)	48–55	30–33	6–10	9–15	50–55
Spruce fir (*Picea excelsa* Lam Link, *Picea glauca*)	49–57	27–33	7–11	10–11	54–63
Pine (*Pinus silvestris Pinus strobes)*	52–55	27–29	8–10	13–16	47–55
Hardwood (deciduous wood)					
Beech (*Fagus silvatica* L, *Fagus grandifolia*)	45–50	21–25	11–20	15–20	43–62
Birch (*Betula verrucosa* Ehrh., *Betula lutea,Betula papirifera*)	45–48	19–23	12–21	20–22	43–46
Oak (*Quercus Robur* L, *Quercus sessiliflora, Quercus petraea, Quercus cerris, Quercus frainetto, Quercus falcate*)	42–45	23–27	9–17	15-21	45–62
Aspen (*Populus tremula* L, *Populus tremuloides, Populus alba L, Populus nigra)*	47–53	18–24	13–18	14–21	44–53
Hornbeam (*Carpenus betulus* L)	43–48	19–21	18–20	12–19	48–52
Sycamore maple tree (*Acer pseudoplatanus* L, *Acer sacharum*, *Acer platanoides* L)	47–53	20–27	13–16	14–15	54–63
Lime (*Tillia cordata* Mill, *Tillia tomentosa* Moench)	52–56	19–21	16–16	13–15	–
Willow (*Salix caprea* L, *Salix alba* L, *Weeping willow*)	46–54	22–29	16–17	14	–
Elm (*Ulmus montana* Stockes, *Ulmus foliacea* Gilb)	49–50	28	11–13	–	–
Locust	46–49	25–27	15–18	12–16	–

[a] These data were determined in laboratories of Technical University Iasi and Institute of Macromolecular Chemistry Iasi from 1964 to 1975

Table 8.2 Lignin content of some woody plants [16, 17]

Wood species	Klason lignin (%)	Wood species	Klason lignin (%)
Hardwoods		*Softwoods*	
Bigleaf maple (*Acer macrophyllum* Pursh)	25	Balsam fir (*Abies balsamea* L. Mill.)	29
Yellow birch (*Betula allerghaniensis* Britton)	21	Western larch (*Larix occidentalis* Nutt.)	27
Quaking aspen (*Populus tremoides* Michx)	19	White spruce (*Picea glauca* (moench) Voss.)	29
Southern red oak (*Quercus falcata* Michx)	25	Jack pine (*Pinus bankasiana* Lamb.)	27
Northen red oak (*Quercus rubra* L.)	24	Eastern white pine (*Pinus strobes* L.)	27
American beech (*Fagus grandifolia* Ehrh)	22	Redwood (*Sequoia sempervirens* (D.Don Endll.)	33
Honey locust (*Gleditsia tricanthos* L.)	21	Eastern hemlock (*Tsuga Canadensis* L. Carr)	33
Yellow poplar (*Liriodendron tulipifera* L)	20	Himalaya ceder (*Cedrus deodora*)	31
Eastern cottonwood (*Populus deletoides* bartr. Ex Marsh.)	23	Himalaya cypress (*Cupressus totulosa*)	35
Black willow (*Salix nigra* March.)	21	Eastern white cedar (*Thuja occidentalis*)	31

deposited after cellulose and hemicellulose have been deposited in the S3 layer. Generally, lignin concentration is higher in the middle lamella (about 70 % of the overall lignin content) and cell corners than in the S2 secondary wall [19–22]. However, because it occupies a larger portion of the wall, the secondary wall has the highest lignin content. Also, it can observe that the secondary walls of vessels generally have higher lignin content than those of fibers [23] (Table 8.3).

The secondary cell walls of angiosperm tension wood are characterized by the presence of an un-lignified gelatinous layer, which is composed of highly crystalline cellulose, whereas lignin distribution is normal in the rest of the secondary cell wall. By contrast, the S2 layer of gymnosperm compression wood is characterized by a highly lignified ring (the S2L layer) [20, 24]. Lignification can be induced of environmental conditions influencing lignin amount and composition. Thus, the alpine growth conditions and autumn temperatures also influence the lignin concentration within the secondary cell wall in latewood tracheids [25]. Examination of the *Pinus radiata* trees growing under drought conditions of severe revealed tracheids with concentric lamellation associated with areas of high and low lignification within the secondary wall. Tracheids with greatest reduction in lignification present evidence of collapse explained by their poor or negligible

Table 8.3 Lignin distribution in White birch [23]

Element	Morphological region	Tissue volume (%)	Lignin conc. (g/g)	
			UV-EDXA	UV
Fiber	S1	11.4	0.14	
	S2	58.5	0.14	0.16
	S3	3.5	0.12	
	ML	5.2	0.36	0.34
	$ML_{cc(F/F)}$	2.4	0.45	0.72
Vessel	S1	1.6	0.26	
	S2	4.3	0.26	0.22
	S3	2.3	0.27	
	ML	0.8	0.40	0.35
	$ML_{cc(F/V)}$	≈0	0.58	
Ray parenchyma	S	8.0	0.12	0.22
	ML	2.0	0.38	
	$ML_{cc(F/R)}$	≈0	0.47	
	$ML_{cc(F/R)}$	≈0	0.41	

S_{1-3} secondary-wall region, *ML* middle lamella; the subscript cc denotes cell corners, *F*/*F* fiber/fiber, *F*/*V* fiber/vessel, *F*/*R* fiber/ray, *R*/*R* ray/ray

Table 8.4 Lignin content (%) in different parts of loblolly pine tree [32]

Normal wood			Compression wood		Opposite wood	
Top juvenile	Bottom juvenile	Bottom mature	Middle juvenile	Middle mature	Middle juvenile	Middle mature
29.6	28.5	27.4	37.5	37.4	28.6	28.4

adhesion due to reduced lignification of middle lamellae [26]. Also, lignification can be a defence response after wounding or pathogen attack [27, 28].

In recently studies, the polar metabolite profiling, new technique was used to investigate the changes in metabolite pools during development or in response to environmental or chemical stress of wood [29, 30]. Thus, Yeh et al. [31] detected the substantial increase in of metabolites (shikimic acid, coniferin and *p*-glucocoumaryl alcohol) associated with an increase lignin production, both quantitatively (higher lignin content) and qualitatively (more H-lignin) in response to compression wood in relation to juvenile wood in loblolly pine. In another papers, Yeh et al. [32] reported that the juvenile and mature compression wood contains significantly higher amounts of lignin (37.5 %, Table 8.4) than normal wood.

Chemical analysis of the wood tissue isolated from loblolly pine showed that the lignin content in the compression wood was 36.6 % (2.3 % H-type lignin) compared with 29.4 % (only 0.1 % H-type lignin) in the normal wood [33].

8.2.2 Lignification Process of Plants

From the botanical standpoint the phenomenon of lignification in tissues is association with evolution of plants with a development of a specialized conduction (vascular) system and solar energy collection devices (leaves, needles and a crown) above ground level.

It is known that lignin is a heterogeneous phenolic polymer composed from three types of monomers (monolignols), p-coumaryl, coniferyl and sinapyl alcohols. Generally, was accepted that during lignin deposition, monolignols are synthesized in the cytoplasm, transported to the cell wall where they undergo oxidation and polymerization reactions to form lignin.

Although, the monolignol biosynthetic pathway has been relatively well elucidated, at least in angiosperms, there is little knowledge about how monolignols are transported through the cell membrane to their polymerization sites. Transportation of small molecules (monolignols) to the cell membrane may occur by at least three different mechanisms: exocytosis, transporter-mediated export, and diffusion. Although, Golgi vesicles are known to be involved in exporting some other components (i.e. hemicelluloses) to cell wall [34], referring to the monolignols, Kaneda et al. [35] promoted the idea that monolignols are exported to the cell wall by membrane-bound transporters, while other researchers suggest [36] that manolignols are able to pass the cell membrane by diffusion. Once transported to the cell wall, monolignols are oxidized to phenolic radicals that then undergo polymerization by chemical coupling. Laccases and peroxidases are involved in the monolignols oxidation reactions [37, 38].

Lignin deposition is one of the final stages of xylem cell differentiation and mainly takes place during secondary wall thickening [20], when microtubule bundles guide the positioning and deposition of cellulose microfibrils at specific sites within the wall where subsequent lignification occurs [39–42], but it is unknown how lignin deposition is directed to these specific sites (i.e. cell corners and another regions).

During deposition, lignin may form chemical bonds with the hemicellulose component in the wall and gradually eliminates water, forming a hydrophobic environment. From these data, one can conclude that lignin deposition, and the relative incorporation of the different monolignols into the polymer, are spatially and temporally regulated. After transport of the monolignols to the cell wall, lignin is formed through dehydrogenative polymerization of the monolignols [43].

Lignification so called is the polymerization process in plant cell walls that takes phenolic monomers, produces radicals, and couples them with other monomer radicals (only during initiation reactions), or more typically cross-couples them with the growing lignin oligomer, to build up a phenylpropanoid polymer [44–47].

In early studies on lignin biosynthesis prepared a lignin like polymer was prepared in vitro, named dehydrogenation polymer (DHP) [46]. Authors concluded that lignin was produced by the random diffusion of monomeric building blocks

over the distance of several cell layers and it had a random poly(oxyphenylpropane) structure. In light of new experimental evidence, it was noted that each individual cells controls the synthesis of lignin precursors and the rate to the lignifying cell wall [23].

Lignin precursors p-coumaryl (p-CA), coniferyl (CA) and sinapyl (SA) alcohols, are synthesized through the shikimate and cinamic acid pathways, starting from phenylalanine which under the action of phenylalanine ammonia-lyase (PAL) is deaminated followed by hydroxylations of the aromatic ring, methylations and reductions of therminal acidic group to an alcohol leading to the formation of the monolignols (Fig. 8.2), [37, 48].

Many studies presented the evidences for the involvement of the enzyme activities in lignification process, for example: hydroxylase (C4H, C3H, F5H), ligase, *O*-methyltransferase types, explaining their role in the lignin biosynthesis [51–53]. These alcohols (monolignols) can radically coupled at several sites each other or with the growing lignin oligomer, to produce a complex polymer with a variety of intermolecular linkages. The dehydrogenation to monolignol radicals has been attributed to different enzyme activities, such as peroxidases, laccases, polyphenol oxidases, and coniferyl alcohol oxidase [43].

After transport into cell wall of the lignin precursors, lignin polymerization takes place by radical reactions. Freudenberg [46] has shown that the formation of lignin precursors undergo dimerization through enzymatic dehydrogenation, which is initiated by an electron transfer and yields resonance-stabilized phenoxy radicals. The formation of radicals is catalysed by oxidative enzymes, such as H_2O_2-dependent peroxidases or O_2-dependent oxidases/laccases [43, 59]. These monolignol free radicals can then undergo radical coupling reactions at several sites each other producing a variety of dimers or with the growing lignin oligomer, to produce a complex polymer with a variety of intermolecular linkages.

Hatfield and Vermerris [54] presented a random model for lignin formation. In their concept the new formed monolignol radicals can follow one of two ways: (a) the lignin polymer is at its base oxidative state, the higher oxidation state on the monolignol can be transferred to the lignin molecule, returning the monolignol to ground state; or (b) the lignin polymer is at a higher oxidation state, the monolignol radical can undergo an oxidative coupling reaction to form a covalent bond.

Recent advances in genetic engineering and mutant experiments led to identify an unforeseen variation in lignin subunits composition. This observation can be explained by the variation of lignin precursors and their distribution into lignified areas from cell walls. These results have significant implications on the traditional definition of lignin and a better understanding of the biosynthesis of lignin precursors.

In this context, the studies on the mutants and transgenic plants permitted to evidence dirigent proteins which are involved in the coupling of monolignols to form lignin polymer [54, 55] (Fig. 8.3).

Also, by the in vitro experiments using of plant tissue-cultured cells and the analysis of mutants and transgenic plants have provided useful information related to lignin structure and several aspects of lignin formation, i.e. monolignol transport,

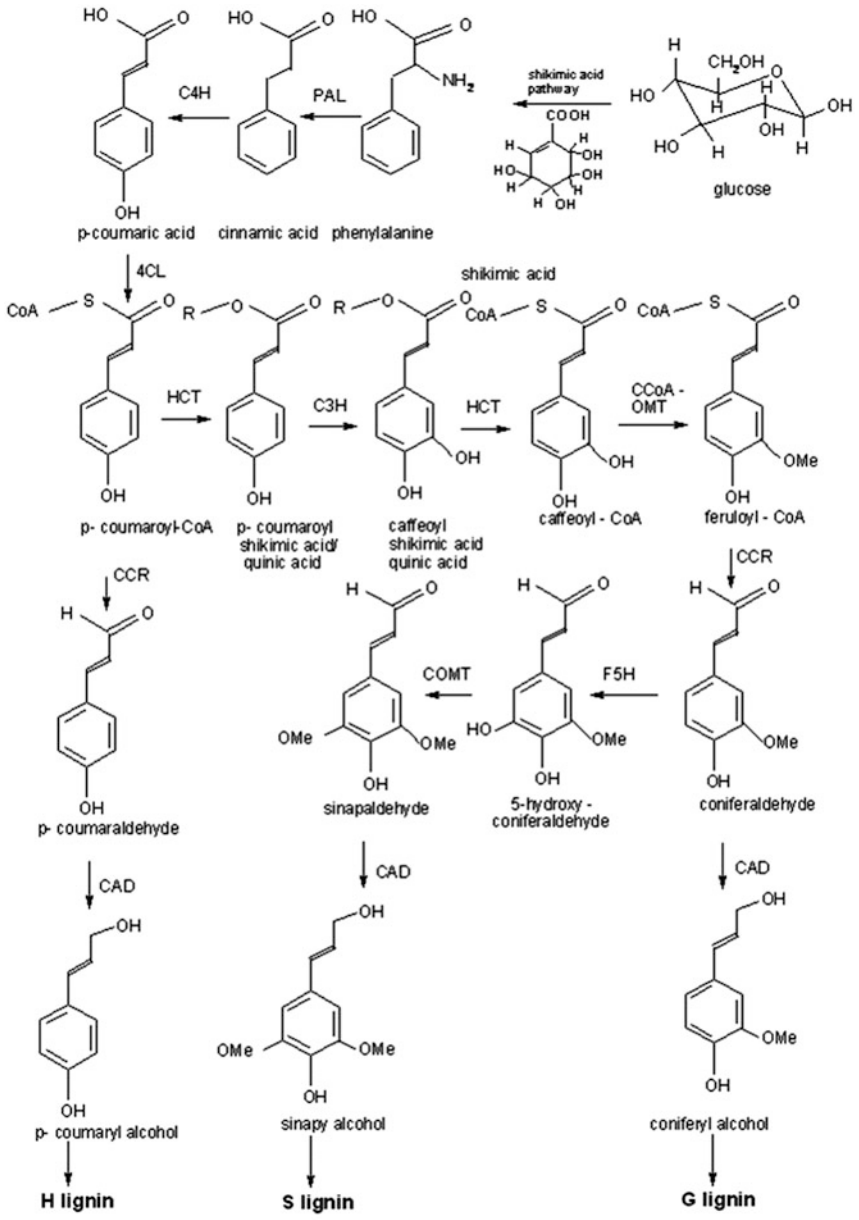

Fig. 8.2 Schematic representation of lignin formation in plants [22, 37, 49, 50]

some indications about the possible mechanisms involved in coupling between monolignol radicals and a radical form of the growing lignin molecule, on the various linkages and their distribution in the lignin polymer [49, 56].

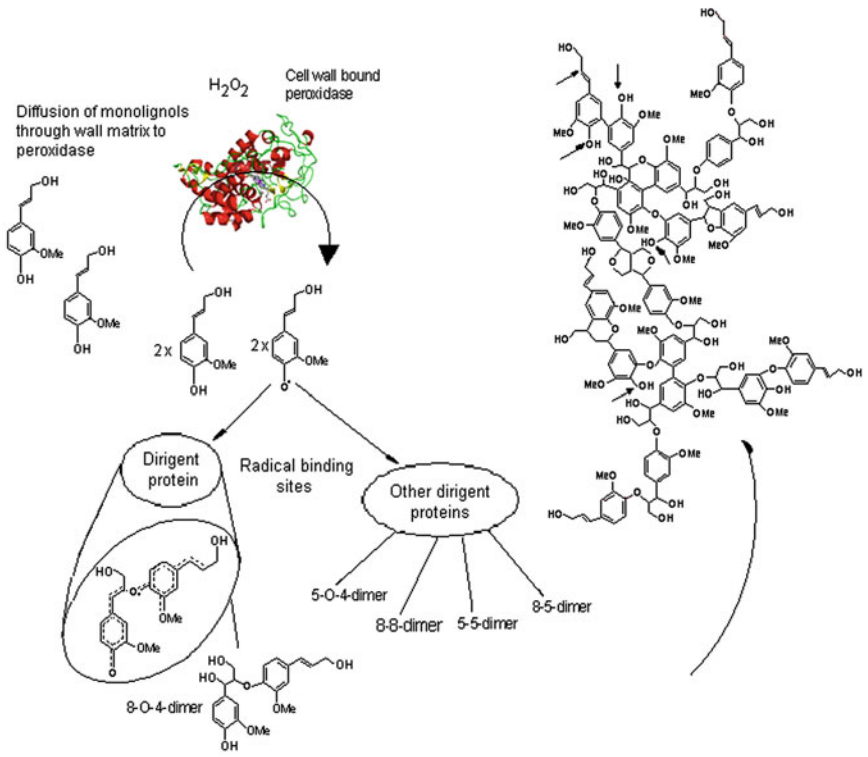

Fig. 8.3 The dirigent protein model for lignin formation proposed by Hatfield and Vermerris [54]

8.2.3 Lignin Composition and its Structural Formulae

Several studies, have dealt with the investigation of lignin structure following: (a) chemical composition of different lignin types from various non-wood/wood species; (b) determination of structural units, the linkages between units and of specific functional groups; (c) synthesis of the lignin model compounds and comparison their chemical reactions of lignin with those of lignin polymer; (d) analysis lignins by destructive/non-destructive methods and analysis of results; (e) to elucidate and to understand the biosynthesis mechanisms of the lignin from plants.

Data obtained have led the conclusion that from chemical point of view, term lignin refers to a complex racemic aromatic of heterogeneous biopolymers that contain limited branching and/or crosslinking, whose content is variable as a function of woody species from which is isolated [3, 57, 58].

Freudenberg [59] defined, in 1928, the native lignin as a macromolecular three-dimensional compound. This definition is maintained at present, as lignin is viewed as a high polymer consisting of a network of three-dimensional aromatic and aliphatic fragments that contain limited branching and or cross-linking.

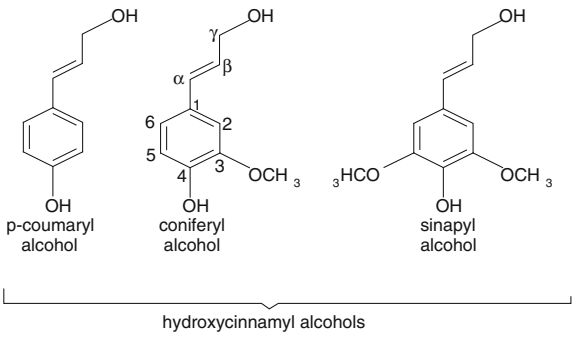

Fig. 8.4 Structures of the hydroxycinnamyl alcohols that form lignin

In the purest sense, lignin is a complex racemic consisting from aromatic heteropolymers produced by free radical coupling reactions initiated by enzymatic dehydrogenation of the three primary precursors, the hydroxycinnamyl alcohol monomers differing in their degree of methoxylation: trans-4-coumaryl alcohol [3-(4-hydroxyphenyl)-2-propenol)], trans-coniferyl alcohol [3-(4-hydroxy-3-methoxyphenyl)-2-propenol)] and trans-sinapyl alcohols [3-(4-hydroxy-3,5-dimethoxyphenyl)-2-propenol)] (Fig. 8.4).

These alcohols lead to the relative abundance of *p*-hydroxyphenyl (H), guaiacyl (G) and syringyl (S) subunits in the lignin. Their amount and composition vary among taxa, cell types, and individual cell wall layers and are influenced by developmental and environmental conditions [60]. The results from numerous studies evidenced the fact that lignin contains the functionalized phenylpropane (C_6–C_3) units connected by various types of linkages leading to a unique and very complex structure [61–64]. The type of the dominant linkages between the phenylpropane units (Fig. 8.5) and their percent abundance are summarized in Tables 8.5 and 8.6.

In the last years, presence of new structures in plant lignins has been reported (Fig. 8.6).

Thus, in 1995, Karhunen et al. [66], discovered a new 8-membered ring linkage in softwood lignin called dibenzodioxocin. The mechanism of formation of this ring linkage involves intramolecular nucleophilic addition to an intermediate quinone methide structure [67]. Results obtained in genetic engineering, evidenced the presence of the benzodioxane units in lignins isolated from poplar (*Populus tremula, Populus alba*) plants deficient in COMT, an *O*-methyltransferase required to produce lignin syringyl units. These structures result from incorporation of 5-hydroxyconiferyl alcohol into the monomer supply and confirm that phenols other than the three traditional monolignols can be integrated into plant lignins [68]. Canapema et al. [65] by the combination of 2D NMR and quantitative ^{13}C NMR spectroscopy were estimated the amounts of various phenolic/etherified noncondensed/condensed guaiacyl and syringyl units for *Eucalyptus grandis* milled wood lignin (MWL). *E. grandis* lignin contained ~0.60/Ar of *β*-O-4 units, small amounts of the other structural units such as pino/syringyresinol (0.03/Ar), phenylcoumaran (0.03/Ar), and a new structure called spirodienone (0.05/Ar). The degree of condensation was estimated at ~21 %, the main condensed

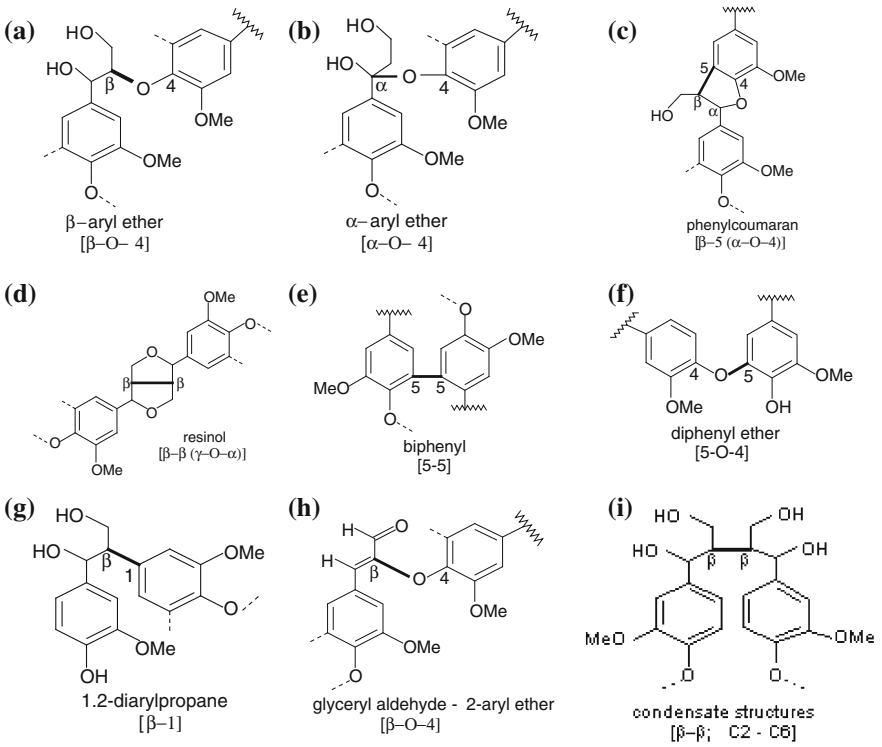

Fig. 8.5 The main bonds between structural units from lignin [16]

Table 8.5 Frequency of interunitary linkages in lignins from gymnosperms and angiosperms (number of linkages per 100 C_9 units) [22]

Linkage type	Substructure	% C_6-C_3 units for lignin from	
		Spruce (softwood)	Birch (hardwood)
β -O-4	Phenylpropane *β*-aryl ether	45–51	60–65
β-5	Phenylcumaran	9–15	6
5-5	Biphenyl	9.5–11	2.3–4.5
α-O-4	Phenylpropane α-aryl ether	6–8	6–8
β-1	1,2-diarylpropane	7–10	7–10
4-O- 5	Diphenyl ether	3.5–8	6.5
β-O-4	Glyceryl aldehyde -2-aryl ether	2	2
β-*β*	Resinol (*β*-*β*-linked structures	3	2–5.5

structures being 4-O-5 moieties (∼0.09/Ar). Comparison data obtained for the structure of *E. grandis* MWL with those of other lignin preparations isolated from various hardwoods reflect both differences between various lignin structures and their dependence on the isolation method, experimental techniques and calculation methods. Also, by the use the 2D NMR analysis correlating different techniques

Table 8.6 Frequency of various interunit linkages in hardwood lignins [65]

Linkages	Beech	Eucalyptus globules	Eucalyptus grandis
β-O-4 total	65	56	61
α-O-4 noncyclic		20	
γ-O-alkyl total			23
5-5′	2	3	3
4-O-5′: guaiacyl/syringyl	1.5	1.5/10	3/6
6(2)-condensed: guaiacyl/syringyl		4/10	3/3
Syringyl:Guiacyl:Hydroxyphenylpropane units ratio		84:14:2	62:36:2

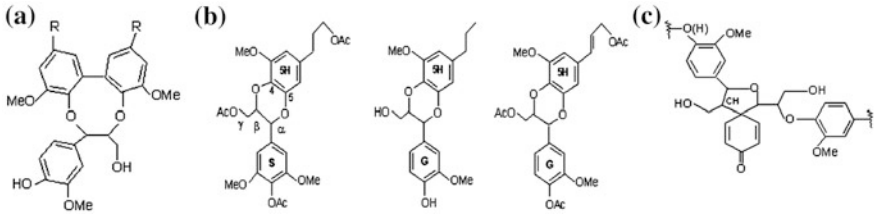

Fig. 8.6 Newly substructures in lignin: **a** dibenzodioxocin; **b** benzodioxane type products; **c** spirodienone

(HMQC, HSQC and TOCSY) can be identified the signals corresponding to spirodienone (β-1′, α-O-α') substructures in the spectra of native lignins from diverse herbaceous plants (i.e. sisal, kenaf, abaca and curaua) [69] and in wood lignins (spruce, birch) [70]. The intensity of spirodienone moieties signals in the spectra of the juvenile hardwoods lignins is much lower than that can be observed in spectrum of a birch MWL isolated from mature wood and of an *E. grandis* MWL samples [71]. The frequency of the substructures in lignin is based an assays and calculations carried out by several authors [72–75]. According to Sarkanen and Hergert [76] there are two main groups of lignins the guaiacyl-type lignins and syringyl lignins. Each class of plants, such as softwoods and hardwoods, grasses contains a lignin rich in one type of alcohol repeat unit. Guaiacyl lignins are generally representative of gymnosperms (softwoods), dicotyledonous angiosperms (hardwoods) posses a mixture of guaiacyl and syringyl lignins, while most non-wood lignins (annually plants and grasses) have significant amounts of p-hydroxyphenylpropane units nuclei in addition to syringyl and guaiacyl units [19]. In normal softwood, usually referred to as guaiacyl lignin the structural elements are derived mainly from coniferyl alcohol (more than 95 % of the total number of structural units), with the remainder consisting mainly of p-coumaryl alcohol type units and trace amounts of sinapyl alcohol derived units [62]. Normal hardwood lignins, termed guiacyl-syringyl lignins, are comprised of coniferyl-alcohol and sinapyl alcohol—derived units in varying ratios [75]. Compression wood conifers, contains a p-hydroxyphenyl-guaiacyl lignin [77].

Lignins from grasses (monocots) incorporate G and S units at comparable levels, and more H units than dicots. Also, grass lignins additionally contain small amounts of residues of p-coumaric acid and ferulic acid attached though ester linkages [78]. Both the amount and the nature of lignin in wood can vary within wide limits and it is influenced by its age such that, for example, in mature poplar wood the syringyl-guaiacyl ratio is high but decreases in the younger xylem and in the phloem [76]. Lignin also is characterized by different functional groups which can be used to carry out modification reactions, or which can be involved in the establishing of bonds with other components of wood. The functional groups attached to the basic phenylpropanoid skeleton include phenolic hydroxyl, benzylic hydroxyl, carbonyl, methoxyl groups (Tables 8.7 and 8.8). The frequency of these groups may vary according to the morphological location of the lignin, wood species and method of isolation.

Based on the results obtained in the investigation of lignin structure have been proposed several structural formula. Thus, in 1961 Adler proposed structural formulae containing the 12 phenylpropanic units connected by C–C and C–O-C bonds [62] and in 1965 Freudenberg proposes a more complex structural model which consists of 18 units for spruce lignin [83] (Fig. 8.7). Lignin polymer structural models have been published by Ludwig [84] based on NMR studies of lignin preparations from softwood, Nimz for beech lignin [75], Simionescu and Anton [85] for reed lignin. Also, Sakakibara [86] proposed a structural model for hardwood lignin based on the analysis of the degradation products obtained by hydrolysis and hydrogenolysis. Glasser [87] through by the computer simulation of the lignin dehydrogenative polymerization designed finals structural model for lignin constituted from 96 phenylpropanic units. Gravitis and Erins [88] have examined various theoretical structural models of lignin. They concluded that under certain conditions these models can form quasi-order regions in the structure lignin. Also, Atalla [89] has shown that the aromatic rings of lignin are tangentially aligned to the cell walls. Based on these observations, he proposed a new model for the lignin assembling, which suggests that variations in the hemicelluloses structure may induce systematic changes both in the cellulose and lignin structure; the author introduced a hierarchical and sequential control, which occurs at multiple levels in different phases and locations separated during lignin biosynthesis [90].

Forss and Fremer [91, 92] have shown that spruce lignin contains ∼24 % lignin with the regular polymer structure and 5 % low molecular weight phenilpropanic compounds called "hemilignins", while the birch lignin contains ∼8 % guaiacyl/syringyl lignin with regular structure and 12 % hemilignins. Characterization of lignin preparations separated shown that lignin is a regular polymer composed from identical repeat units which enantiomeric alternate, fact that explains the lack of optical activity both the lignin and degradation products. In the case of spruce lignin, the guaiacyl lignin, the each repeat unit is composed of 16 guaiacylpropanic units and 2 *p*-coumaryl units (Mw–3325 g/mol and 0.889 OCH_3/C9 content) while for birch lignin, the syringyl/guaiacyl lignin, contains 3 or 6 phenylpropanic units with 1.33 OCH_3/C9 content. Based on these results, the authors proposed a linear structure model (Fig. 8.8).

Table 8.7 Functional groups of hardwood lignin [65]

Functional group	Lignin from:			
	Spruce	Birch	E. globules	E. grandis
Methoxyl	92–96	164	164	160
Total OH		186	117–121	144
Aliphatic OH	15–20	166	88–91	125
Primary		86	68	70
Secondary		80	20	55
Benzylic			16	54
Free hydroxyl phenolic	15–30	20	29–30	19
Total carbonyl	20		24	17
Aldehyde			9	24
Ketone			15	8
α-CO			10	8
Nonconjugated			10	8
COOH			4	5
Degree of condensation			18	21

Table 8.8 Content hydroxyl groups in different type lignins [79–82]

Lignin preparation	OH groups (mol/C_9 unit)		
	Phenolic	Aliphatic	Total
Milled wood lignins (MWL)	0.28	1.18	1.46
Spruce (*Picea glauca*)	0.22	1.11	1.33
Zhong—Yang Mu (*Bischofia polycarpia*)			
Milled bamboo lignin (MBL)	0.36	1.13	1.49
Chinese bamboo (*Phyllostachys pubescens*)			
Willstätter (HCl) lignin	0.12	1.39	1.51
Sweetgums (*Liquidambar styraciflua*)			
Technical lignins	0.58	0.77	1.35
Pine kraft lignin	0.44	0.56	1.00
Bamboo kraft lignin			

The lignin is linked with polysaccharides through arabinose, xylose and galactose units in the hemicellulose components [93].

The chemical nature of the carbohydrate matrix and the orientation of the cellulose microfibrils influence lignin deposition. In the middle lamella and the primary wall, lignin forms spherical structures, whereas in the secondary wall, lignin forms lamellae that follow the orientation of the microfibrils [20, 24, 94].

Because in woody tissues, lignin is intimately associated with polysaccharides it is necessary separation of lignins. There are several methods for the isolation and purification of lignin in the form of: (a) lignin as residue: acid hydrolysis of polysaccharides (H_2SO_4, HCl, HF, CF_3COOH); oxidation of polysaccharides ($Na_3H_2IO_6$); hydrolysis/dissolution of polysaccharides ($NaOH$-H_2SO_4/

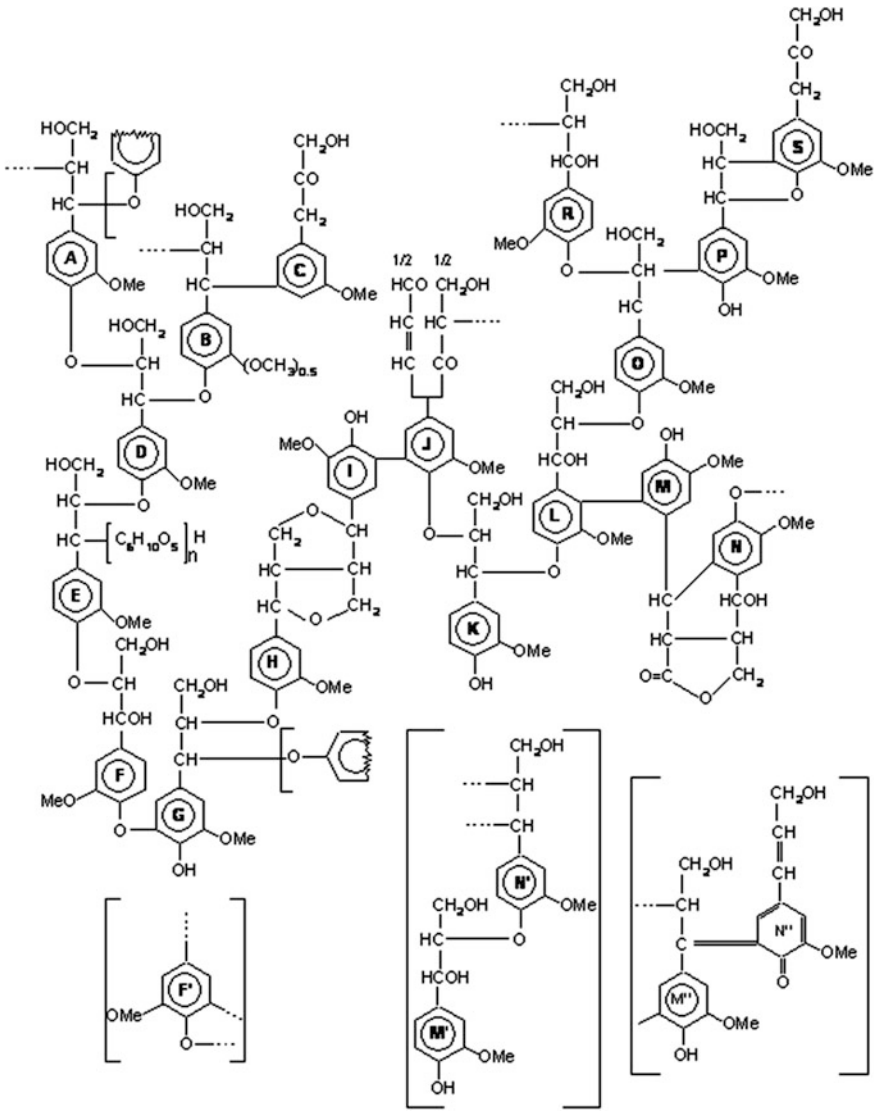

Fig. 8.7 Structural model for spruce lignin proposed by Freudenberg

$Cu(NH_3)_4(OH)$): (b) dissolution lignin: mechanical disintegration (aqueous dioxane); in combination with cellulolytic enzymes; mild acid hydrolysis of lignin-carbohydrate bonds (alcohol, dioxane, phenol, acid acetic with acid catalyst); steam hydrolysis of lignin-carbohydrate bonds (steam- and in situ-generated acetic acid); alkaline hydrolysis of weak ether bonds (NaOH and Na_2S or catalyst); (c) lignin derivative: sulfonation (SO_2-H_2O and base); hioglycolation ($HSCH_2COOH$-HCl).

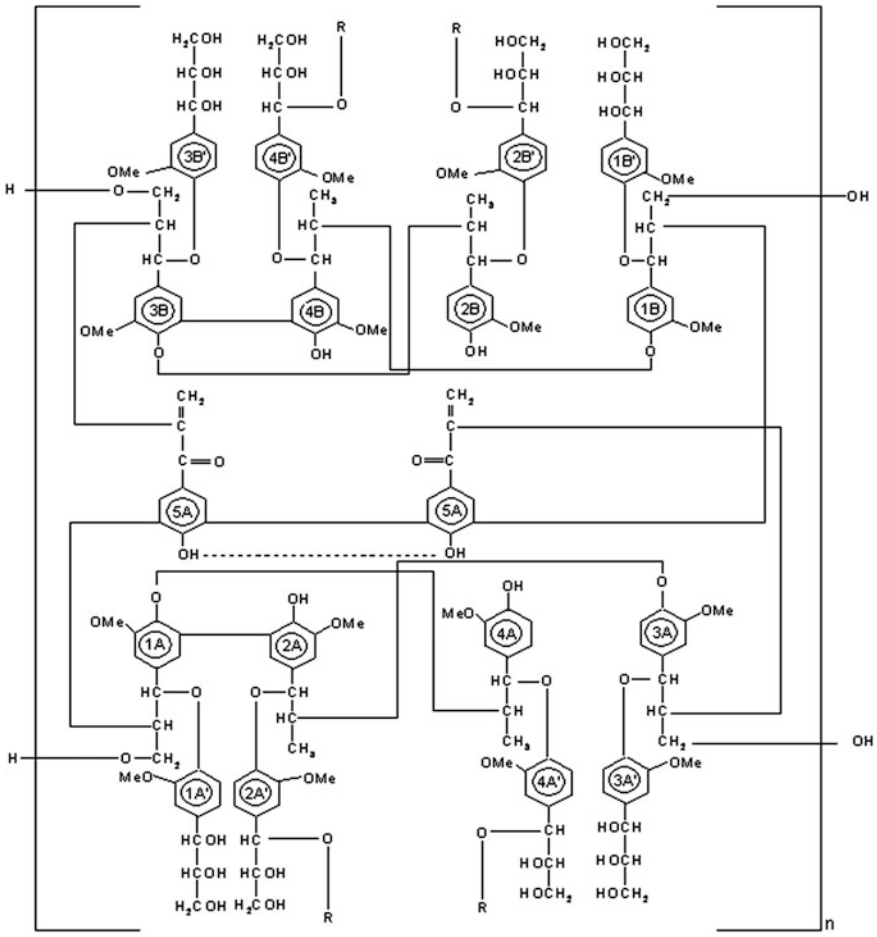

Fig. 8.8 Structural model with the repeat units: R: $H_2[C_{178}H_{194}O_{62}]_n(OH)_{2n}$ [92]

Various industrial processes can be used to remove and to isolate lignin from wood, such as: sulfite (lignosulfonate, SSL) and alkaline (soda or Kraft) pulping and by acidic processes (acid hydrolysis, AHL), by water and steam treatments (autohydrolysis and stream explosion lignin, SEL), organic solvent mixtures (organosolv, OSL) and by mechanical wood milling (MWL). Each process produces lignin material of different composition and properties. Four important factors influence the properties of the lignin preparations: source (woody or annually plants) of lignin; methods used to remove lignin from the plant; methods used to purify the lignin; nature of the chemical modification of the lignin after isolation. It is well known that during lignin separation from wood tissues, complex modification takes place which lead to isolate lignin as a modified product. A new ester pulping process will permit the recuperation of a less modified lignin product in the future [95].

Table 8.9 Characteristics some lignins separated by various procedures

Characteristics	Lignosulfonates	Kraft lignin	Organosolv lignin
Elemental composition	C = 53 % H = 5.4 % S = 6.5 %	C = 66 % H = 5.8 % S = 1.6 %	C = 63 % H = 5.5 % S = –
Impurities	Different products resulted from carbohydrates degradation	Absent	Absent
Functionality:	1.9 %	4.0 %	4.8 %
OH phenolic	7.5 %	9.5 %	5.0 %
OH alcoholic	16.0 %	–	–
SO_3H	–	3.4 %	–
SH	12.5 %	14.0 %	19.0 %
OCH_3			
Solubility	Water	Alkaline solutions	Organic solvent (ethanol)
Molecular mass	400–150,000 range	2,000 (M_N)	700 (M_N)

Lignin preparations can be separated in two groups: the first of pure analytical lignin materials and the second group of the highly modified lignin materials produced by various industrial procedures.

Analytical lignin preparation: Brauns lignin (native lignin); cellulolytic enzyme lignin; dioxane acidolysis lignin; milled wood lignin (Bjorkman lignin—native lignin); klason lignin (lignin structure is markedly changed); periodate lignin.

Industrial lignin preparations: hydrolysis lignin; Kraft lignin; lignosulfonate (from acid sulfite or bisulfite pulping); neutral sulfite semichemical process and alkaline sulfite-alkaline sulfite-anthraquinone pulping pulping; organoslov lignin (ethanol/water, Alcell); alkaline sulfite anthraquinone methanol pulping, (ASAM); methanol/methanol NaOH, anthraquinone pulping, (Organocell); CH_3COOH/HCl pulping); steam explosion lignin (SEL).

During industrial delignification of lignocellulosic materials such as wood, lignin undergoes significant structural changes (Table 8.9).

8.3 Lignin Properties

At present is widely accepted the concept that lignin is a statistical three-dimensional polymeric network. This hypothesis was confirmed by various investigation methods, among them being atomic force microscopy (AFM). AFM measurements indicated that lignin molecules form a slightly different network structure depending on a change in the state of aggregation [96].

Starting from this concept, the lignin properties can be viewed in relation to its structure [97], and the most important are: (a) compatibility determined by amorph structure, solubility/insolubility, molecular mass and its distribution,

macromolecular conformations, and (b) incompatibility characterized by polydispersity, molecular association, topochemistry, ultrastructure at the level of the polymeric network structure.

8.3.1 Amorphous Structure

The structure of lignin consists of phenylpropane units forming a three dimensional polymer network which have not an ordered and regular super-macromolecular structure. The X-ray diffractometry and differential scanning calorimetry (DSC) indicated that the isolated lignins in the solid state are amorphous polymers.

From X-ray diffractrograms one can be observed that the inter-molecular distance in the milled wood lignin in the glassy state is 0.42 nm and that of dioxane lignin corresponds to 0.43 nm, values comparable with those for amorphous synthetic polymers, i.e. polystyrene. In the case of the dioxane lignin a supplementary peak at 0.98 nm was observed, indicating that intra-molecular regularity only local exists. Inter- and intramolecular distance increase discontinuously at the temperature corresponding to the glass transition value [96, 98]. The data obtained by X-ray diffraction are confirmed by DSC studies which characterize lignin as a typical amorphous polymer.

Taking into account the variety of chemical composition and complex structure of lignin, the temperature range of glass transition is broader than that of synthetic amorphous polymers. From this reason, it is recognized that is difficult to detect the glass transition (Tg) for lignins due to the large variety of lignin origin and its extraction methods. Also, Tg value depends on the thermal history of each lignin sample. Goring [99] had first reported the Tg of the different lignins at temperatures around 127–227 °C, and other authors found that Tg varies from 123 to 187 °C [100]. For example, Hatakeyama et al. [98] reported values around 127–147 °C for dioxane lignins, while Irvine [101] found 137 °C for milled Eucalyptus regnans wood lignin and Glasser et al. [102] established a value of 167 °C for kraft pine lignin.

DSC curves presented in Fig. 8.9a indicate behaviour of typical amorphous polymer having a broad spectrum of molecular higher order structure which coaggregates by annealing. Tg values of LS-lignosulfonate and KL-kraft lignin are observed around 100 °C and for HL-hydrolysis lignin samples in a temperature range of 70–85 °C. Hatakeyama [98] remarked that by annealing the enthalpy relaxation is identified as an endothermic shift peak, and by increasing annealing temperature, the endothermic shoulder peak shifts to the high temperature side (Fig. 8.9b).

Vasile and co-workers [103] reported values varying from 102 to 175 °C for different lignins from wood and annual plants, and also, the dependence of Tg values on the phenolic hydroxyl and carboxyl groups have been observed. DSC data evidenced that the Tg values change due to the presence of a small amount of water which can broken up the hydrogen bonds between hydroxyl groups or can blocked the hydroxyl groups.

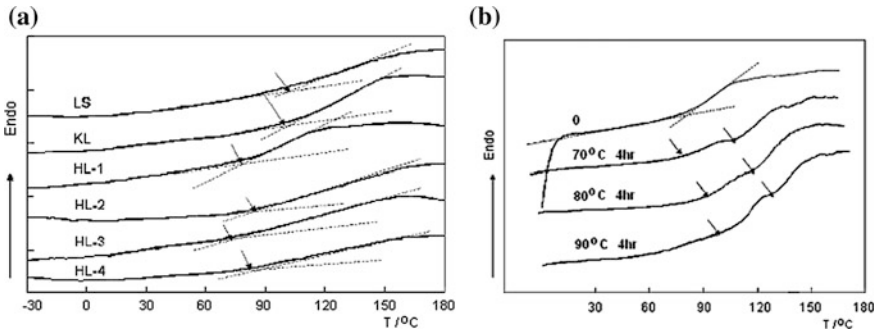

Fig. 8.9 DSC curves recorded for [96]. **a** Na-lignosulfonate (LS), Kraft lignin (KL) and hydrolysis lignins (HL_S) obtained from various industrial plants: LS, KL, HL-1 New Zealand; HL-2, HL-3 and HL-4 Russia. **b** HL-1 annealed at various temperatures and then heated at 10 °C min^{-1}

8.3.2 Lignin Solubility

In literature have been reported numerous results concerning removing lignin from wood and non-wood raw-materials. Usually chemical methods, such as: acid and alkaline hydrolysis, organic solvent treatment, oxidative delignification, lead to substantial degradation and dissolution of lignin. Consequently, solubility of lignin preparations differs in relation to their isolation procedures: (1) lignins insoluble in organic solvents: sulphite, hydrolytic, cuproammoniu and hydrochloric lignin; (2) lignins soluble in organic solvents or in their mixtures: ethanol, methanol, phenol and dioxane lignin; (3) lignins soluble in aqueous solutions: lignosulphonates.

The lignin ability to swell and dissolve depends on its molecular weight and solvent polarity [104]. The solvent ability to interact with OH groups of lignin is a function of cohesive energy (Hildebrand'parameter) and the capacity to form of hydrogen bonds.

Recently, several groups [105, 106] have reported the dissolution of lignins from wood using ionic liquid solvents (ILs). Imidazolium-based cations possess a wide range of lignin and wood flour solubilizing capacity depending on the associated anion [107]. The highest solubility of Kraft lignin was obtained using [Mmim][$MeSO_4$] and [Bmim][CF_3SO_3]; in the case of [Bmim][CF_3SO_3] a higher solubility of lignin was explained by the similarity of the Hildebrand's parameter (δ_H) values for both IL and lignin (24.9 and 24.6, respectively).

Previous observations regarding of characteristics of lignin molecules in solution were included the intrinsic viscosity, branching parameter and the degree of polydispersity.

The low intrinsic viscosities of the different lignins (dioxane, kraft, lignosulfonate, alkali lignins) dissolved in various solvents and the Mark-Houwink exponent (α) ranged between 0 and 0.5 led what allow to conclude that the shape of lignin molecules is between an Einstein sphere and a non free-draining random

coil [97]. This conclusion was confirmed by other parameters, such as sedimentation coefficient and diffusion constants.

The exponential factors of Kuhn-Mark-Houwink-Sakurada (KMHS) equation for kraft lignin are small (0.11–0.11 in DMF and 10.23 in 0.5 N NaOH) indicating that the lignin molecules have a compact spherical structure and approach the limit of an Einstein sphere, a constant-density sphere [108]. By introducing acetylgoups in kraft lignin, organosolv and steam explosion lignins the values of the KMHS exponential factors are in the range of 0.17–0.35 in tetrahydrofuran [109].

The measurements of the branching parameter of various lignin fractions, led to conclusion that the chains of the lignin molecules in solution are densely packed or crosslinked [110, 111]. Rezanowich and co-workers [112] observed by electron microscopy that the lignosulphonates (LS) form spherical particles of a wide range of sizes. Recently, the results obtained using AFM (atomic force microscopy) had confirmed the fact that LS molecules in aqueous solutions form a crosslinked network structure, the shape of LS molecules changing with its concentration in aqueous solution [96].

More authors have observed that the low molecular weight lignin fractions tend to associate by non-covalent linkages (e.g. hydrogen bonds) into complexes with higher molecular weight in certain solvents [113, 114]. The gel permeation chromatography studies evidenced that non-aqueous solvents exhibited multimodal chromatograms, while alkaline aqueous eluents gave rise to broad curves [115]. Other authors have shown that by application various treatments (e.g. esterification or etherification) major changes in the solubility of lignins appeared. Thus, by introduction acetyl or hydroxylpropyl groups in lignin, this becomes soluble in tetrahydrofuran (THF) or other commonly organic solvents [109].

8.3.3 Molecular Weight of Lignin

The establishment of molecular weight of lignins is complicated due to its crosslinked character and poor solubility in non-aqueous solvents. However, data obtained by usual techniques such as viscosimetry [116], size exclusion chromatography, gel permeation chromatography [117, 118], light scattering [119], vapor pressure osmometry [120] and ultracentrifugation [121], suggest that molecular mass of soluble portion of lignin is lower than that of isolated lignin and that it depend not only on plant species but on the isolation procedure and also on measuring method and history of each sample [122]. Fractionation studies of isolated lignin (i.e. lignosulfonates, alkali lignins) have shown that the molecular weight ranging of 10^3–10^6 $gmol^{-1}$. The molecular weight distribution curves for soluble lignins are unimodals and bimodals in some cases [22]. For example, Lindner and Wegner [123] using GPC for fractionated organosolv lignin obtained the average molecular weight (Mw) ranging from 2.7×10^3 to 1.1×10^4 and molecular weight distribution in the ranges from 1.8 to 2.4. Also, Lebo [124] reported that molecular weight distribution for lignosulfonates is large (Mw is

6.4×10^4 gmol^{-1}, *M*w/*M*n ratio 8.8) and for fractionated samples he shown vlaues of Mw from 4.6×10^3 to 4.0×10^5 gmol^{-1}. Molecular weight distribution of lignin in situ was determined by size exclusion chromatography (SEC) and it was found a variation in a range of 1.9–2.4 $\times$ 10^4 [125].

The lignin derivatization with the purpose to enhance its solubility in organic solvents and its characterization was generally accepted. Thus, the acetylated lignin fragments from annual plant were analyzed by size exclusion chromatography associated with ^{31}P-NMR spectroscopy. These lignins had been characterized by molecular weights (Mw) of 7.9–10.4 $\times$ 10^3 and a high polydispersity (3.83–5.87). The polydispersity difference might be due to precipitation of high molecular weight phenolic syringyl components, which are less acidic than high molecular weight units [126]. Sun et al. [127] demonstrated also that the application of a treatment (i.e. alkaline peroxide treatment) on the alkali lignins lead to the degradation of the lignin macromolecules under the conditions given with the decrease of molecular weight (from 3,100 to 2,100 g mol^{-1}) and a polydispersity varying from 1.9 to 4.2.

Glasser et al. [102] studied several types of hydroxyalkyl lignin derivatives synthesized from milled wood, organosolv, steam explosion, acid hydrolysis and kraft lignins. Solubilities in various organic solvents spanning a solubility parameter range from 9.3 to 14.5 and hydrogen bonding index range from 1.5 to 18.7 was established using UV_{280} adsorption of solutions. A greatly enhanced solubility in organic solvents was observed as a consequence of oxyalkylation indicating absence of the gel structure typical for network polymers The lignin derivatives had molecular weights including values between 2 and 5 $\times$ 10^5 and the dispersity factors between 2.5 and 25.

8.3.4 Molecular Conformation of Lignin

It was recognized that lignin by its composition, molecular structure and spatial orientation contributes to wood properties [128]. The presence of the *p*-hydroxyphenylpropane and guaiacylpropane units offers a certain molecular complexity by a great number of intermolecular bonds and crosslinking established with the matrix compounds (polysaccharides).

Studies on the stereochemistry of lignins have been oriented to obtain new information regarding the lignin biosynthesis elucidation. The results of the study concerning the distribution of the diastereomeric forms (*erythro* and *threo* forms of the arylglyceryl β-aryl ethers) suggested that about equal amounts of the two diastereomeric forms in softwood lignins and that *erytrhro* forms are predominant in hardwood lignins [129]. Lundquist and co-workers [130] carried out experiments using the lignin models compounds (β-β, β-1 and β-5 structures) showing that the distribution of diastereomers in lignins differs from that of the equilibrium mixtures for various ratios of the erythro/threo forms. Based on the X-ray crystallographic data on the variety of crystalline lignin models, the authors concluded that the shape of the lignin molecules is influenced by their stereoisomerism and conformation [131].

Micic et al. [132] put forward that the synthetic polymer DHP presents a globule supramolecular assembly. Abreu and co-workers [133] designed a virtual molecule with the β-O-4 structure, which would present a chain with a higher spiral conformation with a low degree of crosslinking, while molecules with a composition of the β-β and β-5 alone would play a low spiral conformation (which have a high possibility to form crosslinking with matrix compound). Starting from this idea, the lignin molecule may have spiral conformation. This presumption was supported by a computer-assisted molecular structure which suggest that lignin biopolymers have a helical structure characteristic of many naturally synthesized molecules [134], while other approaches consider a linear polymer well-defined structure for a synthetic β-O-4 type lignin [135].

8.3.5 Other Properties of Lignins

8.3.5.1 Lignin Antibacterial Properties

Although it is known that a significant amount of lignins from various botanical origins are supplied to the human body by plant foods, little attention was paid to its biological activity and the mechanism of action on human health of lignin or lignin-derived substances. Even if lignin is not digested or absorbed and it is not destroyed by intestinal microflora, it has a special ability to bind bile acids and cholesterol, thus decreasing the absorption of them by intestine [136]. Many vegetables and fruits contain 0.3 % lignin, and for cereal husk a content of 3 % was reported. However, one can imagine that lignin has a health protective effect by its using as a source of bioactive molecules in the pharmaceutical and food additives food.

Lignin is an important source of natural antibacterial compounds. Wood lignin is a phenolic compound containing 11 phenolic monomer fragments with a high content of *p*-coumaric and ferulic acids [137]. In general, phenolic fragments with functional groups containing oxygen (-OH, -CO, COOH) in the side chain are less inhibitory, whereas the most inhibitory phenolic fragments are those containing a double bound in α, β positions of the side chain, and a methyl group in the γ position. Also, it was considered that the antimicrobial activity of lignin is dependent on its extraction methods [138].

Antimicrobial properties of lignin have been studied using a series of model compounds with guiacyl and syringyl structures against different cultures of bacteria, yeasts and fungi. Zemek et al. [139] investigated the antimicrobial effect of phenolic fragments against the following microorganisms: *Escherichia coli*, *Saccharomyces cerevisiae*, *Bacillus licheniformis* and *Aspergillus niger.* The authors found that all lignin fragments exhibit antimicrobial properties; the isoeugenol having the inhibitoriest effect for studied microorganisms in the following order: *B. licheniformis*>*E. coli*=*S. cerevisiae*>*A. niger.* This can be explained by presence of double bond in Cα=Cβ position of the side chain and a methyl group in

γ position [137]. Sláviková and Košiková [140] tested the antibacterial properties of three lignin types (organosolv, sulphite and kraft lignin) against *Staphylococcus aureus, Candida tropicalis, Trichosporon cutaneum şi Candida albicans.*

Also, Nelson and co-workers [141] reported that the Alcell lignin (50 g/L) is capable to inhibit the growth of *Pseudomonas aeruginosa, Escherichia coli,* and *Staphylococcus aureus* colonies. The gel permeation chromatography (GPC) of the rice bran lignin evidenced the modification of molecular weight from about 5,000 to 1,000 and the inhibition of the microorganism growth after 24 h incubation with *E. coli*.

The tests performed on various lignin preparations shown that the antimicrobial activity depends on lignin sample origin, its chemical structure, and its concentration in cultivation medium and type of microorganisms. Thus, it was observed that kraft lignin provided a bactericide effect towards *Erwinia carotovora* and *Xanthomonas vesicatoria* at a lower concentration (0.25 % on nutrition medium), while in the case of *Pseudomonas syringe* şi *Bacillus polimyxa* the lignin did not show inhibitory effect even at the 2 % concentration. Spruce hydrolysis lignin (HL) presented the bactericide activity against *P. syringe* and *X. vesicatoria* in 2 % concentration, but at lower concentration only slight bacteriostatic activity was observed. The modification with quaternary ammonium compound increases bacterial properties of lignins: e.g. for hydrolysis lignin (HL) a stable bactericide effect was achieved at the both concentration used. The fungal species presented different resistance to lignin products and their inhibitory effect being arranged in following order:

Kraft lignin<quaternized hydrolysis lignin<quaternized Kraft lignin.

The antibacterial activity mechanism seems to vary in relation to nature of phenolic compounds. The polyphenolic compounds of lignin cause cell membrane damage and lysis of bacteria with subsequent release of cell content. Some lignin products owing to their microstructure and diversity of sorption centers can realize of simultaneous sorption both of organic pollutants and microorganisms thus activate the process of pollutant biodegradation on interfaces. This was confirmed by sorption experiments carried out with 2,4-D and its bacteria-degrader *Burkholderia cepacia* which was used along with HL and lignin modified with Si-containing compounds [142].

Also, Nada et al. [143] studied the antimicrobial activity of lignin from cotton stalk against *B. subtilis, B. mycoids, E. coli* and *A. niger*. No significant antimicrobial effect of cotton lignins was observed against gram negative bacterium, *E. co*li and fungus A. *niger,* having an effective influence against gram positive bacteria as in the case of bagasse Kraft lignin. Çekmez [144] has been isolated lignin fractions from cotton stalks by alkaline methods at different conditions. Different post treatments such as ultrasonication and TiO_2-assisted photocatalytic oxidation have been applied. The lignins fractions demonstrated different antimicrobial activities towards *Escherichia coli* and *Bacillus pumilus*, depending on the method isolation and post treatment applied (Table 8.10).

Data from Table 8.10 indicated that lignin B had significant antibacterial effect against both *E. coli* and *B. pumilus*. Though preparate A includes a highly toxic compound (sodium borohydride, $NaBH_4$) which inhibits completely growth of both bacteria colonies, lignin A demonstrates very weak antibacterial effect against tested microorganisms.

Table 8.10 The antibacterial effects of cotton stalk lignins and their extraction chemicals against both *E. coli* and *B. pumilus* in liquid medium after 24 h incubation [144]

Compounds and their concentrations concentraţiile (g/L)	Number of *E. coli* cells (CFU/mL) (37 °C)	Microbial log reduction in the number of *E. coli* cells	Number of *B. zpumilus* cells (CFU/mL) (30 °C)	Microbial log reduction in the number *B. pumilus* cells
Lignin A, 50 g/L	1.00×10^9	0.013	9.20×10^8	0.014
Lignin B, 50 g/L	0.00	9.013	0.00	8.978
A, –	0.00	9.013	0.00	8.978
B, –	1.03×10^9	0.00	9.50×10^8	0.000

Initial load of *E. coli* cells: $(1.03 \pm 0.01) \times 1\ 0^9$ CFU/mL; initial load of *B. pumilus* cells: $(9.50 \pm 0.20) \times 10^8$ CFU/mL

Lignin A: lignin isolated from cotton stalks by Zilliox and Debeire (1998) method (24 % KOH + 1 % $NaBH_4$ + acetic acid + ethanol) [145]

Lignina B: lignin isolated from cotton stalks by a modified of Zilliox and Debeire (1998) method (10 % NaOH + 1 % boric acid + acetic acid + ethanol) [145]

FTIR results evidenced the splitting the ester and ether bonds between hydroxycinnamic acids and lignin leading to form of new lignin fractions. On the other hand, FTIR spectra indicated the presence of the C=C bonds in antimicrobial lignin samples suggesting that these bonds might be the reason of the antimicrobial activity. The LC–MS qualitative mass analysis indicated that the antimicrobial lignin fractions might be lignin-derived oligomers.

Lignin B is an antibacterial, natural, renewable and non-toxic product, and for this reason it was integrated into xylan-based biodegradable films obtaining strong antibacterial effect towards tested microorganisms [144] (Table 8.11).

The purified lignins containing low molecular weight monophenolic fragments possess different biological characteristics from those of native lignin. In vivo studies carried out on the different animals confirmed the antibacterial effect of lignin preparations. Thus, purified Alcell lignin has been shown to exhibit prebiotic effects in chickens, favouring growth of beneficial bacteria and improving the morphological structures of the intestines. The animal response to purified lignin action seem to be dependent on dosage, animal species and type and source of the lignin product [146, 147].

8.3.5.2 Lignin Antioxidant Properties

As is known, lignin is a major component in plant fiber and a significant amount of this polymer of various botanic origins is supplied to the human body with vegetable food. Lignin, as phenolic compound, is an effective free radical scavenger that stabilizes the reactions induced by oxygen and its radical species [148], and also it can inhibit the activity of enzymes related to the generation of superoxide anion radicals, acting as a natural antioxidant [149].

The antioxidant effect of different types of lignins has been evaluated by their capacity to inhibit human erythrocyte haemolysis induced by AAPH [2,2′-azobis(2-amidopropane) dihydrochloride], a peroxyl radical initiator (Fig. 8.10) [150], or by hydrogen peroxide [151].

Table 8.11 The antibacterial efect of cotton stalk lignin B-integrated in xylan film against both *E. coli* and *B. pumilus* after 8 h incubation

Film type	Lignin B content (%)	Number of *E. coli* cells (CFU/mL)	Microbial log reduction in the number of *E. coli* cells	Number of *B. pumilus* cells (CFU/mL)	Microbial log reduction in the number of *B. pumilus* cells
Blank xylan film	0.0	9.25×10^8	0.047	8.30×10^8	0.059
Lignin B–integrated xylan film	2.0	2.53×10^8	0.610	1.23×10^8	0.888
Lignin B–integrated xylan film	4.0	8.00×10^8	1.110	4.80×10^8	1.296

Initial load of *E. coli* cells: 1.03×10^9 CFU/mL; initial load of *B. pumilus* cells: 9.50×10^8 CFU/mL; pH–9 for all films

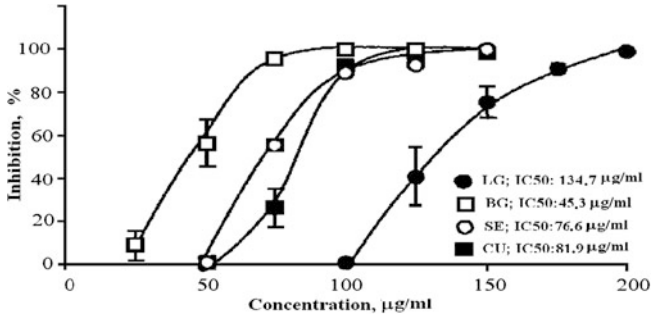

Fig. 8.10 Inhibitory effect of different lignin solutions on haemolysis induced by AAPH: *LG* lignosulfonates; *BG* bagasse lignin; *SE* steam explosion lignin; *CU* Curan a commercial lignin [152]

The highest antioxidant activity was exhibited by bagasse lignin which is characterized by a low IC_{50} value (45.3 µg/mL) (IC50 concentration determining 50 % inhibition on haemolysis induced by AAPH). The haemolysis of erythrocytes induced by AAPH was also studied in the presence of Ligmed-A containing 90 % lignin and what was used as an antidiarrheal drug [152]. The inhibitory effect was dependent on concentration lignin, the greatest IC_{50} value (106.63 µg/mL) being obtained at highest concentration studied [153].

The antioxidant effect of industrial lignins from different sources against lipid peroxidation induced by H_2O_2 was investigated using human red blood cells (RBCs) [152]. From obtained results one can deduced that the high molecular weight was the main factor decreasing the radical scavenging activity. Thus, lignosulfonate with the highest Mn had the lowest antioxidant activity, while the bagasse lignin with the lowest Mn was the strongest antioxidant and Curan and steam explosion lignins which have similar Mn also presented similar antioxidant effect.

Table 8.12 Antioxidant activity (AOA) of some lignins [156]

Plant—raw materials	Sample	AOA, kC per 100 g	
Oats	DL-O	69.4 ± 2.8	0.04
Wheat	DL-W	61.3 ± 2.1	0.03
Fescue meadow (*Festuca pratensis*)	DL-FM	41 ± 2.8	0.07
Hydrolyzed industrial lignin	Polyphen	1.7 ± 0.1	0.04
	Mitofen	87.6 ± 6.6	0.07
DL—dioxan lignin [157]			

A protective effect of lignin against oxidation damage of DNA in the cells of mice has been observed, too [154]. The antioxidant activity of lignin was determination by detection of superoxide anion radicals using the luminal-dependent photochemical method. The preincubation of the isolated cells with lignin led to increase the resistance of both blood lymphocytes and testicular cells to oxidative stress induced by hydrogen peroxide and visible light-excited methylene blue (MB). This was explained by the scavenging both hydroxyl radical and singlet oxygen.

Boeriu et al. [155] followed the ability of lignins to react with the free $ABTS^{+*}$ [ABTS—2,2′-azino-bis(3-ethylbenzo-thiazoline-6-sulphonate)] cation radicals generated by an enzymatic system consisting of peroxidase and hydrogen peroxide. All lignin reacted with $ABTS^{+*}$, but their efficiency was lower (20–30 %) than that measured for the commercial antioxidant BHT (butylated hydroxytoluene). Lignin samples from annual plants (abaca, sisal and jute) and softwoods show the highest scavenging activity against the ABTS radicals.

The antioxidant activity (AOA) of dioxane lignins recovered from Gramineae plants, wheat and oats, was estimated by Kocheva et al. (Table 8.12) [156].

The obtained results showed that the highest AOA value was found for the DL-O 69.4 kC/100 g, followed by DL-W with a value of 61.3 kC/100 g, while for the medical lignin Polyphen, the antioxidant activity was noticeably lower (1.7 kC/100 g). Mitofen lignin [sodium poly(*p*-dihydroxy-*p*-phenylene)-tiosulfonate] has the greatest AOA value (87.6 kC/100 g), and it is widely used in medical practice.

The ESR studies on the lignin structures evidenced its paramagnetism caused by the presence of stable free radicals in the macromolecules. The concentration of paramagnetic centers (PMCs) strongly depends both on the lignin origin and on the procedures of its recovery. For examples, for spruce lignin was found the following concentrations of radicals: Browns lignin 0.5×10^{17} spin g^{-1}, milled wood lignin $(0.23–1.0) \times 10^{17}$ spin g^{-1} and dioxane lignin, 0.83×10^{17} spin g^{-1} and for Gramineae dioxane lignins the PMCs concentration is significant higher $(0.9–2.2) \times 10^{17}$ spin g^{-1} than that in spruce lignins. The PMCs concentration of the grass lignins increases in the same manner of AOA: DL-FM<DL-W<DL-O [156].

The experimental studies on the phenolic lignin model compounds (4-propyl-guaiacol, eugenol, isoeugenol, coniferyl alcohol, coniferyl aldehyde and 4-allyl-2,6-dimethoxyphenol) demonstrated that these compounds had more active antioxidants activity than the commercial inhibitor (2,6-di-*tert*-butyl-4-methyl-phenol) BHT during peroxidation of styrene in chlorobenzene initiated by

azobisisobutyrolnitrilev [158]. The authors also used two dimers and synthetic tetramer models of lignin showing the significant antioxidant properties. The overall relative activity was tetramer>dimers>monomers>BHT.

For the moment, it is not known the mechanism by which lignin acts like antioxidant, but it can be presumed that it can be a scavenger of free radicals thanks to its phenolic structure. Several mechanisms have been proposed [159]: (1) lignin acts like a chelation agent scavenging metals of Fenton's reagent; (2) lignin acts as a "suicide" antioxidant, receiving the attack of the hydroxyl radical avoiding the action of this radical on target molecules, or (3) lignin inhibits enzymes involved in the metabolic pathways able to generate free radicals.

Phenols can scavenge peroxyl radicals due to the presence of hydroxyl groups containing mobile hydrogens. Supplementary, phenols presents capacity to reduce or to chelate necessary divalent ions for several reactions. On the other hand, phenolic antioxidants can interrupt the oxidation reactions by hydrogen atom transfer or by electron transfer with the formation of the radical cation phenoxy, which is fast and reversible deprotonated forming the phenoxy radical. These two mechanisms always happen in parallel but with different rate. Although these mechanisms have the same net results, is preferable to consider the electron transfer because the radical cation formed by electron transfer can be mutagenic.

Telysheva and co-workers [148, 160] followed the capacity to scavenge free stable radicals of DPPH* (1,1-diphenyl-2-picryl hydrazyl) on the different lignin preparations (e.g. methanol soluble fractions from commercial softwood kraft and hydrolysis lignins).

For lignin fractions soluble in methanol it has been confirmed that the OH_{phen} group plays a crucial role in radical scavenger activity of lignin in the DPPH assay.

Antioxidant activity of the isolated lignins can be explained by the presence of π-conjugation system like type stilbens, which could act as catalyst or activators of the lignin phenolic structures interaction with DPPH*. The rate constant for DPPH* disappearance in the case of different lignins depends both the number of phenolic hydroxyls and development degree of π-conjugation systems. The high molecular weight, heterogeneity and polydispersity are among the factors decreasing the radical scavenging activity [161].

8.4 Nanoparticles Based on Lignin and Their Applications

By analogy with materials science, lignin, second major component of the wood, can be defined as a branched, three-dimensional amorphous macromolecular structure what exhibits molecular interactions. From this reason, the lignin can be considered both as a polymer in solution and in solid state providing many opportunities in nanotechnology.

The characteristic features of particles with dimensions below 100 nm are an interesting and important field of studies in wide domains, such as: (a) in medicine to provide drugs; (b) new smart nano-sized coatings beginning to be used on an

industrial scale, and also information technology (IT); (c) cars, cosmetics, chemicals and packaging industries and (d) additives for plastic material industry [162].

The obtaining of nanoparticles based on natural polymer constitutes a major concern for many research teams because of their accessibility and their environmental compatibility. Information on the synthesis of lignin nanoparticles containing products are relatively limited and covered by patents.

8.4.1 Lignin Nanoparticle Properties

One ways of characterization the morphology and aggregation of materials is to determine their sizes. The lignin particles sizes have been studied previously with a variety of methods such as: viscometry, sedimentation, and diffusion measurements in the solution state [163], the box counting method applied on a lignin surface [164], and simulations of the cell wall structure have brought up the idea about fractal lignin [165].

Recently, data regarding the lignin study both in the solid state and solution with the modern and performance techniques, namely the small-angle X-ray scattering (SAXS) and ultra-small-angle X-ray scattering (USAXS) [166], pulsed field gradient spin-echo NMR [167, 168], nano zeta sizer techniques [169] have been reported.

Vainio and co-workers [166] have been summarized the information on the size and shape particle both the dry and dissolved state of the lignin, showing that it is rather difficult to get a general picture of the exact shape and the actual size of an isolated lignin particle. This is due to both the different isolation procedures and the analytical methods used in the measurements of the lignin particle dimensions.

Notley and her group [168, 170, 171] have described the aggregation of kraft lignin particles and they have determined the dimensions of clusters using quasi-elastic light scattering. The aggregation of kraft lignin starts with the self-association of macromolecular kraft lignin into compact colloidal particles in solutions of simple electrolytes. The rapid diffusion-limited colloid (cluster)—colloid (cluster) aggregation is the result of negligible repulsive forces between the colloidal particles, following the von Smoluchowski equations. These particles then associate to aggregates ranging in size from about 100 nm, as deduced from cryogenic transmission electron microscopy photographs. The colloidal stability of dilute solutions of technical lignins depends by alkalinity, ionic strength and temperature [172]. The specific surface area, defined as the total surface area of the sample divided by the mass of the sample, is a measure of the porosity of the material which gives information on the delignification process. Thus, for kraft lignin, by nitrogen absorption experiments a value of 0.77 m^2/g for the specific surface area was obtained [173]. Dry lignins are thought to be composed of subunits of somewhat irregular size and shape. It should be possible to obtain some estimations of the size and shape of the subunits by investigating lignin in the dissolved state. Based on electron microscopy studies, Goring et al. [174, 175] proposed for the first time an

Table 8.13 Surface fractal dimension, Ds, of the lignins at room temperature determined from SAXS and USAXS [166]

Lignin sample		Power-law exponent, α	Region ($Å^{-1}$)	Mass fractal dimension, D_s	Specific surface area, S_I (m^2/g)
CKL	Curan 100 kraft lignin	4.0	0.03–0.2	2	2.4
		3.3	0.009–0.03	2.7	
AOL	Alcell organosolv lignin	4.1	00.3–0.15	2.0	0.5
RSCL	Released suspension culture lignin	4.0	0.02–0.2	2.0	60
MWL	Milled wood lignin	4.1	0.01–0.25	2.0	34
BJO	Björkman lignin	4.1	0.02–0.25	2.0	35
SEL	Steam explosion lignin	4.1	0.005–0.2	2.0	1.3
SOL	Soda lignin	4.0	0.01–0.25	2.0	3.6

oblate shape of the lignosulfonate macromolecules in solution with about 2 nm thick. Garver and Callaghan [167] using field gradient NMR found that the acetylated kraft lignin particles in 1.0 M $CHCl_3$ solution seem to be oblate with an axial ratio of ∼18. They also determined the hydrodynamic radius to be 2.29 nm for kraft lignin (*M*w) 4500) in 1.0 M NaOD.

Using the same method and assuming the shape of the macromolecule to be spherical, Norgren and Lindström [168] established that the hydrodynamic radius of several lignin fractions (concentration, 1.0 wt%) ranged from 1.0 to 2.2 nm in 0.1 M NaOH/NaOD.

Vainio and her group [166] studied by small-angle and ultra-small-angle X-ray scattering (SAXS and USAXS) the morphology of several lignins extracted from plant cell walls using different methods. The average molar masses determined (gel permeation chromatography (GPC)) for the studied lignin samples depend on the isolation procedure and are in the range of 2530–10860 g/mol having a polydispersity index of 1.3–2.8. Vainio obtained two values for power-law exponent (α) indicating a fractal structure which started from about 3.5 nm and continued onto large sizes, probably due to the presence of the pores at the aggregate surfaces. For the rest of lignins, the exponent value was about 4, indicating that the particles are in a form of compact aggregates. The specific surface area of the dry lignins varies with the delignification method (Table 8.13).

By redissolution of the CKL powder the thickness (t) and width (w) of particles have values around 1.3 and 2.5 nm, respectively, indicating an imperfect packing of the particles.

The particle-size distribution pattern in the solution was studied by dynamic light scattering which allows recording particles with sizes within 0.001–10 μm distribution and patterns of the solutions are presented as histograms. Figure 8.11 shows the particle-size distribution pattern for kraft lignin at different temperatures [176]. It can be seen that the modal size of the particles of kraft lignin dispersed at 293 and 313 K is 10 nm; at 333 K it increases to 30 nm. Clearly, rising

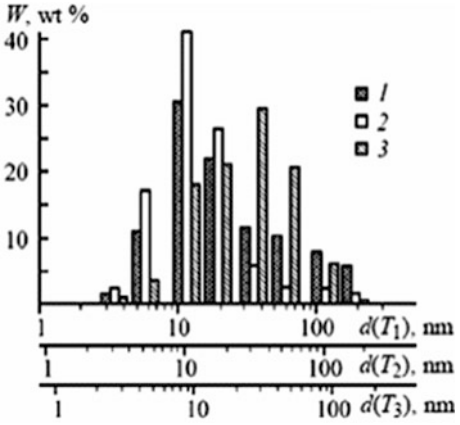

Fig. 8.11 Particle-size distribution pattern *W* for kraft lignin in aqueous alkali solution (pH 12.7) at different temperatures [176]

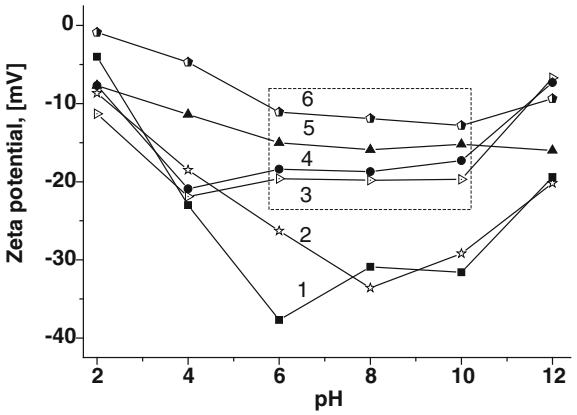

Fig. 8.12 Effect of pH on Zeta (ξ) potential for samples: *1* hardwood Kraft lignin; *2* hardwood hydrolysis lignin; *3* hardwood steam explosion lignin; *4* softwood Kraft lignin; *5* softwood organosolv lignin and *6* soda wheat straw lignin

temperature increases the aggregation instability of the kraft lignin solution, as evidenced by increase in the particle size. This is evidently due to a decrease in the degree of hydration of kraft lignin with rising temperature.

In another work, [177] described the particle-size distribution of sulfate lignin based on thermodynamic model. This model suggests the formation of steady-state microstructure by aggregation of primary lignin particle into metastable clusters (aggregates) closely packed. The distribution of the statistical ensembles of particles is broadened and their average size increase with temperature due to the thermal coagulation process.

Determination of zeta potential shown that organosolv, soda and stream explosion lignins have lower values (0.62–9.78 mV) than those determined for the kraft lignins (20.7–30.4 mV). This means that these lignins are characterized by electrostatic attractive forces among particles leading to the formation of aggregates [169]. The evolution of zeta potential with pH shows a plateau in the range of pH 6–10 indicating a cvasi-stable solution, while at lower values of pH the lignin solutions became unstable due to the precipitation (coagulation) of lignin

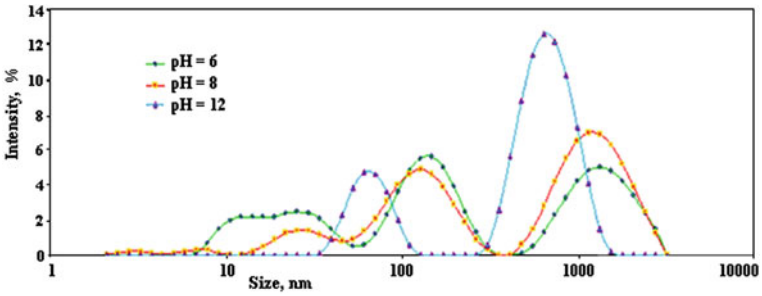

Fig. 8.13 Size distribution of hydrolysis lignin particles in aqueous solutions with various pH values

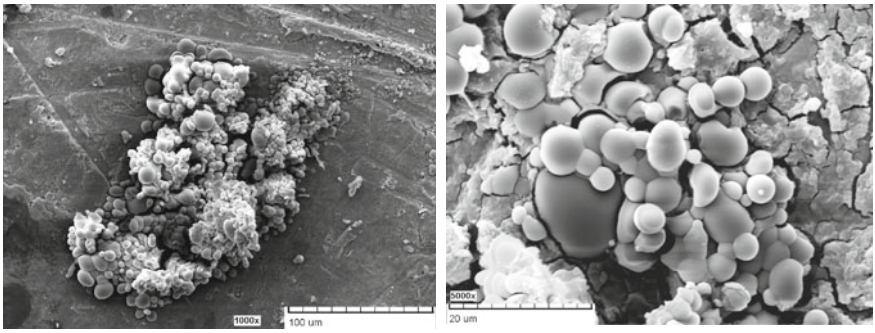

1000x 5000x

Fig. 8.14 SEM images of birch lignin at pH = 6 [179]

(Fig. 8.12). This observation is in a good agreement with the model of reversible aggregation proposed by Bonnikov and Dem'yantseva [177].

Cazacu et al. [169] investigated the aggregation state of the hydrolysis lignin in aqueous solutions depending on pH. All investigated solutions contain nano sized particles. The lignin particle size distribution pattern is bimodal in alkaline medium containing a nano sized lignin fraction with the dimensions of 10–100 nm and a micrometer fraction having a maximum value of about 100 nm indicating the formation of the lignin particles (Fig. 8.13). In the solutions with acid pH the size distribution is trimodal showing presence of the more fractions with size >100 nm due to the forming of lignin association in acid medium.

Shulga et al. [178] confirmed the high degree of the association of the birch lignin particles in water media. The supramolecular structures (Fig. 8.14) are shown as extended cluster consisting from typical globular structures.

The possibilities to obtain lignin or its derivatives based nanoparticles could represent a new research direction with both fundamental and application perspectives. Căpraru [162] subjected different types of alkali lignins from annual

Table 8.14 The average dimensions for nanoparticles obtained from five types of lignins [162]

Samples		Average size, μm
$L1_{nano}$	Wheat straw lignin	0.123
$L2_{nano}$	Sarkanda grass lignin	0.027
$Pb1000_{nano}$	Commercial lignin (Protobind)	0.038
$Pb2000_{nano}$		0.327
$Pb3000_{nano}$		0.329

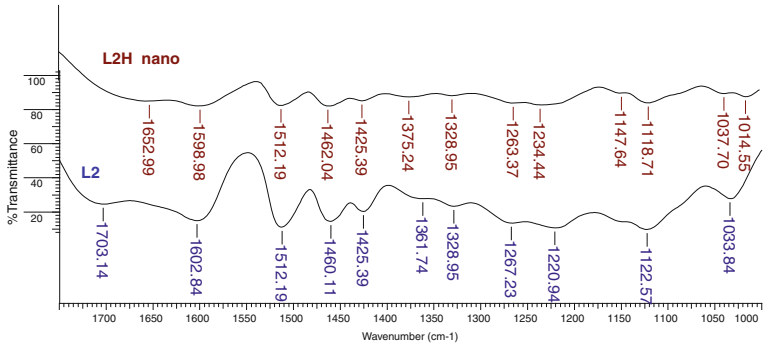

Fig. 8.15 The FTIR spectra of unmodified grass lignin (L2) and modified ($L2H_{nano}$) by hydroxymethylation

plants (wheat straw and Sarkanda grass) and commercial lignins (Protobind) to modification by hydroxymethylation and epoxydation reactions. The chemically-modified lignins were recovered from reaction medium by centrifugation, and were studied from the point of view of the treatment influence on the dimensional distribution of nanoparticles. The first observation was that the size distribution curves can be unimodal or bimodal in relation with the lignin type. The nanoparticles distribution domain for wheat straw lignin was between 0.05 and 0.5 μm, while for Protobind lignins have a broader dimensional distribution range (0.1 ∼ 0.8 μm). The nanoparticles resulted from the other three types of commercial lignin were characterized by a more uniform distribution and the dimensional range was different depending on the nature of the substrate. In Table 8.14 the values of average dimensions for nanoparticles resulted from modification (hydroxymethylation) of the five types of lignin are presented.

In order to obtain more information, these modified products were also studied by FTIR spectroscopy, through which modifications that appeared at a functional level were observed. (Fig. 8.15)

The decrease of intensity of absorptions caharacteristic to the hydroxylic groups and aromatic rings can be correlated with the participations of structural units of lignins in substitutions and condensation reactions and the creation of conditions for obtaining nanoparticles.

At the same time the presence of nanoparticles were signalled in the supernatants resulted from the reaction epoxidation of comercial lignin samples (Prorobind) [162, 179, 180]. The average particle size was about 0.246–0.248 μm. The data emphasizes the fact that nanoparticles, are characterized by uniform distribution, similar to the three studied samples, synthesized derivatives presenting close epoxidation numbers The obtained data indicated the fact that nanoparticles' dimensions and distributions were different depending on the lignin type subjected to hydroxymethylation [181].

8.4.2 Nanolignin Applications

The synthesized derivatives containing hydroxymethylated lignin-based nanoparticles were used in combined with copper ions solutions, with the purpose to achieve biocide systems used to the increasing of biological stability of wood subjected to the action of microorganisms from soil [182]. The birch tree veneer samples treated with hydroxymethylated lignin-based nanoparticle were buried in soil for a few months. At the same time, the birch veneer samples were treated with copper complexes of lignin derivatives, copper solutions ($CuCl_2$ and Cuam) and unmodified lignins. In Figs. 8.16 and 8.17 there are shown mass loss variations as recorded in samples of birch veneer.

The data obtained for samples treated with lignin based nanoparticles and copper compounds shown that the mass losses were lower compared to those of untreated samples. The lower mass losses were due to synergetic toxic effects of copper and lignin derivatives which under complex form limit and inhibit the microorganisms' attack. The treatment of wood surface with copper containing solutions, especially when provided by the chloride derivative and the lignin nanoparticles, proved to be more efficient. Lignin-copper complexes derivatives fall in order as follows: $Pb2000_{nano}$> Pb3000nano> $Pb1000_{nano}$> $L2_{nano}$> $L1_{nano}$, in terms of assurance of wood biological stability. This situation may be correlated with various functionalities of lignins induced through hydroxymetylation, consequently resulting in different degrees of copper complex forming and wood surface interaction [179, 183, 184].

The contact angle data reaches high values (94–116^{o}) for treated samples providing a high biological stability and hidrophobicity of wood surfaces, due to the efficient action of lignin nanoparticles in the presence of copper, that adhere to the wooden layer, ensuring better protection against microbiological attack. Therefore, it can be assumed that the synthesized lignin products provide a high wood surface stability when submitted to the action of soil microorganisms [185, 186].

Treatments performed only with lignin-based nanoparticles are relevant, a value of the contact angle of 115° being registered at a veneer sample treated with $Pb1000_{nano}$ lignin. Compared to the above presented results, the determination of the contact angle, in the case of hydroxymethylated lignin-treated samples or

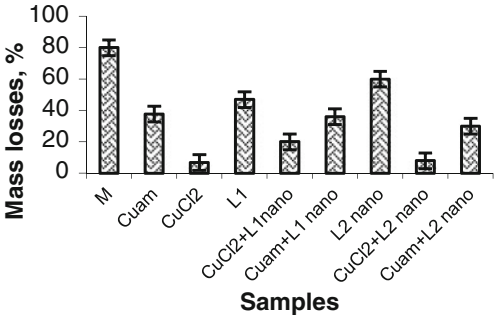

Fig. 8.16 Variation of mass loss for the birch veneer samples non-treated (M) and treated with $CuCl_2$, Cuam, $L1_{nano}$, $CuCl_2L1_{nano}$, $CuamL1_{nano}$, $L2_{nano}$, $CuCl_2L2_{nano}$, $CuamL2_{nano}$

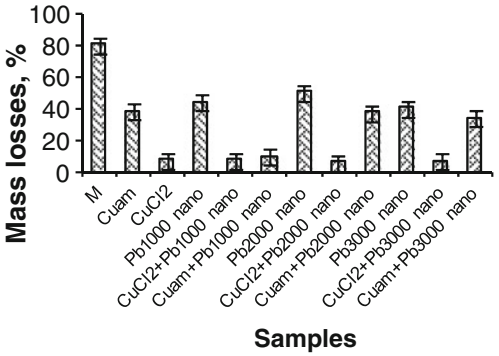

Fig. 8.17 Variation of mass loss for the birch veneer samples non-treated (M) and treated with $CuCl_2$, Cuam, $Pb1000_{nano}$, $CuCl_2Pb1000_{nano}$, $CuamPb1000_{nano}$, $Pb2000_{nano}$, $CuCl_2Pb2000_{nano}$, $CuamPb2000_{nano}$, $Pb3000_{nano}$, $CuCl_2Pb3000_{nano}$, $CuamPb3000_{nano}$

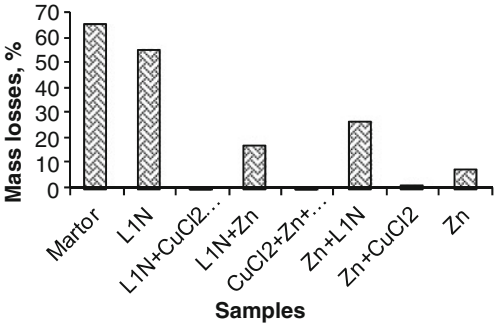

Fig. 8.18 Variation of mass losses for the birch veneer samples non-treated (M) and treated with L1 N, L1N + $CuCl_2$ + Zn, L1N + Zn, $CuCl_2$ + Zn + L1N, Zn + L1N, Zn + $CuCl_2$, Zn

epoxydated ones, evidenced that the values of the contact angle increase significantly at samples treated with lignin-based nanoparticles.

Another experiment was an attempt of treating birch tree veneer samples with hydroxymethylated lignin-based nanoparticles and unmodified and modified lignins through hydroxymethylation, along with copper and zinc compounds. These products were used in wood surface treatments and the effect was followed by the action of microorganisms existing in the soil (Figs. 8.18 and 8.19) [184].

The lower weight losses are due to both lignin modified through hydroxymethylation, that is able to penetrate the veneers surface more easier, granting it

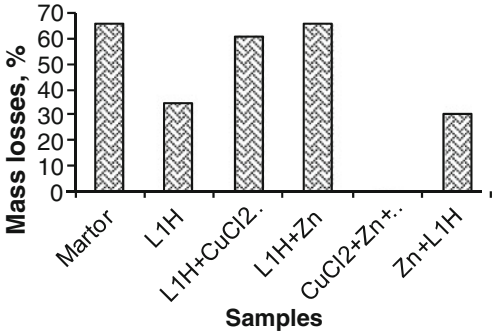

Fig. 8.19 Variation of mass losses for the birch veneer samples non-treated (M) and treated with L1H, L1H + $CuCl_2$ + Zn, L1H + Zn, $CuCl_2$ + Zn + L1H, Zn + L1H

strength, and also due to the cumulated action of copper and zinc ions, known for their protective effect against the microorganisms from soil.

As it can be observed from the data obtained, the mass losses recorded for samples treated with modified lignin nanoparticles and copper and zinc ions solutions led to satisfactory results in terms of birch veneer stability. In this case the biodegradation process is represented by the changes that occur in birch veneer samples in the presence of soil microorganisms. The effectiveness of the wood surface treatment applied depends on the nature of the used product, the order of application and the degree of modification and complexation.

The values of the contact angle of samples treated with copper and zinc complexes lignin derivatives indicated a high stability against microbiological attack, observation confirmed by the data obtained by Yamaguchi and Yaoshino in the case of tannin with copper [187].

The use of copper chloride and zinc acetate intensifies the wood response, probably due to wood tissue penetration and complex forming between wood components, lignin derivatives and metal ions, thus determining an increased biostability. The copper and zinc ions' action might be explained by their retention by wood components' functional groups, lignin playing an important role.

It is known that lignin is a natural absorbent of UV radiation showing antibacterial properties. To improve UV resistance and antibacterial properties of textiles attempts were made to obtain high quality kraft lignin's in nanolignin dispersion to be used in the finishing process of textiles instead of chemical UV absorbers. Lignin with nanostructure obtained by ultrasonic treatment in water solution (<1 g/L nanolignin concentration) was padded on linen fabrics, and for a better fixation of the nanolignin particles on the fabric was used a silicone emulsion [188]. In the last years the major focus on enzyme applications in the pulp and paper field has shifted toward pulp fibre modification with aim of producing improved and/or innovative materials.

Several authors shown that laccase can enhance paper properties through direct lignin oxidation in the fibres or by grafting molecules to lignin, thus creating new types of chemical bonds on the surface [189]. The laccase treatments were performed in the presence of nanofiltered low molecular weight lignin isolated by ultrafiltration of kraft black liquor from softwood pulping. Distribution of the

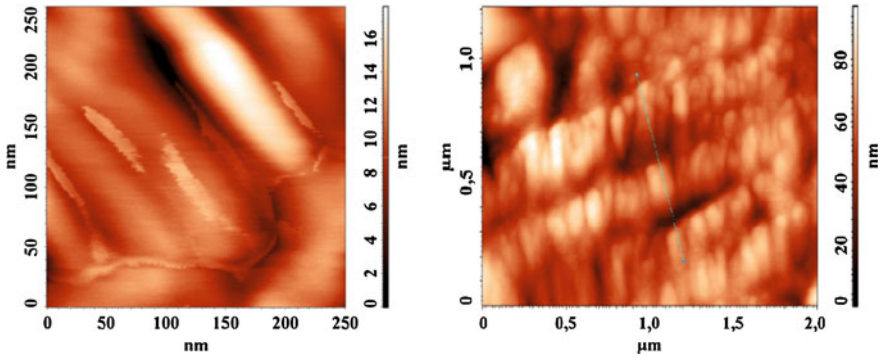

Fig. 8.20 2-D AFM representations of the surface topography for the PVLSE network

average molecular weights of ultra-filtrated lignin (UFL) is quite narrow corresponding to an oligomer formed by approximately 13–15 phenylpropanoid units, and can also contain units like tetramers types. Feature of this product is its size (average molecular weight of 2,500 Da) and high phenolic content (phenols/aromatic ring of 36 %) that it a suitable reactive substrate for lignocellulose fibres crosslinking. The laccase initiated crosslinking of lignin, mediated by UFL lignin lead to a remarkable improvement of wet tensile strength of kraft liner pulp without loosing other critical mechanical properties.

Due to its characteristics (low density, low cost, low abrasive character, nano particles formation, antibacterial and antioxidant properties) lignin was used in the manufacture of composites or blends together with various polymer matrices.

Ciolacu and co-workers [190, 191] studied the possibility to obtain new materials by incorporation of nanolignin particles in synthetic polymer matrices with possible applications in the medical and agriculture areas. Thus, new interpenetrated network hydrogel (PVLS) based on poly(vinyl alcohol) and ammonium lignosulfonate have been realized by crosslinking with epichlorohydrin in alkaline medium. The size distributions of the particles in aqueous solutions containing PVLS hydrogel is unimodal containing particles sizes around 5 nm in diluted solutions and around 100 nm in concentrated ones. By scanning electronic microscopy (SEM) and atomic force microscopy (AFM) was revealed a homogeneous structure that presents a uniform distribution of the lignin particle in PVA matrix. AFM images (Fig. 8.20) showed a fine rugosity of the PVLSE surface with depths around 80 nm.

The enzymatic degradation of these hydrogels in the presence of laccase from *Trametes versicolor* has been studied. The influence of the enzymatic treatment was tested by including and releasing processes of procaine in/from lignin based systems [190]. In another paper are reported the results concerning the obtaining of lignin containing PVA blends (MPL) by melt blending [191, 192]. Aqueous solution of the binary PVA/LSA blends contains particles with the size of around 100 nm, while the solution of the ternary blend PVA/LSA/EP-MA contains the

particles having dimensions of 8–10 nm. This can be explained by the compatibilizing effect of the EP-MA which leads to prevent association and to realize a uniform distribution of the lignin particles. Through the incorporation of the relatively low-molecular mass lignin fractions, a plasticizing effect occurs improving the PVA thermal processability and a significant increase of the tensile properties.

The soy protein isolate (SPI)/hydroxypropyl alkaline lignin (HPL) blends have been prepared by mixing them in aqueous solution containing a small amount of glutaraldehyde as compatibilizer, and then compression-molded to obtain plastic sheets [193]. The investigation of the SPI/HPL blends by FTIR spectroscopy, X-ray diffraction, transmission electron microscopy, and scanning electron microscopy, indicated the existence of amorphous networks and nanoscale HPL dispersion in the SPI matrix. When HPL content was lower than 6 wt%, the HPL-domain occurred in SPI/HPL composites with a dimension of about 50 nm, indicating a high interfacial activity. Differential scanning calorimetry analysis showed that the glass transition temperature of the SPI/HPL sheets increased from 62.5 to 70.4 °C with an increase of HPL content from 0 to 6 wt%. Moreover, the tensile strength of the SPI/HPL nanocomposite sheets with 6 wt% HPL and 3.3 wt% glutaraldehyde was enhanced from 8.4 to 23.1 Mpa.

Incorporation of lignin was investigated with the goal to improve of the starch matrix hydrophobicity. An industrial pine Kraft lignin and its fractions obtained by sequential extraction with organic solvents (dichloromethane and methanol) were used to obtain starch/lignin cast films [194]. The lignin fractions differ both in average hydrodynamic properties and polydispersity. The structural investigation by GC–MS analysis evidenced the presence of the low-molecular weight phenolics (mono- or dilignols) occurring in the kraft lignin fractions. Microscopic observations [195] shown that kraft lignin/starch films have a heterogeneous structure consisting of 1 μm lignin particles dispersed in a starch matrix, and fluorescence microscopy revealed that some phenolic fractions from role. The incorporation of the high molecular weight lignin fraction affects the film properties leading to a very brittle material. The low molecular weight lignin fraction no significantly influenced the film properties, but reduces the water content and water solubility of the film because the high amount of water-soluble phenolics released from this fraction. These compounds interact with the starch matrix by hydrogen bonding leading to increase of its adherence to lignin domains and a plasticizing effect kraft lignin was miscible with starch. Mechanical properties (stress at break and elongation at break) of the lignin/starch films suggested that lignin heterogeneity plays an important [194].

Starch/kraft lignin/glycerol blends were prepared by film casting from aqueous solution and extrusion [196]. Microscopic analyses indicated that the lignin was dispersed into small nanosize domains (0.1–1 μm) within the starch-glycerol matrix. The composites films present good mechanical properties which depended on the ammonium hydroxide amount used to disperse of lignin in the aqueous phase. Lignin improved water resistance relative to starch controls only in starch-lignin blends, in comparison with the ternary blends where glycerol causes a decrease of the water resistance.

Novel transparent composite films based on cellulose, starch and lignin were prepared from an ionic liquid (IL), 1-allyl-3-methylimidazolium chloride (AmimCl), by coagulating in a nonsolvent [197]. By observing the surface morphology of the composites films, it can be seen that all films display uniformity from the interior to the surface that has a dense and homogeneous texture, proving the excellent compatibility in the ternary blend. This can be explained through the fact that the three biopolymers can be dispersed molecularly in AmimCl and the rapid coagulation process determined to establish of the hydrogen bonds between the hydroxyl groups on their molecular chains leading to formation aggregates. The composites films showed good mechanical properties in wet and dry state, the thermal stability and high gas barrier capacity, being recommended to use as food packaging.

Since lignin is a polar polymer has a low solubility in non-polar synthetic polymer matrix. This may limited its reactivity to oxidation reactions and its protective effect of polymer, in comparison with that of synthetic antioxidants. The most commonly polymer matrices used were polyolefines (polypropylene, PP and polyethylene, PE). By using several micro-mechanical models (Halpin–Tsai, Nielsen, Pukánsky) Sánchez and Espósito-Alvarez were able to estimation of the tensile properties and modulus of elasticity of composites based on the polypropylene (PP) and lignin [198]. Lignin content was 10–55 wt%, and the obtained mechanical properties values recommended lignin in various industrial applications, such as: automotive, construction, furniture, packaging and cosmetics. The biodegradation capacity of PP blends films containing 4 % organosolv lignin was confirmed by treatment with enzymes produced from white rot fungi *Phanerochate chrysosporium* [199]. The biodegradation degree of blends films was determined by monitoring their mechanical properties. A correlation between the decrease of the elongation at break and the amount of the lignin fragments released into the extracellular medium has been found.

Investigations on the antioxidant properties of lignin in the polyolefin matrix were carrying out by Pouteau et al. [200]. They have used several types of lignin from wheat (straw and bran) extracted by different procedures and industrial kraft lignin fractions. Mixing a low amount lignin ($\sim$1 wt%) with polypropylene was performed on a micro-extruder obtaining the PP/lignin films which then were pressed at 60 μm. The polydispersity of lignin fractions has a negative effect of its solubility because high molecular weight chains limiting the solubility of active low molecular species. The average surface area of aggregates varies from 57 to 1,395 μm^2. Average dimension of lignin aggregates has been correlated to antioxidant activity. The low molecular weight and low total OH content (aliphatic and phenolic hydroxyl content) tend to improve the compatibility of two partners and consequently the antioxidant activity.

The influence of lignin concentration on the oxidative stability of the PP and recycled PP (recPP) was examined by differential calorimetry under non-isothermal conditions [201]. The results indicated that lignin exerts a stabilizing effect both on the virgin and recycled polypropylene. The antioxidant activity increases up to 5 % lignin content. It was also observed that the presence of lignin influences the Vicat softening temperature of lignin improving the heat resistance of polyolefins.

By blending a commercial polypropylene with lignin (concentration 1 and 2 wt%) made it possible to prepare optically transparent films (thickness 50–60 μm) with acceptable mechanical properties [155]. The lignin takes action as a processing stabilizer during thermo-oxidative aging of polypropylene films. Lignin addition to PP/0.5 wt% Irganox (commercial stabilizer) films enhanced its anti-oxidant efficiency probably due to ability of lignin to modify surface properties of PP influencing the increase of Irganox diffusion into polymer matrix [202]. The mechanical properties (tensile at break and elongation at break) of the films before and after thermo-oxidative aging demonstrated that the PP films containing up to 2 wt% lignin rather stable towards thermo-oxidation in comparison with lignin-free film containing the commercial stabilizer.

A study on the effect of introduction ammonium lignosulfonate (LS-NH_4), epoxy-modified lignosulfonate (LER) on the melt processing of some systems containing polypropylene as matrix and maleated elastomer (ethylene-propylene rubber grafted with maleic anhydride, EP-MA) have been realized [203, 204]. Processing parameters, some tensile parameters (Young Modulus, stress and elongation at break) have been affected by the presence of lignin due to the possible interactions (physical and chemical) at the interphase between the anhydride groups of EP-MA with polar groups of LER or LS-NH_4.Lignin can also act as a plasticizer/melt flow controller, while at low amount (5 wt%) a certain effect as nucleating agent was observed.

8.5 Lignin Applications Perspectives

Though, lignin represents one of the lowest-cost chemical resources available on earth ($ 0.20 on kg), in this moment in worldwide, only 1,000,000 tons/year (<2 % of the total available in separated form) are currently used for non-fuel purpose especially in polymeric form.

Almost all lignin in current commercial use is as lignosulfonates produced from spent sulfite pulping liquor. Most lignosulfonates are obtained from the spent pulping liquor of sulfite pulping operations, although some of them are also produced by postsulfonation of lignins obtained by kraft pulping. Recovered lignosulfonates may be used with little or no additional treatment or they may be converted to specialty materials with the chemical and physical properties adjusted for specific end-use markets.

The world's first investigations into commercial development and application of lignin were performed by Rotschild WI by Marathon Corporation (Borregaard LignoTech's U.S. production facility) in 1927. The first lignin products were used as leather tanning agents. Later, the various products derived from lignosulfonic acid in the form of calcium, sodium, ammonium, iron and chromium salts were applied as dispersants, emulsion stabilizers, battery expanders, concrete mixtures, clay plasticizers and binding agents. In 1970–71, about 10–15 % of the potential lignosulphonate output was used for vanillin. The lignin applications were based on its bulk properties such as solubility, surface activity and solids content.

Lignosulfonates are mainly used as dispersants and binders. Concrete admixtures are the leading market for lignosulfonates, accounting for 38 % of world consumption in 2008. Consumption as binders in copper mining, carbon black and coal is the next largest world market, accounting for 12 % of world consumption in 2008. Dispersant applications of lignosulfonates accounted for 67.5 % of world consumption in 2008 followed by binder and adhesive applications at 32.5 %. Major end-use markets include construction, mining, animal feeds and agriculture. Overall economic performance will continue to be the best indicator of future demand for lignosulfonates. Demand in most downstream markets is greatly influenced by general economic conditions. As a result, demand largely follows the patterns of the leading world economies [205].

It is known that annually huge quantities of kraft lignins are generated and employed as fuel. Because the main functionality in lignins is the hydroxyl groups, this products have been employed as polymeric components in phenol–formaldehyde resins, polyurethanes, epoxies and acrylics. On the other hand, as a consequence of specificity in the intermolecular associative interactions into kraft lignin structure, it can be incorporated into polymeric matrices obtaining kraft lignin-based thermoplastics possessing a broad range of mechanical properties [206].

In Romania, in 1980–1990 period, great quantities of spent liquors obtained from pulping process (especially by bisulphite procedure) and from hydrolysis process of some wood and annual resources with a high content of carbohydrates, lead to approach some studies regarding lignin chemistry. Thus, from ecological and economical point of views some research groups from wood chemistry field have awarded a great attention to capitalization of lignosulfonate complex. In this way, after carbohydrates removing from spent sulphite liquor (by fermentation with the aim to obtain fodder yeast), the lignosulfonates were transformed from lower waste product into raw materials for valuable products. Depending on the specific properties, such as: emulsifying, dispersal, clamminess and absorption capacity, the lignosulfonates (LS) nonmodified or chemically modified were successfully tested in: agriculture—LS-NH_4—as binding agent for mixed fodder granules and modified LS-NH_4 by oxidative oxiammonolysis—fertilizer; wood industry—LS-NH_4 and LS-Ca—in adhesive composition to obtaining fibre boards; chemical industry—LS-Ca—to manufacture vanillin, surfactants and dispersing agents for dyes, pesticides; electrotechnics—expanders for Pb acid batteries; paper industry—as additives for dispersions of resins and to increase of paper resistance; oil and gas extractive industry—LS-Fe, LS-FeCr, LS-NH_4, LS-K, LS-Al—as additives for preparation and treatment of the drilling mud and cement for oil-wells; building materials industry—LS with different cations—additives for concrete mixture.

By application of some reactions characteristic to macromolecular chemistry functionalization of lignin was performed obtaining new products with high value which lead to increasing the possibility to use lignin in different fields, such as: agriculture (plants cultivation and animals forage), wood processing, metallurgy, extractive, textile, etc.

In the last 10 years a new very interesting and actual subject was approached, namely—multicomponent polymeric materials. The development of modern

complex materials by incorporation of lignin products and lignocellulose in synthetic polymers was determined by their large accessibility, low price and possibility to reach of performing proprieties, such as: specific physical–mechanical proprieties, low density, high hardness, good thermal properties, chemical, friction and humidity resistance, or relative high hydrophilicity, etc.

To improve the value-added applications of lignin on medium- and long-term, conversion technologies must be developed, especially for the preparation of low-molecular-weight compounds as an alternative to the petrochemical industry [207].

Based on literature [205] information we can appreciate that the potential lignin-based products were divided into the following three directions:

(a) power, green fuels and syngas—the use of lignin purely as a carbon source using aggressive means (gasification, pyrolysis and hydroliquefication) to break down its polymeric structure leading to products with near-term utilization opportunities;
(b) macromolecules—products with the macromolecular structure and high molecular weight (carbon fibers, polymer fillers, resins, adhesives, composites)—products with medium-term opportunities;

The primarily applications with few or no modification (other than sulfonation or hydroxymethylation) of lignin are as dispersants, emulsifiers/surfactants, binders and sequestrants. These uses represent relatively low value and limited applications, but by the development of appropriate technologies to modify, control and amplify lignin's polyelectrolyte properties, chemical reactivity and compatibility properties with other monomers and polymers, it could be turn into higher-value polymer products.

It is know that lignin is variable by its natural (genetic) origin and also by its isolation and modification processes. From these reasons there are some limitations in the lignin uses in the material industries field, which consist in: (1) molecular incompatibility with thermoplastic polymers in polyblends, and (2) incompatibility/immiscibility/insolubility with crosslinking reagents in thermosets. Some proposed technologies include predictable molecular weight control, facile introduction of reactive functionality (addition of ethoxy, epoxy, vinyl and carbonyl moieties). Molecular weight control leads to improve polydispersity, depolymerization, intermolecular cross-linking and phenolic functionality. The modified lignins can be used in a variety of high-value applications. Applications may include high-strength engineering plastics, heat-resistant polymer, antibacterial surfaces, high-strength and formaldehyde-free adhesives and light- and ultraviolet-resistant polymers (Table 8.15) [205].

Lignin is a potential substitute for oil-based phenols in phenolic and epoxy resins and adhesives [208, 209]. Incorporation of lignin into polymer matrix (polyolefin) offers certain benefits including improved chemical and/or physical properties, UV stabilization, and enhanced biodegradation capacity [209–212].

(c) aromatics and miscellaneous monomers;

Table 8.15 Medium-term conversion technologies: high molecular weight lignin products

Products	Technical challenges
Carbon fiber	– To replace half of the steel in domestic passenger vehicles
Polymer fillers	– Economical modifications to improve solubility and compatibility with other polymers – Control of molecular weight and polymer color – Control of polyelectrolyte properties – Introduction of functional groups in lignin macromolecule
Thermoset resins	– Control of molecular weight and viscosity
Formaldehyde-free resins	– Increase of functional reactivity by carbonylation, carboxylation, de-etherification
Adhesives and binders	– Change to improve oxidative stability, thermal stability, curing rate of resins

Table 8.16 Long-term conversion technologies of lignin

Products	Technical challenges
Phenols, cresols, substituted phenols	– Hydrogenation – Hydrolysis
CH_3COOH, phenol, substituted phenols, CO, CH_4	– Pyrolysis
Vanillin, dimethylsulfide, methyl mercaptan, dimethylsulfoxide	– Oxidative process
Phenolic acids, catechol	– Alkali fusion
Macromolecular lignin product, vanillic, ferulic, coumaric and other acids	– Microbial conversion
Oxidized lignin	– Enzymatic oxidation

The conversion of lignin into high-volume, low-molecular weight aromatic products (monomeric phenolic compounds) is an attractive and viable long-term opportunity [213]. As petroleum resources diminish and their prices increase, this opportunity is very desirable and allow the most complex way of lignin valorization.

Some examples and technical challenges for the aromatics, including BTX (benzene, toluene, and xylene), phenols, monomeric lignin molecules and other low molecular weigh products are presented in Table 8.16.

Lignin is a commercial product and a number of uses currently exist in industry that listed in Table 8.17.

One can affirm that the potential supply of lignin is virtually limitless. The range of lignin uses/applications is "limited by our imaginations" [209]. Lignin suppliers are interested in market size, position on the value-chain, quality *vs* value of lignin product, while lignin consumers are concerned with isolation technology, availability and lignin physical–chemical properties. In the future, suppliers and consumers must coordinate on the lignin product specifications.

Table 8.17 The mainly commercial lignin suppliers

Suppliers	Location	Lignin type (commercial name)	Products
Borreggard-Lignotech Group	USA, Norway Sweden, Swtzerland, Finland, Spain, South Africa, China	Lignosulfonate Kraft lignin (Eucalin)	• Animal nutrition • Additives—ceramics, concrete and gypsum • Dispersing agents—agro chemicals, battery expanders, dyestuffs, water treatments • Binders—carbon black, fertilizers, limestone, mud dispersants • Plant nutrition—humates and micronutrients
Northway Lignin Chemical	Canada	Sulfur-free lignin Na-carbonate lignin (Polybind 300)	• Binders • Emulsifiers, stabilizers, dispersants • Liquid or powder agglomeration/briquetting of fine particles
Tembec	Canada, Europe, North America	NH_4, Na –lignosulfonate steam explosion lignin kraft lignin (Tomlinite)	• Dispersants • Binders • Chelators
Flambeau River Paper Corporation	USA	Lignosulfonates (from hardwoods)	• Binders in ceramics • Medical treatments • Deodorants
MeadWestvaco	USA	Non-sulfonated kraft lignin, lignosulfonates	• Lignin products: hydroxymethylated lignin, propoxylated lignin polyols; additives for cements and animal feeds • Adhesives for particle boards • Wax emulsifier • Dispersants for dyes and pigments, ceramics, refractories and concrete
Northway Lignin Company	USA	Sulfur-free lignin	• Binders • Emulsifiers, stabilizers, dispersants • Liquid or powder agglomeration

(continued)

Table 8.17 (continued)

Suppliers	Location	Lignin type (commercial name)	Products
KMT Lignin Chemical	USA	Lignosulfonate	• Dispersants—concrete admixtures, dust, oil well drilling muds, leather tanning, ceramics, dyestuffs, insecticide sprays • Additives for animal feeds
Melbar	USA	Lignosulfonates (pinewood)	• Dispersants • Emulsifiers and wetting agents • Chelating agents • Animal treatments
Nordin Paper's Backhammar STFI Packfrosk	Sweden	High quality kraft lignin (LignoBoost lignin)	• Chemicals • Carbon fibers • Biofuels
Lennox Polymers LTD	USA	Sulfate lignin (Lenox lignin)	• Formaldehyde-free resins; • Adhesives for wood products (chips, laminates, veneers) • High-performance specialty resins: urethane and polyester molding resins, thermoplastic resins • Traction products: winter tire traction product • Lubricants
Lignol Energy Corporation	Canada	High purity lignin (Lignol)	• Biochemicals • Fuel-grade ethanol
Hubei Aging Chemical Company	China	Lignosulfonates	• Additives for concrete admixtures, feed, leather; reinforcing agents for refractory material asnd ceramics • Dispersants for fertilizers, pesticides
Sanyo Kousaka Nippon Paper Ind.	Japan	Lignosulfonate Steam explosion lignin	• Dispersants • Binders • Chelators
Repap Company	USA	Ethanol lignin (Alcell)	• Analytical grade samples

(continued)

Table 8.17 (continued)

Suppliers	Location	Lignin type (commercial name)	Products
Aldrich Chemical Company	USA	Organosolv lignin autohydrolysis lignin steam explosion lignin	• Analytical grade samples
Asian Lignin Manufacturing India Pvt. Ltd.	India	Lignin lignosulfonate	• Binders—phenolic resin type for plywood, foundry sands
ALM India Pvt. Ltd.	India	High-purity lignin sulphur-free lignin	• Capacity 10,000 t/yr for friction materials and phenolic resins

8.6 Conclusions

From the data presented we can conclude that lignin could represent a valuable product accessible from chemical processing of biomass (delignification and hydrolysis) and new biorefining technologies. For the lignin and its derivatives there are a lot of proposals for utilization in different fields. At the same time, increasing oil prices will favour the uses of lignin in materials if the energy intensity in recovery and conversion is lower than that for the corresponding petroleum-or-coal derived chemicals. This is likely to be the case and lignin can be expected to be used in higher value applications than energy in the future. Properties related to the aromatic nature of lignin can be predicted to be an asset. Therefore, natural systems can teach us something about materials and optimum design. Obviously, lignin along with other plants polyphenols also have a great long-term asset by being solar energy-derived, renewable and ecologically desirable. One can foresee the day when chemical treatments of wood and biomass will be done, not only to produce paper and energy, but also to create sets of products with an optimum combined value for the society.

References

1. Feldman, D., Lacasse, M., Beznaczuk, L.M.: Lignin—polymer systems and some applications. Prog. Polym. Sci. **12**, 271–299 (1986)
2. Chabannes, M., Ruel, K., Yoshinaga, A., Chabbert, B., Jauneau, A., Joseleau, J.P., Boudet, A.M.: In situ analysis of lignins in transgenic tobacco reveals a differential impact of individual transformations on the spatial patterns of lignin deposition at the cellular and subcellular levels. Plant J **28**, 271–282 (2001)
3. Barghoorn, E.S.: Evolution of cambium in geologic time. In: Zimmermann, M.H. (ed.) Formation of Wood in Forest Trees, pp. 3–17. Academic Press, New York (1964)
4. Lopez, M.J., Vargas-Garcia, M.C., Suarez-Estrella, F., Moreno, J.: Biodelignification and humification of horticultural plant residues by fungi. Intern. Biodeter. Biodegrad **57**(1), 24–30 (2006)
5. McMorrow J.M., Al-Roichdi A., Evans M.G., Cutler M.E.: Estimation of humification of exposed upland peat from HyMap and ASD spectra, The airbone imaging spectroscopy workshop, Bruges, October 8, (2004) http://eo.belspo.be/Docs/Resources/Publications/bruhyp2004/McMorrow.pdf
6. Stevenson, F.J., Butler, J.H.A.: Chemistry of humic acids and related pigments. In: Englinton, G.E., Murphy, M.T.J. (eds.) Organic Geochemistry, pp. 534–556. Springer, Berlin (1969)
7. Espiñeira, J.M., Uzal, E.N., Ros, L.V.G., Carrión, J.S., Merino, F., Barceló, A.R., Pomar, F.: Distribution of lignin monomers and the evolution of lignification among lower plants. Plant Biol **13**(1), 59–68 (2010)
8. Martone, P.T., Estevez, J.M., Lu, F., Ruel, K., Denny, M.W., Somerville, C., Ralph, J.: Discovery of lignin in seaweed reveals convergent evolution of cell-wall architecture. Curr. Biol. **19**, 169–175 (2009)
9. Li, X., Chapple, C.: Understanding lignification: challenges beyond monolignols biosynthesis. Plant Physiol. **154**, 449–452 (2010)
10. Weng, J.K., Banks, J.A., Chapple, C.: Independent origins of syringyl lignin in vascular plants. Proc. Natl. Acad. Sci. U. S. A **105**, 7887–7892 (2008)

11. Weng, J.K., Banks, J.A., Chapple, C.: Parallels in lignin biosynthesis: a study in *Selaginella moellendorffii* reveals convergence across 400 million years of evolution. Commun. Integr. Biol. **1**, 20–22 (2008)
12. Vanholme, R., Demedts, B., Morreel, K., Ralph, J., Boerjan, W.: Lignin biosynthesis and structure. Plant Physiol. **153**, 895–905 (2010)
13. Goheen D.W., Hoyt C.H.: Lignin, in encyclopedia of chemical technology, Kirk-Othmer, vol. 14, 3rd edn. pp. 294–312. (1978)
14. Sjöström, E.: In: Sjoström, E. (ed.) Lignin, in Wood Chemistry, Fundamentals and Applications, pp. 71–89. Academic Press, New York (1993)
15. Rozmarin, Gh.: In Macromolecular Fundamentals in Wood Chemistry, pp. 29–40. Technical Publishing House, Bucuresti (1984)
16. Meister, J.J.: Modification of lignin. *J. Macromol. Sci.* Polym. Rev. **C24**(2), 235–289 (2002)
17. Chen C. L.: Lignin: occurrence in woody tissues, isolation, reactions, and structure. In: Lewin M., Goldstein I. S. (eds.) Wood Structure and Composition, pp. 183–261. Marcel Dekker, New York (1991)
18. Campbell, M.M., Sederoff, R.R.: Variation in lignin content and composition. Mechanisms of control and implications for the genetic improvement of plants. Plant Physiol. **110**, 3–13 (1996)
19. Baucher, M., Monties, B., Van Montagu, M., Boerjan, W.: Biosynthesis and genetic engineering of lignin. Crit. Rev. Plant Sci. **17**, 125–197 (1998)
20. Donaldson, L.A.: Lignification and lignin topochemistry—an ultrastructural view. Phytochemistry **57**, 859–873 (2001)
21. Saka, S., Goring, D.A.I.: Localization of lignins in wood cell walls. In: Higuchi, T. (ed.) Biosynthesis and Biodegradation of Wood Components, pp. 51–62. Academic Press, Orlando (1985)
22. Argyropoulos, D.S., Menachem, S.B.: Lignin. In: Kaplan, D.L. (ed.) Biopolymers from Renewable Resources, pp. 2929–322. Springer, Berlin (1998)
23. Wardrop, A.B.: Lignification of the plant cell wall. Appl. Polym. Symp **28**, 1041–1063 (1976)
24. Roussel, M.R., Lim, C.: Dynamic model of lignin growing in restricted spaces. Macromolecules **28**, 370–376 (1995)
25. Gindl, W., Grabner, M.: Characteristics of spruce (*Picea abies* (L.) Karst.) latewood formed under abnormally low temperatures. Holzforschung **54**, 9–11 (2000)
26. Donaldson, L.A.: Abnormal lignin distribution in wood from severely drought stressed *Pinus radiata* trees. IAWA J. **23**(2), 161–178 (2002)
27. Dixon, R.A., Paiva, N.L.: Stress-induced phenylpropanoid metabolism. Plant Cell **7**, 1085–1097 (1995)
28. Vance, C.P., Kirk, T.K., Sherwood, R.T.: Lignification as a mechanism of disease resistance. Ann Rev. Phytopathol. **18**, 259–288 (1980)
29. Fiehn, O., Kopka, J., Dormann, P., Altmann, T., Trethewey, R.N., Willmitzer, L.: Metabolite profiling for plant functional genomics. Nat. Biotechnol. **18**, 1157–1161 (2000)
30. Morris, C.R., Scott, J.T., Chang, H.M., Sederoff, R.R., O'Malley, D., Kadla, J.F.: Metabolic profiling: a new tool in the study of wood formation. J. Agric. Food Chem. **52**, 1427–1434 (2004)
31. Yeh, T.F., Morris, C.R., Goldfarb, B., Chang, H.M., Kadla, J.F.: Utilization of polar metabolite profiling in the comparison of juvenile wood and compression wood in loblolly pine (*Pinus taeda*). Tree Physiol. **26**, 1497–1503 (2006)
32. Yeh, T.F., Braun, J.L., Goldfard, B., Chang, H.M., Kadla, J.F.: Morphological and chemical variations between juvenile wood, mature wood and compression wood of loblolly pine (*Pinus taeda* L.). Holzforschung **60**, 1–8 (2006)
33. Yeh, T.F., Goldfarb, B., Chang, H.M., Peszlen, I., Braun, J.L., Kadla, J.F.: Comparison of morphological and chemical properties between juvenile wood and compression wood of loblolly pine. Holzforshung **59**, 669–674 (2005)
34. Cosgrove, D.J.: Growth of the plant cell wall. Nat. Rev. Mol. Cell Biol. **6**, 850–886 (2005)

35. Kaneda, M., Rensing, K.H., Wong, J.C., Banno, B., Mansfield, S.D., Samuels, A.L.: Tracking monolignols during wood development in lodgepole pine. Plant Physiol. **147**, 1750–1760 (2008)
36. Boija, E., Johansson, G.: Interaction between model membranes and lignin-related compounds studied by immobilized liposome chromatography. Biochim. Biophys. Acta **1758**, 620–626 (2006)
37. Boerjan, W., Ralph, J., Baucher, M.: Lignin biosynthesis. Annu. Rev. Plant Biol. **54**, 519–546 (2003)
38. Ehlting, J., Mattheus, N., Aeschliman, D.S., Li, E., Hamberger, B., Cullis, I.F., Zhuang, J., Kaneda, M., Mansfield, S.D., Samuels, L., Ritland, K., Ellis, B.E., Bohlmann, J., Douglas, C.J.: Global transcript profiling of primary stems from *Arabidopsis thaliana* identifies candidate genes for missing links in lignin biosynthesis and transcriptional regulators of fiber differentiation. Plant J **42**, 618–640 (2005)
39. Gardiner, J.C., Taylor, N.G., Turner, S.R.: Control of cellulose synthase complex localization in developing xylem. Plant Cell **15**, 1740–1748 (2003)
40. Wightman, R., Turner, S.R.: The role of the cytoskeleton during cellulose deposition at the secondary cell wall. Plant J **54**, 794–805 (2008)
41. Gutierrez, R., Lindeboom, J.J., Paredez, A.R., Emons, A.M., Ehrhardt, D.W.: Arabidopsis cortical microtubules position cellulose synthase delivery to the plasma membrane and interact with cellulose synthase trafficking compartments. Nat. Cell Biol. **11**, 797–806 (2009)
42. Pesquet, E., Korolev, A.V., Calder, G., Lloyd, C.W.: The microtubule-associated protein AtMAP70-5 regulates secondary wall patterning in *Arabidopsis* wood cells. Curr. Biol. **20**, 744–749 (2010)
43. Christensen J.H., Baucher M., O'Connell A.P., van Montagu M., Boerjan W.: Control of lignin biosynthesis. In: Jain S.M., Minocha S.C. (eds.) Molecular Biology of Woody Plants, vol. 1 64, pp. 227–267, For. Sci., Dordrecht, Kluwer (2000)
44. Harkin, J.M.: Lignin a natural polymeric product of phenol oxidation. In: Taylor, W.I., Battersby, A.R. (eds.) Oxidative Coupling of Phenols, pp. 243–321. Marcel Dekker, New York (1967)
45. Harkin, J.M.: Lignin. In: Butler, G.W. (ed.) Chemistry and Biochemistry of Herbage, pp. 323–373. Academic Press, London (1973)
46. Freudenberg K., Neish A.C.: Constitution and Biosynthesis of Lignin, Springer, Berlin, p. 129 (1968)
47. Brunow, G.: Oxidative coupling of phenols and the biosynthesis of lignin. In: Lewis, N.G., Sarkanen, S. (eds.) Lignin and Lignan Biosynthesis, pp. 131–147. Am. Chem. Soc, Washington (1998)
48. Rippert, P., Puyaubert, J., Grisollet, D., Derrier, L., Matringe, M.: Tyrosine and phenylalanine are synthesized within the plastids in Arabidopsis. Plant Physiol. **149**, 1251–126 (2009)
49. Kärkönen, A., Koutaniemi, S.: Lignin biosynthesis studies in plant tissue cultures. J. Integrative Plant Biol **52**(2), 176–185 (2010)
50. Vanholme, R., Demedts, B., Morreel, K., Ralph, J., Boerjan, W.: Lignin biosynthesis and structure. Plant Physiol. **153**, 895–905 (2010)
51. Chapple, C.: Molecular-genetic analysis of plant cytochrome P450-dependent monooxygenases, Annu. Rev. Plant Physiol. Plant Mol. Biol **49**, 311–343 (1998)
52. Ro, D.K., Mah, N., Ellis, B.E., Douglas, C.J.: Functional characterization and subcellular localization of poplar (*Populus trichocarpa X Populus deltoids*) cinnamate 4-hudroxylase. Plant Physiol. **126**, 317–329 (2001)
53. Eckardt, N.A.: Probing the mysteries of lignin biosynthesis. The crystal structure of caffeic acid/5-hydroxyferulic acid 3/5-O-methyltransferase provides new insights. Plant Cell **14**, 1185–1189 (2002)
54. Hatfield, R., Vermerris, W.: Lignin formation in plants. The dilemma of linkage specificity. Plant Physiol. **126**, 1351–1357 (2001)

55. Davin, L.B., Lewis, N.G.: Dirigent proteins and dirigent sites explain the mystery of specificity of radical precursor coupling in lignan and lignin biosynthesis. Plant Physiol. **123**, 453–461 (2000)
56. Li, X., Chapple, C.: Understanding lignification: Challenges beyond monolignols biosynthesis. Plant Physiol. **154**, 449–452 (2010)
57. Glasser W.G., Kelley S.S.: Lignin, in encyclopedia of polymer science and engineering. vol. 8, pp. 795–852. Wiley, Wiley Intersci. Publishing, New York (1987)
58. Falkehag, S.I.: Lignin in materials. Appl. Polym. Sci **28**, 247–257 (1975)
59. Freudenberg, K.: Nachtrag zu der Mitteilung über Methylcellulose. Zugleich 6. Mitteilung über Lignin und Celluoses. Liebigs Ann. Chem. **461**, 130–131 (1928)
60. Campbell, M.M., Sederoff, R.R.: Variation in lignin content and composition. Mechanisms of control and implications for the genetic improvement of plants. Plant Physiol. **110**, 3–13 (1996)
61. Boudet, A.M., Lapierre, C., Grima-Pettenati, J.: Biochemistry and molecular biology of lignification. New Phytol. **129**, 203–239 (1995)
62. Adler, E.: Lignin chemistry—past, present and future. Wood Sci. Technol. **11**, 169–218 (1977)
63. Ralph J., Hatfield R.D., Grabber J.H., Jung H.G., Quideau S., Helm R.F.: Cell wall crosslinking in grasses by ferrulate and differulate. In: Lewis N.G., Sarkanen S. (eds.) Lignin and Lignan Biosynthesis, pp. 209–236. American Chemical Society, Washington (1998)
64. Meshitsuka G., Isogai A.: Chemical structure, hemicellulose and lignin. In: Hon D.N.S. (ed.) Chemical Modification of Lignocellulosic Materials, pp. 11–34. Marcel Dekker Inc., New York (1996)
65. Capanema, E.A., Balaksin, M.Yu., Kadla, J.F.: Quantitative characterization of a hardwood milled wood lignin by nuclear magnetic resonance spectroscopy. J. Agric. Food Chem. **53**, 9639–9649 (2005)
66. Karhunen, P., Rummakko, P., Sipilä, J., Brunow, G., Kilpeläinen, I.: Dibenzodioxocins. A novel type of linkage in softwoods lignins. Tetrahedron Lett. **36**(1), 167–170 (1995)
67. Karhunen, P., Rummakko, P., Sipilä, J., Brunow, G., Kilpeläinen, I.: The formation of dibenzodioxocin structures by oxidative coupling. A model for lignin biosynthesis. Tetrahedron Lett. **36**(25), 4501–4504 (1995)
68. Ralph, J., Lapierre, C., Lu, F., Marita, M.J., van Doorsselaere, J., Boerjan, F., Juanin, L.: NMR evidence for benzodioxane structures resulting from incorporation of 5-hydroxyconiferyl alcohol into lignins of O-methyltransferase-deficient poplars. J. Agric. Food Chem. **49**, 86–91 (2001)
69. del Río, J.C., Rencoret, J., Marques, G., Gutiérrez, A., Ibarra, D., Santos, J.I., Jiménez-Barbero, J.: Highly acetylated (acetylated and or p-coumaroylated) native lignins from diverse herbaceous plants. J. Agric. Food Chem. **56**, 9525–9534 (2008)
70. Zhang, L., Gellerstedt, G., Ralph, J., Lu, F.: NMR studies on the occurrence of spirodienone structures in lignins. J. Wood Chem. Technol. **26**, 65–79 (2006)
71. Ammalahti, E., Brunow, G., Bardet, M., Robert, D., Kilpelainen, I.: Identification of side-chain structures in a poplar lignin using three-dimensional HMQC-HOHAHA NMR spectroscopy. J. Agric. Food Chem. **46**, 5113–5117 (1998)
72. Glasser, W.G., Glasser, H.R.: The evaluation of lignin's chemical structure by experimental and computer simulation techniques. Pap. Puu **63**(2), 71–83 (1981)
73. Glasser, W.G., Glasser, H.R., Morohoshi, N.: Simulation of reactions with lignin by computer (SIMREL). 6. Interpretation of primary experimental analysis data. Macromolecules **14**, 253–262 (1981)
74. Erickson, M., Larsson, L., Miksche, G.E.: Zur Struktur des lignins des Druckholzes von *Pinus mugo*. Acta Chem. Scand. **27**, 1673–1678 (1973)
75. Nimz, H.: Beech lignin—proposal of a constitutional scheme. Angew. Chem. Int. Ed. Engl. **13**, 313–321 (1974)

76. Sarkanen K.V., Hergert H.L.: Classification and distribution. In: Sarkanen K.V., Ludwig C.H. (eds.) Lignins. Occurrence, Formation, Structure and Reactions, pp. 43–94. Wiley Interscience, New York (1971)
77. Yasuda, S., Sakakibara, A.: Hydrogenolysis of protolignin in compression wood. IV. Isolation of a diphenyl ether and three dimeric compounds with carbon to carbon linkage. Mokuzai Gakkaishi **23**, 383–387 (1975)
78. Dence C.W., Lin S.Y.: Introduction. In: Lin S.Y., Dence C.W. (eds.) Methods in Lignin Chemistry, pp. 3–17. Springer, New York (1992)
79. Pan, D.R., Tai, D.S., Chen, C.L., Robert, D.: Comparative studies on chemical composition of wood components in recent and ancient woods of *Bischofia polycarpa*. Holzforschung **44**, 7–16 (1990)
80. Tai, D.S., Chen, C.L., Robert, D.: Comparative studies on chemical composition of wood components in recent and ancient woods of *Bischofia polycarpa*. Holzforschung **44**, 7–16 (1990)
81. Tai, D.S., Chen, C.L., Gratzl, J.S.: Chemistry of delignification during kraft pulping of bamboos. J. Wood Chem. Technol. **10**, 75–99 (1990)
82. Robert, D., Brunow, G.: Quantitative estimation of hydroxyl groups in milled wood lignin from spruce and in a dehydrogenation polymer from coniferyl alcohol using ^{13}C-NMR spectroscopy. Holzforschung **38**, 85–90 (1984)
83. Freudenberg, K.: Lignin: Its constitution and formation from p-hydroxycinnamyl alcohols. Science **148**, 595–600 (1965)
84. Ludwig C.H., Nist B.J., McCarthy J.L.: Lignin. XII. The high resolution nuclear magnetic resonance spectroscopy of protons in compounds related to lignin. J. Am. Chem. Scand. **86**, 1186–1196, (1964)
85. Simionescu Cr.I., Anton I.: Das chemische studium des lignins aus schilf. Das Papier, **19**(4), 150–158, (1965)
86. Sakakibara, A.: A structural model of softwood lignin. Wood Sci. Technol. **14**(2), 89–100 (1980)
87. Glasser W.G.: Lignin. In: Casey J.P. (ed.) Pulp and Paper: Chemistry and Chemical Technology, vol. 1, pp. 39–111. Wiley, New York (1980)
88. Gravitis, J., Erins, P.: Topological and conformational structure and macroscopic behaviour of lignin. J. Appl. Polym. Sci.: Appl. Polym. Symp. **37**, 421–440 (1983)
89. Atalla, R.H.: Raman spectroscopy and Raman microprobe: Valuable new tools for characterizing wood and wood pulp fibers. J. Wood Chem. Technol. **7**, 115–131 (1987)
90. Atalla R.H. Cellulose and the hemicellulose: patterns for cell wall architecture and the assemble of lignin. In: Proceedings of 8th International Symposium on Wood and Pulping Chem, Helsinki, vol. 1, pp. 77–84. 6–9 June 1995
91. Forss, K.G., Fremer, K.E.: The nature and reactions of lignin—a new paradigm. Oy Nord Print Ab, Helsinki (2003)
92. Forss, K.J., Fremer, K.E.: Spruce and birch wood lignins—a comparison. Cell Chem. Technol. **40**(9–10), 739–748 (2006)
93. Koshijima T., Watanabe T., Yaku F.: Structure and properties of lignin—carbohydrate complex polymer as an amphipathic substance. In: Glasser W.G., Sarkanen S. (eds.) Lignin Properties and materials, pp. 11–28. ACS Symposium Series 397, (1989)
94. Atalla, R.H., Agarwal, U.P.: Raman microprobe evidence for lignin orientation in the cell walls of native woody tissue. Science **227**, 636–638 (1985)
95. Haggin, J.: Ester pulping process avoids use of sulfur compounds. Chem. Eng. News **64**(4), 25–26 (1986)
96. Hatakeyama H., Hatakeyama T.: Lignin structure, properties and applications. In: Abe A., Dušek K., Kobayashi S. (eds.) Biopolymers. Lignin, Proteins, Bioactive Nanocomposites, vol. 232, pp. 1–63. Springer, Berlin, Adv. Polym Sci. (2010)
97. Goring D.A.I.: Polymer properties of lignin and lignin derivates. In: Sarkanen K.V., Ludwig C.H. (eds.) Lignins. Occurrence, Formation, Structure and Reactions, pp. 695–761. Wiley, New York (1971)

98. Hatakeyama, T., Hatakeyama, H.: Temperature dependence of X-ray difractograms of amorphous lignins and polystyrenes. Polymer **23**, 475–477 (1982)
99. Goring D.A.I.: Thermal softening of lignin, hemicelluloses and cellulose. Pulp Paper Mag. Can. **64**(12) pp. T-517–T-527. (1963)
100. Back, E.L., Salmen, N.L.: Glass transitions of wood components hold implications for molding and pulping processes. TAPPI **65**(7), 107–110 (1982)
101. Irvine, G.M.: The glass transitions of lignin and hemicellulose and their measurements by differential thermal analysis. TAPPI **67**(5), 118–121 (1984)
102. Glasser, W.G., Barnett, C.A., Rials, T.G., Saraf, V.P.: Engineering plastics from lignin. II. Characterization of hydroxyalkyl lignin derivatives. J. Appl. Polym. Sci. **29**(5), 1815–1830 (1984)
103. Vasile C., Popescu M.C., Stoleriu, Gosselink R.: Thermal characterization of lignins. In: Vasile C., Zaikov G.E. (eds.) New Trends in Natural and Synthetic Polymer Science, pp. 135–163. Nova Science Publisher, Inc. (2006)
104. Cernătescu-Asandei, A., Andriescu, A., Rozmarin, G.H., Simionescu, C.I.: Conceptii moderne in domeniul fizico-chimiei ligninei. Studii si Cercetari Chimice **22**(1), 3–74 (1974)
105. Lee, S.H., Doherty, T.V., Linhardt, R.J., Dordick, J.S.: Ionic liquid-mediated selective extraction of lignin from wood leading to enhanced enzymatic cellulose hydrolysis. Biotechnol. Bioengin **102**(5), 1368–1376 (2009)
106. King, A.W.T., Zoia, L., Filpponene, I., Olssszewska, A., Xie, H., Kilpeläinen, I., Argyropoulos, D.S.: In situ determination of lignin phenolics and wood solubility in imidazolium chlorides using ^{31}P NMR. J. Agric. Food Chem. **57**, 8236–8243 (2009)
107. Pu, Y., Jiang, N., Ragauskas, A.J.: Ionic liquid as a green solvent for lignin. J. Wood Chem. Technol. **27**, 23–33 (2007)
108. Rezanovich, A., Goring, D.A.I.: Polyelectrolyte expansion of a lignin sulgonate microgel. J. Colloid Sci. **15**, 452–471 (1960)
109. Glasser, W.G., Dave, V., Frzier, C.E.: Molecular weight distribution of semi-commercial lignin derivatives. J. Wood Chem. Technol. **13**, 545–555 (1993)
110. Gupta, P.R., Robertson, R.F., Goring, D.A.I.: Physicochemical studies of alkali lignins. II. Ultracentrifugal sedimentation analysis. Can. J. Chem. **38**, 259–270 (1960)
111. Pla, F., Robert, A.: Étude du comportement hydrodynamique d'une lignine d'extraction. Cell. Chem. Technol **8**, 3–11 (1974)
112. Rezanovich, A., Yean, W.Q., Goring, D.A.I.: High-resolution electron microscopy of sodium lignosulfonate. J. Appl. Polym. Sci. **81**(4), 1801–1812 (1964)
113. Connors, W.J., Sarkanen, S., McCarthy, K.L.: Gel chromatography and association complexes of lignin. Holzforschung **34**(3), 80–85 (1980)
114. Sarkanen, S., Tellers, D.C., Hall, J.L., McCarthy, J.L.: Associative effects among organosolv lignin components. Macromolecules **14**, 426–434 (1981)
115. Hüttermann, A.: Gel permeation chromatography of water-insoluble lignins on controlled pore glass and sepharose CL-6B. Holzforschung **32**, 108–111 (1978)
116. Dong, D., Fircke, A.L.: Intrinsic viscosity and the molecular weight of kraft lignin. Polym **36**, 2075–2078 (1995)
117. Forss, K., Kokkonen, R., Sagfors, P.E.: Determination of molecular mass distribution studies of lignins by gel permeation chromatography. In: Glasser, W.G., Sarkanen, S. (eds.) Lignin, Properties and Materials, pp. 124–133. American Chemical Society, Washington (1989)
118. Gellerstedt, G.: Gel permeation chromatography. In: Lin, S.Y., Dence, C.W. (eds.) Methods in Lignin Chemistry, pp. 487–497. Springer, Berlin (1992)
119. Pla, F.: Light scattering methods. In: Lin, S.Y., Dence, C.W. (eds.) Methods in Lignin Chemistry, pp. 498–508. Springer, Berlin (1992)
120. Pla, F.: Vapor pressure osmometry. In: Lin, S.Y., Dence, C.W. (eds.) Methods in Lignin Chemistry, pp. 509–517. Springer, Berlin (1992)
121. Himmel, M.E., Tatsumoto, L., Oh, K.K., Grohmann, K., Johnson, D.K., Chum, J.L.: Determination of a polymerr's molecular weight distribution by analytical

ultracentrifugation. In: Glasser, W.G., Sarkanen, S. (eds.) Lignin: Properties and Materials, pp. 82–99. American Chemical Society, Washington (1989)
122. Ben-Ghedalia, B., Yosef, E.: Effect of isolation procedure on molecular weight distribution of wheat straw lignins. J. Agric. Food Chem. **42**, 649–652 (1994)
123. Lindner, A., Wegner, G.: Characterization of lignins from organosolv pulping according to the organocell process. Part 3. Molecular weight determination and investigation of lignins isolated by GPC. J. Wood Chem. Technol. **10**, 331–350 (1990)
124. Lebo, S.E., Braten, S.M., Fredheim, G.E., Lutnaesf, B.F., Lauten, R.A., Myrvold, B.O., McNally, T.J.: Recent advances in the characterization of lignosulfonate, In: Hu, T.Q. (ed.) Characterization of Lignocellulosic Materials, pp. 188–205. Blackwell, Oxford (2008)
125. Westermark, U., Gusafsson, K.: Molecular size distribution of wood polymer in birch draft pulps. Holzforschung **48**, 146–150 (1994)
126. Hattali, S., Benaboura, A., Ham-Pichavant, F., Noumamode, A., Castellan, A.: Adding value to alfa grass (*Stipa tenacissima* L.) soda lignin as phenolic resins. 1. Lignin characterization. Polym. Degrad. Stab. **75**, 259–264 (2002)
127. Sun, R.C., Tomkinson, J., Wang, S.Q., Zhu, W.: Characterization of lignins from wheat straw by alkaline peroxide treatment. Polym. Degrad. Stabil **67**, 101–109 (2000)
128. Bidlack, J., Malone, M., Benson, R.: Molecular structure and component integration of secondary cell wall in plants. Proc. Okla Acad. Sci. **72**, 51–56 (1992)
129. Hauteville, M., Lundquist, K., von Unge, S.: NMR studies of lignins. 7. ^{1}H-NMR spectroscopic investigation of the distribution of erythro and threo forms of β-O-4 structures in lignins. Acta Chem. Scand. **B40**(1), 31–35 (1986)
130. Lundquist, K., Langer, V., Li, S., Stomberg, R.: Lignin stereochemistry and its biosynthetic implications. In: The 12th International Symposium on Wood and Pulping Chemistry, Madison, 9–12 June 2003, pp. 239–244
131. Langer, V., Lundquist, K., Parkås, J.: The stereochemistry and conformation of lignin as judged by X-ray crystallographic investigations of lignin model compounds: arylglycerol β-guaiacyl ethers. BioResources **2**(4), 590–597 (2007)
132. Micic, M., Radotic, K., Jeremic, M., Djikanovic, D., Kämmer, S.B.: Study of the lignin model compound supramolecular structure by combination of near-field scaning microscopy and atomic force microscopy. Coll. Surfac. B: Bionterfaces **34**, 33–40 (2004)
133. Abreu, S.H., Latorraca, V.F.J., Pereira, P.W.R., Moneiro, O.M.B., Abreu, A.F., Amparado, F.K.: A supramolecular proposal of lignin structure and its relation with the wood properties. Ann. Braz. Acad. Sci. **81**(1), 137–142 (2009)
134. Faulon, J.L., Hatcher, P.G.: Is there any order in the structure of lignin. Energy Fuel **8**, 402–407 (1994)
135. Kishimoto, T., Uraki, Y., Ubukata, M.: Chemical synthesis of β-O-4 type artificial lignin. Org. Biomol. Chem. **4**, 1343–1347 (2006)
136. Escudero-Alvarez, E., Gonzàlez-Sànchez, P.: Dietary fibre. Nutri. Hosp **21**, 60–71 (2006)
137. Jung, H.G., Fahey, G.C.: Nutritional implications of phenolic monomers and lignin: a review. J. Anim. Sci. **57**, 206–219 (1983)
138. Balat, M.: Gasification of biomass to produce gaseous products. Energy Sources, Part A **31**, 516–526 (2009)
139. Zemek, J., Košiková, B., Augustin, J., Joniak, D.: Antibiotic properties of lignin components. Folia Microbiol. **24**, 483–486 (1979)
140. Sláviková, E., Košiková, B.: Inhibitory effect of lignin by-products of pulping on yeast growth. Folia Microbiol. **39**(3), 241–243 (1994)
141. Nelson, J.L., Alexander, J.W., Gianotti, L., Chalk, C.L., Pyles, T.: Influence of dietary fiber on microbial growth in vitro and bacterial translocation after burn injury in mice. Nutrition **10**, 32–36 (1994)
142. Telysheva, G., Dizhbite, T., Lebedeva, G., Niokolaeva, V.: Lignin products for decontamination of environment objects from pathogenic microorganisms and pollutants. In: The 7th ILI Forum-Barcelona, 27–28 Apr 2005, pp. 71–74

143. Nada, A.M.A., El-Diwany, A.I., Elshafei, A.M.: Infrared and antimicrobial studies on different lignins. Acta Biotechnol. **9**, 295–298 (1989)
144. Çekmez, U.: Isolation of antimicrobial molecules from agricultural biomass and utilization in xylan-based biodegradable films, thesis master. Middle East Technical University, USA (2010)
145. Zilliox, C., Debeire, P.: Hydrolysis of wheat straw by a thermostable endoxylanase. Adsorbtion and kinetic studies, Enzym. Microbial Technol. **22**, 58–63 (1998)
146. Baurhoo, B., Ruiz-Feria, C.A., Zhao, X.: Purified lignin: nutritional and health impacts on farm animals. Anim. Feed Sci. Technol. **144**(3), 175–184 (2008)
147. Toh, K., Yokoyama, H., Takahashi, C., Watanabe, T., Noda, H.: Effect of herb lignin on the growth of enterobacteria. J. Gen. Appl. Microbiol. **53**, 201–205 (2007)
148. Dizhbite, T., Telyesheva, G., Jurkjane, V., Viesturs, U.: Characterization of the radical scavenging activity of lignins-natural antioxidants. Bioresour. Technol. **95**, 309–317 (2004)
149. Lu, F.J., Chu, L.H., Gau, R.J.: Free radical-scavenging properties of lignin. Nutr. Cancer **30**, 31–38 (1998)
150. Vinardell, M.P., Ugartondo, V., Mitjans, M.: Antioxidant and photoprotective action of lignins from different sources assessed in human red blood cells. In: 7th ILI Forum, Barcelona, 27–28 Apr 2005, pp. 75–77
151. Ugartondo, V., Mitjans, M., Vinardell, M.P.: Applicabilitz of lignins from different sources as antioxidants based on the protective effects on lipid peroxidation induced bz oxzgen radicals. Ind. Crops Prod. **30**, 184–187 (2009)
152. Mitjans, M., Garcia, L., Marrero, E., Vinardell, M.P.: Study of ligmed-A, an antidiarrheal drug based on lignin, on rat small intestine enzyme activity and morphometry. J. Vet. Pharmacol. Therap. **24**, 349–351 (2001)
153. Garcia, L., Abajo, C., del Campo, J., Mitjans, M., Marrero, E., Vinardell, M.P.: Antioxidant effect of ligmed—a on humane erythrocytes in vitro. Pharmacology **3**, 514–519 (2006)
154. Košiková, B., Lábaj, J.: Lignin-stimulated protection of polypropylene films and DNA in cells of mice against oxidation damage. BioResouces **4**(2), 805–815 (2009)
155. Boeriu, C., Bravo, D., Gosselink, R.J.A., van Dam, J.E.G.: Characterisation of structure-dependent functional properties of lignin with infrared spectroscopy. Ind. Crops Prod. **20**, 205–218 (2004)
156. Kocheva, L.S., Borisenkov, M.F., Karmanov, A.P., Mishurov, V.P., Spirikhin, L.V., Monakov, Zu.B.: Structure and antioxidant characteristics of wheat and oat lignins. Rus. J. Appl. Chem. **78**(8), 1343–1350 (2005)
157. Pepper, J.M., Baylis, P.E., Adler, E.: The isolation and properties of lignins obtained by the acidolysis of spruce and aspen woods in dioxane-water medium. Can. J. Chem. **37**(8), 1241–1245 (1959)
158. Barclay, L.R.C., Xi, F., Norris, J.Q.: Antioxidant properties of phenolic lignin model compounds. J. Wood Chem. Technol. **17**(1–2), 73–90 (1997)
159. Perez-Perez, E.M., Rodriguez-Malaver, A.J., Dumitrieva, N.: Antioxidant activity of lignin from black liquor. In: ILI 7th International Forum, Barcelona, 27–28 Apr 2005, pp. 191–194
160. Telysheva, G., Dizhbite, T., Tirzite D., Jurjane V.: Applicability of a free radical (DPPH·) method for estimation of antioxidant activity of lignin and its derivatives. 5th International lignin institute, Forum, Commercial outlets for new lignins and definitions of new projects, Bordeaux, France, Proceedings, pp. 153–160. (2000)
161. Pan, X., Kadla, J.F., Ehara, K., Gilkes, N., Saddler, J.N.: Organosolv ethanol lignin from hybrid poplar as a radical scavenger: Relationship between lignin structure, extraction conditions and antioxidant activity. J. Agric. Food Chem. **54**, 5806–5813 (2006)
162. Căpraru A.M. Disertation thesis: Contributions on lignin modification by hydroxymethylation and epoxydation reactions GH. Asachi Technical University, Iasi, Romania, (2010)
163. Gravitis, J.: Lignin structure and properties from the viewpoint of general disordered systems theory. In: Kennedy, J.F., Phillips, G.O., Williams, P.A. (eds.) Lignocellulosic Science, Technology, Development and Use, pp. 613–627. Ellis Horwood, New York (1992)

164. Radotić, K., Tasić, M., Jeremić, M., Budimlija, Z., Simić-Krstić, J., Bolžović, Z.: Fractal analysis of STM images of lignin polymer obtained by in vitro synthesis. Gen. Physiol. Biophys. **19**(2), 171–180 (2000)
165. Jurasek, L.: Morphology of computer-modeled lignin structures: fractal dimensions, orientation and porosity. J. Pulp Paper Sci **22**, J376–J380 (1996)
166. Vainio, U., Maximova, N., Hortling, B., Laine, J., Stenius, P., Kaarina, S.L., Gravitis, J., Serimaa, R.: Morphology of dry lignins and size and shape of dissolved kraft lignin particles by X-ray scattering. Langmuir **20**, 9736–9744 (2004)
167. Garver, T.M., Callaghan, P.T.: Hydrodynamics of kraft lignins. Macromolecules **24**, 420–430 (1991)
168. Norgren, M., Lindström, B.: Physico-chemical characterization of a fractionated kraft lignin. Holzforschung **54**, 528–534 (2000)
169. Cazacu G., Nita L., Pintilie M., Vasile C.: Physico-chemical characterization of lignin. Size lignin particles determination on the Zetasizer nano, COST FP0901 Meeting, Paris, January pp. 25–26. (2011)
170. Notley, S.M., Norgren, M.: Lignin: Functional biomaterial with potential in surface chemistry and nanoscience. In: Lucia L.A. (ed.) The Nanoscience and Technology of Renewable Biomaterials, pp. 173–206. Blackwell Publishing Ltd., Wiley (2009)
171. Norgren, M., Edlund, H., Wågberg, L., Lindström, B., Annergreen, G.: Aggregation of kraft lignin derivatives under conditions relevant to the process. Part 1. Phase behaviour. Colloids Surf. A **194**, 85–86 (2001)
172. Norgren, M., Edlund, H., Wågberg, L.: Aggregation of lignin derivatives under alkaline derivatives. Kinetic and aggregate structure. Langmuir **18**, 2856–2865 (2002)
173. Šćiban, M., Klašnja, M.: Wood sawdust and wood originate materials as adsorbent for heavy metal ions. Holz Roh Verkst **62**, 69–73 (2004)
174. Goring, D.A.I., Vuong, R., Gancet, C., Chanzy, H.: The flatness of lignosulfonate macromolecules as demonstrated by electron microscopy. J. Appl. Polym. Sci. **24**(4), 931–936 (1979)
175. Favis, B.D., Goring, D.A.I.: A model for the leaching of lignin macromolecules from pulp fibers. J. Pulp Paper Sci **10**(5), J139–J143 (1984)
176. Yu, E., Dem'yantseva, N.P., Lysogorskaya, V.V., Klyubin, S., Zaitseva, V.: A dynamic light scattering study of the temperature dependence of the size-distribution pattern and aggregation stability of sulfate lignin and wood resin in aqueous alkali solution. Russ. J. Appl. Chem. **75**(1), 149–15 (2002)
177. Bonnikov, S.V., Dem'yantseva, E.Yu.: Particle size distribution of wood resin and sulfate lignin in aqueous alkaline solution. Russ. J. Appl. Chem. **78**(3), 492–495, (2005)
178. Shulga, G., Skudra, S., Shakels, V., Brovkina, J., Belkova, L., Cazacu, G., Vasile, C., Nita, L.: Self-organization of birch lignin and its water solution properties. 11th EWLP, August 16–19, Hamburg, Germany, Proceedings, pp. 577–580. (2010)
179. Căpraru, A.M., Ungureanu, E., Popa, V.I.: Aspects concerning some biocides systems based on natural aromatic compounds aromatic compounds and their copper complexes. 15th International Symposium on Wood, Fibre and Pulping Chemistry, Oslo, Norway, Proceedings CD 15–18 June, 2009
180. Măluţan, Th., Nicu, R., Popa, V.I.: Contribution to the study of hydroxymethylation reaction of alkali lignin. Bio/Resources **3**(1), 13–20 (2008)
181. Schilling, P.: Submicron lignin-based binders for water-based black ink formulation. US Patent, 5192361/March 9 1993
182. Popa, V.I., Căpraru, A.M., Grama, S., Măluţan, T.: Studies concerning the obtaining of nanoparticles with biocides properties based on modified lignins. 3rd International Conference on Advanced Composite Materials Engineering, COMAT, vol. 2, pp. 193–197. Braşov, Proceedings, 27–29 October 2010
183. Popa, V.I., Măluţan, Th., Nicu, R.: Study of hydroxymethylation reaction of alkali lignin. 8th Forum ILI the ILI umbrella programme and other existing or new approaches in lignin research, pp. 209–212. Rome, Italy, Proceedings, 10–12 May 2007

184. Ungureanu, E., Căpraru, A.M, Popa, V.I.: Aspects concerning some bioprotection agents based on natural aromatic compounds and their copper complexes. COST 50/ILI Joint meeting, p. 40. Switzerland, Abstracts, 27–29 October 2008
185. Ungureanu, E., Popa, V.I., Todorciuc, T.: Biocides systems based on natural products with application in protecting the lignocellulose materials. The 7th Romanian-Italian Seminar on Pulp and Paper, Iasi, Romania 6–8 Sept 2007
186. Ungureanu, E., Ungureanu, O., Căpraru, A.M., Popa, V.I.: Chemical modification and characterization of straw lignin. Cellul. Chem. Technol. **43**(7–8), 261–267 (2009)
187. Yamaguchi, H., Yaoshino, K.: Influence of tannin-copper complexes as preservatives for wood on mechanism of decomposition by brown-rot fungus *Fomitopsis palustris*. Holzforschung **55**(5), 4644–470 (2001)
188. Kozlowski, R., Zimniewska, M.: Cellulose fibre textiles containing nanolignins, a method of applying nanolignins onto textiles and the use of nanolignins in textile production. International Patent WO 2008/140337 A1, 20.11.2008
189. Elegir, G., Bussini, D., Antonsson, S., Lindström, Z.L.: Laccase-initiated crosslinking of lignocellulose fibres using a ultra-filtered lignin isolated from kraft black liquor. Appl. Microbiol. Biotechnol. **77**(4), 809–817 (2007)
190. Ciolacu, D., Anghel, N., Cazacu, G.: Enzymatic degradation of the hydrogels based on poly(vinyl alcohol) and lignin. Workshop of the COST ActioBioBIO (FP0602), Varenna (Lecco) Italy 2–4 Sept, 2009
191. Ciolacu, D., Darie, R.N., Cazacu, G.: Polymeric systems based on lignin—poly(vinyl alcohol). In: Totolin, M., Cazacu G., (eds.) Binders, Composites and Other Applications Based on Lignins, pp. 170–194. MPIM Publising, Iasi, ISBN 606-520-740-3, (2010)
192. Darie, R.N., Cazacu, G., Vasile, C.: Melt processing and physico-chemical characterisation of some synthetic polymer (PVA)/natural polymer (lignin) systems. Iasi academic days, Progress in organic and polymer chemistry, 22nd edn. Iasi, 8–10 Oct, 2009
193. Chen, P., Zhang, L., Peng, S., Liao, B.: Effects of nanoscale hydroxypropyl lignin on properties of soy protein plastics. J. Appl. Polym. Sci. **101**(1), 334–341 (2006)
194. Baumberger, S., Lapierre, C., Monties, B.: Utilization of pine kraft lignin in starch composites: Impact of structural heterogeneity. J. Agric. Food Chem. **46**, 2234–2240 (1998)
195. Baumberger, S., Lapierre, C., Monties, B., Della, V.G.: Use of kraft lignin as filler for starch films. Polym. Degrad. Stab. **59**, 273–277, (1998)
196. Stevens, E.S., Willett, J.L., Shogren, R.L.: Thermoplastic starch—kraft lignin—glycerol blends. J. Biobased Mat. Bioen **1**(3), 351–359 (2007)
197. Wu, R.L., Wang, X.L., Li, F., Li, H.Z., Wang, Y.Z.: Green composite films prepared from cellulose, starch and lignin in room-temperature ionic liquid. Bioresource Technol. **100**, 2569–2574, (2009)
198. Sánchez, C.G., Espósito Alvarez, L.A.: Micromechanics of lignin/polypropylene composites suitable for industrial application. Angew. Makromol. Chem. **272** (nr. 4758), 65–70, (1999)
199. Mikulàšová, M., Košíková, B.: Biodegradability of lignin-polypropylene composite films. Folia Microbiol. **44**(6), 669–672 (1999)
200. Pouteau, C., Dole, P., Cathala, B., Averous, L., Boquillon, N.: Antioxidant properties of lignin in polypropylene. Polym. Degrad. Stab. **81**, 9–18 (2003)
201. Gregorová, A., Cibulková, Y., Košiková, B., Šimon, P.: Stabilization effect of lignin in polypropylene and recycled polypropylene. Polym. Degrad. Stab. **89**, 553–558 (2005)
202. Košiková, B., Rvajová, A., Demianová, V.: The effect of adding lignin on modification of surface properties of polypropylene. Eur. Polym. J **31**, 953–956 (1995)
203. Darie, R., Cazacu, G., Vasile, C., Kozlowski, M.: Blends with polypropylene matrix and lignin additive. Italic 4, Science and Technology of Biomass: Advances and Challenges, Monte Porzio catone, pp. 215–218. Rome, Italy, Proceedings, 8–10 May, 2007
204. Darie, R.N., Vasile, C., Cazacu, G., Kozlowski, M.: Effect of lignin incorporation on some physico-mechanical properties of blends containing synthetic polymers. 7th International Conference APT 2007 Advances in Plastics Technology, Katowice, Poland 12–15 Nov, 2007

205. Bozell, J.J., Holladay, J.E., Johnson, D., White, J.F.: Top value-added chemicals from biomass. Vol II—Results of screening for potential candidates from biorefinery, 2007 http://www1.pnl.gov/main/publications/external/technical_reports/PNNL-16983.pdf
206. Li, Y., Sarkanen, S.: Thermoplastics with very high lignin contents. In: Glasser, W.G., Northey, R.A., Schultz, T.P. (eds.) Lignin: Historical, Biological and Materials Perspectives, pp. 351–366.ACS Symposium Series 742, Am. Chem. Soc. Washington (1999)
207. Calvo-Flores, F.G., Dobado, J.A.: Lignin as renewable raw material. ChemSusChem **3**(33), 1227–1235 (2010)
208. Pye, E.K.: Industrial lignin production and applications. In: Kamm, B., Gruber, P.R., Kamm M., (eds.) Biorefineries—Industrial Processes and Products. Status Quo and Future Directions, vol. 2, pp. 165–200. Wiley-VCH Verlag Gmbh & Co KGaA, Weinheim, ISBN 3-527-31027-4, (2006)
209. Stewart, D.: Lignin as a base material for materials applications. Chemistry, application and economics. Ind. Crops Prod. **27**, 202–207 (2008)
210. Cazacu, G., Pascu, M.C., Profire, L., Vasile, C.: Environmental friendly polymer materials. I. Polyolefins-lignin based materials. Environ. Prot. Ecol. **3**(1), 242–248 (2002)
211. Cazacu, G., Pascu, M.C., Profire, L., Kowarski, A.I., Mihăeş, M., Vasile, C.: Lignin role in a complex polyolefin blend. Ind. Crops Prod. **20**, 261–273 (2004)
212. Cazacu, G., Mihaeş, M., Pascu, M.C., Profire, L., Kowarski, A.I., Vasile, C.: Polyolefin/lignosulfonate blends. IX. Functionalized polyolefins/lignin blends. Macromol. Mat. Engin. **289**(10), 880–889, (2004)
213. Kleinert, M., Barth, T.: Phenols from lignin. Chem. Eng. Technol. **31**(5), 736–745 (2008)

Chapter 9
Recent Studies on Hemicellulose-Based Blends, Composites and Nanocomposites

Kirsi S. Mikkonen

9.1 Introduction

Hemicelluloses are the most abundant plant polysaccharides other than cellulose. They are biosynthesized in large quantities in the majority of trees and terrestrial plants. In spite of their abundance, the industrial utilization of hemicelluloses is minor in comparison with the use of starch and cellulose. In many lignocellulosic refining processes, hemicelluloses are partly degraded, they are removed and burnt, or further used as feed raw material. However, methods for separation and isolation of high molar mass hemicelluloses have been developed [1, 2]. Hemicelluloses can be extracted from plant material with alkali; parts of them are extracted also with water. The amount of potential raw material from forestry and agricultural side streams is significant and researchers are currently aiming at finding potential uses for it. Unlike starch, hemicelluloses are not digested by humans but function as a dietary fiber. Therefore they are an interesting raw material e.g. for the chemical industry. Potential applications include paper making, biodegradable packaging materials, coatings, hydrogels, absorbents, and emulsifiers [3].

Cellulose is the main component of cell walls and is responsible for their stiffness and strength [4]. Hemicelluloses are a structurally versatile group of polysaccharides. By cross-linking cellulose and lignin they contribute to the cell wall flexibility. Hemicelluloses form the hydrophilic component of the cell wall. Hemicelluloses are classified to different groups according to their structure: xylans, mannans, galactans, arabinans, and β-glucans. The polymer is based on consecutive D-xylose, D-mannose, D-galactose, L-arabinose, or D-glucose units,

K. S. Mikkonen (✉)
Department of Food and Environmental Sciences, University of Helsinki,
Latokartanonkaari 11, P.O. Box 27 Helsinki, Finland
e-mail: kirsi.s.mikkonen@helsinki.fi

S. Thomas et al. (eds.), *Advances in Natural Polymers*,
Advanced Structured Materials 18, DOI: 10.1007/978-3-642-20940-6_9,

respectively [5]. Most hemicelluloses are branched with side groups of 1–2 monosaccharide units. Many hemicelluloses also contain acetyl groups. The most abundant hemicelluloses are xylans and mannans. In addition to hemicelluloses, mannans are found as storage polysaccharides in the endosperm of certain legume seeds [6] and in the tuber of *Amorphophallus konjac* [7]. These mannans have similar chemical structure to that of hemicelluloses, but according to their properties, they are classified as plant gums.

In recent ten years, xylans and mannans have been studied as potential raw materials for biodegradable films. Sometimes they are blended with other polymers or mixed with nanoparticles to achieve enhanced properties. This chapter covers the occurrence, structure and properties of xylans and mannans as well as recent studies on xylan- and mannan-based blends, composites, and nanocomposites.

9.2 Xylans and Mannans

9.2.1 Occurrence

Hemicelluloses are a structurally heterogeneous group of polysaccharides varying in their monosaccharide composition, substitution pattern, and the degree of polymerization. The primary structure of hemicelluloses depends on the type of plant and may also vary between different parts of the same plant. The most common hemicelluloses are xylans and they are considered to be the second most abundant biopolymer in the plant kingdom. Xylans constitute 25–35 % of the dry biomass of woody tissues of dicots and lignified tissues of monocots. Many agricultural crops such as straw, sorghum, sugar cane, corn stalks and cobs, hulls and husks from starch production, as well as forest and pulping waste products from hardwoods, are good sources for xylans (Table 9.1). Up to 50 % of some tissues in cereal grains consist of xylans [8]. Xylans are minor components in the entire cereal grains, but they constitute an important part of the thin cell walls that surround the cells in the starchy endosperm [9]. Xylose comprises 65–90 % of the total sugars in the hemicellulosic fractions of wheat straw [10]. Softwoods contain 5–10 % arabinoglucuronoxylan. Depending on the hardwood species, the xylan content varies within the limits of 15–30 % of the dry wood [11]. White birch (*Betula papyrifera*) and silver birch (*Betula verrucosa*) contain as much as 35 % of xylan [12].

The predominant hemicelluloses in softwoods are galactoglucomannans (GGM) (about 20 %). Hardwoods contain 2–5 % of glucomannan [11, 12]. Legume seeds contain plant gums, the most abundant and commercially the most important of which are those consisting of galactomannans. These include locust bean gum (LBG) i.e. carob bean gum, guar gum (GG), tara gum, fenugreek gum, mesquite gum, and cassia gum [13]. The most important of these are GG and LBG,

Table 9.1 Major sources of xylans and mannans

Compound	Source
Arabinoxylan	Cereal endosperms
Glucuronoxylan	Hardwoods
Arabinoglucuronoxylan	Cereal straws and husks, grasses, softwoods
Glucomannan	Hardwoods, konjac tuber
Galactomannan	Leguminous seeds
Galactoglucomannan	Softwoods

whose endosperm content can be 40–48 % of the weight of the seed [14]. GG is galactomannan isolated from the seeds of *Cyamopsis tetragonolobus*, which is native to India and Pakistan, but nowadays it is also grown in the semi-arid regions of southwestern United States (Texas) and in Malawi, South Africa and Mexico. Carob tree (*Ceratonia siliqua*) is native to the Mediterranean and Middle East, but its commercial exploitation has developed in a number of countries around the world [13]. Konjac glucomannan (KGM) is a polysaccharide isolated from the tuber of *Amorphophallus konjac*. KGM constitutes 60–80 % of the konjac tuber. The konjac plant has been cultivated in the Far East for many centuries [15]. Mannans also occur in the seeds of several other plants, such as date, tomato, and coffee. They function as a nutrient reserve during germination and protect the seed from mechanical damage [16].

9.2.2 Structure

Xylan consists of β-D-xylopyranose units, linked by (1 → 4)-bonds, and different side groups [11]. Certain *Plantago* seeds also contain xylan with β-(1 → 3)-linkages in the backbone [17]. Xylans consisting of only xylose are extremely rare. Most xylans contain side groups attached with α-(1 → 2)- and/or α-(1 → 3)-linkages [18]. Common side groups are L-arabinofuranosyl and 4-*O*-methyl-D-glucopyranosyluronic acid (Fig. 9.1). The uronic acids and the arabinose units can occur on the same or different xylose units [19]. Although most arabinose residues in arabinoxylans are found as monomeric substituents, a small proportion of oligomeric side-chains, consisting of two or more arabinose residues linked via (1 → 2)-, (1 → 3)-, and (1 → 5)-linkages, has been reported for some arabinoxylans [9]. Maize bran xylan has disaccharide and trisaccharide side chains composed of arabinose, xylose, and galactose units [20]. In addition, arabinoxylans contain p-coumaryl and feruloyl groups attached with ester bonds to the C-5 positions of arabinose units [21]. Xylans from grasses and cereal straws have similar backbone to that of wood xylans. However, they contain smaller proportions of uronic acids, but are more highly branched and contain large proportions of L-arabinofuranosyl units [21].

The degree of polymerization of wood arabinoglucuronoxylan is about 100 and that of glucuronoxylan is about 200 [11]. Seven out of ten xylose residues of

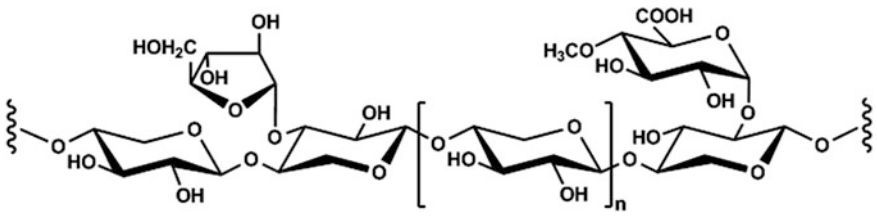

Fig. 9.1 Arabinoglucuronoxylan

hardwood xylans contain an *O*-acetyl group at C-2 or, more frequently, at C-3 of xylose. Softwood xylans do not contain acetyl groups [12].

The backbone of mannans consists of D-mannopyranosyl units that are most commonly linked with β-(1 → 4)-bonds. The backbones of some mannans contain also β-(1 → 3)-bonds and β-(1 → 2)-bonds [6]. Galactomannans contain single D-galactopyranosyl units attached to the backbone with α-(1 → 6)-linkage [6, 13]. The individual galactomannans differ from each other in their mannose:galactose ratio and distribution pattern of the galactose residues along the mannan chain. Mannose:galactose ratios of LBG and GG are approximately 3.5:1 and 1.5:1, respectively [22]. Results from studies on the distribution of galactose side groups along the mannan backbone are contradictory. It was previously believed that side-chain units of GG were disposed alternately along the mannan backbone, whereas those of LBG were disposed in uniform blocks [23]. Daas et al. [22] however, suggested instead that GG has a block wise distribution of galactose side groups and LBG can show random, block wise, and ordered distributions.

The backbones of GGM and glucomannan consist of alternating D-glucopyranosyl and D-mannopyranosyl units attached with β-(1 → 4)-bonds (Fig. 9.2) [18]. GGM in pine contains regions in which two or three glucose units are linked together, and regions with several successive mannose residues [24]. The glucose:mannose ratio of hardwood glucomannan varies between 1:2 and 1:1, depending on wood species. Softwood GGM contain D-galactopyranosyl units α-(1 → 6)-linked to the backbone mannose units and can be roughly divided into two fractions having different galactose contents. In the fraction which has a low galactose content the ratio galactose:glucose:mannose is about 0.1:1:4 whereas in the galactose-rich fraction the corresponding ratio is 1:1:3. The former fraction with low galactose content is often referred to as glucomannan [11]. The degree of polymerization of GGM is about 150 [12]. The hydroxyl groups of softwood GGM at C-2 and C-3 positions in the chain units are partially substituted by O-acetyl groups, on the average one group per 3–4 backbone hexose units [11]. It has been documented that only the mannosyl units bear acetyl groups [3].

The backbone of KGM consists of β-(1 → 4)-linked mannose and glucose units with a glucose:mannose ratio of about 1:1.6. KGM contains small amounts of acetyl groups [7]. Plant gum galactomannans have longer chain than wood mannans, about 1,000–1,500 sugar units [13].

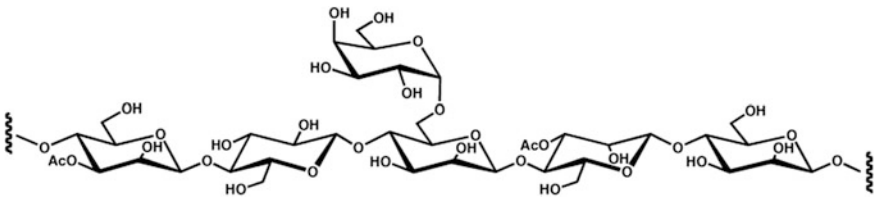

Fig. 9.2 Galactoglucomannan

9.2.3 Properties

Like cellulose, most hemicelluloses function as supporting material in the cell walls [11]. Because of their ability to absorb large amounts of water, they may reduce brittleness and provide some degree of elasticity and resistance of plant tissues to bending abuses. They could also be of some aid in allowing transport of dissolved metabolites and nutrients through the porous hydrated molecular network they establish around the cellulose crystallites [9]. It has also been postulated that certain structural features of arabinoxylans permit some intermolecular alignment between polymer chains of non-covalent interactions of arabinoxylans with other polysaccharides (β-glucan, cellulose) and, therefore, formation of multicomponent gels in the complex matrix of the walls. In addition, the presence of ferulic acid residues on the arabinoxylan chains provides potential for covalent polysaccharide–polysaccharide, polysaccharide-protein, or polysaccharide-lignin interactions [25].

The chemical and thermal stability of hemicelluloses is generally lower than that of cellulose, presumably due to their lack of crystallinity and lower degree of polymerization. In addition, hemicelluloses generally differ from cellulose with respect to their solubility in alkali. This characteristic property is most commonly utilized when fractioning different polysaccharides in lignin-free samples. This, however, results in modification i.e. de-esterification and further reduces solubility to water. Some hemicelluloses, such as cereal arabinoxylans and acetylated hardwood xylan, are partly or even totally water-soluble [26]. Hemicelluloses contain numerous free hydroxyl groups, which makes them hydrophilic [27]. Highly substituted hemicelluloses are more water-soluble and bind less tightly to cellulose, whereas molecules with infrequent side chains are less water-soluble and bind more tightly to cellulose [10]. The solubility normally increases when the degree of polymerization is decreased [28]. In addition to water, acetylated hemicelluloses are soluble in dimethyl sulfoxide, formamide, and *N,N*-dimethylformamide [21].

Hemicelluloses occur in all plants and thus also in common diet. In the human nutrition, the cell wall polysaccharides contribute to the dietary fiber, which is considered to be of salutary importance in the mobility of digesta through the alimentary tract and may have other desirable attributes, for example, in lipid metabolism [25].

Table 9.2 Xylan-based blends and composites

Xylan	Blended compounds	Ref.
Birch glucuronoxylan	Chitosan	[29]
Aspen glucuronoxylan	Chitosan	[30]
Birch glucuronoxylan, grass xylan, corn cob xylan	Gluten	[31]
Arabinoxylan (source not specified)	Agar, starch	[32]

9.3 Xylan-Based Blends and Composites

Xylan accounts for roughly one-third of renewable biomass available on earth but does not have enough applications in the industry. Xylan has been found to form films, and to improve the film formation and properties, xylan has been blended with other natural polymers (Table 9.2). The aim has been to create biodegradable materials with strong interactions, enhanced mechanical performance, and decreased water vapour permeability.

Pure alkali extracted birch glucuronoxylan did not form films, so xylan was blended with chitosan in acidic conditions [29]. Addition of 5 % chitosan resulted in formation of flakes, and at 10 % chitosan and above, continuous, self-supporting films were achieved. Films with a chitosan content below 30 % swelled in water and formed hydrogels. Above 30 % chitosan, the samples started to dissolve gradually during swelling measurements and pure chitosan films were readily dissolved in water. Electrostatic interactions between glucuronic acid functionalities of xylan and amino groups of chitosan, studied by Fourier transform infrared spectroscopy (FTIR), were suggested to be responsible for network formation. However, dynamic mechanical analysis (DMA) and atomic force microscopy (AFM) indicated discrete xylan and chitosan phases. Similar results were obtained for blends of aspen glucuronoxylan and chitosan [30]. Film formation took place at the same chitosan content as with birch xylan. Hydrogel formation was noted at chitosan contents of 5–20 %, and dissolution of films at chitosan contents of more than 20 %. The crystallinity of the films decreased with increasing chitosan content.

The use of xylan as an additive in biodegradable wheat gluten film production was tested to reduce the cost of the films [31]. Birch glucuronoxylan was added to wheat gluten in different combinations, from 0 to 40 wt%, and films were cast under acidic and alkaline conditions (pH of 4 and 11, respectively) and dried at ambient and elevated temperature (80 °C). Xylans alkali extracted from grass and corn cob were used at 20 %, the films were cast at pH 11 and dried at ambient temperature. More uniform films were formed from birch xylan and gluten when cast at high pH than at low pH. Xylan:gluten ratio did not affect the tensile strength of the films. However, the elongation at break of films decreased with increasing xylan content. The tensile strength and Young's modulus of films containing birch xylan were higher than those of films containing grass xylan or corn cob xylan. In contrast, the elongation at break of films with corn cob xylan was clearly higher

than that of the other films. The xylan-gluten films did not lose their integrity in aqueous solution after 24 h and solubility was seen to depend on the drying conditions of the film as well as the source of xylan. The water vapour transfer rate (WVTR) was not significantly affected by the addition of xylan. The authors concluded that it is possible to produce suitable films from wheat gluten by using xylan as an additive.

Some polymer blends have shown improved mechanical properties and gas/moisture barrier properties when compared to the pure materials. Therefore, three low cost polysaccharides were combined as binary blends; namely agar, cassava starch, and arabinoxylan [32]. The source of arabinoxylan was not specified. The main film-forming components were agar and starch, in which arabinoxylan was added at low ratios as an additive. When viewed with scanning electron microscopy (SEM), arabinoxylan and starch formed homogeneous blends, whereas arabinoxylan and agar showed a heterogeneous structure in which arabinoxylan seemed to be dispersed in continuous agar phase. Water vapour permeability (WVP) of agar-based films was reduced by adding arabinoxylan, suggesting interactions between the two polymers leading to a coupled network formation and a compact structure. However, the mechanical properties were not improved by the mixing of polymers but on the contrary; some decrease in the mechanical performance of the films took place with the addition of arabinoxylan. Arabinoxylan could be considered as an additive for agar-based films to increase moisture barrier efficiency.

9.4 Mannan-Based Blends and Composites

Recent studies on mannan-based blends and composites are emphasized on the use of KGM as a film forming component, with a few studies on other mannans (Table 9.3). Even though films from pure KGM have excellent mechanical properties, the improvement of those properties has been sought by blending KGM with other polysaccharides, proteins, or synthetic polymers.

Ye et al. [33] prepared blends of KGM and chitosan and studied the miscibility of the polymers as well as the mechanical properties and biocompatibility of the films. The blend film obtained from the KGM:chitosan ratio of 80:20 (wt%) showed the highest miscibility and blend homogeneity when studied with SEM and differential scanning calorimetry (DSC). FTIR showed that strong intermolecular hydrogen bonds took place between the amino groups of chitosan and the hydroxyl groups of KGM. The tensile strength also achieved its maximum at this ratio. Mouse fibroblast cells attached and spread on the KGM:chitosan 80:20 blend film and grew well in the culture medium which contained almost all the soluble compounds of that film, whereas only a fraction of cells could attach on the pure KGM membrane. Addition of 20 % chitosan made it possible to apply KGM film to biomaterial.

Table 9.3 Mannan-based blends and composites

Mannan	Blended compounds	Ref.
Konjac glucomannan	Chitosan	[33]
Konjac glucomannan	Chitosan, soy protein isolate	[34]
Konjac glucomannan	Sodium alginate	[35]
Carboxymethyl konjac glucomannan	Sodium alginate	[36]
Konjac glucomannan	Sodium alginate, collagen	[37]
Konjac glucomannan	Carboxymethyl cellulose	[38]
Konjac glucomannan	Carboxymethyl cellulose, palm olein	[39, 40]
Konjac glucomannan	Cellulose	[41]
Konjac glucomannan	Xanthan	[42]
Konjac glucomannan	Starch	[43]
Konjac glucomannan	Gellan	[44]
Konjac glucomannan	Gelatin	[45, 46]
Konjac glucomannan	Sericin, beeswax	[47]
Konjac glucomannan	Poly(vinyl alcohol)	[48, 49]
Konjac glucomannan	Poly(vinylpyrrolidone)	[50]
Konjac glucomannan	Quaternized poly(4-vinyl-*N*-butyl) pyridine	[51]
Carboxymethyl konjac glucomannan	Waterborne polyurethane	[52]
Konjac glucomannan	Poly(diallydimethylammonium chloride)	[53, 54]
Locust bean gum galactomannan	Starch	[55]
Guar gum galactomannan	Chitosan	[56]
Spruce galactoglucomannan	Alginate, carboxymethyl cellulose	[57, 58]
Spruce galactoglucomannan	Konjac glucomannan, corn arabinoxylan, poly(vinyl alcohol)	[59, 60]
Spruce galactoglucomannan	Carboxymethyl cellulose, chitosan	[61, 62]

Jia et al. [34] prepared ternary blends from KGM, chitosan and soy protein isolate (SPI). They studied the effect of the blend composition, the type of plasticizer, the amount of glycerol, and the pH of film forming solution on the water vapour permeability (WVP) and mechanical properties of the films. Incorporation of SPI to the polymer matrix at low concentration decreased the WVP. At KGM:chitosan:SPI weight ratio of 1:1:1, the blend film showed the lowest WVP. Both the tensile strength and elongation at break also decreased with increasing SPI content. The use of sorbitol as plasticizer resulted in lower WVP than the use of other plasticizers, but glycerol was chosen as suitable plasticizer because its use resulted in relatively low WVP and good mechanical properties. Increasing glycerol content decreased the WVP and tensile strength, and increased the elongation at break of films. The WVP was the lowest and the elongation at break the highest at pH 5, while the tensile strength reached its maximum at pH 3.

Native [35] and carboxymethylated KGM (CMKGM) [36] were blended with sodium alginate. The mechanical properties, moisture content, and water swelling capacity of the blend films were higher than those of pure KGM film [34]. The interaction from the intermolecular hydrogen bonds existing between the COO^-

groups of sodium alginate and the hydroxyl groups of KGM resulted in the enhancement of mechanical properties of the blend film. Two fruit types, namely lychee and honey peach, were coated with the blend film. Results of the film-coating preservation showed that the weight loss rate and fruit rot rate of lychee and honey peach both decreased, and the brown-altering of the pericarp was delayed. The high tensile strength in dry state, good water solubility, biodegradability, and water-holding ability of the blend film made it a promising fruit preservative film material.

CMKGM and sodium alginate were crosslinked using 5 wt% calcium chloride aqueous solution [36]. The mechanical properties and the thermal stability of the films were improved by blending sodium alginate with CMKGM due to the intermolecular hydrogen bonds between the two polymers. The crosslinked blend films, compared with the uncross linked ones, exhibited further improved physical properties due to the formation of semi-interpenetrating networks. The swelling degree of the crosslinked blend films increased dramatically with the increase of CMKGM content, suggesting that the crosslinked films have potential application for water storage materials with good thermal and mechanical properties.

Blends were made from KGM with collagen and sodium alginate using calcium chloride as the crosslinking agent [37]. FTIR analysis proved calcium crosslinking, strong hydrogen bonding, and electrostatic force between the film polymers. Blending of the three polymers changed or destroyed the original crystalline structure of collagen and sodium alginate resulting in decreased molecular arrangement order, increased amorphous area and significantly lowered crystallinity. Light transmittance measurements showed that the blend films were transparent in appearance, indicating good compatibility between the polymers. High KGM content was associated with high light transmittance of the blend films. The blend with a KGM:collagen:sodium alginate ratio of 25:50:25 (wt%) resulted in the highest tensile strength. The water absorption of the blend films greatly decreased with increasing content of sodium alginate, due to the higher hydrophilic property of collagen and KGM. Films made from collagen, KGM, or collagen together with KGM completely dissolved after being kept in water for 24 h.

Clear, transparent, and water-soluble films were obtained from KGM with sodium carboxymethyl cellulose (CMC) at different ratios [38]. Based upon FTIR, it seemed that the COO– and OH groups in CMC participated in intermolecular hydrogen bonds with the OH and $COCH_3$ groups in KGM. The crystallinity of films decreased with increasing KGM content. Due to hydrogen bonding interactions between the polymers, the thermal stability of the blend films was better than that of the pure KGM and CMC films. Both the tensile strength and elongation at break reached a maximum at CMC content of 10 wt%. SEM showed that high miscibility occurred at low CMC contents. As the CMC content increased, the morphology of the blend film surfaces changed from smooth to rough, indicating phase separation.

Cheng et al. [39] used potassium hydroxide (KOH) in KGM-CMC films to deacetylate KGM and further increase the hydrogen bonding between polymers. Alkali treatment increased the crystallinity of the films. It was suggested that the

alkaline deacetylation of the KGM polymer reduced steric hindrance and the polymer chains became freer to associate. The moisture uptake of pure KGM films decreased with the use of KOH, but the effect of alkali on moisture sorption appeared to be negated in the presence of CMC. Incorporation of CMC increased the WVP of films. The presence of CMC decreased the tensile strength of films in the absence of KOH, but when KOH was used, CMC increased the tensile strength of films. CMC and KOH had interactive effects in modifying the properties of KGM-based films.

Palm olein lipid was emulsified in KGM and KGM-CMC films prepared with and without KOH treatment [40]. Interactions between deacetylated KGM and CMC resulted in a stable emulsion, with CMC functioning as an emulsifier. With alkaline deacetylated KGM and CMC as the base polymers for the emulsion, small lipid globules, with a homogeneous distribution, increased the apparent hydrophobicity of an emulsion film for water molecule transmission, thereby resulting in reduced WVP. Use of palm olein decreased the tensile strength and somewhat increased the elongation at break of films.

Ionic liquid 1-allyl-3-methylimidazolium chloride was successfully used as a solvent in the preparation of blend films from cotton linter cellulose and KGM [41]. The films were coagulated and washed with water. Good compatibility and strong interactions between cellulose and KGM, studied with gravimetric, FTIR, and XRD analyses, resulted in almost no loss of the water-soluble KGM from the blend films even after the water coagulating and washing. However, SEM portrayed phase separations in the blend films, namely, egg-like new phase particles were embedded in a continuous matrix base. DSC suggested that relatively low molar mass part of both cellulose and KGM formed the continuous phase, whereas the egg-like new phase particles were patterns of relatively high molar mass part of both polymers. The egg-like particles were considered to act as physical crosslinks to strengthen the blend material.

Because the rheological and biological properties of KGM are strongly dependent on its molar mass, its backbone was hydrolyzed enzymatically before blending with xanthan [42]. Decreasing the molar mass of KGM increased hydrogen bonding between KGM and xanthan. DSC showed enhancement of thermal stability of the blend films in contrast to the pure KGM films. The crystallinity of the blend films decreased with the increasing content of non-degraded KGM. The mechanical performance of the films was also improved by blending. Decrease in the molar mass of KGM increased the tensile strength of the blends, but the elongation at break had a maximum at the highest molar mass of KGM.

The structure and properties of pea starch-based films were modified and improved by blending starch with KGM [43]. The results from FTIR, XRD, and SEM indicated that strong hydrogen bonding took place between the polymers resulting in a good miscibility of the blends. The melting temperature of the starch crystallites decreased with increasing KGM content. The tensile strength and elongation at break were the highest at 70 wt% KGM content with 10 and 20 wt% glycerol as plasticizer, respectively.

KGM and gellan have shown synergistic effects in hydrosol or gel, so they were used to form blend films [44]. The FTIR, XRD, DSC, and transparency analyses showed that intermolecular hydrogen bonding took place between KGM and gellan. The interaction was strongest at KGM content of 70 wt%. In addition, the tensile strength reached a maximum and moisture uptake was low at that KGM content. Nisin was incorporated in the films to make them antimicrobial. The release of nisin and the antimicrobial activity against *Staphylococcus aureus* increased with increasing gellan content.

KGM was blended with gelatin to form transparent films [45]. The crystallinity of the films decreased with the increase of the KGM content. The thermal stability of films was improved by blending KGM with gelatin. Moisture uptake, degree of swelling, and elongation at break of films increased with increasing KGM content, but tensile strength reached a maximum at KGM content of 30 wt%. SEM showed that as the KGM content increased, the morphology of the blend film surfaces changed from being smooth to becoming microphase separated. Li et al. [46] discovered that the addition of gelatin made KGM films heat sealable. They found that at 40 wt% KGM content the hydrogen bonding interaction was strengthened and the blend films had the best miscibility, good tensile strength, heatseal, and the smallest WVTR. All the blend films showed excellent water-solubility and could dissolve in not more than 30 s.

Sothornvit and Chollakup [47] aimed at utilizing sericin, a by-product from silk production, by preparing biopolymer films. Sericin could not form stand-alone films, so it was blended with KGM with and without using glycerol as plasticizer. Beeswax was added in order to study its effect on the WVP of films. Blending sericin with KGM resulted in yellow, transparent, and flexible films. High sericin content generally indicated high WVP. Surprisingly, adding beeswax did not improve the water vapour barrier properties of the films but somewhat increased the WVP. Tensile tests implied that KGM provided the strength for the film and sericin provided the flexibility, i.e. sericin acted as a plasticizer.

KGM—poly(vinyl alcohol) (PVOH) blends were studied by Xiao et al. [48] and Li and Xie [49]. Microscopic studies by Xiao et al. showed phase separation of PVOH and KGM [48]. They found with FTIR that there was some hydrogen bonding between the two polymers, but not as much as between KGM and other polysaccharides. However, the thermal stability of the blend films was better than that of pure KGM film at PVOH content below 20 wt%. The crystallinity, tensile strength, and elongation at break of films reached maximum values at 20 wt% PVOH. Li and Xie obtained miscible blends from KGM and PVOH by using glutaraldehyde as a crosslink agent [49]. The tensile strength, elongation at break, and moisture uptake of the crosslinked blends were clearly higher than those of films from the pure polymers or uncross linked blends.

A certain degree of interaction existed between KGM and poly(vinylpyrrolidone) (PVP), arising from hydrogen bonding between the hydroxyl groups and carbonyl groups of KGM and the carbonyl groups of PVP [50]. The blend film containing 10 wt% PVP had the lowest crystallinity, 6.7 %, indicating that intermolecular interaction destroyed the regularity of the two polymers. The

tensile strength and elongation at break of films reached a maximum at 10 wt% PVP content. The thermal stability of the blends was higher than that of KGM film. The blend with 10 wt% PVP showed a smooth morphology, but with increasing PVP content the morphology changed to rough.

KGM and quaternized poly(4-vinyl-*N*-butyl) pyridine (QPVP) were miscible when the content of QPVP was less than 30 wt% or in excess of 70 wt%, as confirmed by SEM and XRD [51]. The thermal stability and tensile strength of the films were reduced with increasing content of QPVP, but the elongation at break was the highest at QPVP content of 30 wt%. FTIR indicated that the electrostatic interaction of QPVP and KGM impaired the partial hydrogen bond interaction of KGM. The blend films were able to decrease the lychee fruit weight loss rate and rot rate.

CMKGM was combined with waterborne polyurethane (WPU) to form blend films with enhanced properties [52]. CMKGM was of critical importance to enhance the strength and stiffness of the blends and thus the tensile strength, Young's modulus, and thermal stability of the films increased significantly with an increase in CMKGM content, attributed to intermolecular hydrogen bonding between CMKGM and WPU. The tensile strength reached a maximum at 80 wt% CMKGM content. At low CMKGM contents, phase separation took place, but the blend films with 80 wt% CMKGM exhibited good miscibility. The degree of swelling of the blend films remained at low level, even though the films were immersed in ethyl acetate and toluene for 24 h.

A novel preservative film was prepared by blending KGM with poly (diallydimethylammonium chloride) (PDADMAC) [53, 54]. Density determination, SEM, and XRD showed that the blends were miscible when the PDADMAC content was less than 70 wt% and the highest miscibility appeared when the PDADMAC content was 20 wt% [53]. Strong intermolecular hydrogen bond interaction occurred between KGM and PDADMAC. The maximum tensile strength was obtained for films with 20 wt% PDADMAC and the thermal stability of the blends was higher than that of pure KGM films. Results from a film-coating preservation experiments with lychee and grapes showed that the weight loss rate of the coated fruit was lower than that of the uncoated fruit, indicating that the blend film had good water-holding and preservative ability. The antibacterial activity of the films against *Staphylococcus aureus*, *Bacillus subtilis*, *Escherichia coli*, *Pseudomonas aeruginosa*, and *Saccharomyces* were measured by the halo zone test and the double plate method [54]. The films exhibited an excellent antibacterial activity against *B. subtilis* and *S. aureus* but not against *E. coli*, *P. aeruginosa* or *Saccharomyces*.

LBG was used as an additive in starch-based films [55]. The film solutions were treated with irradiation, which resulted in continuous and smooth films. The presence of LBG increased the tensile strength, but reduced the elongation at break of films. A small addition of LBG decreased the WVP of the blend films, but applying higher concentration of LBG increased the WVP. The results indicated that the irradiation technology can be a useful tool as a cross-linking agent with starch and LBG to improve the functional properties of a starch-based film.

Chitosan is a promising film forming material with antimicrobial activity, but it is expensive. Therefore 0–50 % GG was blended with chitosan to form biopolymer films [56]. All studied films blocked the ultraviolet light transmission at 190–300 nm, which could be beneficial for food product preservation in some food applications. The films with 50 % GG showed the highest transparency, followed by films with 40 and 25 % GG, while films with 15 % GG were the least transparent. Incorporation of GG to chitosan films improved the oxygen barrier properties of the films, and the effect was the greatest at low GG contents. In contrast, the water vapor permeability was not affected by the addition of GG. The tensile strength of films was the highest at 15 % GG content. Moreover, the films with 15 % GG showed high antimicrobial activity against *Escherichia coli* and *Staphylococcus aureus*.

Hartman et al. [57] considered spruce GGM films blended with either alginate or CMC to have interesting oxygen barrier and mechanical strength properties. Phase separation was not observed, which was accounted for by all the components being rich in hydroxyl functionalities. Polyol plasticizers were needed to decrease the brittleness of films and to make them easier to handle. On the other hand, the addition of plasticizers made the films more susceptible to moisture. The oxygen permeability (OP) of the blend films was low. Characterization of the mechanical properties of films using humidity scan dynamic mechanical analysis showed that blend films from GGM with alginate or CMC were less moisture sensitive than the plasticized films from pure GGM.

In another study by Hartman et al. [58] GGM-alginate and GGM-CMC blends were modified by either vapor-phase grafting with styrene or plasma treatment followed by styrene grafting, aiming to create oxygen barrier materials that show high resistance toward moisture-rich conditions. Benzylation of GGM was undertaken with benzyl chloride in alkaline solution, which resulted in deacetylation of GGM, rendering it susceptible to benzylation (BnGGM). A blend of alginate and GGM was additionally benzylated and then cast as film. BnGGM was laminated on GGM-alginate film by soaking the film in a BnGGM solution. The oxygen barrier properties of BnGGM films were less sensitive to moisture than those of the unmodified GGM. The vapour-phase-grafted films showed better tolerance toward humidity than the plasma-treated ones. Lamination of GGM-alginate film by BnGGM resulted in low OP even at high RH (83 %).

Blends were made from GGM also with KGM, corn arabinoxylan (cAX), and PVOH in order to improve the mechanical properties of GGM films [59]. Microscopy and DMA showed good miscibility of GGM with KGM and cAX, but phase separation with PVOH (Fig. 9.3). Adding other polymers increased the elongation at break of GGM blend films. The tensile strength of films increased with increasing amount of KGM and PVOH, but the effect of cAX was the opposite. Blending GGM with KGM was considered to be an effective way to increase the elongation at break and tensile strength of GGM-based films.

Addition of PVOH to GGM decreased the WVP of films [60]. The WVP of GGM-KGM films was lower than that of pure KGM-based films at the RH gradient of 0/54 %, but not at 33/86 %. GGM and KGM seemed to have some synergism, as the

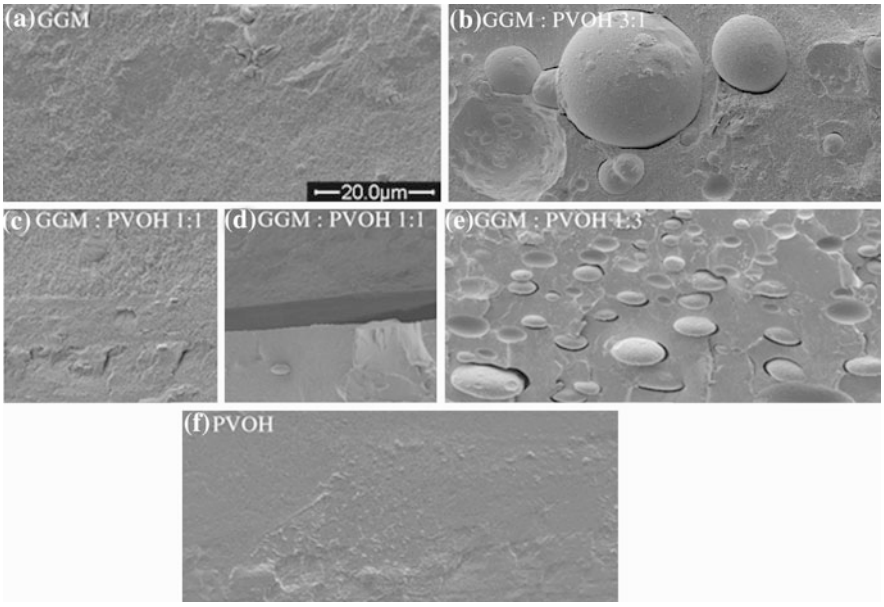

Fig. 9.3 Scanning electron micrographs of cross-sections of films from **a** GGM; **b** GGM: PVOH 3:1; (**c** and **d**) GGM : PVOH 1:1; **e** GGM : PVOH 1:3 and **f** PVOH. Scale bar = 20 μm. All images are at the same magnification [59]

OP of their blends was lower than that of films from either of the raw materials alone. The effect of PVOH on the OP of films depended on the blend ratio. At the ratio of GGM:PVOH 1:3, PVOH formed the continuous phase and GGM was located as small spheres inside the film, whereas at the ratio of 3:1, GGM formed the continuous phase and the PVOH formed large particles (Fig. 9.3) [59]. In the latter case, the OP was high and most of the replicate films leaked during the measurement, while with PVOH as the continuous phase, the OP was lower than that of pure GGM films [60].

Spruce wood was subjected to hydrothermal treatment, which yielded an oligo- and polysaccharide-rich, noncellulosic fraction that was called wood hydrolysate and was expected to consist mainly of GGM, with some of the hemicellulose-lignin interactions preserved [61, 62]. Wood hydrolysate formed brittle and fragile films by itself, and was blended with CMC and chitosan to form stronger free-standing films as well as coatings on polyethylene terepthalate (PET). Using CMC as the co component, CMC contents of 20–50 wt% produced cohesive, smooth, and transparent films. With chitosan as the co component, film homogeneity was impaired by the higher viscosity and 50 wt% chitosan did not yield homogeneous films. According to Hansen's solubility parameter calculations, wood hydrolysate was more compatible with CMC than with chitosan. The thermal stability of wood hydrolysate blends was also higher with CMC than with chitosan. Increasing the content of CMC or chitosan improved the mechanical properties of the films.

Table 9.4 Xylan-based nanocomposites

Xylan	Reinforcement	Ref.
Aspen glucuronoxylan	Bacterial cellulose	[63, 64]
Oat spelt arabinoxylan	Cellulose nanowhiskers	[65–68]
Oat spelt arabinoxylan, birch glucuronoxylan	Montmorillonite	[69]
Rye arabinoxylan	Bacterial cellulose	[70]

When applied onto PET, both types of mixtures produced thin and flexible coatings. Wood hydrolysate-based coatings clearly decreased the OP and somewhat decreased the WVTR of PET films compared with uncoated PET.

9.5 Xylan-Based Nanocomposites

Combination of hemicelluloses with nanosized cellulose creates nanocomposites that mimic natural plant cell wall structures (Table 9.4). The preparation of these nanocomposites has aimed at studying the interactions of the components or at improving the functional properties of hemicellulose-based films, such as tensile strength or water vapour barrier properties.

Nanocomposites were prepared from aspen glucuronoxylan and bacterial cellulose (BC) produced by *Acetobacter xylinum* [63]. In comparison, delignified aspen wood fibers, i.e. holocellulose, was studied. The materials were examined using microscopy, moisture scanning DMA, dynamic vapour sorption (DVS), and dynamic FTIR. Atomic force microscopy (AFM) showed BC microfibrils arranged in bundles with a diameter of approximately 60–100 nm. In the aspen xylan-BC composite, the bundles were covered with an evenly distributed layer of glucuronoxylan. On the contrary, the microfibrils in the aspen holocellulose sample had a thinner diameter and cavities between the microfibrils were visible, resulting from the removal of lignin and/or lignin/polysaccharide matrix. A pronounced decrease in modulus was detected for the film from pure aspen glucuronoxylan at about 85 % RH. The presence of BC had an impact on the softening behaviour, resulting in a less steep decline of the modulus curve. The softening of the holocellulose appeared at approximately the same humidity as for the composite and was considered to be due to the moisture-induced glass transition of the glucuronoxylan. Addition of BC also decreased the moisture content of the films at 90 % RH. According to dynamic FTIR, no clear indication for BC–xylan interactions could be observed [63]. When the nanocomposites were extracted with water, loosely present xylan was removed, leaving only the strongly associated xylan left [64].

Oat spelt arabinoxylan was used for nanocomposites with cellulose nanowhiskers (CNW) [65–68]. Films prepared from oat spelt arabinoxylan alone have poor film forming ability, which has been attributed to insufficient chain length of the polymer, high glass transition temperature, or poor solubility. The

reinforcement effect of CNW prepared by sulphuric acid hydrolysis was compared to that of CNW produced by hydrochloric acid (HCl) hydrolysis of cellulosic fibers (HCl-CNW) [65]. The CNW content was varied from 0 % to 10 % (wt%) and sorbitol was used as a plasticizer at 50 wt%. The films were characterized by tensile testing and microscopy. The addition of CNW resulted in an improvement in the strength properties of the nanocomposite film. The effect was more pronounced with the CNW prepared by sulphuric acid hydrolysis than with CNW produced by HCl hydrolysis. The improvement in strength properties was attributed to a rigid hydrogen-bonded network of CNW to form an integrated matrix. This trend was not, however, as evident with HCl-CNW which showed poor dispersibility because of lack of bulk charge on the HCl-CNW, which made the CNW to contact and interact extensively with each other leading to the formation of loose and bulky aggregates. Due to the formation of hydrogen-bonded network, the OP of films from oat spelt arabinoxylan was greatly decreased by the addition of sulfonated CNW [67]. Saxena and Ragauskas [66] and Saxena et al. [68] prepared oat spelt arabinoxylan films with sulphuric acid hydrolyzed CNW and with bleached kraft softwood fibers at 0–50 wt% using sorbitol as plasticizer. AFM analysis showed that the CNW had a rod-like structure with an average length of 150–200 nm and a width of less than 20 nm. Incorporation of sulfonated CNW into xylan decreased the specific WVTR of films. In contrast, the addition of pulp fibers increased the WVTR of films. The specific density analysis showed that the xylan-10 % CNW films were denser than the control and the xylan-10 % softwood fiber films. The xylan-softwood fiber films exhibited fiber aggregation, which was speculated to be the reason for the higher WVTR of the films in comparison to those reinforced with CNW. The authors concluded that the high degree of crystallinity of CNW, dense composite structure formed by CNW, and the rigid hydrogen bonded network of CNW could cause the CNW to form integrated matrix which contributed to the reduction of WVTR.

Montmorillonite clay particles (MMT) modified with distearyldimethylammonium chloride (DSDMAC) were used as reinforcement of oat spelt arabinoxylan and birch glucuronoxylan films [69]. The incorporation of the nanoparticles to the films were facilitated by treating them with a biodegradable non-ionic surfactant, organically modified inulin. Films were prepared at acidic, neutral, and basic pH. Both xylan types formed films at acidic pH, whereas at neutral and basic pH, films were only obtained from birch xylan. On the other hand, the incorporation of MMT resulted in homogeneous films only from oat spelt arabinoxylan, so the rest of the investigation was performed on them. The surface free energy of the films was evaluated by measuring the contact angles of water, formamide, and diiodomethane on the films. The addition of inulin-coated MMT led to a considerable reduction of the contact angle of water on the films.

Native and enzymatically debranched rye arabinoxylan (rAX and rDAX, respectively) were mixed with 5 and 15 % BC using high-pressure homogenizer to prepare cohesive and transparent nanocomposite films [70]. SEM imaging of the film cross-sections showed that the fibrous phase of the reinforcing BC was more aggregated in the film from native rAX than in the film from debranched rDAX,

Table 9.5 Mannan-based nanocomposites

Mannan	Reinforcement	Ref.
Konjac glucomannan	Silver nanoparticles	[71]
Carboxymethyl konjac glucomannan	Montmorillonite	[72]
Konjac glucomannan	Cadmium sulfide	[73, 74]
Konjac glucomannan, spruce galactoglucomannan	Cellulose nanowhiskers	[60, 75]
Spruce galactoglucomannan	Microfibrillated cellulose	[76]

which was explained by improved interaction between AX and BC when the arabinose side groups were removed. The crystallinity of xylan in the films was studied by subtracting the BC component from the XRD patterns. The xylan crystallinity was found to be dependent on the degree of arabinose substitution, but not on the addition of BC. Incorporation of BC in the nanocomposite films increased their stiffness, as seen from stress–strain curves obtained by tensile testing and confirmed by moisture-scanning DMA.

9.6 Mannan-Based Nanocomposites

Mannans have been combined with inorganic nanoparticles as well as with cellulose to form nanocomposites (Table 9.5). The effect of added nanoparticles e.g. on the mechanical properties and thermal stability of films was studied.

Tian et al. [71] were the first research group to prepare nanocomposites with KGM as the matrix. They added silver nanoparticles in the dilute hydrosol of KGM using photochemical reduction of Ag^+. Transmission electron microscopy (TEM) indicated that the morphology and the agglomerated state of the silver nanoparticles in the composites changed with the concentrations of Ag^+ and KGM as well as with the time of photochemical reduction. The silver nanoparticles were finely dispersed inside the KGM films with different shapes, such as sphere-like and star-like. FTIR showed that the interactions between the silver nanoparticles and oxygen atoms of the hydroxyl groups of KGM became stronger with increasing amount of silver ions. In thermal gravimetric analysis (TGA), the pure KGM film had 47 % loss of weight at 333.3 °C, whereas there were two weight lost peaks for the nanocomposite: first at 213.4 °C with 20 % loss of weight and the second one at 334 °C with 40 % loss of weight.

Lu and Xiao [72] studied the structure and properties of nanocomposites made from CMKGM and MMT. TEM showed that MMT dispersion in CMKGM was mainly in the intercalated state and depended on the CMKGM/MMT weight ratio. At 5 wt% MMT, most MMT layers existed as tactoids; however, some intercalation was seen. At 15 wt% MMT, there were still some tactoids, exfoliation was observed a little; in some parts, MMT layers were separated by ultrathin CMKGM, and intercalation was seen clearly. Pure MMT had a sharp XRD peak at $2\theta = 7.1°$, corresponding to a basal spacing of 1.25 nm. All diffraction peaks of

nanocomposites shifted toward lower angle values and became broad. XRD and DSC provided evidence that low loading of MMT promoted KGM crystallization. According to FTIR, hydrogen bonds were formed between KGM and the hydroxyl groups in the silicate layer of MMT. The thermal stability of the nanocomposites, studied with TGA, was improved by the addition of MMT. That was due to thermal resistance of MMT and the nanodispersion of MMT layers in the CMKGM matrix. Another aspect was the strong hydrogen bond interaction between MMT and CMKGM. MMT acted as physical crosslinking sites to retard the thermal decomposition of CMKGM to a certain extent. The tensile strength, elongation at break, and Young's modulus of the nanocomposites were enhanced with the increase of the MMT content, and the maximum values were observed at 15 wt% MMT content. The degree of swelling of the nanocomposite films became higher than that of pure CMKGM in weak acidic solution and was also highest at 15 wt% MMT. The nanocomposite films of CMKGM/MMT were considered to have potential application as water storage materials with good thermal and mechanical properties.

Nanocomposite films of KGM and cadmium sulfide (CdS) were prepared by one-step synthesis in order to create stealthy materials e.g. for military applications [73]. SEM and TEM indicated that hexagonal CdS nanoparticles with the sizes of 10–100 nm were evenly dispersed in KGM. FTIR showed evidences of chelations of Cd^{2+} to the hydroxyl groups of KGM. Infrared emissivity values of the samples were carried out on an infrared emissometer and the results indicated that both KGM and CdS nanoparticles had high emissivity, but that of KGM/CdS nanocomposite film was much lower. That could be attributed to the KGM wrapping on the surface of CdS nanoparticles. Strong synergism effect existed also between KGM/chitosan and CdS particles, as detected by the low infrared emissivity value [74].

CNW were added to GGM- and KGM-based films to form reinforced nanocomposites [75]. The incorporation of CNW interestingly changed the visual appearance of mannan films indicating interactions between mannan and cellulose. In KGM-based films, the formation of fiber like structures with lengths of several millimeters was induced. In GGM-based films, rodlike structures with lengths of several tens of micrometers were formed. However, XRD study showed that the degree of mannan crystallinity was not significantly increased by the addition of CNW and so increase in crystallinity could not be responsible for the formation of the fibrous structures. Polarizing optical microscopy suggested that the formation of the structures was due to reorganization of crystalline components in the films. Unexpectedly, the remarkable differences in the film structure did not indicate great changes in the thermal and mechanical properties of the films. Glycerol was used as plasticizer and it seemed to have accumulated in the CNW-matrix interface [75]. Addition of CNW did not affect the WVP of sorbitol-plasticized GGM films, but somewhat decreased the WVP of KGM films at 0/54 % RH [60]. The use of CNW did not significantly affect the OP or light transmittance of GGM- or KGM-based films, but slightly increased the haze of films.

In contrast to CNW, microfibrillated cellulose (MFC) was able to improve the mechanical performance of GGM-based films [76]. Two levels of added MFC

were studied, namely 5 wt% and 15 %. The lower level of MFC addition did not affect the tensile properties of the films, but 15 % MFC clearly increased the tensile strength and Young's modulus of the films. The preparation and analysis of films from GGM with 15 % MFC was successful with low plasticizer content (10 % glycerol). XRD analysis revealed that GGM in the films was semicrystalline (ca. 20–25 %), i.e. there were regions of very small GGM crystallites surrounded by amorphous regions. In the nanocomposite film with 15 % MFC, the diffraction intensity of cellulose was fitted in order to eliminate the effect of the cellulose on the calculation of GGM crystallinity. The addition of MFC did not induce the crystallization of GGM in the films, but on the other hand, the increase in glycerol content of films seemed to cause a small increase in the mannan crystallinity. The MFC preparation seemed to contain cellulose fiber residues, visualised as large polarizing structures with polarizing OM. The glass transition temperature (T_g), determined with the dielectric analysis (DEA), increased with the addition of MFC indicating a decrease in the macromolecular mobility in the presence of MFC. The moisture-induced softening behaviour of the films was studied using moisture-scanning DMA. Moisture clearly acted as a plasticizer for GGM, which was evident from the decrease in storage modulus. The composite film with 15 % MFC showed lower degree of softening than the pure GGM film.

9.7 Applications

The aim in developing xylan- or mannan-based blends, composites, or nanocomposites has usually been to create environmentally friendly biodegradable materials, such as packaging films to replace conventional synthetic packaging. Some researchers have also considered mannans as potential raw materials for edible films [59], e.g. coatings for fruit [35, 50, 52] or edible inner packagings for instant noodles, instant coffee, instant tea, and instant milk powder [46]. Selectively antibacterial films have also been developed [44, 53, 56]. Materials that swell in water but do not dissolve are called hydrogels [29, 30] and could be used for pharmaceutical and biomedical applications such as contact lenses, wound dressings, artificial organs, and delivery carriers for bioactive reagents [77]. Konjac glucomannan-based nanocomposites with low infrared emissivity have also been prepared in order to develop stealthy materials for military purposes [73, 74].

9.8 Conclusions

Hemicelluloses are abundant natural raw materials that have great potential but currently not enough industrial applications. In this chapter, the use of two most common hemicelluloses, namely xylans and mannans, as components of polymer blends, composites, and nanocomposites, was reviewed. Plant gum mannans were

also included due to their chemical similarity to hemicelluloses. Xylans were blended with other natural polymers, while mannan-based blends were prepared with polysaccharides, proteins, and synthetic polymers. Nanocomposites were made by mixing xylans and mannans with nanosized cellulose or inorganic nanoparticles. In some cases, blending with other polymers was necessary to obtain cohesive self-standing films from hemicelluloses. Often, the hydrophilic character of xylans and mannans enabled the formation of homogeneous blends and strong hydrogen bonding between the blended polymers or with the nanoparticles. The polymers usually had an optimal blend ratio at which the mechanical properties of the films reached a maximum. The addition of cellulose nanowhiskers increased the tensile strength of oat spelt arabinoxylan -based films. Spruce galactoglucomannan –based films were greatly reinforced by micro fibrillated cellulose. The effect of hemicellulose content on the water vapour barrier properties of films depended on the film composition. Spruce galactoglucomannan—based films were generally considered as good oxygen barriers and the oxygen barrier properties of oat spelt arabinoxylan –based films were greatly improved by the addition of cellulose nanowhiskers. Blending xylans and mannans with other polymers or making nanocomposites enlarges the number of potential applications of these polysaccharides.

Acknowledgments Prof. Maija Tenkanen (University of Helsinki, Finland) is thanked for careful reading and commenting this manuscript and Dr. Kirsti Parikka for drawing the chemical structures presented in Figs. 9.1 and 9.2. The Academy of Finland is acknowledged for financial support through the Wood Wisdom-Net Programme (BioPack project).

References

1. Glasser, W.G., Kaar, W.E., Jain, R.K., Sealey, J.E.: Isolation options for non-cellulosic heteropolysaccharide (HetPS). Cellulose **7**, 299–317 (2000)
2. Willför, S., Rehn, P., Sundberg, A., Sundberg, K., Holmbom, B.: Recovery of water-soluble acetylgalactoglucomannans from mechanical pulp of spruce. Tappi J. **2**, 27–32 (2003)
3. Willför, S., Sundberg, K., Tenkanen, M., Holmbom, B.: Spruce derived mannans—A potential raw material for hydrocolloids and novel advanced natural materials. Carbohydr. Polym. **72**, 197–210 (2008)
4. Klemm, D., Schmauder, H.-P., Heinze, T.: Cellulose. In: Vandamme, E.J., De Baets, S., Steinbüchel, A. (eds.) Biopolymers, vol. 6, pp. 275–319. Wiley, Germany (2002). (Polysaccharides II. Polysaccharides from Eukaryotes)
5. Aspinall, G.O.: Structural chemistry of the hemicelluloses. Adv. Carbohydr. Chem. **14**, 429–468 (1959)
6. Dea, I.C.M., Morrison, A.: Chemistry and interactions of seed galactomannans. Adv. Carbohydr. Chem. Biochem. **31**, 241–312 (1975)
7. Takigami, S.: Konjac mannan. In: Phillips, G.O., Williams, P.A. (eds.) Handbook of Hydrocolloids, pp. 413–424. Woodhead Publishing, Cambridge (2000)
8. Eberingerová, A., Heinze, T.: Naturally occurring xylans structures, isolation procedures and properties. Macromol. Rapid Commun. **21**, 542–556 (2000)
9. Izydorczyk, M.S., Biliaderis, C.G.: Cereal arabinoxylanase: advances in structure and physicochemical properties. Carbohydr. Polym. **28**, 33–48 (1995)

10. Lawther, J.M., Sun, R.C., Banks, W.B.: Extraction, fractionation, and characterization of structural polysaccharides from wheat straw. J. Agric. Food Chem. **43**, 667–675 (1995)
11. Sjöström, E.: Wood Chemistry Fundamentals and Applications. Academic Press, Inc, San Diego (1993)
12. Timell, T.E.: Recent progress in the chemistry of wood hemicelluloses. Wood Sci. Technol. **1**, 45–70 (1967)
13. Dierckx, S., Dewettinck, K.: Seed gums. In: De Baets, S., Vandamme, E.J., Steinbüchel, A. (eds.) Biopolymers (Polysaccharides II. Polysaccharides from Eukaryotes), vol. 6, pp. 322–340. Wiley-VCH Verlag GmbH, Weinheim (2002)
14. Neukom, H.: Galactomannans: properties and applications. LWT Food Sci. Technol. **22**, 41–45 (1989)
15. Nishinari, K., Williams, P.A., Phillips, G.O.: Review of the physico-chemical characteristics and properties of konjac mannan. Food Hydrocolloids **6**, 199–222 (1992)
16. Buckeridge, M.S., Dietrich, S.M.C., Lima, D.U.: Galactomannans as the reserve carbohydrate in legume seeds. In: Gupta, A.K., Kaur, N. (eds.) Carbohydrate reserves in plants—synthesis and regulation, pp. 283–316. Elsevier, Amsterdam (2000)
17. Sandhu, J.S., Hudson, G.J., Kennedy, J.F.: The gel nature and structure of the carbohydrate of Ispaghula husk *ex Plantago ovata* forsk. Carbohydr. Res. **93**, 247–259 (1981)
18. Stephen, A.M.: Other plant polysaccharides. In: Aspinall, G.O. (ed.) The Polysaccharides, pp. 97–193. Academic, New York (1983)
19. Robyt, J.F.: Essentials of Carbohydrate Chemistry. Springer, New York (1998)
20. Fredon, E., Granet, R., Zerrouki, R., Krausz, P., Saulnier, L., Thibault, J.F., Rosier, J., Petit, C.: Hydrophobic films from maize bran hemicelluloses. Carbohydr. Polym. **49**, 1–12 (2002)
21. Sun, R.C., Sun, X.F., Tomkinson, J.: Hemicelluloses and their derivatives. In: Gatenholm, P., Tenkanen, M. (eds.) Hemicelluloses: Science and Technology, ACS Symposium Series 864, pp. 2–22. American Chemical Society, Washington (2004)
22. Daas, P.J.H., Schols, H.A., Jongh, H.H.J.: On the galactosyl distribution of commercial galactomannans. Carbohydr. Res. **329**, 609–619 (2000)
23. Baker, C.W., Whistler, R.L.: Distribution of D-galactosyl groups in guaran and locust-bean gum. Carbohydr. Res. **45**, 237–243 (1975)
24. Tenkanen, M., Makkonen, M., Perttula, M., Viikari, L., Teleman, A.: Action of *Trichoderma reesei* mannanase on galactoglucomannan in pine kraft pulp. J. Biotechnol. **57**, 191–204 (1997)
25. Fincher, G.B., Stone, B.A.: Cell walls and their components in cereal grain technology. In: Pomeranz, Y. (ed.) Advances in Cereal Science and Technology, American Association of Cereal Chemists Inc., St Paul, pp. 207–295 (1986)
26. Alén, R.: Structure and chemical composition of wood. In: Stenius, P. (ed.) Forest Products Chemistry, pp. 12–57. Fapet Oy, Helsinki (2000)
27. Fang, J.M., Sun, R.C., Fowler, P., Tomkinson, J., Hill, C.A.S.: Esterification of wheat straw hemicelluloses in the N, N–dimethylformamide/lithium cloride homogeneous system. J. Appl. Polym. Sci. **74**, 2301–2311 (1999)
28. Tenkanen, M.: Enzymatic tailoring of hemicelluloses. In: Gatenholm, P., Tenkanen, M. (eds.) Hemicelluloses: Science and Technology, ACS Symposium Series 864, American Chemical Society, Washington, pp. 292–311 (2004)
29. Gabrielii, I., Gatenholm, P.: Preparation and properties of hydrogels based on hemicelluloses. J. Appl. Polym. Sci. **69**, 1661–1667 (1998)
30. Gabrielii, I., Gatenholm, P., Glasser, W.G., Jain, R.K., Kenne, L.: Separation, characterization and hydrogel-formation of hemicellulose from aspen wood. Carbohydr. Polym. **43**, 367–374 (2000)
31. Kayserilioğlu, B.Ş., Bakir, U., Yilmaz, L., Akkaş, N.: Use of xylan, an agricultural by-product, in wheat gluten based biodegradable films: mechanical, solubility and water vapour transfer rate properties. Bioresour. Technol. **87**, 239–246 (2003)

32. Phan, D., Debeaufort, F., Voilley, A., Luu, D.: Biopolymer interactions affect the functional properties of edible films based on agar, cassava starch and arabinoxylan blends. J. Food Eng. **90**, 548–558 (2009)
33. Ye, X., Kennedy, J.F., Li, B., Xie, B.J.: Condensed state structure and biocompatibility of the konjac glucomannan/chitosan blend films. Carbohydr. Polym. **64**, 532–538 (2006)
34. Jia, D., Fang, Y., Yao, K.: Water vapour barrier and mechanical properties of konjac glucomannan-chitosan-soy protein isolate edible films. Food Bioprod. Process. **87**, 7–10 (2009)
35. Xiao, C., Gao, S., Zhang, L.: Blend films from konjac glucomannan and sodium alginate solutions and their preservative effect. J. Appl. Polym. Sci. **77**, 617–626 (2000)
36. Xiao, C., Weng, L., Zhang, L.: Improvement of physical properties of crosslinked alginate and carboxymethyl konjac glucomannan blend films. J. Appl. Polym. Sci. **84**, 2554–2560 (2002)
37. Wang, B., Jia, D.-Y., Ruan, S.-Q., Qin, S.: Structure and properties of collagen-konjac glucomannan-sodium alginate blend films. J. Appl. Polym. Sci. **106**, 327–332 (2007)
38. Xiao, C., Lu, Y., Liu, H., Zhang, L.: Preparation and characterization of konjac glucomannan and sodium carboxymethylcellulose blend films. J. Appl. Polym. Sci. **80**, 26–31 (2001)
39. Cheng, L.H., Karim, A.A., Norziah, M.H., Seow, C.C.: Modification of the microstructural and physical properties of konjac glucomannan-based films by alkali and sodium carboxymethylcellulose. Food Res. Int. **35**, 829–836 (2002)
40. Cheng, L.H., Karim, A.A., Seow, C.C.: Characterisation of composite films made of konjac glucomannan (KGM), carboxymethyl cellulose (CMC) and lipid. Food Chem. **107**, 411–418 (2008)
41. Yu, Z., Jiang, Y., Zou, W., Duan, J., Xiong, X.: Preparation and characterization of cellulose and konjac glucomannan blend film from ionic liquid. J. Polym. Sci., Part B: Polym. Phys. **47**, 1686–1694 (2009)
42. Li, Q., Qi, W., Su, R., He, Z.: Preparation and characterization of enzyme-modified konjac glucomannan/xanthan blend films. J. Biomater. Sci. **20**, 299–310 (2009)
43. Chen, J., Liu, C., Chen, Y., Chen, Y., Chang, P.R.: Structural characterization and properties of starch/konjac glucomannan blend films. Carbohydr. Polym. **74**, 946–952 (2008)
44. Xu, X., Li, B., Kennedy, J.F., Xie, B.J., Huang, M.: Characterization of konjac glucomannan–gellan gum blend films and their suitability for release of nisin incorporated therein. Carbohydr. Polym. **70**, 192–197 (2007)
45. Xiao, C., Lu, Y., Gao, S., Zhang, L.: Characterization of konjac glucomannan–gelatine blend films. J. Appl. Polym. Sci. **79**, 1596–1602 (2000)
46. Li, B., Kennedy, J.F., Jiang, Q.G., Xie, B.J.: Quick dissolvable, edible and heat sealable blend films based on konjac glucomannan—gelatin. Food Res. Int. **39**, 544–549 (2006)
47. Sothornvit, R., Chollakup, R.: Properties of sericin-glucomannan composite films. Int. J. Food Sci. Technol. **44**, 1395–1400 (2009)
48. Xiao, C., Liu, H., Gao, S., Zhang, L.: Characterization of poly(vinyl alcohol)—konjac glucomannan blend films. J. Macromol. Sci. Part A Pure Appl. Chem. **37**, 1009–1021 (2000)
49. Li, B., Xie, B.: Synthesis and characterization of konjac glucomannan/poly(vinyl alcohol) interpenetrating polymer networks. J. Appl. Polym. Sci. **93**, 2775–2780 (2004)
50. Xiao, C., Liu, H., Lu, Y., Zhang, L.: Characterization of poly(vinylpyrrolidone)—konjac glucomannan blend films. J. Appl. Polym. Sci. **81**, 1049–1055 (2001)
51. Liu, C., Xiao, C.: Characterization of konjac glucomannan—quaternized poly(4-vinyl-*N*-butyl) pyridine blend films and their preservation effect. J. Appl. Polym. Sci. **93**, 1868–1875 (2004)
52. Yang, G., Huang, Q., Zhang, L., Zhou, J., Gao, S.: Miscibility and properties of blend materials from waterborne polyurethane and carboxymethyl konjac glucomannan. J. Appl. Polym. Sci. **92**, 77–83 (2004)
53. Lu, J., Zhang, J., Xiao, C.: Preparation and characterization of konjac glucomannan/poly(diallydimethylammonium chloride) blend films. J. Appl. Polym. Sci. **106**, 1972–1981 (2007)

54. Lu, J., Wang, X., Xiao, C.: Preparation and characterization of konjac glucomannan/poly(diallydimethylammonium chloride) antibacterial blend films. Carbohydr. Polym. **73**, 427–437 (2008)
55. Kim, J.K., Jo, C., Park, H.J., Byun, M.W.: Effect of gamma irradiation on the physicochemical properties of a starch-based film. Food Hydrocolloids **22**, 248–254 (2008)
56. Rao, M.S., Kanatt, S.R., Chawla, S.P., Sharme, A.: Chitosan and guar gum composite films: Preparation, physical, mechanical and antimicrobial properties. Carbohydr. Polym. **82**, 1243–1247 (2010)
57. Hartman, J., Albertsson, A.-C., Söderqvist Lindblad, M., Sjöberg, J.: Oxygen barrier materials from renewable sources: Material properties of softwood hemicellulose-based films. J. Appl. Polym. Sci. **100**, 2985–2991 (2006)
58. Hartman, J., Albertsson, A.-C., Sjöberg, J.: Surface- and bulk-modified galactoglucomannan hemicellulose films and film laminates for versatile oxygen barriers. Biomacromolecules **7**, 1983–1989 (2006)
59. Mikkonen, K.S., Yadav, M.P., Cooke, P., Willför, S., Hicks, K.B., Tenkanen, M.: Films from spruce galactoglucomannan blended with poly(vinyl alcohol), corn arabinoxylan, and konjac glucomannan. BioResources **3**, 178–191 (2008)
60. Mikkonen, K.S., Heikkilä, M.I., Helén, H., Hyvönen, L., Tenkanen, M.: Spruce galactoglucomannan films show promising barrier properties. Carbohydr. Polym. **79**, 1107–1112 (2010)
61. Edlund, U., Ryberg, Y.Z., Albertsson, A.-C.: Barrier films from renewable forestry waste. Biomacromolecules **11**, 2532–2538 (2010)
62. Zhu Ryberg, Y.Z., Edlund, U., Albertsson, A.-C.: Conceptual approach to renewable barrier film design based on wood hydrolysate. Biomacromolecules **12**, 1355–1362 (2011)
63. Dammström, S., Salmén, L., Gatenholm, P.: The effect of moisture on the dynamical mechanical properties of bacterial cellulose/glucuronoxylan nano composites. Polymer **46**, 10364–10371 (2005)
64. Dammström, S., Salmén, L., Gatenholm, P.: On the interactions between cellulose and xylan, a biomimetic simulation of the hardwood cell wall. BioResources **4**, 3–14 (2009)
65. Saxena, A., Elder, T.J., Pan, S., Ragauskas, A.J.: Novel noncellulosic xylan composite film. Compos. Part B **40**, 727–730 (2009)
66. Saxena, A., Ragauskas, A.J.: Water transmission barrier properties of biodegradable films based on cellulosic whiskers and xylan. Carbohydr. Polym. **78**, 357–360 (2009)
67. Saxena, A., Elder, T.J., Kenvin, J., Ragauskas, A.J.: High oxygen nano composite barrier films based on xylan and nano crystalline cellulose. Nano-Micro Lett. **2**, 235–241 (2010)
68. Saxena, A., Elder, T.J., Ragauskas, A.J.: Moisture barrier properties of xylan composite films. Carbohydr. Polym. **84**, 1371–1377 (2011)
69. Viota, J.L., Lopez-Viota, M., Saake, B., Stana-Kleinschek, K., Delgado, A.V.: Organoclay particles as reinforcing agents in polysaccharide films. J. Colloid Interface Sci. **347**, 74–78 (2010)
70. Stevanic, J.S., Joly, C., Mikkonen, K.S., Pirkkalainen, K., Serimaa, R., Rémond, C., Toriz, G., Gatenholm, P., Tenkanen, M., Salmén, L.: Bacterial nano cellulose-reinforced arabinoxylan films. J. Appl. Polym. Sci. **122**, 1030–1039 (2011)
71. Tian, D., Hu, W., Zheng, Z., Liu, H., Xie, H.-Q.: Study on in situ synthesis of konjac glucomannan/silver nano composites via photochemical reduction. J. Appl. Polym. Sci. **100**, 1323–1327 (2006)
72. Lu, J., Xiao, C.: Preparation and characterization of carboxymethyl konjac glucomannan/sodium montmorillonite hybrid films. J. Appl. Polym. Sci. **103**, 2954–2961 (2007)
73. Zhang, F.-Y., Zhou, Y.-M., Cao, Y., Chen, J.: Preparation and characterization of KGM/CdS nanocomposite film with low infrared emissivity. Mater. Lett. **61**, 4811–4814 (2007)
74. Zhang, F.-Y., Zhou, Y.-M., Sun, Y.-Q., Chen, J., Ye, X.-Y., Huang, J.-Y.: Preparation and characterization of chitosan/konjac glucomannan/CdS nano composite film with low infrared emissivity. Mater. Res. Bull. **45**, 859–862 (2010)

75. Mikkonen, K.S., Mathew, A.P., Pirkkalainen, K., Serimaa, R., Xu, C., Willför, S., Oksman, K., Tenkanen, M.: Glucomannan composite films with cellulose nano whiskers. Cellulose **17**, 69–81 (2010)
76. Mikkonen, K.S., Stevanic, J.S., Joly, C., Dole, P., Pirkkalainen, K., Serimaa, R., Salmén, L., Tenkanen, M.: Composite films from spruce galactoglucomannans with micro fibrillated spruce wood cellulose. Cellulose **18**, 713–726 (2011)
77. Yu, H., Lu, J., Xiao, C.: Preparation and properties of novel hydro gels from oxidized konjac glucomannan cross-linked chitosan for in vitro drug delivery. Macromol. Biosci. **7**, 1100–1111 (2007)

Chapter 10
Bacterial Nanocellulose for Medical Implants

Bibin Mathew Cherian, Alcides Lopes Leão, Sivoney Ferreira de Souza, Gabriel Molina de Olyveira, Ligia Maria Manzine Costa, Cláudia Valéria Seullner Brandão and Suresh S. Narine

Abstract Bacterial cellulose (BC) has established to be a remarkably versatile biomaterial and can be used in wide variety of applied scientific endeavours, especially for medical devices. In fact, biomedical devices recently have gained a significant amount of attention because of an increased interest in tissue-engineered products for both wound care and the regeneration of damaged or diseased organs. Due to its unique nanostructure and properties, microbial cellulose is a natural candidate for numerous medical and tissue-engineered applications. Hydrophilic bacterial cellulose fibers of an average diameter of 50 nm are produced by the bacterium *Acetobacter xylinum*, using a fermentation process. The microbial cellulose fiber has a high degree of crystallinity. Using direct nanomechanical measurement, determined that these fibers are very strong and when used in combination with other biocompatible materials, produce nanocomposites particularly suitable for use in human and veterinary medicine. Moreover, the nanostructure and morphological similarities with collagen make BC attractive for cell immobilization and

B. M. Cherian (✉) · A. L. Leão
Department of Natural Resources, School of Agricultural Sciences, São Paulo State University (UNESP), Botucatu, SP 18610-307, Brazil
e-mail: bmcherian@gmail.com

S. F. de Souza · G. M. de Olyveira · L. M. M. Costa
Department of Nanoscience and Advanced Materials, Universidade Federal do ABC (UFABC), Santo André, SP 09210-170, Brazil

C. V. S. Brandão
Department of Veterinary Surgery and Anesthesiology, School of Veterinary Medicine and Animal Science, São Paulo State University (UNESP), Botucatu, SP 18618-000, Brazil

S. S. Narine
Trent Center for Biomaterials Research, Departments of Physics & Astronomy and Chemistry, Trent University, 1600 West Bank Drive Peterborough, Ontario K9J 7B8, Canada

S. Thomas et al. (eds.), *Advances in Natural Polymers*,
Advanced Structured Materials 18, DOI: 10.1007/978-3-642-20940-6_10,

cell support. The architecture of BC materials can be engineered over length scales ranging from nano to macro by controlling the biofabrication process. The chapter describes the fundamentals, purification and morphological investigation of bacterial cellulose. This chapter deals with the modification of microbial cellulose and how to increase the compatibility between cellulosic surfaces and a variety of plastic materials. Furthermore, provides deep knowledge of fascinating current and future applications of bacterial cellulose and their nanocomposites especially in the medical field, materials with properties closely mimic that of biological organs and tissues were described.

10.1 Introduction

Nanocellulose, such as that produced by the bacteria *Gluconacetobacter xylinus* (bacterial cellulose, BC), is an emerging biomaterial with great potential in several applications. The performance of bacterial cellulose stems from its high purity, ultra-fine network structure and high mechanical properties in dry state [1]. This feature allows its applications in scaffold for tissue regeneration, medical applications and nanocomposites. A few studies have used bacterial cellulose mats to reinforce polymeric matrices and scaffolds with wound healing properties. These advances are reviewed and prospects with future development in these areas are proposed.

BC is pure cellulose made by bacterial fabrication via biochemical steps and self-assembling of the secreted cellulose fibrils in the medium. Shaping of BC materials in the culture medium can be controlled by the type of cultivation and kind of bioreactor and then it obtained BC hydrogel or BC in dry state by methods like freeze-drying [1].

Although chemically identical to plant cellulose, the cellulose synthesized by bacterial has a fibrillar nanostructure which determines its physical and mechanical properties, characteristics which are necessary for modern medicine and biomedical research [2, 3]. In this book chapter, the structural features of microbial cellulose and its properties are discussed in relation to the current and future of its application in medicine.

10.2 Bacterial Cellulose

10.2.1 Bacterial Cellulose Synthesis

Cellulose is found in groups of microorganisms like fungi, bacteria, and algae. In green algae, cellulose, xylan, or mannan may serve as structural cell wall polysaccharides. Cellulose is found, although in small quantities, in all of the brown

algae (Phaeophyta), most of the red algae (Rhodophyta), and most of the golden algae (Chrysophyta (Chrysophytes)). It was also reported to be present in some fungi, forming inner cell wall layer [4].

Microbial cellulose is an exopolysaccharide produced by various species of bacteria, such as those of the genera *Gluconacetobacter* (formerly *Acetobacter*), *Agrobacterium*, *Aerobacter*, *Achromobacter*, *Azotobacter*, *Rhizobium*, *Sarcina*, and *Salmonella* [5].

Many Gram-negative bacteria secrete extracellular polysaccharide material, but only a few have been shown to produce cellulose. *A. xylinum*, the most studied of bacterial cellulose producers, is a Gram-negative, aerobic, rod-shaped organism [6].

A. xylinum has been applied as model microorganism for basic and applied studies on cellulose. It is most commonly studied source of bacterial cellulose because of its ability to produce relatively high levels of polymer from a wide range of carbon and nitrogen sources [5].

The bacteria consume the sugar or carbohydrate from fruits as their main food. BC is formed on the air–liquid medium interface when the HS liquid medium (noted by Hestrin and Schramm [7], consisting of D-glucose, peptone, yeast extract, disodium phosphate, citric acid) and distilled water is inoculated with a strain of *Acetobacter xylinum*. Glucose functions as the bacteria's carbon source, peptone as a nitrogen source, yeast extract as a vitamin source and citric acid and disodium phosphate as a buffer system for the medium. The bacterium increases its population by consuming the glucose and oxygen initially dissolved in the liquid medium. When the oxygen has diminished, only the bacteria with access to air can continue their BC-producing activity. The bacteria below the surface are considered dormant, but can be reactivated by using the liquid as inoculums for a new culture medium [8].

Cellulose synthesis by *Acetobacter* is a complex process and involves (a) the polymerization of glucose residues into linear β-1,4-glucan chains, (b) the extracellular secretion of these linear chains, and (c) crystallization of the glucan chains into hierarchically composed ribbons [2].

Acetobacter xylinum produces two forms of cellulose: (1) cellulose I, the ribbon-like polymer, and (2) cellulose II, the thermodynamically more stable amorphous polymer [9]. They can be divided according to their morphological localization as: intracellular polysaccharides located inside, or as part of the cytoplasmic membrane; cell wall polysaccharides forming a structural part of the cell wall; and extracellular polysaccharides located outside the cell wall. Extracellular polysaccharides occur in two forms: loose slime, which is non-adherent to the cell and imparts a sticky consistency to bacterial growth on a solid medium or an increased viscosity in a liquid medium; and microcapsules or capsules, which adhere to the cell wall.

The differences in the assembly of cellulose I and cellulose II outside the cytoplasmic membrane are described in Fig. 10.1.

Microfibrillar structure of bacterial cellulose is responsible for most of its properties such as high tensile strength, higher degree of polymerization and crystallinity index.

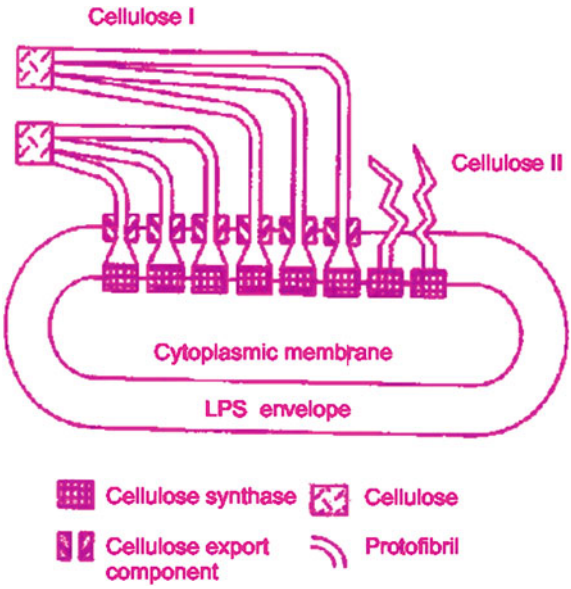

Fig. 10.1 Assembly of cellulose microfibrils by *A. xylinum* [9]

10.2.1.1 Cellulose Biosynthesis

Cellulose is a linear homopolysaccharides which consists of glucose (D-glucopyranose) linked by glycosidic β (1-4). In this connection, the hydroxyl at C-1 (anomeric carbon) of one molecule of glucose is in the β conformation and reacts with the hydroxyl at C-4 of the second molecule.

The size of the cellulose molecule is normally expressed in terms of their degree polymerization (DP), i.e, the number of anhydroglucose units present in a chain. However, the conformational analysis of cellulose indicates that cellobiose (4-O-α-D-glucopyranosyl-α-D-glucopyranose, Fig. 10.2a) is its basic structural unit [10]. The conformation of the repeating unit of cellulose can be explained if we consider the model proposed for the biosynthesis of glucose [11].

The active site of the enzyme cellulose synthase, responsible for the synthesis of cellulose, contains two consecutive sites of binding to uridine-diphosphoglucose precursor (UDP-glucose, Fig. 10.2b), positioned at 180° from each other, and a binding site the non-reducing end of β-glucan (Fig. 10.3). The hydroxyl at C-5 of glucose residues linked to these sites are activated by a mechanism of general base catalysis by promoting the dephosphorylation of UDP-glucose units and establishing new links β (1-4). The resulting β-glucan and had little affinity binding sites for UDP-glucose, moves to a better place, the binding site for β-glucan. Two new units of UDP-glucose can then be added, continuing the synthesis.

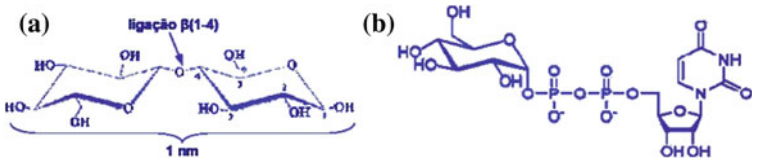

Fig. 10.2 **a** Cellobiose. **b** UDP- Glucose [11]

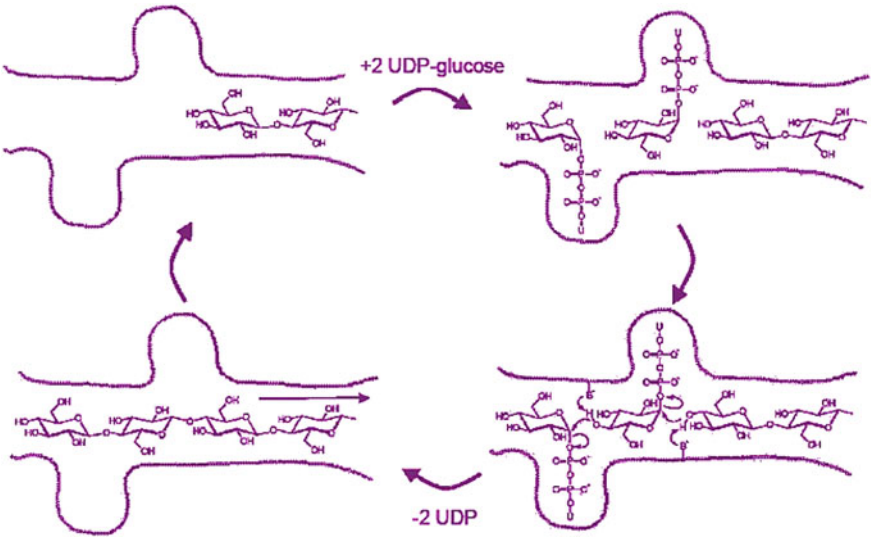

Fig. 10.3 Cellulose biosynthesis [11]

Hydroxyls present in the structure of cellulose are distributed equatorially in a quasi-planar arrangement that allows the formation of a linear chain, in which adjacent chains are aligned to form crystalline structures stabilized by hydrogen bonds inter-and intramolecular [12]. These links lead to a crystalline structure compact and extremely stable having on its surface hydrophilic, but hydrophobic inside, which makes cellulose insoluble in water. Thermodynamic limitations on the growth of these structures make occur, alternating with these crystalline regions, amorphous regions where the molecules are randomly distributed [11]. The process includes the formation of UDP-Glucose, which is the precursor in the formation of cellulose, followed by glucose polymerization into the β (1-4) glucan chain and a nascent chain which forms ribbon-like structure of cellulose chains formed by hundreds or even thousands of individual cellulose chains, their extrusion outside the cell, and self-assembly into fibrils.

Pathways and mechanisms of uridine diphosphoglucose (UDP-Glucose) synthesis are relatively well known, whereas molecular mechanisms of glucose polymerization into long and unbranched chains still need exploring.

10.2.1.2 Fermentative Production and Purification

There are several factors that affecting cellulose production like growth medium, environmental conditions and byproducts. Generally, medium containing high carbon between others (often nitrogen) is favourable for polysaccharide production. Conversion of 60–80 % of the utilized carbon source into biopolymers is commonly found in high yielding polysaccharide fermentations.

The optimal design of the medium is very important for the growth of a microorganism. Nutrients required for the growth of a microorganism are carbon, nitrogen, phosphorus, sulphur, potassium and magnesium salts.

Effect of Components

The fermentation medium contains carbon, nitrogen and other macro- and micronutrients required for the growth of organism. Secretion of bacterial cellulose is usually most noticeable when the bacteria are supplied with an abundant carbon source and minimal nitrogen source [13]. Some authors uses a complex medium supplying amino acids and vitamins is also used to enhance the cell growth and production.

Usually, glucose and sucrose are used as carbon sources for cellulose production, although other carbohydrates such as fructose, maltose, xylose, starch and glycerol have also been tried. The effect of initial glucose concentration on cellulose production is also important, since the formation of gluconic acid as a byproduct in the medium decreases the pH of the culture and ultimately decreases the production of cellulose. Cellulose yields at initial glucose concentrations of 6, 12, 24 and 48 g/L were studied, and the consumption of glucose was found to be 100, 100, 68 and 28 % of the initial concentration, respectively [14].

Nitrogen is a main component of proteins necessary in cell metabolism, and comprises 8–14 % of the dry cell mass of bacteria. The effect of various nitrogen sources on the production of bacterial cellulose has been reported; casein hydrolyzate gave yield of 5 g/L, and peptone gave yield of 4.8 g/L of cellulose in *A. xylinum* [13]. The addition of extra nitrogen favours the biomass production, but diminishes cellulose pr oduction.

The addition of precursor molecules is of considerable importance in the polysaccharide synthesis in terms of metabolic driving. Amino acids have been used by some researchers as a nitrogen source or as a stimulator for improving biopolymer yield [15]. Methionine has an important effect on the cellulose production by *Acetobacter xylinum* ssp. *sucrofermentans*, accounting alone for 90 % of cell growth and cellulose production [16]. Nicotinamide has also been found to be important for cellulose production. Evaluation of nicotinamide in the fraction range of 0.00001–0.00008 % showed that maximal bacterial cellulose production was at 0.00005 % [13]. Besides of these factors, microorganisms respond rapidly to environmental changes in many aspects such as induction and repression of protein synthesis, and changes in cell morphology. The main environmental

parameters of interest are pH, temperature, dissolved oxygen, as well as stirrer speed in fermentative process.

Purification

The microbial cellulose obtained after fermentation is not pure; it contains some impurities like cells and/or the medium components. The fermented medium has to be purified to obtain pure cellulose. The most widely used process of purification of bacterial cellulose in the culture medium is the treatment with alkali (sodium hydroxide or potassium hydroxide), organic acids like acetic acid or repeated washing of the mixtures with reverse osmosis water or hot water for a period of time. The above purification steps can be used alone or in combination [17]. Bacterial cellulose containing entrapped cells was treated with solutions like NaOH/KOH/Na_2CO_3 at 100 °C for 15–20 min to kill the cells; thereafter the solution was filtered using an aspirator to remove the dissolved materials. The filter was repeatedly washed with distilled water until the pH of the filtrate became neutral. The dry mass of bacterial cellulose without any microbial cells was measured after drying for 4–6 h. As such, the dry cell mass was considered to be the difference between the mass of the dried bacterial cellulose containing the cells and the dried bacterial cellulose after the treatment with NaOH [18, 19]. The culture medium was treated with acetic acid after the addition of NaOH solution for neutralization and then with distilled water [20]. The cells can be treated with aqueous solution of SDS and washed with aqueous NaOH, followed by neutralization with acetic acid or by repeated washing with distilled water and then drying in the air or at 60–80 °C to a constant mass [21]. Medical application of bacterial cellulose requires special procedure to remove bacterial cells and toxins. One of the most effective protocols is gentle processing of cellulose pellicle between absorbent sheets to expel about 80 % of the liquid phase and then immersing the mat in 3 % NaOH for 12 h. This procedure is repeated 3 times and after that the pellicle is incubated in 3 % HCl solution, pressed and thoroughly washed in distilled water. The purified pellicle is sterilized in autoclave.

Modification of BC

Alterations of BC morphology during its biogenesis investigate various polymers to the facet of cellulose formation whether in plant cell wall or in BC (see Table 10.1). As miscible polymers such as hemicelluloses, cellulose derivatives and dyes are added into the BC-producing bacterium growth medium, the aggregation of nanofibers is altered due to the competitive adsorption of polymers in the medium. Polymerization and crystallization are separate mechanisms in BC biogenesis [22]. Therefore, subsequent to BC polymerization, the polymer added in the medium can associate and co-crystallize with BC, producing an intimately blended composite material. The modification of bacterial cells is another way to

Table 10.1 Modification of BC biogenesis

Modification BC growth medium with:	Resulting properties or modification (when compared to pure BC)
Hemicellulose	
Xylogincan	–Crystallite size of fibrils changed
	–Aggregation of fibrillar units into ribbon assemblies broke down
	–Lower stiffness or breaking stress
	–Increased extensibility in uniaxial tension
Xylan	–Ribbons were coherent, heavy bundles instead of flat and twisting
	–Ribbon width decreased as aggregation of fibril subunits was controlled
Pectin	–Increased extensibility and decreased breaking stress compared to pure BC
Phosphomannan	–Fibrils are oriented in parallel
	–Aggregation time of fibrils is delayed
Glucomannan, galactomannan	–Induced coalescence of fibrils and dramatic reduction of crystallinity
Other Hemicellulosic polysaccharides: glucuronoxylan, arabinogalactan	–Crystallinity of BC was modified
Celulose derivatives	
Carboxymethyl Cellulose (CMC)	–In vivo cellulose ribbon formation prevented normal fasciation of fibril bundles into a typical ribbon
	–Thinner ribbon width and smaller crystallite fibril size
	–Aggregates and pellicle show birefringence, and contain crossed, superimposed layers of cellulose fibrils oriented in parallel
	–Less resistant to stress
Cellulose derivatives (hydroxyethylcellulose, methylcellulose)	–In vivo cellulose ribbon formation was altered
	–Fibril size was modified, and diameter was thinner
Dyes	
Calcofluor White ST	–Morphology of BC is changed by preventing assembly of fibrils prohibiting crystallization, but BC is crystalline when dried
Congo Red	–Formation of the ribbon was prevented
Tinopal	–Support van der Waals force as initial step in cellulose crystallization
Antibiotics	
Nalidixic acid, chloramphenicol	–Elongates *A. xylinum* cells producing thicker, larger BC ribbons
Theinamycin, mecillinam	–Shortened *A. xylinum* cells producing thicker BC ribbons

alter BC morphology. However, this research concentrates on using miscible polymer to alter BC biogenesis. Manipulating BC biogenesis can be a useful approach for fine-tuning BC properties to appropriate applications or for producing BC composites with tailored characteristics. A few researchers have undertaken this approach, including Ciechanska [23], who fabricated modified BC by growing it in a chitosan-modified growth medium for wound dressing application, and Seifert et al. [24], who produced modified BC in a carboxymethylcellulose-, methylcellulose- and poly(vinyl alcohol)-modified medium to produce water-content-controlled BC for medically useful biomaterials. Biogenesis manipulation can produce BC composites of nanoscale polymer interaction, given that BC fibrils and polymer can co-crystallize during ribbon formation and the fact that ribbon dimensions are in the nano scales. Moreover, the composites produced will have dispersed BC fibrils, as aggregation of the fibrils is controlled, which reduces dispersion (the major challenge in composite fabrication) [25].

Bodin et al. obtained BC tubes with different shapes and sizes depending on the product requirements, which has made BC interesting to be explored for use in other biomedical applications such as bone graft material and a scaffold for tissue engineering of cartilage and blood vessels [26]. Beyond controlling the size and shape of the BC, the microscopic morphology can also be changed in several ways. A high oxygen ratio during static cultivation has been shown by both Watanabe and Yamanaka [27] and Hult et al. [28] to increase the density and subsequently the toughness of the BC membrane. Shaking velocities and the addition of dyes has further been shown to have a profound effect on the aggregating of the sub-elementary microfibrils, thereby reducing the crystallinity of the BC network [29, 30]. Different structures of BC obviously affect its mechanical properties as well as cell attachment into the material. Tang et al. [31] obtained BC mats with different pore size and porosities changed fermentation conditions (cultivation time and inoculation volume) and post-treatment methods (alkali treatment and drying methods). Backdahl et al. [32] produced a novel method to introduce microporosity in BC tubes intended as scaffolds for tissue-engineered blood vessels, by placing paraffin wax and starch particles of various sizes in a growing culture of *Acetobacter xylinum,* bacterial cellulose scaffolds of different morphologies and interconnectivity were prepared. Paraffin particles were incorporated throughout the scaffold, while starch particles were found only in the outermost area of the resulting scaffold.

10.3 Properties of Bacterial Cellulose

Microbial cellulose possesses high crystallinity, high tensile strength, and extreme insolubility in most of the solvents, moldability and high degree of polymerization. The thickness of cellulose fibrils is generally 0.1–10 mm, one hundred times thinner than that of cellulose fibrils obtained from plants with good shape retention [33]. The biopolymer degrades at higher temperatures (>300 °C), although the alkali-treated

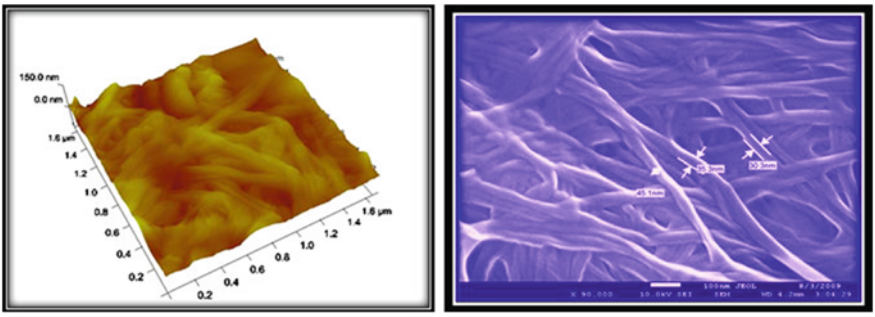

Fig. 10.4 AFM and SEM images from Nanoskin®

cellulose membrane is more stable (between 343 and 370 °C). Composites prepared by adding bacterial cellulose increase mechanical properties like bending strength and Young modulus [34, 35]. The mechanical properties of cellulose are due to the uniqueness of uniform nanoscale network structure, which is oriented bi-dimensionally when compressed. Its water holding capacity is over 100 times (by mass) higher. Figure 10.4 shows AFM and SEM images from Nanoskin®—Bacterial Cellulose produced by Innovatećs—Biotechnology Research and Development.

10.4 Surface Modification of Bacterial Cellulose and Nanocomposites of Bacterial Cellulose

Organic polymers have interesting properties such as flexibility, low density, high hardness, excellent mechanical and optical properties such as transparency and high refractive index. So arrays are attractive for the preparation of novel composites [36]. From this point of view, cellulose is emerging as a promising material. This polysaccharide is relatively inert compared to many solvents, has high mechanical properties, good heat resistance, low density, biodegradable, and is the most abundant natural polymer on earth [37, 38]. Natural fibers of cellulose present morphology of nanometer order. This morphology allows relatively simple methods, environmentally friendly, low cost, which can lead to formation of sophisticated nanostructures [39].

Composites of natural cellulosic fibers may have the best option to the array because the nanofibers can interact with other natural materials to form highly ordered structures. The cellulose microfibrils have hydroxyl groups (OH) on their surface, which can form covalent bonds with the matrix. In literature, three alternative routes for the preparation of composites of cellulose are known [40]. The first route refers to the incorporation of hydrophobic fibers in matrices such as polyethylene, polypropylene and polystyrene. In this case, it is necessary to a chemical or physical treatment, so that the surfaces of the matrix and the fibers

become compatible. The second route consists in the preparation of composite materials where the cellulose fibers act as reinforcement material. It relies on the introduction of polymerizable alkenes on the fiber surface. A third route for preparation of composites of cellulose targets the coupling between the matrix and fiber. In this case it uses a matrix reactive as hydroxypropyl cellulose (HPC) that are coupled leading to the formation of urethane or ester. Finally, a last approach that has been commonly used consists of solvent casting BC and a polymer solution into solid shapes. There is in the literature numerous papers involving the production of cellulose composite materials. Hutchens and collaborators published patent involving composite bacterial cellulose for application as biomaterial. They bacterial cellulose incubated in a solution of sodium hydrogen phosphate and calcium chloride in later. Through X-ray diffraction confirmed the incorporation of calcium and phosphate in the bacterial cellulose [41]. Bacterial cellulose has shown very promising characteristics for reinforcement material for composites with optical functions. Recently a paper entitled: "optically transparent composites reinforced with bacterial cellulose nanofibers, which showed the characteristics of the composite formed, such as transparency and low coefficient of expansion, are due primarily to networks of chains of semicrystalline materials nanofibers produced by the bacterium *Acetobacter xylinum*" [42]. Ifuku et al. obtained acetylated BC sheets to enhance the properties of optically transparent composites of acrylic resin reinforced with the nanofibers [43].

Narkato et al. produced bacterial cellulose composites with excellent mechanical strength of cellulose membranes impregnated in phenolic resin at a pressure of 100 MPa. The authors credited these results to the tapes that have uniform size, are extremely thin and are packaged in cellulose microfibrils arranged linearly [43]. Campos and colleagues have prepared and characterized niobium oxide coated cellulose fiber. The authors showed a possible increase in the degree of crystallinity of the composite Nb_2O_5/cellulose by reacting the reagent with the precursor amorphous phase of cellulose fibers [44]. The synthesis and application of new materials for electromagnetic devices could be observed in the article: "cellulose fibers coated with metals for use in composites technology for microwave applications". Based on the cellulose fibers in metallic materials, the authors obtained robust, lightweight, simple to obtain and inexpensive. The composites show interesting dielectric properties and good conductivity [45]. An alternative route for the preparation of composites of bacterial cellulose has been the sol-gel method. In the literature some papers have been generated. Kemell et al. used a sol-gel method to prepare composites of photocatalytic cellulose/TiO_2. In this study, they used atomic layer deposition (ALD), combining the benefits of surface sol-gel technique and by chemical vapor deposition (CVD) [39].

Zhang and Qi synthesized hybrid bacterial cellulose/titania. They obtained mesoporous Titania networks consisting of nanowires, using as a "template" bacterial cellulose membrane. The network obtained shows Titania photocatalytic activity [46]. Composites of cellulose acetate/silica were obtained by sol-gel method [47]. Tanaka and Kozuka precipitated silica by acid catalysis of tetraethyl orthosilicate (TEOS). The composites of cellulose acetate/silica showed

micrometer particles of silica dispersed on the cellulose fibers, exhibited a plastic-elastic character, excellent for cutting and manufacturing, with low processing cost. Yano and colleagues [36] have prepared hybrid organic/inorganic hydroxypropyl cellulose (HPC) and silica through sol-gel process. Presented a simple method of mixing organic polymer (HPC) with metal alkoxides, for example, TEOS.

Hybrids derived from sol-gel process are developed for practical applications such as coatings, contact lenses and nonlinear optics, electrochromic materials and electroconductivity [36]. Persson recently appealed to the sol-gel method for the mineralization of wood and wood pulp. In his thesis entitled "Strategies for modification of cellulose fiber, wood samples and wood pulp were immersed in silicon alkoxide and subsequently characterized by various techniques. It was observed that silica is distributed on the surface and compacted by the cellulose fibrils [48]. Simonsen et al. [49] developed a bio nanocomposites based on thermoplastic starch and bacterial cellulose nanofibers. The bacterial cellulose was obtained from *Acetobacter xylinum* cultures. Cassava starch and glicerol were used for the production of thermoplastic starch films. X-ray diffractometry of the films showed the development of starch crystallinity induced by the fibers, which may contribute to improve mechanical properties. Electron scanning microscopy of the disrupted films showed good adhesion between fiber and matrix and good dispersion of the nanofibers. Hisano [50] developed a new biocomposites based on hydrated BC membranes and PU resins were prepared. An improvement of the interface between the BC and the PU resin was obtained from solvent exchange process. Results obtained by FTIR revealed the presence of main bands of urethane bond and disubstituted urea in the biocomposites. Additionally, the observed reduction of the hydroxyl band (3,500 cm^{-1}) suggests an interaction between the BC and the NCO-free groups in the resin. The biocomposites presented a non-crystalline character, while the thermal characterization indicates a significant increase in the glass transition temperature. Mixing of a polymer solution and a BC suspension followed by solvent casting is another common method to prepare BC nanocomposites. Due to the synthesis and nature of thermoplastic polymers, this approach has been more common for preparing BC/thermoplastic nanocomposites and has involved both natural and synthetic polymers.

Stokke and Groom [51] prepare the BC/xylans nanocomposites consisted of first homogenizing the bacterial cellulose in a blender after which the xylan solutions were added in different ratios and the blends were allowed to interact for 30 min and solution casted. Xylans were found to aggregate on BC to produce a laminated structure. Besides, the incorporation of xylans in the composites reduced the tensile strength of homogenized bacterial cellulose from ca 110 to 65 MPa in nanocomposites containing 50 % xylans. However, Young modulus increased from ca 4 GP to 6.5 Gpa when the xylan content increased to 30 % after which the modulus was found to decrease again. Chitosan, has also been used in several works to create BC/chitosan nanocomposites. While it has been shown that incorporation of chitosan in the culture medium of bacterial cellulose leads to

the incorporation of N-acetyl glucosamide into the cellulose chain, other studies [52, 53] have shown that true nanocomposites can be formed by immersing a purified BC pellicle in a chitosan solution followed by solvent casting. The resulting nanocomposites were considered ideal for wound dressing applications. Chitosan lowered the mechanical properties of the membrane from a tensile strength of 74–54 MPa while elongation at break increased from 6.8 to 7.4 %. Hutchens et al. [54], by incubation cycles of alternating layers of nanocellulose in solutions of calcium and phosphate, demonstrated that the combination of hydroxyapatite, and bacterial nanocellulose provides a framework that allows the formation of organized deficient calcium hydroxyapatite (CDHAP). The application of this structure in bone defects showed promising because CDHAP promoted new bone formation, demonstrating the potential of this biomaterial.

Proteins have also been used in combination with bacterial cellulose to develop high mechanical strength double hydrogels or dry nanocomposites [55, 56]. While bacterial cellulose in the wet state has high tensile properties, its compressive properties are low limiting its utilization in various biomedical applications. Nakayama et al. [56] have immersed a purified BC pellicle in a gelatin solution after which it was chemically crosslinked. The resulting bacterial cellulose mats combined the tensile properties of BC with very high compressive strength. The gelatin did not affect the crystalline structure of BC. The compressive modulus was 1.7 MPa, that is over 200 times higher than that of BC alone. The fracture strength of the BC/gelatin network was also very largely improved compared to that of the gelatin gel alone, being 30 times higher. Jung et al. [57] evaluated composites of silk fibroin and BC in the dry and in the wet state. Silk protein, a mixture of glycine, alanine and serine, can take various conformations, amorphous and crystalline, and has generated interest in the biomedical field as membranes due to its biocompatibility, permeability in the wet state and high mechanical properties. BC/silk fibroin nanocomposites was prepared by immersing a purified and never dried bacterial cellulose pellicle into aqueous silk fibroin solution (8 wt %) and then drying the nanocomposites into films. The morphology changed from a mostly amorphous coil structure to a crystalline structure as a β-sheet structure as demonstrated by X-ray diffraction and FTIR spectroscopy.

As a result the mechanical properties of the nanocomposites differed from those of the pure silk protein or bacterial cellulose films. In the dry state, the tensile modulus of the composite film (465 $\pm$ 57 MPa) was higher than that of the neat BC film (118 $\pm$ 9 MPa) or silk fibroin film (355 $\pm$ 56 MPa). However, the composite films were more brittle than the silk fibroin film. On the other hand, in the hydrated state, the composite was tougher and more flexible with an elongation at break reaching 13.5 $\pm$ 2.9 % but exhibited very low tensile strength and modulus. Tomé et al. [58] produced a modified bacterial cellulose membranes with tailored properties, regarding their surface and barrier properties. It was prepared by controlled heterogeneous esterification with hexanoyl chloride.

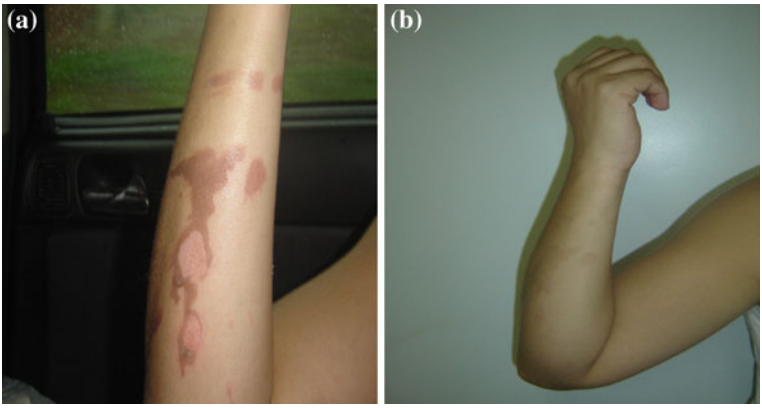

Fig. 10.5 Burns second degree, after 7 days was completely healing with treatment using Nanoskin®

10.5 Medical Application of Bacterial Cellulose

10.5.1 Human Medicine

Bacterial Cellulose mats is very effective in promoting autolytic debridement, reducing pain, and accelerating granulation, all of which are important for proper wound healing. These nanobiocellulose membranes can be created in any shape and size, which is beneficial for the treatment of large and difficult to cover areas of the body.

Bacterial Cellulose has been shown to be a highly effective wound dressing material. In fact, the results of burns, diabetic ulcer, healing process can be show in Figs. 10.5 and 10.6a,b. The biomedical applications of BC include meniscus replacements (pig meniscus on the left, BC meniscus on the right), artificial blood vessels and wound dressing for skin healing [12, 20, 21] (Fig. 10.7).

Figure 10.8a shows the 6 mm BC graft which has been retrieved after 4 weeks used as an infrarenal aortic bypass. There were no problems with mechanical performance of the graft. There was no leakage and no mechanical rupture which show that the BC tube provides sufficient mechanical properties to be used as vascular graft. The tube was cut open longitudinal and there was no sign of thrombosis. The internal surface of lumen of BC looked very smooth and had a nice single layer of cells as seen in the histology section, Fig. 10.8b. This indicates that the smooth inner layer of BC produced in the vertical bioreactor described in this study is advantageous with regards to performance as vascular graft.

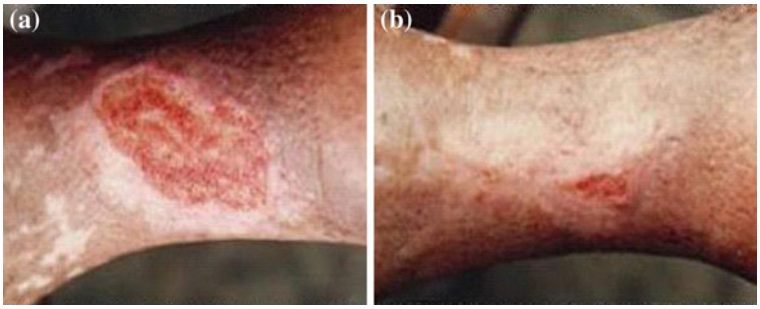

Fig. 10.6 Diabetic Ulcer varicose treatment using Nanoskin®. After 3 months we can see the completely healing

Fig. 10.7 Examples of biomedical applications of BC are meniscus replacements (pig meniscus on the *left*, BC meniscus on the *right*), artificial blood vessels and wound dressing for skin healing [76–78]. Nanocellulose (bacterial cellulose, BC), such as that produced by Acetobacter xylinum, has shown promising results as a replacement material for small diameter vascular grafts (Fig. 10.8). These BC tubes have been tested in a pig model as an infrarenal aortic bypass and show promising results for use as vascular grafts in the future

10.5.2 Veterinary Medicine

Biosynthetic membranes show good acceptance by the body, protecting and aiding the repair of damaged areas by selective permeability, and prevent contamination by microorganisms [59, 60]. The biosynthetic membrane based on cellulose was used in experiments in dogs trochleoplasty, not interfering in biomechanics and even in the intra-articular [61]. Moreover, it accelerated the initial repair of the trochleoplasty area, showing good integration of newly formed tissue with the adjacent cartilage. However, as a single part, is not effective to promote complete regeneration of articular cartilage [61]. According to Helenius et al. [62], the cellulose membrane obtained from bacteria has good compatibility and has promising potential for use in tissue engineering.

The cellulose membrane showed slight fibrotic reaction when used as a substitute for dura mater in dogs [63], and therefore to be considered suitable material for dural graft. The analysis of these histological features suggests that cellulose is degraded in the animal organism by biochemical process to clarify. The finding of refractile particles of cellulose in the cytoplasm of giant cells in mice implanted

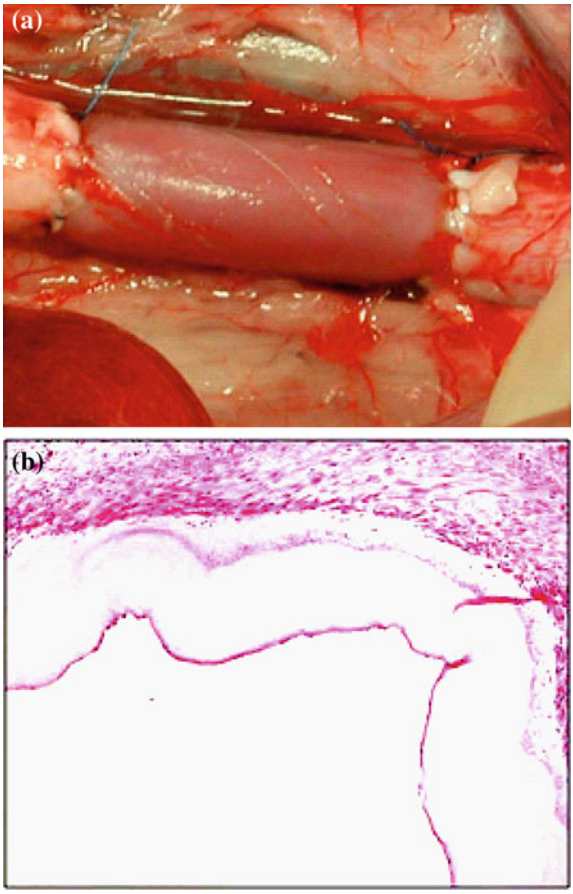

Fig. 10.8 **a** A 6 mm BC graft as an infrarenal aortic bypass. **b** Routine histology showing a nice single layer of cells on the interior of the BC surface after 1 month implantation in the pig aorta [78]

with cellulose in the liver, suggested absorption of the material by phagocytosis [64]. In the study by Salata et al. [65], it was shown that the model of bone repair found in the group of cellulose membranes was predominantly endochondral ossification. In contrast, the membrane of poly-tetrafluoroethylene expanded (e-PTFE) induced bone formation directly (intramembranous ossification). The formation of cartilage during bone healing is regarded as the result of low oxygen tension in tissue. Sandberg et al. [66] observed areas of cartilage in experimental mandibular defects in rats, coated membrane. The presence of cartilage may be due to low oxygen tension generated by the sealing of the periosteal blood supply.

Salata et al. [65] concluded that due to the presence of severe inflammation, probably due to biodegradation of the membrane, the requirements for the accumulation of morphogenetic protein, were not found with the use of cellulose membrane. All these effects combined can lead to the formation of cartilage instead of bone deposition directly in the defects covered with membrane. The results of this study suggest the possibility of (GTR) of cartilage tissue, which has

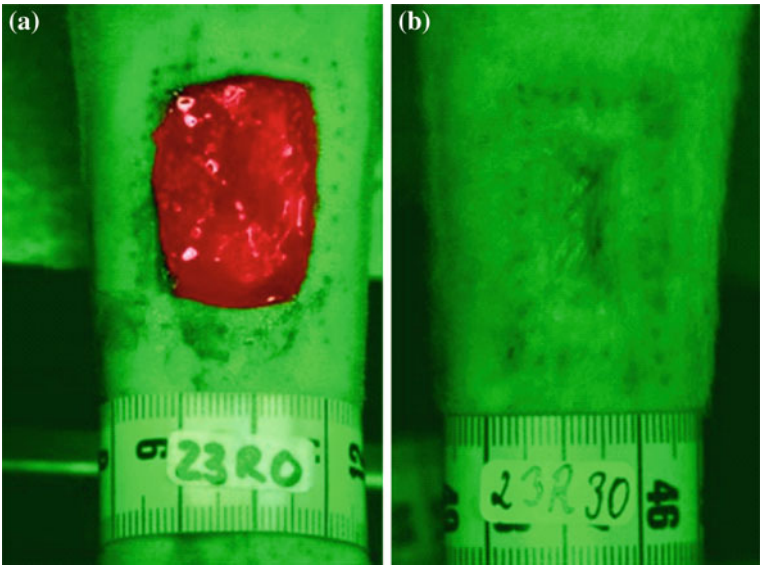

Fig. 10.9 Wound healing of sheep. **a** Fresh artificial wound (day 0). **b** Wound area after treatment with BC dressing (day 30)

limited capacity for repair after injury. Svensson et al. [67] developed a study to assess the potential of the cellulose membrane in the repair of cartilage in vitro, observing a significant increase of viable chondrocytes.

The cellulose membrane was applied in trochleoplasty experimental dogs proved to be clinically feasible, since it did not affect the biomechanics and even in the intra-articular [61]. Furthermore, the membrane accelerated the initial repair of the trochleoplasty area, showing good integration of newly formed tissue with the adjacent cartilage. However, the authors concluded that, as a single part, are not effective to promote complete regeneration of articular cartilage [61] but can be used as a framework for the introduction of cells or other chondrogenic factors.

The randomized study with sheep was the subject of a special animal experiment (Fig. 10.9). Comparable artificial wounds were created and the process of healing was controlled. In this way, the permeability to microorganisms, the extent of wound bleeding, and the characteristics (duration and degree) of the healing process were investigated [68]. In practice, further important aspects of BC are the focus of interest, concerning cooling of overtaxed muscles and particularly wound treatment of animals such as horses, sheep, cows, cats, and dogs. Extremely highly infected wounds are frequent in dogs after car crashes or similar accidents [69]. Furthermore, treatment of badly healing and permanent wounds, e.g., ulcers, and in the clinical and home-care sector both for human and veterinary medicine, as well as specific applications in tissue engineering will be major future developments.

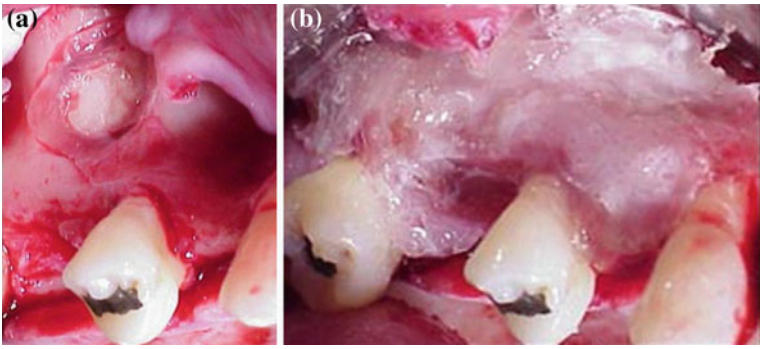

Fig. 10.10 Bacterial cellulose used in dental tissue regeneration in 38 year old male patient

10.5.3 Dental Medicine

Based on the results with artificial skin in burns or skin tissue loss, bacterial cellulose was tested in dental tissue regeneration. Microbial cellulose produced by the *Gluconacetobacter xylinus* strain, can be used to regenerate dental tissues in humans (Fig. 10.10). Nanocellulose product Gengiflex® and Gore-Tex® has intended applications within the dental industry. It was developed to aid periodontal tissue recovery [70]. A description was given of a complete restoration of an osseus defect around an IMZ implant in association with a Gengiflex® therapy. The benefits included the reestablishment of aesthetics and function of the mouth and that a reduced number of surgical steps were required. The bandage, called Gengiflex®, consists of two layers: the inner layer is composed of bacterial cellulose, which offers rigidity to the membrane, and the outer alkali-cellulose layer is chemically modified [71]. Salata et al. [72], in 1995, compared the biological performance of Gengiflex® and Gore-Tex® R membranes using the in vivo non-healing bone-defect model proposed by Dahlin et al. [73].

The study showed that Gore-Tex® membranes (a composite with polytetrafluoroethylene, urethane and nylon) were associated with significantly less inflammation and both membranes promoted the same amount of bone formation during the same period of time. A greater amount of bone formation was present in bone defects protected by either Gore-Tex® or bacterial cellulose membrane, when compared to the control sites. Gore-Tex® is better tolerated by the tissues than Gengiflex®. Recently, in a similar vein, Macedo et al. [74] also compared bacterial cellulose and polytetrafluoroethylene (PTFE) as physical barriers used to treat bone defects in guided tissue regeneration. In this study, two osseous defects (8 mm in diameter) were performed in each hind-foot of four adult rabbits, using surgical burs with constant sterile saline solution irrigation. The effects obtained on the right hind-feet were protected with PTFE barriers, while Gengiflex® membranes were used over wounds created in the left hind-feet. After 3 months, the histological evaluation of the treatments revealed that the defects covered with

PTFE barriers were completely repaired with bone tissue, whereas incomplete lamellar bone formation was detected in defects treated with Gengiflex® membranes, resulting in voids and lack of continuity of bone deposition. This demonstrated that the non-porous PTFE barrier is a more effective alternative to treat osseous defects than a bacterial cellulose membrane.

10.5.4 Conclusion

The aim of the chapter was to demonstrate the current state of research and development in the field of nanocelluloses especially in medical, dental and veterinary fields. Bacterial cellulose has proven to be a remarkably versatile biomaterial and can be used in a wide variety of biomedical devices. The extraordinary supramolecular nanofiber network structure and the resulting valuable properties have led to a real challenge and extensive global activity. The ultrafine 3-D BC network structure with its native unique properties is exploited for the synthesis of materials analogous to human and animal soft and hard tissues. It is the intention of this work to broaden knowledge in this subject area and stimulate the practical application of nanocelluloses in medicine. From the scientific and economic perspective, these innovative polymers, which are exciting examples of the large and significant biopolymer family of cellulosics, are on the threshold of a breakthrough that is also being driven by recent extraordinary activities in the field of nanosized materials.

References

1. Gatenholm, P., Klemm, D.: Bacterial nanocellulose as a renewable material for biomedical applications. MRS bulletin. **35**(3), 208–213 (2010)
2. Czaja, W.K., Young, D.J., Kawecki, M., Brown, R.M.Jr.: The future prospects of microbial cellulose in biomedical applications. Biomacromolecules, **8**(1), 1–12 (2007)
3. Shoda, M., Sugano, Y.: Recent advances in bacterial cellulose production. Biotechnol. Bioprocess Eng. **10**(1), 1–8 (2005)
4. Richmond, P.A.: Occurrence and Functions of Native Cellulose. In: Weimer, P.J., Haigler, C.H. (eds.) Biosynthesis and biodegradation of cellulose. Marcel Dekker, pp. 5–23. Inc. New York, USA (1991)
5. Bielecki, S., Krystynowicz, A., Turkiewicz, M., Kalinowska, H.: Bacterial cellulose. In: Steinbüchel, A., Rhee, S.K. (eds.) Polysaccharides and Polyamides in the Food Industry, pp. 31–85. Wiley- VCH Verlag, Weinheim (2005)
6. Ross, P., Mayer, R., Benziman, M.: Cellulose biosynthesis and function in bacteria. Microbiol. Mol. Biol. Rev. **55** (1), 35–58 (1991)
7. Puri, V.P.: Effect of crystallinity and degree of polymerization of cellulose on enzymatic saccharification. Biotechnol. Bioeng. **26**(10), 1219–1222 (1984)
8. Forng, E.R., Anderson, S.M., Cannon, R.E.: Synthetic medium for *Acetobacter xylinum* that can be used for isolation of auxotrophic mutants and study of cellulose biosynthesis. Appl. Environ. Microbiol. **55**(5), 1317–1319 (1989)

9. Iguchi, M., Yamanaka, S., Budhiono, A.: Bacterial cellulose—A masterpiece ofnature's arts. J. Mater. Sci. **35**, 261−270 (2000)
10. Fengel, D., Wegener, G.: Wood: chemistry, ultrastructure, reactions. Walter de Gruyter, Berlin (1989)
11. Koyama, M., Helbert, W., Imai, T., Sugiyama, J., Henrissat, B.: Parallel-up structure evidences the molecular directionality during biosynthesis of bacterial cellulose. Proc. Natl. Acad. Sci. USA **94**(17), 9091–9095 (1997)
12. Zugenmaier, P.: Conformation and packing of various crystalline cellulose fibers. Prog. Polym. Sci. **26**(9), 1341–1417 (2001)
13. Ramana, K.V., Tomar, A., Singh, L.: Effect of various carbon and nitrogen sources on cellulose synthesis by *Acetobacter xylinum*. World J. Microbiol. Biotechnol. **16**(3), 245–248 (2000)
14. Masaoka, S., Ohe, T., Sakota, N.: Production of cellulose from glucose by *Acetobacter xylinum*. J. Ferment. Bioeng. **75**(1), 18–22 (1993)
15. Son, H.J., Kim, H.G., Kim, K.K., Kim, H.S., Kim, Y.G., Lee, S.J.: Increased production of bacterial cellulose by *Acetobacter* sp. V6 in synthetic media under shaking culture conditions. Bioresour. Technol. **86**(3), 215–219 (2003)
16. Matsuoka, M., Tsuchida, T., Matsushita, K., Adachi, O., Yoshinaga, F.: A synthetic medium for bacterial cellulose production by *Acetobacter xylinum* subsp. *sucrofermentans*. Biosci. Biotechnol. Biochem. **60**(4), 575–579 (1996)
17. Kongruang, S.: Bacterial cellulose production by *Acetobacter xylinum* strains from agricultural waste products. Appl. Biochem. Biotechnol. **148**(1–3), 245–256 (2008)
18. De Wulf, P., Joris, K., Vandamme, E.J.: Improved cellulose formation by an *Acetobacter xylinum* mutant limited in (keto) gluconate synthesis. J. Chem. Technol. Biotechnol. **67**(4), 376–380 (1996)
19. Sakairi, N., Asano, H., Ogawa, M., Nishi, N., Tokura, S.: A method for direct harvest of bacterial cellulose filaments during continuous cultivation of *Acetobacter xylinum*. Carbohydr. Polym. **35**(3), 233–237 (1998)
20. Keshk, S.M.A.S., Sameshima, K.: Evaluation of different carbon sources for bacterial cellulose production. Afr. J. Biotechnol. **4**(6), 478–482 (2005)
21. Jung, J.Y., Park, J.K., Chang, H.N.: Bacterial cellulose production by *Gluconoacetobacter hansenii* in an agitated culture without living non-cellulose producing cells. Enzyme Microb. Technol. **37**(3), 347–354 (2005)
22. Haigler, C.H., White, A.R., Brown, R.M.: Alteration of in vivo cellulose ribbon assembly by carboxymethylcellulose and other cellulose derivatives. J. Cell Biol. **94**(1), 64–69 (1982)
23. Cienchanska, D.: Multifunctional bacterial cellulose/chitosan composite materials for medical applications. Fibres Text. East. Europe **12**(4), 69–72 (2004)
24. Seifert, M., Hesse, S., Kabrelian, V., Klemm, D.: Controlling the water content of never dried and reswollen bacterial cellulose by the addition of water-soluble polymers to the culture medium. J. Polym. Sci. Part A: Polym. Chem. **42**(3), 463–470 (2004)
25. Stell, G., Rikvold, P.A.: Polydispersity in fluids, dispersions, and composites; some theoretical results. Chem. Eng. Commun. **51**(1–6), 233–260 (1987)
26. Bodin, A., Bäckdahl, H., Fink, H., Gustafsson, L., Risberg, B., Gatenholm, P.: Influence of cultivation conditions on mechanical and morphological properties of bacterial cellulose tubes. Biotechnol. Bioeng. **97**(2), 425–434 (2007)
27. Watanabe, K., Yamanaka, S.: Effects of oxygen tension in the gaseous phase on production and physical properties of bacterial cellulose formed under static culture conditions. Biosci. Biotechnol. Biochem. **59**(1), 65–68 (1995)
28. Hult, E.-L., Yamanaka, S., Ishihara, M., Sugiyama, J.: Aggregation of ribbons in bacterial cellulose induced by high pressure incubation. Carbohyd. Polym. **53**(1), 9–14 (2003)
29. Watanabe, K., Tabuchi, M., Morinaga, Y., Yoshinaga, F.: Structural features and properties of bacterial cellulose produced in agitated-culture. Cellulose **5**(3), 187–200 (1998)
30. Haigler, C.H., Brown, R.M.Jr., Benziman, M.: Calcofluor White ST alters the in vivo assembly of cellulose microfibrils. Science **210**(4472), 903–906 (1980)

31. Tang, W., Jia, S., Jia, Y., Yang, H.: The influence of fermentation conditions and post-treatment methods on porosity of bacterial cellulose membrane. World J. Microbiol. Biotechnol. **26**(1), 125–131 (2010)
32. Bäckdahl, H., Esguerra, M., Delbro, D., Risberg, B., Gatenholm, P.: Engineering microporosity in bacterial cellulose scaffolds. J.Tissue Eng. Regen. Med. **2**(6), 320–330 (2008)
33. Schrecker, S.T., Gostomski, P.A.: Determining the water holding capacity of microbial cellulose. Biotechnol. Lett. **27**(19), 1435–1438 (2005)
34. Orts, W.J., Shey, J., Imam, S.H., Glenn, G.M., Guttman, M.E., Revol, J-F.: Application of cellulose microfibrils in polymer nanocomposites. J. Polym. Environ. **13**(4), 301–306 (2005)
35. Nakagaito, A.N., Iwamoto, S., Yano, H.: Bacterial cellulose: the ultimate nano-scalar cellulose morphology for the production of high-strength composites. Appl. Phys. A Mater. Sci. Process. **80**(1), 93–97 (2005)
36. Yano, S., Iwata, K., Kurita, K.: Physical properties and structure of organic-inorganic hybrid materials produced by sol-gel process. Mater. Sci. Eng. C **6**(2–3), 75–90 (1998)
37. Eichhorn, S.J., Baillie, C.A., Zafeiropoulos, N., Mwaikambo, L.Y., Ansell, M.P., Dufresne, A., Entwistle, K.M., Herrera-Franco, P.J., Escamilla, G.C., Groom, L., Hughes, M., Hill, C., Rials, T.G., Wild, P.M.: Current international research into cellulosic fibers and composites. J. Mater. Sci. **36**(9), 2107–2131 (2001)
38. Nishino, T., Matsuda, I., Hirao, K.: All cellulose composite. Macromolecules **37**(20), 7683–7687 (2004)
39. Kemell, M., Pore, V., Ritala, M., Leskelä, M., Lindén, M.: Atomic layer deposition in nanometer-level replication of cellulosic substances and preparation of photocatalytic TiO2/cellulose composites. J. Am. Chem. Soc. **127**(41), 14178–14179 (2005)
40. Borges, J.P., Godinho, M.H., Martins, A.F., Trindade, A.C., Belgacem, M.N.: Cellulose based-composite films. Mech. Compos. Mater. **37**(3), 257–264 (2001)
41. Hutchens, S. A., Woodward, J., Evans, B. R., O'neill, H. M.: Composite material. US n. 2004096.509, 15 Nov (2002)
42. Yano, H., Sugiyama, J., Nakagaito, A.N., Nogi, M., Matsuura, T., Hikita, M., Handa, K.: Optically transparent composites reinforced with networks of bacterial nanofibers. Adv. Mater. **17**(2), 153–155 (2005)
43. Ifuku, S., Nogi, M., Abe, K., Handa, K., Nakatsubo, F., Yano, H.: Surface modification of bacterial cellulose nanofibers for property enhancement of optically transparent composites: dependence on Acetyl-Group DS. Biomacromolecules **8**(6), 1973–1978 (2007)
44. Campos, E.A., Gushikem, Y., Gonçalves, M.C., Castro, S.C.: Preparation and characterization of niobium oxide coated cellulose fiber. J. Colloid Interface Sci. **180**(2), 453–459 (1996)
45. Zabetakis, D., Dinderman, M., Schoen, P.: Metal-coated fibers for use in composites applicable to microwave technology. Adv. Mater. **17**(6), 734–738 (2005)
46. Zhang, D., Qi, L.: Synthesis of mesoporous titania networks consisting of anatase nanowires by templating of bacterial cellulose membranes. Chem. Commun. **21**, 2735–2737 (2005)
47. Taneka, K., Kozuka, H.: Sol-gel preparation and mechanical properties of machinable cellulose/silica and polyvinylpyrrolidone/silica composites. J. Sol-Gel. Sci. Technol. **32**(1–3), 73–77 (2004)
48. Persson, P.: Strategies for cellulose fiber modification. 2004. Doctoral thesis (Doctor of Chemistry) Fiber- och polymerteknologi, Stockholm. Trita-FPT.**7**, 1–52 (2004)
49. Simonsen, J.: Bio-based nanocomposites: challenges and opportunities. Available: http://woodscience.oregonstate.edu/faculty/simonsen/Nanocomposites. Accessed: 19 mar (2007)
50. Hisano, C.: Desenvolvimento de materiais compósitos baseados em celulosebacteriana produzida por *Acetobacter xylinum*, 2006. Masters dissertation—Institute of Chemistry, São Paulo State University, Araraquara (2006)
51. Stokke, D.D., Groom, L.H.: Preparation and properties of cellulose/xylan nanocomposites. In: Dammström, S., Gatenholm, P. (ed.) Characterization of the cellulosic cell wall. Blackwell Publishing: pp. 53–66 (2008)

52. Hamlyn, P.F., Crighton, J., Dobb, M.G., Tasker, A.: Cellulose product. GB Patent 2314856, 14.01.1998 (1998)
53. Dubey, V., Pandey, L.K., Saxena, C.: Pervaporative separation of ethanol/water azeotrope using a novel chitosan-impregnated bacterial cellulose membrane and chitosan-poly (vinyl alcohol) blends. J. Membr. Sci. **251**(1–2), 131–136 (2005)
54. Hutchens, S.A., Benson, R.S., Evans, B.R., et al.: Biomimetic synthesis of calcium-deficient hydroxyapatite in a natural hydrogel. Biomaterials **27**(26), 4661–4670 (2006)
55. Gong, J.P., Katsuyama, Y., Kurokawa, T., Osada, Y.: Double-network hydrogels with extremely high mechanical strength. Adv. Mater. **15**(14), 1155–1158 (2003)
56. Nakayama, A., Kakugo, A., Gong, J.P., Osada, Y., Takai, M., Erata, T., Kawano, S.: High mechanical strength double-network hydrogel with bacterial cellulose. Adv. Funct. Mater. **14**(11), 1124–1128 (2004)
57. Jung, R., Jin, H.-J.: Preparations of silk fibroin/bacterial cellulose composite films and their mechanical properties. Key Eng. Mater. **342–343**, 741–744 (2007)
58. Tomé, L.C., Brandão, L., Mendes, A.M., Silvestre, A.J.D., Neto, C.P., Gandini, A., Freire, C.S.R., Marrucho, I.M.: Preparation and characterization of bacterial cellulose membranes with tailored surface and barrier properties. Cellulose **17**(6), 1203–1211 (2010)
59. Aslan, M., Simsek, G., Dayi, E.: Guided bone regeneration (GBR) on healing bone defects: a histological study in rabbits. J. Contemp. Dent. Pract. **5**(2), 114–123 (2004)
60. Carvalho, R.S., Nelson, D., Kelderman, H., Wise, R.: Guided bone regeneration to repair an osseous defect. Am. J. Orthod. Dentofacial Orthop. **123**(4), 455–467 (2003)
61. Iamaguti, L.S., Brandão, C.V.S., Pellizzon, C.H., Ranzani, J.J.T., Minto, B.W.: Histological and morphometric analysis for the use of a biosynthetic cellulose membrane in experimental trochleopasty. Pesq. Vet. Bras. **28**(4), 195–200 (2008)
62. Helenius, G., Bäckdahl, H, Bodin, A., Nannmark, U., Gatenholm, P., Risberg, B.: In vivo biocompatibility of bacterial cellulose. J. Biomed. Mater. Res. A. **76**(2), pp. 431–438 (2006)
63. Mello, L.R., Feltrin, L.T., Fontes Neto, P.T.L., Abreu, A.R.: Experimental study of byosinthetic cellulose to duraplasty and brain protection. Arq. Bras. Neurocirurg. **15**, 14–21 (1996)
64. Mello, L. R., Feltrin, Y., Selbach, R., Macedo Jr., G., Spautz, C., Haas, L.: J. Uso da cellulose liofilizada em lesões de nervos periféricos com perda de substância. Arq Neuro-Psiquiatr. **59**(2B), (2001)
65. Salata, L.A., Hatton, P.V., Devlin, A.J., Craig, G.T., Brook, I.M.: In Vitro and in vivo evaluation of e-PTFE and alkali-cellulose membranes for guided bone regeneration. Clin. Oral Implants **12**(1), 62–68 (2001)
66. Sandberg, E., Dahlin, C., Linde, A.: Bone regeneration by the osteopromotion technique using bioabsorbable membranes: an experimental study in rats. J. Oral Maxillofac. Surg. **51**(10), 1106–1114 (1993)
67. Svensson, A., Nicklasson, E., Harrah, T., Panilaitis, B., Kaplan, D.L., Brittberg, M., Gatenholm, P.: Bacterial cellulose as a potential scaffold for tissue engineering of cartilage. Biomaterials **26**(4), 419–431 (2005)
68. Cockbill: Evaluation in vivo and in vitro of the performance of interactive dressings in the management of animal soft tissue injuries. Vet. Dermatol. **9**(2):87–98 (1998)
69. Goodrich, L.R., Moll, H.D., Crisman, M.V., Lessard, P., Bigbie, R.B.: Comparison of equine amnion and a nonadherent wound dressing material for bandaging pinch-grafted wounds in ponies. Am. J. Vet. Res. **61**(3), 326–329 (2000)
70. Novaes, Jr. A.B.: Novaes AB.: Soft tissue management for primary closure in guided bone regeneration: surgical technique and case report. Int. J. Oral Maxillofac. Implants **12**(1), 84–87 (1997)
71. Novaes Jr. A.B., Novaes A.B.: IMZ implants placed into extraction sockets in association with membrane therapy (Gengiflex) and porous hydroxyapatite: A case report. Int. J. Oral Maxillofac. Implants, **7**(4), 536–540 (1992)

72. Salata, L.A., Craig, G.T., Brook, I.M.: Bone healing following the use of hydroxyapatite or ionomeric bone substitutes alone or combined with a guided bone regeneration technique: an animal study. Int. J. Oral Maxillofac. Implants. **13**(1), 44–51 (1998)
73. Dahlin, C., Linde, A., Gottlow, J., Nyman, S.: Healing of bone defects by guided tissue regeneration. Plast. Reconstr. Surg. **81**(5), 672–676 (1988)
74. Macedo N.L., Matuda F.S., de Macedo L.G.S., Monteiro A.S.F., Valera M.C., Carvalho Y.R.: Evaluation of two membranes in guided bone tissue regeneration: Histological study in rabbits. Braz. J. Oral Sci. **3**(8), 395–400 (2004)
75. Bodin, A., Concaro, S., Brittberg, M., Gatenholm, P.: Bacterial cellulose as a potential meniscus implant. J. Tissue Eng. Regen. Med. **1**(5), 406–408 (2007)
76. Johannesson, S.: GLP production in bioreactor and evaluation of cellulose grafts. CHALMERS Chemical and Biological Engineering. http://www.chalmers.se/chem/EN/divisions/biopolymer-technology/tissue-engineering/bbv-scientific-teams, visited 07/02/2011
77. Aung, B.J.: Does A New Cellulose Dressing Have Potential In Chronic Wounds? Podiatry Today **17**(3), 20–26 (2004)
78. Bäckdahl, H., Risbergb, B., Gatenholm, P.: Observations on bacterial cellulose tube formation for application as vascular graft. Mater Sci Eng C. **31**(1), 14–21 (2011)

Chapter 11
Polylactic Acid Based Blends, Composites and Nanocomposites

Azman Hassan, Harintharavimal Balakrishnan and Abozar Akbari

Abstract Biopolymers are expected to be an alternative for conventional plastics due to the limited resources and soaring petroleum price which will restrict the use of petroleum based plastics in the near future. PLA has attracted the attention of polymer scientist recently as a potential biopolymer to substitute the conventional petroleum based plastics. The chapter aims to highlight on the recent developments in preparation and characterization of PLA blends (biodegradable and non-biodegradable blends), PLA composites (natural fiber and mineral fillers) and PLA nanocomposites (PLA/montmorillonite, PLA/carbon nanotubes and PLA/cellulose nanowhiskers).

11.1 Introduction

Polylactic acid (PLA) has caught the attention of polymer scientist and proving to be a viable alternative biopolymer to petrochemical based plastics for many applications. PLA is produced from lactic acid, that is derived itself from the fermentation of corn or sugar beet and due to its biodegradation ability, PLA presents the major advantage to enter in the natural cycle implying its return to the biomass. The life-cycle of PLA is shown in Fig. 11.1.

It is known that agricultural raw materials such as sugarcane or corn can be used as basic materials in PLA production. However, waste biomass such as whey and cellulose waste can also be utilized. These basic materials will be transferred

A. Hassan (✉) · H. Balakrishnan · A. Akbari
Enhanced Polymer Research Group (EnPRO), Department of Polymer Engineering,
Faculty of Chemical Engineering, Universiti Teknologi Malaysia,
81300 Johor Bahru, Johor, Malaysia
e-mail: azmanh@cheme@utm.my

S. Thomas et al. (eds.), *Advances in Natural Polymers*,
Advanced Structured Materials 18, DOI: 10.1007/978-3-642-20940-6_11,

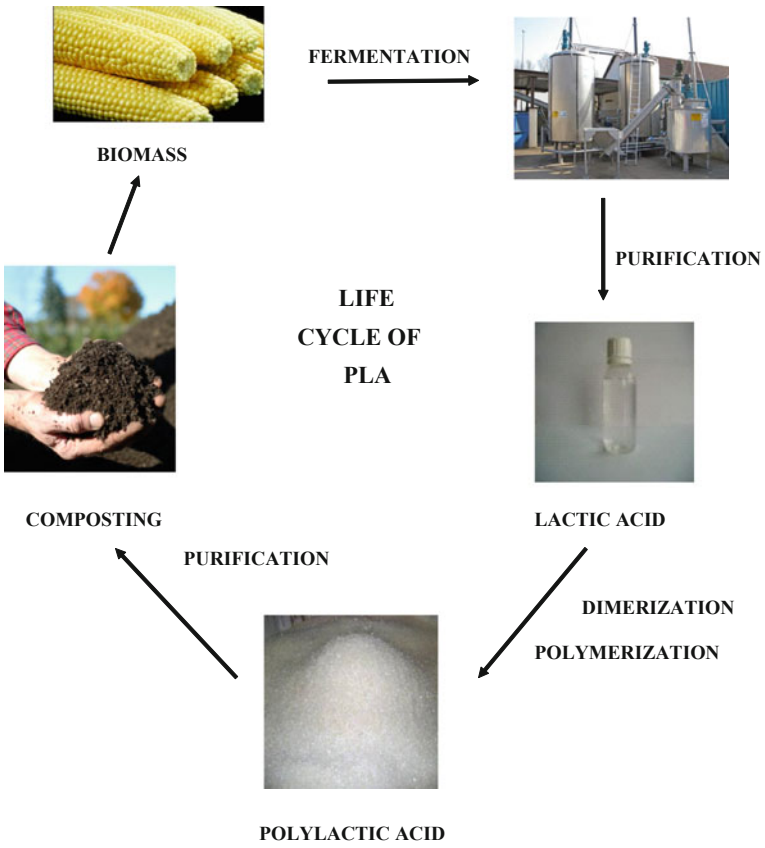

Fig. 11.1 Life cycle of PLA

by means of a bacterial fermentation process into lactic acid which is the basic monomer needed for PLA production. Lactic acid can then be altered into lactide, the cyclic dimer of lactic acid through a combined process of oligomerization and cyclization. Preparation of PLA can be conducted by (1) ring-opening polymerization (ROP) of the dehydrated ring-formed dimer or dilactide, (2) polycondensation and manipulation of the equilibrium between lactic acid and polylacide by removal of reaction water using drying agents, or (3) polycondensation and linking of lactic acid monomers. Due to the existence of a chiral carbon in lactic acid, the repeating unit of PLA can have two different configurations (D-(dextro) or L-(levo)) and the relative amount and distribution of these stereo-isomers influences various properties of the resulting PLA. In general, PLA built with L-stereoisomer monomer is referred to as poly(L-lactic acid) (PLLA), whereas, PLA which containing both D- and L-stereoisomer monomers is referred to as (PDLLA). The stereoisomers can be used as a great tool to verify the properties of

Table 11.1 Mechanical properties of PLA (material datasheet by Biomer for L9000)

Properties	Values
Young's Modulus (MPa)	3600
Tensile Strength (MPa)	70
Elongation at break (%)	2.4
Flexural Strength (N/mm^2)	98
Impact strength (kJ/m^2)	16.5
Notched impact strength (kJ/m^2)	3.3
MFI (g/10 min)	3–6
Density (g/cm^3)	1.25
Moisture absorption (%)	0.3

PLA to certain extend without the introduction of additives or other polymers. Although two general terms of polylactic acid and polylactide used to refer to PLA, the irony is, polylactides are prepared via ROP process while polylactic acid refers to PLA produced through polycondensation of lactic acid.

Recent researches in life cycle assessments (LCA) have also focused to enable PLA to find its place among traditional commodity polymers for many applications in the agricultural sector as well as in the packaging field (the food and non-food sector). It was found that PLA can be processed like all other thermoplastic polymers with extrusion, injection molding, blow molding, thermoforming or fiber spinning processes into various products.

The products can also be recycled after use for second time and they can even be hydrolyzed back into lactic acid which is the basic monomer. Nevertheless, the recycled lactic acid can be re-introduced into the polymerization process of PLA. The last possibility is to introduce PLA into the natural life cycle of all biomass where it degrades into carbon dioxide and water. Thus, the diversity of PLA becomes obvious as it can be recycled and also decomposed like all other organic matter. Besides that, it will do no harm if burned in an incineration plant or introduced into a classical waste management system (Jacobsen et al. [1]). The typical values of mechanical properties of PLA are displayed in Table 11.1.

Despite its origin form the nature, PLA's good stiffness and strength has enabled it to compete with other existing chemically based commodity plastics. Previous study on the mechanical properties of neat PLA by Jacobsen et al. [1] showed that PLA has great potential to be a substitute polymer for petroleum based plastics. The respective values of mechanical properties of PLA [2] with comparison of other petroleum based plastics e.g. polypropylene (PP) [3], polystyrene (PS) [4], high density polyethylene (HDPE) [5], polyamide (PA6) [6] shown in Fig. 11.2.

It can be observed from Fig. 11.2 that the elongation at break of PLA is lower than PS indeed, proving that it is more brittle than PS. Thus, although biopolymers such as PLA have great commercial potential to substitute conventional petroleum based polymers, but some of the properties such as brittleness and low heat distortion temperature had restrict their use in a wide-range of applications.

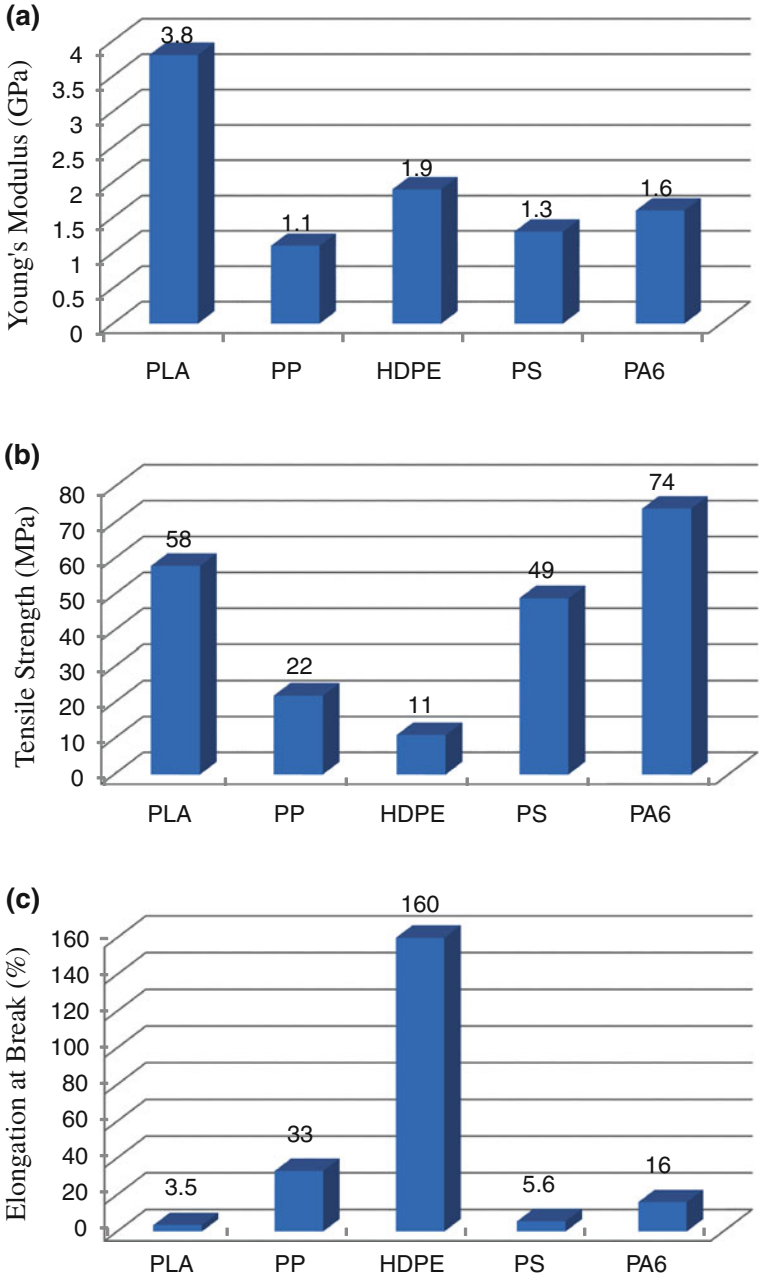

Fig. 11.2 Mechanical properties of PLA and other commodity plastics. **a** Young's modulus. **b** Tensile strength. **c** Elongation at break

Therefore, modification of these biopolymers through innovative technology is a formidable task for materials scientists.

11.1.1 Plasticized PLA

An improvement in terms of flexibility for PLA may widen its application as a biodegradable packaging and film material. The addition of plasticizers has been investigated lately in order to improve the fragility and increase the elongation of break or elasticity of PLA. Previous researchers have shown that addition of plasticizers such as polyethylene glycol (PEG), glucosemonoesters and partial fatty acid esters had successfully overcome the brittleness and widen PLA's application [2, 7, 8].

Jacobsen and Fritz [2] had studied on the introduction of plasticizers such as polyethylene glycol (PEG), glucosemonoesters and partial fatty acid esters into PLA. They revealed that the elongation at break of PLA increased from 3.3 to 40 % with 10 wt% addition of polyethylene glycol (PEG). Interestingly, their study also showed that 2.5 wt% addition of PEG to PLA lead to a decrease in impact resistance but with 10 wt% of added PEG, the plasticizing effect becomes the dominant aspect. The impact resistance increased significantly up to the level that the samples were unbreak under the chosen condition.

The work of Baiardo et al. [7] had investigated on the thermal and mechanical properties of PLA with the use of two different plasticizers, Acetyl tri-n-butyl citrate (ATBC) and poly-(ethyleneglycol) (PEG). PLA shows high elastic modulus and tensile strength and is quite brittle. Plasticizer addition favorably changes the mechanical properties. With increasing plasticizer content, a common trend is shown by all systems investigated: the tensile modulus and tensile strength decreased, while elongation at break increased. Besides that, an analysis of the glass transition temperatures of the different plasticized PLA systems showed that the abrupt change of elongation occurs in all blends when T_g is around 35 °C illustrated that when the glass transition decreased down to 35 °C, the mechanical behavior of plasticized PLA changed from fragile to ductile.

Recently, Kulinski and Piorkowska [8] had investigated the crystallization, structure and properties of PEG plasticized PLA. The tensile properties demonstrated that the plasticizers enhancing the segmental mobility of PLA chains increased the ability of amorphous PLA to the plastic deformation, decreasing the yield stress and increasing the elongation at break. They also found that the plasticized semicrystalline samples gained the ability to plastic deformation, leading to about 20 % elongation at break with the addition of 10 wt% plasticizer content.

Even though the addition of plasticizers for plasticization of PLA will overcome the brittleness but, it comes with a sacrifice of stiffness of the material which

Table 11.2 Summary of reported mechanical properties for blends of PLA with PC

Material	Blend component	σ_b (MPa)	ε_b (%)	E (GPa)	Charpy (kJm^{-2})
PLA	None	60	5	1.3	–
PLA	PCL (20 %)	30	175	1.1	–
PLA	PCL (30 %)	–	2	1.4	1.1
PLA	PCL (20 %, NR)	–	28	–	–
PLA	None	35	3	3.1	1.8
PLA	PCL (20 %)	31	10	2.1	–
PLA	None	70	10	–	–
PLA	PCL (30 %)	55	20	–	–
PLA	None	45	2.1	3.7	–
PLA	PCL (5 %)	52	2.9	3.3	–
PLA	Clay (4.75 %)	40	1.7	4.4	–
PLA	PCL (4.75 %)/Clay (4.75 %)	54	3.2	4.1	–

is also equally important for structural applications. The tensile modulus representing the stiffness of the PLA dropped dramatically from 3800 to 1200 MPa with 10 wt% addition of PEG as plasticizer [2]. Kulinski and Piorkowska [8] also observed a decrease in stiffness and yield strength of PLA with addition of PEG. They also reported that an increase of PEG content to 10 wt% further decreased the yield stress to about 18–20 MPa. Thus, the development of an impact modifier is significantly required to improve the toughness of the material without extensively forfeiting the stiffness of PLA.

11.2 PLA Blends

11.2.1 PLA/Biodegradable Blends

There are generally two classes of polymer blends containing PLA; blends with other degradable/renewable resource polymers and blends with non-degradable polymers. A large portion of the studies on polymer blends with PLA have been on completely degradable/renewable resource blends.

The most widely studied polymer blends of PLA are those containing polycaprolactone (PCL). PCL is also degradable polyester and due to its low T_g it exhibits rubbery characteristics with an elongation at break of approximately 600 %, which makes it an ideal candidate for toughening PLA. However, immiscibility of PLA and PCL in binary blends, courses phase separation, and tends to lower the fracture properties and in generally lead to insignificant improvements in mechanical properties. Due to this drawback, current researches

have tried to improve compatibility between PLA and PCL in PLA/PCL blends. Mechanical properties of various on PLA/PCL blends are summarized in Table 11.2.

Takayama and Todo [9] used lysine triisocyanate (LTI) as an additive in PLA/PCL blends to improve the compatibility between PLA and PCL. They evaluated the impact fracture properties of PLA/PCL/LTI blend and compared to those of PLA/PCL blend to assess the effect of LTI. They reported that the dissipated energies in both crack initiation and fracture stage, dramatically improved by LTI addition. The miscibility and ductile deformation of PLA/PCL improved through cross-linking of PLA and PCL induced by chemical reaction between the hydroxyl group of PLA and PCL and the isocyanate groups of LTI. A following study by Takayama et al. [10] revealed that the bending modulus and strength of PLA/PCL/LTI blends further improved due to polymerization and cross-linking effect of LTI and crystallization by annealing strengthen the microstructure, resulting in the dramatic improvement of the impact strength of PLA/PCL/LTI blends.

In similar work, Semba et al. [11] have investigated the effect of dicumyl peroxide (DCP) on PLA/PCL blend. In this reactive blending, DCP act as a crosslinking agent to generate high performance material. They revealed that addition of 0.2 parts per hundred (phr) on DCP had synergistic effect on 70/30 PLA/PCL blend. They reported that with addition 0.2 phr of DCP to the 70/30 PLA/PCL blend with the elongation at break increases to 160 %. The tensile modulus and yield stress were unaffected with slight decrease in Izod impact strength observed.

In order to obtain a toughen PLA, Chen et al. [12] reacted PLA with a small amount of methacryloyloxyethyl isocyanate (MOI). They reported that for the PLA modified with 5 % MOL and 8 h reaction time, elongation at break increased (2.5–51 %) tensile strength was decreased from 49 to 26 MPa, Young's modulus was decreased (3.29 GPa–1.64 MPa) impact resistance (notched) improved 1.6 times (44.3–71.2 J/m).

Jiang et al. [13] used poly(butylenes adipate-co-therphthalate) (PBAT) as a natural choice to improve PLA properties without compromising PLA biodegradability. They showed that fracture behavior of the specimen in the tensile tests changed from brittle fracture of the neat PLA to ductile fracture of the blends. It was noticed that even at 5 % of PBAT the elongation of the blend tremendously increased (>200 %) while the elongation at break values continuously increased with increasing PBAT content.

In similar research, Li and Shimizu, [14] used melt blending method to blend PLA with biodegradable polyurethane (PU) in an effort to toughen the PLA without compromising its biodegradability and biocompatibility. They reported that the blend with 10 wt% PU had showed 75 % improvement in Impact strength while the elongation at break improved from 4 to 220 % compared to neat PLA. The elongation at break continuously increased with increasing PU content, and

Table 11.3 Tensile and impact testing properties for PLA/PE blends

Material	Blend component	σ_b (MPa)	ε_b (%)	E (GPa)	MLT[b] (μm)	Izod (kJm^{-2})
PLA	None	–	–	–	–	12
PLA	LLDPE (20 %)	–	–	–	3.3	35
PLA	LLDPE (19 %)/LE[b] (5 %)	–	–	–	0.4	540
PLA	None	62	4	2.40	–	20
PLA	LLDPE (20 %)	22	23	1.68	1.1	490
PLA	LLDPE (19 %)/LE[b] (5 %)	24	31	1.32	0.4	760
PLA	HDPE (20 %)	42	2.9	1.71	1.2	12
PLA	HDPE (19 %)/LP[b](5 %)	25	13	1.39	0.8	64

MLT matrix ligament thickness, *LE*^{b} PLLA-b- diblock copolymer, *LP*^{b} PLA-b-PEP diblock copolymer

reached to maximum value of 363 % at 30 wt% PU. Liu et al. [15] have studied on blends of PLA with poly(tetramethylene adipate-co-terephthalate) (PTAT) and discussed the resultant mechanical properties. They reported that the (75/25) PLA/PTAT blend, had a tensile strength of 25 MPa and elongation at break of 97 %, compared to 28 MPa and 19 % respectively for neat PLA.

11.2.2 PLA/Non-biodegradable Blends

Blending PLA with nondegradable polymers has not been as extensively studied as degradable/renewable resource polymer blends; however, a few have been reported. For example, Polyethylene oxide (PEO) and polypropylene oxide (PPO) have been blended with PLA. Low molecular weight glycols (300–1000) are miscible with PLA and have been used as a polymeric plasticizer while high molecular weight PEO at high levels of incorporation is immiscible with PLA.

Although the idea of blending PLA with non-biodegradable polymers seem defeat the purpose developing a fully degradable blend/composites. The aim of these studies is to improve the impact strength of PLA. Liner low density polyethylene (LLDPE) is a soft but tough plastic with high elongation at break. Because of this, the addition of LLDPE may improve the toughness the materials without significantly sacrificing the stiffness. There are many reports about researches that have been done about introduction of LLDPE to thermoplastics as impact modifiers.

Anderson et al. [16] had performed melt blending on PLA/LLDPE in an effort to toughen PLA. The results indicated that, for the amorphous PLA, the toughening effect was achieved only when a polylactic acid-b-polyethylene (PLA-PE) block compolymer was used as a compatibilizer. They have reported that impact strength of 80/20 wt% PLA/LLDPE blend reach 35 ± 15 kJm^{-2} compare to the homopolymer (12 ± 4 kJm^{-2}). They also showed that addition of 5 wt% of

polylactide-b-propylene (PLA-b-PE) copolymer as a compatibilizer, improve compatibility between PLA an LLDPE and resulting better dispersion of the LLDPE in the PLA matrix, and significantly increase impact resistance up to 540 ± 100 kJm^{-2}. They observed appreciable improves in toughening of PLA/LLDPE blends, as without any compatibilizer, impact strength reach to 490 ± 200 kJm^{-2}. However, addition of a PLA-b-PE block copolymer compatibilized the blend resulting in better PLA/LLDPE interfacial adhesion, better dispersion of the LLDPE in the PLA matrix and an appreciable improve in impact resistance of blend, as impact values were reach up to 760 ± 50 kJm^{-2}. Table 11.3 shows result of different researches of PLA/PE that recently been done.

Ishada et al. [17] had performed melt blending of rubber with PLA in effort to toughen PLA. They melt PLA with four rubber component, ethylene-propylene copolymer, ethylene–acrylic rubber, acrylonitrile-butadiene rubber (NBR), and isoprene rubber (IR) and observed that all the blend samples exhibited distinct phase separation indication partial compatibility between PLA and rubber. The Izod impact testing showed the toughening was achieved only when PLA was blended with NBR, which showed the smallest particle size in the blend sample. In agreement with the morphological analysis, the value of the interfacial tension between the PLA phase and NBR phase was the lowest, and this suggested that the rubber with the high polarity was more suitable for toughening PLA. Under the tensile stress conditions, PLA blend with rubber which did not have crosslinking like NBR and IR, showed higher ability to induce plastic deformation before the break as well as high elongation properties. The authors suggested that the intrinsic mobility of the rubber was important for the dissipation of the breaking energy. Interestingly, the researchers also found that PLA in the NBR blend was not in a completely ductile state. It was deduced that the impact strength of a NBR blend could increase if the NBR particles size becomes smaller.

Recently, melt blending of PLA and LLDPE was performed by our group [18] to investigate the effects of LLDPE loadings on the morphology, mechanical and thermal properties of PLA/LLDPE blends. LLDPE was blended with PLA from 5 to 15 wt% and prepared by counter-rotating twin-screw extruder followed by injection molding into test samples. The mechanical properties of the blends were assessed through tensile, flexural and impact testing while thermal properties were analyzed using differential scanning calorimetry (DSC) and thermogravimetric analysis. Scanning electron microscope was used to study the dispersion and particle size of LLDPE in PLA matrix. The impact strength of PLA improved by 53 % with the addition of 10 wt% LLDPE. However, the tensile modulus and strength, and elongation at break of PLA/LLDPE blends decreased with increasing weight ratio of LLDPE. Similarly, flexural modulus and strength also dropped with addition of LLDPE. DSC results showed that glass transition temperature (T_g) and crystallinity (X_c) of PLA increased with blending of LLDPE. The LLDPE particles size was seen to increase with increasing loadings of LLDPE.

Recently, the largest manufacturer of PLA, Nature Works, has studied the effect of toughening agents on PLA [19]. Especially, they investigated the use of high rubber content (35–80 %) impact modifiers for resins such as polyvinylchloride (PVC), polycarbonate, and aromatic polyesters. In this case, Blendex 338, an acrylonitrile–butadiene–styrene terpolymer containing 70 % butadiene rubber, is the most effective impact modifier. Natureworks [19] reported that with 20 wt% of the Blendex 338, the notched Izod impact strength increased from 26.7 kJm^{-2} of notch for PLA up to 518 kJm^{-2} of notch and the elongation at break increased to 281 from 10 % for PLA. Pellethane 2102-75A, a PU commercially available from Dow chemical company, is another toughening agent that was studied by Nature Works. They reported that with 30 wt% of the polyurethane, the notched Izod impact strength and elongation at break were significantly improved, as impact strength and elongation at break reach 769 kJm^{-2} and 410 %, respectively.

Biomax Strong 100 is an ethylene copolymer which when used at the recommended levels, one to five percent of weight, is said to outperform competing products with improved toughness and minimal effect on transparency. Dupont commercialized Biomax for modifying PLA [20]. As it is mentioned, transparency is the one of the important properties for packaging industrial that addition of impact modifier exacerbate this property and Biomax as an impact modifier is aiming to address. In the product data sheet for Biomax Strong 100, the Spencer Impact (a method used to measured film's resistance to impact-puncture penetration) increases from 1250 gmm^{-1} for unmodified PLA up to 3500 gmm^{-1} for PLA containing 2 % of the additive. While the haze, the measure of the transparency, increased to 45 % at the same additive level, up to 5 % for the unmodified PLA.

11.3 PLA Composites

11.3.1 PLA/Natural Filler Composites

Natural fillers have always experienced a large variation in quality parameters such as strength, fineness, color, and trash content. These variations have been a barrier to large-scale application because of their impact on the quality of the final product. The combination of natural fillers like kenaf, flax, jute, rice husk, pineapple leaf fiber, and etc. with PLA to produce a new material that is competitive with non-renewable polymers, is gaining attention over the last decade. In this context, natural fiber are attracting increasing interest for combination with PLA to apply in the automotive, building materials, and other industries. Reasons for interest in natural fiber filled-PLA composites including stiffness enhancement relative to the parent polymer, and reduce cost along with maintaining the degradability of PLA.

As an extension to the considerable amount of research undertaken on processing and properties of natural filler composites, in this last decade, a number of researchers have explored the concept of natural filler-reinforced PLA composites. An outstanding one is the project FAIR-CT-98-3919 (New functional biopolymer-natural fiber composites from agriculture resources) by European Union, in which one of the key objectives was to manufacture demonstration parts on a pre-competitive level with the automotive industry as the main potential market. Within this project, Lanzillotta et al. [21] prepared biocomposites with flax fibers and PLA as the biopolymer matrix. The research focused on the idea of converting biocomposites into products for real automotive applications.

Tokoro et al. [22] used three types of bamboo fibers (BF) as reinforcement to improve the impact strength of PLA at not only room but also elevated temperatures. There different types of BF were extracted from raw bamboo by either sodium hydroxide (NaOH) treatment or steam explosion in conjunction with mechanical processing. The fibers were designated as "short fiber bundle", "alkali-treated filament" and "steam-exploded filament" respectively. They reported that, among the three bamboo fibers, steam-exploded filament most significantly increases the bending strength of PLA matrix composites due to the highest interfacial strength between PLA and stream-exploded filament. They revealed that impact strength of PLA was not greatly improved by addition of short fiber bundles as well as both filaments. In other to improve impact strength, they alternatively fabricated composites samples by hot pressing using medium length bamboo fiber bundles (MBF) to avoid the decrease in fiber length at fabrication. They reported that impact strength of PLA/MBF composites significantly increased.

Graupner et al. [23] used a compression molding method, combining PLA with different kinds of natural fibers like cotton, hemp, kenaf and man-made cellulose fibers (Lyocell) with various characteristics with a fiber mass proportion of 40 % wt%. Additionally, they were investigated the composites were made of fiber mixtures (hemp/kenaf, hemp/Lyocell). They reported that, the best characteristics values were measured in Lyocell-PLA composites. Nevertheless, achieving a good bonding between Lyocell fiber and matrix was problematic. They measured high elongation at break in cotton-PLA composites. However, tensile strength, Young's modulus and impact strength could be marginally improved compared to the pure matrix. They also reported that the higher value for tensile strength, elongation at break and Young's modulus are related to hemp/kenaf-PLA and kenaf-PLA composites, in compare to cotton-PLA.

In an alternative work, the compatibility and mechanical properties of green coconut fiber (GCF) blended with PLA and maleic anhydride-modified PLA (PLA-g-MA) were evaluated by Wu [24]. He investigated FTIR, NMR, and XRD analysis and revealed that the formation of ester groups, via reactions between the –OH groups in GCF and the anhydride carboxyl groups in PLA-g-MA, which significantly altered the crystal structure of the composite material. Also, Wu

observed good adhesion between GCF phase and PLA-g-MA matrix by SEM images. Finally, Wu [24] concluded that the PLA-g-MA copolymer described herein would be a useful material for lowering the cost and improving the physical properties of PLA/GCF blends.

Qin et al. [25] modified rice straw fiber (RSF) by suspension polymerization of butyl acrylate (BA) monomer, and then prepared biodegradable composites with the modified rice straw fiber (MRSF) and PLA to improve the mechanical and thermal properties of PLA. They observed that the tensile strength of PLA/RSF composites increases at the first and then decreases with the increase of the percentage of weight of PBA reacted of RSF (W(%)). The tensile strength of PLA/RSF composites significantly increased to 6 MPa when W(%) = 7.98. But tensile strength of PLA/RSF rapidly decreased while the content of PBA was over W(%) = 7.98, whereas the elongation at break increased slowly. The researchers also investigated the thermal stability of PLA/RSF composites by TGA and DSC tests. They concluded that thermal stability of PLA/RSF composites increased with the PBA increasing and also, RSF played a role as a nucleating agent and PBA made crystallization of PLA more difficult and incomplete.

Sawpan et al. [26] investigated the mechanical properties of chemically treated and untreated random short fiber and aligned long hemp fiber reinforced PLA composites, over a range of fiber content (0–40 %). The fibers were silane treated (SIL) or alkali treated (ALK) or untreated (FB). They revealed that impact strength, tensile strength and Young's modulus of short hemp fiber reinforced PLA composites increased with increased fiber content (10–30 %), and these properties are higher in case of treated fiber compare with untreated fiber. This is due to good adhesion in between treated fibers and PLA. Among the al samples, the PLA/alkali treated short hemp fiber composites (70:30) had highest tensile strength, Young's modulus, and impact strength, which were 75.5 MPa, 8.2 GPa, and 2.63 kJ/m^2, respectively, about 10.5, 8.2 and 14 % higher than those of the PLA/FB composites. In next stage, they extended their investigations to produce high strength alkali treated hemp fiber/PLA composites using aligned long fibers. They concluded that the alignment of long fibers was found to be effective technique to improve the mechanical properties of PLA/hemp fiber composites compared to those of short hemp fiber/PLA composites. Meanwhile, the highest mechanical properties were obtained with 35 wt% aligned long alkali treated fiber composites with tensile strength of 85.4 MPa, Young's modulus of 12.6 GPA and impact strength of 7.7 kJ/m^2.

Previous publication by our group [27] compared the performances of PLA/kenaf (PLA-K) and PLA/rice husk (PLA-RH) composites in terms of biodegradability, mechanical and thermal properties. Composites with natural fiber weight content of 20 % with fiber sizes of less than 100 μm were produced for testing and characterization. The flexural modulus of the PLA increased with the addition of natural fibers, while the flexural strength decreased. The highest impact strength (34 J/m), flexural modulus (4.5 GPa) and flexural strength (90 MPa) were obtained for PLA-K, which means kenaf natural fibers are potential to be used as an alternative filler to enhance mechanical properties. On the other hand PLA-RH

composite exhibited lower mechanical properties. The impact strength of PLA has decreased when filled with natural fibers; this decrease is more pronounced in the PLA-RH composite. In terms of thermal stability it was found that the addition of natural fibers decreased the thermal stability of virgin PLA and the decrement was more prominent in the PLA-RH composite. Biodegradability of the composites increased 1.2 and 0.8 % for PLA-K and PLA-RH, respectively for a period of 90 days while SEM micrographs showed poor interfacial between the polymer matrix and natural fibers.

As it was mentioned previously, one feasible method of producing plastics that retain the necessary mechanical properties but have high biodegradability is the blending of plastic polymer materials with organic fillers such as starch. Starch is an abundant, inexpensive, renewable and fully biodegradable natural raw material, but its hydrophobic character leads to poor adhesion with hydrophobic polymers in starch-polymer blends. Such blends therefore require a compatibilizer and/or toughener, a reactive functional group introduced into the synthetic polymer, to enhance the compatibility between the two phase and hence to improve the mechanical properties of the composite. Meanwhile, there are many studies that have used different compatibilizers to improve compatibility between PLA and starch.

In this context, Wu [28] investigated the effect on the structure and properties of PLA/starch composites of replacing pure PLA in the blend with acrylic acid grafted PLA (PLA-g-AA). They evaluated the effect of starch content on tensile strength at break for PLA/starch and PLA-g-AA/starch composites. Both composites suffered a decrease in tensile strength at breakpoint as the starch content increased, due to a concomitant increase in the starch phase diameter, but the decrease in tensile strength of PLA/starch was greater than for PLA-g-AA/starch. The tensile strength at breakpoint of PLA/Starch decreased to about 24 and 17 MPa with 40 and 50 wt% Starch, compare with 40 and 38.5 MPa for PLA-g-AA/starch composites.

In similar work, Shi et al. [29] investigated the effect of poly (ethylene ocyane) (GPOE) on mechanical properties of PLA/thermoplastic starch (TPS) blends. GPOE acted as a grafting agent and improve compatibility between PLA and TPS. They reported that, for 10–15 wt% GPOE, the blend with 20 wt% TPS content, have dramatically improved mechanical properties. It had nearly 400 % elongation at break and more than 10 kJ/m^2 in impact strength compared with 12 % and 4.5 kJ/m^2 for PLA/TPS (80/20).

11.3.2 PLA/Mineral Filler Composites

Mineral fillers such as mica, kaolin, calcium carbonate, and talc are frequently incorporated in thermoplastics to reduce the costs and improve the properties of the polymers such as rigidity, durability, and hardness [30]. Talc is common filler in plastics as it serves as the most cost effective filler. Previous researchers have

shown that addition of talc has successfully improved the stiffness, strength, and thermal resistance and widen PLA's application [31, 32]. The addition of talc has been effective for maintaining the stiffness and tensile modulus of PLA on toughening process. However, more studies are needed to be done in order to realize how the talc or other mineral additives interact in PLA/talc.

Audrey et al. [32] have studied on the introduction of talc into PLA. They revealed that the tensile modulus of PLA increased 92 % with 30 wt% of added talc. In this case flexural strength and flexural modulus of PLA also increased 14.5 and 196 %, respectively. Interestingly, their study also showed that 30 wt% addition of talc as a stiff additive to PLA has too little negative effect on impact resistance of PLA. They also reported 37.8 % increase in HDT of PLA matrix with 30 wt% addition of talc.

Fowlks and Narayan [33] used maleic anhydride-functionalized PLA (MAPLA) as an interfacial additive to improve compatibility between PLA and talc particles in PLA/talc composite. The effect of MAPLA was investigated based on evaluation of composite properties and examination of the microstructure using scanning electron microscopy. The incorporation of MAPLA contributed to an increase in the crystallinity of PLA in the composites, and when added in optimal concentration, showed improved tensile strength. DSC results revealed that the talc acted as nucleating agent and improved crystallinity of PLA from 16 to 26 %. They suggested that MAPLA is in lower molecular weight and act as a lubricating agent on the PLA matrix and to contributed more freely moving polymer chains and enhanced chain mobility permitting higher molecular orientation and better dispersion, which in turn led to increased crystallization activity. In next step, they investigated the effect of varying amount of MAPLA on mechanical behavior of PLA/talc composite. Generally, the incorporation of talc tend to decrease the strength of the composites due to their lower ability to support stress transferred from the polymer matrix. Interestingly, they revealed that the sole addition of talc had no significant effect on the tensile strength. But, adding MAPLA, increased the tensile strength, from 66 MPa at 3 % MAPLA up to 72 MPa at 5 % MAPLA (compared with 58.7 MPa for neat PLA), at which the tensile strength reached a maximum; beyond which it dramatically dropped to 24 MPa. They resulted that increasing the amount of anhydride groups in the system increases the number of the acid–base interactions and the degree of hydrogen bonding, which leads to stronger interaction between the filler and the matrix. They found that the most prominent physical effect of the talc was the stiffening effect. The Young's modulus increased from 7 GPa for PLA/talc (60:40) composite up to 10.1 and 11.1 GPa at 3 and 5 % MAPLA addition, in compared with 3.6 GPa for neat PLA. This is because the Young's modulus of talc (170 GPa) is significantly higher than that of PLA and nucleating effect of talc particles to improve crystallinity of PLA. On the other hand, MAPLA improve interaction between PLA and talc particles, resulted in more stress transfer from PLA matrix to stiff talc particles.

In similar research, Huda et al. [34] evaluated the effect of the addition of silane treated and untreated talc as the filler on the mechanical properties of PLA/

recycled newspaper cellulose fiber (RNCF)/talc hybrid composites. They incorporated 10 wt% of a talc with and without silane treatment into PLA/RNCF (60/30 wt%) composites that were processed by a micro-compounding and molding system. They reported that the flexural and impact properties of hybrid composites found significantly higher than that made from either PLA/RNCF. The flexural strength of PLA/PNCF composite increased from 77.7 MPa up to 116 and 132.6 MPa, respectively, with addition 10 wt% untreated talc and, simultaneously, flexural modulus increased from 6.7 GPa up to 12.3 and 15.3 GPa. These improvements in flexural behaviors could be due to the effects of hybridization. Meanwhile, flexural modulus of the hybrid composite containing treated talc was significantly higher than those containing untreated talc. In next stage, they investigated the notched Izod impact resistance of composites and revealed that the impact properties of PLA based composites improved in the presence of talc and RNCF. Silane treated talc showed greater improvement compared untreated talc. They reported that the impact strength of PLA/RNCF composites reached to 24.6 and 26.2 J/m with addition 10 wt% untreated and treated talc, respectively, compared with 25.7 J/m for neat PLA. They suggested that improved filler-matrix adhesion favored the impact property of the RNFC reinforced talc filled PLA composites. Since the impsct strength of the particle size and uniform dispersion in matrix, silane treated talc might help to increase impact strength of hybrid composite. In final, they concluded that the addition of silane treated talc to RNCF reinforced PLA composites improves the interaction at the polymer/talc interphase, and thus improve the mechanical properties of the composites.

Calcium carbonate ($CaCO_3$) is another widely used mineral fillers which is associated with substantial cost reduction. It can function either as extender filler or reinforcing filler when used in polymers. Kim et al. [35] used treated and untreated micron-sized (3–4 μm in diameter) $CaCO_3$ to improve mechanical of (L-lactid) (PLA) and $CaCO_3$ particles were coated or uncoated with calcium stearate. In this study, they investigated the role of $CaCO_3$ particles as a reinforcing and calcium stearate as a surface treatment, on PLA/treated calcium carbonate (PLAC) and PLA/untreated calcium carbonate (PLAH) composites. They reported that with addition 5 and 10 wt% of treated $CaCO_3$, tensile modulus of the PLA reached to 2.34, 2.73 GPa, respectively, compared with 2.19 GPa for neat PLA. Simultaneously, the tensile modulus of PLAH reached to 2.38 and 3.34 GPa, respectively. On the other hand, tensile strength of PLAC and PLAH composites significantly improved by incorporation $CaCO_3$ fillers, since in case of 10 wt% filler, tensile strength of PLAC and PLAH reached to 58.3 and 60 MPa compared with 51.5 MPa for neat PLA.

In another research, Wang et al. [36] investigated the effect of carbon black (CB) on mechanical and thermal properties of plasticized PLA. They used two different plasticizer, acetyl tributyl citrate (ATBC) and poly(1,3-butylene adipate) (PBA) and revealed the plasticizers improved interaction existed between PLA and CB. The FT-IR spectra revealed that with increasing CB content in each

composite, the the characteristics of all FT-IR peaks all shifted towards lower wave number. These shifts of stretching absorption to lower wavenumber indicated the more interaction between PLA and CB. With increasing plasticizers content in PLA/CB composites, the wavenumber of the characteristics peak vs. CB content plots basically located lower. It also indicated that plasticizers could improve the interaction between the PLA and CB particles. They concluded from SEM images that, although there were interaction between PLA and CB particles, it was not enough to disperse CB well in the PLA phase. Because of that, the macro agglomerations of CB particles were located in the PLA phase like the islands in the sea without the connections. Mechanical tests revealed that although plasticizers decreased tensile strength of PLA but CB maintained it in moderate value. DMTA showed that the storage improved by increasing CB contents. This improvement in stiffness was associated with the interaction between plasticized PLA matrix and CB. On the other hands, this interactions, caused to increase T_g of plasticized PLA.

11.4 Nanocomposites

Nanocomposites are gaining acceptance in the mainstream of the global plastics processing industry and there has been a great recognition of their enormous potential in relation to a wide range of product development. The term 'Nanocomposite' relates to the dispersion of nano-sized particles within the polymer matrix [37]. In the last few years, a large number of nanomaterials consisting of particles measuring a billionth of a meter (one nanometer) or less have been commercialized. The new polymeric materials made by using these particles in an appropriate matrix may be classified as advanced materials because of their superior tensile strength, modulus and dimensional stability compared with conventional composite materials. The nanoparticles are so small and their aspect ratio is so high that the material properties improve even when the filler component is very low compared to conventional reinforcements like talc and glass. These nanocomposite materials also offer increased modulus, strength and heat resistance, decreased gas permeability and flammability [38]. Nanocomposites have been attracting attention since the 1990s when Toyota, for the first time, produced polyamide-6/MMT nanocomposites, used them to manufacture timing belt housings for the automotive industry, and demonstrated their unprecedented thermomechanical properties. This event proved to be the signal for a great deal of international academic and industrial research in the field of nanocomposites.

Regardless the improvements and technologies advances succeeded in the field of nanocomposites, increasing amount of plastic waste has become a major global environmental problem. There are two approaches that can be used for keeping the environment free from these plastic wastes: First one is the storage of wastes at landfill sites. However, due to the rapid development of society, satisfactory landfill sites are also limited. Besides that, burial of plastics wastes in landfill is a

time bomb as today's problems being shifted onto the shoulders of future generations. Another approach is to find a solution through waste management which can also be divided into two steps; incineration and recycling. Incineration of the plastic wastes always produces a large number of carbon dioxide and creates global warming, and sometimes produces toxic gases, which again contribute to global pollution. On the other hand, recycling seem to be the practical solution for the problem even though it requires considerable expenditure of labor and energy; removal of plastics wastes, separation according to the types of plastics, washing, drying, grinding and, only then, reprocessing to final product. Indirectly, this makes packaging more expensive and the quality of the recycled plastic is also lower than that of the material produced directly by the primary manufacturer. The dependency on petroleum as the building source for plastics also questions the future of these materials as petroleum becomes scarce and more expensive. For these reasons, throughout the world today, the development of green biodegradable materials from renewable resources, with controlled properties has been a subject of great research challenge to the community of material scientists and engineers.

Preparation of blends or conventional composites using inorganic or natural fillers, respectively are among the routes to improve some of the properties of biodegradable polymers. Improved thermal stability, gas barrier properties, mechanical strength and low melt viscosity are among the properties that can be achieved by these multiphase systems. Nanoreinforcements of biodegradable polymers have strong promise in designing eco-friendly green nanocomposites for several end-use applications. A fairly new area of composites has emerged in which the reinforcing material has the dimensions in nanometric scale.

Most biodegradable polymers have excellent properties comparable to many petroleum-based plastics and readily biodegradable, and may soon be competing with commodity plastics. So, biodegradable polymers have great commercial potential for bio-plastic, but some of the properties such as brittleness, low heat distortion temperature, high gas permeability, low melt viscosity for further processing etc. restrict their use in a wide-range of applications. Therefore, modification of the biodegradable polymers through innovative technology is a formidable task for materials scientists. On the other hand, nanoreinforcement of pristine polymers to prepare nanocomposite has already proven to be an effective way to improve these properties concurrently. So, preparation to processing of biodegradable polymer-based nanocomposites, that is, green nanocomposites from renewable resources are the wave of the future and considered as the next generation materials.

11.4.1 PLA Nanocomposites

PLA nanocomposites hold the future in biopolymer nanocomposites as there is an urge for the development of 'green' technology from sustainable and renewable

resources. Nano-sized filler-based technology has enabled the application of both organic/inorganic fillers with at least one of its dimension in the scale of nanometer, into PLA leading to the formation of PLA nanocomposites. Various types of nanofillers are incorporated into PLA by researchers to explore the suitable nanofiller which contribute to the desired properties of the engineering PLA nanocomposites. In the past decades, layered clay such as montmorillonite (MMT) is commonly used as reinforcement materials due to its nanoscale size and intercalation/exfoliation properties. In its pristine form, they are hydrophilic in nature, and this property makes them very difficult to be well dispersed in PLA. The most common strategy to overcome this difficulty is to replace the interlayer MMT cations with quaternized ammonium cations, preferably with long alkyl chains. The presence of hydrophobic chain within the interlayer of MMT enables PLA chains to diffuse in resulting in separation of the layers.

The development of PLA/carbon nanotubes (CNT) nanocomposites is favored due to CNT's unique structure and properties. Recent studies have focused on the functionalization of CNT, and then, the modified CNT are used to replace MMT in PLA. Nevertheless, the addition of CNT as reinforcing nanofillers into PLA has been less quantitatively understood, especially with respect to its effect on the thermal and mechanical behaviors. Cellulose nanowhiskers (CNW) on the other hand have attracted significant attention in the last decade as potential nano-reinforcement in PLA as cellulose is abundant in nature and it can also be produced by bacteria. It is believed that CNW has good mechanical properties attributed to the binding forces of neighboring atoms within CNW resulting in improved mechanical properties. However, the use of CNW as nanofillers in PLA is still a new field in nanotechnology and as a result, there are still many obstacles remaining to their use.

These new families of green nanocomposite materials exhibit remarkable improvements of mechanical and material properties when compared with virgin polymers or conventional micro- and macro-composites. The field of PLA-based nanocomposites has gained its popularity among scientist and industrials. These nano-biocomposites are obtained by adding nanofillers to PLA, resulting in very promising materials with improved properties with preservation of PLA's biodegradability, without eco-toxicity. The nanoscale distribution of such high aspect ratio nanofillers also brings up some large improvements to the polymer matrix in terms of mechanical, fire retardant, rheological, gas barrier and optical properties, especially at low content (as small as 5 wt%) in comparison with conventional composites (>30 wt% of microfiller). Thus, it can be said that PLA nanocomposites also represent a strong and emerging answer for improved and eco-friendly materials which may also replace the current petroleum based plastics in future. This chapter reports on an aspect of the state of the art in wide field of nano-biocomposites materials, namely PLA-based nanocomposites with MMT, CNT and CNW as nanofillers.

11.4.2 PLA/MMT Nanocomposites

Preparation PLA nanocomposites with organically modified montmorillonite (OMLS) as nanofillers has been studied extensively recently. Ogata et al. [39] first prepared PLA/OMLS blends by dissolving the polymer in hot chloroform in the presence of dimethyl distearyl ammonium modified MMT ($2C_{18}$MMT). In the case of PLA/MMT composites, WAXD (wide angle X-ray diffraction) and SAXS (small angle X-ray scattering) results showed that the silicate layers could not be intercalated using solution method. In other words, MMT existed in the form of tactoids, consisting of several stacked silicate monolayers. These tactoids are responsible for the formation of particular geometrical structures in the blends, which lead to the formation of superstructures in the thickness of the blended film. This kind of structural feature increases the Young's modulus of the hybrid. Later, Bandyopadhyay et al. [40] reported the preparation of intercalated PLA/OMLS nanocomposites with much improved mechanical and thermal properties.

In recent studies, Pluta et al. [41] developed PLA/MMT nanocomposites loaded with 3 wt% organomodified MMT and PLA/MMT microcomposites containing 3 wt% sodium montmorillonite by melt blending. They investigated the morphological and thermal properties of the nanocomposites and microcomposites and compared them with the unfilled PLA. They observed that the unmodified MMT filled PLA formed a microcomposite with a phase-separated microstructure. They also reported that PLA is a polymer that readily interacts during melt blending with a montmorillonite organomodified with dimethyl 2-ethylhexyl (hydrogenated tallowalkyl) ammonium cation, leading to the formation of at least an intercalated structure which led to the formation of a nanocomposite. The processing properties of the nanocomposite were excellent and comparable to those of the microcomposite and unfilled PLA. Thermal investigations showed an improvement in the nanocomposite thermal stability under oxidative conditions in comparison to those for the microcomposite and unfilled PLA.

Ray et al. [42] had successfully prepared PLA/MMT nanocomposites by simple melt extrusion of PLA wherein the silicate layers of the MMT were intercalated and randomly distributed in the matrix. They also showed that the incorporation of very small amounts of oligo(ε-caprolactone) (o-PCL) as compatibilizer in PLA led to a better parallel stacking of the silicate layers and also much stronger flocculation due to the hydroxylated edge–edge interaction of the silicate layers. The PLA/MMT nanocomposites also exhibited remarkable improvement of materials properties in both solid and melt states compared to the matrix without MMT.

Maiti and co-workers [43] investigated the effect of organic modifiers of various chain lengths in different types of clays, smectite, MMT, and mica on the degree of dispersion of clay in PLA. They observed that the nanocomposites of MMT and mica are intercalated and well-ordered compared to smectite. The

layered structure and gallery spacing of organo-MMT in PLA nanocomposites shows that, with a modifier of the same chain length, the gallery spacing of the organoclay was largest for mica and smallest for smectite because of the higher ion-exchange capacity of mica and physical jamming of the modifier due to a restricted conformation at the core part of the clay of larger size. However, the increment of the modulus in a smectite nanocomposite, compared to that of PLA, is higher than MMT or mica nanocomposite due to better dispersion in a smectite system for the same clay loading. Being a well-dispersed system, smectite nanocomposites have better gas barrier properties than the MMT or mica systems, which are larger in size but stacked in nature in their nanocomposites.

Nam et al. [44] studied the detailed crystallization behavior and morphology of pure PLA and one representative PLA/C18-MMT nanocomposites. They concluded that the overall crystallization rate of neat PLA increases after nanocomposite preparation with C18-MMT. These behaviors indicate dispersed MMT particles act as a nucleating agent for PLA crystallization in the nanocomposites. Lee and co-workers ([45]) who investigated the thermal and mechanical characteristics of PLA nanocomposite scaffold, reported that the recrystallization temperature (T_c) of quenched PLA and its nanocomposite systems decreased by the addition of MMT clay. The nanosized layered MMT platelets provide large surface area due to their small size and thus it is reasonable to consider that the MMT particles could act as effective nucleating sites of PLA crystallization. The increased nucleating sites are likely to facilitate the PLA crystallization process in the nanocomposite systems.

Krikorian and Pochan [46] explored the effect of compatibility of different organic modifiers on the overall extent of dispersion of aluminosilicate layers in a PLA matrix. Three different commercially available MMT were used as a reinforcement phase. According to TEM and XRD studies an increase in miscibility of the organic modifier with the PLA matrix increased the tendency of the aluminosilicate layers to exfoliate. They also reported an enthalpic interaction between diols present in the organic modifier with the C=O bonds present in the PLA backbone is a significant factor for driving the system toward exfoliation. According to the DSC measurements the addition of MMT did not alter the melting point of PLA, which suggests intact crystalline lamellae thickness, in accordance with corresponding XRD crystalline peaks of PLA. The mechanical properties of the nanocomposites show significant improvements compared to neat PLA due to the nanometer range dispersion of the MMT platelets. They concluded that a higher MMT incorporation and degree of exfoliation gave rise to stiffer materials with optically transparent properties.

In another study by Di et al. [47] revealed that the exfoliation of MMT in PLA matrix has been achieved due to the strong interaction between the MMT and polymer matrix. They also stressed that the high surface area of MMT layers had reduced molecular mobility of PLA leading to unique properties for the PLA/MMT nanocomposites. The exfoliated MMT platelets act as nucleating agents at

low content by increasing the crystallization rate of PLA. However, at high MMT content, they become the crystallization retardant acting as physical hindrance to restrict the molecular chain mobility of PLA because of the increased interaction sites. Therefore, there is an optimal amount of MMT for PLA/MMT nanocomposites to achieve the greatest improvements in their properties. Besides that, the melt viscosity and dynamic shear modulus of PLA/MMT nanocomposites are also enhanced significantly by the exfoliation of MMT. These results have been attributed to the strong interaction between PLA and exfoliated MMT layers which lowers the molecular mobility of PLA and forms an interconnected structure within the PLA matrix.

Peterson and Oksman [48] had compared the mechanical, thermal and barrier properties between layered silicate and microcrystalline (MCC) in PLA nanocomposites by incorporating 5 wt% of each nanoreinforcement. The results showed that there was a difference in exfoliation and in the interaction with the PLA matrix between layered silicates and MCC. This has resulted in a large difference in the mechanical properties between the two nanocomposites. The layered silicate system showed great improvements in both tensile modulus and yield strength, while the MCC nanocomposite only improved the yield strength. However, they also found that the two materials also had very different effects on the elongation to break. The MCC system showed a more satisfactory behaviour compared to the layered silicate which reduced the elongation to break greatly. The difference seen was due to layered silicates' larger surface area which will allow the nanoreinforcement to interact with a larger amount of polymer chains and thereby having a larger effect on the mechanical properties. Besides that, the layered silicate is organically modified to be compatible with polymers like PLA and will therefore have better interaction with the PLA matrix. Good interaction between the reinforcing phase and the matrix in a composite will allow for good stress transfer to take place in the composite. This gives rise to large improvements in the mechanical properties of the weaker matrix.

Pluta [49] studied the structure and properties of PLA/MMT nanocomposites and showed an effective enhancement of MMT dispersion with prolongation of the blending time (from 6 to 30 min). They stressed that this was possible due to strong interaction between PLA-MMT and shearing forces during melt compounding. The nanostructure was induced by the intercalation followed by tactoids formation and exfoliation of MMT, as confirmed by TEM analysis and XRD. The studies performed also clearly revealed the influence of MMT's dispersion in the PLA matrix on the physical properties of the nanocomposites formed as the improved MMT's dispersion (at their constant concentration) had increased the thermal stability of the nanocomposites under oxidative and nonoxidative conditions was improved with MMT's dispersion. Besides that, the crystallization ability of PLA also improved with incorporation of MMT.

Wu and Wu [50] have successfully prepared and characterized PLA/chitosan modified MMT nanocomposites through the solution insertion of PLA polymer

chains into organically-modified montmorillonite, which was first treated by n-hexadecyl trimethylammonium bromide (CTAB) cations and then modified by biodegradable chitosan to improve the chemical similarity between the PLA and organically modified MMT. The mechanical properties and thermal stability of the PLA/m-MMT nanocomposites analyzed by dynamic mechanical analysis (DMA) and thermogravimetric analysis (TGA) showed significant improvements in the storage modulus and 50 % loss in temperature when compared to the neat PLA. They also observed that the degradation rates of PLA/MMT nanocomposites are slower than that of PLA matrix.

Besides that, the structure, dielectric, vicsoelastic and thermal properties of PLA/MMT nanocomposites also had been investigated by Pluta et al. [51]. They found that the X-ray investigations exhibited an exfoliated nanostructure in 3 wt% MMT filled PLA nanocomposites. The degree of exfoliation of the MMT also improved due to combined interactions of the MMT's surfactant with PLA chains. However, mixed intercalated and exfoliated nanostructures were detected in 10 wt% MMT filled nanocomposites due to the high concentration of the filler. They also found that the nanocomposites show a significant increase of viscosity and reinforcement of the molten PLA matrix with increasing MMT content due to the presence of the dispersed MMT. The viscoelastic spectra from DMA showed a gradual increase of the storage and loss modulus with the increase of the MMT content and improved dispersion. Dielectric properties of the nanocomposites show a weak influence of the MMT on segmental and local relaxations in PLA, except for the highest MMT content. The researchers concluded that the dielectric properties of all the nanocomposites in the high temperature range are dominated by the processes related to ionic species present in the MMT.

Lately, Jiang et al. [52] investigated the reinforcing effects and toughening mechanisms by comparison of PLA/nano-sized calcium carbonate and PLA/MMT nanocomposites. They reported that the semicrystalline PLA exhibits high tensile strength and modulus but very low strain-at-break and toughness. The researchers also revealed the intercalation of MMT by PLA and a good dispersions of both MMT and NPCC nanoparticles were achieved when the filler concentration was lesser than 5 wt%. However, more large agglomerates were observed with increasing concentration of the filler. The strain-at-break of PLA increased with NPCC concentration ranging from 0 to 7.5 wt%, whereas it only increased with MMT concentration up to 2.5 wt% and decreased at higher concentrations and it was observed that the tensile strength of PLA nanocomposites also decreased with MMT content up to 5 wt%. Interestingly, stress yielding was noted in PLA/MMT nanocomposites at 2.5 wt% MMT with significant necking but, with 5 and 7.5 wt% MMT, however, the strain at break was dramatically reduced and the nanocomposites fractured in completely brittle manner without yielding. They also concluded that the different reinforcing effects of MMT and NPCC could be mainly attributed to the differences in microstructures and interactions between the nanoparticles and PLA in the respective nanocomposites. It was observed that the MMT stacks located between the microvoids and prevented their coalescence, allowing large scale shear yielding but at

higher MMT concentrations. However, the agglomerates of MMT induced premature material failure occurred before the shear yielding was able to start.

Recently, Chow and Lok [53] investigated the flexural, morphological and thermal properties of PLA/MMT nanocomposites prepared by using solution (toluene) intercalation and melt intercalation methods. They showed that the PLA/MMT nanocomposites prepared by solution intercalation shows higher flexural modulus than PLA/MMT nanocomposites prepared by melt intercalation. The researchers summarized that this was attributed to the better dispersion of MMT layered silicate in PLA. They found that an optimum loading, 1 wt% of MMT can achieve a good balance between flexural properties (e.g. flexural modulus, yield stress and yield displacement) for PLA nanocomposites prepared by both solution and melt intercalation method. They also observed the morphological transformation in PLA matrix by the incorporation of MMT through field emission scanning electron microscope (FESEM) micrographs. The increment of d-spacing observed from XRD diffractograms indicates that the PLA polymer chains were successfully intercalated in between the intergallery of MMT. The DSC thermograms showed that the addition of MMT did not influence the glass transition temperature (T_g) and melting temperature (T_m) of PLA nanocomposites but, the crystallization temperature (T_c) of PLA was reduced with th presence of MMT. The researchers also concluded that although the PLA/MMT nanocomposites prepared by solution intercalation method show better MMT intercalation and flexural properties. However, the melt intercalation method also produced PLA/MMT nanocomposites with comparable flexural properties. Thus, the melt intercalation method could be an acceptable method to produce PLA/MMT nanocomposites consequent to its environmental friendly nature and its compatibility to the current industrial compounding techniques.

11.4.3 Plasticized PLA/MMT Nanocomposites

Regardless of the improvements achieved in the development of PLA nanocomposites, PLA's brittleness had become more inherent, limiting its application for structural applications. Thus, the addition of plasticizers into PLA nanocomposites may provide a way to improve the elongation at break and toughness of the material. However, only several studies which had been contributed recently in the development of plasticized PLA nanocomposites [54–58] but the mechanical properties of these nanocomposites were yet to be studied in detail.

Paul et al. [54] developed the plasticized PLA nancomposites by melt blending of PLA with 20 wt% of poly(ethyleneglycol) 1000 (PEG 1000) and different amounts of MMT to investigate the thermal and morphological properties of the plasticized PLA nanocomposites. X-ray diffraction (XRD) has pointed out that all the studied MMT led to intercalated nanostructures, even the unmodified MMT had produced an intercalated structure. The researchers stressed that the particular

intercalation was provoked by the interlayer migration of poly(ethyleneglycol) 1000 plasticizer. The differential scanning calorimeter (DSC) results confirms that the MMT content does not greatly influence the T_g and the T_m of the plasticized PLA nanocomposites. However, these temperatures are noticeably altered at higher MMT content (10 wt%) which was due to the preferential intercalation of PEG 1000 in MMT, which renders it less available to plasticize the PLA matrix. It results a remarkable increase of the T_g, particularly at 10 wt% of loading. It is stated that at lower MMT content, the proportion of plasticizer intercalated into the interlayer space of the MMT remains insufficient to affect the T_g of the PLA. Besides that, the morphological analyses performed on the plasticized nanocomposites showed a possible competition between PLA and the plasticizer for the intercalation between the MMT layers.

Pluta [55] investigated the morphology and properties of PLA modified by thermal treatment, filling with MMT and plasticization with 10 wt% of PEG. The researchers showed that melt filling of PLA by organomodified nanoparticles had led to the formation of an intercalated nanostructure. They also observed that an intercalated nanostructure formed in plasticized PLA nanocomposites as the molecules of PEG stimulated the intercalation process. The presence of inorganic MMT particles reduce the crystallization of PLA and this effect was more pronounced in nanocomposites due to the intercalated nanostructure with provides higher surface area of interaction. Besides that, the addition of plasticizer facilitates the crystallization process of both plasticized PLA and plasticized PLA nanocomposites. The crystallization process by heating up from the glassy amorphous state led to the formation of the same crystalline modification in PLA. They also observed a reinforcing effect of MMT in the intercalated plasticized PLA nanocomposites as the storage modulus from DMA analyses registered higher value for MMT filled plasticized PLA compared to the unfilled plasticized PLA. The observed increase in modulus contributes to the rigidity of the material.

Thellen et al. [56] had investigated the influence of MMT layered silicate on plasticized PLA blown films and concluded that the plasticized PLA/MMT nanocomposites did not see highly significant enhancements with addition of MMT but the toughness is at least maintained in the nanocomposites unlike other MMT filled polymeric systems. They found that the plasticization effect reduced the brittleness of the nanocomposites as the elongation at break of the prepared nanocomposites did not reduce significantly as expected. The researchers concluded that although the plasticized PLA/MMT nanocomposites did not see highly significant enhancements, the toughness is at least maintained unlike in the unfilled PLA/MMT nanocomposites… Their studies also show that the addition of MMT compensates the loss of rigidity in PLA due to the plasticizing effect plasticizers. Although the addition of plasticizer improves the toughness of PLA but it comes with a sacrifice in stiffness which is also an important trait for structural applications. Thus, the addition of an impact modifier to substitute plasticizers may improve the toughness of PLA nanocomposites without significantly forfeiting the stiffness of the nanocomposites.

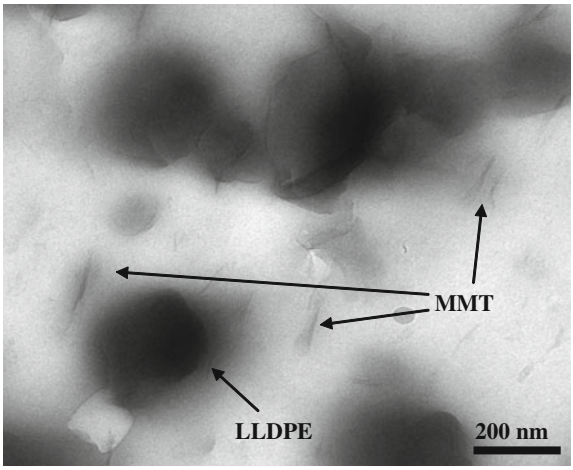

Fig. 11.3 TEM image of PLA/LLDPE/MMT nanocomposites

11.4.4 Toughening of PLA/MMT Nanocomposites

Up to date, very few studies done so far on the toughening of PLA nanocomposites via elastomeric materials to overcome the brittleness [59]. As discussed earlier, the blending of an elastomeric material into PLA nanocomposites would eventually improve the toughness without significantly forfeiting the stiffness of the nanocomposites. Recently, Li et al. [60] had investigated on three types of composites, namely, PLA/MMT, PLA/core–shell rubber, and PLA/MMT/core–shell rubber in their effort to toughen PLA. In comparison with pure PLA, both types of PLA/5 wt% nanoclay composites had an increased modulus, similar impact strength, slightly reduced tensile strength, and significantly reduced strain at break. On the other hand, PLA/core–shell rubber composites with a rubber loading level of 10 wt% or higher had a much higher impact strength and strain at break, but a lower modulus and strength when compared with pure PLA. This proves the excessive loadings of elastomeric materials would significantly sacrifice the stiffness of the neat material. However, the researchers found that simultaneous addition of 5 wt% of MMT and 20 wt% of core–shell rubber resulted in a PLA composite with a 134 % increase in impact strength, a 6 % increase in strain at break, a similar modulus, and a 28 % reduction in tensile strength in comparison with pure PLA.

Lately, the used of LLDPE had been explored by our group [61] in toughening PLA/MMT nanocomposites. We found that the blending of the tough LLDPE compensated the brittleness caused by MMT in the nanocomposites by improving the impact strength of the nanocomposites. The Young's and flexural modulus improved with increasing content of MMT indicating that MMT is effective in increasing stiffness of LLDPE toughened PLA nanocomposite even at low content. LLDPE improved the impact strength of PLA nanocomposites with a sacrifice of tensile and flexural strength. The tensile and flexural strength also decreased with

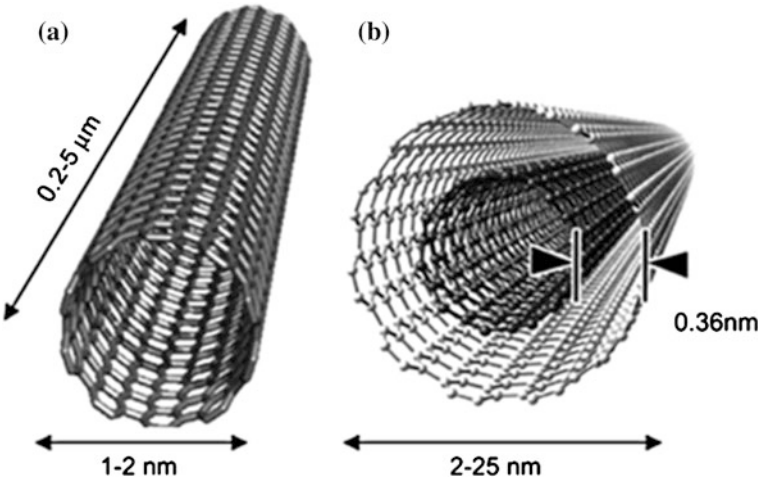

Fig. 11.4 Dimensions of **a** CNT, and **b** MWCNT

increasing content of MMT in PLA/LLDPE nanocomposites. The impact strength and elongation at break of LLDPE toughened PLA nanocomposites also declined steadily with increasing loadings of MMT. The crystallization temperature and glass transition temperature dropped gradually while the thermal stability of PLA improved with addition of MMT in PLA/LLDPE nanocomposites. The storage modulus of PLA/LLDPE nanocomposites below glass transition temperature increased with increasing content of MMT. XRD and TEM (Fig. 11.3) studies revealed that an intercalated LLDPE toughened PLA nanocomposite was successfully prepared at 2 phr MMT content.

Thus, the development of PLA/LLDPE nanocomposites with the correct addition of LLDPE and MMT would engineer a material with targeted and optimal performance for any specific requirements of different applications. Thus, it's inflicted that the optimum toughened PLA nanocomposites formulation hold the future as potential replacement for petroleum based plastics in the near future.

Polylactic acid (PLA)/montmorillonite (MMT) nanocomposites toughened with Biostrong (an ethylene copolymer from DuPont) was also developed by our group [62]. PLA, Biostrong and MMT were melt blended using twin-screw extruder followed by injection molding. Impact strength improved with 2 phr MMT in PLA/Biostrong. It was found that the flexural modulus of PLA/Biostrong nanocomposites increased while the strength decreased with MMT. PLA chains were intercalated in MMT. The presence of Biostrong and MMT improved the thermal stability and crystallinity (X_c) of PLA. The storage modulus (E') values of PLA at 25–50 °C dropped with Biostrong while incorporation of MMT compensated the loss. It was also found that the biodegradation rate and permeability of PLA/Biostrong nanocomposites decreased with MMT.

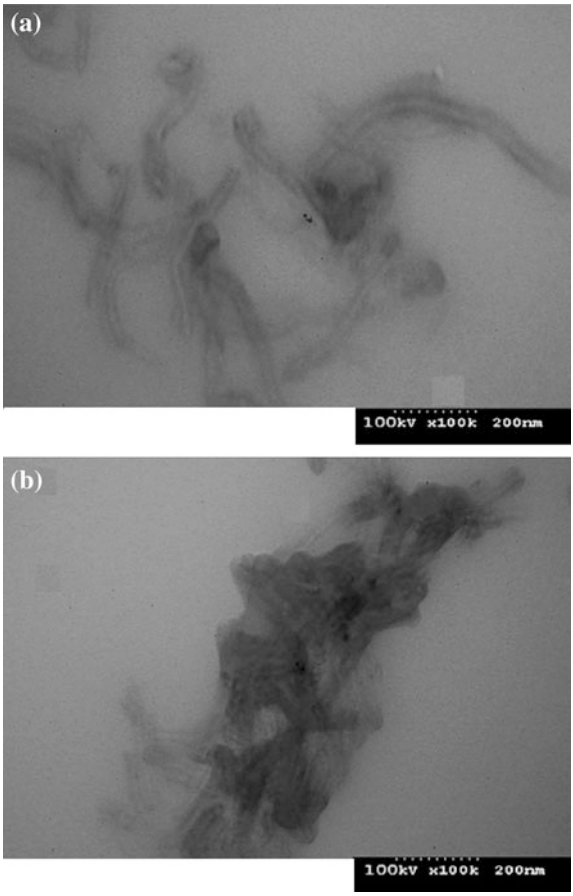

Fig. 11.5 **a** PLA/1 wt% MWCNT and **b** PLA/3 wt% MWCNT nanocomposites (Wu and Liao [71])

11.4.5 PLA/CNT Nanocomposites

Since their discovery in 1991 [63], carbon nanotubes have generated huge activity in most areas of science and engineering due to their unprecedented physical and chemical properties. No previous material has displayed the combination of enhanced mechanical, thermal and electronic properties attributed to them [64]. Carbon nanotubes also possess high flexibility, low mass density, and large aspect ratio (typically ca. 300–1000) as illustrated in Fig. 11.4. CNT have a unique combination of mechanical, electrical, and thermal properties that make nanotubes excellent candidates to substitute or complement the conventional nanofillers in the fabrication of multifunctional polymer nanocomposites. Some nanotubes are stronger than steel, lighter than aluminum, and more conductive than copper [65]. In particular, this combination of properties makes them ideal candidates as advanced filler materials in nanocomposites and the first polymer nanocomposites using carbon nanotubes as reinforcing filler were reported in 1994 by Ajayan et al. [66].

Song et al. [67] prepared PLA/CNT nanocomposites by one step based on in situ polycondensation of the commercially available lactic acid monomer in the presence of purified CNTs. The TEM image (Fig. 11.5) of core/shell nanostructures clearly indicates that the coating of grafted polymer was uniform both on the CNT's sidewall and tip. It was suggested that the incorporation of CNT into PLA will improvement its solubility and biocompatibility as it may promise a good future in biomedical systems and the development of bio-nanomaterials. The researchers also suggested that the current method of PLA/CNT nanocomposites preparation should be favored in industrialization as it takes less steps and cheaper.

Another study by Kobashi et al. [68] investigated the electrical resistance of melt-processed PLA/multi walled (MWCNT) nanocomposites. The researchers found good responses, reversibility and reproducibility of the resistance in 0.5–2.0 wt% MWCNT filled PLA/MWCNT nanocomposites depending on the kind of solvent as well as immersion and drying time. The MWCNT loading had a significant influence on the resistance change as larger changes were registered at lower MWCNT loadings with higher signal noises. It was also reported that PLA/MWCNT nanocomposites can sense poor solvents for PLA like ethanol, *n*-hexane, and water as well as good solvents like toluene, chloroform, tetrahydrofuran, and dichloromethane.

Kuan et al. [69] successfully prepared PLA/MWCNT nanocomposites through melt blending performed with co-rotating extruder. The researchers used water-crosslinking reaction in their effort to perform silane-grafting to improve interfacial adhesion of MWCNT with PLA. Mechanical analysis showed that the addition of 1phr of MWCNT would improve the tensile strength of PLA/MWCNT nanocomposites by 13 % while the degradation temperature of PLA improved with increasing MWCNT content. The researchers also found that the heat deflection temperature (HDT) of PLA (62 °C) improved to 106 °C with the addition of 1 phr MWCNT in PLA/MWCNT nanocomposites after 7 h of cross-linking reaction. This finding is useful in the application of biodegradable container. However, further addition of MWCNT can reduce the degree of water-crosslinking thus, the tensile strength of PLA/MWCNT nanocomposites has no significant improvement after long water-crosslinking reaction time and at higher loadings of MWCNT.

The effects of nano-structured carbon fillers [fullerene C60, single wall carbon nanotube (SWCNT), carbon nanohorn (CNH), carbon nanoballoon (CNB), and ketjenblack (KB) and conventional carbon fillers [conductive grade and graphitized carbon black (CB)]] on conductivity (resistance), thermal properties, crystallization, and proteinase K-catalyzed enzymatic degradation of PLA films were investigated by Tsuji et al. [70]. The researchers found that the addition of 1 wt% SWCNT effectively decreased the resistivity of PLA film compared with that of conventional CB. The crystallization of PLA further decreased the resistivity of films. The addition of carbon fillers, except for C60 and CNB at 5 wt%, lowered the glass transition temperature, whereas the addition of carbon fillers, excluding

C60, elevated softening temperatures, if an appropriate filler concentration was selected. On heating from room temperature, cold crystallization temperature was determined mainly by the molecular weight of PLA, whereas on cooling from the melt, the carbon fillers, excluding KB, elevated the cold crystallization temperature, reflecting the effectiveness of most of the carbon fillers as nucleating agents. Despite the nucleating effects, the addition of carbon fillers decreased the enthalpy of cold crystallization of PLA on both heating and cooling. The addition of CNH, CNB, and CB elevated the starting temperature of thermal degradation of PLA, whereas the addition of SWCNT reduced the thermal stability. Furthermore, the addition of C60 and SWCNT enhanced the enzymatic degradation of PLA, whereas the addition of KB and CNB disturbed the enzymatic degradation of PLA.

Wu an Liao, [71] successfully prepared biodegradable PLA/multi-walled carbon nanotubes (PLA/MWNTs) hybrids were prepared by means of a melt blending and acrylic acid grafted polylactide (PLA-g-AA) and the multihydroxyl-functionalized MWNTs (MWNT-OH) were developed for a comparative purpose to investigate the compatibility between PLA and MWNTs. The researchers found that the formation of ester bonds through dehydration of carboxylic acid groups in the PLA-g-AA matrix with grafted hydroxyl groups in the MWNT-OH resulted in better adhesion of MWNT-OH in PLA-g-AA compared to the adhesion of MWNTs in PLA. The TEM examination also proves that the formation of agglomerates of carbon nanotubes can be observed for hybrids with higher (>1 wt%) MWNT-OH content. As the result of DSC analysis, it can be also be found that the gap between Tg and Tm of the PLA-g-AA/MWNTseOH hybrid is smaller than that of the PLA/MWNTs hybrid implying that the compatibility between PLA and MWNTs has been enhanced. TGA tests showed that the PLA-g-AA/MWNT-OH hybrid with 1 wt% MWNT-OH gives an increment of 77 °C for the initial decomposition temperature. The effect of MWNTse OH content on tensile strength at break of PLA-g-AA/MWNTseOH hybrids was also similar. Maximum values of tensile strength of hybrid occurred at about 1 wt% of MWNTseOH and excess MWNTseOH reduced the compatibility of hybrid due to the inevitable aggregation of carbon nanotubes.

Another study by Wu et al. [72] focused on the development of the PLA nanocomposites with various functionalized MWCNTs prepared by melt mixing for morphological, rheological and thermal measurements. The surface functionalization influences the dispersion state of MWCNTs in the PLA matrix strongly as the carboxylic functionalized MWCNTs show relatively better dispersion than that of hydroxy and purified MWCNTs, which is due to the nice affinity between carboxylic group and PLA. For all composites, no remarkable improvement in thermal stability is seen at the initial stage of degradation, while with increase of decomposition level, the presence of carboxylic and purified MWCNTs retards the thermal depolymerization of PLA due to their barrier and thermal conductive effects, respectively.

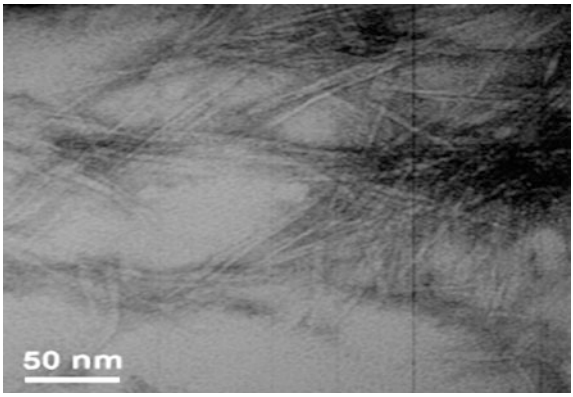

Fig. 11.6 TEM bright-field image of a microtomed foil of the solution cast cellulose whiskers-PLA nanocomposite (Kvien et al. [74])

11.4.6 PLA/CNW Nanocomposites

In effort to develop a fully green and biodegradable PLA nanocomposites, the field of PLA/cellulose nanowhiskers (CNW) had been explored. Cellulose nanowhiskers (CNW) have attracted significant attention during the last decade as potential nanoreinforcement in different polymers. Cellulose is abundant in nature, and is found in plants and can also be produced by bacteria. Cellulose nanowhiskers have good mechanical properties due to the binding forces of neighboring atoms [73]. As a result cellulose whiskers have far better mechanical properties than a majority of the commonly used reinforcing materials. In order to produce fully renewable and biodegradable nanocomposites both the polymer matrix and the nanoreinforcement have to be derived from renewable resources.

The use of cellulose nanowhiskers as nanoreinforcement is a new field in nanotechnology and as a result there are still many obstacles remaining to their use. Namely, cellulose nanowhiskers are not commercially available and their production is time consuming with low yields. In addition, they are difficult to be deployed in systems that are not water based due to their strong intermolecular hydrogen bonding thus, the CNW have to be transferred from water to an appropriate solvent for this type of PLA. In the past decade, the field of PLA/CNW still remained sow in progress due to these obstacles.

Unfortunately, both these modifications are complicated processes to carry out. There is also a negative side effect of using modified cellulose whiskers. It has been shown that modified whisker have less reinforcing effect than unmodified whiskers. Grunert and Winter [74] prepared nanocomposites with a hydrophobic thermoplastic matrix using trimethylsilylated cellulose whiskers. They found that unmodified whiskers showed a better reinforcing performance than the trimethylsilylated whiskers. Similarly, the mechanical properties of nanocomposites containing chemically modified chitin whiskers from crab shell were found to be inferior to the unmodified nanocomposites [75].

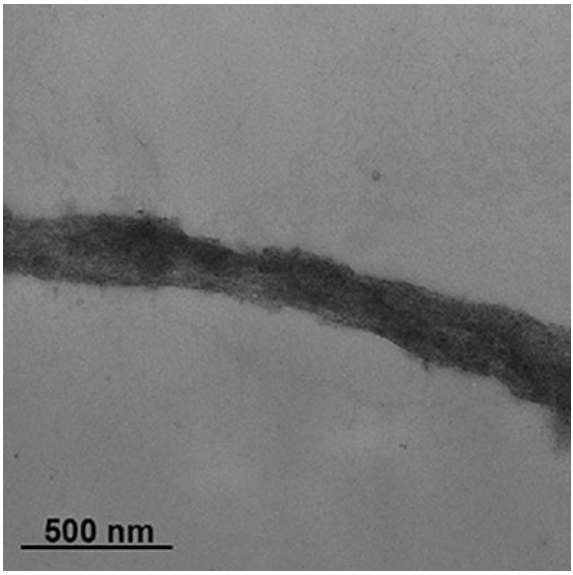

Fig. 11.7 TEM image of PLA/CNW nanocomposite film. (Petersson et al. [77])

Previous study by Kvien et al. [76] prepared CNW by acid hydrolysis of microcrystalline cellulose from wood and analyzed its structure and their nanocomposites with PLA via TEM and FE-SEM. From TEM images (Fig. 11.6), it was possible to identify individual whiskers, which enabled determination of their sizes and shape. TEM in such composite materials where contrast between the whiskers and the matrix is limited and the beam sensitivity is a major challenge.

FE-SEM allowed for a quick examination giving an overview of the sample; however, the resolution was considered insufficient for detailed information. FESEM applied on fractured surfaces allowed some insight into the morphology of the nanocomposite. The researchers revealed that the information obtained was restricted due to the influence of the metal coating applied on the fractured surfaces. An effort was made to obtain images without metal coating by lowering the accelerating voltage. However, the resolution appeared then to be insufficient.

Another study by Petersson et al. [77] revealed the preparation of PLA/CNW nanocomposites via solution casting using chloroform as solvent. The researchers also found that a compatibilizer or chemical treatment of the CNW is required in order to produce a stable suspension of cellulose whiskers in chloroform. FESEM and TEM (Fig. 11.7) revealed that the whiskers were best dispersed in the surfactant added PLA/CNW nanocomposites. It was expected that the surfactant would hinder hydrogen bonding between the CNW during freeze drying and further aid the distribution of the CNW in chloroform. When studying the surfactant added PLA/CNW material, it is believed that the surfactant did not have access to single whiskers but rather encapsulated several whiskers that were held together by hydrogen bonding. In order to make sure that single whiskers are

modified either a more efficient modifier has to be used or the whiskers have to be more vigorously stirred after the surfactant has been added to the water solution.

It is important when creating biodegradable nanocomposites that high demands are placed on the environmental impact of the surfactant. The DMA performed to investigate the thermal properties of the produced materials showed that the introduction of CNW were able to improve the storage modulus of PLA in the plastic zone. The researchers stated that the well dispersed CNW have a large potential in improving the mechanical properties of biopolymers such as PLA.

11.5 Future Directions

Despite the current efforts by researchers and polymer engineers in realizing the commercial potential of PLA to create a sustainable environment, there are a number of challenges which lie ahead to be overcome. Challenges from economic and technicality have to be faced to enable PLA to compete with petroleum based plastics in the near future. The high price of PLA at the current market is attributed to the tedious process of obtaining lactic acid and the polymerization process to produce PLA. Whereas from technical point of view, the limited toughness (i.e: impact strength) has urged researchers to developed a biodegradable impact modifier in the recent decade. Another challenge is to be able to identify and utilize process additives (i.e: compatibilizers, plasticizers) including PLA blends, that are derived from renewable resources to be consistent with the concept of sustainable materials. The introduction of natural fibers in PLA however, will have to meet several performance requirements such as expected degradability (biodegradability when required and not before). Resistance to moisture absorption, flame retardancy and embrittlement are also the major setbacks to be tackled. The development of PLA nanocomposites is ought to hold the future in the effort to develop the future material. Nevertheless, due to low number of effective applications, the acceptance of PLA nanocomposites has been relatively slow. Despite the setback, the properties of these nanocomposites up to now confirm that the promise of a dream material for the 21st century can be fulfilled. Further research is therefore necessary to develop a proper understanding of the formulation/structure/property relationship/toughening mechanisms and interactions involved in PLA nanocomposites system.

References

1. Jacobsen, S., Degée, P., Fritz, H.G., Dubois, P., Jerome, R.: Polylactide (PLA)-a new way of production. Polym. Eng. Sci. **39**(7), 1311–1319 (1999)
2. Jacobsen, S., Fritz, H.G.: Plasticizing polylactide-the effect of different plasticizers on the mechanical properties. Polym. Eng. Sci. **39**(7), 1303–1310 (1999)

3. Lim, J.W., Hassan, A., Rahmat, A.R., Wahit, M.U.: Morphology, thermal and mechanical behavior of polypropylene nanocomposites toughened with poly (ethylene-co-octene). Polym. Int. **55**, 204–215 (2006)
4. Hasegawa, N., Okamoto, H., Kawasumi, M., Usuki, A.: Preparation and mechanical properties of polystyrene–clay hybrids. J. Appl. Polym. Sci. **74**, 3359–3364 (1999)
5. Gupta, K., Rana, S.K., Deopura, B.: Mechanical properties and morphology of high-density polyethylene/linear low-density polyethylene blend. J. Appl. Polym. Sci. **46**, 99–108 (1992)
6. Wahit, M.U.: Rubber toughened polyamide 6/polypropylene nanocomposites: Mechanical, thermal and morphological properties. Ph.D. thesis. Universiti Teknologi Malaysia, Skudai (2006)
7. Baiardo, M., Frisoni, G., Scandola, M., Rimelen, M., Lips, D., Ruffieux, K., Wintermantel, E.: Thermal and mechanical properties of plasticized poly(L-lactic acid). J. Appl. Polym. Sci. **90**, 1731–1738 (2003)
8. Kulinski, Z., Piorkowska, E.: Crystallization, structure and properties of plasticized poly(L-lactide). Polymer **46**, 10290–10300 (2005)
9. Takayama, T., Todo, M.: Improvement of impact fracture properties of PLA/PCL polymer blend due to LTI addition. J. Mater. Sci. **41**, 4989–4992 (2006)
10. Takayama, T., Todo, M., Tsuji, H.: Effect of annealing on the mechanical properties of PLA/PCL and PLA/PCL/LTI polymer blends. J. Mech. Behav. Biomed. Mater. **4**, 255–260 (2011)
11. Semba, T., Kitagawa, K., Ishiaku, U.S., Hamada, H.: The Effect of crosslinking on the mechanical properties of polylactic acid/polycaprolactone blends. J. Appl. Polym. Sci. **101**(3), 1816–1825 (2006)
12. Chen, B.K., Shen, C.H., Chen, S.C., Chen, A.F.: Ductile PLA modified with methacryloyloxyalkyl isocyanate improves mechanical properties. Polymer **51**, 4667–4672 (2010)
13. Jiang, L., Wolcott, M.P., Zhang, J.: Study of biodegradable polylactide/poly(butylene adipate-co-terephthalate) blends. Biomacromolecules **7**, 199–207 (2006)
14. Li, Y., Shimizu, H.: Toughening of polylactide by melt blending with a biodegradable poly(ether)urethane elastomer. Macromol. Biosci. **7**, 921–928 (2007)
15. Liu, T.Y., Lin, W.C., Yang, M.C., Chen, S.Y.: Miscibility, thermal characterization and crystallization of poly(l-lactide) and poly(tetramethylene adipate-co-terephthalate) blend membranes. Polymer **46**(26), 12586–12594 (2005)
16. Anderson, K.S., Lim, S.H., Hillmyer, M.A.: Toughening of polylactide by melt blending with linear low-density polyethylene. J. Appl. Polym. Sci. **89**, 3757–3768 (2003)
17. Ishada, S., Nagasaki, R., Chino, K., Dong, T., Inoue, Y.: Toughening of poly(L-lactide) by melt blending with rubbers. J. Appl. Polym. Sci. **113**, 558–566 (2009)
18. Balakrishnan, H., Hassan, A., Wahit, M.U.: Mechanical, thermal and morphological properties of polylactic acid/linear low density polyethylene blends. J. Elastomers Plast. **42**(3), 223–229 (2010)
19. Natureworks LLC Website.: Technology Focus Report: Toughened PLA. http://www.natureworkspla.com. (2007). Accessed June 2011
20. Dupont Website.: Product Data Sheet. Dupont Biomax Strong 100. http://www2.dupont.com/DuPont_Home/en_US/index.html (2007). Accessed June 2011
21. Lanzillotta, C., Pipino, A., Lips, D.: New functional biopolymer natural fiber composites from agriculture resources. In: Proceeding of annual technical conference of the society of plastics engineers, vol. 60, pp. 2185 (2002)
22. Tokoro, R., Vu, D.M., Okubo, K., Tanaka, T., Fujii, T., Fujiura, T.: Mechanical properties of polylactic acid/bamboo fibers. J. Mater. Sci. **43**, 775–787 (2008)
23. Graupner, N., Herrmann, A.S., Mussig, J.: Natural and man-made cellulose fibre-reinforced poly(lactic acid) (PLA) composites: An overview about mechanical characteristics and application areas. Compos. A **40**, 810–821 (2009)
24. Wu, C.S.: Renewable resource-based composites of recycled natural fibers and maleated polylactide bioplastic: Characterization and biodegradability. Polym. Degrad. Stab. **94**, 1076–1084 (2009)

25. Qin, L., Qiu, J., Liu, M., Ding, S., Shao, L., Lu, S., Zhang, G.: Mechanical and thermal properties of poly(lactic acid) composites with rice straw fiber modified by poly(butyl acrylate). Chem. Eng. J. **166**(2), 772–778 (2011)
26. Sawpan, M.A., Pickering, K.L., Fernyhough, A.: Improvement of mechanical performance of industrial hemp fibre reinforced polylactide biocomposites. Compos. A **42**, 310–319 (2011)
27. Yussuf, A.A., Massoumi, I., Hassan, A.: Comparison of polylactic acid/kenaf and polylactic acid/rise husk composites: The influence of the natural fibers on the mechanical, thermal and biodegradability properties. J. Polym. Environ. **18**(3), 422–429 (2010)
28. Wu, C.S.: Improving polylactide/starch biocomposites by grafting polylactide with acrylic acid–characterization and biodegradability assessment. Macromol. Biosci. **5**, 352–361 (2005)
29. Shi, Q., Chen, C., Gao, L., Jiao, L., Xu, H., Guo, W.: Physical and degradation properties of binary or ternary blends composed of poly (lactic acid), thermoplastic starch and GMA grafted POE. Polym. Degrad. Stab. **96**, 175–182 (2011)
30. Rothon, R.N.: Particulate-Filled Polymer Composites. Longman Scientific & Technical, U.K. (1995)
31. Velasco, J.I., Desaja, J.A., Martinez, A.B.: Crystallization behavior of polypropylene filled with surface-modified talc. J. Appl. Polym. Sci. **61**, 125–132 (1996)
32. Audrey, W., Rahul, B., Amar, K.M.: Novel talc-filled biodegradable bacterial polyester composites. Ind. Eng. Chem. Res. **45**, 7497–7503 (2006)
33. Fowlks, A.C., Narayan, R.: The effect of maleated polylactic acid (PLA) as an interfacial modifier in PLA-talc composites. J. Appl. Polym. Sci. **118**, 2810–2820 (2010)
34. Huda, M.S., Drzal, L.T., Mohanty, A.K., Misra, M.: The effect of silane treated- and untreated- talc on the mechanical and physic-mechanical properties of poly(lactic acid)/newspaper fibers/talc hybrid composites. Compos. B **38**, 367–379 (2007)
35. Kim, H.S., Park, B.H., Choi, J.H., Yoon, J.S.: Mechanical properties and thermal stability of poly(L-lactide)/calcium carbonate composites. J. Appl. Polym. Sci. **109**, 3087–3092 (2008)
36. Wang, N., Zhang, X., Ma, X., Fang, J.: Influence of carbon black on the properties of plasticized poly(lactic acid) composites. Polym. Degrad. Stab. **93**, 1044–1052 (2008)
37. Giannelis, E.P.: Polymer-layered silicate nanocomposites: Synthesis, properties and applications. Appl. Organomet. Chem. **12**(10–11), 675–680 (1998)
38. Alexandre, M., Dubois, P.: Polymer-layered silicate nanocomposites: preparation, properties and uses of a new class of materials. Mater. Sci. Eng., R **28**(1–2), 1–63 (2000)
39. Ogata, N., Jimenez, G., Kawai, H., Ogihara, T.: Structure and thermal/mechanical properties of poly(L-lactide)-clay blend. J. Polym. Sci., Part B: Polym. Phys. **35**, 389–396 (1997)
40. Bandyopadhyay, S., Chen, R., Giannelis, E.P.: Biodegradable organic-inorganic hybrids based on poly(L-lactide). Polym. Mater. Sci. Eng. **81**, 159–160 (1997)
41. Pluta, M., Galeski, A., Alexandre, M., Paul, M.A., Dubois, P.: Polylactide/montmorillonite nanocomposites and microcomposites prepared by melt blending: Structure and some physical properties. J. Appl. Polym. Sci. **86**, 1497–1506 (2002)
42. Ray, S.S., Maiti, P., Okamoto, M., Yamada, K., Ueda, K.: New polylactide/layered silicate nanocomposites. 1. Preparation, characterization, and properties. Macromolecules **35**, 3104–3110 (2002)
43. Maiti, P., Yamada, K., Okamoto, M., Ueda, K., Okamoto, K.: New polylactice/layered silicate nanocomposites: Role of organocalys. Chem. Mater. **14**(11), 4654–4661 (2002)
44. Nam, J.Y., Ray, S.S., Okamoto, M.: Crystallization behavior and Morphology of biodegradable polylactide/layered silicate nanocomposite. Macromolecules **36**, 7126–7131 (2003)
45. Lee, H.J., Park, T.G., Park, H.S., Lee, D.S., Lee, Y.K., Yoon, S.C., Nam, J.: Thermal and mechanical characteristics of poly (L-lactic acid) nanocomposite scaffold. Biomaterials **24**, 2773–2778 (2003)
46. Krikorian, V., Pochan, D.J.: Poly(L-lactic acid)/layered silicate nanocomposite: Fabrication, characterization, and properties. Chem. Mater. **15**, 4317–4324 (2003)

47. Di, Y., Iannace, S., Maio, E.D., Nicolais, L.: Poly(lactic acid)/organoclay nanocomposites: Thermal, rheological properties and foam processing. J. Polym. Sci., Part B: Polym. Phys. **43**, 689–698 (2005)
48. Petersson, L., Oksman, K.: Biopolymer based nanocomposites: Comparing layered silicates and microcrystalline cellulose as nanoreinforcement. Compos. Sci. Technol. **66**, 2187–2196 (2006)
49. Pluta, M.: Melt compounding of polylactide/organoclay: Structure and properties of nanocomposites. J. Polym. Sci., Part B: Polym. Phys. **44**, 3392–3405 (2006)
50. Wu, T.M., Wu, C.Y.: Biodegradable poly(lactic acid)/chitosan-modified montmorillonite nanocomposites: Preparation and characterization. Polym. Degrad. Stab. **91**, 2198–2204 (2006)
51. Pluta, M., Jeszka, J.K., Boiteux, G.: Polylactide/montmorillonite nanocomposites: Structure, dielectric, viscoelastic and thermal properties. Eur. Polymer J. **43**, 2819–2835 (2007)
52. Jiang, L., Zhang, J., Wolcott, M.P.: Comparison of polylactide/nano-sized calcium carbonate and polylactide/montmorillonite composites: Reinforcing effects and toughening mechanisms. Polymer **48**, 7632–7644 (2007)
53. Chow, W.S., Lok, S.K.: Flexural, morphological and thermal properties of polylactic acid/organo-montmorillonite nanocomposites. Polym. Polym. Compos. **16**(4), 263–270 (2008)
54. Paul, M.A., Alexandre, M., Degée, P., Henrist, C., Rulmont, A., Dubois, P.: New nanocomposite materials based on plasticized poly(L-lactide) and organo-modified montmorillonites: Thermal and morphological study. Polymer **44**, 443–450 (2003)
55. Pluta, M.: Morphology and properties of polylactide modified by thermal treatment, filling with layered silicates and plasticization. Polymer **45**, 8239–8251 (2004)
56. Thellen, C., Orroth, C., Froio, D., Ziegler, D., Lucciarini, J., Farrell, R., D'Souza, N.A., Ann, J.: Influence of montmorillonite layered silicate on plasticized poly(L-lactide) blown films. Polymer **46**, 11716–11727 (2005)
57. Pluta, M., Paul, M.A., Alexandre, M., Dubois, P.: Plasticized polylactide/clay nanocomposites. I. the role of filler content and its surface organo-modification on the physico-chemical properties. J. Polym. Sci., Part B: Polym. Phys. **44**, 299–311 (2006)
58. Pluta, M., Paul, M.A., Alexandre, M., Dubois, P.: Plasticized polylactide/clay nanocomposites. II. the effect of aging on structure and properties in relation to the filler content and the nature of its organo-modification. J. Polym. Sci., Part B: Polym. Phys. **44**, 312–325 (2006)
59. Balakrishnan, H., Hassan, A., Imran, M., Wahit, M.U.: Toughening of polylactic acid nanocomposites: A short review. Polym. Plast. Technol. Eng. **51**(2), 175–192 (2012)
60. Li, T., Turng, L.S., Gong, S., Erlacher, K.: Polylactide, nanoclay, and core–shell rubber composites. Polym. Eng. Sci. **46**(10), 1419–1427 (2006)
61. Balakrishnan, H., Hassan, A., Wahit, M.U., Yussuf, A.A., Abdul Razak, S.B.: Novel toughened polylactic acid nanocomposites: Mechanical, thermal and morphological properties. Mater. Des. **31**, 3289–3298 (2010)
62. Balakrishnan, H., Masomi, I., Yussuf, A.A., Imran, M., Hassan, A., Wahit, M.U.: Ethylene copolymer toughened polylactic acid nanocomposites. Polym. Plast. Technol. Eng. **51**(1), 19–27 (2012)
63. Iijima, S.: Helical microtubules of graphitic carbon. Nature **354**, 56–58 (1991)
64. Coleman, J.N., Khan, U., Blau, W.J., Gunko, Y.K.: Small but strong: A review of the mechanical properties of carbon nanotube–polymer composites. Carbon **44**, 1624–1652 (2006)
65. Moniruzzaman, M., Winey, K.I.: Polymer nanocomposites containing carbon nanotubes. Macromolecules **39**, 5194–5205 (2006)
66. Ajayan, P.M., Stephan, O., Colliex, C., Trauth, D.: Aligned carbon nanotube arrays formed by cutting a polymer resin—nanotube composite. Science **265**, 1212–1214 (1994)
67. Song, W., Zheng, Z., Tang, W., Wang, X.: A facile approach to covalently functionalized carbon nanotubes with biocompatible polymer. Polymer **48**, 3658–3663 (2007)

68. Kobashi, K., Villmow, T., Andres, T., Pötschke, P.: Liquid sensing of melt-processed poly(lactic acid)/multi-walled carbon nanotube composite films. Sens. Actuators, B **134**, 787–795 (2008)
69. Kuan, C.F., Chen, C.H., Kuan, H.C., Lin, K.C., Chiang, C.L., Peng, H.C.: Multi-walled carbon nanotube reinforced poly(L-lactic acid) nanocomposites enhanced by water-crosslinking reaction. J. Phys. Chem. Solids **69**, 1399–1402 (2008)
70. Tsuji, H., Kawashima, Y., Takikawa, H., Tanaka, S.: Poly(L-lactide)/nano-structured carbon composites: Conductivity, thermal properties, crystallization, and biodegradation. Polymer **48**, 4213–4225 (2007)
71. Wu, C.S., Liao, H.T.: Study on the preparation and characterization of biodegradable polylactide/multi-walled carbon nanotubes nanocomposites. Polymer **48**, 4449–4458 (2007)
72. Wu, D., Wu, L., Zhang, M., Zhao, Y.: Viscoelasticity and thermal stability of polylactide composites with various functionalized carbon nanotubes. Polym. Degrad. Stab. **93**, 1577–1584 (2008)
73. Azizi Samir, M.A.S., Alloin, F., Dufresne, A.: Review of recent research into cellulosic whiskers, their properties and their application in nanocomposite field. Biomacromolecules **6**, 612–626 (2005)
74. Grunert, M., Winter, W.T.: Nanocomposites of cellulose acetate butyrate reinforced with cellulose nanocrystals. J. Polym. Environ. **10**, 27–30 (2002)
75. Gopalan, N.K., Dufresne, A., Gandini, A., Belgacem, M.N.: Crab shell chitin whiskers reinforced natural rubber nanocomposites. 3. Effect of chemical modification of chitin whiskers. Biomacromolecules **4**, 1835–1842 (2003)
76. Kvien, I., Tanem, B.S., Oksman, K.: Characterization of cellulose whiskers and their nanocomposites by atomic force and electron microscopy. Biomacromolecules **6**, 3160–3165 (2005)
77. Petersson, L., Kvien, I., Oksman, K.: Structure and thermal properties of poly(lactic acid)/cellulose whiskers nanocomposite materials. Compos. Sci. Technol. **67**, 2535–2544 (2007)

Chapter 12
Polyhydroxyalkanoates: The Natural Polymers Produced by Bacterial Fermentation

Bijal Panchal, Andrea Bagdadi and Ipsita Roy

12.1 Introduction

Polymers are mainly divided into two groups, natural polymers, such as proteins, cellulose, silk and synthetic polymers, such as polystyrene, polyethylene, and nylon. In some cases, naturally occurring polymers can also be produced synthetically. An important example is natural rubber which is known as polyisoprene in its synthetic form.

A plastic material is any of a wide range of synthetic or semi-synthetic organic solids used in the manufacture of industrial products [1]. They have been a necessity in our life, due to their versatility, outstanding mechanical properties and relatively low price. Plastics have been used universally for different purposes such as components in automobiles, home-appliances, computer equipment, packages, construction, sports and leisure equipment and also in medical applications [2]. Currently, the worldwide demand of plastics has increased to more than 100 million tonnes per year [3]. Although plastics are fantastic commercial materials for a large variety of applications, their inappropriate disposal has threatened the world's natural environment. Plastics of petrochemical origin are non-biodegradable in nature. In the UK, average households' packaging waste is around 3.2 million tonnes annually, while industries produce around 150 million tonnes of packaging waste annually [4]. Moreover, the rising price of the crude oil, depletion of the world's oil reserves and public awareness of the environmental effects of synthetically produced materials has created a lot of interest in the development of biodegradable plastics [4, 5]. Biodegradable plastics synthesised from renewable resources are now being considered as a potential replacement for commercial synthetic plastics due to

B. Panchal · A. Bagdadi · I. Roy (✉)
Applied Biotechnology Research Group, School of Life Sciences,
University of Westminster, London W1W 6UW, UK
e-mail: royi@wmin.ac.uk

S. Thomas et al. (eds.), *Advances in Natural Polymers*,
Advanced Structured Materials 18, DOI: 10.1007/978-3-642-20940-6_12,

their biodegradability and non-toxicity. This would help in sorting out the problem of plastic waste disposal [2].

Some synthetic polymers like, polyurethanes, specifically polyether-polyurethanes, are likely to be degraded by microbes but not completely. However, several polymers such as, polyamides, polyfluorocarbons, polyethylene, polypropylene, and polycarbonate are highly resistant to microbial degradation. Natural polymers are generally more biodegradable than synthetic polymers specifically, polymers with ester groups like aliphatic polyesters [1]. Therefore, several natural polymers such as cellulose, starch, blends of those with synthetic polymers, polylactate, polyester-amide, and polyhydroxyalkanoates (PHAs) have been the focus of attention in the recent years [3].

In 1920s, a French scientist called Maurice Lemoigne isolated a polymer of 3-hydroxybutyric acid (3HB) from the Gram-positive bacterium *Bacillus megaterium* [4, 5]. But it took nearly 30 years to commercialise the polymer. Later a PHA with 3HB and 3-hydroxyvalerate (3HV) was discovered from activated sludge [5]. Further, mcl-PHAs were discovered in 1983, more than 100 different monomers units have been incorporated into mcl-PHAs in order to produce PHAs with different physical as well as mechanical properties, to be utilized in various applications. PHAs are naturally occurring biodegradable and biocompatible polymers commonly found as storage compounds of carbon and energy in various microorganisms. These are produced in the presence of excess carbon and other nutrient limiting conditions for e.g. nitrogen, phosphorus, sulphur, magnesium or oxygen [6, 7]. There are more than 100 different known types of PHA monomers and more than 300 different PHA producing microorganisms known. The known producers of PHA include *Ralstonia eutropha* reclassified from *Alcaligenes eutrophus*, *Alcaligenes latus*, *Azotobacter vinelandii*, *Azotobacter chroococcum*, *Methylotrophs*, *Pseudomonads*, *Rhodobacter sphaeroides* and recombinant *Escherichia coli* [8]. The main properties of PHAs are biodegradability, insolubility in water, nontoxic, biocompatibility, piezoelectric, thermoplastic and/or elastomeric nature, which makes them favourable to be used in the packaging industry, medicine, pharmacy, agriculture, food industry and the paint industry [9].

12.2 Properties

PHAs are polyesters composed of several units of hydroxyalkanoate monomers linked to each other through ester linkages. Figure 12.1 represents PHA's general formula where 'n' is the number of monomer units in each polymer chain, which varies between 100 and 30,000, 'R_1' and 'R_2' the side chain that includes alkyl groups with 1–13 carbons and 'x' in the main chain which ranges from 1 to 4.

Numerous microorganisms synthesize PHAs by the fermentation of a carbon source and then accumulate them as intracellular carbon reserve inclusion bodies. In order to accumulate PHAs, in most bacteria an excess supply of carbon and limitation of nitrogen, phosphorus, oxygen or magnesium is required. These unfavourable growth conditions result in a decrease in cell growth and division, and a

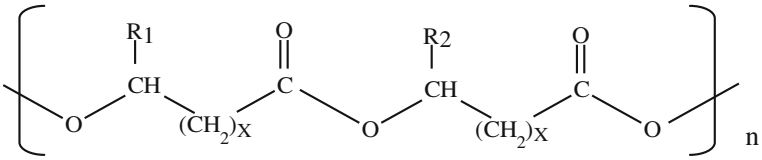

Fig. 12.1 General formula for PHAs. R_1/R_2: Alkyl groups C_1–C_{13}, x: 1–4, n: 100–30,000

redirection of their metabolism towards the biosynthesis of the PHAs [10]. The stored PHA can be degraded by intracellular depolymerases and metabolized as carbon and energy source when needed [11].

The properties of PHAs vary depending on the distance between ester groups in the molecule, the structure of the side groups and the number of monomer units in the polymer chain. For example, the length of the side chain and its functional group has a direct effect in the polymers physical properties such as flexibility, crystallinity, melting point and glass transition temperature [12]. The nature and proportion of the PHA monomers are influenced by the type and relative quantity of carbon sources supplied to the growth media, the organism used and the culture conditions provided [13]. For instance, based on growth conditions and the used microorganism, the molecular weight of the polymers can vary from 2×10^5 to 3×10^6 daltons [11].

PHAs can be either thermoplastic or elastomeric materials with variable mechanical, thermal stability and durability properties. They are water insoluble and impermeable to oxygen [14]. Due to the stereospecificity of the PHA synthase, all the hydroxyalkanoate monomers incorporated in the polymer are in the R(−) configuration, resulting in an optically pure polymer [15]. Additionally, they are biodegradable; hence, they can be degraded and metabolized by microbes and by enzymes within the human body; biocompatible, they do not generate toxic by-products and some of them are piezoelectric, a property known to stimulate cell growth [4].

Based on the number of carbon atoms in the monomer units PHAs can be divided in two main different groups: the short chain length polyhydroxyalkanoates (scl-PHAs), which consist of C_3–C_5 atoms, and the medium chain length polyhydroxyalkanoates (mcl-PHAs) consisting of C_6–C_{14} atoms [13]. Also, it has been observed that some organisms produce copolymers including both scl and mcl monomers, these are referred to as scl-mcl-PHAs. These groups are a consequence of the PHA synthase substrate specificity, which accepts precursors of a certain range of carbon length [16].

Poly(3-hydroxybutyrate) (P(3HB)), the simplest and most common example of the scl-PHAs, is highly crystalline, brittle, stiff and piezoelectric material with a melting temperature of 177 °C, glass transition temperature of 4 °C tensile strength of 40 MPa and elongation at break of 6 %. Its biological properties include, complete biodegradability, water resistance, high biocompatibility and a suitable substrate for tissue engineering which enhances cell adhesion, migration, proliferation and differentiation functions [17]. The mcl-PHAs such as poly(3-

Table 12.1 Comparison of the physical properties of P(3HB), a scl-PHA, P(3HO), a mcl-PHA and polypropylene [13, 23]

	scl-PHAs P(3HB)	mcl-PHAs P(3HO)	Polypropylene
Melting point (°C)	175	49	176
Glass-transition temp (°C)	15	−36	−10
Crystalline (%)	81	30	70
Young's modulus (GPa)	3.5	1.4	1.7
Tensile strength (MPa)	40	9	34.5
Elongation to break (%)	6	276	400

hydroxyhexanoate) (P(3HX)) or poly(3-hydroxyoctanoate) (P(3HO)) are thermoplastic elastomers with melting point, T_m ranging between 40 and 60 °C and glass transition temperature, T_g ranging between −50 and −25 °C. The mcl-PHAs have lower crystallinity with higher flexibility and softness. They are more thermally stable than scl-PHAs with an elastomeric nature which increases with the length of the side chain. These are also biodegradable, water resistant and biocompatible, which could be utilized in medical implants, such as scaffolding for the regeneration of arteries and nerve axons [18]. Table 12.1 describes the physical properties of P(3HB), a scl-PHA, P(3HO),a mcl-PHA, and polypropylene, a commonly used synthetic polymer. The crystallinity and tensile strength of P(3HB) are similar to those of propylene, however, the elongation to break is significantly lower than that of propylene. On the other hand, the Young's modulus and elongation to break values for, P(3HO) are comparable to those of propylene and dissimilar in terms of crystallinity and tensile strength. The scl-mcl PHA copolymers have properties intermediate between scl and mcl-PHAs [19]. Nowadays, most of the studies focus in the development of different types of copolymers for the production of tailor made materials to suit different applications. For example, one of the most commonly produced copolymers that is commercially available, is Poly(3-hydroxybutyrate-co-3-hydroxyvalerate)(P(3HB)-co-P(3HV)).This copolymer is more ductile, elastic and flexible than P(3HB) due to the presence of the 3HV groups [20]. Moreover, it has been reported that the increment in 3HV units results in a melting temperature, crystallinity and the tensile strength reduction, but an increment in flexibility, impact strength and ductility of the material [21]. These approaches make PHAs suitable for a wider range of applications and a promising class of new emerging biomaterial [22].

12.3 Biosynthesis of PHAs

PHA biosynthesis has been intensively studied over the years. Different metabolic pathways were described and the particular pathway used for PHA production was found to depend on the particular metabolic pathways that are operating in a

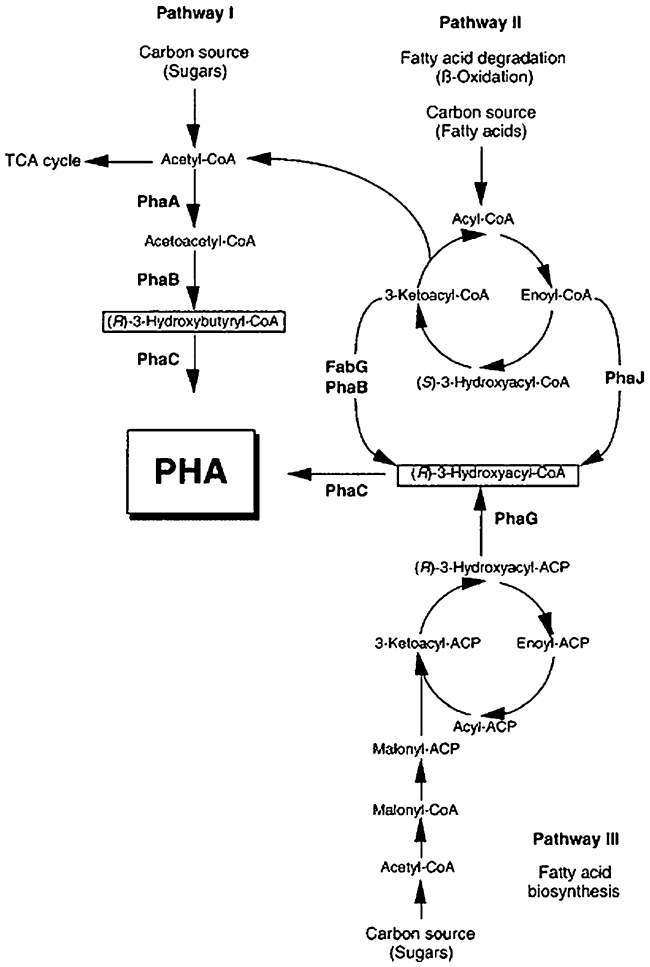

Fig. 12.2 Metabolic pathways involved in the biosynthesis of PHAs from related and unrelated carbon sources (adapted from [28])

particular microorganism and the carbon source provided. PHA biosynthesis can be divided in two main steps. The first step involves the synthesis of hydroxyacyl-CoA, the PHA's activated monomer units. The second step involves a reaction catalyzed by the PHA synthase which use the hydroxyacyl-CoA units as substrates and catalyze their polymerization into PHAs with the concomitant release of CoA [16]. The synthesis of the 3-hydroaxyl CoA units can occur mainly by three different pathways (Fig. 12.2) [24–27]. Two of the pathways involve the production of PHAs using carbohydrates as a carbon source and a third using fatty acids.

In the first pathway, PHA biosynthesis occurs from carbohydrates unrelated in structure to the final PHA monomer [28]. Three key enzymes are implicated:

β-ketothiolase, NADPH-dependent acetoacetyl-CoA reductase, and PHA synthase. The β-ketothiolase catalyzes the condensation of two acetyl-CoA molecules from the tricarboxylic acid cycle. The resulting acetoacetyl-CoA subunits are then converted to 3-hydroxybutyryl-CoA and the PHA synthase catalyzes the esterification of these subunits leading to the formation of P(3HB) [4]. This pathway can also be utilised for the synthesis of P(3HB-co-3HV).

The second pathway involves the production of PHAs via the fatty acid degradation pathway. In this case, the resulting monomers in the polymer chain were similar in structure to the carbon source or shortened by 2, 4 or 6 carbon atoms [29]. In this pathway the fatty acids are first converted to the corresponding acyl-CoA which are then oxidised by the β-oxidation pathway via enoyl-CoA, (*S*)-3-hydroxyacyl-CoA and 3-ketoacyl-CoA precursors. Finally, enzymes like the enoyl-CoA hydratase, hydroxyacyl-CoA epimerase, and β-ketoacyl-CoA reductase connect the β-oxidation pathway with the medium-chain length PHA biosynthesis through the PHA synthase [30].

The third pathway involves mcl-PHA production via the fatty acid de novo biosynthesis metabolic pathway. This pathway is of significant interest due to the ability of producing mcl-PHAs from carbohydrates that are structurally unrelated to the carbon source and are inexpensive [28]. In this pathway, the carbohydrates are first oxidized to acetyl-CoA molecules that enter into the fatty acid de novo biosynthesis. The fatty acid de novo biosynthesis leads to the formation of R-3-hydroxyacyl-ACP precursor which is then linked to the PHA synthase for the mcl-PHA biosynthesis via the (R)-3-hydroxyacyl-ACP-CoA transacylase [14].

12.4 Production of PHAs

Since the discovery of PHAs in 1926, production of PHAs has been widely studied in many living organisms. But the main candidates for the large-scale production of PHAs are plants and bacteria. Due to very low productivity of PHAs by plant cells (recombinant plants) [31], bacterial source of PHA production have been preferred in the world of PHAs research and development [32, 33]. However, PHA synthesis in crop plants is seen as an attractive system for the sustained production of large amounts of polymers at low cost. Moreover, awareness of the cost of the production and need of industrialisation of the polymer have reinforced the interest in scientists to develop cheap PHAs, equivalent in cost to starch which is extracted from crop plants. There have been some investigations on the possibility of producing P(3HB) in transgenic plants. A small oil seed plant (transgenic plant-*Arabidopsis thaliana*) was engineered to harbour the *A. eutrophus* PHA biosynthesis genes, this was found to accumulate P(3HB) granules. This shows that production of PHA by transgenic plants may be economically viable if efforts are concentrated on improving this process [13]. A variety of PHAs having different physical properties have now been synthesized in a number of transgenic plants, including *Arabidopsis thaliana*, rape seed and corn. This has been accomplished

through the creation of novel metabolic pathways either in the cytoplasm, plastid or peroxisome of plant cells. Beyond its impact in biotechnology, PHA production in plants can also be used to study some fundamental aspects of plant metabolism [34]. Despite all of the hindrances in the production cost of the PHAs, relatively high productivity has been achieved for P(3HB), (P(3HB-co-3HV)) and poly(3-hydroxyhexanoate-co-3-hydroxyoctanoate) (P(3HHx-co-3HO)) [5, 13].

PHAs are insoluble granules accumulated by bacteria as carbon and energy storage compounds in the cytoplasm under nutrient limiting conditions such as depletion of nitrogen for some bacteria e.g. *Azotobacter* spp. (most common limitation), phosphorous or oxygen (most effective limitation) while an excess amount of a carbon is maintained [4, 13, 33, 35]. However, there are some bacteria such as *A. eutrophus*, *A. latus* and mutant strain of *Azotobacter vinelandii* are known to accumulate PHAs even in the absence of nutrient limitation [13]. A wide variety of bacteria, both Gram-negative and Gram-positive have been studied for PHA production such as *Bacillus* spp., *Alcaligenes* spp., *Pseudomonas* spp., *Aeromonas hydrophila, Rhodopseudomonas palustris, Escherichia coli, Burkholderia sacchari* and *Halomonas boliviensis* [4, 33]. But *Cupriavidus necator* (formerly known as *Ralstonia eutropha* or *Alcaligenes eutrophus*) [36, 37] is the most widely studied organism [33]. Spore-forming *Bacillus* strains are known to produce a novel terpolymer but because of the polymer production and spore forming events going on simultaneously in the cells, there is a noticeable decrease in the polymer synthesis. Therefore, non-spore forming mutants of *Bacillus* have been of interest to get PHAs [33, 38]. Moreover, *Bacillus cereus* SPV was found to be capable of using a wide range of carbon sources including fructose, sucrose and gluconate for the production of 3HB, 3HV and 4-hydroxybutyrate (4HB)-like monomer units [39]. Also, different culture conditions of potassium, nitrogen, sulphur and phosphate limitations led to the production of both 3HB and 3HV monomers from the structurally unrelated carbon source, glucose [40]. Also, genetic engineering has been used to improve polymer production by optimising microbial metabolism. For example, *Escherichia coli* strains [41] have been genetically modified to produce ultra high molecular weight P(3HB) with an M_w up to 10^7 Da using glucose as the carbon source to make very strong films [33, 42].

As compared to traditional petro-chemically synthesised plastics, microbially synthesised PHAs are rather expensive and less in yield which restricts their use for industrial applications. Therefore, it needs further investigation to overcome these disadvantages and try an extensive range of PHA production with varying characteristics to be utilised for mass production at the industrial level [5]. Several strategies have been tried to improve conditions for efficient PHA production with the cost effectiveness [13, 43–45]. Several factors need to be considered such as the type of microorganisms (e.g. Gram-negative or Gram-positive) with the ability to utilize an inexpensive carbon source and with high growth rate and with high polymer synthesis rate. In addition, media ingredients, fermentation conditions, modes of fermentation (batch, fed-batch, continuous) and recovery also effect the cost of PHA production and their commercial utilisation [5, 13].

The choice of media is very important not only to supply optimal conditions for production of a variety of PHAs in different bacteria but also to do so with high volumetric productivity to provide a final product that is economically competitive with the traditional plastics [5]. Some workers have also derived an equation that can predict the PHA yield on several carbon sources [46] which could be used for the preliminary calculation of PHA yields and know the target cost of the production [13]. As the major cost in the production is the medium, recently researchers have been exploring cultivation strategies involving inexpensive, renewable carbon substrates in order to reduce production cost and obtain high productivity [7, 13]. Low cost media including molasses, corn steep liquor, whey, wheat, rice bran, starch, starchy wastewaters, effluents from olive mill, palm oil mill activated sludge and swine waste have been developed [5, 13, 22, 47]. The choice of media also depends on the type of the microorganism i.e. whether the producing organism is wild type or recombinant and whether it needs nutrient limiting conditions [48]. Therefore, it is now possible to produce different types of homopolymers and copolymers with different molecular weights and more than 100 different types of monomers using different media [39, 48–50].

In order to reduce the overall cost, there has been many fermentation techniques developed to produce PHAs with high productivity and high yield such as batch, fed-batch and continuous cultivations [5, 13]. Two stage fermentation is the most common and highly productive method to generate high density culture as well as increased amount of PHAs.

Recovery of PHAs should also be considered because it significantly affects the overall process economics [13]. Initially, for extraction and purification of P(3HB), solvent extraction has been carried out using solvents including chloroform, methylene chloride, propylene carbonate, and dichloroethane. In this method the cell walls are broken and the polymer was then extracted and purified. However, large amount of solvent is required due to the high viscosity of PHAs, this makes the method economically unattractive. Sodium hypochlorite has also been used during the recovery process. Although the use of sodium hypochlorite significantly increased PHA degradation, polymer purity greater than 95% was achieved [5, 13]. Therefore, organic solvent extraction, enzymatic digestion, pretreatment of cells, cell disruption, chemical or enzymatic digestion of non-polyhydroxyalkanoates in the system, spontaneous liberation of P(3HB), dissolved air flotation and extraction using supercritical CO_2 are the interesting downstream processes that have been developed to recover the PHAs [5, 13].

12.5 Composites of PHAs

After the discovery of PHAs in 1920s, it took nearly 30 years to commercialise P(3HB). However, the brittleness of P(3HB) inspired scientists to develop polymer composites in order to improve polymer property [51].

P(3HB) has been used to make natural fibre/biopolymer composites using flax and P(3HB). The biopolyesters consisting of the homopolyester P(3HB) and its copolymers with 5 and 12 % 3HV, P(3HB-co-3HV), showed better adhesion with the fibres than the analogous polypropylene composites. This composite was characterised using SEM and observed results showed good adhesion, increased nucleation, improved melting temperature, bending modulus and storage modulus [52, 53].

The fragility of P(3HB) and its poor bioactivity restrict its application in bone-tissue repair. Hence, composites were prepared by incorporating bioactive ceramic materials in order to achieve higher strength, increased bioactivity, and altered degradation behaviour. Hydroxyapatite (HA) has been used to make composites with PHAs because it is the principal crystalline constituent of bone and provides compression strength to the bone by forming strong chemical bonds with surrounding bone. In one study HA, tricalcium phosphate (TCP) and coral powder were incorporated into P(3HB) to generate a bioactive and biodegradable composite for applications in hard tissue replacement and regeneration which showed great results in vitro as well as in vivo. Addition of HA increased bonelike apatite formation on the composite within a short period demonstrating increased in vitro bioactivity of the composite. It is possible to vary mechanical and bioactivity properties by using different concentrations of HA particles in composite making [54–57]. In other instance, three composites of P(3HB) with HA, HA/glass and carbon fibre reinforced polysulfone (CFRP) were implanted in the femur of mature Japanese white rabbits for 8 weeks. There was an increase in interfacial shear strength (ISS) observed but carbon fibre reinforced polysulfone (CFRP) composite showed better results due to their surface morphology allowing deep in growth of the soft tissue [58].

Moreover, P(3HB)/HA and P(3HB-co-3HV)/HA composites have also been considered for fracture fixation application since they have a mechanical strength in compression of 62 MPa, which is about the same order of magnitude of several human bones [59]. In vivo study on HA/P(3HB-co-3HV) composite was tested into tibias of rabbits. Regenerative ability of the composite was found good morphologically, biologically and chemically. Moreover, the composites remained active throughout the period of study which showed increased thickness of the newly formed bone from about 130 mm at 1 month to about 770 mm at 6 months [60]. Another approach of using bioactive ceramics has also been explored by preparing composite films of P(3HB)/Bioglass® particles (5 and 20 wt% concentrations). The presence of Bioglass® in the polymer matrix reduced the degree of crystallinity of the polymer, increased the glass transition temperature and reduced the Young's modulus of the composite. A 28 days in vitro bioactivity study in simulated body fluid (SBF) confirmed the bioactivity of the composites by the formation of HA crystals on the composites' surface [58].

The approach of making porous composites of P(3HB-co-3HV) with sol–gel bioactive glass (SGBG) and calcium phosphate-loaded collagen (CaP-Gelfix) foams have been tried for bone-tissue engineering. It was found to be useful since it showed formation of a HA layer on the surface of P(3HB-co-3HV)/SGBG

composite after 12 h immersion in SBF. Moreover, fibrous tissue formation was observed within 6 weeks of implantation in vivo and increased reattachment of the osteoblast cells respectively [61–64].

Natural polymers such as starch and protein are potential alternatives to petroleum-based polymers for a number of applications. Unfortunately, their high solubility in water limit their use for water sensitive applications. To solve this problem thermoplastic starches have been laminated using water-resistant, biodegradable polymers. For example, polylactic acid and P(3HB-co-3HV) were utilised as the outer layers of the stratified polyester/PWS (plasticized wheat starch)/polyester film structure in order to improve the mechanical properties and water resistance of PWS which made it useful for food packaging and disposable articles [65]. Moreover, improved physic-chemical interactions between P(3HB-co-3HV) and wheat straw fibres were achieved with high temperature treatment. It resulted in increased P(3HB-co-3HV) crystallization, increased Young's moduli and lowered values of stress and strain to break than the neat matrix of P(3HB-co-3HV). There was no difference in the biodegradation rate of the polymer [66].

12.5.1 Blends

The difficulty in finding new materials with specific characteristics for different applications has been traditionally overcome by the blending of the existing ones. PHA blending is a technique which allows an optimization of the chemical, structural, mechanical, morphological and biological properties of a material by improving the material's desirable properties or by minimizing the undesirable ones [67]. The blending of two or more materials in different ratios can result in changes in the final product degradation rates, stiffness and elasticity, among other properties, allowing their exploitation in a wider range of applications.

According to the level of miscibility of the different compounds, blends can be divided into three groups, including miscible, partially miscible and immiscible. For miscible blends the constituent polymers mix at a molecular level to form a homogeneous material. In contrast, in the case of immiscible blends the constituent polymers do not mix. In most of the cases a miscible blend will have properties between those of the two unblended materials and these properties will be directly related to the ratio of each compound in the resulting blend. In the case of an immiscible blend the material will present different properties which in most cases will correspond to each unblended material. For example, the blend obtained using P(3HO) and poly(lactid acid) (PLA) exhibit two glass transitions temperatures corresponding to those of pure P(3HO) and PLA [68].

Varieties of blends with different types of PHAs have been produced. P(3HB) is the most common, lowest cost and commercially available member of the PHAs. Although P(3HB) can be considered as a polymer of high potential for numerous applications, its low crystallization rate and brittle nature is a disadvantage in some cases [69]. Several studies were carried out to enhance P(3HB) mechanical and

processability properties through blending the polymer with other biodegradable or non-biodegradable polymers. Among the biodegradable materials used for blending with P(3HB) are: different types of PHAs, poly(ethylene-oxide), poly(ε-caprolactone), polylactide, cellulose-ester, poly(vinyl alcohol), chitosan, chitin and polyglutamate. On the other hand, the non-biodegradable polymers used for the P(3HB) blends include poly(vinyl acetate), poly(vinyl acetate-co-vinyl alcohol), polymethacrylate and poly(vinyl phenol) [70].

Several PHAs were also blended with P(3HB). For example, Satoh et al. 1994 [71] describes the possibility of regulating P(3HB) biodegradability by blending this material with P(3HB)-co(3HV). They have concluded that the rate of degradation of the polymer blend was accelerated with respect to P(3HB) alone. In addition, they have proven that there is a linear correlation between crystallinity and degradation rate.

Blends containing poly(ethylene-oxide) (PEO) have also been investigated due to the material hydrophilicity and low toxicity. These blends were studied in terms of thermal and mechanical behaviour. It was described that these blends were immiscible and that both melting temperature and glass transition temperature decreased proportional to the amount of PEO in the blend. They also observed a reduction in the crystallinity of P(3HB) in the presence of PEO [72–74].

Poly(ε-caprolactone) (PCL), on the other hand, is a semi-crystalline biodegradable polymer. This material is commonly used as plasticizer. The P(3HB)/PCL blend exhibited partial miscibility, however, the elongation at break was increased about 81 % in comparison with pure P(3HB) [43].

One of the most studied blends has been the one composed of P(3HB) and polylactide, both commercially available polymers with superior thermal and mechanical properties than other commercial polymers. Polylactide is a chemically synthesized, biodegradable thermoplastic and derived from renewable resources. It has been shown that this blend exhibited greater flexibility and hydrolytic biodegradation than the Polylactide or P(3HB) alone [75].

In terms of the P(3HB) blending with non-biodegradable polymers, it was observed that some of the materials become biodegradable after blending with biodegradable ones. This indicates that the degradation properties of a material can be modified by blending [76]. Poly(vinyl acetate) has also been used to create blends with P(3HB). This resulting blend can form a completely miscible system. In this case, it has also been observed that a small addition of poly(vinyl acetate) results in an increment in the tensile strength [77].

12.5.2 Applications of PHAs

As mentioned in the introduction section that commercial plastics became a necessity in our life due to their versatility, outstanding technical properties and relatively low price. This has resulted in an increased worldwide demand of plastics more than 100 million tonnes per year and expanding at around 4–5 % per

annum [4, 78]. In 1990, about 25 % of the plastics market (about 7.5 million tonnes) was consumed by the packaging industry. In 1993, it was predicted that the demand for biodegradable materials would increase within 3 years and a major portion of that demand would be from the packaging industry [4]. More use means more waste and so it made plastic waste a global problem. Therefore, in recent years, there has been more interest in developing biodegradable polymers rather than synthetic non-degradable plastics costing twice as much for their waste disposal.

12.5.3 Bulk Applications

The PHAs are non-toxic, biocompatible, biodegradable thermoplastics that can be produced from renewable resources. They have a high degree of polymerization, are highly crystalline, optically active and isotactic (stereochemical regularity in repeating units), peizoelectric and insoluble in water. These features make them highly competitive with polypropylene, the petrochemical-derived plastic. PHAs have a wide range of applications owing to their novel features. Initially, PHAs were used in packaging films mainly in bags, containers and paper coatings. Similar applications of PHAs as conventional commodity plastics include the disposable items, such as razors, utensils, diapers, feminine hygiene products, cosmetic containers—shampoo bottles and cups [48, 79, 80]. The first consumer product made out of PHAs was launched in April 1990 by Wella AG. They tested their Sanara range of biodegradable shampoos in bottles made of Biopol (ICI, UK). Over the last decade, applications have increased both in variety and specialisation. PHA latex can be used to cover paper or cardboard to make water-resistant surfaces as opposed to the combination of cardboard with aluminium that is currently used and is non-biodegradable. This also works out be cost-effective since a very small amount of PHAs is required for this purpose. PHAs can be used to make foils, films and diaphragms [22, 81]. The polymer thus produced is used to make articles such as combs, pens and bullets. The polymer pellets are sold commercially for use in classical transformation processes. The melted polymers have low viscosity, permitting the injection moulding of objects with thin walls. The end product is very hard and can be used at temperatures from −30 to 120 °C. This product degrades within 2 months in the environment [4, 82]. Metabolix, a US-based company, now markets among others, Metabolix PHA which is a blend of P(3HB) and P(3HO). This is an elastomer that has been approved by the FDA for production of food additives [4, 80, 81].The polymer poly(3-hydroxybutyrate-co-3-hydroxyhexanoate) (P(3HB-3HHx)) is used to make flushables, nonwovens, binders, flexible packaging, thermoformed articles, synthetic paper and medical devices. It is also possible to use PHAs to make the following articles due to their piezoelectric nature: pressure sensors for keyboards, stretch and acceleration measuring instruments, material testing, shock wave sensors, lighters, gas lighters; acoustics: microphone, ultrasonic detectors, sound pressure measuring

instruments; oscillators: headphones, loudspeakers, for ultrasonic therapy and atomization of liquids. The gas barrier property of P(3HB-co-3HV) is useful for applications in food packaging and for making plastic beverage bottles. The same property can be exploited to make coated paper and films which can be used for coated paper milk cartons. P(3HB) or its copolymers can be used to make the non-woven cover stock and the plastic film moisture barriers in nappies and sanitary towels along with some speciality paramedical film applications in hospitals.

Copolymer of PHAs containing mainly P(3HB) and small quantities of MCL monomers has been used as biodegradable mulch films known as Nodax^{TM} for agricultural purposes such as a coating for urea fertilizers to be used in rice fields or for herbicides and insecticides. Insecticides could also be mixed into P(3HB-co-3HV) pellets which could then be sown along with the seeds of the crops. This will help in the controlled release of insecticides. Furthermore, studies have been carried out to increase the nitrogen fixation in plants by *Azospirillum brasilense* (nitrogen fixing organism) inoculants containing high amounts of intracellular PHA in order to enhance crop yield. Intracellular PHA helps bacterial cells to survive for long time in stressful environmental conditions such as desiccation and hot conditions [59, 81–83].

12.5.4 Biomedical Applications

PHAs are natural polymers which are also present in vivo, hence their metabolism and elimination are well understood. Therefore PHAs are attractive materials for biomedical applications because of their natural origin, enhanced biocompatibility, biodegradability, lack of cytotoxicity, ability to support cell growth and cell adhesion [9]. PHAs have been utilized in different biomedical applications such as medical device development including sutures, stents, nerve repair devices and wound dressing [9]. Moreover, PHAs provide cell adhesion, migration, differentiation and proliferation functions [17].

12.5.4.1 Cardiovascular

One of the main medical application of PHAs are as cardiovascular products due to increasing threats of death caused by cardiovascular diseases worldwide. There have been several research developments in order to obtain alternative materials as opposed to synthetic polymers which are unable to repair, regenerate and have high risks of immune responses. The ideal properties required for a cardiovascular product are long lasting, resistance to infection, lack of immunogenicity, induce regeneration and repair by increasing cell adhesion and growth [84–86]. PHAs have been studied as cardiovascular products, such as pericardial patches to prevent postsurgical adhesions between the heart and the sternum, artery augmentation, atrial septal defect repair, vascular grafts and heart valves, but pericardial

patch made from biodegradable P(3HB) has been the most advanced and important development in cardiovascular devices. These patches are used after heart surgery to seal the pericardium and prevent adhesions between heart and sternum [9, 87]. To study tissue response towards the P(3HB) patch, in vivo work on 18 sheep were carried our initially, showing less inflammation, no infection and lack of adhesion formation in the test animals receiving P(3HB) patches compared to control animals in which the pericardium was left open. Apart from animal studies, 39 human patients were also examined for post surgical adhesions after heart bypass or vascular replacement. 19 patients were implanted with P(3HB) patch and 20 patients were left without P(3HB) patch. The group of patients receiving the P(3HB) patch showed lower incidence of postsurgical adhesions than patients without the P(3HB) patch [9, 87]. Biodegradable non-woven P(3HB) patches were also utilized for artery augmentation to regenerate arterial tissue in low-pressure systems [9, 87]. P(3HB) patches were compared against standard Dacron patches showing good regeneration of endothelial layers on both sides and native arterial tissue regeneration with smooth muscle cells, collagen and elastic fibres on it. P(4HB) in a highly porous foam form was also tried in artery augmentation giving very good tissue regeneration without any thrombus, dilation or stenosis [8, 9, 87]. A non-woven P(3HB) patch has also been used to repair atrial septal defects giving complete endothelial regeneration on both sides of atrium with sub-endothelial collagen layer and smooth muscle cells [87]. Cardiovascular stents made of metallic materials have problems of restenosis due to excessive growth of the blood vessel wall which has inspired scientists to develop alternative absorbable materials to prevent reocclusion of the vessel wall. For that, initially a homopolymer of P(3HB) and P(3HB-co-3HV) with drug delivery systems were tried as biodegradable stents in vivo resulting in temporary proliferation of the atrial cells and rapid degradation of the polymers on site within 4 weeks [87]. Nowadays, vascular grafts are being used to repair or replace compromised blood vessels in arterial or venous systems that have been damaged or diseased, for example atherosclerosis, aneurysmal disease or traumatic injury. Hence, poly(3-hydroxybutyrate-co-4-hydroxybutyrate) (P(3HB-4HB) were evaluated as cardiovascular graft coating showing early degradation within 2 weeks of implantation but poly(3-hydroxyoctanoate-co-3-hydroxyheptanoate) (P(3HO-co-3HH)) showed mild tissue reaction with later degradation at 6 months. P(3HO-co-3HH) has also been combined with non-woven PGA, Poly(glycolic acid) mesh on the inside layers and then seeded with endothelial cells, smooth muscle cells and fibroblasts. On the 7th day after seeding, these conduits were transferred to abdominal aortic segment in lambs and checked for tissue response. The end results were productive, giving less inflammatory reactions and increased cell density, collagen formation and native aorta like mechanical properties [9, 87]. Moreover, recently P(4HB) scaffolds were also tried in sheep models and resulted in fully functional native aorta like growth [9]. The most extraordinary cardiovascular application of the PHA polymers is the use of them in making of heart valves to repair deficiencies in mechanical properties of the valves or even outgrown valves in the young children. Although initially scientists tried PGA-PLA (Poly(glycolic acid)-Poly(lactic acid))

to replace single pulmonary valve leaflet in lambs, attempt of replacing all 3 valves failed due to the high rigidity and stiffness of the PGA-PLA material. This led scientists towards PHAs to overcome these mechanical property problems [88]. P(3HO-co-3HH) film in between the two layers of the PGA mesh showed great potential for replacing the defective heart valves. In in vitro conditions, this scaffold showed good vascular cell growth in the direction of the flow. Improvement in the design of the valve scaffold has also been investigated with porous P(3HO-co-3HH) resulting in growth of the vascular cells in the pores of the polymer scaffold, forming a solid layer in the direction of the pulsatile flow [9, 87]. However, the most amazing result to date for heart valve is the regenerated fully functional trileaflet heart valve resembling the native valve after 20 weeks of in vivo implantation using P(4HB) coated on a PGA mesh [9, 87].

12.5.4.2 Wound Treatment

The ideal properties for the wound healing sutures are easy handling, lack of immunogenic reactions, good tensile strength, absorbability and knot security. There are two types of sutures, natural and synthetic. Early researchers in the mid 1960s led to the recommendation of P(3HB) as an absorbable suture. P(3HB) and P(3HB-co-3HV) sutures were implanted in the female wistar rats and compared with absorbable catgut and nonabsorbable silk sutures. P(3HB) and P(3HB-co-3HV) sutures showed positive results including less inflammatory reactions, necrosis and carcinogenesis. Moreover, P(3HB-co-4HB) film was also used in the abdominal cavity of the rat after surgery in the intestine to prevent adhesion between skin and intestine which showed healing after 1 month but failed to degrade even after 1 year which demanded further improvement in the polymer properties [9]. In 1986 Webb and Adsetts investigated use of volatile solutions of P(3HB) and P(3HB-co-3HV) that forms thin film over the naked wound in case of emergency to prevent air borne bacterial contamination. However, this process was risky due to the health hazards associated with chlorinated solvents. Steel and Norton-Berry in 1986 also described wound dressings based on P(3HB) prepared in nonwoven fibrous form which could be used as swabs, gauze, lint or fleece [87].

12.5.4.3 Nerve Tissue Engineering

There has been interesting progress in neurological science to cure peripheral nerve injuries as well as spinal cord injuries. Nerve regeneration is a complex phenomenon which needs four major components such as a scaffold for axonal proliferation, support cells like Schwann cells, growth factors and extracellular matrix [89, 90]. The peripheral nervous system damage is easy to cure compared to spinal cord injuries which lead to the disruption of continuous axonal growth and therefore it is life threatening for the patient. While peripheral nerve injuries can regenerate on their own if injuries are small, for larger injuries, nerve grafts from

elsewhere in the body can need to be used in order to repair the injured nerves [91]. Two major products such as conduits and carrier scaffolds have been developed to repair both peripheral as well as spinal cord nerve injuries [9]. Many natural (e.g. collagen, chitosan, alginate, laminin, fibronectin) and synthetic (e.g. silicone, ethylene vinyl co-acetate, ethyl vinyl acetate-co-polymer, poly(lactide-co-glycolide) [PLG]) polymers have been used for nerve tissue engineering as they enhance cell adhesions and direct neurite growth. Unfortunately, the conduits and carrier scaffolds made of these polymers can bridge only limited distance in the nerve gap and produce acidic end products after degradation which enhance inflammatory reactions [89, 90]. Therefore the biocompatible, biodegradable and piezoelectric polymers, PHAs, have great potential for use in the treatment of nerve injuries [9].

In many cases in vivo work has been carried out using P(3HB) to regenerate nerve tissues, for example P(3HB) has been used to repair transected superficial radial nerves in cats for an experimental period of 12 months which showed normal inflammatory response and axonal regeneration of 2–3 mm nerve gap [92, 93]. While another experiment on rat sciatic nerve showed axonal regeneration of 10 mm nerve gap with low inflammation [92, 93]. P(3HB) has also been used as the carrier scaffold for nerve regeneration after spinal cord injury in which matrix components and cell lines were coated in the polymer material to support neuronal survival. Grafts made of P(3HB) coated with alginate hydrogel and fibronectin was implanted in adult rat with a cervical spinal-cord injury to check neuronal regeneration. To compare the results, animals were treated intrathecally with neurotrophic factors such as brain derived neurotrophic factor (BDNF) or neurotrophin-3 (NT-3) [94]. This experiment showed that P(3HB) decreased cell loss up to 50 % and caused regeneration of axons along the entire length of the P(3HB) graft, after addition of neonatal Schwann cells. Not only P(3HB) but P(4HB) has also been explored for nerve regeneration which showed more axonal regeneration and restoration of sensory functions than P(3HB) [95]. P(4HB) has also been used as carrier scaffolds because of its high tensile strength and less inflammatory reactions in vivo compared to synthetic polymers e.g. poly(L-lactic acid) (PLLA) and poly(glycolic acid) (PGA). These examples show that PHAs have great potential as materials for nerve tissue engineering. Previous research has also mentioned that high porosity of these materials can increase nerve regeneration by allowing accessibility of growth factors and nutrients to cells from the surrounding tissues [96]. Therefore many nano-fibre polymers have been tested to achieve high surface area with high porosity which could support neuron growth, more specifically than the solvent cast polymer films. The electrospinning technique can be used generate polymeric fibres of 100 nm–1 μm which could enhance cell migration, proliferation and differentiation [97–99]. Hence, many electrospun polymers such as chitosan, poly(3-caprolactone), poly(L-lactide-co-glycolide) (PLGA) and PHAs have already been tried in nerve tissue engineering to get better nerve regeneration. Electrospun scl-PHAs were used to check the behaviour of rat cerebellar granule neurons (rCGNs) which showed higher viability of these cells on electrospun PHA membranes than PHA films [100].

12.5.4.4 Drug-Delivery Systems

In traditional methods drugs have been given intravenously or via extravascular routes to the patients which unfortunately doesn't allow the required concentration of the drugs at the target site for longer periods of time. This disadvantage in the drug delivery systems has inspired the development of controlled release of the drug at the target site extending its time of action. Biodegradable polymers such as homo- and copolymers of lactate and glycolate are widely used in commercially available sustained release products for drug delivery providing 30 day release at the site. However, lactate and glycolate co-polymers degrade by bulk hydrolysis. Hence drug release cannot be fully controlled. Therefore, scientists started looking for an alternative material for controlled release of the drug. All the efforts became productive when PHAs started being used as the carrier material due to their biodegradability, biocompatibility and their degradation by surface erosion in early 1990s. Compressed P(3HB) tablets were investigated for in vitro and in vivo release of 7-hydroxyethyltheophylline. This study concluded that drug release is dependent on matrix porosity, copolymer composition and the molecular weight of the drug and was independent of the molecular weight of the polymer. P(3HB) was also tested for long term controlled release of metoclopramide in the treatment of cattle disease (fescue toxicosis caused by cattle feeding on endophyte-infected pastures) when implanted subdermally in cattle. Rods made of poly(3-HB-co-22 mol %-3-HV) were loaded with sulbactam-cefoperazone antibiotic and implanted into a rabbit tibia in order to study the change in chronic osteomyelitis. After 15 days of implantation, the infection decreased and within 30 days there was complete healing. Moreover, P(4HB), (P(3HB-co-4HB)) and poly (4-hydroxybutyrate-co-glycolate) (P(4HB-co-glycolate)) have been recently considered for the drug release systems and showed improved sustained release of tetracycline compared to the previously reported drug release systems. [4, 9]

PHAs have also been considered as drug carriers in the form of microspheres due to their biodegradability and biocompatibility in the early 1990s. Microspheres of P(3HB) loaded with rifampicin were investigated for their use as a chemo-embolizing agent by using the solvent evaporation technique with polyvinyl alcohol as an emulsifier, distilled water as the dispersion medium and methylene chloride as the solvent. The granule size varied between 5 and 100 mm and the drug release of all microspheres was very rapid with almost 90 % of the drug released within 24 h. However, controlled drug release was possible by regulating the drug loading and the particle size. P(3HB-co-3HV) has also been tested for tetracycline release in the acidic and neutral form showing rapid release of drug without any particle degradation [3].

12.5.4.5 Dental Materials

Periodontosis is a disease in which the alveolar bone and periodontium regress by bacterial infection. Gottlow et al. found that these regressed tissues can be

regained if the space for their regeneration is preserved. This technique is called guided tissue regeneration (GTR) or guided bone regeneration. The membrane for the space making has to function not only as a barrier but also as a permeable membrane, in order to shut out the inner growth of soft tissues and to supply nutrients, simultaneously. Hence, barrier membranes made from PHAs are being used to encourage regeneration of the periodontal ligament by making a space or pocket [3, 87]. P(3HB-co-3HV) membranes were compared with polytetrafluoroethylene membranes which showed better regeneration and tolerance. Moreover, non-porous P(3HB-co-3HV) films have been tried to keep soft tissues and bone separated until the regeneration is completely finished. P(3HB-co-3HV) films proved better than polylactic acid or polycaprolactone in terms of mechanical properties and tissue response [87]. Not only periodontal ligament defects but jaw bone defects can also be treated by these barrier membranes by regenerating new bone as well as increase height and width of the alveolar ridge. This has been proven by using P(3HB-co-3HV) membranes which showed complete regeneration of new bone in jaw bone defects [87]. P(3HB-co-3HV) membranes were also used to investigate the treatment of mandibular defects as well as increase the height of the rat mandible which resulted in increased bone fill within 15–181 days and completely filled space with regenerated new bone by 6 months respectively [87].

12.6 Conclusion

Petro-chemically synthesised plastics have become a necessity in our life because of their versatility, outstanding technical properties and relatively low price. Therefore, they have been used universally for different purposes such as, components in automobiles, home-appliances, computer equipment, packaging, construction, sports and leisure equipment, and also the medical applications, which made the discard of plastic wastes generated, a global problem. Even though plastics are fantastic commercial materials for almost everything, the inappropriate discard of the plastic wastes has threatened the world's natural environment since they are non-biodegradable in nature. Moreover, the extremely high price of the crude oil and the rapid depletion of the world's oil reserves as well as public awareness of the environmental effects of synthetically produced materials has created much interest in the development of biodegradable polymer plastics.

PHAs have rapidly gained interest both in research and industry due to their structural versatility and characteristics such as biodegradability, insolubility in water, nontoxicity, biocompatibility, piezoelectric property, thermoplasticity and or elastomeric properties, which make them favourable to be used in the packaging industry, medicine, pharmacy, agriculture, food industry and in the paint industry. The chemical and physical properties of the polymer are dependent on the monomeric composition which is determined by the producing microorganism and their nutrition. So far scl-PHAs are being studied extensively due to their easier

handling and higher crystallization rates. However, the degradation rate of scl-PHAs in vitro and in vivo has been found to be very slow probably due to the high crystallinity. Therefore, the less crystalline mcl-PHA has become the better prospective material for medical applications with required rate-controlled degradation. Hence, one major step forward for PHAs is the production of composites and blends to overcome or minimise drawbacks in properties that limit their application. In order to tailor the property of the polymer according to the application, blends and composites of PHAs have been studied which has helped in the progress of tissue engineering, sustained and controlled drug delivery and in other areas of medical/biomedical applications such as the development of devices, artificial organs and therapeutic uses.

However, the high production cost of the PHAs has triggered interest in using cheap raw materials including a variety of waste and byproducts as carbon sources for PHA production. Several strategies have been tried to improve conditions for economical PHA production including different bacterial species for different types of PHA production and recombinant strains, transgenic plants harbouring the microbial PHA biosynthesis genes, inexpensive carbon sources with high growth rate and with high polymer synthesis rate, media ingredients, fermentation conditions, modes of fermentation (batch, fed-batch, continuous) and recovery. And so far, despite all of the hindrances in the production cost of the PHAs, relatively high productivity at large scale has been achieved for P(3HB), P(3HB-co-3HV) and P(3HHx-co- 3HO).

In conclusion, PHAs are the environmentally friendly, next generation future green material with a range of applications.

12.7 Future Perspectives

Petro-chemical plastic production is estimated to increase with an annual growth rate of 9 % [101]. Much effort is made to reduce its consumption without any success due to their versatile properties suitable for an ample range of applications. However, it is possible to replace oil derived plastics with a material with similar properties but biodegradable characteristics which allow it to degrade without generation of toxic by-products. Among the various types of biodegradable polymers, PHAs have attracted a lot of attention as material for various applications for substitution of oil-derived polymers due to its ample range of monomer compositions appropriate for different kind of applications. PHAs have been proposed as material for several devices ranging from packaging materials to medical devices. However, they have not had a wide application mainly because of their production costs. For this reason, currently, only a few PHAs are available in the market. Although at the present petrochemical plastics are a more economically feasible choice than biodegradable ones, future lack in oil supply will result in a drastic increase in the petrochemical plastic production costs. On the other hand, further research on microbial strains, inexpensive substrates sources, diverse

fermentations strategies, polymer recovery and purification can substantially reduce the production cost and make PHAs commercially relevant. In addition, the development of genetically improved organisms to increase process efficiency can result in larger product yields and lower the cost of production.

The high cost of PHA production has led to most of the current studies to be focused on applications that conventional plastics cannot perform and where their properties are more important than the cost, such as medicine and pharmacology. In the medical field, the biocompatibility, biodegradability and adjustable mechanical properties of the PHAs have make them superior candidates for several applications. Research over the past years focused on the PHA metabolic pathways, PHAs polymerase substrate specificity and carbon sources provided to the media which are directly related to the final monomer composition. Altering monomer composition of PHAs can results in the development of polymers with favourable mechanical properties, biocompatibility and desirable degradation rates. In the future much more work needs to be done in developing tailor made materials to suit each particular application. Additionally, PHA blends and composites can widen PHA properties and applications. In the past years, PHAs have been proposed as materials for producing medical devices to replace several tissues and different studies in animals reveal PHA compatibility with a range of tissues. However, pyrogenic compounds co-purified with PHAs may cause immunogenic reactions and can limit their application in several cases. Future work thus also needs to develop different strategies to produce ultrapure PHAs using scalable, industry-friendly methods.

Hence, in the near future PHAs can be used to replace the currently used petrochemical-based plastics for certain suitable bulk applications and medical applications. These are certainly the natural green polymers of the future with a huge potential.

References

1. Langstaff, E., Ostrum, G.: Access to polymer information in chemical abstracts. J. Chem. Inf. Comput. Sci. **19**, 60–64 (1979)
2. Abou-Zeid, D.M.: Anaerobic biodegradation of natural and synthetic polyesters. Dissertation, Technische Universität Carolo-Wilhelmina zu Braunschweig, Germany (2001)
3. Zinn, M., Witholt, B., Egli, T.: Occurrence, synthesis and medical application of bacterial polyhydroxyalkanoates. Adv. Drug Deliv. Rev. **53**(1), 5–21 (2001)
4. Philip, S., Keshavarz, T., Roy, I.: Polyhydroxyalkanoates: biodegradable polymers with a range of applications. J. Chem. Technol. Biotechnol. **82**, 233–247 (2007)
5. Keshavarz, T., Roy, I.: Polyhydroxyalkanoates: bioplastics with a green agenda. Curr. Opin. Microbiol. **13**, 321–326 (2010)
6. Du, G., Si, Y., Yu, J.: Inhibitory effects of medium-chain-length fatty acid on synthesis of polyhydroxyalkanoates from volatile fatty acid by *Ralstonia eutrophus*. Biotechnol. Lett. **23**, 1613–1617 (2001)

7. Salehizadeh, H., Van Loosdrecht, M.: Production of polyhydroxyalkanoates by mixed culture: recent trends and biotechnological importance. Biotechnol. Adv. **22**, 261–279 (2004)
8. Stock, U., Sakamoto, T., Hastuoka, S., Martin, D., Nagashima, M., Moran, A., Moses, M., Khalil, P., Schoen, F., Vacanti, J., Mayer, J.: Patch augmentation of the pulmonary artery with bioabsorbable polymers and autologous cell seeding. J. Thorac. Cardiovasc. Surg. **120**, 1158–1168 (2000)
9. Valappil, S., Misra, S., Boccaccini, A., Roy, I.: Biomedical applications of polyhydroxyalkanoates, an overview of animal testing and in vivo responses. Expert Rev. Med. Devices **3**(6), 853–868 (2006)
10. Jurasek, L., Marchessault, R.: Polyhydroxyalkanoate (PHA) granule formation in Ralstonia. Appl. Microbiol. Biotechnol. **64**, 611–617 (2004)
11. Byrom, D.: Polyhydroxyalkanoates. In: Mobley, D.P.(ed.) Plastic from Microbes: Microbial Synthesis of Polymers and Polymer precursors, pp. 5–33. Hanser Munich (1994)
12. Volova, T.: Properties in polyhydroxyalkanoates-plastic materials of the 21st century: production, properties, applications, pp. 79–95. Nova Science Publishers, New York (2004)
13. Ojumu, T., Yu, J., Solomon, B.: Production of polyhydroxyalkanoates, a bacterial biodegradable polymer. Afr. J. Biotechnol. **43**, 18–24 (2004)
14. Chen, G.: Plastics completely synthesized by bacteria: polyhydroxyalkanoates. Microbiol. Monogr. **14**, 17–37 (2010)
15. Zinn, M., Hanry, R.: Tailored material properties of polyhydroxyalkanoates through biosynthesis and chemical modification. Adv. Eng. Mater. **7**, 408–441 (2005)
16. Rehm, B.H.A., Steinbüchel, A.: PHA synthases—the key enzymes of PHA synthesis. In: Steinbüchel, A., Doi, Y. (eds.) "Biopolymers", (Polyesters I), vol. 3a, pp. 173–215. Wiley, Heidelberg (2001)
17. Saad, B., Neuenschwander, P., Uhlschmid, G., Suter, U.: New versatile, elastomeric, degradable polymeric materials for medicine. Int. J. Biol. Macromol. **25**, 293–301 (1999)
18. Witholt, B., Kessler, B.: Perspectives of medium chain length poly(hydroxyalkanoates), a versatile set of bacterial bioplastics. Curr. Opin. Biotechnol. **10**, 279–285 (1999)
19. Nomura, C., Tanaka, T., Gan, Z., Kuwabara, K., Abe, H., Takase, K., Taguchi, K., Doi, Y.: Effective enhancement of short-chain-length-medium-chain-length polyhydroxyalkanoate copolymer production by coexpression of genetically engineered 3-ketoacyl-acyl-carrier-protein synthase III (fabH) and polyhydroxyalkanoate synthesis genes. Biomacromolecules **5**(4), 1457–1464 (2004)
20. El-Hadi, A., Schnabel, R., Straube, E., Müller, G., Henning, S.: Correlation between degree of crystallinity, morphology, glass temperature, mechanical properties and biodegradation of poly (3-hydroxyalkanoate) PHAs and their blends. Polym. Test. **21**, 665–674 (2002)
21. Conti, D., Pezzin, S., Coelho, L.: Mechanical and morphological properties of poly (3-hydroxybutyrate)/poly(3-hydroxybutyrate-co-3-hydroxyvalerate) Blends. Macromol. Symp. **245–246**, 491–500 (2006)
22. Akaraonye, E., Keshavraz, T., Roy, I.: Production of polyhydroxyalkanoates: the future green materials of choice. J. Chem. Technol. Biotechnol. **85**, 732–743 (2010)
23. Rai, R., Yunos, D., Boccaccini, A., Knowles, J., Barker, I., Howdle, S., Tredwell, G., Keshavarz, T., Roy, I.: Poly-3-hydroxyoctanoate P(3HO), a medium chain length polyhydroxyalkanoate homopolymer from *Pseudomonas mendocina*. **13**;**12**(6), 2126–2136 (2010)
24. Kim, D.Y., Kim, H.W., Chung, M.G., Rhee, Y.H.: Biosynthesis, modification, and biodegradation of bacterial medium-chain-length polyhydroxyalkanoates. J. Microbiol. **45**(2), 87–97 (2007)
25. Doi, Y., Abe, C.: Biosynthesis and characterization of a new bacterial copolyester of 3-hydroxyalkanoates and 3-hydroxy-ω-chloroalkanoates. Macromolecules **23**, 3705–3707 (1990)
26. Poirier, Y., Nawrath, C., Somerville, C.: Production of polyhydroxyalkanoates, a family of biodegradable plastics and elastomers in bacterial and plant. Biotechnol **13**, 142–150 (1995)

27. Steinbüchel, A.: Polyhydroxyalkanoic acids. Biomaterials: novel materials from biological sources, pp. 124–213. Stockton, New York (1991)
28. Kazunori, T., Takeharu, T., Ken'ichiro, M., Sumiko, N., Seiichi, T., Yoshiharu, D.: Investigation of metabolic pathways for biopolyester production. Ecomolecular Sci.Res. **42**, 71–74 (2001)
29. Huisman, G., Leeuw, O., Eggink, G., Witholt, B.: Synthesis of poly-3-hydroxyalkanoates is a common feature of fluorescent *pseudomonads*. Appl. Environ. Microbiol. **55**, 1949–1954 (1989)
30. Rehm, B.: Biogenesis of microbial polyhydroxyalkanoate granules: a platform technology for the production of tailor-made bioparticles. Curr. Issues Mol. Biol. **9**, 41–62 (2007)
31. Bohmert, K., Balbo, I., Tischendorf, G., Steinbuchel, A., Willmitzer, L.: Constitutive expression of the beta- ketothiolase gene in transgenic plants. A major obstacle for obtaining polyhydroxybutyrate-producing plants. Plant Physiol. **128**, 1282–1290 (2002)
32. Steinbuchel, A., Lutke-Eversloh, T.: Metabolic engineering and pathway construction for biotechnological production of relevant polyhydroxyalkanoates in microorganisms. Biochem. Eng. J. **16**, 81–96 (2003)
33. Verlinden, R., Hill, D., Kenward, M., Williams, C., Radecka, I.: Bacterial synthesis of biodegradable polyhydroxyalkanoates. J. Appl. Microbiol. **102**, 1437–1449 (2007)
34. Poirier, Y.: Polyhydroxyalknoate synthesis in plants as a tool for biotechnology and basic studies of lipid metabolism. Prog. Lipid Res. **41**, 131–155 (2002)
35. Shang, L., Jiang, M., Chang, H.: Poly(3-hydroxybutyrate) synthesis in fed-batch culture of *Ralstonia eutropha* with phosphate limitation under different glucose concentrations. Biotechnol. Lett. **25**, 1415–1419 (2003)
36. Vandamme, P., Coenye, T.: Taxonomy of the genus *Cupriavidus*: a tale of lost and found. Int. J. Syst. Evol. Microbiol. **54**, 2285–2289 (2004)
37. Vaneechoutte, M., Kampfer, P., De Baere, T., Falsen, E., Verschraegen, G.: Wautersia gen. nov., a novel genus accommodating the phylogenetic lineage including *Ralstonia eutropha* and related species, and proposal of Ralstonia [*Pseudomonas*] syzygii (Roberts et al. 1990) comb. nov. Int. J. Syst. Evol. Microbiol. **54**, 317–327 (2004)
38. Labuzek, S., Radecka, I.: Biosynthesis of copolymers of PHB tercopolymer by Bacillus cereus UW85 strain. J. Appl. Microbiol. **90**, 353–357 (2001)
39. Valappil, S., Peiris, D., Langley, G., Herniman, J., Boccaccini, A., Bucke, C., Roy, I.: Polyhydroxyalkanoates (PHA) biosynthesis from structurally unrelated carbon sources by a newly characterised Bacillus spp. J. Biotechnol. **127**, 475–487 (2007)
40. Valappil, S., Rai, R., Bucke, C., Roy, I.: Polyhydroxyalkanoate biosynthesis in *Bacillus cereus* SPV under varied limiting conditions and an insight into the biosynthetic genes involved. J. Appl. Microbiol. **104**, 1624–1635 (2008)
41. Park, S., Choi, J., Lee, S.: Engineering of *Escherichia coli* fatty acid metabolism for the production of polyhydroxyalkanoates. Enzyme Microb. Technol. **36**, 579–588 (2005)
42. Kahar, P., Agus, J., Kikkawa, Y., Taguchi, K., Doi, Y., Tsuge, T.: Effective production and kinetic characterization of ultra-high-molecular-weight poly (R)- 3-hydroxybutyrate in recombinant *Escherichia coli*. Polym. Degrad. Stab. **87**, 161–169 (2005)
43. Du, G., Chen, J., Yu, J., Lun, S.: Continuous production of poly-3- hydroxybutyrate by *Ralstonia eutrophus* in a two-stage culture system. J. Biotechnol. **88**, 59–65 (2001)
44. Du, G., Yu, J.: Green technology for conversion of food scraps to biodegradable thermoplastic polyhydroxyalkanoates. Environ. Sci. Technol. **36**, 5511–5516 (2002)
45. Yu, J.: Production of PHA from starch wastewater via organic acids. J. Biotechnol. **86**, 105–112 (2001)
46. Yu, J., Wang, J.: Metabolic flux modelling of detoxification of acetic acid by *Ralstonia eutrophus* at slightly alkaline pH levels. Biotechnol. Bioeng. **73**, 458–464 (2001)
47. Bhubalan, K., Lee, W., Loo, C., Yamamoto, T., Doi, Y., Sudesh, K.: Controlled biosynthesis and characterization of poly(3-hydroxybutyrate-co-3-hydroxyvalerate-co-3-hydroxyhexanoate) from mixtures of palm kernel oil and 3HV-precursors. Polym. Degrad. Stab. **93**, 17–23 (2007)

48. Reddy, C., Ghai, R., Rashmi Kalia, V.: Polyhydroxyalkanoates: an overview. Bioresour. Technol. **87**, 137–146 (2003)
49. Madison, L., Huisman, G.: Metabolic engineering of poly(3-hydroxyalkanoates): from DNA to plastic. Microbiol. Mol. Biol. Rev. **63**, 21–53 (1999)
50. Taguchi, S., Doi, Y.: Evolution of polyhydroxyalkanoate (PHA) production system by "enzyme evolution": successful case studies of directed evolution. Macromol. Biosci. **4**, 145–156 (2004)
51. Long, Y., Katherine, D., Lin, L.: Polymer blends and composites from renewable resources. Prog. Polym. Sci. **31**, 576–602 (2006)
52. Shanks, R., Hodzic, A., Wong, S.: Thermoplastic biopolyester natural fiber composites. J. Appl. Polym. Sci. **91**(4), 2114–2121 (2004)
53. Wong, S., Shanks, R., Hodzic, A.: Properties of poly(3-hydroxybutyric acid) composites with flax fibres modified by plasticiser absorption. Macromol. Mater. Eng. **287**, 647–655 (2002)
54. Al-Salihi, K., Samsudin, A.: Coral-polyhydroxybutrate composite scaffold for tissue engineering: prefabrication properties. Med. J. Malaysia. **59**(Suppl. B), 202–203 (2004)
55. Chen, L., Wang, M.: Production and evaluation of biodegradable composites based on PHB–PHV copolymer. Biomaterials **23**, 2631–2639 (2002)
56. Luklinska, Z., Bonfield, W.: Morphology and ultrastructure of the interface between hydroxyapatite-polyhydroxybutyrate composite implant and bone. J. Mater. Sci-Mater. M. **8**, 379–383 (1997)
57. Ni, J., Wang, M.: In vitro evaluation of hydroxyapatite reinforced polyhydroxybutyrate composite. Mater. Sci. Eng. C-Bio. S. **20**, 101–109 (2002)
58. Knowles, J., Hastings, G., Ohta, H., Niwa, S., Boeree, N.: Development of a degradable composite for orthopaedic use: in vivo biomechanical and histological evaluation of two bioactive degradable composites based on the polyhydroxybutyrate polymer. Biomaterials **13**, 491–496 (1992)
59. Galego, N., Rozsa, C., Sanchez, R., Fung, J., Vazquez, A., Tomas, J.S.: Characterization and application of poly(b-hydroxyalkanoates) family as composite biomaterials. Polym. Test. **19**, 485–492 (2000)
60. Luklinska, Z., Schluckwerder, H.: In vivo response to HApolyhydroxybutyrate/ polyhydroxyvalerate composite. J. Microsc-Oxford. **211**, 121–129 (2003)
61. Kose, G., Ber, S., Korkusuk, F., Hasirci, V.: Poly(3-hydroxybutyric acid-co-3-hydroxyvaleric acid) based tissue engineering matrices. J. Mater. Sci-Mater. M. **14**, 121–126 (2003)
62. Kose, G., Korkusuz, F., Korkusuz, P., Hasirci, V.: In vivo tissue engineering of bone using poly(3-hydroxybutyric acid-co-3- hydroxyvaleric acid) and collagen scaffolds. Tissue Eng. **10**, 1234–1250 (2004)
63. Kose, G., Korkusuz, F., Korkusuz, P., Purali, N., Ozkul, A., Hasirci, V.: Bone generation on PHBV matrices: an in vitro study. Biomaterials **24**, 4999–5007 (2003)
64. Zheng, Y., Wang, Y., Chen, X., Ren, Y., Wu, G.: Chemical reaction of PHBV/sol–gel bioglass foams for born tissue engineering in simulated body fluid. Chem. J. Chin. U. **24**, 1325–1328 (2003)
65. Martin, O., Schwach, E., Averous, L., Couturier, Y.: Properties of biodegradable multilayer films based on plasticised wheat starch. Starch **53**, 372–380 (2001)
66. Avella, M., Rota, G., Martuscelli, E., Raimo, M., Sadocco, P.: Poly(3-hydroxybutyrate-co-3-hydroxyvalerate) and wheat straw fibre composites: thermal, mechanical properties and biodegradation behaviour. J. Mater. Sci. **35**, 829–836 (2000)
67. Eidelman, N.: Characterization of combinatorial polymer blend composition gradients by FTIR microspectroscopy. J. Res. Natl. Inst. Stand. Technol. **109**, 219–231 (2004)
68. Renard, E., Walls, M., Guérin, P., Langlois, V.: Hydrolytic degradation of blends of polyhydroxyalkanoates and functionalized polyhydroxyalkanoates. Polym. Degrad. stab. **85**(2), 779–787 (2004)

69. Padermshoke, A., Katsumoto, Y., Harumi, S., Ekgasit, S., Noda, I., Ozaki, Y.: Melting behavior of poly(3-hydroxybutyrate) investigated by two-dimensional infrared correlation spectroscopy. Spectrochim. Acta Part A Mol. Biomol. Spectrosc. **61**, 541–550 (2005)
70. Ha, C., Cho, W.: Miscibility, properties, and biodegradability of microbial polyester containing blends. Prog. Polym. Sci. **27**(4), 759–809 (2002)
71. Satoh, H., Yoshie, N., Inoue, Y.: Hydrolytic degradation of blends of poly (3-hydroxybutyrate) with poly(3-hydroxybutyrate-co-3-hydroxyvalerate). Polymer **35**(2), 286–290 (1994)
72. Avella, M., Martuscelli, E.: Poly-d(-)(3-hydroxybutyrate)/poly(ethylene oxide) blends: phase diagram, thermal and crystallization behavior. Polymer **29**(10), 1731–1737 (1988)
73. Avella, M., Martuscelli, E., Greco, P.: Crystallization behaviour of poly(ethylene oxide) from poly(3-hydroxybutyrate)/poly(ethylene oxide) blends: phase structuring, morphology and thermal behaviour. Polymer **32**(9), 1647–1653 (1991)
74. Peoples, O., Snell, K.: Progress on plant based PHA production systems. In: International symposium on biological polyesters. minneapolis, Minnesota, US (2006)
75. Babu, R., Woods, T.: Polymer blends with improved mechanical properties. Society of plastics engineers. Plastics research online, pp. 1–2 (2011)
76. Premraj, M., Doble, M.: Biodegradation of polymers. Indian J. Biotechnol. **4**, 186–193 (2005)
77. Sivalingam, G., Karthik, R., Madras, G.: Blends of poly(ε-caprolactone) and poly(vinyl acetate): mechanical properties and thermal degradation. Polym. Degrad. Stab. **84**(2), 345–351 (2004)
78. Ren, Q., Grubelnik, A., Ruth, K., Hoerler, M., Hartmann, R., Felber, H.: Bacterial poly(hydroxyalkanoates) as a source of chiral hydroxyalkanoic acids. Biomacromol **6**, 2290–2298 (2005)
79. Rehm, R.: Genetics and biochemistry of polyhydroxyalkanoate granule self-assembly: the key role of poly-ester synthases. Biotechnol. Lett. **28**, 207–213 (2006)
80. Clarinval, A., Halleux, J.: Classification of biodegradable polymers, in biodegradable polymers for industrial applications. In: Smith, R. (ed.) CRC. pp. 3–56. Fl, USA (2005)
81. Chen, G.: Polyhydroxyalkanoates, in biodegradable polymers for industrial applications. In: Smith, R. (ed.) CRC. pp. 32–56. Fl, USA (2005)
82. Scholz, C.: Poly(β-hydroxyalkanoates) as potential biomedical materials: an overview. In: Scholz, C., Gross, R.A. (eds.) Polymers from renewable resources–biopolymers and biocatalysis, ACS series, vol. 764, pp. 328–334 (2000)
83. Steinbuchel, A.: Perspectives for biotechnological production and utilization of biopolymers: metabolic engineering of polyhydroxyalkanoate biosynthesis pathway as a successful example. Macromol. Biosci. **1**, 1–24 (2001)
84. Kofidis, T., Akhyari, P., Wachsmann, B.: A novel bioartificial myocardial tissue and its perspective use in cardiac surgery. Eur. J. Card. Thorac. Surg. **22**, 238–243 (2002)
85. Morosco, G.: Conquering heart disease: a call to action. Prev. Cardiol. **5**, 31–36 (2002)
86. Smaill, B., Mcfin, D., LeGrice, I.: The effect of synthetic patch repair of coarctation on regional deformation of the aortic wall. J. Thorac. Cardiovasc. Surg. **120**, 1053–1063 (2000)
87. Williams, S., Martin, D.: Applications of PHAs in medicine and pharmacy. Medicine **4**, 1–38 (1996)
88. Stock, U., Nagashima, M., Khalil, P., Nollert, G., Herden, T., Sperling, J., Moran, A., Lien, J., Martin, D., Schoen, F., Vacanti, J., Mayer, J.: Tissue engineered valved conduits in the pulmonary circulation. J. Thorac. Cardiovasc. Surg. **119**, 732–740 (2000)
89. Yang, F., Murugan, R., Wang, S., Ramakrishna, S.: Electrospinning of nano/micro scale poly(L-lactic acid) aligned fibersand their potential in neural tissue engineering. Biomaterials **26**, 2603–2610 (2005)
90. Yang, Y., De Laporte, L., Rives, C., Jang, J., Lin, W., Shull, K., Shea, L.: Neurotrophin releasing single and multiple lumen nerve conduits. J. Controlled Release **104**, 433–446 (2005)

91. Schmidt, C., Leach, J.: Neural tissue engineering: strategies for repair and regeneration. Rev. Biomed. Eng. **5**, 293–347 (2003)
92. Hazari, A., Johansson, R., Junemo, B.: A new resorbable wrap around implant as alternative nerve repair technique. J. Hand. Surg. **24**, 291–295 (1999)
93. Hazari, A., Wiberg, M., Johansson, R., Green, C., Terenghi, G.: A resorbable nerve conduit as an alternative to nerve autograft in nerve gap repair. Br. J. Plast. Surg. **52**, 653–657 (1999)
94. Novikov, L., Novikova, L., Mosahebi, A., Wiberg, M., Terenghi, G., Kellerth, J.: A novel biodegradable implant for neuronal rescue and regeneration after spinal cord injury. Biomaterials **23**, 3369–3376 (2002)
95. Opitz, F., Schenke-Layland, K., Richter, W.: Tissue engineering of ovine aortic blood vessel substitutes using applied shear stress and enzymatically derived vascular smooth muscle cells. Ann. Biomed. Eng. **32**, 212–222 (2004)
96. Maquet, V., Martin, D., Malgrange, B., Franzen, R., Schoenen, J., Moonen, G., Jerome, R.: Peripheral nerve regeneration using bioresorbable macroporous polylactide scaffolds. J. Biomed. Mater. Res. **52**, 639–651 (2000)
97. Ding, B., Wang, M., Wang, X., Yu, J., Sun, G.: Electrospun nanomaterials for ultrasensitive sensors. Mater. Today **13**(11), 16–27 (2010)
98. Queen, H., Master thesis. Electrospinning chitosan-based nanofibers for biomedical applications. North Carolina state University (2006)
99. Vondran, J., Rodriguez, M., Schauer, C., Sun, W.: Preparation of electrospun chitosan-PEO fibers in bioengineering conference. Proceedings of the IEEE 32nd annual Northeast, pp 87–88. (2006)
100. Bo-Yi, Y., Chi-Ruei, C., Yi-Ming, S., Tai-Horng, Y.: The response of rat cerebellar granule neurons (rCGNs) to various polyhydroxyalkanoate (PHA) films. Desalination **245**, 639–646 (2009)
101. Chanprateep, S.: Current trends sin biodegradable polyhydroxyalkanoates. J. Biosci. Bioeng. **110**(6), 621–632 (2010)

Editors Biography

Sabu Thomas, (PhD) is a Professor of Polymer Scienceand Engineering at the School of Chemical Sciences, as well as the Director of Centre for Nanoscience and Nanotechnology, Mahatma Gandhi University, India. He received his Ph.D. in 1987 in Polymer Engineering from the Indian Institute of Technology (IIT), Kharagpur, India. He is a fellow of the Royal Society of Chemistry, London and a member of the American Chemical Society. He has been ranked no 5 in India with regard to the number of publications (most productive scientists). He also received the coveted Sukumar Maithy Award for the best polymer researcher in the country for the year 2008. The research group of Prof. Thomas has received numerous awards and honors for excellent work in polymer science and engineering.

Visakh P. M. (MSc, MPhil) is a Research Fellow at the School of Chemical Science Mahatma Gandhi University. He edited 2 books with Sabu Thomas from Wiley and more than 8 books in press, (from Wiley, Springer, American Chemical Society and Royal Society of Chemistry and Elsevier) He has been invited as a visiting student in Italy (2009, 2012), Argentina (2010) Sweden (2010, 2011, 2012), Switzerland (2010), Spain (2011, 2012), Slovenia (2011), France (2011), Belgium (2012), and Austria (2012) for his research work and he published more than 5 publications and more than 5 book chapters. He has attended and presented more than 25 conferences. His research interests include: polymer nanocomposites, bio-nanocomposites, rubber based nanocomposites, fire retardant polymers and liquid crystalline polymers.

S. Thomas et al. (eds.), *Advances in Natural Polymers*,
Advanced Structured Materials 18, DOI: 10.1007/978-3-642-20940-6,

Aji. P. Mathew (Ph.D) is an Associate Professor in the field of Bionanocomposites at Luleå University of Technology, Luleå, Sweden. She recieved her Ph.D in Polymer Chemistry, in 2001 from Mahathma Gandhi University, Kottayam, Kerala, India. She worked as Postdoc. at CNRS, Grenoble, France and Norwegian University of Science and Technology (NTNU), before taking up the faculty position at Luleå University of Technology. Prof. Mathew is active in the field of biobased nanoreinforcments, nanocomposites, membranes and medical implants and products and published about 50 papers in these research areas.